FI 9703077-3/CD   SA-PUB -- 6/95

CCNF-9505257--

INTERNATIONAL CONFERENCE ON PAST, PRESENT AND FUTURE CLIMATE

MASTER

Proceedings of the SILMU conference held in Helsinki, Finland,
22–25 August 1995

S I L M U

The Finnish Research Programme on Climate Change

Pirkko Heikinheimo (Ed.)

INTERNATIONAL CONFERENCE ON PAST, PRESENT AND FUTURE CLIMATE

Proceedings of the SILMU conference held in Helsinki, Finland,
22–25 August 1995

Ministry of Education
The Academy of Finland

2nd edition

DISCLAIMER

**Portions of this document may be illegible
in electronic image products. Images are
produced from the best available original
document.**

Preface

The International Conference on Past, Present and Future Climate was organized to serve at least two purposes. Firstly, it was the fourth meeting in a series of Nordic climate conferences. Earlier Nordic meetings had been held in Copenhagen (1978), Stockholm (1983) and Tromsö (1990). Secondly, the conference formed part of the integration activities of the Finnish Research Programme on Climate Change (SILMU).

Four central themes were selected for the conference: 1) Climatic changes since the last glaciation inferred from proxy data, 2) Detection of climate change from the instrumental record, 3) Changes in atmospheric composition and 4) Predicting future climate.

The Finnish Research Programme on Climate Change was in its sixth and final year at the time of the conference. One of the aims of the meeting was to foster the communication of SILMU's results to the scientific community at large. On the other hand, feedback from overseas colleagues was expected to be beneficial for the final reporting of the results of the research programme.

The conference was held in the Hotel Aurora, Helsinki. Altogether 117 scientific contributions were submitted and more than 140 scientists attended the conference. SILMU hosted the conference, and additional support was received from the Ministry of Education and from the Research Council for the Environment and Natural Resources.

The organizers would like to thank all those who contributed to the different phases of the conference. Special thanks are due to the congress secretary, Jouni Pirttijärvi, for all his work.

This report contains all the papers and posters presented in the conference, organized according to the logic of the main theme: Past, Present and Future. Individual papers are arranged in alphabetical order. About one fourth of the papers are contributions by SILMU scientists.

Helsinki, 30 June 1995

Pirkko Heikinheimo

452844D

The organizing committee

Prof. Matti Eronen (chairman)
Department of Geology
FIN-00014 University of Helsinki
Phone (+358- 0)-191 3460
Fax: (+358-0)-191 3466
Email: matti.eronen@helsinki.fi

Dr. Martti Heikinheimo (secretary)
Finnish Meteorological Institute
P.O. Box 503, FIN-00101 HELSINKI
Phone (+358-0)-1929661
Fax: (+358-0)-1929 537
Email: martti.heikinheimo@fmi.fi

Dr. Tim Carter
Finnish Meteorological Institute /
Agricultural Research Centre

Dr. Raino Heino
Finnish Meteorological Institute

Prof. Eero Holopainen
Department of Meteorology
University of Helsinki

Dr. Markku Kanninen
SILMU Project Manager
Academy of Finland

Dr. Markku Kulmala
Department of Physics
University of Helsinki

Dr. Esko Kyrö
Finnish Meteorological Institute

Dr. Petteri Taalas
Finnish Meteorological Institute

Contents:

CLIMATE CHANGE RESEARCH: THE NATIONAL AND INTERNATIONAL CONTEXT

PAST CLIMATIC CHANGES

CLIMATIC CHANGES SINCE THE PLEISTOCENE TIMES

HOLOCENE CLIMATIC CHANGES

TREE RINGS

HISTORICAL CLIMATOLOGY

DETECTION OF CLIMATE CHANGES FROM THE INSTRUMENTAL RECORD

ANALYSIS OF CLIMATE RECORDS; LOCAL AND REGIONAL ASPECTS

ANALYTICAL METHODS / ANALYSIS OF OBSERVATION

CHANGES IN ATMOSPHERIC COMPOSITION

OZONE AND AEROSOL STUDIES

UV RADIATION

PREDICTING FUTURE CLIMATE

CLIMATE MODELS - DIAGNOSTICS, VALIDATION AND SENSITIVITY STUDIES

CLIMATE PROJECTIONS AND SCENARIOS

Climate change research: the national and international context

IPCC Scientific Assessment - a view from the inside

Bruce A. Callander
Head of the Technical Support Unit of IPCC WGI

Abstract

The Second IPCC Scientific Assessment, due to be completed at the end of 1995, will be the fourth report compiled by Working Group I of the Intergovernmental Panel on Climate Change since its inception in 1988. During those seven years the *political* climate (quite apart from the physical climate) has certainly changed. On the one hand, the Framework Convention on Climate Change is now in force and likely, over time, to lead to significant reductions in greenhouse gas emissions. On the other hand, pressure groups from both extremes of the climate change debate are still active in a vociferous campaign to capture the minds of those who make or influence policy . Such groups, usually with a better instinct for grabbing headlines than the average scientist, often fuel their campaigns with a mix of truths, half-truths and oversimplifications. The general public, meanwhile, perceive that global warming is a proven fact, even if they do tend to attribute it to 'the ozone hole'. Against this background, this talk will offer an overview of the key policy-related messages of the IPCC science assessments and whether these have changed significantly over the period of the four reports.

Regarding questions such as: why was IPCC invented? who participates in it? and who is its chief audience? it is clear that there is still some confusion and misunderstanding even among scientists. The process will be described by which IPCC science assessments, including their Summary for Policymakers, are drafted, reviewed, revised and, finally, formally approved by IPCC . Some personal observations will be offered on the strengths and weaknesses of the process, and how successfully it communicates policy-relevant scientific information. Evidence will also be produced in support of the case that IPCC science assessments remain the best available means of objectively assessing current scientific knowledge and understanding of climate change.

The talk will conclude with a brief outline of the threats and opportunities facing IPCC, its workplan post-1995 and its evolving relationship with the Conference of the Parties to the Climate Convention.

The International Coordination of Climate Model Validation and Intercomparison

W. L. Gates*

Program for Climate Model Diagnosis and Intercomparison
Lawrence Livermore National Laboratory Livermore, CA, USA

Climate modeling, whereby basic physical laws are used to integrate the physics and dynamics of climate into a consistent system, plays a key role in climate research and is the medium through which we seek to express our accumulating experience of how the climate has behaved and how it is expected to behave in the future. Depending upon the portion(s) of the climate system being considered, climate models range from those concerned only with the equilibrium globally-averaged surface temperature to those depicting the 3-dimensional time-dependent evolution of the coupled atmosphere, ocean, sea ice and land surface. Here we consider only the latter class of models, which are commonly known as general circulation models (or GCMs).

The validation (or determination of the degree of truth or validity) of climate models is a normal part of model development, but has not generally been carried out in a systematic manner. Ideally, each modeled physical or dynamical relationship should be tested against observational data, and the model's solutions for the overall spatial distribution and time evolution of the climate should be verified with corresponding observations. Here we consider only "whole model" validation in terms of the portrayal of systematic errors in the time averages of primary climatic variables, although a more complete validation would also include an examination of errors in the model's average variability and other statistics. A distinction may also be made between a "level 1" intercomparison in which models' results are assembled without regard to the experimental conditions, and a "level 2" intercomparison in which models' performance under common standardized conditions are considered. Once a model error has been identified, there remains the question of determining its statistical significance with respect to the model's stability and the uncertainty of the observational estimates.

The international coordination of climate modeling and model validation is appropriately carried out by the World Climate Research Programme (WCRP). Of the WCRP's many activities related to modeling, perhaps the best known is the Atmospheric Model Intercomparison Project (AMIP) initiated in 1989 (Gates, 1992). In this level-2 intercomparison, which expands an earlier WCRP level-1 intercomparison reported by Boer et al. (1992), all current atmospheric GCMs are being run over the ten-year period 1979-1988 subject to the same sequence of observed monthly-mean distributions of sea-surface temperature and sea ice (and with common values of the CO_2 concentration and solar constant). The

---

30 atmospheric GCM groups currently participating in AMIP have also agreed to calculate a common set of output that includes the surface heat, momentum and fresh water fluxes, the surface and top-of-the-atmosphere radiative fluxes, and the temperature, moisture, winds and pressure at selected tropospheric levels. In comparison to concurrent observational data, AMIP provides a comprehensive assessment of the accuracy of atmospheric GCMs as of the early 1990s, and is serving to document the improvement of many of the models whose revised versions are being used to revisit the AMIP simulation.

The AMIP results are illustrated in Fig. 1 for the zonally-averaged mean zonal wind at 200 hPa during December-January-February. Here most models are seen to agree with the observed distribution to within a few ms^{-1} at all latitudes, although a few models are evident outliers. Variables for which there is less agreement among models (and for which the observed data are less well known) include precipitation and cloudiness. An array of diagnostic subprojects are engaged in the detailed analysis and validation of the AMIP results, with emphasis on the models' performance in specific geographical regions and their portrayal of specific processes and/or phenomena. The initial results of AMIP were presented at an international scientific conference in May 1995 and will be summarized in the conference proceedings and in related reports and publications. Beginning in 1996, it is planned to launch AMIP II in which the surface boundary conditions will be made compatible with those being used in current reanalysis projects and in which the standard model output and diagnostics will be expanded. Although not formally coordinated through the WCRP, other ongoing intercomparisons of atmospheric models include the Climate of the Twentieth Century Project in which several GCMs are using the GISST sea-surface temperatures observed during the 1900s in extended integrations similar to those in AMIP.

The systematic validation and intercomparison of ocean GCMs are less advanced than those of atmospheric models, due to the availability of fewer observational data and to the difficulty of formulating suitable surface boundary conditions. This is illustrated by the WCRP intercomparison of 7 ocean models reported by Stockdale et al. (1993), in which the models systematically overestimate the sea-surface temperature in the western tropical Pacific. In a preliminary level-1 intercomparison of coupled global ocean-atmosphere models (Gates et al., 1993), on the other hand, the mean sea-surface temperature was simulated with reasonable accuracy only by those models employing empirical surface flux corrections, while the internal ocean circulation showed significant differences among the models. Major difficulties to be overcome in future (level-2) coupled model intercomparisons are the specification of suitable initial conditions in view of the relatively long spin-up times required by the deeper ocean, and the assembly of observational oceanic data suitable for model validation. The preliminary steps toward such an intercomparison being taken within the WCRP CLIVAR program will require coordination with the emerging Global Climate Observing System (GCOS), and should be designed to accommodate models of the more complete global climate system in the future.

References

Boer, G.J., K. Arpe, M. Blackburn, M. Déqué, W.L. Gates, T.L. Hart, H. Le Treut, E. Roeckner, D.A. Sheinin, I. Simmonds, R.N.B. Smith, T. Tokioka, R.T. Wetherald and D. Williamson, 1992: Some results from an intercomparison of the climate simulated by 14 atmospheric general circulation models. J. Geophys. Res., 97, 12771-12786.

Gates, W.L., 1992: AMIP: The Atmospheric Model Intercomparison Project. Bull. Amer. Meteor. Soc., 73, 1962-1970.

Gates, W.L., Cubasch, G.A. Meehl, J.F.B. Mitchell and R. Stouffer, 1993: An intercomparison of selected features of the control climates simulated by coupled ocean-atmosphere general circulation models. WCRP-82, WMO/TD-No. 574, World Meteor. Organization, Geneva, 46 pp.

Stockdale, T., D. Anderson, M. Davey, P. Deleluse, A. Kattenberg, Y. Kitamura, M. Latif and T. Yamagata, 1993: Intercomparison of tropical ocean GCMs. WCRP-79, WMO/TD - No. 545, World Meteor. Organization, Geneva, 43 pp.

Mean Zonal Wind at 200 hPa (m/sec)
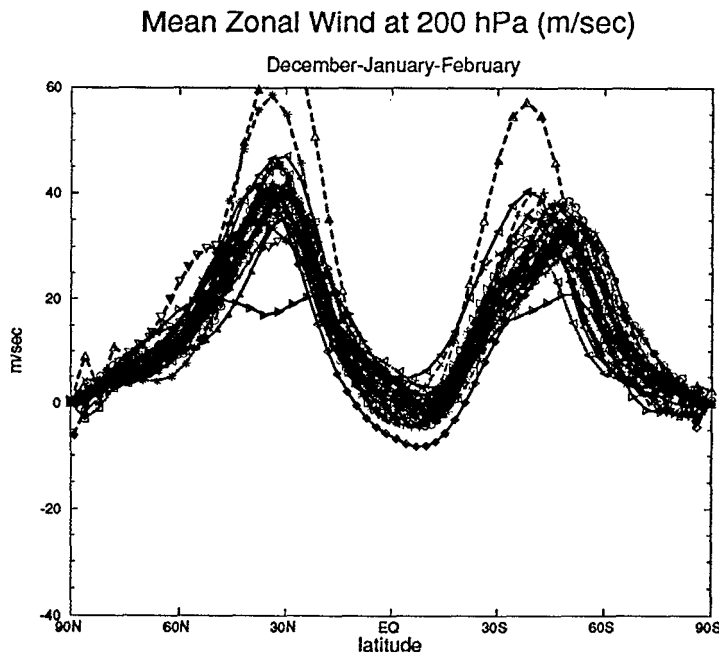
Fig. 1. The zonally-averaged zonal wind at 200 hPa as simulated in AMIP by 30 atmospheric GCMs for December, January and February of 1979-1988. The observed zonal wind is close to the mean of the models at all latitudes.

EUROPEAN NETWORK FOR RESEARCH IN GLOBAL CHANGE (ENRICH)

Anver Ghazi
Head, ENRICH Office

European Commission
DG XII/JRC
Rue de la Loi 200, B - 1049
Belgium

While approaching the beginning of the twenty first century, the scientific community is faced with the formidable tasks of monitoring and detecting, understanding and predicting changes in the Earth System and its interactions with human beings. A crucial challenge is to make scientific research results accessible and usable for those involved in the decision making process related to the concept of Sustainable Development. Major international scientific programmes under the umbrella of ICSU, such as the IGBP and WCRP, are dealing with these issues.

Although there exist many well developed global change research programmes in several European countries and effective collaboration networks between research institutes, there is an urgent need for overall communication with a view to promoting wider international links ensuring complementarity, synergy and coherence.

Recognising the importance of promoting coherence in research and utilising research results for various European Union (EU) policies, the European Commissioner responsible for Science, Research and Development wrote in March 1992 to all the EU Research Ministers to propose an initiative in this domain. In a rapid response, a group of Senior Experts from the EU Member States was set up in April 1992. This Group established a Task Force to develop the concept of the European Network for Research In Global CHange (ENRICH) which was approved in July 1993.

This concept is based on three fundamental principles:

- improvement of communication, collaboration and coordination with the aim to increase synergy and coherence;
- promotion of partnership; and
- promotion of capacity building in the geographical regions concerned.

The overall objective of ENRICH is to pursue a major coherent European contribution to international actions on global change research. As well as considering the needs of European Commission (EC) programmes and activities, and taking into account

the existing activities of the EU and EFTA Member States, ENRICH aims to support the knowledge base for the development of EU policy objectives. It intends to do so by acting as a clearinghouse for the exchange of information and by promoting cooperation in research and capacity building. In addition to promoting collaboration in Western Europe (EU and EFTA), ENRICH also aims to encourage the endogenous research capabilities in developing countries mainly, but not exclusively in Africa and in the Mediterranean Basin and to promote support for relevant research initiatives in the countries of Central and Eastern Europe and the New Independent States of the former Soviet Union (NIS).

The main objectives of ENRICH are:

i)   to promote a pan-European contribution to the international global change research programmes;
ii)   to foster collaboration between and promote support for global change research in Western Europe, Central and Eastern Europe and NIS, Africa and other developing countries;
iii)   to promote the establishment of Communication links/networks;
iv)   to improve the access by the scientific community to EU mechanisms for support to global change research.

The European Commission is initiating the implementation of ENRICH in the context of its Fourth Framework Programme for Research and Development (1995-1998) with a view to focussing the EU's research efforts in this area. In particular, the specific programme for Environment and Climate research is to be the main vehicle for ENRICH actions.

ENRICH's Implementation Plan was adopted in February 1995 by the ENRICH Council which is made up of high-level representatives of the EU and EFTA countries and Commission services. The Plan includes a list of concrete actions with respect to the four main objectives mentioned earlier and is a logical continuation of activities already undertaken in 1994 such as: support to several workshops and meetings of international programmes (eg. IGBP/START) in Europe and Africa, organisation of the ENRICH Regional Seminar for Central and Eastern Europe (Budapest,1994) with the aim to promote joint research with Western Europe, studies on EC level research on Human Dimensions of Global Change and the preparation of an inventory on global change research networks in Europe and pilot projects on terrestrial ecosystems and land-ocean interactions.

The Implementation Plan and other information about ENRICH is accessable through the ENRICH Home Page on Internet (address:http://www.enrich.hi.is/).

Thus, this initiative of the European Commission is meant to facilitate and enable climate and global change research networking and will encourage, promote and augment the effectiveness of similar undertakings elsewhere in the world.

The ATMOSPHERE subprogramme of the Finnish Research Programme on Climate Change (SILMU): some remarks

Eero Holopainen (Subprogramme Head)

Department of Meteorology,
P.B. 4 (Hallituskatu 11), FIN-00014 University of Helsinki

Content of the ATMOSPHERE subprogramme of SILMU

The Finnish Research Programme on Climate Change (SILMU) consists of four subprogrammes: (1) ATMOSPHERE, (2) WATERS, (3) TERRESTRIAL ECOSYSTEMS and (4) HUMAN INTERACTIONS. The International Conference on Past, Present and Future Climate is organized by the ATMOSPHERE subprogramme.

In the second phase of SILMU programme (1993-95) the ATMOSPHERE subprogramme has consisted of some 15 projects falling roughly in three groups:

A. Climate data and climate models
- *Dendrocronological climate history of the Fennoscandian subarctic region*
- *The variation of carbon isotope ratios in the tree rings*
- *Microclimate models*
- *Climate changes in the northern Europe*
- *Climate models and scenarios*
- *Statistical weather generator*

B. Ozone
- *Changes in the stratospheric ozone in northern Europe*
- *UV radiation in Finland*
- *Accurate measurements of the solar UV-radiation and the carsinogenic effects of the radiation*
- *Tropospheric chemistry*

C. Aerosols
- *Chemical and physical aerosol processes in cold conditions, and the effect of radiation on these processes*
- *Mathematical models for atmospheric aerosol*

Some highlights of the results obtained

Many of the results obtained in various projects of SILMU/ATMOSPHERE will come up in the oral and poster presentations at this conference. Within each group A, B and C only one of the main results is mentioned here:

A) Estimates of lowfrequency natural climate variability from tree rings

Tree rings in northern Finland are known to provide proxy data of summer temperatures. When SILMU ends, a 7000 year long time series of tree rings and, hence, of summer temperatures may be available providing estimates of natural lowfrequency temperature variability in northern Europe. Such estimates are particularly important in connection with the "detection issue".

B) Anthropogenic depletion of the Arctic ozone layer

SILMU/ATMOSPHERE researchers have participated in the international field campaigns and modelling studies aimed at finding out indications of possible anthropogenic depletion of the Arctic ozone layer, by now wellknown in the Antarctic atmosphere. Some evidence for such depletion has indeed been found.

C) The cooling effect of aerosols on climate

Studies within SILMU/ATMOSPHERE have shown that atmospheric aerosol particles generated by anthropogenic air pollution can have a direct and possibly even an indirect cooling effect on climate.

General comment

Usual difficulties of an interdisciplinary approach have been encountered within SILMU, not only in connections between the various subprogrammes but also within the subprogrammes themselves. Nevertheless, the ATMOSPHERE subprogramme has, besides producing important scientific findings, also created significant interaction between various disciplines and institutes involved.

Past climatic changes
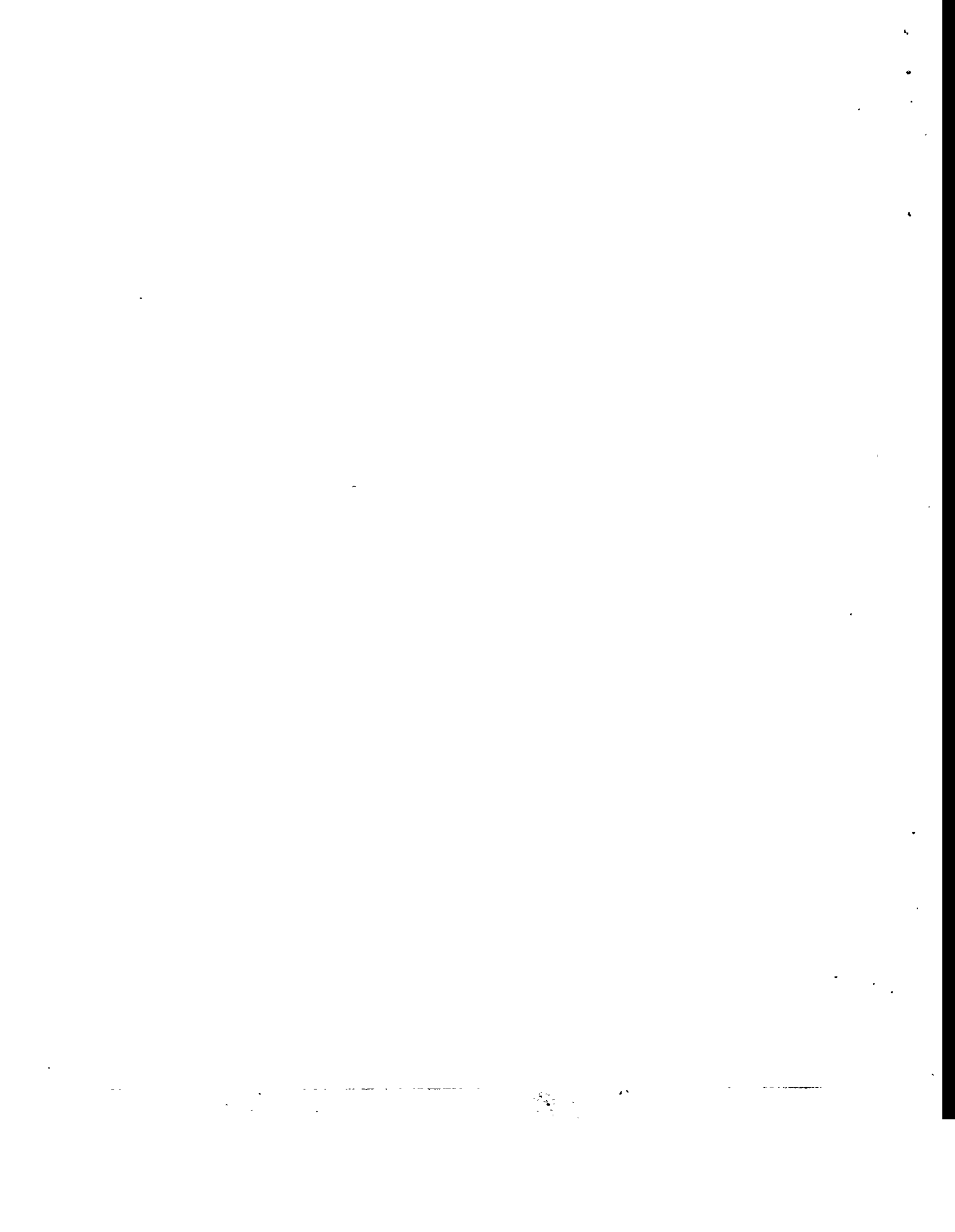
Transient response of the LLN model over the last 200 kyr and next 100 years

André Berger, Marie-France Loutre and Xuesong Li

Institut d'Astronomie et de Géophysique Georges Lemaître
Université catholique de Louvain
2 Chemin du Cyclotron
B-1348 Louvain-la-Neuve, Belgium

The LLN climate model is a two-dimension (latitude-altitude) sectorially averaged model of the northern hemisphere which links the atmosphere, the ocean mixed layer, the sea ice, the ice sheets and their underlying bedrock (a global model including the deep-ocean circulation and a carbon cycle is in development). Simulation shows that the model is able to reproduce the main characteristics of the present-day climate and general circulation. Its response to a CO_2 doubling ($\sim 2°C$) lies in the lowest range of sensivity of the equilibrium general circulation models, but is in full agreement with the transient simulation made with atmosphere-ocean GCM's.

Used to test the Milankovitch theory, the 2-D LLN model shows that orbital and CO_2 variations induce, in the climate system, feedbacks sufficient to generate the low frequency part of the climatic variations over the last glacial-interglacial cycles. This model clearly shows that long-term changes in the Earth's orbital parameters lead to variations in the amount of solar radiation received at the top of the atmosphere, which in turn act as a pacemaker for climatic variations at the astronomical frequencies, through induced albedo-temperature and greenhouse gases-temperature feedbacks. In order to demonstrate the ability of the model to generate the 100 kyr cycle, the transient response of the climate system to both the astronomical and CO_2 forcings was simulated over the last 800 kyr. It is particularly significant that spectral analysis of the simulated northern hemisphere global ice-volume variations reproduces correctly the relative

intensity of the peaks at the orbital frequencies as seen in SPECMAP data. Except for variations with time scales shorter than 5 kyr, the simulated long-term variations of total ice volume are comparable to that reconstructed from deep-sea cores. For the last 200 kyr for example, the model simulates glacial maxima of similar amplitudes at 134 kyr BP and 15 kyr BP, followed by abrupt deglaciations. Using different CO_2 reconstructions over the two last glacial-interglacial cycles, the model seems to be not too sensitive to the glaciological time scale of the Vostok ice core. It is definitely driven by the astronomical forcing, the CO_2 variations helping to produce a better amplitude in the long-term temperature change and a more accurate southward extend of the northern american ice sheet. For the Middle and Late Pleistocene, the atmospheric CO_2 concentration was reconstructed from a regression between Vostok CO_2 data and the marine oxygen isotope values. The results of the simulation suggest that the amplitude between glacial and interglacial stages was increasing, the interglacials were related to high eccentricity and the northern hemisphere mean temperature has slightly increased.

For the future, if the CO_2 concentration of the last interglacial-glacial cycle is used, the next "natural" glacial stage is happening at about 60 kyr AP, is followed by a glacial maximum just after 100 kyr AP and by a rapid deglaciation leading to an interglacial and the disappearance of the northern hemisphere ice-sheets at 120 kyr AP.

Historical Climatology in Europe: Recent findings and developments

Christian Pfister

Institute of History, University of Bern
Unitobler, CH 3000 Bern 9

Introduction

A recent survey of the evidence presented by Hughes & Diaz (1994) indicates that the pattern of regional differences in the character of climatic anomalies during the ninth through fourteenth century, indeed shows spatial and temporal differentiation in much the same way as the Little Ice Age (Bradley & Jones 1995). However, it is not clear, how far these findings can be extrapolated to the **whole** of Europe. Significant progress towards an area covering climate history of Europe for the last 500 years is being obtained from a cooperation among historical climatologists in the framework of the Euro-Climhist data-base. Less effort is spent on the Middle Ages despite the fact that the so called Medieval Optimum is the only warm period of purely natural climate that can be investigated in some detail.

Methodology and Data

Documentary data often include observations of hydrological or biological features that may be calibrated with instrumental series (e.g. Pfister 1992; Vesajoki & Tornberg 1994). An appropriate statistical tool for quantifying both proxy data and descriptive information in their combination is not available. A rather robust solution to this problem consists in rating both types of data available for a specific period with an index (Wanner et al. 1995).

Moreover, the usual time series approach needs to be complemented with an effort to explore the spatial dimension of climatic change. Data for a specific time interval are displayed in form of charts that provide an initial framework for the reconstruction of synoptic pressure distribution (e.g. Lamb 1987; Kington 1988). The difficulties in developing this approach are closely related to the deficiencies of the available material. Systematic observations of wind direction (Jönsson 1994, Frich & Frydendahl 1994) or cloud direction (Pfister & Bareiss 1994) are particularly valuable in this respect. Gaps in the distribution of long term instrumental records are being closed for the Baltic (Tarand 1993; Vesajoki 1995), Iceland (Jonsson, in prep.) and the Iberian Peninsula (Barriendos, in prep). Evidence is still not sufficient for Russia and for the Balkans.

A pilot study for the late Maunder Minimum (1675-1715) included 220'000 documentary and early instrumental data from 17 countries of Europe as well as tree ring data (Frenzel et al. 1994). For the winter and spring months in the period 1675-1704 a systematic reconstruction of surface pressure patterns was attempted (Wanner et al. 1995).

The lack of data for the Iberian peninsula was a major shortcoming for this approach. A promising, area covering type of proxy data has been explored: Anomalous spells of

weather such as droughts in the winter half year or long periods of rain in summer which endangered the outcome of the harvests were systematically monitored. The church was asked to organize rogations appropriate for every type and level of environmental stress. The analysis of this indicator allows a systematic reconstruction of climatic anomalies from the sixteenth to the nineteenth century (Martin Vide & Barriendos 1995, Rodrigo et al. 1995).

Results

Iceland
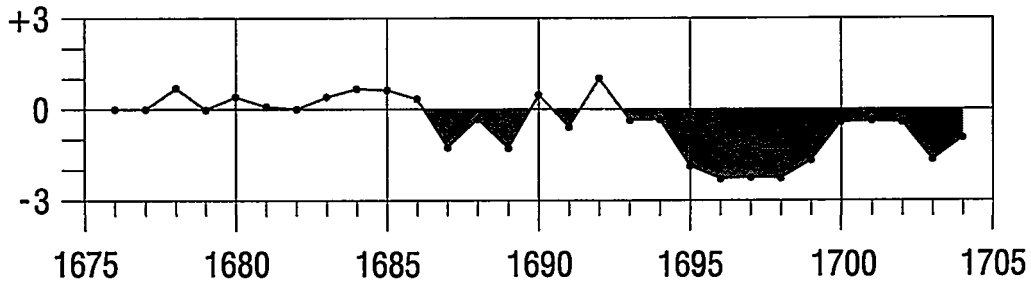
England
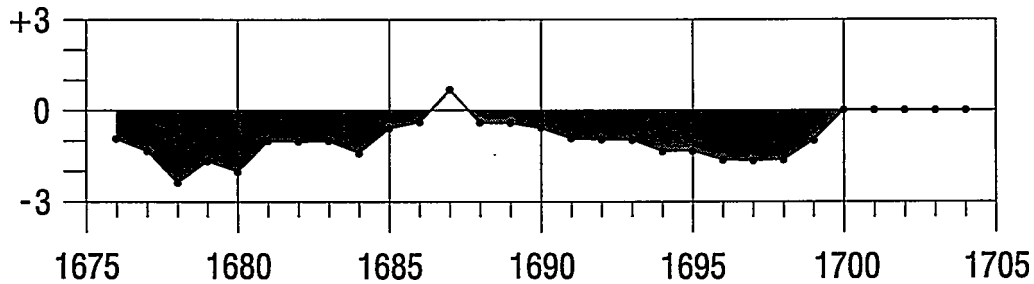
Switzerland
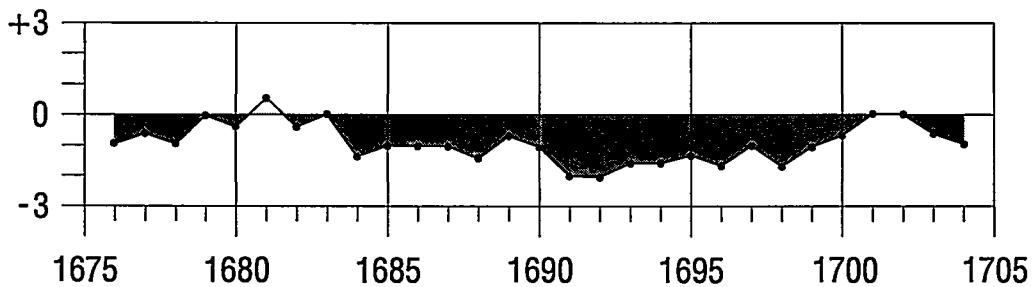
Fig. 1: Three year moving averages of winter temperature indices for Iceland, England and Switzerland. Positive indices stand for warm, negative ones for cold conditions. The Icelandic curve is based upon descriptive information, the English one on thermometric measurements, the Swiss one on documentary proxy data (freezing of lakes, duration of snow-cover).

Fig. 1 displays moving averages of the indices for three typical regions (oceanic, coastal, continental) for the period of the Late Maunder Minimum. Winter temperatures show a clear 'below normal behavior'. The temperature decline started first in England and was then continued in Switzerland. In Iceland winters were not persistently cold except in the late 1690's.

Moses & Kiladis (1987) stated that the strong wintery reversals in the monthly pressure field with high pressure over Iceland represent an extreme mode of the North Atlantic Oscillation (NAO). It is concluded from the analysis of some analogues in the more recent past and from the example of the Late Maunder Minimum (Fig. 2) that the most severe winters of the 'long' Little Ice Age (from the early fourteenth century) were strongly influenced by pressure reversals over Iceland and blocking actions with dominating northeasterly flow and cold air advection (Pfister et al. 1995).
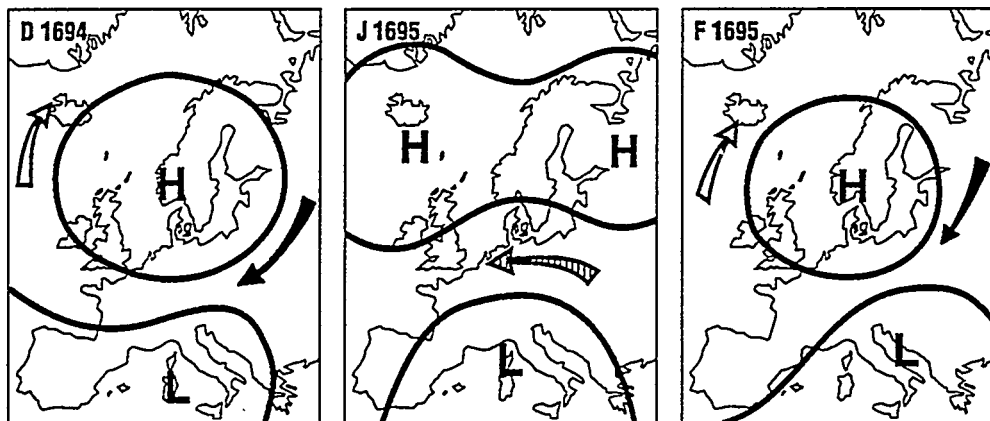
Fig. 2: Reconstructed surface pressure pattern for winter 1694/95. From December 1694 to February 1695 Europe was mainly dominated by blocking anticyclones centered over Southern Scandinavia. This lead to a sustained inflow of cold continental air-masses from NE or E, whereas the SW of Iceland was rather warm.

Severe winters frequently clustered within a period of 20 to 25 years and were then followed by runs of milder winters. The timescale of 40-60 years suggest that these oscillations are related to variations in the thermohaline circulation in the North Atlantic (Stocker 1994).

References

Bradley, R.S. & Jones, P. D. 1995: Recent developments in studies of climate since A.D. 1500. In Climate since A.D. 1500. 2nd revised ed., Routledge, London, pp. 666-680.

Frenzel, B., Pfister, C. & Glaeser, B. (eds.) 1994: Climate in Europe 1675-1715. Special Issue. ESF Project European Palaeoclimate and Man, Fischer, Stuttgart.

Frich, P. & Frydendahl, K. 1994: The summer climate in the Oresund region of Denmark, A.D. 1675-1715. In: Frenzel B., Pfister, C., Glaeser B. (eds). Climatic trends and anomalies in Europe 1675-1715, Fischer, Stuttgart, pp. 33-42.

Hughes, M.K. & Diaz, H.F. (1994): The Medieval Warm Period. Special Issue: Climatic Change Vol. 26/2-3, 1994. Kluwer, Dordrecht.

Jönsson, P. 1994: Wind Climate During the Instrumental Period and Recent Wind Erosion in Southern Scandinavia. University Press, Lund.

Kington, J. 1988: The Weather of the 1780s over Europe. CUP, Cambridge.

Lamb, H.H. 1987: What can Historical Records Tell us About the Breakdown of the Medieval Warm Climate in Europe in the Fourteenth and Fifteenth Centuries - An Experiment. In: Beitr. Phys. Atmosph. 60/2, pp. 131-143.

Martin Vide, J. & Barriendos, M. 1995: Rogation Ceremony Method based on Environmental Factors. In: Climatic Change, in press

Moses, T. & Kiladis, G.N. 1987: Characteristics and frequency of reversals in mean sea level pressure in the north atlantic sector and their relationship to long-term temperature trends. In: Journal of climatology, Vol. 7, 1987, pp. 13-30.

Pfister, C. 1992: Monthly temperature and precipitation patterns in Central Europe from 1525 to the present. A methodology for quantifying man made evidence on weather and climate. In: Bradley R.S., Jones P.D. (eds.) Climate since 1500 A.D., Routledge, London, pp. 118-143.

Pfister, C. & Bareiss W. 1994: The Climate in Paris between 1675 and 1715 after the Meteorological Journal of Louis Morin, In: Frenzel, B., Pfister, C. & Glaeser, B. (eds.), Climate in Europe 1675-1715. Fischer, Stuttgart, pp. 151-172.

Pfister C., Kington J., Kleinlogel G., Schüle H. & Siffert, E. 1994: The creation of high resolution spatio-temporal reconstructions of past climate from direct meteorological observations and proxy data. In: Frenzel, B., Pfister, C. & Glaeser, B. (eds.), Climate in Europe 1675-1715. Fischer, Stuttgart, pp. 329-376.

Pfister, C, Schwarz-Zanetti G., F. Hochstrasser & Wegmann M. 1995: The most severe winters of the fourteenth century in Central Europe compared to some analogues in the more recent past: in: B. Frenzel, E. Wishman, M.M. Weiss (eds.), Documentary climatic evidence for 1750-1850 and the 14th century, Fischer, Stuttgart, in press.

Rodrigo, F.S., Estban-Parra, M.J. & Castro-Diez, Y. 1995: The onset of the Little Ice Age in Andalusia (southern Spain) detection and characterization from documentary sources. In: Annales Geophysicae 13, 1995: 330-338.

Stocker, T.F. 1994: The variable ocean. In: Nature, Vol 367, January 1994, p. 221-222.

Tarand, A. 1993: Precipitation Time Series in Estonia in 1751-1990. In: Zeszyty Naukowe Uniwersytetu Jagiellonskiego, MCXIX, Prace Geograficzne, Z.95, pp.139-149. Tallinn.

Vesajoki, H., Tornberg, M. 1994: Outlining the climate in Finland during the pre-instrumental period on the basis of documentary sources, In: Frenzel, B., Pfister, C. & Glaeser, B. (eds.), Climate in Europe 1675-1715. Stuttgart (Fischer), pp. 51-60.

Vesajoki, H. 1995: The early temperature records of Turku, in: in: B. Frenzel, E. Wishman, M.M. Weiss (eds.), Documentary climatic evidence for 1750-1850 and the 14th century, in press

Wanner, H., Pfister, C., Brazdil, R., Frich, P., Frydendahl, K., Jonsson, T., Kington, J., Lamb, H.H., Rosenom, S. & Wishman, E. 1995: Wintertime European Circulation Patterns during the Late Maunder Minimum (1675-1704) cooling period. In: Theoretical and Applied Climatology, in press

Paleoclimates and chronology interpreted from the loess-paleosol sequence, North Central China

Nat Rutter

Department of Geology
University of Alberta
Edmonton, Alberta, Canada T6G 2E3

Introduction

The Baoji section is judged to be the most complete pedostratigraphic section in the Loess Plateau of north-central China. It is located about 5 km north of the city of Baoji and consists of 37 field identified paleosols formed during the last 2.5 Ma (Rutter et al., 1991a; Fig. 1). The variation of the paleosols suggests climatic cycles of varying intensity and duration; but generally warmer and moister conditions when compared with the loess units that suggest colder and drier periods.

Geochronological control is based largely on magnetostratigraphy with the Brunhes, Matuyama and Gauss epochs, and Jaramillo and Olduvai events clearly recognized (Rutter et al., 1991b). The Baoji paleosols can be correlated with equivalent pedostratigraphic units throughout the Loess Plateau by a combination of magnetostratigraphy, magnetic susceptibility, and the character, position and association of the Pedostratigraphic units within the Quaternary succession. By utilizing various proxies within the sequence it has been possible to elucidate on paleoclimate and monsoonal variations, determine forcing mechanisms, develop an orbital time scale, and speculate on linkages between various climatic elements.

Results

Based on macro- and micromorphological observations, the major pedogenic processes involved in the formation of the Baoji paleosols are believed to be carbonate eluviation and illuviation, clay translocation, pseudogleization and rubification (Rutter and Ding, 1993). The diagnostic B horizons of the 37 soils are classified into four types - Bw, or weak Bt, moderate Bt, strong Bt and very strong Bt. The Holocene soil at Baoji contains a moderately developed Bt, which was formed under steppe-forest vegetation. Most of the soils with comparable Bt horizons to the Holocene soil are interpreted to be developed under forest and/or steppe-forest environments.
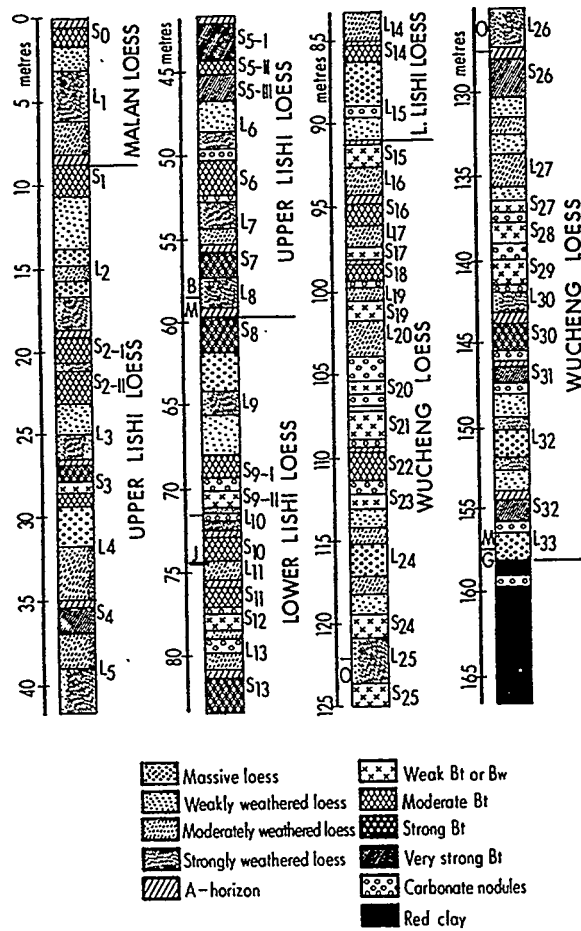
Fig. 1. Loess-paleosol sequence at Baoji with designation of the major soil horizons. Paleomagnetic reversals are indicated — B = Brunhes, M = Matuyama, J = Jaramillo, O = Olduvai, G = Gauss.

Particle size measurements of some typical loess-soil samples taken in different localities of the Chinese Loess Plateau show that the grains are concentrated almost completely in the fractions below 50 μm. The fraction ranging from 50 to 10 μm, and smaller than 2 μm show the most variability, with the variability within the fraction between 10 and 2 μm being minor. The measurements also suggest that pedogenic weathering can only make a limited or negligible contribution to the grain size distribution of loess deposits. The ratio of the fraction smaller than 2 μm (%) to the fraction greater than 10 μm (%) was used as a grain size index, and the grain size distribution in the Baoji and Weinan (50 km east of Baoji) loess-soil sections was analyzed. Results show that this grain size index is very sensitive to loess-soil alternations, with loess units being coarser than soils (Ding et al., 1994; Fig. 2).

Analytical results also suggest that during soil-forming periods, aeolian dust accumulation was still substantial, though at a reduced rate, and hence loess deposition can be regarded

as a nearly continuous process in the Loess Plateau of north-central China. As previous studies have demonstrated, loess deposits in the Loess Plateau were shifted from the inland deserts of northwestern China by cold-dry winter monsoonal winds (Liu et al., 1985; An et al., 1991). The grain size profiles are then employed to represent the glacial-interglacial cyclic variations in the intensity of the East Asia winter monsoon.
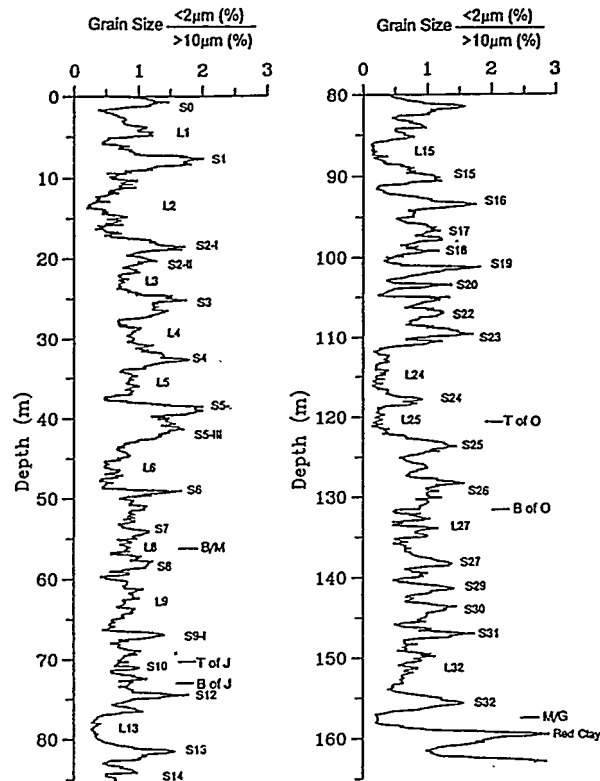
Fig. 2. Grain size variation of the Baoji loess-soil section, plotted on a depth scale with the numbering of the loess (L) and soil (S) units. Grain size index expressed in the ratio of the fraction smaller than 2 μm (%) to that larger than 10 m (%). Major magnetic reversals (Brunhes/Matuyama boundary, Jaramillo and Olduvai subchrons, and Matuyama/Gauss boundary) tied to the loess-soil sequence are shows.

The grain size record is thus employed as a proxy indicator of the winter monsoon circulation and tuned to the orbital records calculated recently by Berger and Loutre (1991). An orbital time scale was developed (Ding et al., 1994; Fig. 3). The tuning is independent of any correlation with $\delta^{18}O$ signals in the deep-sea sediments. The grain size time scale is tightly constrained, as suggested by the following facts: (1) the filtered obliquity and precession components from the grain size data on the orbital time scale closely match the theoretical orbital records; (2) ages of the major magnetic reversals estimated from the grain size time scale are in good agreement with the K/Ar-dated ages; (3) there is close coherence between the Baoji grain size time series and the orbital variations at the orbital frequency bands over the entire 0-2.5 Ma period; and (4) the grain size record on the orbital time scale shows a close similarity to the orbitally-tuned DSDP Site 607 and ODP Site 677 $\delta^{18}O$ records.
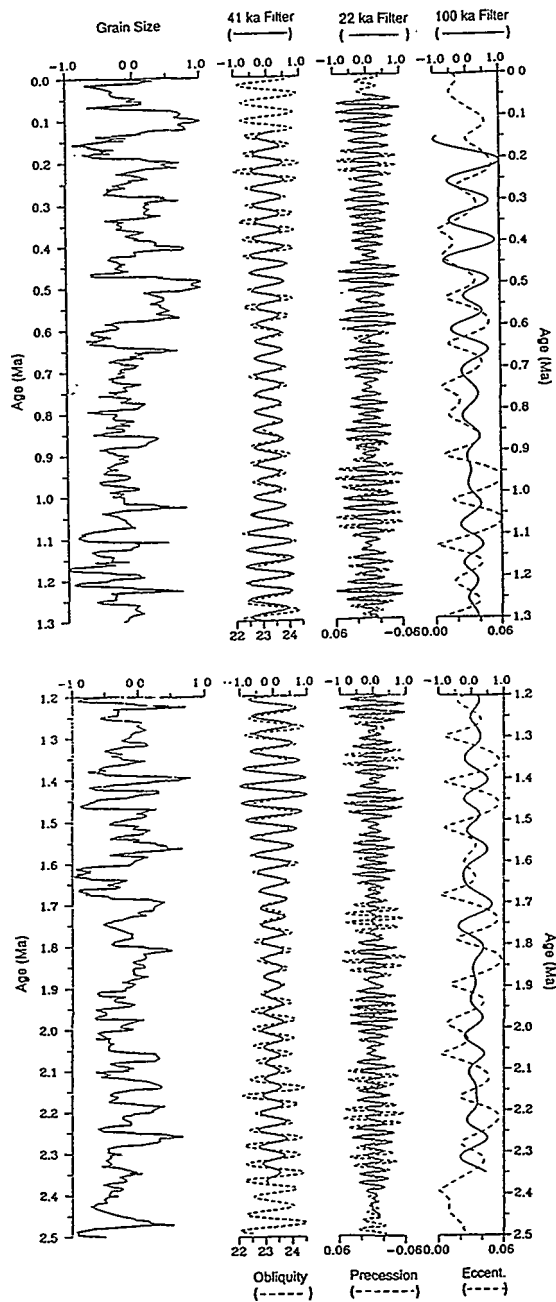
Fig. 3. Baoji grain size data plotted on BJGS time scale in the past 2.5 Ma: (left to right) normalized grain size data, filtered obliquity signal from the grain size data with a central period of 41 ka (solid line) versus lagged orbital obliquity (dashed lines), filtered precessional signal with a central period of 22 ka (solid line) versus lagged and inverted orbital precision, and filtered eccentricity signal with a central period of 100 ka (solid line) versus orbital eccentricity (dashed line). The filtered signals are normalized.

The somewhat abrupt commencement of loess deposition on a large scale in north-central China is palaeomagnetically measured at about 2.5 Ma. The formation of the dynamical conditions responsible for windblown loess processes implies a reorganization of the atmospheric circulation over eastern Asia. It is speculated that at that time, the accelerated uplift of the Tibetan Plateau had reached a threshold height, giving rise to the intensification and northward shift of the Siberian high and deepening of the cyclone in the lee of the Tibetan Plateau. The uplift of Tibet and the resulting reorganization of atmospheric circulation at about 2.5 Ma would initiate a coupled environmental system: Tibetan Plateau-inland desert-Loess Plateau in eastern Asia that could be a key system in understanding the onset of glaciation in Northern Hemisphere and climatic change in the Quaternary. Therefore, the climatic shift from near-continuous warm condition before 2.5 Ma to frequent and chaotic fluctuations after is speculated to be triggered to a significant extent by the uplift of the Tibetan Plateau.

The high-resolution East Asian winter monsoon record reconstructed from the Baoji section shows two major shifts in climate modes over the past 2.5 Ma, one occurring at about 1.7-1.6 Ma BP and the other at about 0.8-0.5 Ma BP. The 1.7-1.6 Ma shift is characterized by a rather abrupt transition of winter monsoon variability from various periodicities to dominant 41-ka cycles, and accompanied by a substantial increase in intensity of winter monsoon winds as manifested by an increase in average loess grain size. The 0.8-0.5 Ma event shows relatively gradual transition from constant 41-ka cycles to predominant 100-ka climatic oscillations with a significant increase in amplitude. The 0.8-0.5 Ma shift matches that registered in deep-sea $\delta^{18}O$ records, whereas the 1.7-1.6 Ma shift is absent in global ice volume changes. This comparison suggests that at about 1.6 Ma BP, the ice sheets in the Northern Hemisphere may have reached a critical size that were sufficient to modulate changes in the global climate system. The discrepancy suggests that the older Matuyama climate evolution cannot be understood simply by a regular 41-ka cycle model on the global scale.

The orbital time scale based on grain size was compared with the isotopic SPECMAP record (Imbrie et al., 1984; Fig. 4). Good agreement between the two records was obtained in both the time and frequency domains. In particular, the winter monsoon variations are characterized by a dominant 100 ka period in the past 800 ka. It is concluded that the winter monsoon changes are forced not directly by changing orbital geometry, but are phase-locked by glacial-age boundary conditions, particularly the dynamics of ice volumes in the Northern Hemisphere. Ice volume-Siberia high-meridional wind linkage is explained by the coherent variability between global ice volume and the East Asia winter monsoon.
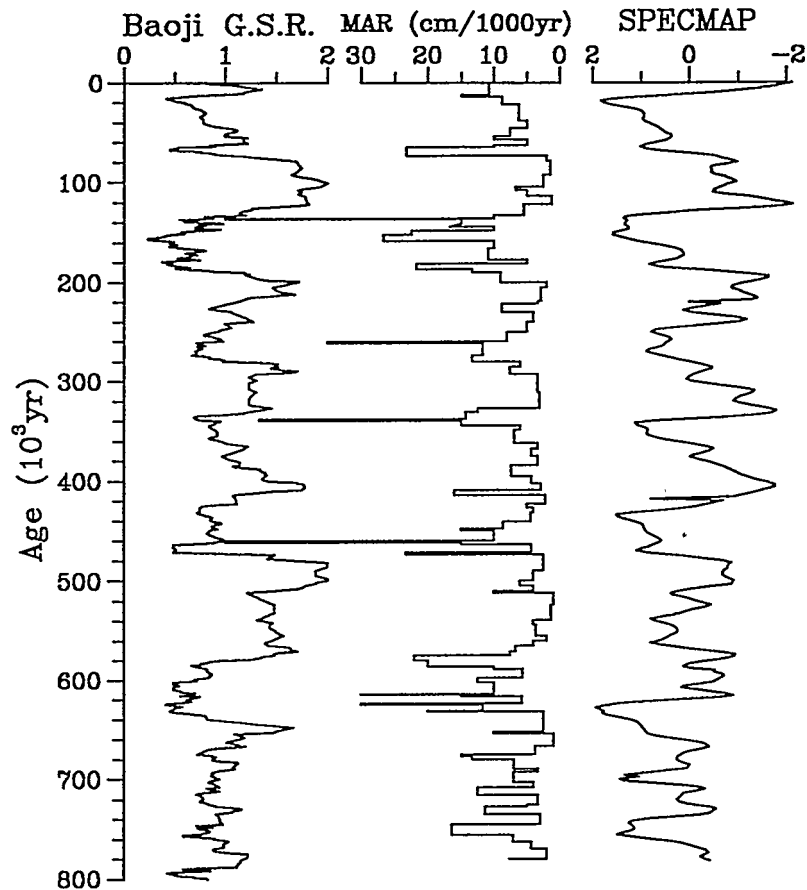
Fig. 4. Correlation of the grain size record and changes in the mass accumulation rate of the Baoji section with the isotopic SPECMAP stack in the past 800,000 years. The Baoji MAR record is calculated on the basis of the time control points introduced in tuning an astronomical time scale.

References

An, Z.S., Kukla, G., Porter, S.C. & Xiao, J.L. 1991. Late Quaternary dust flow on the Chinese Loess Plateau. Catena 18: 125-132.

Berger, A. & Loutre, M.F. 1991. Insolation values for the climate of the last 10 million years. Quaternary Science Reviews 10: 297-317.

Ding, Z., Yu, Z., Rutter, N.W. & Liu, T. 1994. Towards an orbital time scale for Chinese loess deposits. Quaternary Science Reviews 12: 39-70.

Imbrie, J., Hays, J.D., Martinson, D.B., McIntyre, A., Mix, A.C., Morley, J.J., Pisias, N.G., Prell, W.L. & Shackelton, N.J. 1984. The orbital theory of Pleistocene climate: Support from a revised chronology of the marine delta ^{18}O record. In: Berger, A., Imbrie, J., Hays, J.,

Kukla, G. & Saltzman, B. (eds.), Milankovitch and Climate: 269-305. D. Reidel Publ. Company, Dordrecht, Netherlands.

Liu, T.S. et al. (unnamed) 1985. Loess and the Environment. Science Press, Beijing, 215 pp.

Rutter, N., Ding, Z., Evans, M.E. & Liu, T. 1991. Baoji-type Pedostratigraphic Section, Loess Plateau, North-Central China. Quaternary Science Reviews 10: 1-22.

Rutter, N., Zhongli, D., Evans, M.E. & Yuchan, W. 1991. Magnetostratigraphy of the Baoji-type pedostratigraphic section, Loess Plateau, North-Central China. Quaternary International 7/8: 97-102.

Rutter, N. & Ding, Z. 1993. Paleoclimates and Monsoon Variations Interpreted from Micromorphogenic Features of the Baoji Paleosols, China. Quaternary Science Reviews 12: 853-862.
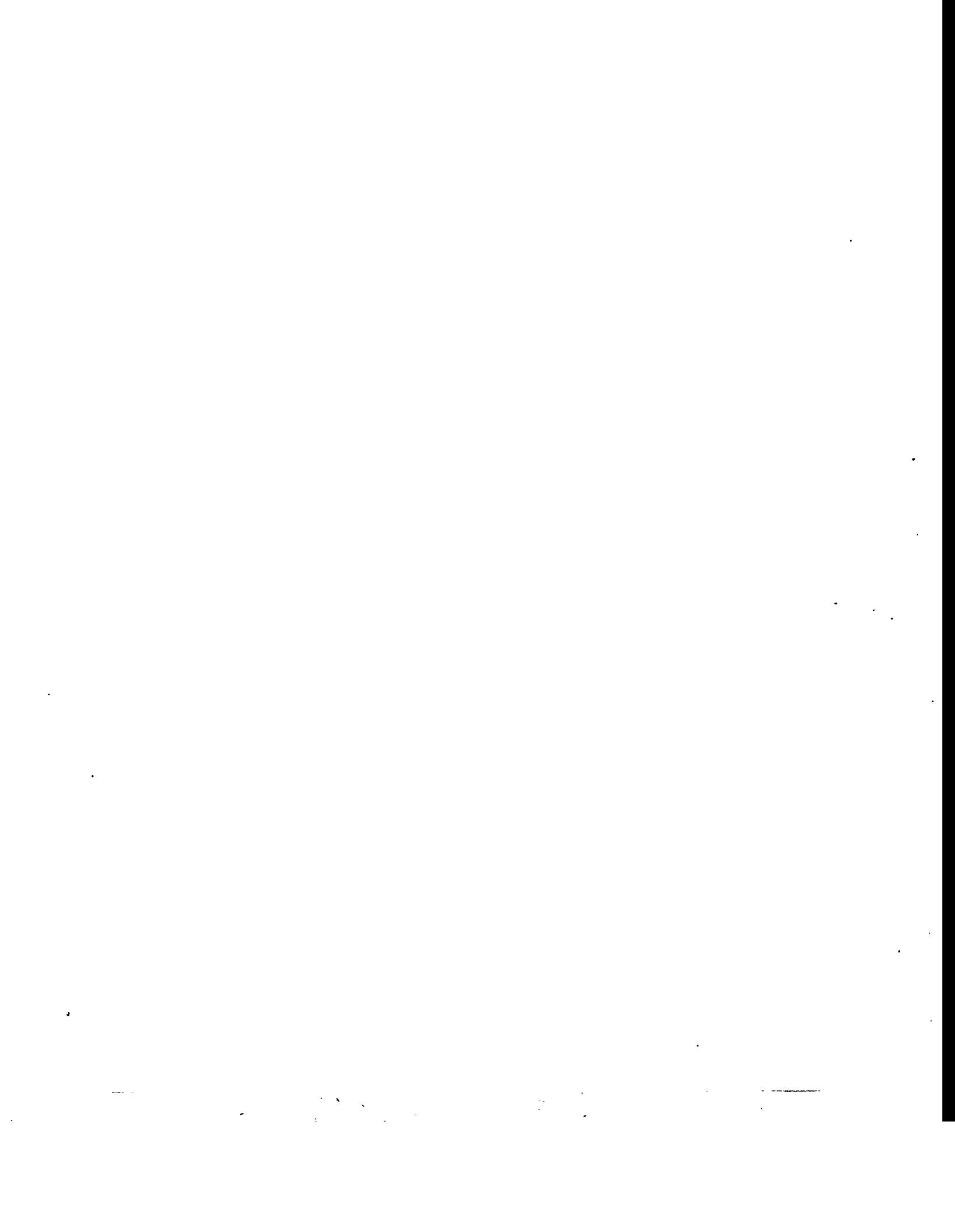
Climatic changes since the Pleistocene times
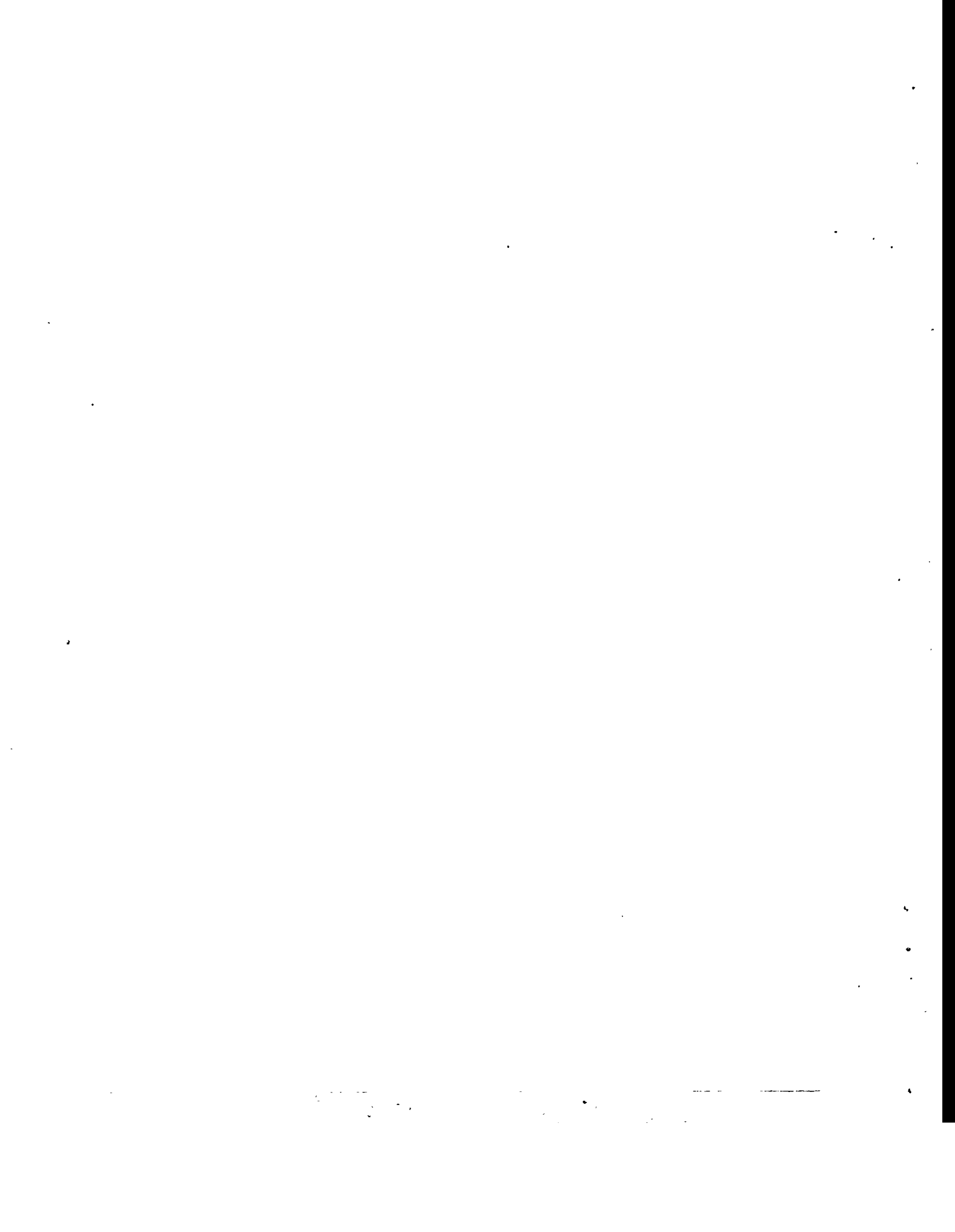
TAPHONOMY AND PALEOECOLOGY OF SAN JOSECITO CAVE, NUEVO LEON, MEXICO

Joaquín Arroyo-Cabrales and Eileen Johnson
Subdirección de Laboratorios y Apoyo Académico, I.N.A.H., Moneda # 16, Col. Centro, 06060 México, D. F., México, and Museum of Texas Tech University, Box 43191, Lubbock, Texas 79409, U.S.A.

Introduction

The hypothesis in this study was that the paleoenvironment at the mid-Wisconsinan (40,000 to 25,000 years BP) was similar to present ambient conditions, allowing the presence of similar faunal elements.

To test this hypothesis, it was decided to reexamine the available evidence from San Josecito Cave (northeastern México), one of the most important paleontological sites for the late Pleistocene of North America (Kurtén and Anderson, 1980). Most of its importance was based on the high number of taxa represented (at least 128 species, including 65 mammals). However, the locality potentially was important in developing a regional paleoenvironmental model. New excavations allowed insight into the taphonomic history and provided data to initiate a paleoenvironmental reconstruction.

Results and Discussion

A careful reexamination of the materials and available documentation has provided information on the cave. past excavations. and bone taphonomy as well as additional knowledge on the fauna itself (Arroyo-Cabrales and Johnson, 1995). Further analyses are warranted, but the complete curation of the original collection is mandatory.

Stratigraphically-controlled excavation methodology was utilized in the recent excavation in order to collect the greatest possible data to understand the taphonomic factors acting on the bones, and to infer the best possible paleoenvironmental scenario at the time of sediment deposition. An important contribution to field paleontology is the use of taphonomic boxes to gain detailed collected data. A taphonomic box is a much smaller

subunit (10x10 cm) within the test unit that is used for collecting matrix samples ; it allows the maintenance of a closer relationship between disarticulated bones from microvertebrates.

Analysis of the sediments showed a large internal contribution through limestone and breccia dissolution, with very minimal addition from external sources. Biological contributions were important, and such contributions seemed to be derived mainly from the vertebrates (Nelson et al., 1994). Botanical and insect studies did not provide useful information.

Radiocarbon dates obtained for several strata constitute the first radiometric control available for the cave, and provide the basis for faunal comparisons and paleoenvironmental inferences (Arroyo-Cabrales et al., 1995). The strata dated between 28,000 to 44,000 years BP, encompassing what is known as the Pre-Pleniglacial stage or mid-Wisconsinan period (Harris, 1993).

The identification of 20 new species of birds and mammals for the cave, based on both past and recently-collected materials, indicates that the faunal assemblages found in the cave have not been exhausted and deserve further research. Furthermore, each of the strata contain a faunal assemblage whose composition changed through the stratigraphic section. Also, the enormous fossiliferous content below the excavated units points to the great potential for developing a continuous late Pleistocene faunal record for the Pre-Pleniglacial Period.

Taphonomic analyses were undertaken, including quantification, breakage patterns, and spatial distribution. The different quantification methods provided comparable results if relative values were utilized. Breakage patterns appeared to point to the presence of avian predators as major agents in bone accumulation in stratum 720.

Faunal comparisons show a great similarity between San Josecito Cave stratum 720 local fauna and the fauna from U-Bar Cave (Harris, 1987) in southwestern New Mexico, U.S.A. Similarly, the stratum 720 local cave fauna appears to be composed of faunal elements predominantly occupying the Rocky Mountain Forests. Presently, this biome is found in the region where the cave is located. However, four specific associations within the Rocky Mountain Forests occur, and those cannot be identified with the ecological data available for recent and past taxa.

Conclusions

The significance of the new San Josecito Cave faunal data is to provide the first inference on paleoclimate at the Mid-Wisconsin of northeastern México. It appears that the paleoclimate regime at about 28,000 years BP supported the same kind of vegetational association that presently occurs in the cave region. That paleoclimate was probably similar to the present one with a continental climatic regime. Such a paleoclimate supported a harmonious fauna. With the onset of the Glacial Maximum at about 18,000 years BP, disharmonious communities apparently appeared with elements from tropical climates. Lastly, the concept of a San Josecito Cave Local Fauna (Jakway, 1958) as a single time-related entity is invalid and the stratified series of cave sediments represents a sequence of changing faunal communities.

Further studies on the materials from San Josecito Cave should include the identification and comparisons of the faunas from the different excavated strata. as well as the recovery of any stratigraphic data that can be inferred from the remaining breccia left intact in the cave. An excavation of a test unit should try to reach the bottom of the fossiliferous sediments.

Overall, the study of the San Josecito Cave and its faunal data have demonstrated the need for detailed studies of single localities in building paleoenvironmental models. Furthermore, the recognition of San Josecito Cave as an important late Pleistocene vertebrate paleontological locality is enhanced with the consideration of its faunal data for paleoenvironment reconstruction and possible contribution to Quaternary paleoclimatic modeling. In addition, the new field and analytical methodology demonstrates the importance of very detailed paleontological excavations, with precise spatial and temporal controls, to assess the taphonomic history of a site and to infer the paleoecological conditions during the time span considered.

insensitive, and occurs if adequate water is available.

Stomatal density (number per unit area) was measured on *Salix herbacea* leaves that had grown at known CO_2 concentrations (Neftel *et al.*, 1988; Boden *et al.*, 1991) over the last 200 years of CO_2 increase. Specimens were obtained from Herbaria, and also from high altitudes where the partial pressure of CO_2 is reduced. One full-glacial fossil was measured and plotted against the glacial CO_2 concentration obtained from ice-core measurements. The regression obtained is statistically significant, and an inverse regression can be used as a transfer function to reconstruct CO_2 concentration from measurements of stomatal density on the fossil leaves.

Fossil *Salix herbacea* leaves were extracted by gentle sieving of the sediments from 30 levels in the Kråkenes core, covering the interstadial Allerød period 11700 - 10700 ^{14}C yr BP, the Younger Dryas 10700 - 10000 ^{14}C yr BP, and the early Holocene 10000 - 9600 ^{14}C yr BP. The cuticles were isolated and mounted, and stomatal density was measured using a Leitz Quantimet image analyser, usually for 3 leaves per level, for a total of 80 leaves.

The measurements were used to reconstruct CO_2 concentrations. The results were plotted stratigraphically, and a LOWESS scatter plot smoother (Cleveland, 1979) was put through to demonstrate the trends in the data.

Results

Reconstructed CO_2 concentrations in the Allerød were at interglacial levels, at ca. 280 ppmv. Near the end of the Allerød, concentrations fell at a rate of ca. 0.35 ppmv per ^{14}C year, a rate similar to the current rate of rise of CO_2 today due to human activity. CO_2 concentrations reached ca. 220 ppmv at the start of the Younger Dryas, approaching glacial concentrations. In the mid Younger Dryas, concentrations started to rise at a rate of 0.09 ppmv per ^{14}C year, much slower than the earlier fall. Values reached 270 ppmv at the Holocene boundary, and the increase continued steadily until ca. 280 ppmv was attained at 9600 ^{14}C yr BP.

Discussion

The CO_2 decrease at the end of the Allerød seems to occur slightly before the major temperature drop at the Younger Dryas boundary, as assessed from other palaeoenvironmental indicators. Temperatures remain very low throughout the Younger Dryas, and rapidly increase by 5-7°C at the opening of the Holocene. The gradual rate of rise in CO_2 concentrations does not change during this major climatic change. The total change in CO_2 concentration would only affect global temperatures

directly by 0.5-1.0°C acting alone. If CO_2 changes are involved in the late-glacial climatic changes, it is probably through feedback mechanisms related to changes in ocean circulation. However, if the late Younger Dryas rise in CO_2 concentration did play a role in global warming, its build-up could have contributed to the sudden switch to interglacial conditions when a certain threshold was reached of e.g. meltwater influx, and shifts in atmospheric and ocean circulation (e.g. Zahn, 1992). At present, the mechanisms of our CO_2 record are unexplained. Nevertheless, these temporally-detailed reconstructions of rapid late-glacial atmospheric CO_2 changes should now be included as a further constraint in global climate-atmosphere-ocean models seeking a mechanistic explanation of the origin of the Younger Dryas.

References

Boden, A., Sepanski, R.J. & Stoss, F.W. (eds) Trends '91: a Compendium of Data on Global Change (Carbon Dioxide Information and Analysis Center, Oak Ridge, Tenessee).

Birks, H.H. + 23 others (1995). J. Paleolimnology (in press).

Cleveland, W.S. (1979). J. Amer. Statistical Ass. 74, 829-836.

Leuenberger, M., Siegenthaler, U, & Langway, C.C. (1992). Nature 357, 488-490.

Neftel, A. et al. (1988). Nature 331, 609-611.

Woodward, F.I. (1987). Nature 327, 617-618.

Zahn, R. (1992). Nature 356, 744-746.

The Neoproterozoic glacial record and the Passo da Areia Sequence in the Lavras do Sul region, southern Brazil

Toni T. Eerola(1) and Mauro R. Reis(2)

(1)International Division, Geological Survey of Finland
   FIN-02150 ESPOO

(2)Residência de Porto Velho, Geological Survey of Brazil (CPRM)
   Av. Lauro Sodré, 2561, B. Tanques, 78904.300 Porto Velho-RO,
   Brazil

Introduction

Recently, international attention has been focused on the climatic changes, tectonics and polar wandering paths that occurred in the Precambrian-Cambrian transition and in the reflection of these tranformations in the Cambrian evolutionary explosion. In this period, continental drift was faster than today (Gurnis & Torsvik 1994), there were important differences in oceanic and atmospheric chemistry in comparison to the Neogene (Grant 1994) and glacial diamictites occurred on all continents, even in low latitudes (Hambrey & Harland 1985). This glacial record was recently observed in southern Brazil (Eerola 1995). In this work, this deposit is tentatively correlated with the coeval glacial record in the context of supercontinent Rodinia. The work is intended to be a contribution to view presented recently by Young (1995) on Laurentia-Gondwana interaction and its relation to Neoproterozoic climate.

Neoproterozoic glaciogenic deposits

In the Neoproterozoic-Cambrian, four main glacial periods have been recognized: Lower Congo (*ca.* 900 Ma), Sturtian (750-700 Ma), Varangerian (650-630 Ma) and Sinian (625-550 Ma) (Hambrey & Harland 1985, Meert & Van der Voo 1994). Some researchers have proposed worldwide glaciations (e.g. Hambrey & Harland 1985) and others, the occurrence of mountain glaciers in rift- and orogenic zones (e.g. Eyles & Young 1994, Schemerhorn 1983).

Glaciogenic deposits with ages of *ca.* 600 Ma form a zone which begins in Baltica and passes through Greenland, Scotland, eastern Laurentia and western Gondwana, coinciding with collisional/rifting zone between these areas (Young 1995) in the reconstructed supercontinent Rodinia (*cf.* Dalziel et al. 1994). This zone is here denomined as the *Varangian-Sinian Glacial Zone* (VSGZ) and is extended to southern Brazil, Uruguay, Argentina and Namibia (Fig. 1).
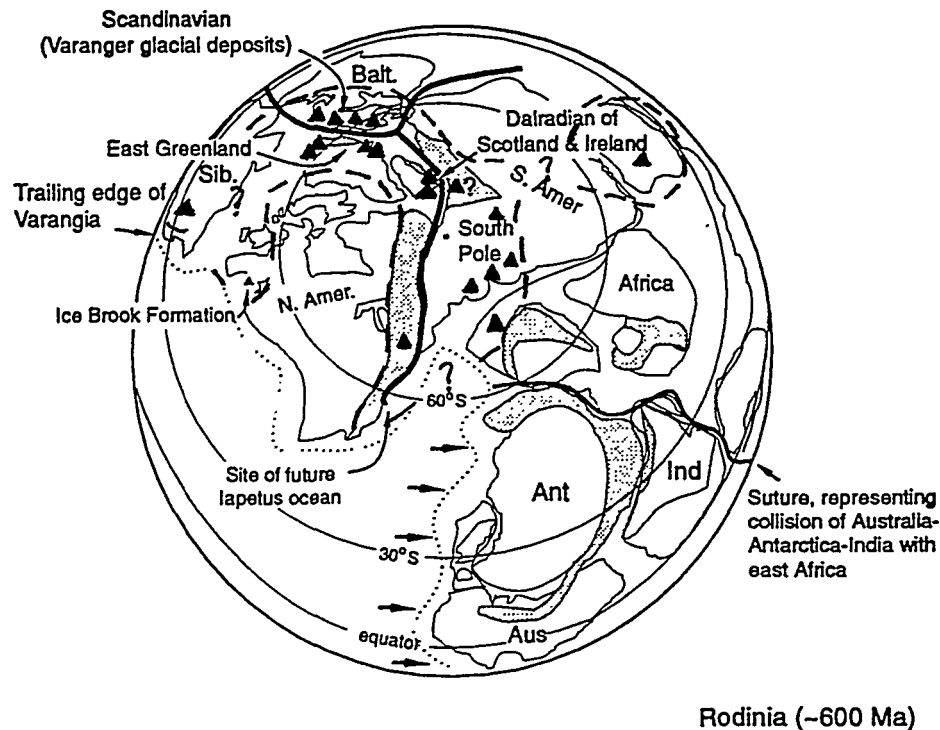
Rodinia (~600 Ma)

Fig. 1. The Neoproterozoic supercontinent, Rodinia, at *ca.* 600 Ma and its coeval glaciogenic record, "the Varangian-Sinian Glacial Zone" (after Young 1995). Data on Gondwana from Alvarenga & Trompette (1992), Eerola (1995), Kröner (1981) and Spalletti & Del Valle (1984).

The Neoproterozoic glacial record in southern Brazil - The Passo da Areia Sequence (*ca.* 600 Ma)

The first Neoproterozoic glacial record in the Rio Grande do Sul Shield (RGSS) is the Passo da Areia Sequence (Eerola 1995) in the Lavras do Sul region, southern Brazil. It consists of conglomerates, sandstones, rhythmic shales, diamictites and probable dropstones. The basal facies appears to represent fluvial outwash deposits. Diamictites associated with rhythmic shales with clasts suggest a glacio-lacustrine origin. Alternating shales and fine-grained sandstones probably represents turbidite deposits in a lacustrine pro-glacial delta-front.

The Passo da Areia Sequence is overlain by the red beds (also with diamictites) of the Santa Bárbara Formation and the aeolian deposits of the Guaritas Formation. The succession is similar to that of the Schwarzrand Subgroup of the Nama Group in Namibia (see Kröner 1981).

Correlations and implications

There is coeval glaciogenic record in regions which were situated close to the RGSS in Neoproterozoic times, including Laurentia and Namibia (Fig. 1). In Gondwana, coeval glaciogenic deposits are located in western Brazil (Alvarenga & Trompette 1992), Tandilia region of Argentina (Spalletti & Del Valle 1984), Uruguay (Preciozzi, pers. comm. 1994) and Namibia (Kröner 1981). This record forms extension to Varangian-Sinian Glacial Zone, in which RGSS appears to belong (Fig. 1). As the Sequence has an age of *ca*. 600-550 Ma, there is the case for correlation with various coeval glaciogenic deposits as the Numees Formation of the Gariep Supergroup or with the Schwarzrand Subgroup of the Nama Supergroup in Namibia (Kröner 1981), with the La Tinta Group of the Tandilia region (Spalletti & Del Valle 1984) and the Puga and Jangada Formations in western Brazil (Alvarenga & Trompette 1992). As all these appear to belong to the VSGZ, there is a possible correlation with coeval glaciogenic deposits in Laurentia, Greenland, Scotland and Baltica. The extensive coeval glaciogenic record occur also in Taoudenni basin, western Africa (see Alvarenga & Trompette 1992), although Bertrand-Sarfati et al. (1995) has recently considered it as being of Cambrian age.

To date, the Passo da Areia Sequence, which may also occur in other regions (Eerola 1995) has only been described locally. Therefore, it is still not clear if its deposition was due to continental glaciation or mountain glaciers, as has been proposed for most of the Varangian-Sinian glacial deposits (e.g. Eyles & Young 1994, Meert & Van der Voo 1994, Young 1995). Most of these deposits are though to have been generated by glaciers that originated in the uplifted borders of the rifting/colliding parts of Rodinia (Eyles & Young 1994, Young 1995). In the case of the RGSS and Namibia, glacial sequences are related to uplifted basin borders formed during the post-collisional stage of the Brasiliano - Pan-African Orogeny. This uplift could be reached the altitude of snowline, which, due to CO_2 depletion, could have been lower in Neoproterozoic - Cambrian times (*cf*. Schemerhorn 1983). This process could have generated glaciers by the accumulation of snow in uplifted highs. This model may explain the paradox of a Neoproterozoic glacial record in low latitudes and the association of warm climate indicators with these deposits. However, this model is problematic because many of the deposits are glaciomarine, which infers that the glaciers reached the sea-level in a warm climate: an improbable scenario. As seen in Figure 1, the major part of the glacial record is situated near the south pole in reconstruction of Dalziel et al. (1994). Despite the fact that many of paleomagnetic reconstructions still remain controversial, the possibility for the occurrence of continental ice-sheet at *ca*. 600 Ma must not be neglected.

Conclusions

The Passo da Areia Sequence in the Lavras do Sul region seems to indicate glacial deposition in southern Brazil at around 600 Ma. This deposit can be correlated with other coeval glaciogenic deposits in Gondwana, Laurentia, Baltica and Scotland, forming the so called "Varangian-Sinian Glacial Zone" of the Rodinia, which probably has importance in deciphering the Gondwana-Laurentia interaction and related climatic changes during the Neoproterozoic-Cambrian transition.

Studies of past climatic effects using sedimentary rocks could contribute to the understanding and prevention of present and future climate changes. The Neoproterozoic-Cambrian era is a key position in this research.

References

Alvarenga, C.J.S. & Trompette, R. 1992 Glacially influenced sedimentation in the Later Proterozoic of the Paraguay belt (Mato Grosso, Brazil). Palaeogeography, Palaeoclimatology, Palaeoecology 92:85-105.

Bertrand-Sarfati, J., Moussine-Pouchkine, A., Amard, B. & Aït Kaci Ahmed, A. 1995 First Ediacaran fauna found in western Africa and evidence for an early Cambrian glaciation. Geology 23:133-136.

Dalziel, I.W.D., Dalla Salda, L.H. & Gahagan, L.M. 1994 Paleozoic Laurentia-Gondwana interaction and the origin of the Appalachian-Andean mountain system. Geological Society of America Bulletin 106:243-252.

Eerola, T.T. 1995 From ophiolites to glaciers? Review on geology of the Neoproterozoic-Cambrian Lavras do Sul region, southern Brazil. In: Autio, S. (ed.) Geological Survey of Finland, Current Research 1993-1994. Geological Survey of Finland, Special Paper 20:5-16.

Eyles, N. & Young, G.M. 1994 Geodynamic controls on glaciation in Earth history. In: Deynoux, M., Miller, J.M.G., Domack, E.W., Eyles, N., Fairchild, I.J. & Young, G.M. (eds.) Earth's glacial record. London, Cambridge University Press, pp. 1-27.

Grant, S.W.F. 1994 Neoproterozoic to early Cambrian carbon, sulphur and strontium isotopes. Terra Abstracts 3:3-4.

Gurnis, M. & Torsvik, T.H. 1994 Rapid drift of large continents during the late Precambrian and Paleozoic: Paleomagnetic constraints and dynamic models. Geology 22:1023-1026.

Hambrey, M.J. & Harland, W.B. 1985 The Late Proterozoic glacial era. Palaeogeography, Palaeoclimatology, Palaeoecology 51:255-272.

Kröner, A. 1981 Late Precambrian diamictites of South Africa and Namibia. In: Hambrey, M.J. & Harland, W.B. (eds.) The Earth's Pre-Pleistocene glacial record. London, Cambridge University Press, pp. 167-177.

Meert, J.G. & Van der Voo, R. 1994 The Neoproterozoic (1000-540 Ma) glacial intervals: no more snowball earth? Earth and Planetary Science Letters 123:1-13.

Schemerhorn, L.J.G. 1983 Late Proterozoic glaciation in the light of CO2 depletion in the atmosphere. In: Medaris, L.G., Byers, C.W., Mickelson, D.M. & Shanks, W.C. (eds.) Proterozoic Geology: Selected papers from an International Proterozoic Symposium. The Geological Society of America, Memoir 161, pp. 309-315.

Spalletti, L.A. & Del Valle, A. 1984 Las diamictitas del sector oriental de Tandilia: caracteres sedimentologicos y origen. Revista da Associación Geologica Argentina 39:188-206.

Young, G.M. 1995 Are Neoproterozoic glacial deposits preserved on the margins of Laurentia related to the fragmentation of two supercontinents? Geology 23:153-156.

Model reconstruction of the temperature and ozone profiles in the last glacial and interglacial periods

Igor L. Karol, Victor A. Frolkis, and Andrey A. Kiselev

Main Geophysical Observatory
St. Petersburg, 194018, Russia

Several observational and model reconstructions of paleoatmosphere composition of the Earth have been based on various assumptions and indirect evidences about the gas content variations in the past. Recent air temperature reconstructions, measurements of CO_2, CH_4, and N_2O, and of various aerosol concentrations in the air bubbles of ice cores, drilled from the deep layers of the Antarctic and Greenland continental ice sheets, provide the direct evidence about the temperature and concentration evolution of these gases (and some aerosols) at the ground level polar air during the last 150-200 ka (Raynaud et al. 1993, Jouzel et al. 1993, Lenenberg & Siegenthaler 1992).

This paper contains the pilot results of vertical profile reconstructions of temperature and of atmospheric trace gas concentrations in the 0 to 50-km atmospheric layer for four periods, (1) the contemporary (C) period of 1985, (2) the preindustrial (PI) period of 1850, (3) the glacial (G) period of 18-20 ka B.P., and (4) the interglacial (IG) period of 125-130 ka B.P., using the 1-D Radiative Photochmical Model (RPM), which models the radiative and photochemical processes in the globally averaged troposphere and stratosphere. The prescribed ground surface air concentrations of CO and NO_y are necessary for the reconstruction of the paleoatmospheric composition. Special of studies the model sensitivity to large variations of these and other nonmeasured input concentrations and parameters have been carried out. A comparison of our results with those of Valentin (1990) and of Crutzen & Brühl (1993) is presented. Our study was carried out quite independently of the latter. Our first paper was submitted for publication (Karol et al. 1994) before we knew about the Crutzen and Brühl work.

The nonstationary annually and globally averaged one-dimensional photochemical block of the model is extended from the Earth's surface up to 50-km level with 2 km vertical step, and it contains 141 gas phase reactions among oxygen, nitrogen, hydrogen, carbon, chlorine, and bromine compounds. The

stratospheric water vapor content is calculated, but in the troposphere the contemporary climatic relative humidity is prescribed and conserved for all the calculated variants. Reaction rates and cross sections are taken from De More et al. (1994). A full description of the model is given by Karol (Ed. 1986) with some updating from Frolkis & Rozanov (1993). Parameters used in the model and calculated variants are indicated in Tables 1 and 2 in (Karol et al. 1994).

The vertical profiles of ozone concentration deviation from its preindustrial standard, demonstrated in Figure 1, show that the total ozone stability is ensured by only small changes of ozone concentration in the layer 20-30 km of its maximum. The tropospheric ozone deficit in paleoperiods is compensated partly by the ozone content increase in the middle and upper stratosphere at altitudes of 30-44 km. The same total ozone stability during glacial and interglacial periods was noted also by Crutzen & Brühl (1993).

The largest deviations of vertical temperature profile from the preindustrial profile occur in the upper stratosphere and also in the troposphere of the glacial period and the current atmosphere (see Figure 2). The stratospheric temperature increase during the glacial period does not depend on the choice of tropospheric lapse rate. Significant tropospheric temperature vertical changes are due to various used lapse rate effects. The preindustrial temperature profile used as a standard is calculated with standard y_s = 6.5 K/km, being close to the profile with y_m, but temperature profiles, presented in Figure 2, are obtained with y_m and y_d for glacial and with y_m for interglacial periods. The tropospheric temperature with y_d = 9.8 K/km decreases with height much more quickly than that with y_s. Therefore the difference between the temperature profiles with y_d and y_s increases up to tropopause and reaches about 25 K at 8 km. In the lower troposphere y_m is lower than y_s, but in the upper troposphere, y_m approaches y_d.

The tropospheric temperature is strongly connected with the water vapor content, the configuration of temperature deviation and of corresponding water vapor change profiles being similar. Calculations show the low sensitivity of tropospheric ozone to the CO surface source intensity. The NO_x surface source intensity determines [NO_x] in the troposphere only, but stratospheric [NO_x] is determined by the [N_2O] tropospheric content. The [N_2O] and [CH_4] profiles are determined by their prescribed surface air concentrations and change only slightly with altitude. The model results show that in spite of the significant changes in atmospheric composition the total ozone remained almost constant during all the time considered here before the last decade.
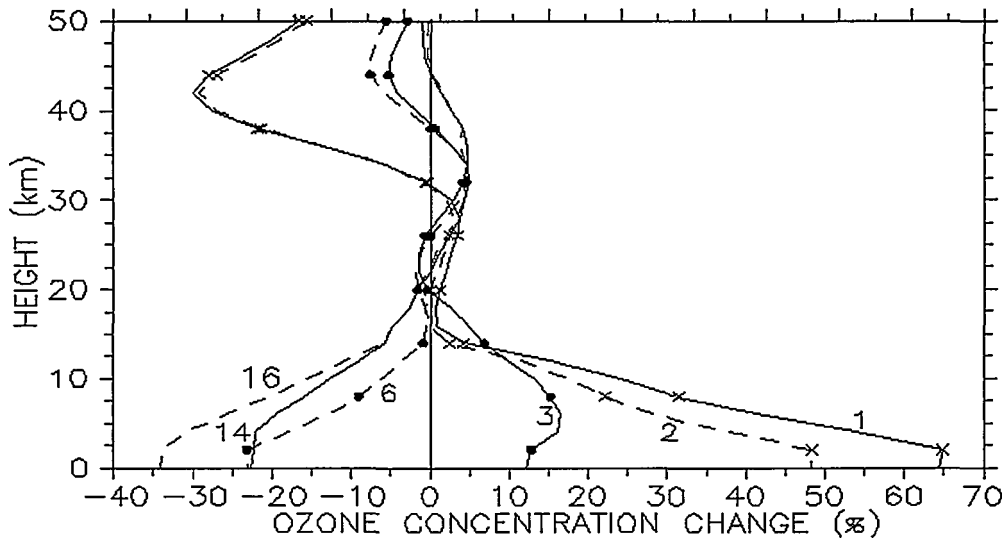
Figure 1. Vertical profiles of calculated ozone concentration changes from the preindustrial profile: 1, 1985 period, Y_s, no aerosols; 2, 1985 period, Y_m, no aerosols; 3, glacial period, Y_d, dust; 6, glacial period, Y_m, dust; 14, interglacial period, Y_m, sulfate aerosols; 16, interglacial period, Y_m, no aerosols, reduced NO_x emission. Numbers near curves indicate the number of variants in Table 2 in Karol et al. (1994).
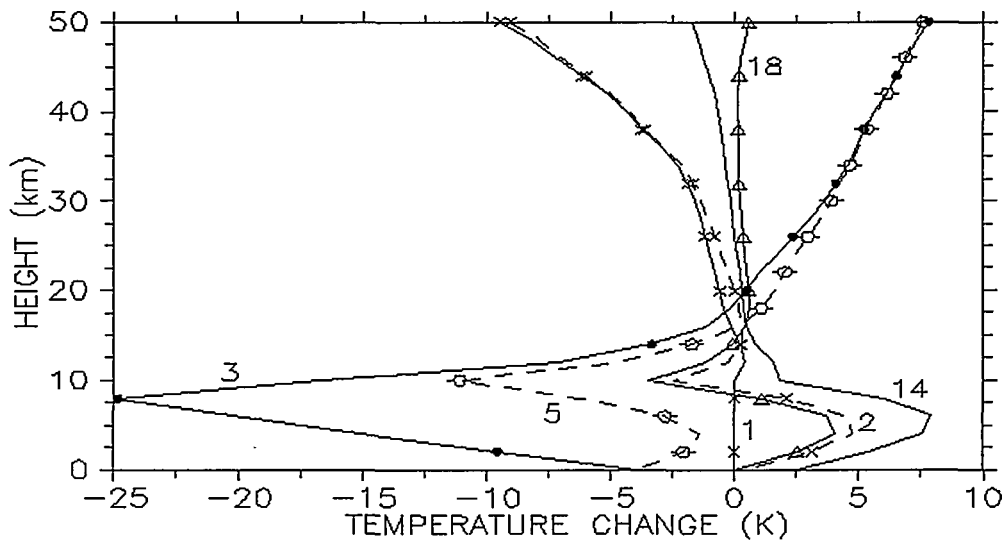
Figure 2. Vertical profiles of calculated temperature changes from the preindustrial profile: 1, 1985 period, Y_s, no aerosols; 2, 1985 period, Y_m, no aerosols; 3, glacial period, Y_d, dust; 5, glacial period, Y_m, no aerosols; 14, interglacial period, Y_m, sulfate aerosols; 18, preindustrial period, Y_m, no aerosols. Numbers near curves indicate the number of variants in Table 2 in Karol et al. (1994).

References

Crutzen, P.J. & Brühl C. 1993. A model study of atmospheric temperatures and the concentrations of ozone, hydroxyl, and some other photochemically active gases during the glacial, the preindustrial holocene, and the present. Geophys. Res. Lett. 20:1047-1050.

De More, W.B., Sander S.P., Golden D.M., Hampson R.F., Kurylo M.J., Howard C.J., Ravishankara A.R., Kolb C.E. & Molina M.J. 1994. Chemical kinetics and photo-chemical data for use in stratospheric modeling. JPL Publ., 94-1, Jet Propul. Lab., Pasadena, Calif., 218 pp.

Frolkis, V.A. & Rozanov, E.V. 1993. Radiation code for climate and general circulation models. In IRS'92 Current Problems in Atmospheric Radiation (Proceed-ings, International Radiation Symposium, Tallinn, Estonia 1992), edited by S. Keevallik & O. Kärner. A. Deepak, Hampton, Va. pp. 176-179.

Jouzel, J. et al. 1993. Extending the Vostok ice-core record of palaeoclimate to the penultimate glacial period. Nature 364:407-412.

Karol, I.L., Kiselev, A.A. & Frolkis, V.A. 1994. Model reconstructions of the global tropospheric and stratospheric composition and temperature in the last glacial and int-erglacial periods (in Russian), Dokl. Ross. Akad. Nauk 336:525-528.

Lenenberg, M. & Siegenthaler U. 1992. Ice age atmospheric concentration of nitrous oxide from an Antarctic ice core. Nature 360:449-451.

Raynaud, D., Jouzel J., Barnola J.M., Chappelaz J., Delmas R. & Lorius C. 1993. The ice record of greenhouse gases. Science 259:926-934.

Valentin, K. M. 1990. Numerical modeling of the climatological and anthropogenic influence on the chemical composition of the troposphere since the last glacial maximum. Ph.D. thesis, Univ. of Mainz, Germany.

Stable isotope content of segregated ice: a new terrestrial paleothermometer

Vladimir I. Nikolaev and Dmitry V. Mikhalev *

Institute of Geography, Russian Academy of Sciences
Staromonetny per. 29, Moscow 109017, Russia;
*Geography Faculty, Moscow State University
Moscow 119899, Russia

Introduction

The mean isotopic composition of annual precipitation in polar regions is highly correlated with the mean annual air temperature near the ground surface (Dansgaard 1964, Nikolayev & Kolokolov 1993) and this robust correlation constitutes a solid basis for using stable isotopes as a sign of ground moisture origin in active layer.

In this paper we propose to use oxygen isotope composition ($\delta^{18}O$) of ground ice (ice cement, as well as segregated ice) for reconstruction of winter paleotemperature in permafrost areas.

The oxygen composition of recent ground ice from seasonally frozen unlithified sediments has complex nature. In permafrost areas freshly deposited snow is subjected to great deflation and drifting by wind. Moreover melting and freezing within the snow cover and the active layer of the ground can lead to isotopic fractionation. However, these considerable isotopic differences are evidently smoothed out by snow melt and runoff.

The $\delta^{18}O$ of ground water collected during summer in the Kolymian Lowland and the Yenisei estuary area was practically equal to the $\delta^{18}O$ of the summer precipitation in these areas. By the beginning of the cold season, the ground water $\delta^{18}O$ values correspond to mean values for summer-autumn precipitation. Analyses of ice seldom reveal more than 2-3‰ isotopic differences across the active layer in the early winter. By the onset of the thawing season these differences reach values as great as 5-6‰. The most probable reason for this process is freeze-drying of the frozen sediments. The freeze-drying decrease moisture content of active layer and creates favorable conditions for penetration of snowmelt into frozen sediments.

In spring and early summer, as well as during the thaw period, additional ice can form in the frozen part of the active layer. This new ice has low $\delta^{18}O$ values due to the movement of isotopically light snowmelt into frozen zone. The significance of the role of winter precipitation in forming ground ice sharply increases due to migration of this water. In the lower part of active layer, the $\delta^{18}O$ of ice is less affected by water migration.

Our $\delta^{18}O$ investigations of recent ground ice revealed systematic variations with topographic position and sediment lithology, as well as organic content. Ground ice from low areas (e.g., floodplains, river bars, alases - large flat-bottomed kettles) tends to be isotopically heavier than ice from high levels (e.g., near drainage divides and high river terraces). Ice from organic or peat-rich ground is generally 1-2‰ heavier isotopically than is ice from other sediments.

Results and its paleoclimatic applications

Despite the above-mentioned processes altering the original isotopic (temperature) signal, we proposed to correlate the averaged $\delta^{18}O$ values for recent ground ice (segregated ice & ice-cement) with the mean temperatures of the cold (frosty) season (T_c), of January (T_j), of the calendar winter (T_w), of the warm season (T_s), and the mean annual temperature (T_{av}). For this purpose, we use observation from the nearest meteorological station, generally within several tens of kilometers of a field site. For each region of our investigations (17 polar regions, extending from the mouth of Lena River area to Chukotka) we collected as many samples of segregated ice as we could from the different geomorphic settings and types of ice-containing sediments. We correlate average $\delta^{18}O$ with temperature (up to 55 single isotopic analyses) (see Fig.). The correlation coefficients are 0.953 (T_c); 0.883 (T_j); 0.875 (T_w); -0.426 (T_s); 0.406 (T_{av}). These results allow us for the first time to calculate regression equations and to use segregated ice $\delta^{18}O$ as a paleothermometer:

$$\delta^{18}O = (0.84 \pm 0.06)T_c - (1.78 \pm 0.24)$$
$$\delta^{18}O = (0.60 \pm 0.06)T_j - (0.87 \pm 0.25)$$
$$\delta^{18}O = (0.61 \pm 0.06)T_w - (0.84 \pm 0.25)$$

We also recalculated δ/T slopes for primary ice veins using published data (e.g., Vasilchuk 1992) from 35 Russian polar regions, extending from the mouth of the Pechora River area to Chukotka and from the Arctic islands to the Aldan River.

The δ/T slopes for both segregated ice and primary ice veins range from 0.83 to 0.86‰ per degree centigrade in the case of mean temperature of frosty season (T_c) and about 0.5-0.6‰ per degree centigrade in the case of mean temperature of T_j and T_w values. These data are in a good agreement with ones from simple Rayleigh model for precipitation (Dansgaard 1964).

From our results, we also conclude that the dominant source of moisture for both segregated ice and ice veins is snowmelt which is not obvious, as discussed in recent cryological literature (Mackay 1983, Michel 1982, Parmuzina 1979). Evidently, there is
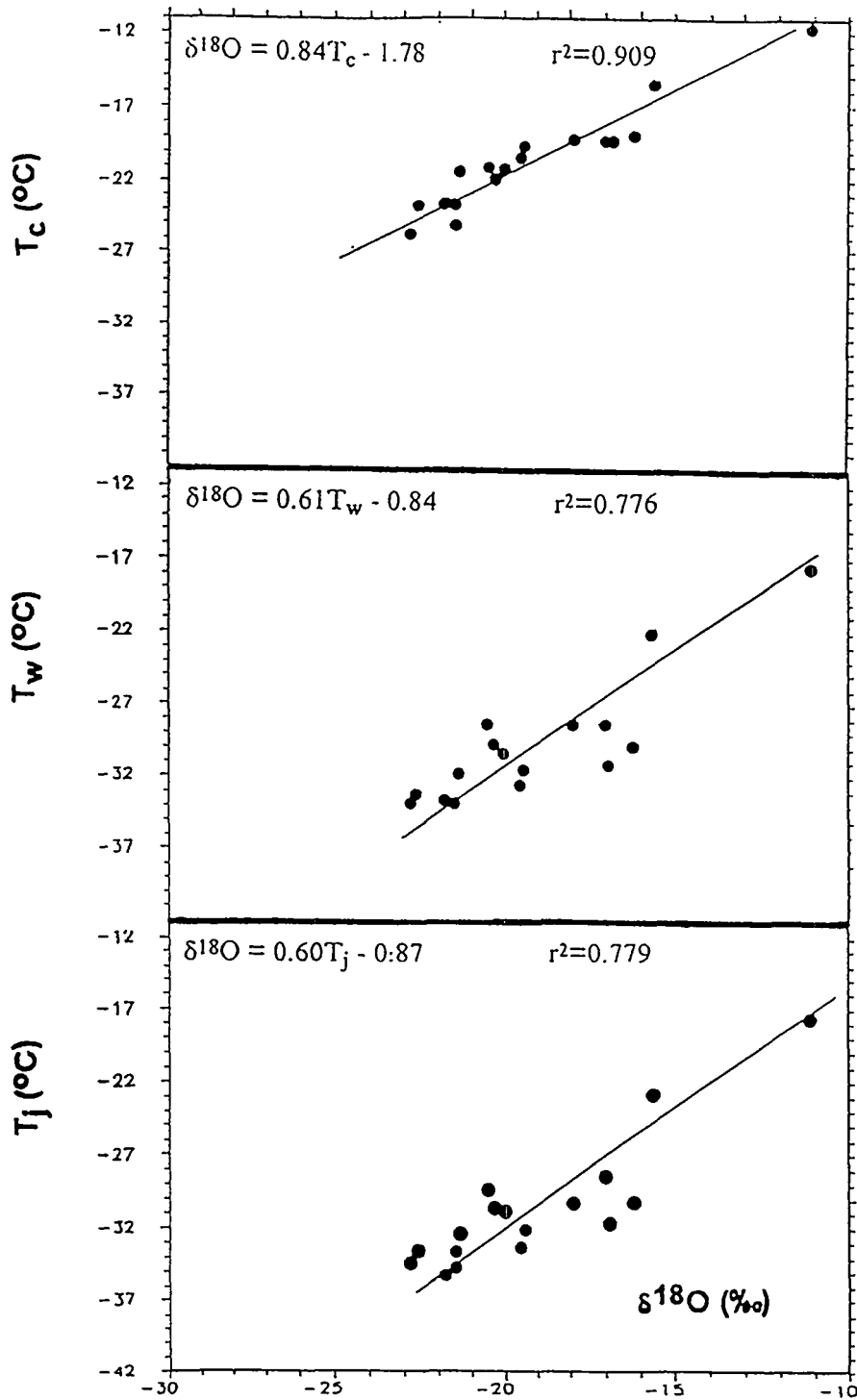
Fig. Mean $\delta^{18}O$ of recent ground ice (ice cement and segregated ice) from Yakutia versus mean temperatures of the cold (frosty) season (T_c), of January (T_j) and of the calendar winter (T_w)

a regional homogenization of $\delta^{18}O$ of H_2O in the active layer, probably due to recurrent water migration in melting or freezing ground. As a result, average values of $\delta^{18}O$ in these types of ice reflect the mean temperature at which snow forms. Hence, any of the δ/T slopes from our Eqs. can be used for paleotemperature calculation.

To test this new paleothermometer, we collected all of our data, as well as other data known to us, pertaining to the $\delta^{18}O$ of segregated ice from Holocene and Pleistocene sediments in Yakutia and Chukotka. We also took into account correction for changes of the average ocean water $\delta^{18}O$ and evaporation conditions during the ice ages compared with recent time (about 1.5‰). Our reconstruction shows that during cold Pleistocene stages the mean temperatures of January were 10-14° lower than recent values in interior regions and 18-20° near the present coast line. For the Last Interglaciation, our estimates of T_j values are about 1‰ in $\delta^{18}O$, i.e., 2°C warmer than present.

We conclude that paleotemperature reconstructed from $\delta^{18}O$ of segregated ice is reasonable and, hence, that ground ice $\delta^{18}O$ is a new paleothermometer useful in paleoclimatic reconstruction of vast high-latitude land areas in Eurasia and North America. Because individual samples show considerable scatter, averaging of at least 10 samples is required to obtain meaningful paleotemperature reconstruction.

Acknowledgments

References

Dansgaard, W. 1964. Stable isotopes in precipitation. Tellus 16:436-468.

Mackay, J.R. 1983. Oxygen-isotopic variations in permafrost Tuktoyaktuk peninsula area, North-West Territories. Geological Survey of Canada, Current Research 83(1B):67-76.

Michel, F.A. 1982. Isotope investigations of permafrost waters in Northern Canada. Ph. D. Thesis. University of Waterloo, Ontario, 424pp.

Nikolayev, V.I. & Kolokolov, S.L. 1993. Paleoclimatic interpretation of isotope-oxygen data on ice cores obtained from polar glaciers: methodological aspects. Data of Glaciological Studies 76:146-154.

Parmuzina, Q.Yu. 1979. About redistribution of moisture in frozen ground by natural observations. Problems of Cryolithology 8:194-197.

Vasilchuk, Yu. K. 1992. Oxygen Isotopic Composition of the Ground Ice (an Experience of Palaeocryological Reconstructions). Moscow, Vol. 1, 421pp., Vol. 2, 250pp.

A 30,000 climatic record from Dome B ice core (East Antarctica)

Rein Vaikmäe[1], Jean Jouzel[2,3], Jean-Robert Petit[3], Michel Stievenard[2] and Margus Toots[1]

[1] Institute of Geology, Estonian Academy of Sciences
7 Estonia Avenue, EE0100 Tallinn, Estonia

[2] Laboratoire de Modélisation du Climat
CEA/DSM CEN Saclay, 91191, Gif sur Yvette Cedex, France

[3] Laboratoire de Glaciologie et Géophysique de l'environnement,
BP96, 38402 Saint Martin d'Hères Cedex, France

Interpretation of the data obtained from three deep Antarctic ice cores, Byrd, Dome C and Vostok has given continuous detailed long-term environmental records extending back to the last glacial period (Johnsen et al. 1972, Lorius et al. 1979, Jouzel et al. 1989, Jouzel et al. 1992, Hammer et al. 1994). Here we introduce a new $\delta^{18}O$ profile obtained along the Dome B ice core.

The Dome B drilling site is located on the high East Antarctic plateau (77°05'S and 94°55'E, 3600 m elevation). The bedrock relief is flat at the drilling site and the character of the radioecho reflection lets us to presume that there is a lake about 20 km in length under the ice.

During the 1987-1988 Austral season, a 780m-deep ice core was drilled using the thermodrill by the 33th SAE. Sampling was performed on 1 and 2 m ice increments.

Oxygen-18 and deuterium determinations were performed simultaneously on all the samples of 1 m increments and only oxygen-18 analyses on the samples of 2 m increments. Here we shall mainly discuss the results of of oxygen-18 analyses on samples of 2 m increments.

The $\delta^{18}O$ profile in figure 1 is presented as a function of sample depth. Down to the bottom, the basic features of the $\delta^{18}O$ profile of the Dome B core are very similar to those of Dome C and Vostok. A dominating feature, well expressed is the Last Glacial Maximum (LGM) to Holocene transition in the depth interval of 410 to 570 m which is interrupted by the Antarctic cold reversal (ACR) in the depth interval of 440 to 480 m. Such a two-step character of the

last deglaciation is well recognized in Western Europe, in Greenland and in the North Atlantic (Ruddiman & McInture 1981, Rind et al. 1986, Dansgaard et al. 1989). A detailed isotopic record analysed in a new ice core drilled at Dome B fully demonstrates the existence of cold reversal also in Antarctica. These results suggest that the two-step shape of the last deglaciation has a worldwide character but they also point out to noticeable interhemispheric differences (Jouzel et al. 1995).

Another characteristic feature of Dome B isotope profile besides the ACR is a well expressed warm period just after the transgression in the depth interval of 320 to 410 m . This compares well with previous results at Dome C, Vostok and Byrd indicating that in contrast with the hypsithermal optimum for Europe and North America showing higher temperature during the mid-Holocene, in Southern Hemisphere high latitudes the climate optimum existed just at the end of the last deglaciation (Lorius et al. 1984, Ciais et al. 1992).
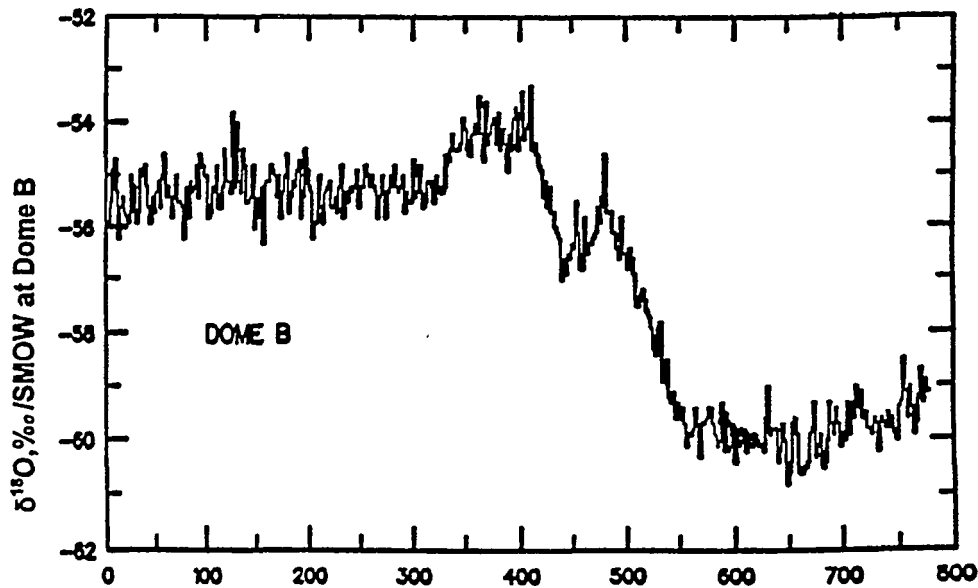
Fig. 1. The δ¹⁸O profile at Dome B with respect to depth

References

Ciais, P., Petit, J.R., Jouzel, J., Lorius, C., Barkov , N.I., Lipenkov, V. & Nicolajev, V. 1992. Evidence for an early Holocene climatic optimum in the Antarctic deep ice core record, Climate Dynamics 6:169-177.

Dansgaard, W., White, J.W. & Johnsen, S.J. 1989. The abrupt termination of the Younger Dryas climate event. Nature 359: 532-534.

Hammer, C.U., Clausen, H.B. & Langway, C.C.J. 1994. ECM stratigraphic dating of the Byrd station ice core. Ann. Glaciol. 20:115-120.

Johnsen, S.J., Dansgaard, W., Clausen, H.B. & Langway, C.C. 1972. Oxygen isotope profiles through the Antarctic and Greenland ice sheets, Nature 235: 429-434.

Jouzel, J., Petit, J.R., Barkov, N.I., Barnola, J.M., Chappellaz, J., Ciais, P., Kotlyakov, V.M., Lorius, C., Petrov, N., Raynaud, D. & Ritz, C. 1992. The Last Deglaciation in Antarctica: Evidence for a "Younger Dryas" Type Climatic Event. In:Absolute and Radiocarbon Chronologies, NATO ASI Series 1 ed. by E. Bard and W.S. Broecker, Springer-Verlag, Berlin:229-266.

Jouzel, J., Raisbeck, G., Benoist, J.P., Yiou, F., Lorius, C., Raynaud, D., Petit, J.R., Barkov, N.I., Korotkevitch, Y.S., & Kotlyakov, V.M. 1989. A comparison of Deep Antarctic Ice Cores and Their Implications for Climate between 65,000 and 15,000 Years Ago, Quat. Res. 31:135-150.

Jouzel, J., Vaikmäe, R., Petit, J.R., Martin, M., Duclos, Y., Stievenard, M., Lorius, C., Toots, M., Mélières, M.A., Burckle, L.H., Barkov, N.I. & Kotlyakov, V.M. 1995. The two-step shape and timing of the last deglaciation in Antarctica. Climate Dynamics, in the press.

Lorius, C., Jouzel,J., Ritz, C., Merlivat, L., Barkov, N.I., Korotkevitch, Y.S. & Kotlyakov, V.M. 1985. A 150,000 year climate record from Antarctica ice, Nature 316: 591-596.

Lorius, C., Raynaud, D., Petit, J.R., Jouzel, J. & Merlivat, L. 1984. Late glacial maximum - Holocene atmospheric and ice thickness changes from Antarctic ice core studies, Annals of Glac. 5:88-94.

Rind, D., Peteet, D., Broecker, W., McInture, A. & Ruddiman, W. 1986. Impact of cold North Atlantic Sea surface temperatures on climate implications for the Younger Dryas cooling, Climate Dyn. 1:3-33.

Ruddiman, W.F. & McInture,A. 1981. The North Atlantic ocean during the last glaciation, Palaeogeogr. Palaeoclim. Palaeoecol. 35:145-214.

Climate variations last Late Pleistocene cryochron 40-10 Kyr B.P. in Northern Eurasia

Yurij K.Vasil'chuk[1] and Alla C. Vasil'chuk[2]

[1]Theoretical Problems Department. The Russian Academy of Sciences. Vesnina 12, 121002, Moscow. and [2]Institute of Cell Biophysics. The Russian Academy of Sciences 142292, Pushchino, Moscow Region.

Introduction

There are quite little data concerning paleoclimatic information for the vast areas of Northern Eurasia cryolithozone (zone of permafrost distribution). We have studied about 50 reference permafrost sequences of syngenetic Late Pleistocene sediments from Yamal and Gydan Peninsulas, North and Central Yakutia, Chukotka, Magadan and Transbaikal Regions. The combination of oxygen isotope analysis of syngenetic ice wedges with radiocarbon dating of organic matter of enclosing sediments (peat, wood, bones, allochthonous detritus), allowed to receive detailed temporal reconstructions of Late Pleistocene paleoclimate dynamics. The special interest of this study deals with the syngenetic permafrost sediments. In the northern Eurasia thick ice wedges, cutting through the entire stratum, are the dominant form of ice (its heights exceed 20-30 m).

Results and discussion

Our hypothesis consists of the new conception of formation mechanism for thick syngenetic ice wedges and has been worked out for Late Pleistocene and Holocene syngenetic (cyclesyngenetic) sediments. It is most possible to describe the ice wedge forming as periodic (and cyclic) or repeated injection of thin

elemental cuneiform veins having penetrated in just
existed wedges. The active forming of ice wedges
proceeded in subaerial conditions during the
accumulation of peat or peat sedimentations. During the
forming of ice wedges system the subaerial conditions
some times were changed to subaquaeous. At subaquaeous
regime (Fig.1) the accumulation of the most part of
ice wedges stopped and for some of them decreased
considerably. When subaerial regime returned the active
accumulation of ice wedges renewed. If the thickness of
previously sedimented subaerial strata is thin enough
the tails of newly forming ice wedges penetrate into
fossil ice wedges of previous phase with forming of
large continuous (transit) ice wedges. If this
subaquaeous layer is great enough the multistage system
of ice wedges is formed.
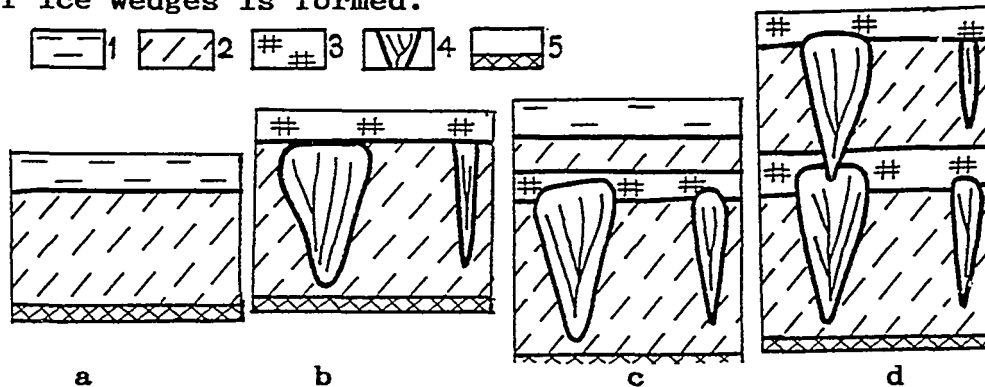
Fig.1 Schematic cycle of formation of thick syngenetic
ice wedge. The intensive ice wedge development occurred
in subaerial conditions ("b" and "d" stages), arrest
of ice wedge development and intensive sedimentation in
subaquaeous regime ("a" and "c" stages): 1 - water, 2 -
sandy loam, loam; 3 - peat, peaty sediment; 4-ice
wedge, 5 - indigenous rocks. We consider the whole
process of accumulation of ice wedges as macrocycling.
Mineral layer thickness are 3-7 meters, as a rule
subaerial organic interbanded thickness are 1-2 meters.

The $\delta^{18}O$ trend in Late Pleistocene ice wedges is more
negative from West to East by 8-10 promilles, from -19
to -25 promilles, in Western Siberia ice wedges to
-30 to -35 promilles, in Northern Yakutia. Than it

reaches the value as high as -28 to -33 promilles, in North Chukotka and central areas of Magadan Region, and up to -23 to -29 promilles, in the East of Chukotka. These data suggest that the air mass transport was similar to the modern one at the end of the Late Pleistocene through whole Asia Subarctic. The $\delta^{18}O$ values in modern ice wedges in Northern Yakutia are oscillated from -28 to -24 promilles, in the North of Western Siberia from -20 to -16 promilles. Paleotemperature reconstructions are based on equation of regression which is received for modern ratio of winter temperatures and $\delta^{18}O_{iw}$ in recent ice veinlets (Vasil'chuk, 1992):

$$t^o_{mean\ winter} = \delta^{18}O_{iw} \quad (\overset{+}{-} 2\ ^oC)$$

The mean winter temperatures during the 40-10 Kyr B.P. were about 6-8^oC less,than the modern ones (from -22^oC in Western Siberia to -33 ^oC in Northern Yakutia), and the total winter temperatures were less than modern ones by 2000-3000^oC in Late Pleistocene cryochron. The mean summer temperatures which are reconstructed by palynological method were about 1-5^oC less than modern ones. The mean annual surface air temperatures were about 5-9^oC lower during Late Pleistocene cryochron (40-10 Kyr B.P.).

a   b
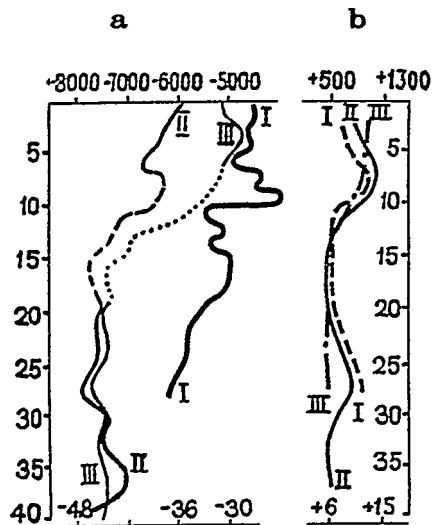
Fig.2. The paleotemperature records plotted for the 40-10 Kyr B.P.: a - b - total negative (a-winter seasons) and total positive (b - summer seasons) near soil air temperatures in some regions of Northern Eurasia cryolithozone: I - in north of Western Siberia, II - in North Yakutia, III-in North Chukotka; bottom horizontal scale shows values of mean January and mean July air temperatures(approximately)

We have studied the dependence between permafrost area

and temperatures of air and permafrost ground for different periods:Late Pleistocene cryochron (pal.) and the present(mod.) at the main regions of Eurasia (Tab.)

Table

The dependence between width of permafrost area (1) and temperatures of the permafrost ground (t_{gr}) of different regions in 40-10 Kyr B.P. (pal.) and the present (mod.)

area of ice wedge distr.	$\delta^{18}O_{iw}$ ‰		1, km		t_{mw}, °C		t_{gr}, °C		$1/t_{gr}$, km/°C	
	mod.	pal.	mod.	pal.	mod.	pal.	mod.	pal.	mod.	pal.
E.Eur.	-15	-18	240	2000	-15	-21	-6	-9	60	220
W.Sib.	-18	-23	800	3000	-18	-25	-10	-15	80	200
N.Yak.	-26	-32	2500	5000	-26	-33	-13	-21	190	270
N.F.E.	-17	-26	1200	3200	-16	-27	-8	-16	170	200

Note: E.Eur.-Eastern Europe, W.Sib.-Western Siberia, N.Yak.- Northern Yakutia, N.F.E.-Northern Far East

The Late Pleistocene cryolithozone was similar to Yakutia type. Just as modern Yakutia cryolithozone it had vast extension from North to South and rather moderate gradient of mean annual ground temperature increase in the same direction. The dominantly continental climate of Western Europe and corresponded climate of permafrost conditions were determined in Late Pleistocene by Northern Atlantic iciness. By this means Yakutia type cryolithozone extended from Atlantic to Pacific and had the width which was varied from about 2000 in Western Europe to 5000 km in Siberia.

References

Vasil'chuk, Yu.K. (1992) Oxygen isotope composition of ground ice (application to paleogeocryological reconstructions). Moscow. Vol.1.- 420 p.p. Vol.2.- 264 p.p. (In Russian, with English the contents, all figure captions and appropriately summary).

Carbonate nodules in Chinese loess as isotopic indicators of the Quaternary palaeoclimate

ZHANG, Hongping   IHEG, Shigang Street 150, Shijiazhuang 050061, Hebei; China
   present address: IFAQ-ETI, VUB, Pleinlaan 2, 1050 Brussels, Belgium
PAEPE, R.   BGD-SGB, Jennerstraat 13, B-1040 Brussels, Belgium
ZHANG, Zonghu   IHEG, MGMR, Zhengding 050803, Hebei, P.R.China
KEPPENS, E.   CHRO, VUB, Pleinlaan 2, 1050 Brussels, Belgium
HAESAERTS, P.   IRSNB-KBIN, rue Vautier 29, B-1040 Bruxelles, Belgium
HUS, J.   KMI-IRM, B-5670 Dourbes, Belgium.

Introduction

Much of our quantitative knowledge of climate fluctuations in the past has been derived from the long and detailed isotope recordes preserved in deep-sea sediments and some continental deposits such as ice sheets. The main palaeoclimate indicator has been the oxygen and carbon stable isotopes of water and carbonates. The stable isotope record in land deposits is less well-developed, but has, nevertheless, shown some potential as an indicator of past climatic variations. In addition to the studies of marine sediments, recent major advances in the understanding of the palaeoclimatic history of the Quaternary era have been made from the sequences of loess. Of special importance are the findings from the Chinese Loess Plateau, which is situated in the north part of the East Asian monsoon as the largest accumulation of loess in the world (Liu T.S *et al.*, 1984, Kukla *et al.*, 1989, Zhang Z.H. *et al.*1980). Generally, soil carbonates form under arid to sub-humid climatic conditions (Birkland, 1974, Jenny 1980) in relatively dry soils where mean annual rainfall is < 75 cm, grasses or mixed grasses and shrubs are the dominant vegetation. The isotopic composition of soil or paleosol carbonate, if unaltered after burial, can be used as a sensitive palaeoclimatic indicator to reconstruct certain aspects of the palaeoenvironment of soil formation. Chinese Loess deposits are characterized by the concentration of well developed pedogenic carbonate nodules, whose stable isotopic geochemistry is useful for the study and reconstruction of the Quaternary palaeoclimate and palaeoenvironment.

The palaeoclimatic evolution since the Quaternary has initiated the depositon of the loess sediments in China. The continuous loess-paleosol sequences in the Loess Plateau of China recorded geological and climatological events since about 2.4 Ma. B.P.: each cold/dry to warm/humid climatic cycle represents a complete glacial-interglacial cycle. In the present study, a well-defined loess stratigraphic sequence, the Huangling section is examined, from which at least 27 loess-paleosol cycles above the Red Clay can be counted, i.e. at least 27 glacial (cold) - interglacial (warm) cycles in the past 2.4 Ma. may be documented. Systematic analysis is carried out in order to (1) document the isotopic composition of pedogenic carbonate nodules in loess deposits; (2) identify its palaeoenvironmental implications; (3) examine the utilization of soil carbonate in loess deposits as one of the continental isotopic indicators of climate (CIICs).

The study area, lying at the Yuan Area of the Loess Plateau in North-Central China, enjoys

a semi-arid continental climate. Sampling was done by collecting carbonate nodules systematically horizon by horizon along the 4 profiles of the whole Huangling section. Round, compact dense non-layered calcareous concretions were selected preferentially because such kind of samples are suitable for isotope study (Zheng, S. H. et al.,1987). In addition, some carbonate-rich calcic sediments were taken from certain positions. From each nodule sample, five isotope samples are taken on the cutting surface from outer, middle, inner and different positions respectively. The carbon and oxygen isotopic analyses are performed on CO_2 prepared from the carbonate samples by treatment with 100% phosphoric acid following McCrea's (1950) classical procedure, and measured by Finnigan MAT Delta-E mass spectrometer with results reported in the conventional δ notation (‰) relative to the PDB standard.

Results and discussion

The analytical results are plotted in the figure. The $\delta^{13}C$ values vary from -8.887‰ to -2.588‰ with a range of 6.299, averaging -6.106‰; while $\delta^{18}O$ change between -11.063‰ to -7.911‰ with a range of 3.152, averaging -9.211‰. It can be seen clearly from the Fig.1 that the general tendency of both oxygen and carbon isotope stratigraphy of carbonates in loess deposits changing with position is according with the alternation of loess and paleosol quite well. Loess layer normally responds with higher value of $\delta^{13}C$ and lower value of $\delta^{18}O$, but paleosol layer goes the other way round. Because each loess or paleosol layer stands for a major climatic event independently, therefore, the changing isotope curve of the Huangling section might be thought as the record of Quaternary climatic events, suggesting the basic pattern of climatic changes at certain time span at certain distinguishing ratio. It seems that most of the information on important palaeoenvironmental and palaeoclimatic evolution can be reflected by stable isotopes, especially by the carbon isotopes. For instance, some climatic-optimum events like S2, S5, and L9, L15, S17 and so on are clearly indicated by isotope records. The isotopic analyses also reflect rather clearly the Pleistocene climatic changes, which are characterized by the alternation of dry-cold (glacial loess) period and warm-wet (interglacial paleosol) period. On the figure, if the standard presented by the average value of $\delta^{18}O$ and $\delta^{13}C$ is chosen, it can be seen that most of the $\delta^{18}O$ and $\delta^{13}C$ values are below the average values basically before the formation of paleosol S15; From loess L15 to S9, and from L9 to L6, most of the $\delta^{18}O$ and $\delta^{13}C$ values are alternative around the average; From paleosol S5 to L2, $\delta^{18}O$ values higher than the average value are in the majority, but $\delta^{13}C$ values change sharply within a significant range. Above loess L2 to S0, most of $\delta^{18}O$ and $\delta^{13}C$ values are below the average value. The regular variation of $\delta^{18}O$ and $\delta^{13}C$ with position on the sequence means that the Quaternary palaeoclimatic changes could possibly be divided into four major different climatic environmental periods, which can be expressed by four major stable isotope assemblages. According to the palaeomagnetic ages of the loess sections in the Loess Plateau, corresponding time can be designated roughly as follows: (1) the Stable Isotope Assemblage I (S1 to S0: from 0.13 Ma. to the present): representing a cold / dry environment; (2) the Stable Isotope Assemblage II (S5 to L2: 0.62 - 0.13 Ma. B.P.): representing a warm / wet environment; The most dramatic climatic changes occurred in this assemblage; (3) the Stable Isotope Assemblage III (S15 to L6: 1.35 - 0.62 Ma.B.P.): An alternation of cold / dry and warm / wet periods; This assemblage is likely to be divided into two sub-assemblages mainly based on the lithostratigraphic assemblages, i.e. the sub-Assemblage 2 (S15 to S9), and the Sub-Assemblage 1 (L9 to L6); (4) the Stable Isotope Assemblage IV (L27 to L16, before about 1.35 Ma.B.P): representing a cold / dry environment. In general, it is apparent from both $\delta^{18}O$ and $\delta^{13}C$ curves that the Quaternary palaeoclimatic changes have a general tendency to become drier during the alternation of cold / dry and warm / humid climatic circles. The changes of stable isotopic
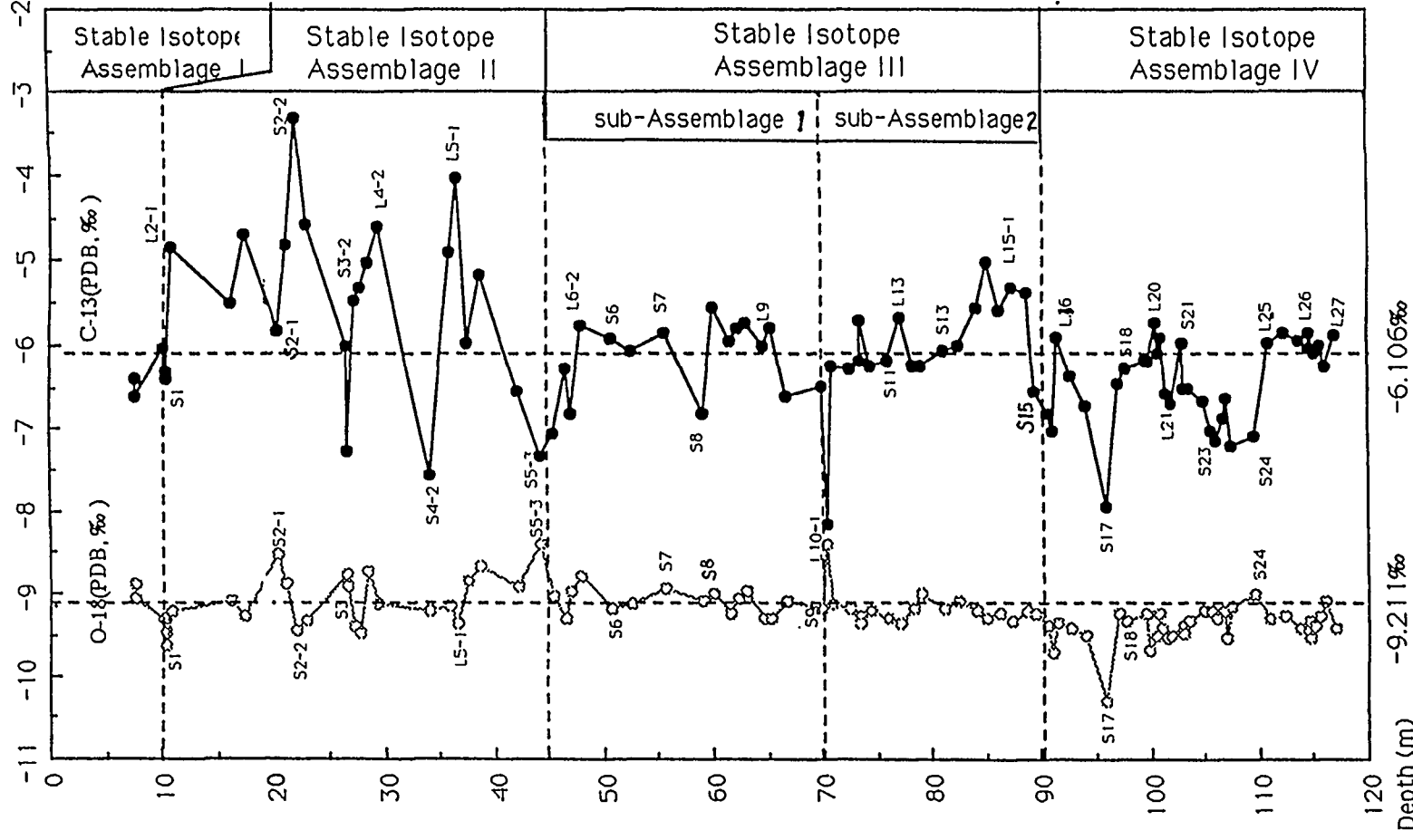
Fig. Stable isotope assamblages of the Huangling loess section in Central China, corresponding to the Quaternary palaeoclimatic changes.

composition of carbonate nodules are recording the environmental changes. The oxygen and carbon isotope study results, especially the four major stable isotope assemblages of the Huangling loess section do coincide quite well with that of lithostratigraphic record, *i.e.* the four main stratigraphic assemblages of the Huangling Section.

Because the oxygen isotopic composition of soil carbonate is related to the isotope of meteoric waters, which are related to climate, especially to the mean annual temperature, and the carbon isotopic composition of soil CO_2 during the growing season is related to the carbon isotopic composition of the biomass which is related to the proportion of plants that use the C3 and C4 photosynthetic pathways, the paleoenvironmental, paleoecological conditions, and paleoclimates, e.g. paleotemperature, precipitation and humidity of the past can be quantitatively or semi-quantitatively evaluated based on adequate data. A preliminary attempt has been made , in a tentatively quantitative way, to estimate the annual mean temperatures and precipitations, under which paleosols were formed. The palaeoecological environment is also evaluated in terms of C3 / C4 biomass proportions. The results show a mixed C3 and C4 flora with C3 as dominant (C3 >50%). Since all trees and most shrubs use the C3 photosynthetic pathway regardless of temperature during the growing season (Wang and Zheng, 1989), this could be indicative of a flora that pedominantly consisted of trees and shrubs, or it might indicate a mixed C3 and C4 prairie. It is only during the well developed paleosols such as S4 and S5 formations there seems to be a little more forests. The significant proportion (30-45%) of C4 biomass means that the vegetation differences between different paleosol formation is apparent. Such a high C4 biomass fraction may indicate that grasses were an important part of the ecosystem.

Here, a preliminary attempt is also made to correlate the stable isotope records of the Huangling loess section with the standard reference - deep sea oxygen isotope stratigraphy record. This land/sea correlation shows that the Quaternary climatic changes revealed by the Huangling Section are synchronous rather well with those in the deep sea and hence of worldwide significance.

References

Cerling, T.E.. 1984. The stable isotopic composition of modern soil carbonate and its relationship to climate. Earth Planet. Sci.Lett.. 71, 229-40.

Cerling, T.E., Quade, J., Wang, Y., & Bowman, J.R.. 1989. Carbon isotopes in soils and paleosols as ecology and palaeoecology indicators. Nature, 341, 138-9.

Haesaerts, P., Hus, J., Zhang Hongping, Shi Jiansheng *et al.*. 1993. Working report of 1992-93 for the Sino-Belgian joint loess project.

Han Jiamao. 1991. Palaeoclimatic impact on the magnetic and stable isotopic characteristics of the Chinese loess. Doctoral thesis. Free University of Brussels, 242pp.

Kukla, G. & An, Zhisheng. 1989. Loess stratigraphy in central China. Palaeogeogr. Palaeoclimatol. Palaeoecol. 72, 203-25.

Liu Tungsheng. *et al.* 1985a. Loess and the environment. China Ocean Press, Beijing.

Paepe, R., Mariolakos, I. , Van Overloop, E. & Keppens, E. 1990. Last interglacial-glacial north-south geosoil traverse (from stratotypes in the North Sea basin and in the Eastern Mediterranean). Quat. Intern.. 5, 57-70.

Wang Yang & Zheng Shuhui. 1989. Paleosol nodules as Pleistocene paleoclimatic indicators, Luochuan, P.R.China. Palaeogeogr. Palaeoclimatol. Palaeoecol.. 76. 39-44.

Zhang Hongping *et al.* 1989. Stable isotopes in Precipitation in China. Investigation Science Technology. 6.

Zhang Zonghu *et al.* 1980. The geomorphological map of the loess plateau. Geological Publishing House, Beijing.

Holocene climatic changes
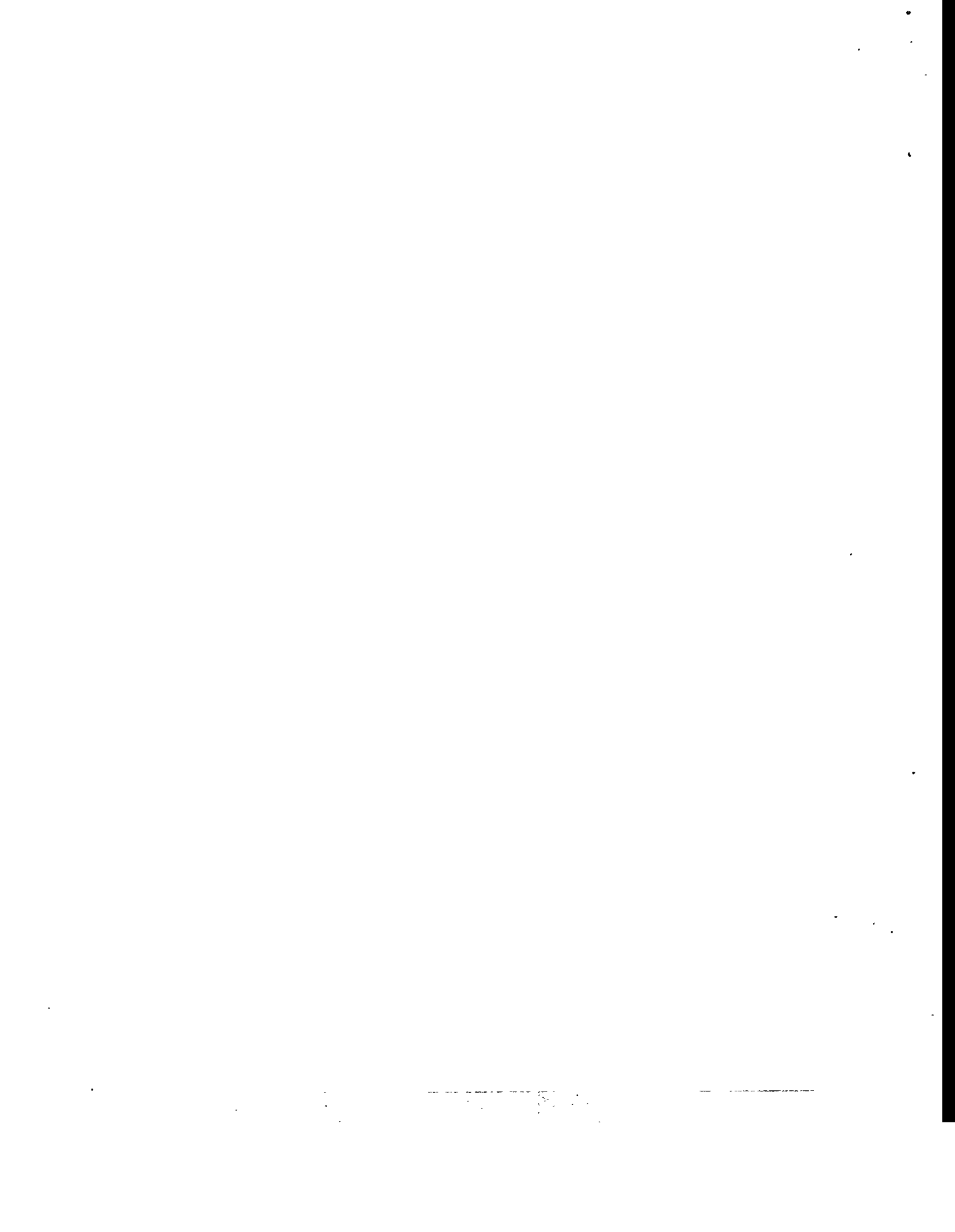
Length of the ice-cover period inferred from varved boreal lake sediments, Finland

Itkonen, A. and Salonen, V-P

University of Turku
Department of Geology
FIN-20500 TURKU Finland

Introduction

Modelling of future climate conditions requires evaluation where simulated past changes can be tested against observed ones. This can be done by using proxy information (tree ring series, ice cores, corals etc). Instrumental records on climatic parameters normally extend back not more than 50-100 years. Lakes with annually laminated sediments provide valueable proxy records of long-term climatic variation because, in addition to being chronometers, varves also provide a compositional framework for climatic variability connected to their formation (Dean et al. 1984).

The deposition of lake sediments is controlled by atmospheric processes, the geology, and the hydrology within the lake's catchment. Climatic signals can be reconstructed using geochemical, biological or sedimentological techniques. For example, calcium carbonate precipitating from open water gives direct information about precipitation and lakewater temperature (Kelts 1991). Diatom taxa respond indirectly to climate through, for example, salinity changes (evaporation/precipitation) in semiarid regions (Wilson et al. 1994). Chironomid assemblages in sediments of shallow headwater lakes are sensitive to variations in summer lake water temperatures (Walker et. al., 1991).

Perkins and Sims (1983) presented the hypothesis that in areas where lakes receive runoff from partly glacier-covered terrain, temperature, averaged over the summer, is the main control in varve thickness variation. This hypothesis has lately been verified by, for example, Desloges (1994), Desloges & Gilbert (1995) and Bradley et al (in press).

Respectively, in the boreal zone, climatic forcing effects varved sedimentary sequences (Petterson et al. 1993). Already Saarnisto et al. (1977) observed that varve thickness variations in a small Finnish boreal lake were related to climatic fluctuations: thin varves coincide to years with a crop failures. Itkonen and Salonen (1994) found

that warm winter months indicating a short ice-cover period had the strongest control on varve thickness in three Finnish boreal lakes. Short ice-cover period favours thick varves. Here we discuss further the forcing mechanisms and application of these records in estimating past variations of winter severity in southern Finland.

The lakes

The studied lakes differ in nutrient status; lake Pääjärvi is oligotrophic, lake Päijänne mesotrophic, and lake Pyhäjärvi eutrophic. All three lakes are relative deep with anoxic conditions at the bottom, and the seasonal cycle of sediment flux preserved in the varves. The varves in Ristiselkä and Pääjärvi are composed of light summer layers consisting of allochtonous mineral material and diatoms, and thin dark winter layers rich in organic material and sulfides. In Pyhäjärvi the thin, grey summer laminae are composed almost entirely of diatom layers.

Key results and discussion

The natural trend caused by compaction was removed from the varved sequences by using the equation presented by Håkanson & Källstrom (1978). The time series for original, corrected and smoothed time series show that there is a lot of noise in the record. However, certain long term variations in varve thickness can be observed. The laminae are thicker than average from AD 1300 - 1500, thinner than average from A.D. 1500 - 1870, and then again become thicker towards the surface in the most recent sediments.

In multivariate regression analysis, the corrected varve thickness measurements were regressed against measured monthly variations in Helsinki temperature (1829-1992), precipitation (1844-1992) (Heino 1994), and information on the length of the freezing time from lake Kallavesi, Central Finland (AD 1834-1959; Kuusisto, pers comm).

The statistically significant regressions show that the sediment thickness variation in all three lakes is a function of the observed spring temperatures. Warm springs and short winters lead to thick varves in sediments. This was further demonstrated by significant negative correlations between the observed ice cover time and the varve thickness. Thick varves were formed when the lake was ice-free until December.

All three series indicate that the length of freezing period (which in the area varies between 90 and 200 days) has become shorter since the 1850's. The winters corresponding with the Little Ice Age between AD 1570 and 1730 (Bradley & Jones 1993) were clearly more severe than the winters of the present century. The curves also indicate that the mildness of present day winters is exceptional. Moreover, the overall increase in field erosion since the beginning of the 19th century has accelerated the rate of sedimentation by a factor of 1.5 to 2 in lakes Pääjärvi and Päijänne. Correspondingly, the proportion of allogenic clastic components has increased in the sediments during the last 200 years.

It is clear, that the varve thickness reflects climatic parameters in all the lakes studied. The composition of the varves show, that both organic matter and allogenic clastic components increase in thick varves. This is probably the result of an increased sensitivity to wind induced resuspension when ice-cover time is short (Itkonen & Salonen, 1994). Storms, which are common during autumn and spring, can be responsible of major part of the whole year sediment accumulation (eg. Bengtsson et al., 1990, Page et al., 1994).

The proportions of nutrients (authigenic P, total N and organic C) have regularly strong positive correlations with the varve thickness in all three studied lakes. This indicates that the ice cover time has a significant control on lake trophic status. Furthermore, the sediment bioproduction component (evidenced by biogenic silica, N:P and C:N ratios) has a positive correlation and a significant control on sedimentation in the meso-eutrophic lakes Päijänne and Pyhäjärvi. Scavia et al. (1986) found, that prolonged ice cover decreased sediment resuspension resulting in lower total P, reduced chlorophyll-a and increased water transparency. Nevertheless, the results indicate the possibility of increased nutrient availability and bioproduction, if the greenhouse effect shortens the ice cover time in boreal lakes.

Boreal lakes filter a lot of climatic variability, but in certain circumstances they demonstrate a strong signal of the length of the freezing period. Long, even Holocene-length records providing annual proxy information on winter freezing time could thus be obtained from lacustrine cores. Three conditions must be met in order to obtain this information; first, the catchment soils have to be susceptible to erosion, second, there has to be a significant year-to-year variation in the length of the lake freezing period, and third, the lake with annually laminated sediments has to be large enough to smooth local interferences.

References

Bengtsson, L., Hellström., T. & Rakoczi, L., 1990. Redistribution of sediments in three Swedish lakes. Hydrobiologia 192: 167-181.

Bradley, R.S. & Jones, P.H. 1993. 'Little Ice Age' summer temperature variations: their nature and relevance to recent global warming trends. The Holocene 3,4, 367-376.

Bradley, R.S., Hardy, D.R., Lamoureux, S.F., Ludlam, S.D., Retelle, M.J. & Zolitschka, B. Summer paleotemperatures in the Canadian High Arctic from varved lake sediments. Science, in press.

Dean, W.E., Bradbury, J.P., Anderson, R.Y. & Barnosky, C.W., 1984. The variability of Holocene climatic change: evidence from varved lake sediments. Science 226: 1191-1194.

Dean, W.E., Bradbury, J.P., Anderson, R.Y., Ramirez Bader, L. & Dietrich-Rurup, K., 1994. A high-resolution record of climatic change in Elk Lake, Minnesota for the last 1500 years. U.S. Department of the interior. U.S. Geological Survey. Open-file report 94-578.

Desloges, J. 1994. Varve Deposition and the Sediment Yield Record at Three Small Lakes of the Southern Canadian Cordillera. Arctic and Alpine Research, Vol 26, 130-140.

Desloges, J. & Gilbert, B. 1995. The sedimentary record of Moose Lake: implications for glacier activity in the Mount Robson area, British Columbia. Canadian Journal of Earth Sciences 32,

Håkanson, L. & Källström, A. 1978. An equation of state for biologically active lake sediments and its implications for interpretations of sediment data. Sedimentology 25, 205-226.

Heino, R. 1994. Climate in Finland during the period of meteorological observations. Finnish Meteorological Institute Contributions, 12. Helsinki 212 pp.

Itkonen, A. & Salonen, V-P. 1994. The response of sedimentation in three varved lacustrine sequences to air temperature, precipitation and human impact. Journal of Paleolimnology 11, 323-332.

Kelts, K. 1991.Reading pages from limnogeological archives. INQUA XIII, Special Proceedings Review Reports, 10-19.

Page, M.J., Trustrum, N.A. & DeRose, R.C., 1994. A high resolution record of storm-induced erosion from lake sediments, New Zealand. Journal of Paleolimnology 11: 333-348.

Perkins, J.A. & Sims, J.D. (1983). Correlation of Alaskan varve thickness with climatic parameters, and use in paleoclimatic reconstruction. Quaternary Research 20:308-321.

Petterson, G., Renberg, I., Geladi, P., Lindberg, A. & Lindberg, F., 1993. Spatial uniformity of sediment accumulation in varved lake sediments in northern Sweden. Journal of Paleolimnology 9: 195-208.

Saarnisto, M., Huttunen, P., & Tolonen, K. 1977. Annual lamination of sediments in Lake Lovojärvi, southern Finland, during the past 600 years. Annales Botanici Fennici 14, 35-45.

Scavia, D., Fahnenstiel, G.L., Evans, M.S., Jude, D.J. & Lehman, J.T., 1986. Influence of salmonine predation and weather on long-term water quality trends in Lake Michigan. Can. J. Fish. Aquat. Sci. 43: 435-443.

Walker, I.R., Mott, R.J. & Smol, J.P. 1991. Allerød-Younger Dryas Lake Temperatures from Midge Fissils in Atlantic Canada. Science 253, 1010-1012.

Wilson, S.E., Cumming, B.F. & Smol, J.P. 1994. Diatom-salinity relationships in 111 lakes from the Interior Plateau of British Columbia, Canada: the development of diatom-based models for paleosalinity reconstructions. Journal of Paleolimnology 12, 197-221.

Deglaciation chronology and climate change in the Norra Storfjället area, Northern Sweden

Volli Kalm*, William C. Mahaney**, Judith Earl-Goulet** and Patrick Julig***

*Tartu University, Institute of Geology, Vanemuise 46, EE2400, Tartu, Estonia
**Geomorphology and Pedology Laboratory, York University, 4700 Keele Street, North York, Ontario, Canada, M3J 1P3
***Laurentian University, Department of Sociology & Anthropology, Sudbury, Ontario, Canada, P3E 2C6

Introduction

The Norra Storfjället massif (Fig. 1), located on the leeward side of the Caledonian Mountains at 65°N, 15°E, includes the birch forest at elevations below 700 m a.s.l., alpine vegetation above to elevations of 1000 m a.s.l., small cirque glaciers, and exposed bedrock at higher elevations up to 1600 m a.s.l. The deglaciation and climate history of the Norra Storfjället area is reconstructed (Fig. 2) from a complex record based on glacial geomorphological, sedimentological, pedological and archaeological evidence and C^{14} dates (cal C^{14}-dendrochronologically calibrated dates). The Holocene chronozone boundaries are given after Mangerud et al. (1974).

Results and discussion

In the Norra Storfjället region (Fig. 1), the Weichselian glacier thinned during the Boreal Chronozone, and began to operate as several individual valley glaciers.The Umeälven Valley 160-300 km SE of the area studied, at 225-265 m a.s.l. was deglaciated between 9500 and 9200 yr BP (Zale, 1988). During the Early Boreal the ice retreat left valleys below 600 m a.s.l. largely free of ice. In the Umeälven Valley a glacial lake was dammed up in the Tärnaby region. Deposition of varved clays (Fig. 1, sections HEM5, 6, 7) at 470-480 m a.s.l., according to the number of annual layers in site HEM5, lasted 122 years as a minimum. The bottommost peat layer on top of the varved clays yielded the cal C^{14} age of 8610±110 yr BP(HEM7). Consequently, the glacier receded from this valley and deposition of varved clays started at ca. 8730 yr BP as the latest (Fig. 2). Piece of wood 10 cm above the clay/peat boundary revealed the early Atlantic Chronozone age 7770±140 yr BP and the respective timberline was not lower than 470-500 m a.s.l. According to H. Agrell (1979) the Pre-Boreal chronozone) is characterized by the rapid immigration of the northern coniferous forest (pine/birch) over the central Sweden, probably advancing close to the receding ice front. Still in the early Atlantic Chronozone the water table in the Stor-Laisan (Fig. 1) lowered, Tärnaan river became the only outlet from the valley above Tärna, and a peat accumulation started (7424±70 yr cal C^{14} BP) on a saddle west of Tärnaby (site TBY4).
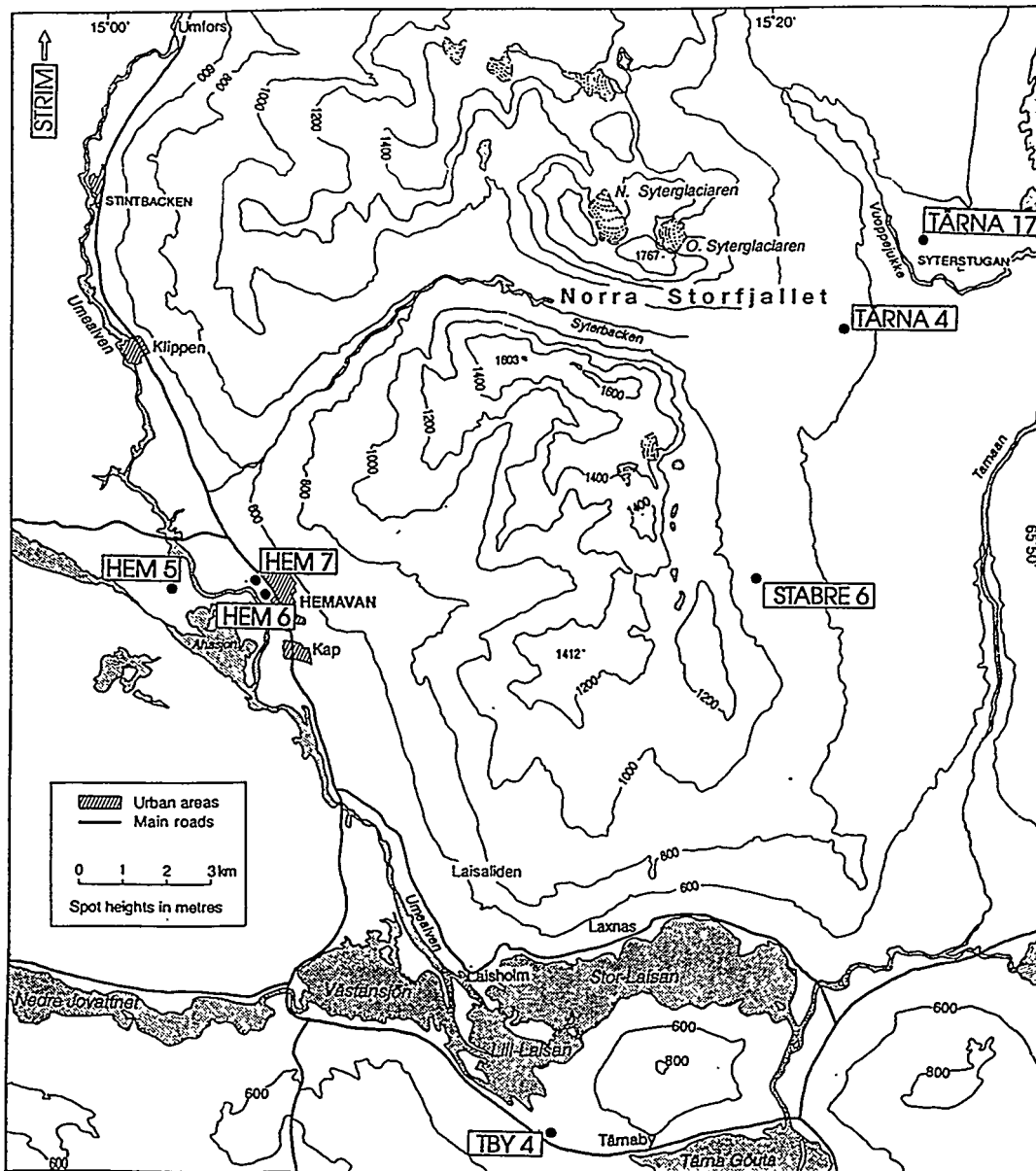
Fig. 1. Norra Storfjället massif and location of investigated sites.

The area above present-day timberline contains podzolic (Spodosols) paleosols that formed in well-protected areas of swales and in depressions. The podzols above the timberline have been recorded in several studies in Sweden and Norway (Caseldine and Matthews, 1987; Kullman, 1993). Ellis (1985) indicates a possible expansion of the conifer forest in southern Norway to 1150 m a.s.l., 400 m higher than its present extent. The podzolic paleosols (e.g. Fig. 1, TÄRNA 4 profile, 920 m a.s.l.) are fossil soils, formed during the Atlantic Chronozone when an elevated timberline produced a dwarf pine and birch forest as high as 900 m a.s.l. (Fig. 2). During the Climatic Optimum in the Atlantic Chronozone (ca. 6000-5000 yr BP) the timberline was situated approximately +200 m higher than at present, as is obvious from
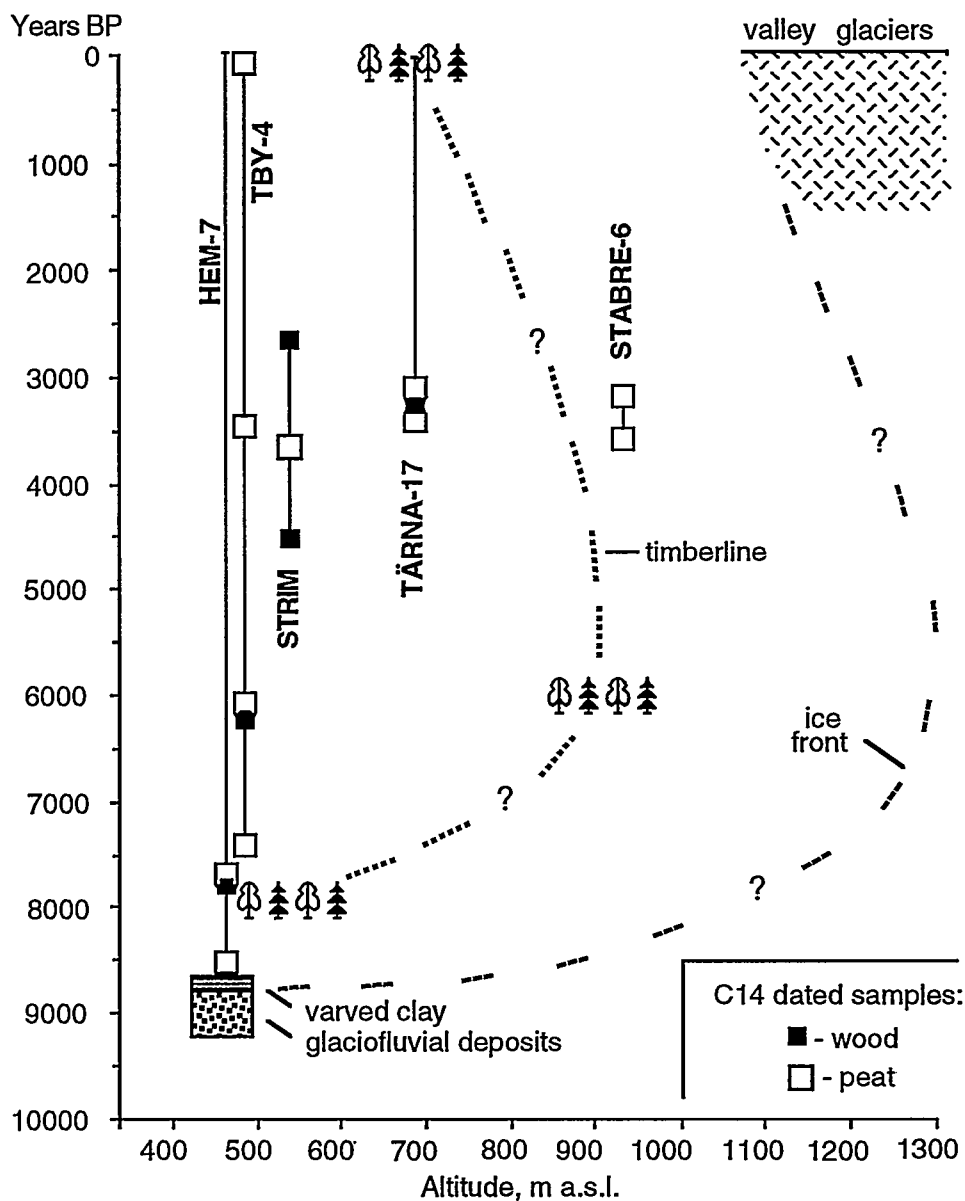
Fig. 2 Tentative diagram illustrating the general extension of ice and the change of timberline position over the Norra Storfjället area. Time span of the main dated sections is shown. STRIM - section at Strimasund (from Worsley, 1974).

still-present pine stumps (Lundqvist, 1969; Karlén, 1976). The archaeological finds and the stone technologies indicate use of the uplands by Late Mesolithic, from the Atlantic Chrono-zone (8,000-5,000 yr BP) as well as later Neolithic and Bronze age inhabitants (Holm, 1991). This temporal placement is also supported by the recovery of a quartz artifact from 70 cm depth in a peat bog (TBY-4), dating to the Climatic Optimum, and recovery of keeled scra-pers at quarry sites in upland locations at Hemavan. With the beginning of the Sub-Boreal Chronozone, temperature and precipitation dropped and the soil forming potential above 650 m a.s.l. could produce only Inceptisols and Entisols. The paleopodzols have retained their podzolic genetic horizonation showing E/Bs/Cox/Cu profiles even after the disappearance

of the forest and reappearance of alpine tundra at approximately 5000 yr BP. Accelerated solifluction during the Sub-Boreal produced development of turf-banked lobes and terraces burying pre-existing Spodosolic and Inceptisolic profiles. We have radiocarbon dates of 3150±100 and 3650±100 yr BP in these solifluction lobes (1.5 m inside the lobe front) at an altitude of 930 m (Stabre 6). A rapid change in the climate, characterized by falling temperature and an increasing humidity, occurred at the transition to the Sub-Atlantic Chronozone (ca. 2500 yr BP). This is obvious also from archaeological evidence, since a relatively long period at the transition from the Bronze Age to the Iron Age is very poor in artifacts, with metal tools replacing stone. However, there is archaeological evidence of continued use of upland regions in the form of hunting pits and habitation features (Mahaney et al., 1995). At present the Mean Annual Temperature at Hemavan (475 m a.s.l.) is -0.4°C. Mean Annual Precipitation is 681 mm (Sveriges Meteorologiska och Hydrologiska Institutionen). Current snowline with walley glaciers is situated between 400-450 m above the timberline.

References

Agrell, H. 1979. The Quaternary of Sweden. Sver. Geol. Unders., Serie C, 770, 29 pp.

Caseldine, C.J. & Matthews, J.A. 1987. Podzol development, vegetation change and glacier variations at Hanabreen, southern Norway. Boreas16:215-230.

Ellis, S. 1985. An altitudinal sequence of podzolic soils, Hardargervidda, southern Norway. Norsk Geogr. Tidsskr. 39:141-154.

Holm, L. 1992. The use of stone and hunting of reindeer. Archaeology and Environment 12, Department of Archaeology, Umeå University, Umeå, 199 pp.

Karlén, W. 1976. Holocene climatic fluctuations indicated by glacier and tree-limit variations in northern Sweden. Univ. of Stockholm, Dept. of Physical Geography, Rep. 23, 9 pp.

Kullman, L. 1993. Holocene thermal trend inferred from tree-limit history in the Swedish Mountains. Global Ecology and Biogeography letters 2:181-188.

Lundqvist, J. 1969. Description of the map of the Quaternary deposits of the county of Jämtland, Central Sweden. Swer. Geol. Unders., Serie Ca, 45, 418 pp.

Mahaney, W.C., Earl, J., Kalm, V. and Julig, P.J. 1995. Geoecology of the Norra Storfället Area, northern Sweden. Mountain Res. and Development 15, 2:165-174.

Mangerud, J., Andersen, S.T., Berglund, B.E. & Donner, J.J. 1974. Quaternary stratigraphy of Norden, a proposal for terminology and classification. Boreas 3:109-128.

Zale, R. 1988. Bedrock-related irregularities of the highest shoreline along the Umeälven valley, northern Sweden. Geol. Fören. i Stockh. Förh. 110, 3:203-206.

Worsley, P. 1974. Absolute dating of the Sub-Boreal climatic deterioration - fossil pine evidence from Strimasund, Västerbotten County, Sweden. Geol. Fören. i Stockh. Förh. 96, 4:399-403.

Fine scale pollen diagrams related to the environmental changes

Tiiu Koff

Institute of Ecology, Estonian Academy of Sciences
Kevade 2, EE0001 Tallinn, Estonia

Introduction

To better understand the impact of different scale climatic processes on the environment palaeoenvironmental data are widely used. In principal it is possible, using different palaeogeographical information sources and methods, to study the changes in the past environment on different time scales, characterize and understand former natural variability and alteration. The pollen data are the basic material for such research. The interpretation of pollen data simply in terms of climate is not possible due to other factors like competitive interactions between plant species; the influence of grazers and plant pathogens, etc. that need to be constantly taken into consideration. Only the development of absolute techniques of pollen analysis, like pollen concentration and accumulation rates allow us to interpret such data in terms of the population dynamics.

The main aim of the present study of lake sediments is to assess the extent of the influence of fire as a typical short term natural disturbance on the state and development of vegetation and ecosystems. Pollen analysis together with charred particles and diatom analysis leads to an understanding of vegetation successions and their causes, the regularities of the changes in vegetation after natural fires, the inertness and restoration time of primary successions.

Site description, field and laboratory techniques

The study object, a small Lake Kuradijärv covering 1.4 ha, is situated in north-eastern Estonia in the Kurtna Kame Field area. It is a closed lake, surrounded by forests, with a small watershed and paludified shores. The lake is shallow (1-2 m), the water depth increasing over 6 m only in the central part of it. The lake sediment consist mainly of

gyttja with some plant remains like *Drepanocladus sp.* mosses. At the northern shore of the lake a small mire is situated. The core of the mire sediments contained some very distinct burnt layers with a quantity of charred plant remains. That means there certainly existed fires in the nearest vicinity of the lake. For detailed investigation we took a core from the central part of the lake 3.35 m deep and its sediment 5.50 m thick consisting of homogenous dark brown gyttja lying on the sand bottom. For sampling an Byelorussian type corer was used (inner diameter 7 cm and length 50 cm). The sampled cores were preserved in plastic tubes in a deep freezer. For detailed investigations the sampling core obtained 5.50-6.00 m deep was chosen. The macroscopic charred particles found at the depth of 5.661-5.664 m were sent for AMS ^{14} C dating to the University of Arizona. Using special equipment 3 mm continuous sampling was made, samples being dried and weighed. For calculating pollen concentration values 2 *Lycopodium* tablets were added and samples prepared using the standard method of acetolysis. Pollen diagrams were drawn using the TILIA program by Eric Grimm. A widely employed procedure for counting charred particles has been applied to measure particle areas of different size. Four area size classes: 130, 250, 650 and bigger than 1000 μm^2 were calculated. In the concentration diagram they are expressed in $\mu m^2 \ g^{-1}$. From the same samples also diatom analysis were made.

Results

The fine scale studies cover the period of around 6000 years BP (according to the AMS ^{14} C dating is 6155±75 (AA-15048) at the depth of 5.660 m). If the accumulation rate was constant then its rate is approximately 0.37 mm yr^{-1} and one sample represents 8 years. All the analysed sediment interval covers 500 years. According to our studies in this region (Koff 1994) the human impact at that time was absent or very weak. Therefore natural fires may have been the main cause of changes in the vegetation.

Remarkable are the changes in the pollen concentration diagram (Fig. 1). Here the distribution of the areas of charred particles allows us to distinguish four zones. Zones A and C are characterised by high and zones B, D by low values of the areas of charred particles as well as of their concentrations.

In the pollen concentration diagram zone A is characterised by increasing *Salix, Tilia* and *Corylus* values. *Salix* and *Corylus* are species of very rapid growth and they belong to the pioneer vegetation communities. High values of *Tilia* pollen content coinciding with charcoal peaks can be possibly explained by long distance transport. After fire due to the openness of the landscape around the lake the share in the pollen spectra of the species not growing immediately in the nearest vicinity increased. This assumption is supported also by the presence of some pollen grains of *Fagus* and *Carpinus.* All these species are not growing on such sandy soils that surround the Kuradijärve lake. Their possible habitats are some kilometres away. After fire *Rumex* and Umbelliferae have find some places where to live. *Calluna* pollen values are
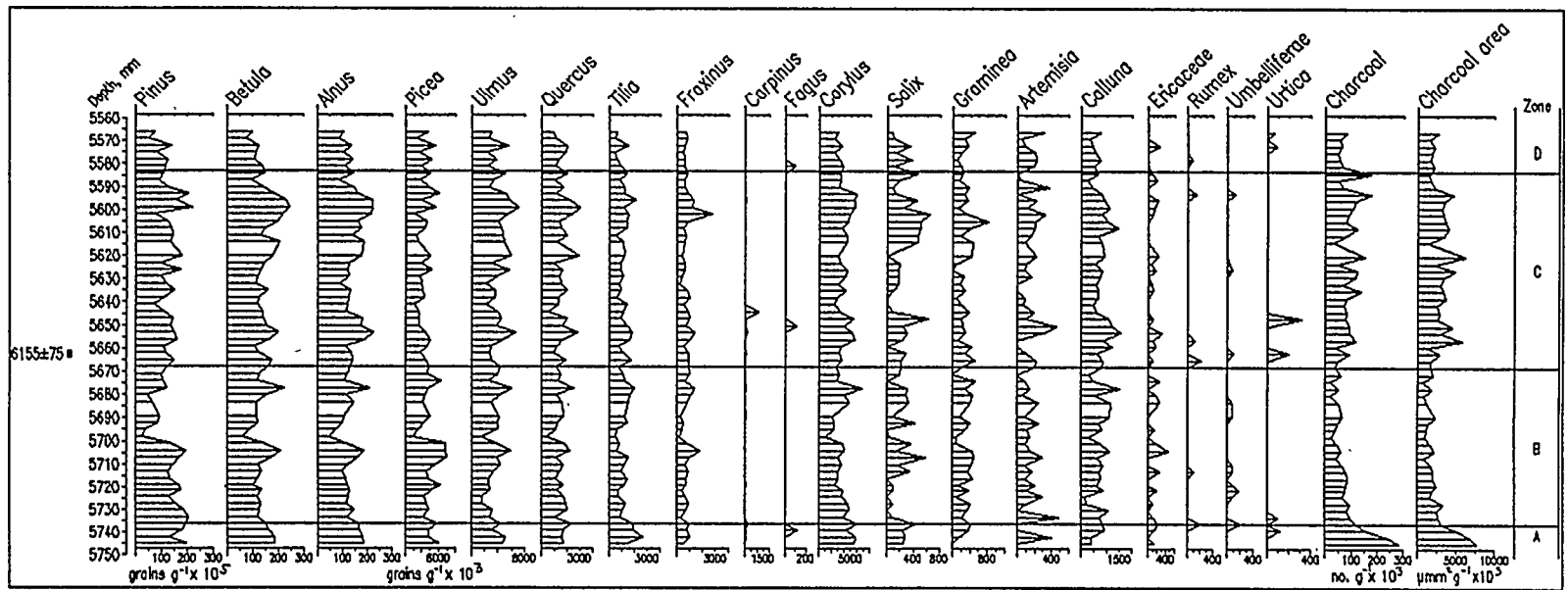
Fig. 1 Pollen concentration diagram of major pollen types from Lake Kuradijärv.

increasing after a short period of 10-20 years (one sample covering 8-10 years). Zone B is characterised by low background values of charred particles without essential fluctuations. Increased pollen concentrations can be traced for all species at the depth 5.700-5.710 m. If, according to ^{14}C data, we take the sedimentation rate as 0.37 mm yr^{-1}, this increase must have taken place approximately 70-80 years later, that is enough for local trees like *Picea, Pinus, Betula, Alnus* to recover from forest fire. The decrease of pollen content following the increase is very noticeable for *Pinus, Betula, Alnus*. This stage without dramatic evidence of forest fires describes the natural succession stages in plant communities. After about 200 years the plant community became stabilized. Zone C like zone B is characterised by high charcoal content. There certainly had occurred at least three local fires but also its regional background of fires is higher. The happening of local fires can be proved by peaks in charred particle content at the depths of 5.665m, 5.620 m and 5.595 m. Shortly after these charcoal maximums pollen content of *Salix* increases. Also the pollen of *Carpinus* and *Fagus* appear in the lake sediment showing the increased openness of the landscape and growing share of the long-distance pollen. *Calluna* and *Artemisia* content increase after charcoal maximum. Pollen of *Urtica* and *Rumex* also seem be connected with the pioneer vegetation after fires. Zone D is characterised by a lower content of charcoal particles. These values are the same as in the zone B. Signs of the last wildfire (charcoal peak at the level of 5.595m) can be observed by an increase of *Salix, Artemisia* and presence of *Rumex* and Umbelliferae pollen. The growth of *Salix* pollen values seems to be very regular. Roughly speaking it happens 30-40 years after fire. Pollen of the main trees are decreasing and the pollen of *Ulmus, Tilia* and *Quercus* have more fluctuating values.

Conclusions

The results obtained demonstrate that using the fine-scale sampling and pollen concentration data it is possible to study the reaction of different plant species to natural wildfires even in dense forest areas. The response of the pollen influx after fires has been caused by two principal reasons: 1) the destruction of more sensitive species creates the conditions for the development of new species, the most obvious is the appearance of *Salix* and some herbs (*Calluna, Artemisia*) pollen in the diagram immediately after the charred particles maximum; 2) burning of the forest nearby makes landscape more open and will increase the share of the long transported pollen. The changes in the pollen content are rather short-lived after a period of some 40-50 years following the fire the pollen spectra will reach their stationary state.

References

Koff, T. 1994. The development of vegetation . In: Punning, J.M. (ed.) The influence of natural and anthropogenic factors on the development of landscapes. Institute of Ecology, Estonian Academy of Sciences, Publ. 2: 24-57.

Deglaciation and late Pleistocene-Holocene environmental change on Franz Josef Land, Russia: Timing of Barents Ice Sheet disintegration

Johan L. Kuylenstierna, Jens-Ove Näslund and Arjen P. Stroeven

Department of Physical Geography, Stockholm University
S-106 91, Stockholm, Sweden

Introduction

Considerable uncertainty still exists concerning the spatial distribution of ice during the last glacial maximum and the timing of the deglaciation, especially for the postulated Barents and Kara Sea ice sheets. The deglaciation of Svalbard has been studied in more detail than any other region bordering the Barents Ice Sheet. Deglaciation occurred between 13 ka years BP and 10 ka years BP, but might have commenced earlier (e.g., Blake, 1961; Hyvärinen, 1968; Lehman and Forman, 1987; Miller et al., 1987; Salvigsen and Österholm 1982; Salvigsen et al., 1991; Salvigsen and Elgersma, 1993). Although the deglaciation of the Svalbard region may have been initiated by globally rising sea levels (Lehman and Keigwin, 1992a, b), rapid deglaciation appears to have followed the initiation of the Norwegian Current around 13.5 ka years BP. At present, evidence for a Younger Dryas stadial is lacking on Svalbard, suggesting that glaciers were small by this time (Salvigsen and Elgersma, 1993).

In comparison to Svalbard, the glacial history of Franz Josef Land, located at the northern rim of the postulated Barents Ice Sheet, is relatively unknown. Until recently the only available results were obtained during the International Geophysical Year (e.g., Grosswald et al., 1973). However, recent political development in the former Soviet Union reopened this vast region for international research co-operation. We have used that opportunity to investigate the timing of deglaciation on Alexandra Land, the western most island of the Franz Josef Land archipelago (e.g., Glazovskiy et al., 1992). From this and other studies it is clear that the deglaciation occurred earlier than previously documented (Näslund et al., 1994), and may have predated the Holocene (Forman et al., 1992). In this study we employ environmental data stored in lake sediments to yield a continuous record of environmental change since the deglaciation.

Results

Four lakes on Alexandra Land (Fig 1) were cored, all situated below the highest postglacial marine limit at 23.5 m a.s.l. The sediments from two of these, Sledge lake and Walrus lake were analysed for organic- and salt content in one centimeter increments, thereby achieving a continuous environmental record reaching back possibly to the time of the last deglaciation. Two different sediment sections are evident within the core from Sledge Lake, a lower from 155-58 cm, showing a relative high organic content, and an upper section (58-0 cm) with considerably lower values. To a great extent, the salt content follows the same pattern, with an exception between 82-55 cm showing intermediate salinity values. The organic content in Walrus Lake is much lower than in Sledge lake and shows a different pattern. A different and more complicated pattern is also evident for the paleosalinity of this lake (Fig. 2).
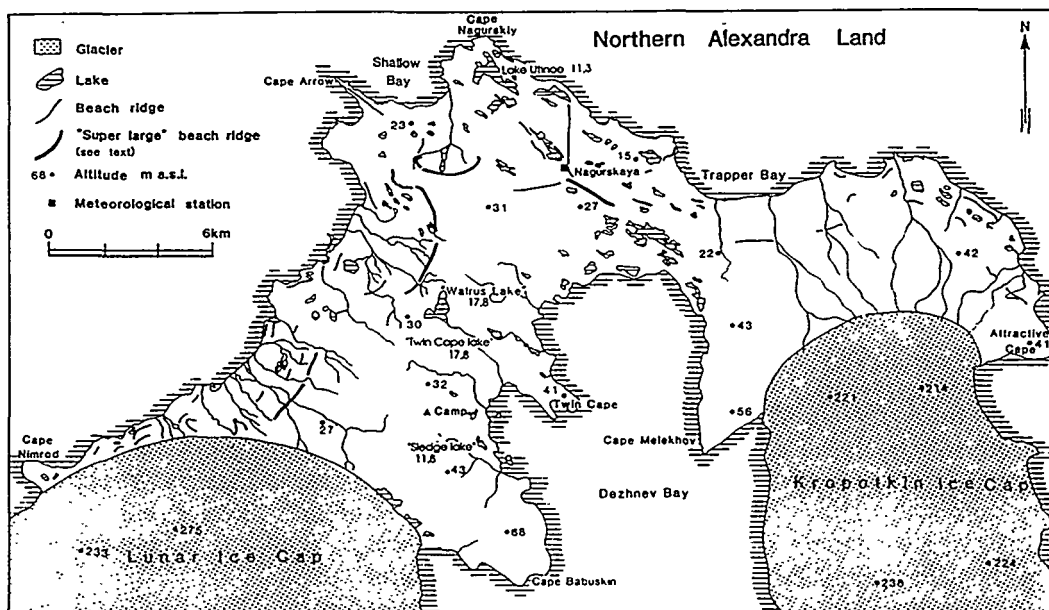
Figure 1. Map of northern Alexandra Land with cored lakes

Chronology

Accelerator Mass Spectrometry (AMS) radiocarbon dates on six bulk samples and one macro fossil sample did not provide a consistent chronology. We have therefore derived a provisional chronology by using the land emergence rate for Alexandra Land (Glazovskiy et al. 1992) and by assuming that a significant and permanent drop in core salinity signifies the transition from a marine to a lacustrine environment. In the cores (Fig. 2), this transition occurs at 56 cm and 70 cm below the sediment surface,

respectively. A tentative chronology further involves the assumption of a constant sedimentation rate. Following a land emergence rate of 3 mm/year as calculated by Glazovskiy *et al.,* (1992) for the last 8600 years, we estimate that this transition in Walrus lake occurred around 5950 years BP and in Sledge lake around 3950 years BP. Allowing for these assumptions, the age span of the Walrus lake core will be about 13000 years and for the Sledge lake core about 11000 years. From this we infer an early deglaciation, in line with evidence from central parts of Franz Josef Land (Forman *et al.* 1992) and Svalbard (*e.g.,* Blake, 1961; Hyvärinen, 1968; Lehman *et al.,* 1987; Miller *et al.,* 1987; Salvigsen and Österholm 1982; Salvigsen and Elgersma, 1993).

Organic- and salt content, Walrus Lake, Franz Josef Land

——organic content (%)
——salt content (g/l)

Organic- and salt content, Sledge Lake, Franz Josef Land

——organic content (%)
——salt content (g/l)
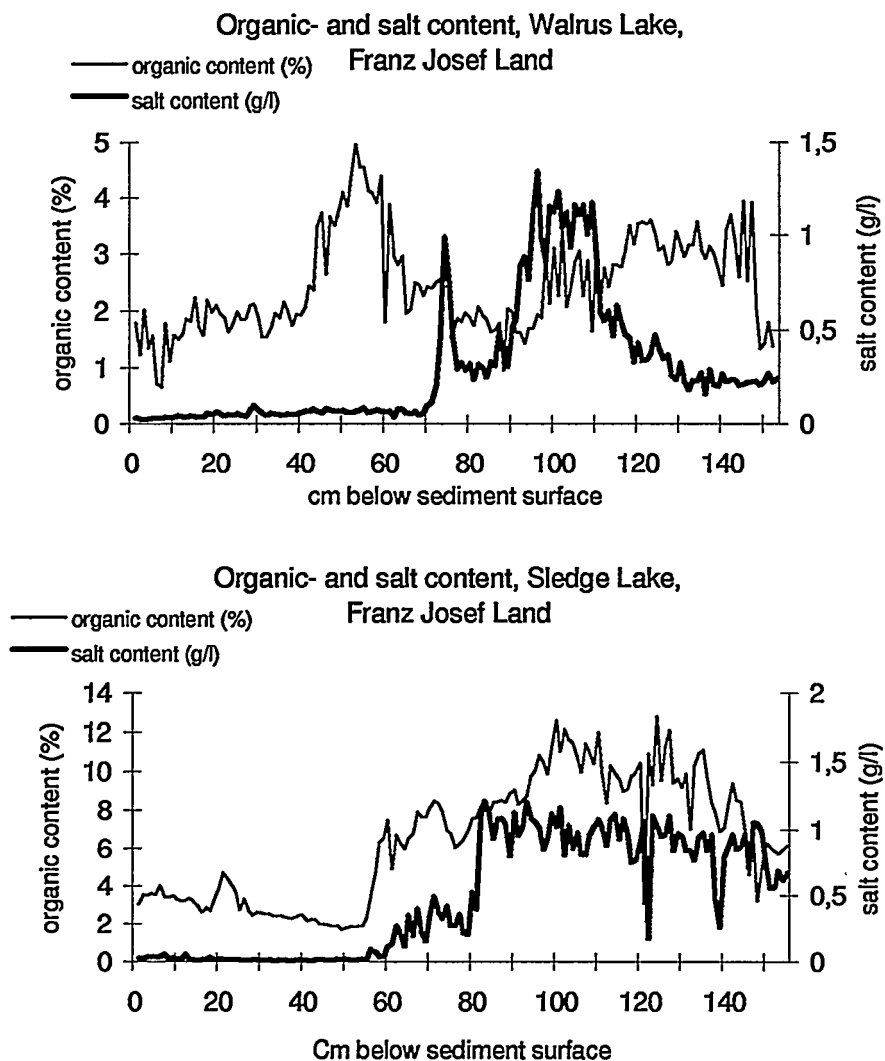
Figure 2. Organic and salt content in Walrus Lake and Sledge Lake, Franz Josef Land

Discussion

We have interpreted salt content variations in the sediments of Walrus Lake to signify variations in meltwater input to the Barents- and Kara sea region. Low values in salt content in the lower section of the Walrus Lake core indicate a high fresh water input from a nearby melting Barents ice-sheet, creating a freshwater lid in the Barents Sea. The diatom flora in this section indicates a slightly brackish-water environment. The subsequent slow increase in salt content is interpreted to be a result of a diminishing meltwater input from vanishing ice sheets or possibly a colder climate with decreased melt rates. At 112 cm below the sediment surface, a sharp increase in salt content indicates that the meltwater input from the large ice sheets had stopped and that subsequent variations are due to variations in melt water input in Dezhnev Bay from local glaciers (Fig. 1). The sharp drop in salt content after 97 cm marks the onset of isolation, *i.e.* a "lagoonal stage" with low salt values. The short but significant increase in salt content between 77-72 cm reinforces an earlier inference for a mid-Holocene transgression (Näslund *et al.,* 1994) that occurred around 6800 years BP. The final isolation of Walrus Lake took place at about 5950 years BP at 70 cm.

If our inferences on regional ice decay, reflected in the Walrus Lake sediments, are correct, one could expect to obtain a similar stratigraphy from nearby lakes. However, analyses from Sledge Lake reveal a marked absence of major paleosalinity variations in the marine section of the core and no salinity peak relating to the transgression prior to 5950 years BP. Because the melt water release resulted in a less saline upper layer of the sea water, we believe that, in early Holocene time, Sledge Lake was located at a depth greater than the mixing depth of the meltwater. Evidence for the transgression is not found due to the same reason. In Sledge lake, the sharp drop in salt content at 82 cm marks the transition from the marine to the lagoonal stage. The final isolation of this lake occurred at 56 cm around 3950 years BP.

Conclusion

We suggest that lake sediments below the highest marine limit from Franz Josef Land can provide useful information on deglaciation. Variations in the salt content of Walrus Lake can be interpreted as variations in the meltwater input to the Dezhnev Bay and the Barents Sea from ice sheets in the vicinity. The location of Franz Josef Land, on the edge of the postulated Barents Sea and Kara Sea ice sheets possibly indicates that results from this study apply to the decay of this ice. One major problem is the establishment of a reliable radiocarbon-dated chronology. However, based on primitive principles, we tentatively suggest that the obtained sediment sequences span up to 13000 years, and probably represent most of the time since deglaciation in that region.

References

Blake, W., Jr. 1961. Radiocarbon dating of raised beaches in Nordaustlandet, Spitsbergen. Gilbert O. Raasch (ed.). Geology of the Arctic. Proceedings of the First International Symposium on Arctic Geology. University of Toronto Press: 133-145.

Forman, S. L., Snyder, J., Miller, G. H., Lubinski, D., Matishov, G. G., Korsun, S. and Myslivets, V. 1992. Late Weichselian glaciation and deglaciation of Franz Josef Land, Russia. Abstract. Annual Meeting of the Geological Society of America, Abstracts with Programs: A346.

Glazovskiy, A., Näslund, J.-O. and Zale, R. 1992. Deglaciation and shoreline displacement on Alexandra Land, Franz Josef Land. Geografiska Annaler, 74A (4): 283-293.

Grosswald, M. G., Krenke, A. N., Vinograd, O. N., Markin, V. A. Psareva, T. V., Razumeyko, N. G. and Sukhodrovskiy, V. L. 1973. The glaciation of Franz Josef Land. Nauka Publishing House, Moscow: 352 pp.

Hyvärinen, H. 1968. Late-Quaternary sediment cores from lakes on Björnöya. Geografiska Annaler, 50A: 235-244.

Lehman, S. J. and Keigwin, L. D. 1992a. Deep circulation revisited. Nature, 358: 197-198.

Lehman, S. J. and Keigwin, L. D. 1992b. Sudden changes in North Atlantic circulation during the last glaciation. Nature, 356: 757-762.

Lehman, S. J and Forman, S. L. 1987. Glacier extent and sea level variation during the Late Weichselian on northwest Spitsbergen. Polar Research 5 n.s.: 271-272.

Miller, G. H., Sejrup, H. P., Lehman, S. J. and Forman, S. L. 1987. The last glacial-interglacial cycle, western Spitsbergen, Svalbard archipelago. Polar Research 5 n.s.: 279-280.

Näslund, J.-O., Zale, R. and Glazovskiy, A. 1994. The mid Holocene transgression on Alexandra Land, Franz Josef Land, Russia. Geografiska Annaler, 76A (1-2): 97-101.

Salvigsen, O. and Österholm, H. 1982. Radiocarbon date raised beaches and glacial history of the northern coast of Spitsbergen, Svalbard. Polar Research, No. 1: 97-115.

Salvigsen, O., Elgersma, A. and Landvik, J. Y. 1991. Radiocarbon dated raised beaches in northwestern Wedel Jarlsberg land, Spitsbergen, Svalbard. In J. Repelewska-Pekalowa & K. Pekala (Eds.): Polar Session. Arctic Environment Research. Institute of Earth Sciences, Marie Curie-Sklodowska University. Lublin: 316 pp.

Salvigsen, O. and Elgersma, A. 1993. Radiocarbon dating of deglaciation and raised beaches in the north-western Sörkapp land, Spitsbergen, Svalbard. Prace Geograficzne z. 94. Zeszyty Naukowe Uniwerytetu Jagiellonskiego: 39-48.

Sedimentary chironomids as indicators of climatically induced changes in deep Finnish lakes

Virpi Marttila and Jarmo J. Meriläinen

Institute for Environmental Research, University of Jyväskylä, P.O.Box 35, FIN 40351 Jyväskylä, Finland

Introduction

Chironomid head capsules are usually present at high abundances in lake sediments. Chironomids are sensitive for changes in profundal conditions and a number of studies made in deep, stratified lakes (Wiederholm 1980, Meriläinen 1987, Meriläinen & Hamina 1993a) have shown the information value of chironomids for interpreting the biological and developmental changes in a lake.

These results are mainly based on the Holocene record of Lake Päijänne and the short core sediment samples of few lakes in Saimaa lake complex. The 720 cm long core sample from the Ristiselkä basin of Lake Päijänne at a depth of 73 m was dated by paleomagnetic and radiocarbon methods. In order to interpret the changes in the lake basin and its catchment area, sedimentary pollen, diatom, chironomid and chemical analysis were performed as described in Itkonen et al. (in press). The recent eutrophication history of Lake Päijänne is described in Meriläinen & Hamina (1993a).

Results and discussion

The abundance and influx of chironomid head capsules was low in the oldest studied sample in Lake Päijänne core dated c. 7500 BP (8200 cal BP) (Fig. 1). After that the influx began to increase and reached its maximum about 6700-5700 BP (7500-6500 cal BP), which corresponds the end of Ancient Lake Päijänne phase. The mean abundance of individuals could be assessed to be considerably higher than the present mean abundance in the profundal area. According to this the profundal area was productive 6700-5700 BP, but that kind of changes, which could imply to the shifts in the trophic level of the lake did not occur. *Heterotrissocladius subpilosus*, typical species living in the large, oligotrophic boreal lakes, dominated accounting c. 50% of the head capsules. The Holocene climatic optimum has been reached nearly simultaneously to the termination of the transgression c. 6000-5000 BP, which complicates the interpretations of climatic responses. The high accumulation rate of chironomids, biogenic silica and

organic carbon supports the idea of high bioproductivity however. The yearly growing season was long due to light and warm springs but the net organic sedimentation remained low, under 50 g $m^{-2}a^{-1}$. The critical value of organic sedimentation for *Heterotrissocladius subpilosus* was 50 g $m^{-2}a^{-1}$ both in northern Lake Päijänne and in Lake Haukivesi in Saimaa lake complex. The species disappears when the organic sedimentation exceeds this rate and *Sergentia coracina* displaces it (Meriläinen & Hamina 1993a, Marttila & Meriläinen unpubl.)
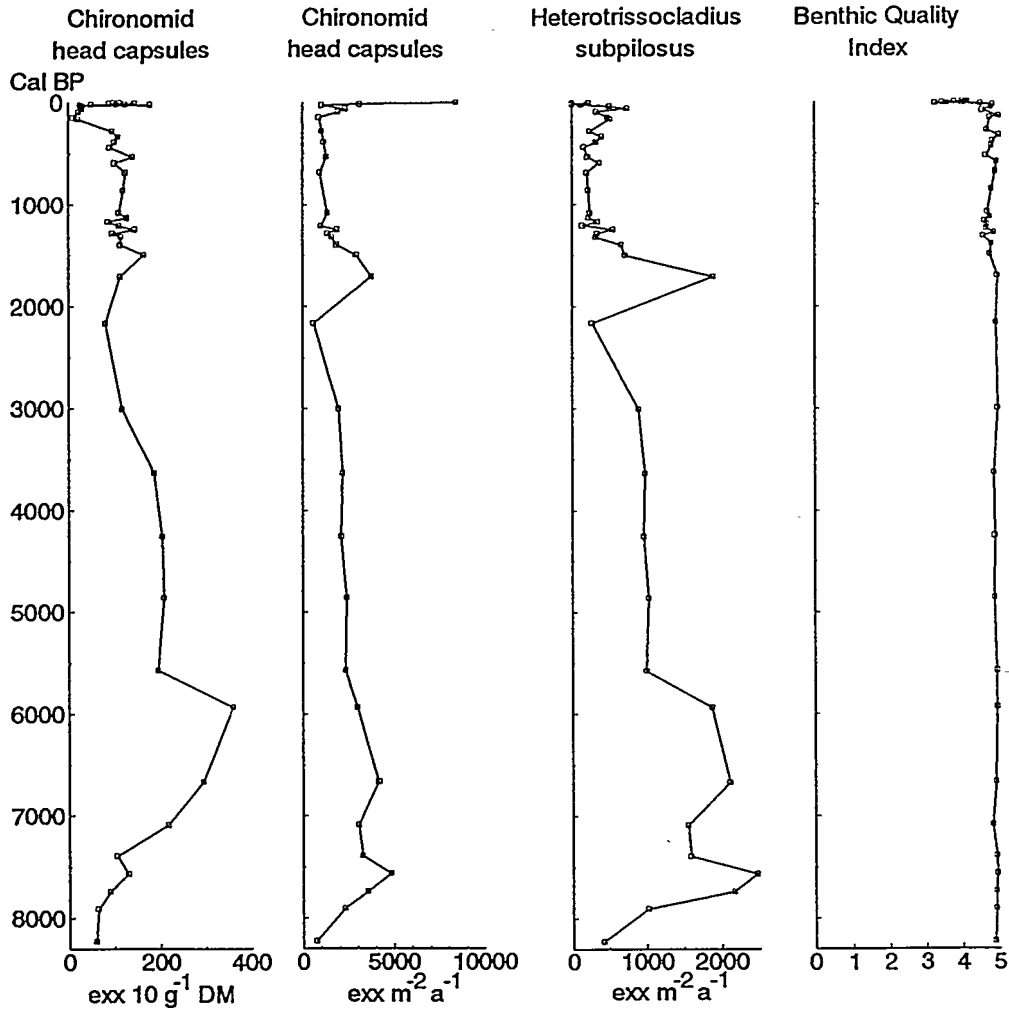
Fig. 1. Characteristics of subfossil chironomid assemblages and the Benthic Quality Index showing the biological condition of the profundal area of the Lake Päijänne during the Holocene (0-7500 BP, 0-8200 cal BP).

Ancient Lake Päijänne phase was followed by a stable period in the chironomid succession 5300-3300 BP (6000-3500 cal BP). The influx of head capsules and the accumulation of biogenic silica into the sediment slightly decreased but in the whole there were no distinct changes during this period.

In the sample dated around 2200 BP (2200 cal BP) the influx of chironomids was at its lowest during the Holocene. According to Eronen et al. (1992) the instability of climate might have been great c. 2500 BP. This or cooler and more humid climate prevailing over large areas at that time as showed by many proxy data might have decreased the production of profundal areas. After that the influx increased and was high 1800-1600 BP (1700-1500 cal BP). After 1600 BP it decreased again and remained low until the last decades. The influx of littoral fauna exceeded the influx of profundal fauna after 1600 BP in Ristiselkä. The proportion of the epiphytic diatom flora was high and the mineral matter of the sediment became more coarse. These changes could imply to increased erosion and changes in the lake water level. The human activity in the catchment area could also affect to observed changes.

The most distinct changes in Ristiselkä have occurred during the last 30 years as a result of waste water. *Heterotrissocladius subpilosus* was replaced by *Sergentia coracina* and the Benthic Quality Index (BQI) (Wiederholm 1980) which was near to its maximum values almost the whole Holocene reached its minimum value, 3.25, based on the subfossil assemblages, at the beginning of 1970's (Fig. 1). The sedimentation of organic matter reached its maximum, 113-155 g $m^{-2}a^{-1}$ in 1972-1975.

Itkonen & Salonen (1994) found significant positive correlation between annual sediment varve thickness and temperature in Lake Päijänne but according to the chironomid data the climatically induced changes in the profundal conditions were small in Ristiselkä. The observations made in Lake Puruvesi (in Saimaa) where the volume of the hypolimnion is small relative to that of the trophogenic layer showed that the natural changes in biological conditions in the profundal zone of a lake can be fairly high and can complicate the assessment of human interference in such rather shallow lakes (Meriläinen 1992, Meriläinen & Hamina 1992). Thick trophogenic layer leads to relatively abundant sedimentation of organic matter in Lake Puruvesi and this results in fairly high oxygen consumption in the hypolimnion as the organic matter mineralizes and explains the low hypolimnetic oxygen values in winter. According to Meriläinen (1992) oxygen saturation in this layer in winter is greatly affected by the hypolimnetic temperature, which explained 50% of the observed variation in Lake Puruvesi. The hypolimnetic temperature in winter is in turn highly affected by the weather condition prevailing, before the freezing of the lake.

References

Eronen, M., Zetterberg, P. & Lindholm, M. 1994. Climate history from tree rings in the subarctic area of Fennoscandia. Julkaisussa: Kanninen, M. & Heikinheimo, P. (toim.), The Finnish Research Programme on Climate Change. Publications of the Academy of Finland 1/94, 13-19.

Itkonen, A., Marttila, V., Eriksson, B., Grönlund, T., Ilmasti, M., Kankainen, T., Saarinen, T., Meriläinen, J.J. & Salonen, V.-P. 1995. Päijänteen Ristiselän jääkauden jälkeinen kehitys (Abstract: Holocene development of Lake Päijänne ecosystem). Geological Survey of Finland, Report of Investigation (in press).

Itkonen, A. & Salonen, V.-P. 1994. The response of sedimentation in three varved lacustrine sequences to air temperature, precipitation and human impact. J. Paleolimnol. 11: 323-332

Meriläinen, J.J., 1987. The profundal zoobenthos used as an indicator of the biological condition of Lake Päijänne. Biol. Res. Rep. Univ. Jyväskylä 10:87-94.

Meriläinen, J.J. 1992. Niukkaravinteinen, kirkas Puruvesi tuottaa mesotrofisen järven profundaalifaunan (Abstract:Lake Puruvesi - a nutrient poor, clear-water lake with a profundal benthos typical of a mesotrophic lake). University of Joensuu, Publications of Karelian Institute 103:109-116.

Meriläinen, J.J. & Hamina, V. 1993a. Recent environmental history of a large, originally oligotrophic lake in Finland: A palaeolimnological study of chironomid remains. J. Paleolimnol. 9: 129-140.

Meriläinen, J.J. & Hamina, V. 1993b. Changes in biological condition of the profundal area in an unpolluted, nutrient-poor lake during the past 400 years. Verh. Internat. Verein. Limnol. 25: 1079-1081.

Wiederholm, T. 1980. Use of benthos in lake monitoring. J. Wat. Pollut. Cont. Fed. 52: 537-547.

The substantiation of various hierarchical climatic processes in the composition and structure of lake and mire sediment profiles

Jaan-Mati Punning

Institute of Ecology, Estonian Academy of Sciences
Kevade 2,EE0001 Tallinn,Estonia

Introduction

The most widely used paleoecological indicators are peat and lacustrine sediment profiles. Their composition and structure are primarily determined by variances in the physical environment. Based on geochemical and paleobiological data from sediment profiles, it is possible, in principal, to reconstruct the paleogeographical conditions related to certain past temporal-spatial systems.

A great deal of study has been devoted to the interpretation of paleoecological data in an attempt to determine past environmental conditions (Aaby 1976, Berglund 1986, Delcourt & Delcourt 1985, Chamber 1993). It has been shown that in general, it is not possible to demonstrate cause and effect relationships between exogenous environmental factors and past ecosystem changes. This is as a result of the environmental variability of time and space factors related to the ecosystems and the impact of the physical environment. These variabilities have been greatly determined by the multihierarchical characteristics of exogenous factors, such as climate, as well as anthropogenic and physico-biological consideration. The success of interpreting paleoecological data is dependent upon the analyst's ability to separate climatic and non-climatic factors for a given effect.

As the development of landscapes varies over time and space, the sequence in which sediments are formed in a particular landscape unit will be determined by the different geographical spatial-temporal systems (Delcourt & Delcourt 1988). As a consequence these systems have been influenced by a wide range of external forces and their ability to adapt may differ greatly. It is therefore to neccessary interpret not only the

paleogeographic information (geochemical, paleobiological, isotopic etc), obtained by study the sediments, but also to examine the entire sequence.

This paper presents a number examples that to demonstrate the complications arising from the interpretation of paleoclimatic data due to the spatial development of landscapes.

Results and discussions

Microclimatic studies that have been carried out in deep-sloped contemporary landscape formations (Rikkinen 1989), indicate the essential deviations of falling radiation on the different slopes and the importance that an influx of cold air to the hole what might cause. A decrease in temperature from 4-8oC can occur at the bottom of a depression as compared with the surrounding areas.

Our comprehensive palaeoecological study of a 17 m deep peat profile in the kettle-hole in Haanja Heights in SE Estonia (Punning et al 1995) demonstrated that the temporal distribution of falling radiation on the surface of filling-up the kettle-hole organic sediments is variable, especially during the initial stage of formation of organeous deposits. The difference between the radiation falling on different slopes at the bottom of the studied kettle-hole are comparable to the total radiation during one spring or autumn month. It must be mentioned that the analysis above concerns only variations of the solar radiation and does not account such additional factors as changes in the formation, melting of the snow cover in the kettle-hole, suffusion of cold air and other impacts.

The impact of the microclimatic conditions on vegetation growth in the small depressions, particularly the early formation of vegetation, was remarkable and increased in course of filling-up the depression.

Many of the factors affecting the structure of landscapes such as the vertical movements of the Earth's surface, changes in hydrological regime, paludification etc. can cause changes in the spatial structure of landscapes over time. Our detailed investigations in Kurtna Kame Field (NE Estonia) with its jointed relief and numerous glaciokarstic depressions demonstrated the importance of obtaining paleogeographic information from the general structure of landscapes (Punning 1994).

In order to study the influence of the development of landscapes the formation of the pollen spectra are the most widely used paleoclimatic indicators. The lake and mire sediment cores were analysed, and changes in the sizes of studied lakes and mires during the Holocene period reconstructed. Data demonstrates that an expansion of the mires and lakes was significant and the spatial extent differs greatly in different objects. These changes in the area covered by lakes or mires will increase the distance between the tree stand and the site studied now.

Using the pollen data obtained by T.Koff (1994) it is possible to assess the relationships between the maximum values of the AP pollen sum and the sizes of the studied lakes and mires in the corresponding time intervals. The data analysis show, that there are sharp changes in values of the pollen influxes if the sizes of the object studied are less than 200 m. This means that in the beginning of the Holocene when the sizes of studied objects were small , the dominant in pollen spectra was the impact of local pollen rain all over the area of studied landscape element(lake, mire). In the case of the expansion of lakes and mires in the central area the share of regional and even global influx will increase. It is therefore not correct to compare different parts of pollen diagrams as they basically reflect different non-climatic situations (Fig.1).
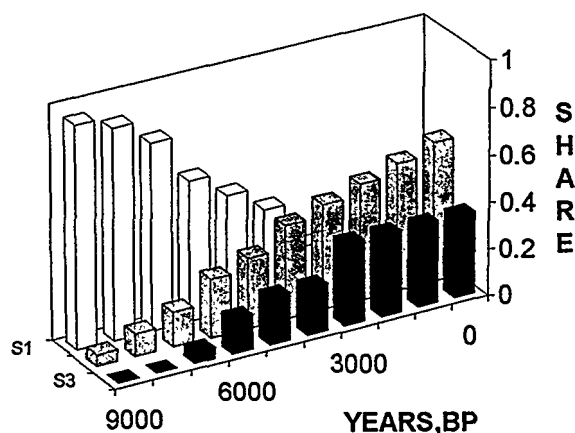
Fig.1.In course of spatial expansion of studied landscape the origin of atmospheric transported particles will change.S1-extralocal; S2-local; S3-regional factor.

The remarkable impact with development of landscape on paleoclimatic record in sediment cores is from quick uplifting small islands. Our study of the Island Naissaar (Gulf of Finland), which emerged from sea 7500-7700 BP show that the spatio-temporal regularities of extension of terrestrial area have a direct influence on the development of vegetation there. Similarity of pollen content during the first stages of development at the studied mire, about 7000-5000 BP, with present one on coastal areas in northern and western Estonia demonstrate clearly, that climatic conditions did not play the primary role on the forming of pioneer vegetation on the open coastal areas. The divergence of open coast from the studied site in course of emergence the land, development of soils and their wetness might be the reasons of development of the mixed forest around the mire later. The spatial extent of mire leads to the supplementation of the desidous trees by coniferous one. Besides climatic factors, the formation of vegetation non-climatic factors have dominance. Here one must account also that factors as the reaching pioneer flora, concurence and competition etc. In study of lake and bog sediments in the coastal areas and islands it must be accounted also the factor of terrestrialization and rapid changes in maritimity.

Conclusions

Due to the variability of landscapes some non-climatic factors will complicate the paleoclimatic interpretations of geochemical and paleobiological data obtained by study of lake and peat sediment cores. As the non-climatic factors change in course of development of the environmental conditions and landscapes, in the different parts of sediments in the same core samples, non-climatic factors differs so much that the interpretation of data needs more paleogeographic information.

In course of development of past studied landscapes, the adaptation ability of ecosystems will change and lead to the changes in the sensitivity of ecosystem to the impact of climatic factors e.g.to the changes in the cause-consequencial relationships.

References

Aaby, B. 1976. Cyclic climatic variations in climate over the last 5500 years reflected in raised bogs. Nature 263:281-284.

Berglund, B.E.(ed.). 1986. Handbook of Holocene palaeoecology and palaeohydrology. John Wiley & Sons,New-York, 869p.

Chambers, F.M.(ed). 1993. Climate change and human impact on the landscapes. Chapman & Hall, London, 303p.

Delcourt, H.R. & Delcourt, P.A. 1985. Comparison of taxon calibrations, modern analogue techniques, and forest-stand simulation models for the quantitative reconstruction of past vegetation. Earth Surf. Proc. Landforms !0:293--304.

Delcourt, H.R. & Delcourt, P.A. 1988. Quaternary landscape ecology: relevant scales in space and time. Landscape ecology 2:23-44.

Koff, T. 1994. The development of vegetation. In: J.-M.Punning(ed).The influence of natural and anthropogenic factors on the development of landscapes. Inst. of Ecology, Publ.2, Tallinn:24-57.

Punning, J.-M. 1994(ed.). The influence of natural and anthropogenic factors on the development of landscapes. Inst.of Ecology, Publ.2, Tallinn:227p.

Punning, J.-M., Koff, T., Ilomets, M., Jôgi, J. 1995. On the influence of multihierarchic factors on organogenic sedimentation in the Vällamäe kettle hole, Estonia. Boreas:1.

Palaeoclimatic interpretation of the Holocene litho- and biostratigraphic proxy data from Estonia

Leili Saarse, Atko Heinsalu and Siim Veski

Institute of Geology, Estonian Academy of Sciences,
7 Estonia Ave, EE0100, Tallinn, Estonia

Introduction

Lakes respond to fluctuations in the local hydrologic balance by changing in depth and area (Saarse, Harrison 1992). Records of these changes are commonly printed in sediment lithology, biological remains and/or shorelines. Lake-level fluctuations provide information on trophic stage and productivity changes in lakes and serve as an useful tool for the moisture balance control. Changes in lake level may be caused by climatic or non-climatic factors (tectonic, karst phenomena, changes in basin morphometry and hydrology or human activities; Harrison et al. 1991). But regionally synchronous changes argue strongly for climatic control. These climatically-induced changes could last from annual to millennial time scale.

For reconstructing lake-level fluctuation Digerfeldt (1986, 1988) recommends to use transects of cores of relatively small lakes (100 ha) and mostly relay on three lines of evidence: changes in sediment composition, the position of sediment limit and the distribution of aquatic vegetation recorded by macrofossil and pollen analyses. This method is time-consuming and thus has been used only at a few sites in Europe.

Our lake level reconstructions are based on single cores, combining several lines of evidence, as sediment lithology, aquatic pollen, plant macrofossils, molluscs and diatom records (if available). Such approach yields estimation of relative long-term regional trend in lake levels in spite of several limitations (Harrison et al. 1991; Saarse, Harrison 1992). It is not appropriate for a shallow infilling and overgrown basins which uppermost sequence lithological and biostratigraphic proxy data commonly point to the low lake level and thus shadow the real lake-level fluctuation trend.

Depending on the evidence available, lake-level fluctuations have been divided into 3-5 status categories and for each site the low water depth is recorded as 1. Afterwards these lake status categories have been grouped into three status classes: low, intermediate and high. The class "high" corresponds to the upper quartile and "low" to the lower quartile of lake record during the entier period coded. Such approach was used in the lake-level data base documentation (Tarasov et al. 1994) and enables to compare our data set with that of the other regions (Street-Perrott et al. 1989).

Results and discussion

Ten sequences (among those 3 overgrown basins) from Estonia have been used for lake-level (Harrison et al. 1991; Saarse & Harrison 1992; Tarasov et al. 1994) and past climatic reconstructions (Harrison et al. 1993). In the present report we eliminated all the overgrown basins and made reconstructions   on 6 new lacustrine cores. The results of lake-level fluctuations based on 12 lakes (Ermistu, Maardu, Järveotsa, Kaali, Karujärv, Kirikumäe, Punso, Päidre, Raigastvere, Tõhela, Äntu Sinijärv, and Ülemiste) are presented in Figure. The most pronounced lake-level lowering occurred about 9000-8000 and 4000-3500 yr BP with a less significant lowering around 7000 and 2500 yr BP. The similar two low-water periods are traceabe on the lake-level record from southern Sweden, the first between 9000-8500 yr BP, and the second 2500-2500 yr BP (Digerfeldt, 1988). The high water stand in Estonian lakes occurred about 9500, 7000, 4500, 3000 yr BP and during the present. In southern Sweden high lake- levels appeared 10000, 6500 yr BP and at present (Digerfeldt, 1988), whereas the magnitude of changes was greatest during the Early Holocene (Figure).
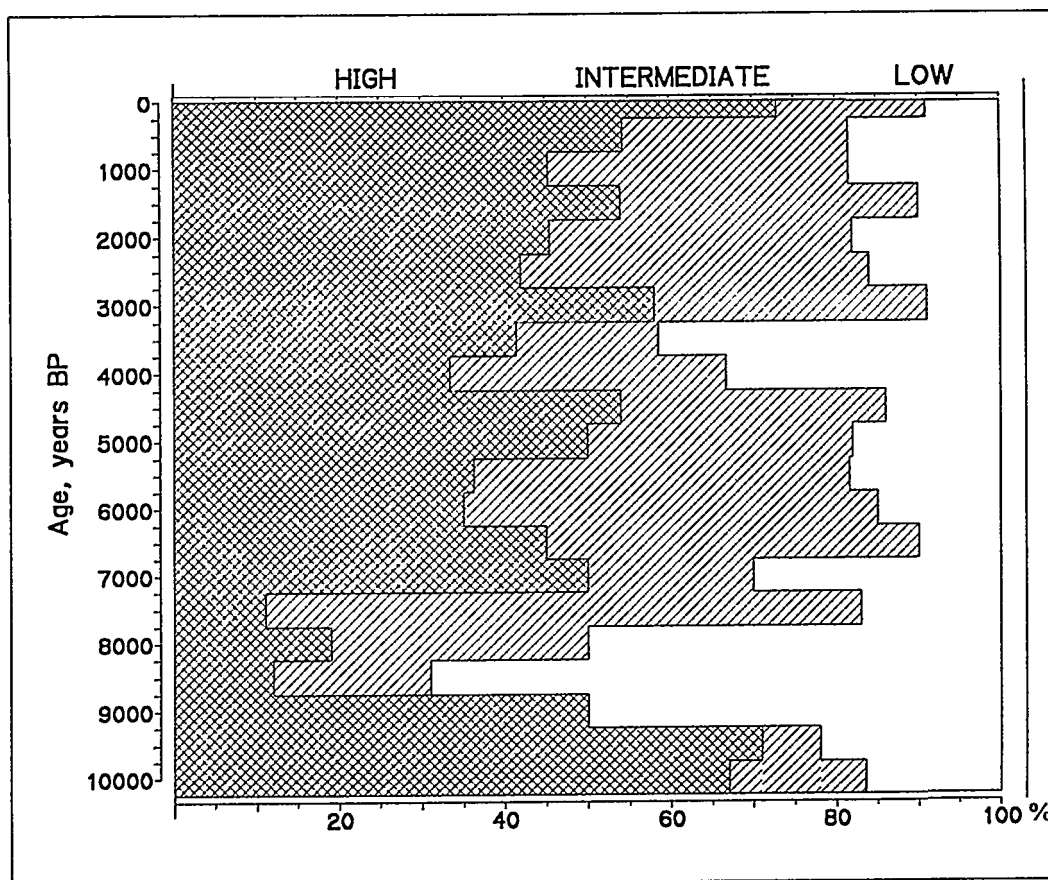
Figure. Relative lake-level changes during the last 10,000 yr BP in Estonia.

Comparision of our results with the pollen-based climatic reconstructions made by J. Guiot on three Estonian sequences reveals that the high lake-level at about 9500 yr BP was caused by low evapotranspiration (July temperature only 14.7 °C, mean annual precipitation value 460 mm/yr^{-1}). The major lake level lowering 1000 years later (8500 yr BP) has almost the same background. Both July and annual temperatures as well as precipitation value rapidly increased, but the potential evapotranspiration was not fully compensated by the latter one. Low lake level between 7000-8000 yr BP is essential, as the precipitation value was almost the same as at present, but July and annual temperatures were considerably higher. The climatic reconstructions do not give the unequivocal answer to the lake-level fluctuations between 6500-7000 yr BP. The amount of precipitation close that at present, and almost 1 °C higher July temperature should have induced low, not high-lake level stand, as it was suggested by GCM experiments (Kutzbach, Guetter, 1986).

The constant decrease in precipitation and increase in July temperature is consistent with low lake level 3500-4000 yr BP, but do not explain the slight lake-level rise around 4500 yr BP. The fluctuations around 1500 and 1000 yr BP and at present are in good accordance with the palaeoclimatic parameters.

Lake-level based reconstruction shows the wetter conditions 9500, 7000, 4000, 3000 yr BP and at present and drier conditions 8500 and 4000 yr BP in Estonia. The lake-level records, left after elimination of overgrown basins, suggest that during the Late Holocene the water level was high not intermediate as presented in our earlier reconstructions (Saarse, Harrison 1992).

In general, the results induced from the lake-level records are consistent with the pollen-based palaeoclimatic data. The descrepancy between the different trends in the middle Holocene needs a plausible explanation in the future.

References

Digerfeldt, G. 1986. Studies on past lake-level fluctuations. In: Berglund B.E. (ed), Handbook of Holocene Palaeoecology and palaeohydrology. John Wiley, Chichester, 127-143.

Digerfeldt, G. 1988. Reconstruction and regional correlation of Holocene lake-level fluctuations in Lake Bysjön, South Sweden. Boreas 17:165-182.

Harrison, S.P., Prentice I.C., Guiot, J. 1993. Climatic controls on Holocene lake-level changes in Europe. Climatic Dynamics 8:189-200.

Harrison, S.P., Saarse, L., Digerfeldt, G. 1991. Holocene changes in lake level as climate proxydata in Europe. Paläoklimaforschung 6:159-170.

Kutzbach J.E., Guetter P.J. 1986. The influence of changing orbital parameters and surface boundary conditions on climate simulations for the past 18 000 years. J. Atmos. Sci. 43:1726-1759.

Saarse, L., Harrison, S.P. 1992. Holocene lake-level changes in the eastern Baltic region. In: Estonia. Man and Nature. Estonian Geographical Society. Tallinn, 6-20

Street-Perrott F.A., Harrison, S.P. 1985. Lake levels and climatic reconstructions. In: Hecht A.D. (ed), Palaeoclimate analysis and modeling. John Wiley, New York, 291-340.

Street-Perrott, F.A., Marchand, D.S., Roberts, N., Harrison, S.P. 1989. Global lake-level variations from 18,000 to 0 years ago: a palaeoclimatic analysis. U.S. Department of Energy, Technical Report.

Tarasov, P.E., Harrison, S.P., Saarse, L. et al. 1994. Lake Status records from the Former Soviet Union and Mongolia:Data Base Documentation. Boulder, Colorado.

The relationship between Holocene fire frequencies and climatic changes in Finland

Kaarina Sarmaja-Korjonen

Division of Geology and Palaeontology, University of Helsinki
P.O. Box 11, FIN-00014 University of Helsinki, Finland

This paper provides preliminary results of a study examining the relationship between forest fire frequencies and periods of climatic change during early and middle Holocene in Finland. Microscopic charcoal analysis and fire studies have been mainly concentrated on problems concerning the use of fire to clear forested areas during the last three thousand years (e.g. Tolonen 1978, Huttunen 1980). Not much is known about the role of fire in the untouched forests before the onset of agriculture. The changes of climate, the alternating dry and moist periods (where they cool or warm? what was the relationship between precipitation and evaporation?) may have affected the lake-levels and burning cycles of the forests.

To be able to measure the actual fire frequences high-resolution studies (sample thickness of a couple of millimetres) are needed so that years between fires can be estimated. Before a section can be chosen for high-resolution studies a "basic analysis" (sensu Sarmaja-Korjonen 1992), with sample thickness of some centimetres, is needed to get a background to more specific analyses. It can also give a general picture of the commonness of forest fires during the Holocene even though individual fires cannot be distinguished. This paper shows four examples of "basic analyses" and what is known about lake-level and fire history in Finland (Fig. 1).

Lapland, NW Finland

Hyvärinen & Alhonen (1994) studied two lakes from western Lapland and found a dry period about 8000-6000 BP when one of the lakes, Jierstivaara, may have been almost dry. This was shown both by the cladoceran plankton/littoral relation and the diatom composition; the pollen composition also showed signs of a dry period (Mäkelä et al. 1994). The amount of charcoal particles was exceptionally low during the Holocene. The sediment section representing the dry period was also studied more closely (1 cm interval) and no variation in the amount of charcoal (charcoal area) was found with the exception of one peak, during the period 8200-4500 BP. Thus fires must have been

very rare in the area and the role of fire may not have been important in the birch-pine forests above the present coniferous tree line.

Fig. 1. Location of the study sites discussed in text. 1. Lake Jierstivaara, 2. Lake Ylimmäinen Kuivajärvi, 3. Lake Etu-Mustajärvi, 4. Lake Iso Lehmälampi.

Kuusamo, NE Finland

From Kuusamo district Lake Ylimmäinen Kuivajärvi was studied for stable isotopes, pollen and charcoal (Korjonen & Sarmaja-Korjonen, in prep.). Results of the water-level studies are not yet available. The pollen analysis showed a development of vegetation typical to NE Finland: pioneer birch forests followed by the dominance of pine, the middle Holocene reflected by birch, pine and alder, and at last, the arrival of spruce about 5000 BP. The charcoal values were very low as in Lapland, and suggest that fires were very rare throughout the Holocene. Exceptionally low values were found between 5000 BP and 2000 BP. The increasing charcoal after 2000 BP may be caused by human activities.

Lammi area, S Finland

Lake Etu-Mustajärvi was studied for pollen and charcoal (Sarmaja-Korjonen 1995); but, no high-resolution analyses are available. The charcoal record can be divided into four periods: 1) small values in the earliest Holocene, 2) a maximum from about 8500 to 6000 BP, 3) smaller values from about 6000 to 4000 BP, 4) after that values rising towards modern times. An identical behavior of charcoal curve was found from Lake Lamminjärvi in the same parish (Tolonen 1980). Results from Lake Työtjärvi, some 20 km west, showed high water-level from about 8000 BP until a dry period about 6000 BP (Donner et al. 1978). The charcoal maximum (8500-6000 BP) coincides with high water-levels known also from southern Sweden (Digerfeldt 1988, Harrison & Digerfeldt 1993), and disagreed with the common concept "moist period-less fires". The final rise of charcoal towards modern times can be connected to human activities (Tolonen 1978).

Vihti area, S Finland

From Vihti a small lake, Iso Lehmälampi, is being studied (Sarmaja-Korjonen & Alhonen, in prep.) with both basic and high-resolution analyses (pollen, diatoms, Cladocera). The preliminary results of the basic analyses show that the lake has experienced at least two periods of low water in the beginning of the Atlantic chronozone (Mangerud et al. 1974). During the low-water periods *Bryales* peat was formed in the deepest part of the lake (nowadays 8 m deep). The water-level began to rise towards the end of the Atlantic. The charcoal values were high during the treeless stage in the early Holocene; but, stayed low during the Boreal and Atlantic chronozones. The charcoal area increased at the same time when other data suggested rising water-level.

Discussion

The examples above suggest that the relationship between climatic changes and fire has been different in southern and northern Finland. In Lapland and Kuusamo the low charcoal values point to the lesser importance or frequent fires in northern forest ecosystems - even dry periods seem not to have increased fires. In southern Finland fires occurred more often according to the larger amounts of charcoal. Periods of lower and higher values succeed each other clearly. The relationship of forest fire frequency to climatic variation and changes in water-level cannot be determined yet until more precise data are available. It is not entirely ruled out, however, that easier transportation of charcoal through surface runoff may have caused the higher amounts of charcoal during a period of increased precipitation and high water-levels.

Acknowledgements

References

Digerfeldt, G. 1988. Reconstruction and regional correlation of Holocene lake-level fluctuations in Lake Bysjön, South Sweden. Boreas 17:165-182.

Donner, J., Alhonen, P., Eronen, M., Jungner, H. & Vuorela, I. 1978. Biostratigraphy and radiocarbon dating of the Holocene lake sediments of Työtjärvi and the peats in the adjoining bog Varrassuo west of Lahti in southern Finland. Annales Botanici Fennici 15:258-280.

Harrison, S.P. & Digerfeldt, G. 1993. European lakes as palaeohydrological and palaeoclimatic indicators. Quaternary Science Reviews 12:233-248.

Huttunen, P. 1980. Early land use, especially the slash-and-burn cultivation in the commune of Lammi, southern Finland, interpreted mainly using pollen and charcoal analyses. Acta Botanica Fennica 113:1-45.

Hyvärinen, H. & Alhonen, P. 1994. Holocene lake-level changes in the Fennoscandian tree-line region, western Finnish Lapland: diatom and cladoceran evidence. The Holocene 4:251-258.

Mangerud, J., Andersen, S.T., Berglund B.E. & Donner, J.J. 1974. Quaternary stratigraphy of Norden, a proposal for terminology and classification. Boreas 3:109-128.

Mäkelä, E., Sarmaja-Korjonen, K. & Hyvärinen, H. 1994. Holocene forest history of the Pöyrisjärvi area north of the coniferous tree line in western Finnish Lapland: a pollen stratigraphical study. Bulletin of the Geological Society of Finland 66:81-94.

Sarmaja-Korjonen, K. 1992. Fine-interval pollen and charcoal analyses as tracers of early clearance periods in S Finland. Acta Botanica Fennica 146:1-75.

Sarmaja-Korjonen, K. 1995. Pollen and charcoal analyses from Lake Etu-Mustajärvi, southern Finland, with special reference to an early Holocene Urtica pollen maximum. Bulletin of the Geological Society of Finland 67:37-46.

Tolonen, M. 1978. Palaeoecology of annually laminated sediments in Lake Ahvenainen, S. Finland. I. Pollen and charcoal analyses and their relation to human impact. Annales Botanici Fennici 15:177-208.

Tolonen, M. 1980. Postglacial pollen stratigraphy of Lake Lamminjärvi, S Finland. Annales Botanici Fennici 17:15-25.
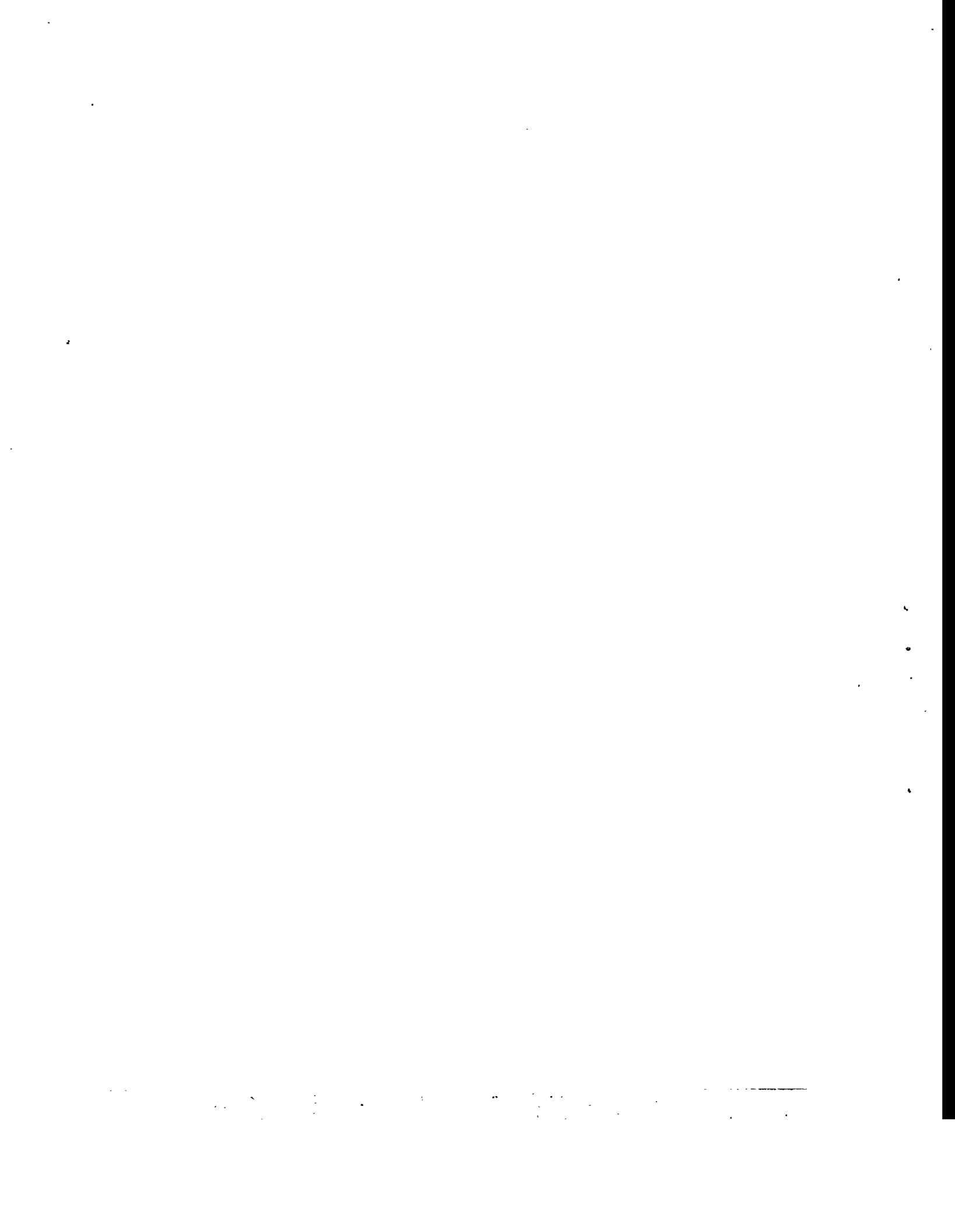
Tree rings
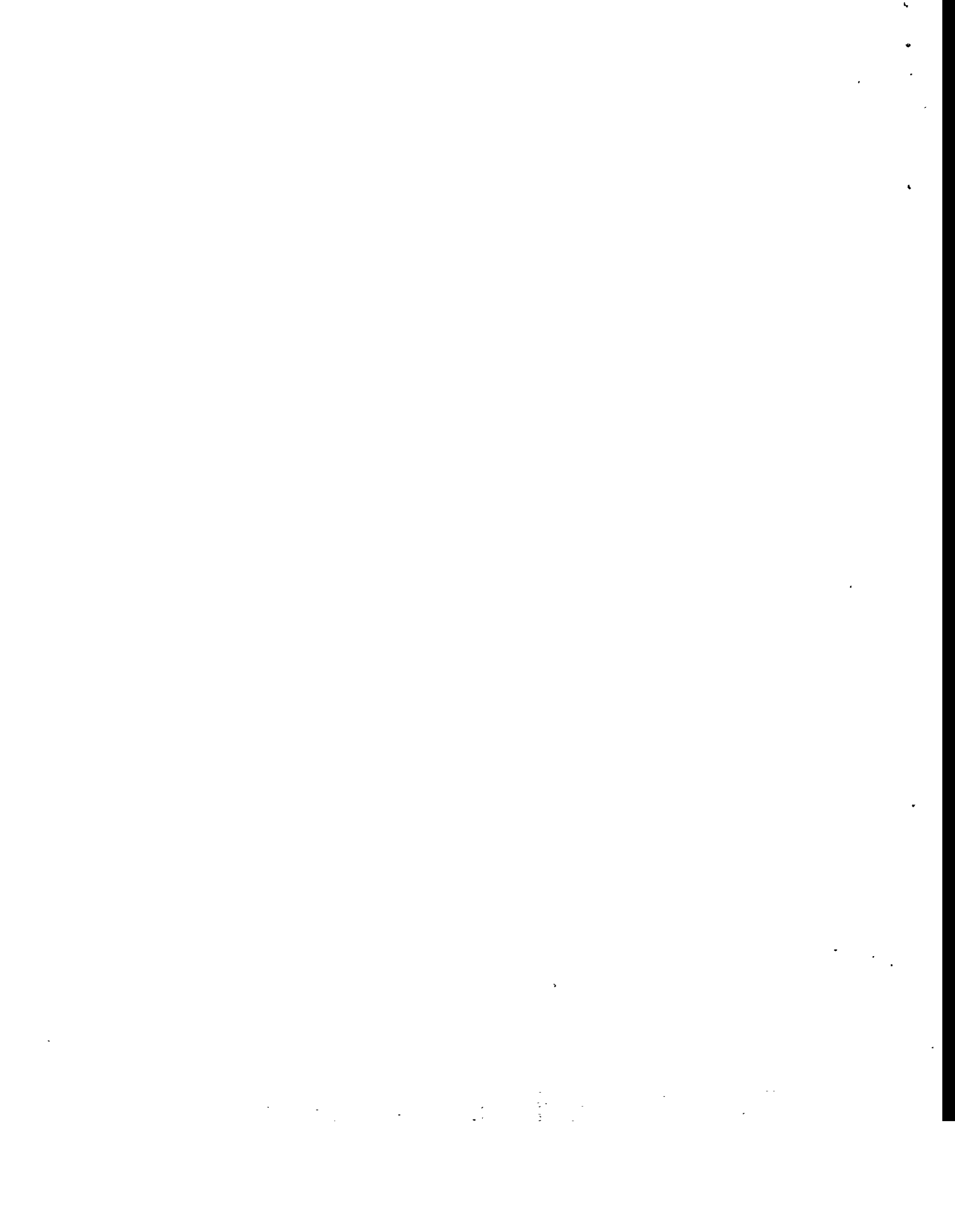
Testate amoebae (Protozoa, Testacea) of Russia and Canada as indicators of climatic changes in Holocene

Anatoly BOBROV
Department of Soil Science, Moscow State University
119899,Moscow, Russia

Rhizopod analysis has less than 100 years history. It has been described in detailes by K.Tolonen (1986). The works of Harnisch (1951), Grospietsch (1953), Tolonen (1966) made an appropriete contribution to the development of this method andits using in paleoclimatic reconstructions. Latter publications (Tolonen, Warner, Vasander, 1992, 1994) devoted to the ecology of Testate amoebae showed new opportunities of using of freswater amoebae as an index of climatic change in peatlands.But untill now this method has certain limits of its use. Such studies have not been carried out in Russia, in Canada they have been developed only in recent years (Warner,1987, Warner, Chmielewski, 1992).

During 1993-1994 samples from two canadian (Ontario) and one russian (north-eastern Siberia) were studing. The research has been carried out in Experimental Lakes Area, peatland 979, site North-East. Samples have been taken at 5 cm interval within upper 1 m layer and than at 10 cm interval on a depth 9 m. The age of peat samples at 9 m depth, asshown by radiocarbon age analysis, was 10 000 years. 150 species, varietes and forms of testate amoebae have been found.

Rhizopodium analysis allowed us to reveal several stages of testate amoebas community. The stage of large oligotrophic lake finished about 8500 years ago. A big species number of Difflugia, Centropyxis indicates aquic conditions of bogdevelopment with minerotrphic type of feeding. The limnic stage finished about 5500 years ago. The species richness of Difflugia genus reached its maximum at this period. This reflects continuing eutrophication of the lake. Intensive developpmentof Centropyxis genus took place at this period simultaneously with decreasing of species richness of Difflugia genus. Occurence of such sphagnophil species as Amphitrema wrigthianum, Heleopera sphagni, Hyalosphenia elegans, Assulina muscorum.werecharacteristic of this period. The early stage of swamp development accompanied by temporal increasing of hydromorphizm appr. 5000 years ago. Intensive development of sphagnofilous species occured appr. 4000 years ago. Only 2 species from Difflugia genus D.globulosa, D.globulus survived, wich are typical for upland bogs with small water areas. A wide representativety of Arcella, Trigonopyxis, Heleopera, Hyalosphenia, Nebela, Pseudodifflugia, Amphitrema

genuses marked the bog stage of ecosystem'sevolution. Simultaneous flushes of Assulina muscorum and Triginopyxis arcula taken place appr. 3500 and 2000 years ago may were due to xeromorphic conditions . Occurence of shells of Euglypha, Trinema, Nebela genuses in the upper layer indicates atthe tendency of the development of the ecosystem studied towards forest peat assosiations (Waldmoos according to Grospietsch).

Evolution of siberian bog has its own pecularities. More humid conditions in Holocene have been confirmed by discovering the reperesentatives of Difflugia genus such as D.elegans and urceolata -typical hydrophilous - at all depths of thecolumn. Profound poorness of species composition of Nebela, Euglypha, Heleopera genuses and wide species variety of Centropyxis genus may be regarded as another peculiarity of taxonomic composition. Lower temperatures in Siberia during Holoceneperiod may account for such a difference in regional faunas of Testate amoebaes, but this suggestion requires further research to confirm.

Cluster analysis allowed us to reveal certain periods in the development of bog ecosystems which practically completely coincided with the periods determined according to pollen analysis.

References

Grospietsch,Th. 1953. Rhizopodenanalytische Untersuchungen an Mooren Ostholsteins.Arch.Hydrobiol., 47, 321-452.

Harnisch, O. 1951. Daten zur Gestaltung der okologischen Valenz der sphagnikolen Rhizopoden im Verlauf des Postglazials.Deutsch.Zool.Z., 1, 222-233.

Tolonen, K. 1966. Stratigraohic and rhizopod analyses on an old raised bog, Varrassuo, in Hollola, South Finland. Ann. Bot. Fennici, 3, 147-166.

Tolonen, K. 1986. Rhizopod analysis. In: Handbook of Holocene Palaeoecology and Palaeohydrology. Chichester, 645-665.

Tolonen, K., Warner, B., Vasander. H. 1992. Ecology of Testaceans (Protozoa:Rhizopoda) in Mires in Southern Finland: 1.Autecology. Arch. Protistenkd. 142 : 119-138.

Tolonen, K., Warner, B., Vasander. H. 1994. Ecology of Testaceans (Protozoa: Rhizopoda) in Mires in Southern Finland: 11. Multivariate Analysis. Arch. Protistenkd. 144: 97-112.

Warner, B.G. 1987. Abudance and diversity of testate amoebae (Rhozopoda, Testacea) in Sphagnum peatlands in southwestern Ontario, Canada. Arch. Protistenkd. 133: 173-189.

Warner, B.G., Chmielewski, J.G. 1992. Testate amoebae (Protozoae) as indicators of change with soil drying in a forested mire, northern Ontario, Canada. Arch.Protistenkd. 141: 179-183.

Regional temperature patterns across Northern Eurasia: tree-ring reconstructions over centuries and millennia

Keith R. Briffa[1], Philip D. Jones[1], Fritz H. Schweingruber[2], Wibjörn Karlén[3], Thomas Bartholin[4], Stepan Shiyatov[5], Eugene A. Vaganov[6], PenttiZetterberg[7] and Matti Eronen[8]

[1]Climatic Research Unit, University of East Anglia,
  Norwich NR4 7TJ, UK

[2]Swiss Federal Institute of Forest, Snow and Landscape Research,
  Zürcherstrasse 11, CH-8903 Birmensdorf, Switzerland

[3]Department of Physical Geography, University of Stockholm,
  S-10691 Stockholm, Sweden

[4]Laboratory of Quaternary Biology, University of Lund,
  Tornavägen 13, S-22363 Lund, Sweden.

[5]Institute of Plant and Animal Ecology, Ural Branch of the Russian
  Academy of Sciences, 8 Marta St., Ekaterinburg 620219, Russia

[6]Institute of Forest, Akagemogorodok, Krasnoyarsk 660036, Russia

[7]Karelian Institute, Secction of Ecology, University of Joensuu,
  PO Box 111, SF-90101 Joensuu, Finland

[8]Department of Geology, P.O. Box 11 (Snellmaninkatu 3), FIN-00014
  University of Helsinki, Finland

Spatial patterns during recent centuries

As part of a continuing European project in dendroclimatology, a network of temperature-sensitive tree-ring collections is being developed, at generally high-latitude or high-altitude sites extending across northern Fennoscandia and northern Russia. Intensive Russian sampling was carried out in 1991 and 1992 as a collaboration between the Swiss Federal Institute of Forest, Snow and Landscape Research, Birmensdorf; the Institute of Plant and Animal Ecology, Ekaterinburg; and the Institute of Forest, Krasnoyarsk. Together with earlier west European collections, this has provided an initial network made up of tree increment core samples at over 100 sites, many with data for different tree species. All of the collections are being analysed to produce tree-

ring density as well as ring-width data, and todate nearly 70 chronologies for each of these variables are available in Russia.

Established multivariate transfer function techniques are being used to associate regional patterns in the tree growth variables with patterns of gridded summer temperature averaged over 'seasons', equating locally to cumulative degree days above a 5(C threshold. The ultimate aim of this work is to apply these transfer functions to past tree growth variations so as to provide a detailed regional picture of year-by-year changes of summer temperatures across northern Eurasia. The results will be produced in the form of detailed anomaly maps and gridpoint temperature series representing annual-to-multidecadal variability with high statistical confidence for periods up to 250-300 years.

At present, the effective spatial resolution of these reconstructions is restricted by the density of site chronologies produced. Todate, this is good west of the Ural Mountains but poor in central and eastern regions (though laboratory analysis and fieldwork are currently underway to improve this). Provisional results of chronology comparisons, intra- and inter-site data analyses, climate calibration and provisional temperature reconstructions are already available and will be described.

The Last Millennium in Northwest Eurasia

At specific locations in northern high-latitude regions it is possible to extend the tree-growth record back beyond the life span of living trees by amalgamating the measurements from overlapping, absolutely-dated series of measurements made on dead wood from historical or archaeological provenances or naturally surviving above ground, in peat or alluvial sediments, orpreserved in lakes. At two locations in northern Eurasia the availability of sufficient subfossil pine material has enabled separate ring-width and maximum-latewood-density chronologies to be produced, each spanning more than 1000 years. The first pair of (ring-width and density) chronologies, made up from samples at several locations adjacent to Lake Torneträsk, northern Sweden, have been used to reconstruct summer (April-August) temperatures representing a large region of northern Fennoscandia (65-70(N; 10-30(E) from A.D. 500 to 1980. Similar data from samples of larch on the eastern slopes of the northern Urals have been used to reconstruct regional summer (May-Sept.) temperatures representing a region of northwestern Siberia (62-68(N; 65-75(E) for the period 914 to 1990. The approach used in constructing these tree-ring chronologies was one in which sample-age bias is removed from the individual tree measurement series but long-timescale (potential climate) variability is preserved in the mean chronology. Hence the temperature reconstructions represent longer timescale temperature variations than would be possible if more 'usual' data processing techniques had been employed.

Both the Fennoscandian and the Russian temperature records show marked high-frequency (interannual - to - century) timescale variability. However, they also demonstrate that marked long-timescale (multicentury) variations in summer

temperatures have been a characteristic feature of climate in each region during the last millennium. On the basis of instrumental temperature comparisons over the present century, we would not expect significant correlation between these records (at least on interannual - to - decadal timescales). However, a comparison of the long-timescale variability in the two records reveals up until about 1600, temperature anomalies were largely out of phase between the regions. This is dramatically illustrated between 950 and 1200 when it was generally warm in northern Fennoscandia and cool over the northern Urals (the period of the so-called Medieval Warm Epoch). However, both areas appear to have experienced very cool conditions during the late 16th and the 17th centuries (though the cool period set in earlier in the Russian series, in the early 18th century). After this time, summers appear to have followed similar long-term paths, warming to the mid 18th century, slight cooling to the end of the 19th and a sharp rise to a period of generally warm summers during the present century. In the context of extended Fennoscandian record, the 20th century warmth is not anomalous. However, the recent temperatures over the northern Urals do appear unusual in the context of the 1000-year record.

Despite cool summers during the late 1960s and 1970s, summer temperatures over the northern Urals, averaged over the whole 20th century todate (1901-90), were warmer than for any other 90-year period in the record. The period from 1919-1968 was also warmer than any other 50-year period, though the warmest 20-year value this century (1948-1967) is only the second warmest (after 1461-1480).

While acknowledging the real uncertainty that is always particularly associated with attempts to capture long-timescale variability in the series, it is still interesting to note that model-based scenarios of future temperature change in these regions is at least consistent with the recent temperature trends that we have reconstructed. Recent long runs of coupled atmosphere-ocean general circulation models with perturbed greenhouse-gas forcing suggest that future warming may be greatest at high-latitudes and continental regions and might be reduced (or absent) in the vicinity of the North Atlantic due to the effects of North Atlantic Deep Water formation. We also note, however, that conditions in Fennoscandia and the polar Urals during the 13th century caution against viewing the recent level of warmth as necessarily evidence of regionally enhanced greenhouse warming.

Fennoscandia during the Holocene

In Fennoscandia, two projects currently underway aim to build continuous multimillennial pine ring-width chronologies, spanning 7-8000 years. The Finnish project is described in another contribution to this meeting (Zetterberg et al.). The current status of the northern Swedish project, centred on the region around Lake Torneträsk will be described.

A continuous, absolutely dated ring-width chronology currently spans the period from A.D. 1 to 1981. Prior to this over 300 subfossil series have been incorporated within two 'floating' chronologies, one 4450 years and the other 823 years long. Based on calibrated conventional radiocarbon dates these probably span the periods 5480-1131 and 1111-289 B.C. The 19-year gap between them is supported by comparison with another floating Finnish chronology that is continuous over this period (based on data supplied by P. Zetterberg, Pers. Comm.). The replication is very poor in certain areas of the early chronologies and they should only be considered as provisional at this point in time. Despite this, they suggest major multicentury variability of climate during the last 7000 years with anomalous warmth at about 5300, 5100, 4650, 3850, 3700, 3400, 2900, 1300 and 750 B.C. A mid Holocene period of protracted warmth is suggested between about 4000 and 3300 B.C., though interrupted by relatively cool conditions after 3600.

The gap in the long chronology after 300 B.C. is coincident with other evidence of poor subfossil wood preservation and independent evidence of wetter conditions and therefore supports the hypothesis of a major widespread climate anomaly at this time. The long chronologies as constructed at present do not show any evidence for millennial-timescale lowering of summer temperatures as would be expected on the evidence of falling alpine tree lines, latitudinal retreating tree lines and calculated summer insolation. To some extent, this reflects a lack of sensitivity in the tree-ring data to very long-term changes in temperature as a result of the way the long chronologies are constructed. Adjusting the data to take account of the elevation of the source material may overcome this to some extent.

Acknowledgements

Intrasecular air temperature changes in the North European Russia over the last Millennium

Margarita Chernavskaya

Laboratory of Dynamical and Historical Climatology, Institute of Geography
Staromonetny pereulok 29, 109017 Moscow, Russia

Introduction

The study of climate variability (trend, amplitude, duration of warming and cooling periods, statistics) over the historical past gives us the possibility for estimation of future climatic changes. Climatic variability may be reconstructed on the base of different proxy data. The joint using of natural and documentary indicators can provide for a reliable reconstruction of the climate of the historical past. The use of palinological data for climatic reconstruction is based on the assumption that there is an evident link between vegetation and climate in contemporary conditions and that this link may be presumed to have existed in the historical past. A variety of combinations of multiple regression techniques and principal components analyses are used to calculate calibration function from a spatial network of modern pollen and climate data and to reconstruct climatic changes (Gajewski,1988; Guiot, 1990; Guiot et al., 1993).

Results and discussion

The results presented in this paper are based on a study of two temporal series of fossil pollen spectra obtained from peatbogs Polistovo (56,8°N, 30,1°E, broad-leaved and coniferous forest) and Panfilovo (55,7°N, 40,5°E, pine forest of middle and southern taiga). More than a hundred modern pollen spectra were used to calibrate pollen data in climatic terms. Percentage represented pollen spectra included the taxa which made up the continual spatial and temporal sequences and revealed the linkage with climate. The procedure of reconstruction was based on stepwise multiple regression on principle components. The Russian chronicles and diaries contained the information on extreme weather phenomena served for confirmation of some revealed climatic anomalies. Time series of ice-free period duration in the North Dvina basin (since 1734) was used for studding thermal conditions changes and reconstruction of dominating circulation processes.

The results of reconstruction shows that annual mean temperature varied with the range of no more than one and a half degree in both sites (Fig.1). There is no obvious trends in curves.
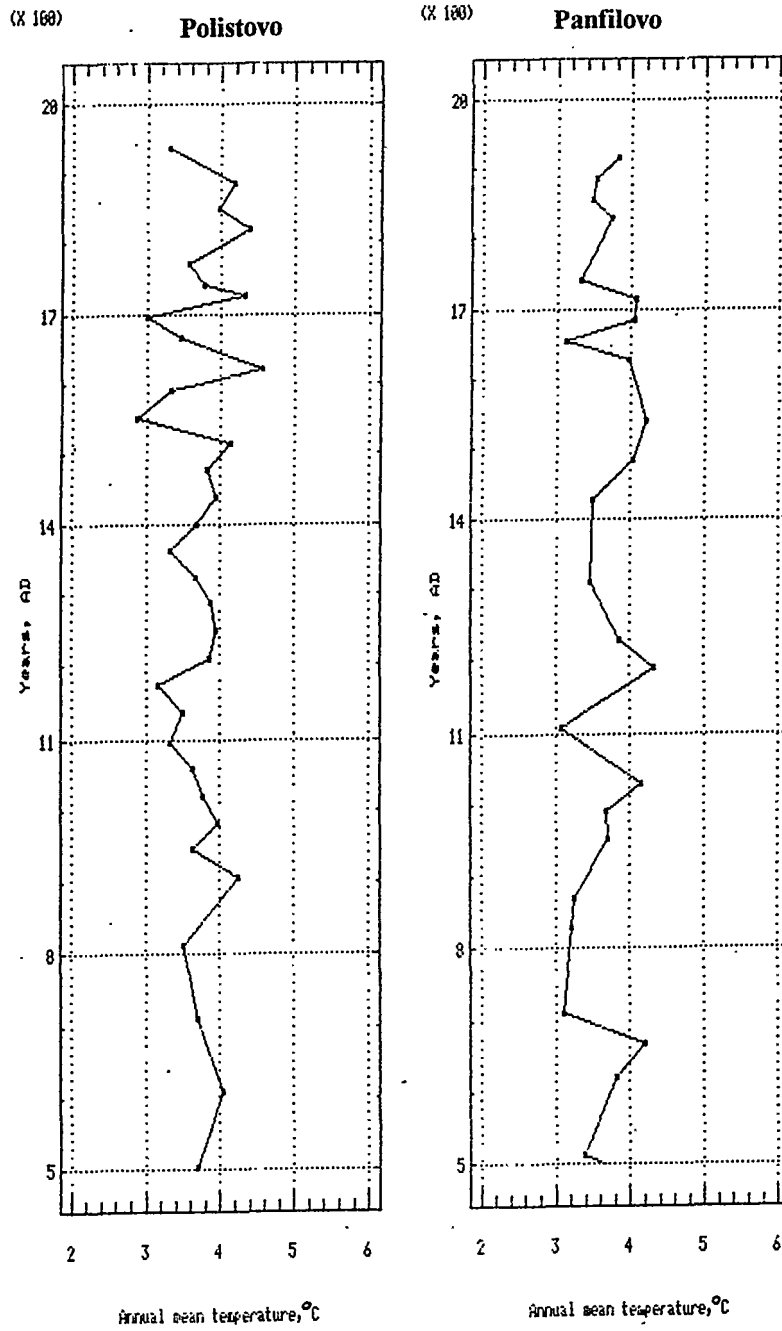
Fig. 1 Annual mean temperature reconstructed on pollen data for Polistovo (the north-west of European Russia) and Panfilovo (the center of European Russia).

Some short-term fluctuations of annual mean temperature are in phase or with a small lag at the sites. It was a period of cooling between the VIII-th and the IX-th centuries, as well as during the XI-th and the XIV-th ones (indicating relative cold). The variability increased in period since the end of the XVI-th century to the first part of the XVIII-th century in both sites. Worthy of mention is the supercooling at the very end of the XVII-th century in Polistovo. According to the documentary sources the last decade of that century was extremely cold (Neumann & Lindgren, 1979; Eronen et al, 1994; Chernavskaya, 1995).

The medieval warming was the most distinctly expressed in the XIII-th century in the north-western part of European Russia (Polistovo) and during the second part of the XII-th century in the central part (Panfilovo). The postmedieval warming observed in Panfilovo was simultaneous to the rather intensive cooling in Polistovo.

Time-series of ice-free period duration in the North Dvina basin confirms some fluctuations of annual mean temperature during the last phase of the little Ice Age. Prevailing of circulation processes with Arctic intrusions was the reason of cooling which was observed in 1730-th to 1760-th in the North Dvina basin as well as in Polistovo and Panfilovo sites.

The most intensive decreasing of July temperature took place during the XIII-th century, at the very beginning of the 17-th and during the XIX-th centuries in north-western Russia.

Acknowledgment

References

Chernavskaya, M. 1995. Weather conditions of 1695-1696 in European Russia. The Jehuda Neumann Memorial Symposium on mesoscale modeling and climate history. Preprints. Extended abstracts. 135-136.

Eronen, M., M.Lindholm, & P.Zetterberg. 1994. Extracting palaeoclimatic information from pine tree-rings in Finland. Climatic trends and anomalies in Europe 1675-1715, edited by B.Frenzel. Gustav-Fischer Verlag, Stuttgart, Jena, New York. 43-50.

Guiot, J. 1990. Methodology of the last climatic cycle reconstruction in France from pollen data. Palaeogeography, Palaeoclimatology, Palaeoecology, 80. 49-69.

Guiot, J., S.P.Harrison, & I.C.Prentice. 1993. Reconstruction of Holocene precipitation patterns in Europe using pollen and lake-level data. Quaternary research 40. 139-149.

Neumann, J., & S.Lindgren. 1979. Great historical events that were significantly affected by the weather: 4. The great famines in Finland and Estonia. 1695-97. Bull. Am. Meteorol. Soc. 60. 775-787.

Tree-ring and megafossil evidence on climatic fluctuations in Northern Fennoscandia

Matti Eronen[1] and Pentti Zetterberg[2]

[1]Department of Geology, P. O. Box 11 (Snellmaninkatu 3), FIN-00014 University of Helsinki, Finland

[2]Karelian Institute, University of Joensuu, P. O. Box 111, FIN-80101 Joensuu, Finland

Subfossil Scots pines (*Pinus sylvestris*, L.) have been collected in the treeline area of northern Fennoscandia in order to construct a continuous dendrochronological master curve extending back over 7000 years. Pine megafossils have been preserved in large quantities in small lakes, where the subaquatic trunks can be easily located by a diver. The trunks have been taken to the shore and sampled by cutting a disc with a chainsaw from the lower part of the tree. In the laboratory the samples have subjected to a dendrochronological analysis. The tree rings of the forest-limit pines are good palaeoclimatic indicators, because the radial growth of those trees is strongly controlled by the thermal conditions of the growing season, especially by the July temperatures (Briffa et al. 1992, Lindholm et al., in press).

A total of 1265 samples of subfossil pines from 38 sites were collected by the end of the 1994 field season. Tree-ring series of almost 1000 samples have been connected to the existing long dendrochronological curves. The continuous "absolutely" dated chronology extends back to the year 165 BC. There also exists a long older part of the master chronology, which has been fixed in time by several ^{14}C dates. There is still a gap of 250-300 years between the "absolute" and "floating" parts of the chronology. The older part of the master chronology covers approx. 5000 years extending back to about 5500 BC (Zetterberg et al. in press).

The variations in tree-ring width can be used for estimation of the variability of climate during the past centuries and millenia. It is difficult to infer the long-term trends of temperature changes from the tree-ring widths, because the rate of growth is different at different sites and thus the material is not homogeneous in this respect. Nevertheless, many interesting observations on the past climatic variations have been made from the present data. The medieval warm period and the Little Ice Age do not stand out as distinct mild and cool periods in the northern pine tree ring data (Briffa et a. 1992, Zetterberg et al. 1994). A marked climatic shift seems to have taken place around 3800 BC (5000 ^{14}C years BP), when the variability of the summer temperatures in the north obviously increased leading gradually to cooler climatic conditions (Zetterberg et al., in press). The gap in the master curve between 2000 and 2500 BP

also falls close to a period of time characterized by a change in the climatic pattern, i. e. the traditional boundary between the Subboreal and Subatlantic periods. This turning point marks the start of a new cooling trend and increase in humidity. The unfavourable climatic conditions may have brought about so many irregularities in the growth of pines that it is very difficult to match the tree-ring series with each other. The collected samples very probably include wood also from this period and attempts are being made to bridge the gap.

The dated megafossils provide information about the past changes in timberline. Before the present extensive dendrochronological dating about 80 radiocarbon dates had been obtained on the subfossil pines found in the timberline zone or beyond it in Finnish Lapland (Eronen & Huttunen 1987, 1993). Now there are nearly 1000 old pines dated by dendrochronology. The megafossils show it in a very concrete manner that pine stands exists even tens of kilometres beyond the present limit of pine in northern Fennoscandia in early and mid-Holocene times. The maximum spread occurred in this region 4000 to 6000 BP (roughly 2500 to 5000 calBC). The latter part of the Holocene is characterised by a gradual retreat of pine from its outermost occurrences. There are regional differences in this development, but no rapid large-scale changes can be distinguished in the megafossil data.

References

Briffa, K. R., Bartholin, T. S., Eckstein, D., Schweingruber, F. H., Karlén, W., Zetterberg, P. & Eronen, M. 1992. Fennoscandian summers from AD 500: Temperature changes on short and long timescales. Climate Dynamics 7, 111-119.

Eronen, M. & Huttunen, P. 1987. Radiocarbon-dated subfossil pines from Finnish Lapland. Geografiska Annaler 69A(2), 297-304.

Eronen, M. & Huttunen, P. 1993. Pine megafossils as indicators of Holocene climatic changes in Fennoscandia. Paläoklimaforschung - Palaeoclimate Research 9, 29-40.

Lindholm, M., Eronen, M., Meriläinen, J. & Zetterberg, P., in press. Climatic calibration of tree-ring width variations in forest-limit pines (Pinus sylvestris, L.) in northern Finnish Lapland. Paläoklimaforschung - Palaeoclimate Research 17.

Zetterberg, P., Eronen, M. & Briffa, K. R. 1994. Evidence on climatic variability and prehistoric human activities between 165 B.C. and A.D. 1400 derived from subfossil Scots pines (Pinus sylvestris, L.) found in a lake in Utsjoki, northernmost Finland. Bulletin of the Geological Society of Finland 66, 107-124.

Zetterberg, P., Eronen, M. & Lindholm, M., in press. The mid-Holocene climatic change around 3800 B.C.: tree-ring evidence from northern Fennoscandia. Paläoklimaforschung - Palaeoclimate Research 17.

A 2,305 year tree-ring reconstruction of mean June-July temperature deviations in the Yamal Peninsula.

Rashit M Hantemirov

Institute of Plant and Animal Ecology, Ural Division of Russian Academy of Sciences, GSP-511, Ekaterinburg 620219, Russia

Introduction

High latitude areas located within the forest-tundra zone are the most suitable ones for reconstruction of summer temperatures on the basis of tree-ring analysis. Air temperatures of the summer months, particularly June and July of the current year growth, make the largest contribution to the tree growth variability (Briffa et al.,1990; Graybill and Shiyatov,1992; Jacoby and D'Arrigo, 1989).

We have made reconstruction of average June-July temperature for 313 BC - AD 1991 using tree-ring width variation of *Larix sibirica* from the south of Yamal Peninsula, close by timberline. It is of considerable interest because it is the longest proxy record of seasonal temperatures for the subarctic. Taking into account that this region is thought to be particularly sensitive to long-term trends and variations in temperature over the arctic and possibly the Northern Hemisphere (Kelly et al., 1982) dendroclimatic long-term reconstruction is of great importance for understanding regional and hemispheric temperature changes.

Material

There is considerable recent and old tree wood material preserved in the Holocene deposits (alluvial, peat) in the southern part of the Yamal Peninsula (Khadyta, Tanlova and Yada rivers basin, 67-68 ° N, 70 °E). At present the polar timberline passes through the most southern part of this peninsula (67°30' N). Open larch and larch-spruce-birch forests are located mainly along the banks above mentioned rivers in the middle and lower parts of valley. The upper reaches of these rivers are treeless.

The species of the wood remains is mainly Siberian larch (*Larix sibirica*). Currently, circa 150 bores and cuts from old living trees and about 1200 subfossil wood cuts have been obtained from the area about 100 x 100 km. Radiocarbon dating has shown that the age of the oldest subfossil wood remains reaches 9000-9400 years.

The presented results are as a first step at building multi-millenial-length tree-ring chronology (up to 8-9 thousand years) for the North of Western Siberia (Shiyatov et al., 1995).

Methods

Individual tree-ring series were initially crossdated with each other and all rings were assigned calendar years based on the known collection dates of the living series. The total time span represented by the living series is AD 1573-1991. Samples from subfossil wood cover the time range of 313 BC-AD 1856. Each series was treated with the Corridor Method of Standardization (Shiyatov, 1986). Seventy-four longest of these series were combined by simple averaging to form a tree-ring index chronology for the region. The order of the pooled autoregressive model that was used for pre-whitening is estimated as AR(2). High positive correlations between obtained ring-width chronology and June-July mean monthly temperature have been found (0.59 for Salekhard and 0.58 for Yar-Sale meteorological stations). This allowed to make a reliable reconstruction of summer temperature.

Results and discussion

Reconstructed summer temperature deviations over the past 2305 years are illustrated in Figure 1.

Most of the constituent tree-ring series forming the chronology range in age from about 200-300 years, although a few are of shorter length. Given this, and the fact that standardization can remove trends that are at the same or greater legth than the series in question, the ability of this reconstruction to mirror longer term trends may be questioned. However fluctuations of summer temperatures on annual, decadal and partly century timescale are notice.

Most cold periods were during the middle of the III century BC, on the border of the III and II centuries BC, the beginning and the end of the V century, the middle of the VII century, the beginning of the IX , X and XI centuries, the middle of the XV century and the beginning of the XIX century. The warm periods are not so marked as the cold ones. It could be noted that during the first half of the II century BC, the second half of the V and XVII centuries were relatively warm.
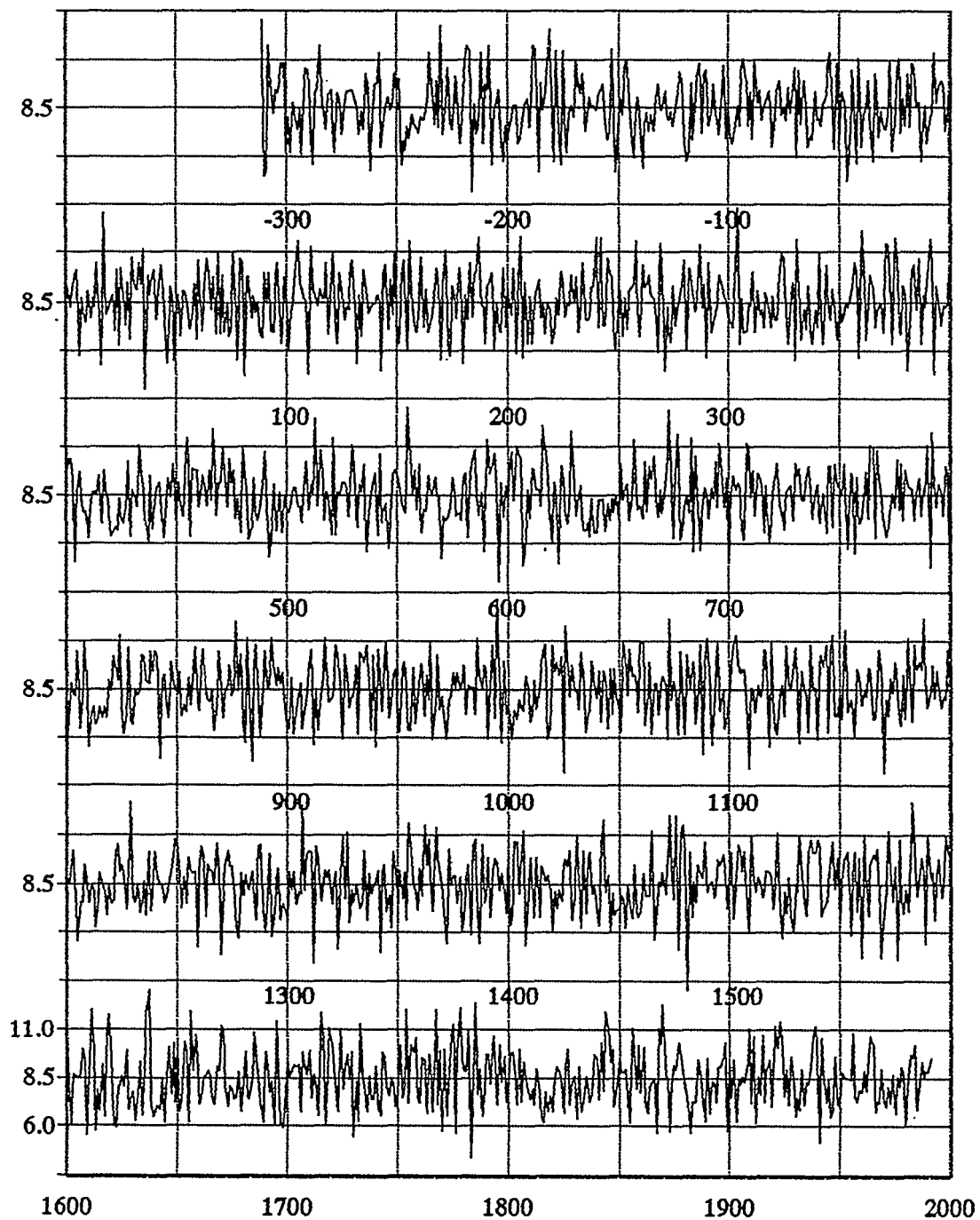
Fig. 1 Reconstructed mean June-July temperature, southern part of Yamal Peninsula, 313 BC - AD 1991. (Scales on the left are for actual °C from observation period.)

The cold and warm periods mentioned above are not quite coincided with the ones well-known for the northwestern Europe. Further evaluation of the results obtained here may be possible as the development and analysis of other long tree-ring chronologies in the subarctic proceeds.

Acknowledgements

References

Briffa, K.R., Bartolin, T.S., Eckstein, D., Scweingruber, F.H. & Zetterberg, P. 1990. A 1,400-year tree-ring record of summer temperatures in Fennoscandia. Nature 346: 434-439.

Graybill, D.A. & Shiyatov, S.G. 1992. Dendroclimatic evidence from the northern Soviet Union. In Bradley, R.S. and Jones, P.D., eds., Climate since A.D. 1500. London: Routledge, 393-414.

Jacoby, G.C., Jr. & D'Arrigo, R.D. 1989. Reconstructed Northern Hemisphere annual temperature since1671 based on high-latitude tree-ring data from North America. Climatic Change 14: 39-59.

Kelly, P.M., Jones, P.D., Sear, C.B., Cherry, B.S.G. & Tavakol, R.K. 1982. Variations in surface air temperatures: Part 2, Arctic regions 1881-1980. Monthly Weather Review 110: 71-83.

Shiyatov, S.G. 1986. Dendrochronology of the upper timberline in the Urals. Moscow: Nauka, 136 pp. (in Russian).

Shiyatov, S.G., Hantemirov, R.M. & Loosli H.H. 1995. The potential of developing long-term tree-ring chronologies in the northwestern part of the West-Siberian Plain. Boreas (in press).

Climatic evidence from stable carbon isotope data of tree rings of Scots pine from northern Finland

Högne Jungner and Eloni Sonninen

Dating Laboratory, University of Helsinki
P.O.B. 11, FIN-00014 Helsinki

The carbon isotope ratio, $^{13}C/^{12}C$, stored in a tree ring depends on the isotopic content of the atmospheric CO_2 at time of growth, and on the degree of isotopic fractionation, which occures during assimilation. The fractionation processes are influenced by plant physiology and environmental conditions at time of growth, as temperature, humidity and precipitation. The isotopic composition of atmospheric CO_2 is a result of exchange of CO_2 between the carbon reservoirs (the ocean, the biosphere and the atmosphere). The increase of CO_2 in the atmosphere during the last hundred years caused by intensified land use and buming of fossil fuels has significantly changed the isotopic composition. As many factors make influence on the isotope ratio, $^{13}C/^{12}C$, during the process, where carbon is taken up from the atmosphere and finally fixed in the cellulose, the use of isotope data from tree rings to obtain information on climatic parameters and atmospheric CO_2 isotopic content has proven difficult.

The tree ring material used is from living and Holocene subfossil Scots pine (Pinus sylvestris L.) from different localities within the tree limit area in northern Finland. Pine from this area has been used to construct a tree ring chronology covering a period from present to about 5000 BC (Zetterberg et al. in press, Eronen & Zetterberg in press). The area is sparsely forested with scarce ground vegetation. The carbon isotope ratios in cellulose from these trees should therefore well reflect the atmospheric CO_2 content and the fractionation in the tree. The tree ring material studied so far covers the following periods: living trees from AD 1840-1993, and subfossil trees from AD 1860-1700, AD 1420-1550, AD 75-160 BC, 1400-1290 BC, 1800-2100 BC and 3450-3700 BC. Single annual rings have normally been used but for some of the subfossil trees five successive rings were combined together. The data given are based on α-cellulose extracted from the ring material. Experimental methods used have been described in previous papers by Sonninen and Jungner (1994, in press).

The isotope records obtained from different trees from same periods show great similarities. The results of isotope measurements on annual rings from recent trees show a few general trends besides the short-term fluctuations. The $\delta^{13}C$ values remains quite stable at a value around -24 ‰ for the period AD 1840-1980, then there is a decreasing trend until present with exception of a period at AD 1910-1940 with increased values. Similar trends have been observed in other tree ring studies (Freyer & Belacy 1983, Stuiver et al. 1984, Leavitt & Long 1989) and they can be related to changes in the isotopic composition of the atmospheric CO_2 measured from air samples (Keeling et al. 1979, Mook et al. 1983) and from air trapped in Antarctic ice (Friedli et al. 1986). The decrease in $\delta^{13}C$ value observed from our tree ring data from 1850 to 1990 is c. 1.6 ‰. This indicates that pines living in an open landscape close to the tree limit in Northern Finland can give a good reflection of the $^{13}C/^{12}C$ isotope ratio of the atmospheric carbon dioxide.

The short-term fluctuations in the $\delta^{13}C$ record may be connected to variations in fractionation during assimilation by the tree. In order to find the correlation between $\delta^{13}C$ and temperature variations we used meteorological data available from AD 1901 onwards. Regression analysis indicates the temperature dependence of the $\delta^{13}C$ value to be of the order of +0.1 ‰ /C when mean temperatures for July were used. As a consequence a positive correlation between ring width and $\delta^{13}C$ value was found both for recent and subfossil trees to be of the order of 1 ‰/mm. No significant influence of the amount of precipitation on the carbon isotope ratio in the ring cellulose could be seen.

The results obtained until now are based on a limited material. The work will be continued with material available from different localities in the tree limit area in order to establish a long carbon isotope record from a region sensitive to climatic variations.

References

Eronen, M. & Zetterberg, P. (in press). Expanding dendrochronological data on Holocene changes in the polar/alpine pine-limit in northern Fennoscandia. Paper presented at The Nordic symposium on Holocene tree-lines, dendrochronology and palaeoclimate. Skibotn, northern Norway, September 6-8, 1993. Paläoklimaforschung / Palaeoclimate Research 17.

Freyer, H.D. & Belacy, N. 1983. $^{13}C/^{12}C$ Records in Northern Hemispheric Trees During the Past 500 Years - Anthropogenic Impact and Climatic Superpositions. J. Geophys. Res. 88:6844-6852.

Friedli, H., Lötscher, H., Oeschger, H., Siegenthaler, U. & Stauffer, B. 1986. Ice core record of the $^{13}C/^{12}C$ ratio of atmospheric CO_2 in the past two centuries. Nature 324:237-238.

Keeling, C.D., Mook, W.G. & Tans, P.P. 1979. Recent trends in the $^{13}C/^{12}C$ ratio of atmospheric carbon dioxide. Nature 277:121-123.

Leavitt, S.W. & Long, A. 1989. The atmospheric $\delta^{13}C$ record as derived from 56 pinyon trees at 14 sites in the southwestern United States. Radiocarbon 31:469-474.

Mook,W.G., Koopmans, M., Carter, A.F. & Keeling, C.D. 1983. Seasonal, Latitudinal, and Secular Variations in the Adundance and Isotopic Ratios of Atmospheric Carbon Dioxide. J. Geophys. Res. 88:10915-10933.

Sonninen, E. & Jungner, H. 1994. Stable carbon isotope ratios in tree rings of pine from northern Finland. In Kanninen, M. & Heikinheimo, P. (eds) The Finnish research programme on climate change, Second Progress Report. Helsinki 1994:20-24.

Sonninen, E. and Jungner, H. in press. Stable carbon isotopes in tree rings of a Scots pine (Pinus sylvestris L.) from northern Finland. In Problems of Stable Isotopes in Tree-Rings, Lake Sediments and Peat-Bogs as Climatic Evidence for the Holocene, Bern 28-30 April, 1993. Paläoklimaforschung/Palaeoclimate Research 15:117-123. Special Issue 10.

Stuiver, M., Burk, R.L. & Quay, P.D. 1984. $^{13}C/^{12}C$ Ratios in Tree Rings and the Transfer of Biospheric Carbon to the Atmosphere. J. Geophys. Res. 89:11731-11748.

Zetterberg, P., Eronen, M. & Lindholm, M. (in press). The Atlantic/Subboreal climatic shift, tree-ring evidence from northern Fennoscandia. Paper presented at The Nordic symposium on Holocene tree-lines, dendrochronology and palaeoclimate. Skibotn, northern Norway, September 6-8, 1993. Paläoklimaforschung / Palaeoclimate Research 17.

Tree-growth and climate relationships and dendro-climatological reconstruction at the northern forest limit in Fennoscandia

Markus LINDHOLM and Jouko MERILÄINEN

Saima Centre for Env. Sci., Univ. of Joensuu,
Linnank. 11, FIN-57130 Savonlinna, Finland.

Introduction

In regions where trees form annual growth layers, the characteristics of those layers may be used to reconstruct the environmental conditions under which they were formed. Sequential variability in annual tree rings frequently coincides in several trees within a region. This indicates that some common set of external factors, such as climate influences growth. Modelling tree rings from climate variables demonstrates how trees have responded to changing climate in the past. At the northern coniferous timberline trees grow at their climatically determined limits of distribution and the external factor having the strongest influences on growth is thermoclimate.

At the present work, ring-width series from living pines and modern climate records of mean monthly temperature and total precipitation were calibrated to determine the patterns of growth response to climatic forcing. 230 trees in all from nine forest stands in the forest-limit zone were measured and analyzed by standard means of tree-ring analysis. The oldest trees had began their growth during the last years of the 13th century and are still growing.

Results and discussion

The results show a most striking similarity of all the nine response functions. The patterns of growth response to intra-annual climatic forcing may be considered consistent and spatially extensive throughout the forest-limit zone. In Fig. 1 the response function analyses suggest that mid-summer temperatures may be usefully reconstructed in the region. However, there exists also other patterns, although less significant, that indicate the possible reconstruction of other periods.
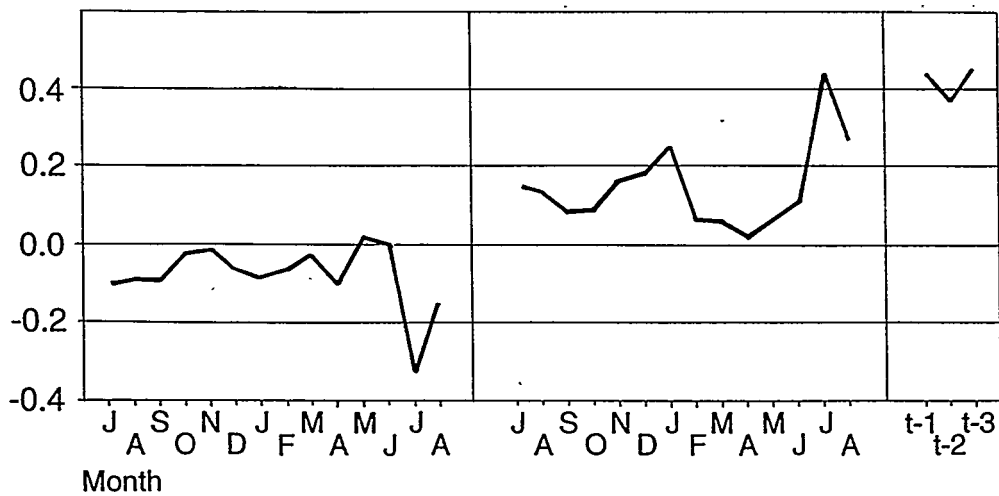
Fig. 1 Patterns of growth response in relation to climatic conditions at the forest-limit zone in Fennoscandia. Growth is expressed as a response to variations in particular climatic variables. Variables for prior growth at lags of 1, 2, and 3 years are introduced as predictor variables along with the variables of climate.

Reconstructed yearly variations of the July-August growing season since 1714 are illustrated in Fig. 2. Instrumental observations during the calibration period are also shown. Both the response and transfer models are statistically highly significant and consistent with those reported by other workers.

Some years, during which the growing-season conditions have been extremely austere, are clearly evident in the reconstruction. These so-called pointer years include: 1723, 1734, 1769, 1773, 1786, 1787, 1790, 1791, 1793, 1794, 1795, 1806, 1813, 1826, 1831, 1837, 1839, 1874, 1881, and 1893. The coldest summer in the instrumental record is 1902. The first decade of the twentieth century as a wholo was the coldest period in both actual and reconstructed data.

RECONSTRUCTED   VS.   OBSERVED TEMPERATURES
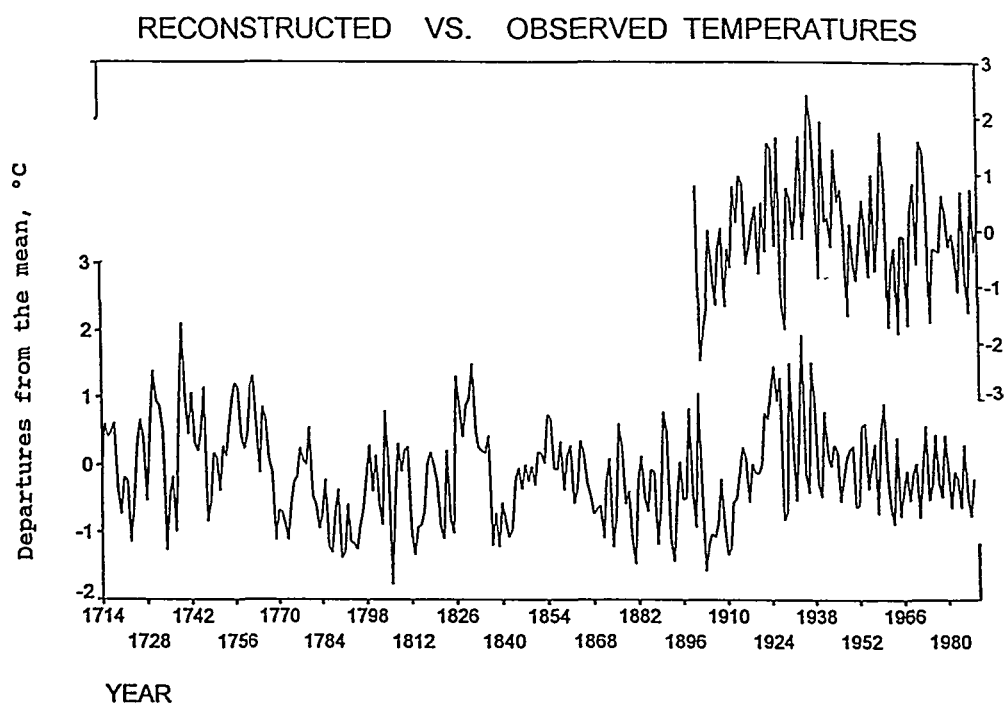
Fig. 2 Reconstructed mean July-August temperatures since 1714. The values are in normalized units, equal to degrees Celsius, as anomalies from the mean for 1901-1990. Measured temperatures available since 1900 are also shown.

Reconstructing Palaeoenvironmental Change using Stable Carbon Isotope variations in *Pinus sylvestris* from Northern Britain.

N.J.Loader & V.R.Switsur

The Godwin Institute of Quaternary Research
The Godwin Laboratory, University of Cambridge,
Cambridge, United Kingdom CB23RS.

Introduction

Attempts to assess the nature and magnitude of man's impact upon the natural environment have increased the need for accurate, quantitative methods of reconstructing palaeoenvironmental change. Whilst a variety of proxy indicators are available for this purpose, few have either the geographical distribution or temporal resolution of tree-rings.

Dendroclimatology has been demonstrated as both a valid and valuable means of reconstructing past environmental change, in extreme or marginal regions where growth may be limited by a single climatic or environmental factor. Unfortunately, in more maritime regions, for example the United Kingdom, such ecological dependencies are rarely evident.

It is known that the stable isotope ratios contained within tree rings vary as a function of the isotopic ratio of the carbon dioxide in the atmoshpere at the time of assimilation and fractionation effects within the arboreal system during photosynthesis (Francey & Farquhar 1982). Since the nature of the arboreal processes are known to be influenced by environmental factors, potential exists for the analysis of stable carbon isotopes in tree rings as a method of reconstructing past environmental variation in less extreme climatic zones.

This paper presents stable carbon isotope analyses from three native Scots Pine (*Pinus sylvestris L.*) from the Ballochbuie forest, Royal Deeside, Scotland and discusses the climatic and environmental signals contained within each. The Ballochbuie Forest, which is located approximately 2km from a long standing meteorological station provides an ideal site for stable isotope dendroclimatology and the future application of these findings to the extensive regions of sub-fossil Scots Pine found across the Cairngorm Region.

Results & Discussion

The isotope profiles obtained from the three trees show a high degree of coherence between trees across both the long- and short term. Consideration of the longer term trends identify the presence of an industrial effect, the magnitude of which is comparable to the findings of Freyer (1989) who considered a variety of plant species and also Jungner & Sonninen (1991) who also worked on Scot's Pine.

The annually resolved sequence (BALIA) demonstrates an erroneous trend post 1969, which is not apparent in either of the isotope sequences (BAL05A) or (BALIB). Ring width data support the hypothesis for a physiological disturbance during this time, the implications of which are discussed. Analysis of the high frequency variation also demonstrates a high degree of similarity between the two annually resolved sequences (BALIA & BALIB).

The nature of this higher frequency variation was investigated further using "pointer year" analysis and a degree of climatic dependence observed. The nature of this relationship was determined using a conventional response/ multivariate transfer function approach and identified a strong significant relationship between Δsummer temperature and Δcarbon isotopes. This relationship was independently verified and a record of summer temperature variation reconstructed back to 1764.

In a manner similar to conventional dendrochronology the two sequences were successfully cross-dated demonstrating the high degree of covariance. The stable carbon isotopes identified how it might be possible in future to extend these findings to the *long* tree-ring chronologies (ie: Bartholin 1987). Whilst this study has identified a number of obstacles which face those reconstructing palaeoenvironments from tree-ring stable isotopes they also demonstrate the potential that exists for the future stable isotope dendroclimatological investigations in the United Kingdom and highlight some of the challenges for the future.

Reconstruction of spatial variations in summer temperatures for the last 300 years in the north of West-Siberian Plain.

Valeri S. Mazepa

Institute of Plant and Animal Ecology, Ural Division of Russian Academy of Sciences, GSP-511, Ekaterinburg 620219, Russia

Introduction

There are only a few meteorological stations in the north of West-Siberian Plain which began to make records before 1930. The longest records are available from Turukhansk (since 1878) and Salekhard stations (since 1883). Others (more than 10) have shorter common periods of observation with many gaps. So the primary goal of this study is to make available preliminary series of maps showing past summer temperatures from the Polar Urals (64-68°N, 64-68°E) to Yenisey River (66-70°N, 86-89°E) based on tree-ring data.

The predictant temperature series were June-July averages from 11 meteorological stations. These stations are uniformly spread on the area mentioned. They are: Rai-Iz (66°57'N, 65°28'E, 882 m a.s.l.), Muzhy (65°23'N, 64°43'E), Salekhard (66°31'N, 66°36'E), Novy Port (67°42'N, 72°57'E), Nadym (65°36'N, 72°44'E), Tazovskoye (67°28'N, 78°44'E), Tarko-Sale (64°55'N, 77°49'E), Sidorovsk (66°36'N, 82°18'E), Dudinka (69°24'N, 86°05'E), Igarka (67°28'N, 86°16'E), Turukhansk (65°47'N, 86°58'E). The elevation of these stations is from 5 to 65 m a.s.l. except Rai-Iz. To fill the gaps we use gridded temperature data (Jones et al. 1991) and data from the nearest stations.

Samples from three species (*Larix sibirica* Ledeb., *Picea obovata* Ledeb., *Pinus sylvestris* L.) were collected during 1991-1993. No less than 15 cores per site were bored. The average distance between sites is about 200 km. Cores were collected from the north forest islands as well as from the forest massifs located 200-400 km to the south from the polar timberline. The samples were taken from 26 sites. Length of chronologies varies from 268 to 486 years.

Results and discussion

June-July mean temperatures for this area have been reconstructed back to 1690 using chronology network. The results are presented in Fig. 1 and 2. The
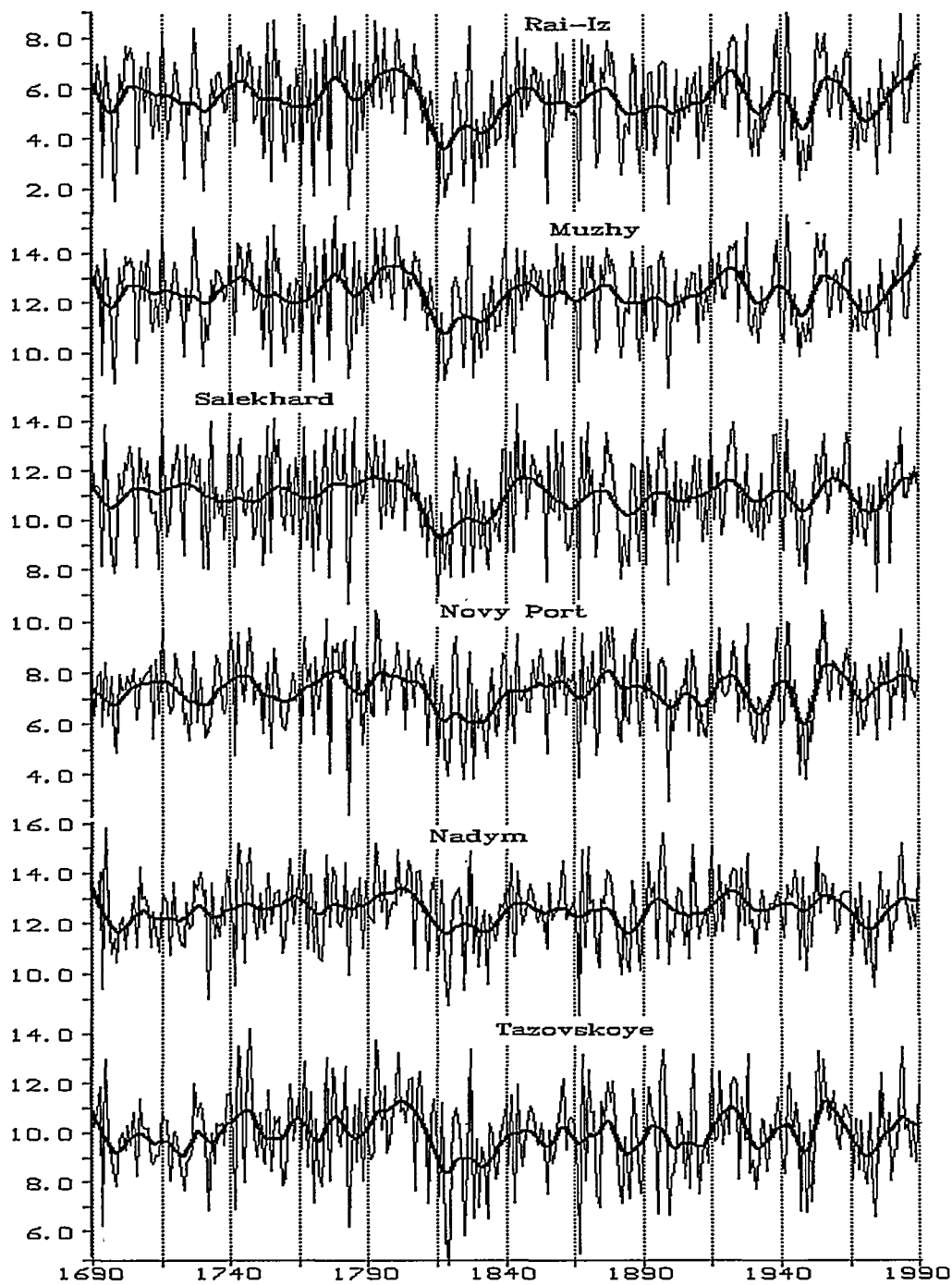
Fig. 1 Reconstructed mean June-July temperatures for selected stations. (Scales on the left are for actual °C from observation period.)
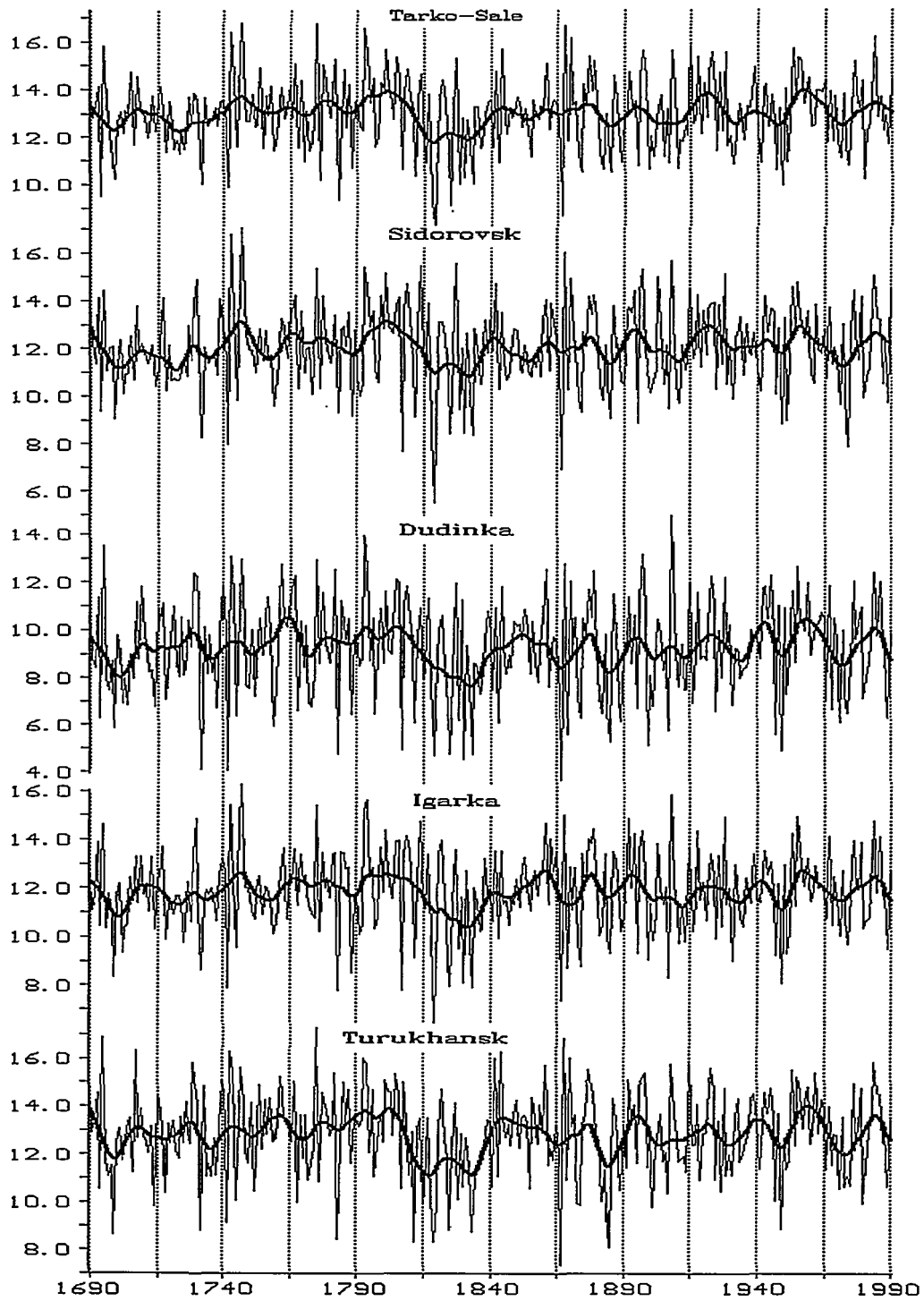
Fig. 2 Reconstructed mean June-July temperatures for selected stations. (Scales on the left are for actual °C from observation period.)

maps are plotted as anomalies from the mean temperature of each station. Reconstructions were produced using the orthogonal spatial regression technique (Briffa et al. 1986). The reconstructions are of good quality at least for the most north temperature records.

Multiple regression technique (Fritts 1976) was used to estimate how the ring width variations are caused by climate where the air monthly average temperatures were as predicators. The developed ring-width chronologies have a strong climatic signal. This is evidenced by the presence of high mean sensitivity values (from 0.27 to 0.45 in larch chronologies and from 0.21 to 0.26 in spruce and pine ones) and high variance explained by climate (from 56 to 72) in response functions. Low first order autocorrelations were recognized (between 0.1 and 0.4). The order of the pooled autoregressive model that was used for prewhitening shows similar variation within the chronology network. It is estimated as AR(2). Only in two cases we choose AR(3) model.

The long term fluctuations of reconstructed series within the area are very similar at separate time periods. But there are distinctions. For instance, very cold period at the boundary of 17th and 18th centuries marked very well at the east part of the area. At the same time this cycle was poor at the west part. The longest cold period was observed during the 19th century first part. At the west part of the area the coldest period occurred in 20-s, and at the east part it occurred in 40-50-s. The highest temperature variability was estimated in the northern regions of West-Siberian Plain. This conforms to the conclusion made earlier (Rubinshtein & Polozova 1966). They analyzed temperature changes using instrumental meteorological data and concluded that the north of West-Siberian Plain with Kara Sea and Barents Sea territories are of regions with the highest temperature variability over the Northern Hemisphere.

Acknowledgements

References

Briffa, K. R., Jones, P.D., Wigley, T. M. L., Pilcher, J. R., Baillie, M. G. L. 1986. Climate reconstruction from tree rings: Part 2, Spatial reconstruction of summer mean sea-level pressure patterns over Great Britain. Journal of Climatology 6: 1-15.

Fritts, H.C. 1976. Tree rings and climate. Academic Press, London, 567 pp.

Jones, P.D., Raper, S.C.B., Cherry, B.S.G., Goodess, C.M., Wigley, T.M.L, Santer, B., Kelly, P.M., Bradley, R.S., Diaz, H.F. 1991. An updated global grid point surface air temperature anomaly data set: 1851-1990. ORNL/CDIAC-37, NDP-020/R1. Carbon Dioxide Information Analysis Center, Oak Ridge National Laboratory, Oak Ridge, Tennessee. 422 pp.

Rubinshtein, E.S., Polozova, L.G. 1966. The recent climatic change. Gydrometeoizdat Press, Leningrad, 267 pp. (in Russian).

Inter- and Intra-Site ^{13}C/^{12}C Relationships in oak

I.Robertson[1], A.C.Barker[2], V.R.Switsur[1], A.H.C.Carter[1,2] and
J.S.Waterhouse[2]

1. The Godwin Institute for Quaternary Research, University of Cambridge, Free
School Lane, Cambridge, United Kingdom CB2 3RS.

2. Centre for Environmental Research, Anglia Polytechnic University, East Road,
Cambridge, United Kingdom CB1 1PT.

Introduction

In recent years, it has been increasingly realised that the long European oak
chronologies created during the 1970's for the purposes of dendrochronology could
serve many other purposes. The first such use was as a calibration device for the
radiocarbon timescale, but more recently attention has turned to their value as proxy
palaeoclimatic records.

Since the isotopic composition (δ^{13}C, δ^{18}O and δD) of α-cellulose in tree rings is
influenced by climatic factors at the time of growth (Ramesh *et al.* 1986) and is
preserved in sub-fossil wood since the time of its formation, the isotopic composition of
α-cellulose in tree rings could be used as a proxy record of past climates.

The aim of this study was to investigate inter- and intra-site δ^{13}C variations in
oak (*Quercus robur*) at an annual resolution for the period 1895-1994.

Paper to be presented by I.Robertson
Poster to be presented by A.C.Barker

Methods

Site Selection

Two sites in north-west Norfolk (52°50'N, 0°30'E) which provided contrasting local environments were selected for the study. The sites were located approximately 3 km apart. Sandringham Park is a dry, freely drained site and Babingley Osier Carr is a wet, poorly drained site.

Chronologies were established for the two sites using 5 mm cores (Carter, A.H.C. *et al.* unpublished results). From these chronologies trees were selected for the stable isotope study for the period 1895-1994. Five 12 mm cores were taken from individual trees at each site for isotope analyses. The trees chosen gave good inter-tree correlations with others at the site and represented, as far as possible, subtle changes in the local environment.

Sample Preparation

The isotopic heterogeneity of the different components of wood makes it necessary to isolate and analyse a single compound (Epstein, Yapp and Hall 1976). α-cellulose is the most abundant component of oak, constituting around 40% of its dry mass (Pettersen 1984), and its carbon, oxygen and carbon-bound hydrogen are resistant to post-formation isotopic exchange. Only the late wood of each ring was used in this study. The carbohydrates that are used in the formation of the early wood may undergo chemical modification during the period between synthesis and utilisation (Lipp *et al.* 1991; Robertson *et al.* in press).

Wood shavings were delignified using a modified version of the acid sodium chlorite oxidation summarised by Green (1963). Samples were placed in glass Soxhlet thimbles and agitated in an ultra-sonic bath (Loader *et al.* unpublished results). Unlike other batch processes (Leavitt and Danzer 1993), an alkaline extraction of holocelluloses using sodium hydroxide to yield α-cellulose was adopted.

Approximately 3 mg of α-cellulose was loaded into 125 mm long x 7 mm bore borosilicate tubes together with 400 mg of pre-heated copper(II) oxide. The loaded tubes were evacuated to $< 10^{-3}$ mbar for approximately one hour to ensure that all traces of absorbed water were removed, sealed with an oxy-gas torch at a length of *ca.* 100 mm and heated in a muffle furnace for six hours at 450°C (Sofer 1980).

Isotope ratios were measured using a VG ISOGAS SIRA II mass spectrometer and are reported in the usual δ notation relative to PeeDee belemnite (PDB) for $^{13}C/^{12}C$ (Craig 1957).

Results

The carbon isotope results to be presented at the International Conference on Past, Present and Future Climate confirm that water stress can induce stomatal closure thus decreasing the ratio of intercellular CO_2 to ambient CO_2 leading to an increase in the $\delta^{13}C$ value of the plant (Schleser 1994).

The two sites of Sandringham Park and Babingley Osier Carr were selected for their different hydrological regimes. The results illustrate that there is a greater intra-site isotopic coherence between trees growing on the dry site of Sandringham Park than there is between the trees growing at the wet site of Babingley Osier Carr. As bog oak constitutes approximately 75% of the wood in the Irish chronology (McCormack et al. 1994), these results have important implications for studies using the long oak chronologies of north-west Europe for climatic reconstruction.

Acknowledgements

References

Craig, H. 1957 Isotopic standards for carbon and oxygen correction factors for mass-spectrometric analysis of carbon dioxide. *Geochimica et Cosmochimica Acta* 12: 133-149.

Epstein, S., Yapp, C.J. and Hall, J.H. 1976 The determination of the D/H ratios of non-exchangeable hydrogen in cellulose extracted from aquatic and land plants. *Earth and Planetary Science Letters* 30: 241-251.

Green, J.W. 1963 Wood cellulose. In Whistler, R.L., ed., *Methods in Carbohydrate Chemistry III.*, Academic Press, New York: 9-21 pp.

Leavitt, S.W. and Danzer, S.R. 1993 Method for batch processing small wood samples to holocellulose for stable-carbon isotope analysis. *Analytical Chemistry* 65: 87-89.

Lipp, J, Trimborn, P., Fritz, P., Moser, H., Becker, B. and Frenzel, B. 1991 Stable isotopes in tree ring cellulose and climatic change. *Tellus* 43B: 322-330.

M^{C}Cormac, F.G., Baillie, M.G.L., Pilcher, J.R., Brown, D.M. and Hoper, S.T. 1994 $\delta^{13}C$ Measurements from the Irish oak chronology. *Radiocarbon* 36(1): 27-35.

Pettersen, R.C. 1984 The chemical composition of wood. In Rowell, R., ed., *The Chemistry of Solid Wood, Advances in Chemistry Series 207, American Chemical Society Symposium Series*, Washington, D.C.: 57-126 pp.

Ramesh, R., Bhattacharya, S.K. and Gopalan, K. 1986 Stable isotope systematics in tree cellulose as palaeoenvironmental indicators - a review. *Journal of the Geological Society of India* 27: 154-167.

Robertson, I., Field, E.M., Heaton, T.H.E., Pilcher, J.R., Pollard, A.M., Switsur, V.R. and Waterhouse, J.S., in press, Isotopic coherence in oak cellulose. In Frenzel B., ed., *Paläeoklimaforschung 15, Special Issue 10*, European Science Foundation, Strasbourg.

Schleser, G. 1994 *Causes of carbon isotope behaviour within tree rings*. In Spieckler, H. and Kahle, P., eds., *Proceedings of the Workshop on Modelling of Tree-Ring Development - Cell Structure and Environment*, Institut für Waldwachstum, Universität Freiburg: 12-23 pp.

Sofer, Z 1980 Preparation of carbon dioxide for stable carbon isotope analysis of petroleum fractions. *Analytical Chemistry* 52: 1389-1391.

Reconstruction of climate and the upper timberline dynamics since AD 745 by tree-ring data in the Polar Ural Mountains

Stepan G. Shiyatov

Institute of Plant and Animal Ecology, Ural Division of the Russian Academy of Sciences, Ekaterinburg, 620219, Russia

Introduction

On the eastern macroslope of Polar Ural Mountains there is a great number of dead trees and wood remnants of Siberian larch (*Larix sibirica* Ledeb.) located on the surface up to 60-80 m above the present upper timberline (Shiyatov 1993). Various direct and indirect evidences (altitudinal position, longevity and calendar life span of dead and living trees, shape of trunk, density and age structure of stand, variability of radial increment and ring-width indices) were used for detailed reconstruction of climate and the upper timberline changes for the last 1250 years. In the area of Rai-Iz Massif (66°50'N, 65°15'E) more than 400 cuts from wood remnants and 350 cores and cuts from living trees have been collected, mapped and absolutely dated by cross-dating procedure. Altitudinal position of the past and recent upper timberlines and individual age generations of larch trees was also mapped. To reconstruct climatic conditions of the past, the longer ring-width chronology was developed for this area (AD 745-1992) in comparison with previously published chronology (Shiyatov 1986, Graybill & Shiyatov 1992).

Results and discussion

Fig.1 shows location of 209 dated wood remnants *in situ* and 16 larch seedlings along the transect 430 m long and 20 m wide. This transect began at an elevation of 340 m a.s.l., where the highest remnants were found, and ended at the present timberline at an elevation of 280 m a.s.l.

During the last 1250 years a significant displacement of the upper timberline took place. The oldest wood remnants (AD 745-935) were only large roots located in the middle part of the transect. At this period the upper timberline was approximately 315 m a.s.l. or 35 m higher compared with its present position (280 m a.s.l.). It is difficult to conclude about stand density at this time as most remnants became rotted. From the middle of the 8th to the end of the 13th centuries there was intensive regeneration of larch, and the

timberline rised up to 340 m a.s.l. The 12th and 13th centuries were most favoralbe for larch trees growth. At this time the altitudinal position of the
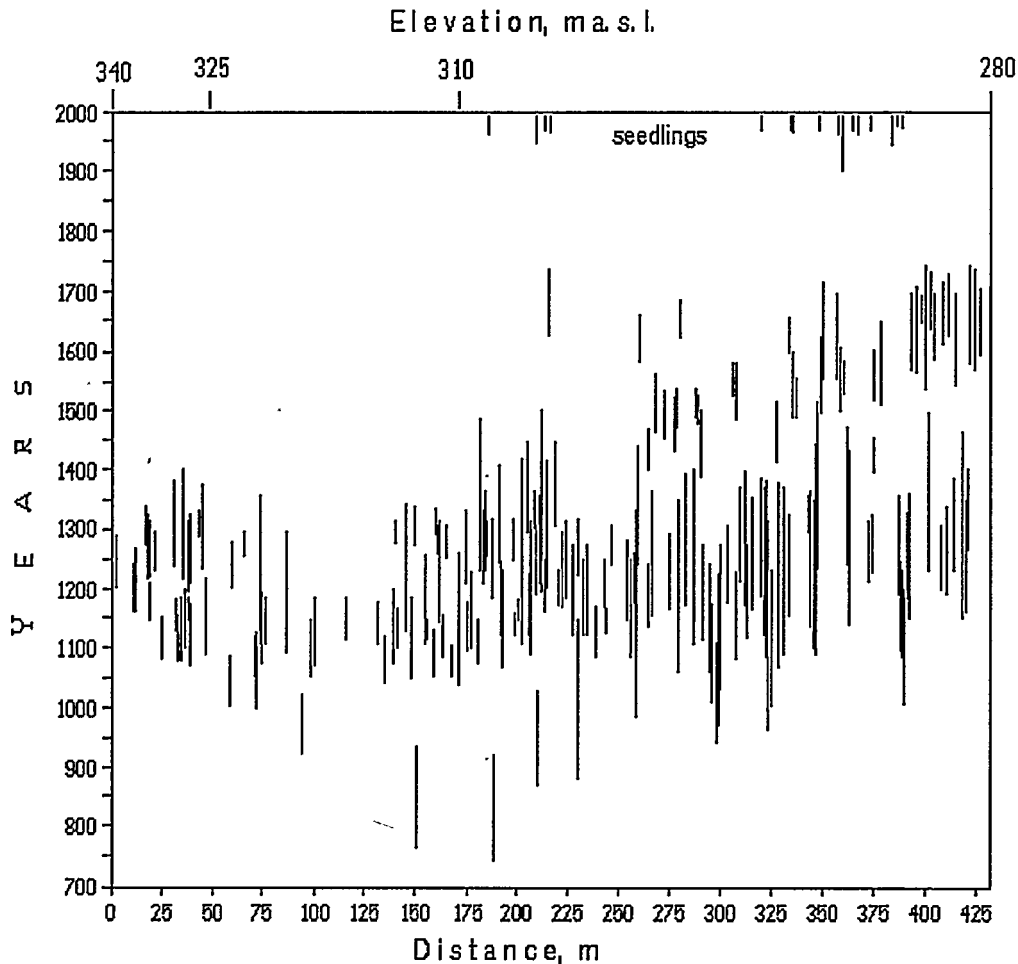
Fig. 1. Location of dated wood remnants and larch seedlings along the transect.

timberline was the highest, stand density the biggest, longevity of trees the longest, sizes of trees the largest, increment in diameter and height the most intensive as compared with other periods under review. At the close of the 13th century growing conditions deteriorated and larches, including young ones, began dying off. During the second half of the 14th century the retreat of timberline was very intensive and the upper timberline retreated up to 310 m a.s.l. Dying off of trees was observed along all parts of the transect. Adverse growing conditions were in the 15th century, and during this period the stand density was low. Only from the end of this century poor larch regeneration started in the lower part of the transect. This process continued during the 16th century and no retreat of the timberline took place. The first half of the
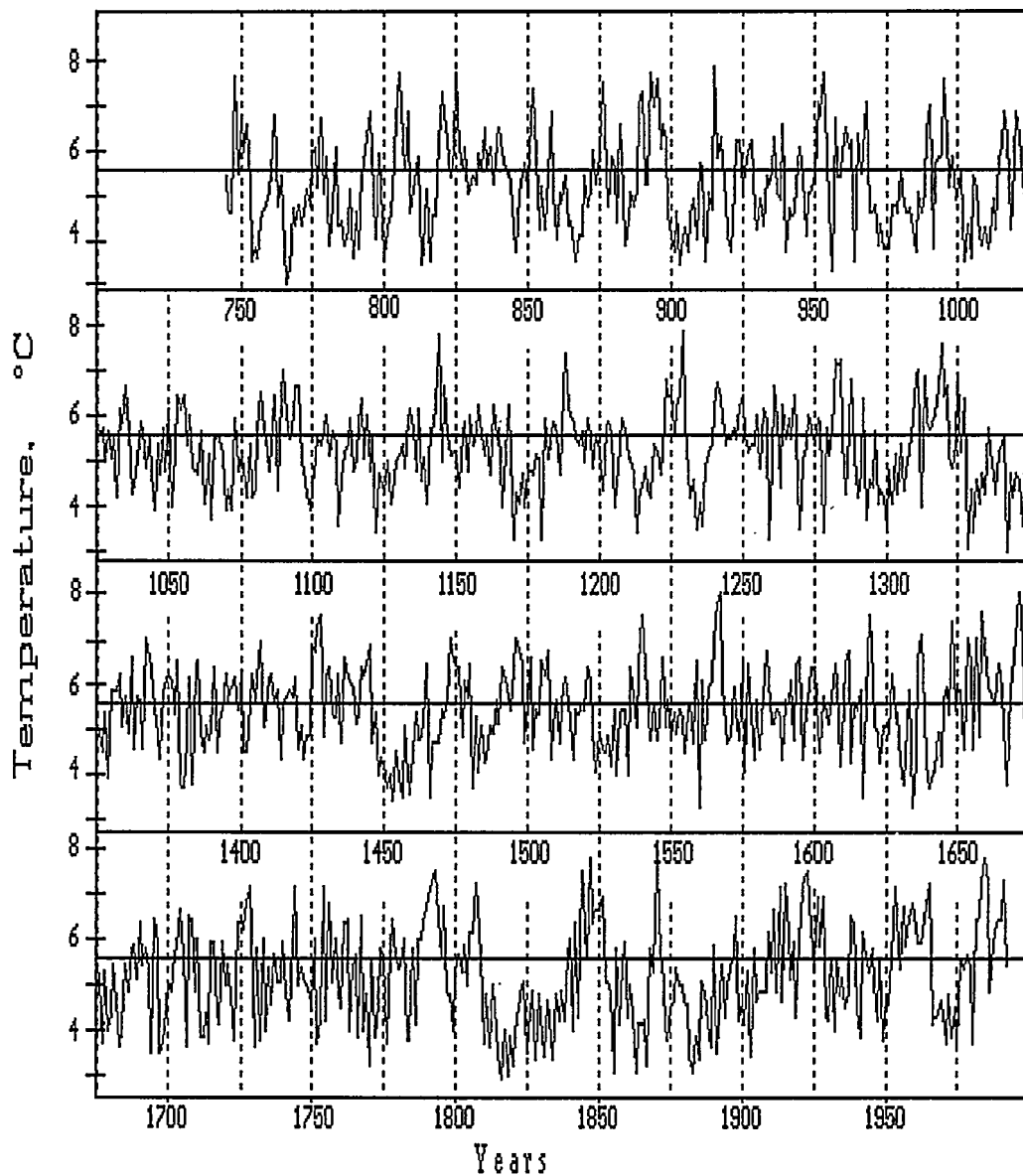
Fig. 2. Reconstructed average June-July temperature for Rai-Iz meteorological station from RAIARS ring-width chronology.

17th century was unfavorable for larch growth and the timberline retreated to 290 m a.s.l. During the second part of this century the decline of larch stand ceased and rather dense larch stand existed in the lowest part of the transect. The 18th century was favorable for trees growth. Most adverse period for the last 1250 years was in the 19th century. At this time there was not a single

living tree over the whole transect, and the upper timberline retreated up to 280 m a.s.l. During the 20th century there was a rather intensive regeneration of larch, and now 16 trees of 30-90 years old grow in the lower half of the transect.

Thus, during the last 1250 years the upper timberline and structure of larch stands altered significantly. The range of displacement of the upper timberline on the transect was 60 m in altitude and 430 m along the slope. In some parts of the Rai-Iz Massif this displacement was bigger (up to 80 m in altitude and 800 m along the slope). In the area of the upper timberline there was no evidence of fires or other catastrophic phenomena, the most probable reason of these displacements is climatic changes.

To reconstruct climatic conditions the mean ring-width chronology AD 745-1992 have been used. This chronology contains strong climatic signal, mainly June-July temperatures of current growth year. Reconstruction of this climatic parameter is shown in Fig.2. During the period investigated there were considerable annual, decadal and secular oscillations of summer temperatures. Changes in stand structure and altitudinal position of the upper timberline are caused by long-term oscillations of climatic conditions. Intensive dying off of trees in the area of the upper timberline coincides with cold periods no less than 20-30 years long. Most favorable climatic period for tree growth was during the 12-13th centuries when periods of long-term cooling were absent. The coldest period was during the 19th century when June-July temperature was 2-3°C below the average for two long periods. The long-term climatic fluctuations which have the biggest influence on forest ecosystem dynamics are rather poorly presented in this chronology due to detrending individual ring-width chronologies.

Acknowledgments

References

Graybill, D.A. & Shiyatov, S.G. 1992. Dendroclimatic evidence from the northern Soviet Union. Climate Since A.D. 1500. Raymond S. Bradley & Philip D. Jones, eds. London & New York: Routledge, pp.393-414.

Shiyatov, S.G. 1986. Dendrochronology of the upper timberline in the Urals. Moscow: Nauka, 136 pp. (in Russian).

Shiyatov, S. G. 1993. The upper timberline dynamics during the last 1100 years in the Polar Ural Mountains. Oscillations of the Alpine and Polar Tree Limits in the Holocene. Burkhard Frenzel, ed. Stuttgart, Jena & New York: Gustav Fischer Verlag, pp.195-203.

Climatic variations during the last 500 years in Finnish Lapland: an approach based on the tree-rings of Scots pine

Mauri Timonen

Finnish Forest Research Institute
Rovaniemi Research Station
P.O.B. 16, FIN-96301 Rovaniemi

Introduction

The tree-rings of Scots pine are sensitive to temperature changes of the summer months June and July (e.g. Hustich 1945, Mikola 1950, Sirén 1961, Lindholm et al. 1994). This is the case particularly in Lapland where temperature is clearly the minimum factor in tree growth while in Southern Finland it is precipitation. The correlation coefficient between tree-ring widths and the mean temperature in June-July may rise up to 0.70 in individual stands.

A typical pine in Lapland lives 200-300 years old, and it is easy to find over 400 years old individuals. The oldest known Scots pine tree ever found in Lapland, age 810 years, was found by professor Gustaf Sirén. Many of the small ponds and lakes of Lapland preserve submerged subfossil pines for thousands of years. This gives possibilities for examining climatic variations in tree-ring width almost to the end of the most recent Ice Age, about 10 000 years ago.

Extending climatic data to longer periods presupposes the use of proxy data , variables giving information indirectly about past climate. Tree-rings represent a reliable form of proxy data. Considered from this point of view. it is quite understandable that dendroclimatologists prefer to construct climatic models from tree-rings.

Trend studies

The research project, *"Variation and trends in tree increment"*, is the main dendroecologically executed project at the METLA (The Finnish Forest Research Institute). Special interest is paid to studying increasing growth and its components as observed in Finnish forests during the 1900s. At least four growth components are believed to have been re cognised: 1) the effect of natural cl imatic variation, 2) the effect of improved silviculture and changed stand structure 3) the effect of possible acidic deposition (e.g. nitr ogen) and 4) the effect of possible atmospheric CO_2 concentration.

The deposition component is expected to be available only in tree-rings of the 1900s. Separating the effects of climatic, acidic deposition and CO_2 components from tree-rings is problematic, because the only possible sources of tree-ring data, the natural forests, include all these components.

Direct temperature data or data other than tree-ring data are needed for estimating the effects of climatic variation in the 1900s. The measured temperature records in Lapland span about 90 years back in time. The oldest regular temperature observations were started in 1908 in Sodankylä.The relatively short time span of measured temperature data

does not enable one to make conclusions as to the causes of low-frequency oscillations in the climate. Do the present day annual climatic variations or the observed trend patterns differ in some way from those of the ancient times? Should the present phenomena be regarded as normal variation within a long time interval, or is something really happening?

Why are these kinds of studies done? Too many unfounded assumptions have been put forward as scientific facts for and against the ongoing climatic phenomena. Too little attention has been paid to the information potential of long-interval time series. In order to try to place present-day growth phenomena in their proper context, for instance the unexplained increasing growth of trees of the 1900s or forecasting of future forest growth, requires that we know what kind of growth patterns there were thousands of years ago. Once we know exactly the long-term influence of climate on tree-rings, we are also in a better position to judge more reliably the effects of environmental changes (e.g. nitrogen deposition). This also means that improvements must be made in adjusting growth models to the changing env ironments.

Modelling climate from tree-rings

Dendroclimatic studies at the METLA are based on nation-wide tree-ring data and advanced techniques for manipulating and analysing data. A very important part is played by the climatic trend surface model developed by Ojansuu and Henttonen (1983). The data of the model originate from the Finnish Meteorological Institute. Simply the geographical coordinates in a kilometer-based grid and the altitude are needed in order to get monthly mean temperatures, monthly precipitations and annual day-degree values from the model. The system covers the years 1880-1993.

The tree-ring data can be analysed by universal statistical packages and by some dendrochronological software. The most commonly used are the DPL (Dendrochronological Program Library), the DYNACLIM software and the KINDSYS package developed by the author.

The purpose in modelling is to construct reliable local chronologies and then use them for constructing temperature maps for the last 500 years. The derived temperatures will be used for calibrating the climatic variation of the 1900s. The time span of 500 years may be too short for this kind of approach. It is, however, possible to extend the span to at least 8000 years, which gives a far more reliable reference.

The quality of the tree-ring material presupposes careful cross-dating. Data, measurement errors and missing rings cause severe problems in pinpointing the climatic signals. Because of large quantities of older and uncrossdated data, it is time-consuming to prepare them for analysis. One of the old techniques, skeleton plotting, developed by A.E. Douglas (1941), has been re-developed further by the author. A new PC-based version, using laser printer techniques, produces sharp images for easy visual cross-dating (Fig.1).

Some basic temperature models from tree-rings (transfer functions) will be presented at the conference. They are based on multiple regression, and ridge regression techniques are used for minimising the effects of multicollinearity.
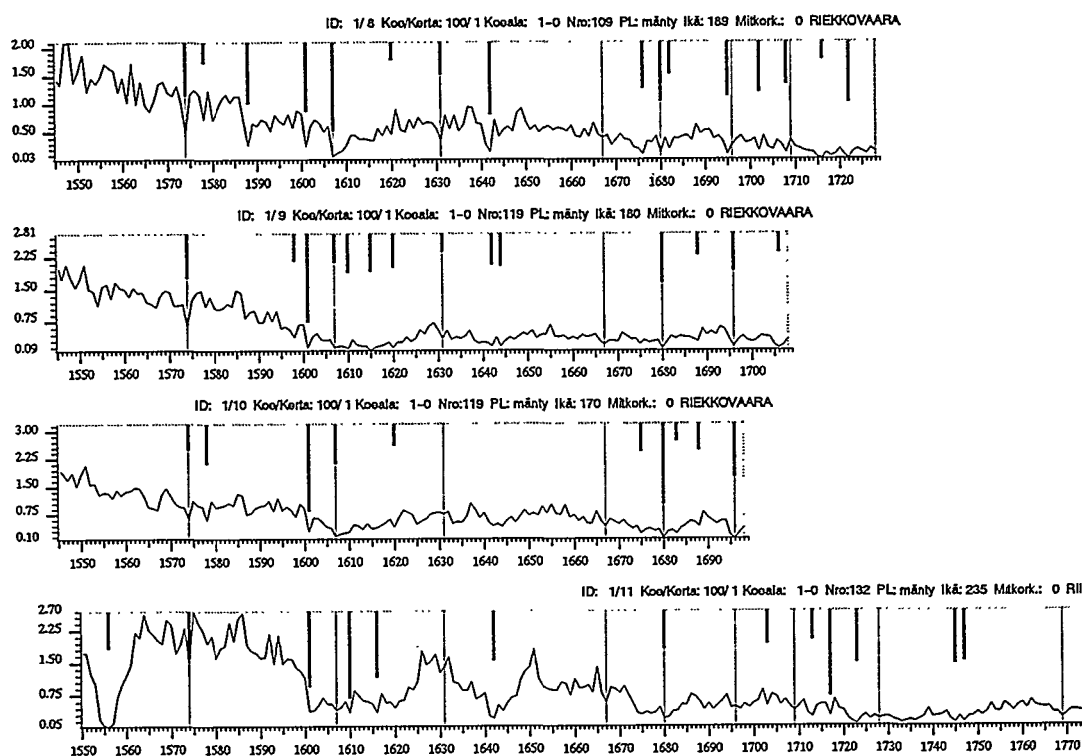
Fig. 1. An example of the skeleton plot technique used in the author's KINDSYS dendro-software. The thick bars indicate minimum points in the tree-ring data. The longer the bar, the deeper is the local minimum. The years where the bars occur frequently, are most probably climatic signals in large data. Other bars may be caused by tree-specific damage. The cross-dating checking is interpreted by the position of the bars: how they hit vertically on the same year.

References

Hustich, I. 1945. The radial growth of the pine at the forest limit and its dependence on the climate. Commentationes Biologicae, Societas Scientiarum Fen nica 9:11, 1-30.

Eronen, M., Zetterberg, P. & Lindholm, M. 1994. Climate history from tree rings in the subarctic area of Fennoscandia. This publ.

Siren, G. 1961. Skogsgränstallen som i ndikator för klimatfluktuationerna i norra fennoskandien under historisk tid. Commun. Inst. Forest. Fenn. 54(2), 1-66.

Ojansuu, R. & Henttonen, H. 1983. Kuukauden keskilämpötilan, lämpösumman ja sademäärän paikallisten arvojen johtaminen Ilmatieteen laitoksen mittaustiedoista. Silva Fennica 17(2).

A 7500-year pine tree-ring record from Finnish Lapland and its applications to palaeoclimatic studies.

Pentti Zetterberg[1], Matti Eronen[2] and Keith R. Briffa[3]

[1]Karelian Institute, Section of Ecology, University of Joensuu, P.O. Box 111, FIN-80101 Joensuu, Finland
[2]Department of Geology, University of Helsinki, P.O. Box 11, FIN-00014 University of Helsinki, Finland
[3]Climatic Research Unit, University of East Anglia, GB-Norwich NR4 7TJ, U.K.

Introduction

Subfossil trees, dated precisely by dendrochronology, can significantly increase our knowledge of climate history. The abundance of subfossil pines (*Pinus sylvestris* L.) in northern Fennoscandia makes it possible to develop long chronologies of tree growth and explore the long-term stand history of pine over thousands of years. The comparison of data from several sites will identify common changes in tree growth which represent important evidence of past climate changes. Pine spread over northern Fennoscandia by 8000-7500 BP. Sites well beyond the limits of the present distribution of pine were popu- lated under favourable climatic conditions 7000-5000 BP. The maximum spread of pine occurred between 6000 to 4000 BP and was.followed by a retreat during the following millennia (Hyvärinen 1976, Eronen & Huttunen 1993). Pine is a relatively long-lived tree species and the ring-width variability is clear, making reliable dendrochronological dating possible. In areas where trees grow in marginal environments the control of annual growth by environmental factors, particularly climate, is strong and clearly discernible. In the polar/alpine pine forest limit in northern Fennoscandia the variations in tree-ring width are very similar across a wide area. Ring-width series correlate over large areas and this allows short gaps in one site-record to be bridged with data from other sites.

Materials and methods

A total of 1265 subfossil Scots pines has been sampled from 38 sites in northern Finland and adjacent areas of Norway. The sampling sites are mostly small lakes in the timberline zone located between 68°30' N and 70°00' N and at elevations ranging from 75 m a.s.l. to 515 m a.s.l. (Fig. 1). Individual lakes normally yielded several tens of subfossil logs. Over 100 pine trunks were collected from five small lakes, the record being a lake where a total of 219 subfossil pine trees were sampled. Best sites for the preservation of subfossil trees are small ponds with a thick layer of mud on the bottom. The trunks totally embedded in the soft sediment can be located by the help of divers. The longest trunks are up to 15 m long and the maximum diameter is more than 50 cm. Sample discs were cut by chainsaw about 1 - 1.5 m above the original root plate and higher up from the trunk in case when the
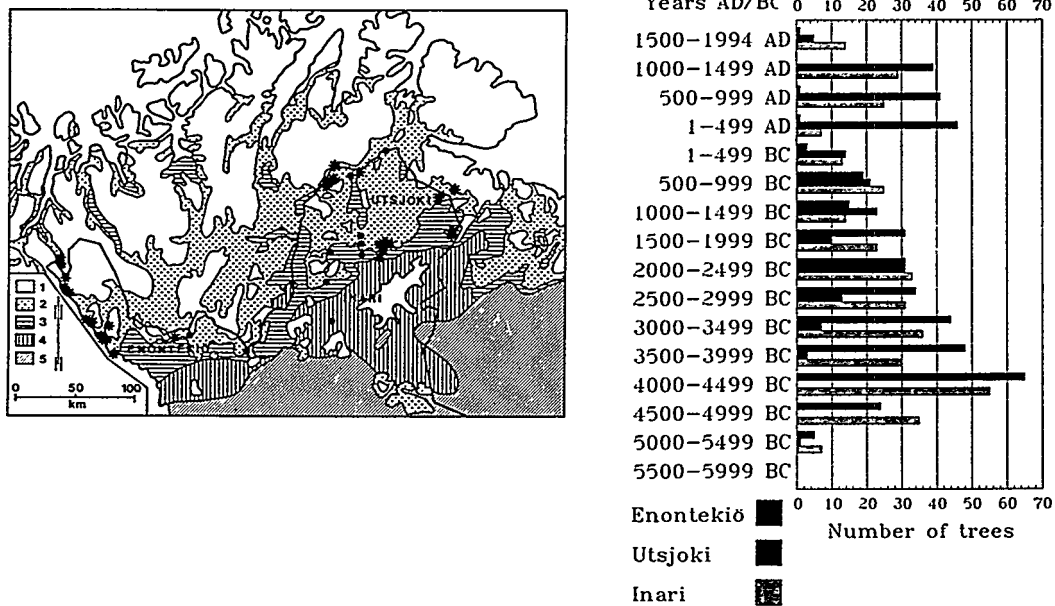
Figure 1 (left). Subfossil pine locations in Finnish Lapland and adjacent areas. The asterisks indicate sites, mainly small lakes, where dendrochronological samples have been collected and black dots show the sites of other pine subfossil dates. The forest vegetation zones of northern Fennoscandia are also shown. 1. Tundra, 2. Birch woodland, 3. Birch and pine forest, 4. Pine forest, 5. Pine and spruce forest.

Figure 2 (right). Age-distribution of dendrochronologically dated subfossil pines from the forest limit zone in subarctic Fennoscandia

lower part of tree was not preserved. Measurements were made under the microscope, along two to four radii. The mean value of these measurements was used to produce the tree-ring curves for individual trees. This replication facilitates the identification of partially 'missing' rings and averaging the data across radii reduces the 'within-tree' noise. The cross-dating of samples was achieved initially by statistical correlation between series but was always confirmed by visual inspection of the ring-width graphs.

Results and discussion

A total of 970 subfossil trees have been dated by dendrochronology in this study. The age distribution of the dated samples is given in Fig. 2. In the Figure the material has been divided in three parts based on the origin of the samples: Enontekiö, Utsjoki and Inari areas. The continuous tree-ring curve based on the dendrochronological dating extends more than 2000 years before present, to the year 165 BC. Over 200 subfossil trees from several sites in northernmost Finland are incorporated within this absolute chronology and sample replication is more than 20 trees in most parts. Thus the northern Finland absolute chronology can be regarded as a master curve and as such it is the longest for northern Europe, so far. Most of the dated trees (ca. 750 samples) belong to the older part of the long master chronology, which is fixed to the time scale by radiocarbon dates. This continuous part of the master chronology extends over more than 5000 years from ca. 7500 calBP. The 150-200 years long gap separating the older part from the younger

absolute chronology can probably be bridged in the near future. Together with the subfossil trees we have also collected tree-ring samples from a large number of living forest-limit pines, which have been used for construction of the youngest part of the Finnish Lapland master chronology. Tree-ring measurements from beams of old houses in northern Lapland were also of great importance in cross-matching the curves derived from living and subfossil trees.

The subfossil pine material has been used for studies on the Holocene climatic history, growth variations, year-to-year variability in ring-widths, periods of germination and mortality, population size and age structure at the sampling sites (Zetterberg et al. 1994) and tree-line changes (Eronen & Zetterberg, in press). These combined data are good indicators of diverse environmental changes in the past. When developing the site chronologies we have not applied any 'standardization' (i.e. correction to remove the age-related trends in individual series) in the chronology construction in order to maintain all possible long-timescale variation (cf. Cook et al. 1995). Thus the data contain some sample-age-related bias in different periods. Detailed tree-ring patterns showing the growth variations in northern Finland are already available for two periods in mid- to late-Holocene times. The data for the period 4500-3000 B.C. suggest increased variability in tree growth after 3800 B.C. The mid-Holocene climatic change at this time may have thus been largely the result of a shift towards less stable growing conditions (Zetterberg et al. in press). For the late Holocene period from 165 B.C. to the present, growth and climate variations have been studied with a dating accuracy of one year (Zetterberg et al. 1994). The mean annual growth has varied notably through time being highly dependent on growing conditions at each site, but when the material is considered as a whole, the mean ring width has remained rather constant in the long term, being approx. 0.6 mm. The data from the Holocene climatic optimum and late Holocene do not differ from each other in this respect. In northern Fennoscandia the growth of tree-limit pines is very strongly correlated with summer temperatures, which has permitted the reconstruction of past summer temperature variations (Briffa et al. 1990, 1992). Climatic stress, such as extremely cold conditions, influences the number of trees dying. The variations in germination and dying off of trees can be used as a complementary source of information on past growing conditions (Zetterberg et al. in press). In marginal environments, such as the polar/alpine tree line, the tree population usually increases during favourable, relatively warm periods than during unstable or cold times. Subfossil logs have been found even tens of kilometres beyond the present limit of pine, and at altitudes above the highest present occurrences of pine trees, indicating more favourable conditions thousands of years ago.The new dated trees corroborate the earlier conclusion that the pine forests reached their maximum extent in northern Fennoscandia during mid-Holocene time, 4900 - 2500 BC (cf. Eronen and Huttunen 1993). The subsequent retreat shows somewhat different patterns in different regions, but the general trend is stepwise dying out and receding from the outmost growing sites (Eronen & Zetterberg, in press).

The future aims of this research include: 1) bridging the short gap in the tree-ring data and extending the chronology further back in time, 2) developing several continuous site chronologies as long as possible, 3) detailed study of the growth variations and their climatic interpretations , 4) comparing the results and combining data with subfossil tree-ring data from the Lake Torneträsk area, northern Sweden (Briffa 1994). The 7500-year pine master chronology is well suitable for dating of subfossil pines and archaeological pine-wood from wide area in northern Fennoscandia already at present even though it is not fully complete.

Acknowledgements

References

Briffa, K.R. 1994. Mid and late Holocene climate change: evidence from tree growth in northern Fennoscandia. In: Funnell, B.M and Kay, R.L.F. (eds.) Palaeoclimate of the last glacial/interglacial cycle. Special Publication of the NERC Earth Sciences Directorate 94/2, 61-65.

Briffa, K.R., Bartholin, T.S., Eckstein, D., Jones, P.D., Karlén, W., Schweingruber, F.H. and Zetterberg, P. 1990. A 1400-year tree-ring record of summer temperatures in Fennoscandia. Nature 346, 434-439.

Briffa, K.R., Bartholin, T.S., Eckstein, D., Schweingruber, F.H., Karlén, W., Zetterberg, P. and Eronen, M., 1992. Fennoscandian summers from AD 500: temperature changes on short and long timescales. Climate Dynamics 7, 111-119.

Cook, E.R., Briffa, K.R., Meko, D.M, Graybill, D.A. and Funkhouser, G., 1995. The 'segment length curse' in long tree-ring chronology development for palaeoclimatic studies. The Holocene, 5: 229-237.

Eronen, M. and Huttunen, P., 1993. Pine megafossils as indicators of Holocene climatic changes in Fennoscandia. Paläoklimaforschung - Palaeoclimate research, 9: 29-40.

Eronen, M. and Zetterberg, P., in press. Expanding megafossil data on Holocene changes at the polar/alpine pine limit in northern Fennoscandia. Paläoklimaforschung - Palaeoclimate Research 20.

Hyvärinen, H., 1976. Flandrian pollen deposition rates and tree-line history in northern Fennoscandia. Boreas 5, 163-175.

Zetterberg, P., Eronen, M. and Briffa, K.R., 1994. Evidence on climatic variability andprehistoric human activites between 165 B.C. and A.D. 1400 derived from subfossil Scots pines (Pinus sylvestris L.) found in a lake in Utsjoki northernmost Finland. Bulletin of the Geological Society of Finland, 66: 107-124.

Zetterberg, P., Eronen, M. and Lindholm, M., in press. The mid-Holocene climatic change around 3800 B.C: tree-ring evidence from northern Fennoscandia. Paläoklimaforschung - Palaeoclimate Research 20.

Historical climatology
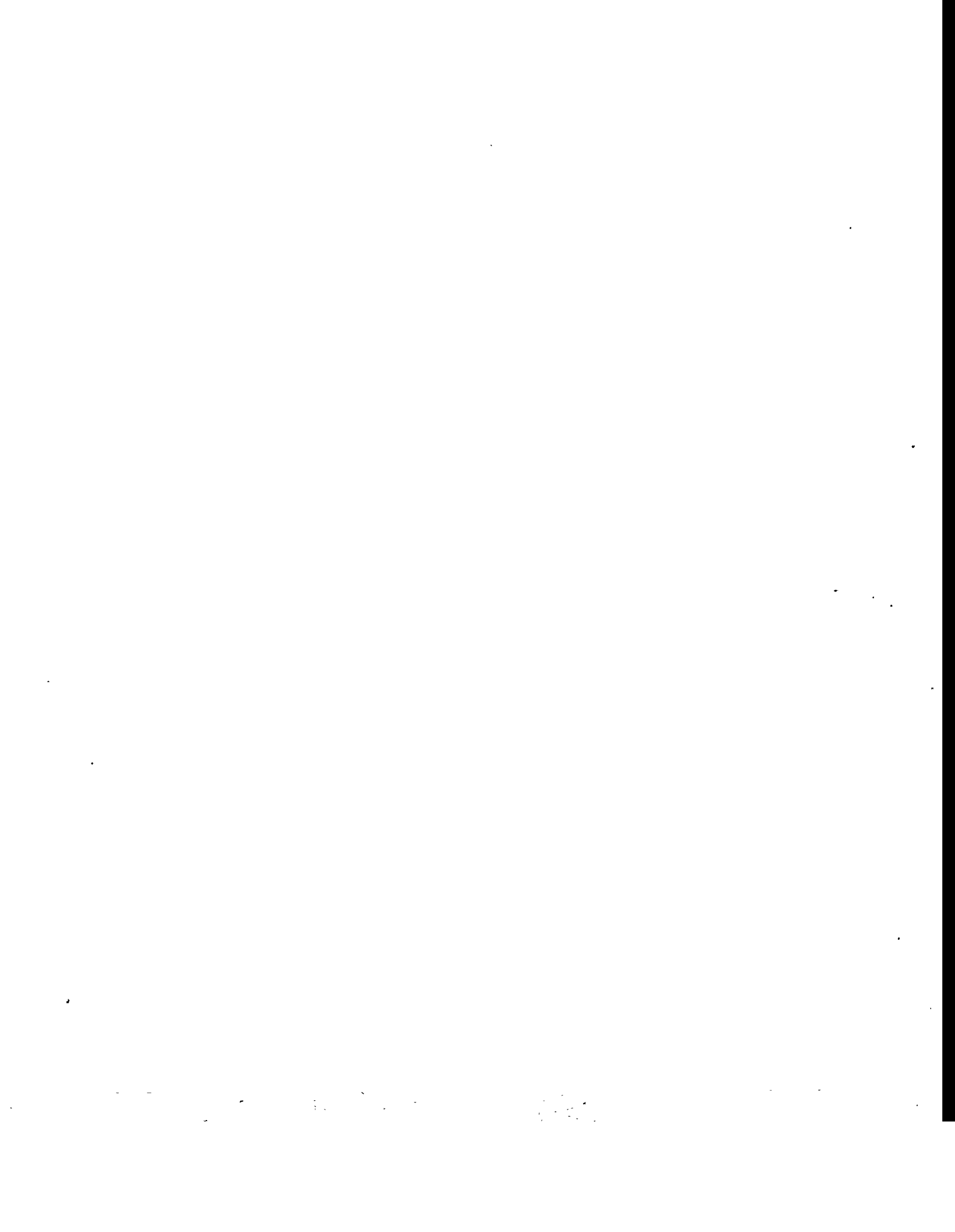
CLIMATIC FLUCTUATION IN THE LAST TWO THOUSAND YEARS

Rudolf Brázdil[1] and Oldřich Kotyza[2]

[1]Department of Geography, Masaryk University, Brno, Czech Republic
[2]District Museum of Local History, Litoměřice, Czech Republic

Introduction

The period of the last 2,000 years is usually divided into the so-called Subatlantic period (about 700 B.C. - 600 A.D.) and the Subrecent period (from 600 A.D. up to the present). From the climatic point of view, a drop in temperature and an increase in precipitation should have occurred in comparison with the preceding Subboreal period. Within the Subrecent period are classically delimited a warmer period, the so-called Medieval Warm Epoch (MWE, about 800-1300 A.D.) and a colder one, the Little Ice Age (LIA, about 1550-1850 A.D.), separated by a period of unsettled and deteriorating climate in the Late Middle Ages (Lamb, 1984). The submitted contribution is an attempt at summarising the knowledge of the fluctuation of the climate in the Czech Lands during the last 2,000 years.

Data

Since the longest continuous instrumental series in the Czech Lands date back to the latter half of the 18th or the beginning of the 19th centuries, the reconstruction of the climate can only be based on different proxy data:

a) Written evidence about weather and related phenomena
The earliest credible written record from the sources of Czech provenience comes from the Monk of Sázava about winter of 974/75 ("very severe and unpleasantly long"). Directly to the territory of Bohemia is related Kosmas report about the great heat on 22-23 August, 1040. The number of reports is very low until the mid-13th century and also for some later time periods of different length (Brázdil 1995, Brázdil & Kotyza 1995).

b) Archaeological evidence
The climate reconstruction can start from the study of: movements of the settlement in higher positions and in the flood plains of water streams; the intensity of settlement reflecting the operation of climatic conditions on the possibilities of agricultural

utilisation of the landscape and on ecological development; the development of the natural environment in connection with human culture (Brázdil & Kotyza 1995).

c) Natural evidence

The existing dendrochronological series reach only to the end of the 18th century, older ones are now analysed. Pollen analyses have limited possibilities due to a strong anthropogenic activities in this region. Rougher climate interpretations are connected with archaeobotanical remnants. More recently, also the analysis of borehole temperatures can be utilised (for natural evidence see Brázdil & Kotyza 1995).

Climate fluctuation during the first millennium A.D.

With the absence of written sources, in the study of the climate in the first millennium A.D., priority sources are archaeological, palynological and sedimentological. Despite their considerable torso character and limitation, they can at least be utilised for characterising general climatic trends. It can be concluded that the whole first millennium was prevailingly warmer and drier (Fig. 1), which is also confirmed by palynological reconstructions for Padrtiny in the Bohemian-Moravian Highlands (Chernavskaya, 1992a). One of the exceptions was a moister and colder period between about 300-425 A.D., characterised by the retreat of settlements from higher positions and from the lowest river terraces (found out also in the near Saxonia - Gühne & Simon 1985). But according to Chernavskaya (1992b) this period was rather dry. Also within long warm and dry periods moister climatic microphases were registered, whose duration, however, did not exceed about 50 years - in the course of the 2nd century, the 8th century, between about 900-950 A.D., and at the turn of the 10th and the 11th centuries. On the whole, in the first millennium A.D. the climate rather approached the long-term central European average, which is also indicated by the results of archaeological and palaeobotanical research studies from Roztoky near Prague (see Sádlo & Gojda 1994).

Climate fluctuation during the second millennium A.D.

The Czech Lands during the greater part of the last millennium experienced rather cold winters and warm summers, indicating a more continental character of the climate. According to written evidence reconstructed Czech series (Fig. 2) do not indicate the existence of the MWE, delimited by Lamb (1984) in central Europe by the period of about 1150-1300. On the other hand, colder and wetter years from the mid-15th century to the beginning and/or the latter half of the 17th century can be probably considered as an expression of the LIA in the Czech Lands (more severe and wetter winters, colder springs and wetter summers). Its last impact fell on the period about the middle of the 19th century, when the lowest temperatures for the whole instrumental period were measured. Then temperature series indicate conspicuous warming, probably overestimated due to the intensification of the urban heat island of Prague-Klementinum. On the other hand, according to interpretation of measurements of 11 borehole temperatures for the Czech Republic, warming was indicated with the peak for 1240±30 and cooling for 1680±40 (Bodri & Čermák 1994). Their results are partly different from our results based on analysis of written evidence (see the MWE).
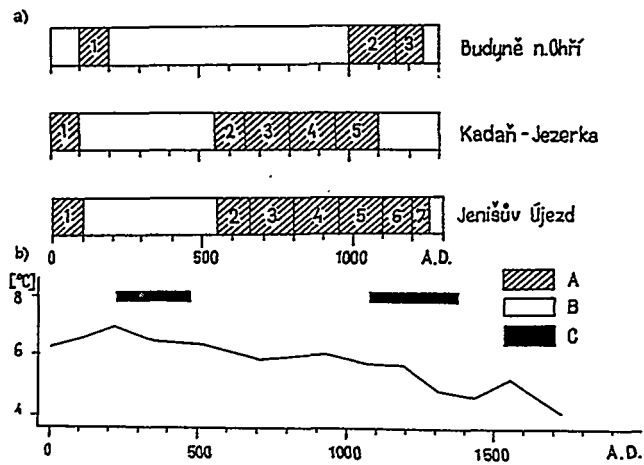
Fig. 1. a) The development of the settlement in the flood plain for selected localities in the Czech Republic: A - settlement, B - hiatus in the settlement (Kotyza 1995); b) Annual air temperature and dry period (C) reconstructions according to high bog stratigraphy at Padrtiny - Bohemian-Moravian Highlands (Chernavskaya 1992a,b)
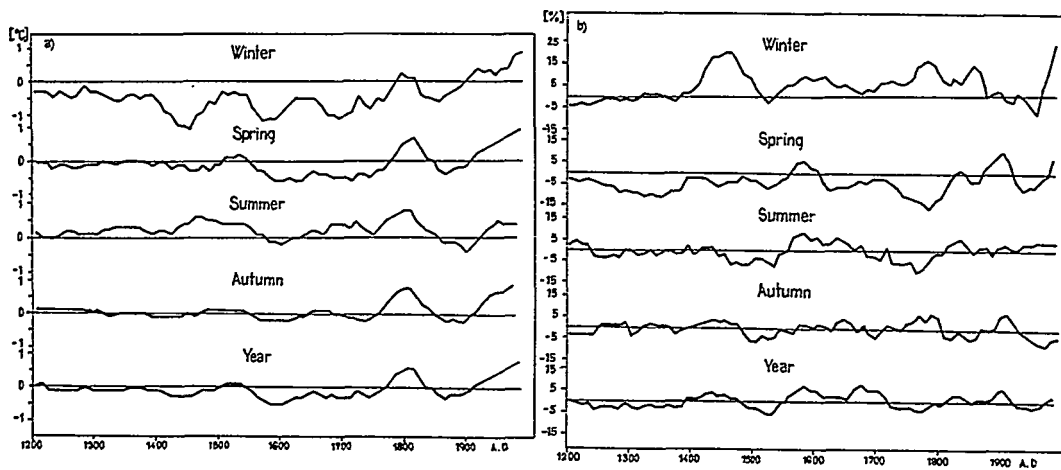
Fig. 2. Fluctuations of air temperature (a) and precipitation (b) for Prague-Klementinum (1200-1989) plotted as anomalies from the 1851-1950 mean, smoothed by running averages of five decades. Reconstruction is based on quantitative interpretation of written records (see Brázdil 1995) and instrumental measurements (from 1771 for air temperature and from 1804 for precipitation)

Conclusion

Presented results of climate fluctuation of the Czech Lands during the last 2,000 years are consequence of possibilities of existing proxy data. They are often insufficient, so different proxy data cannot be cross-checked. But despite this fact, the reconstructed Czech series show a good agreement with the climate fluctuation in a broader European area (see e.g. Willerding 1977, Brázdil 1995). Further improvement

of results depends on possibility to extend amount and quality of proxy data. Above results are in agreement with fact that the available evidence does not support a global character of the MWE or the LIA (Jones & Bradley 1992, Hughes & Diaz 1994).

References

Bodri, L. & Čermák, V. 1994. Climate change of the last millennium inferred from borehole temperatures: results from the Czech Republic. Manuscript.

Brázdil, R. 1995. Reconstructions of past climate from historical sources in the Czech Lands. In: NATO Advanced Research Workshop, Il Ciocco, in press.

Brázdil, R. & Kotyza, O. 1995. History of weather and climate in the Czech Lands I (Period 1000-1500). Zürcher Geogr. Schriften, Zürich, in press.

Chernavskaya, M.M. 1992a. Personal communication.

Chernavskaya, M.M. 1992b. Proyavleniye kolebaniy uvlazhnenosti v stratigrafii verkhovykh bolot. Materialy Meteorol. Issled. 15:110-115.

Gühne, A. & Simon, K. 1985. Frühe Siedlungen am Elbübergang in Dresden-Neustadt. Arbeits- u. Forschungsber. sächs. Bodendenkmalpflege 30:187-343.

Hughes, M.K. & Diaz, H.F. 1994. Was there a 'Medieval Warm Period', and if so, where and when? Climatic Change 26:109-142.

Jones, P.D. & Bradley, R.S. 1992. Climatic variations over the last 500 years. In: Bradley, R.S. & Jones, P.D., eds.: Climate Since A.D. 1500, Routledge, London, 649-665.

Kotyza, O. 1995. Climate fluctuation during the first millennium. In: Růžičková, E., Zeman, A., eds.: Climate change in the last Holocene. Geological Institute CAS, Prague, in press.

Lamb, H.H. 1984. Climate in the last thousand years: natural climatic fluctuations and change. In: Flohn, H., Fantechi, R., eds.: The Climate of Europe: Past, Present and Future, D. Reidel, Dordrecht, Boston, Lancaster, 25-64.

Sádlo, J. & Gojda, M. 1994. Pokus o geobotanickou rekonstrukci vývoje kulturní krajiny (Raný středověk - současnost). Archeol. Rozhl. 46:191-204.

Willerding, U. 1977. Über Klima-Entwicklung und Vegetationsverhältnisse im Zeitraum Eisenzeit bis Mittelalter. In: Jankuhn, H., Schützeichel, R. & Schwind, F., eds.: Das Dorf der Eisenzeit und frühen Mittelalters. Siedlungsform - wirtschaftliche Funktion - soziale Struktur. Göttingen, 357-405.

Natural calamities in history and solar activity (based on chronicle annals)

Dmitrieva I.V., Zaborova E.P., Obridko V.N.

IZMIRAN, Troitsk, Moscow region, Russia.

Introduction

The question of whether solar activity variations exert any effect on the climate has been under investigation since long ago. In a number of recent works (e.g., Lebedeva, 1979, Girskaya, Sazonov et al. 1981; Efanova, 1981; Iasamanov, 1991) the authors tried to establish relation between some natural calamities and solar activity. As a result, it was shown that the solar activity/climate coupling is very complicated and its mechanism is not clear enough. The works cited above are based on the analysis of either too long (several millennia), or too short (several decades) time series. Long series are usually composed of the data from diverse sources, whereas short series are insufficient for reliable rating of the significance of natural phenomena. We made an attempt to overcome this difficulty by comparing information on disastrous natural events and information solar activity available in the chronicle annals, thus introducing some uniformity in the data series.

Data and methods

The chronicle data on natural phenomena observed in Europe and in Russia from year 0 through 1600 were collected and published by Borisenkov and Pasezky (1988). We have analyzed year by year the distribution of severe winters, strong draughts, epidemics, epizootics, and hunger, summarizing the number of events for every 50 years. Since the quality of the chronicle records improved with the development of communication facilities, we normalized the annalistic data to the information trend (assumed linear), and used the normalized data in our further analysis. Solar activity data are the data on sunspots visible by naked eye. They

were reconstructed from Chinese and European chronicles of observations of the Sun (Leftus 1986)& These data were not normalized.

Results and discussion

We have compared the data on draughts and on sunspot numbers. As shown by the analysis, the maximum occurrence of draughts either coincides with the sunspot maximum or is observed in the growth phase of solar activity (see Fig. 1), which is corroborated in (Girskaya, Sazonov et al., 1981). The same study was carried out for very cold winters. However the correlation with solar activity was not as pronounced as in the previous case (see Fig. 1)& One can only state that the greatest number of severe winters is usually recorded in the years close to the maximum or minimum of solar activity.

Comparison of periodograms of the series under investigation obtained by Fourier method also yields interesting results. The data of solar activity and draughts clearly reveals a 250-year period, which is less pronounced in the data for epidemics and epizootics, and is practically absent in the data for hungers and cold winters (see Fig. 2).

As shown by Serdyuk and Kotlar (1981) and by Sazonov and Scheremetova (1985), the principal role among the factors triggering draughts belongs to anticyclone circulation. So long as a certain dependence exists between the atmospheric circulation and the solar activity, the latter should manifest itself in the occurrence of draughts (Molodych 1985), whereas its relation to cold winters is not as direct. The periodicity of epizootics is rather determined by draughts than directly by solar activity. As to hungers, they do not reveal noticeable correlation with any natural factors, either in dynamics or in spectrum. Their cause should be most likely sought for in social and political spheres.

Acknowledgments
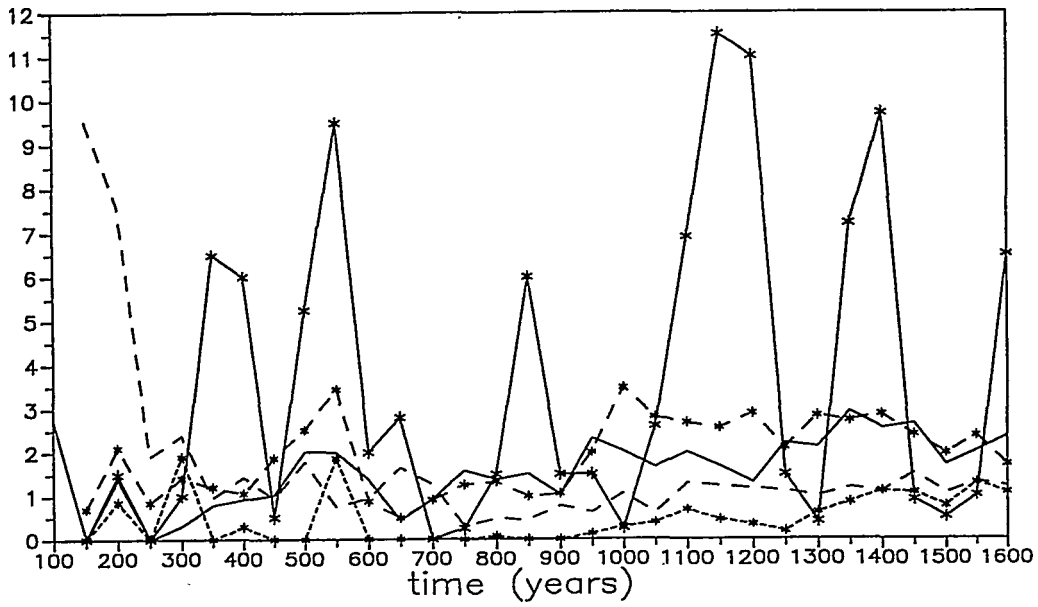
Fig.1 Data versus time: ——*—— sunspots, — —*— — draughts, □□*□□ epidemics and epizootics, ———— colds, — — — — — hungers.
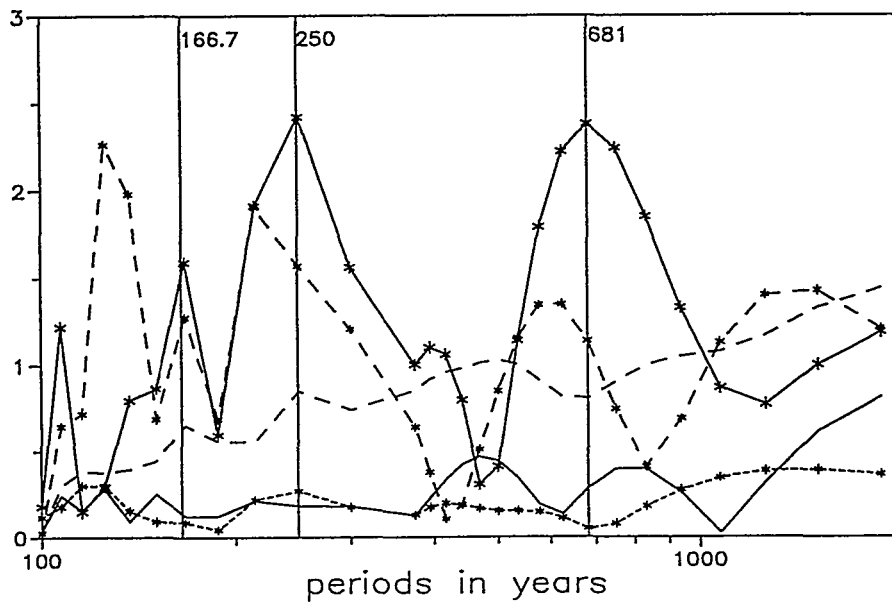
Fig.2   Periodograms: ——*—— sunspots, — —*— — draughts, □□*□□ epidemics and epizootics, ———— colds, — — — — — hungers.

References

Borisenkov E.P. and Pasezky V.N. Thousand-year annals of extraordinary natural phenomena. M.: Mysl, 1988.

Efanova A.V. Relationship between solar activity and severe winters. Trudy GGO (Proceedings of the Main Geophysical Observatory), 1981, issue 443, p. 28-34.

Iasamanov N.A. Climate periodicity. Cycles of natural processes hazardous events, and ecological forecasting, issue 1, Proceedings of the N.D.Kondratyev Centenary International Conference, 1991, p. 81-88.

Girskaya E.I., Sazonov B.I., and Ulianova T.N. Draught Catalogues in the USSR and geomagnetic activity. Trudy GGO (Proceedings of the Main Geophysical Observatory), 1981, issue 443, p. 24-27.

Lebedeva A.N. Relation of the most damaging weather events in the Tatar Republic to sunspots. In: Proceedings of the Kuibyshev HMO, 1979, issue 10, p. 40-47.

Leftus V. Solar activity variations and climatic changes. Studia geoph. et geod. 30, 1986, p.93-110.

Molodych V.A. Some regularities in variations of the continental climate. Trudy GGO (Proceedings of the Main Geophysical Observatory), 1985, issue 486, p. 107-110.

Sazonov B.I. and Scheremetova L.M. Atmospheric circulation conditions in the North hemisphere during draughts. Trudy GGO (Proceedings of the Main Geophysical Observatory), 1985, issue 486, p. 96-99.

Serduk V.N. and Kotlar I.V. Macrosynoptic features in the development and movement of anticyclones during the draughts in 1963, 1972, and 1975. Trudy GGO (Proceedings of the Main Geophysical Observatory), 1981, issue 443, p. 50-59.

Swedish meteorological data since the 18th century: temperature trends and data homogenisation

Anders Moberg[α] and Hans Alexandersson[β]

[α] Department of Physical Geography, Stockholm University,
   S-106 91 Stockholm, Sweden
[β] Swedish Meteorological and Hydrological Institute,
   S-601 76 Norrköping, Sweden

Introduction

The Standard Normal Homogeneity Tests (SNHT) for single shifts (Alexandersson 1986) and trends (Alexandersson, unpublished manuscript A) have been applied to approximately 100 Swedish monthly mean temperature records having minimum lengths of 50 years. A number of similar records from Denmark, Finland and Norway from sites near the Swedish territory were also included in the tests. The temperature records were divided into groups of about 5 to 10 records each, according to the locations and climatic conditions of the individual stations, before the tests were made. Temperature records that exhibited no significant non-homogeneities or only reasonably small non-homogeneities were used for one or two of the following two purposes: 1) Construction of a gridded (5° long X 5° lat) data set of monthly temperature records for the period 1860-1993. This data set consists of six grid box series that represent one part each of the Swedish territory and also (in the case of four of the grid boxes) parts of the territories of the neighbouring contries. 2) Homogenisation of the second half of the long Stockholm temperature record beginning in 1756.

Earlier results and their implications

Grid box temperatures

In a recent study (Moberg and Alexandersson, unpublished manuscript), monthly temperature records were calculated for three of the grid boxes used here. The three temperature records were primarily used for a test of the corresponding temperature records for the same grid boxes selected from the hemispheric gridded data set of Jones (1994). Moberg and Alexandersson found that only a small part of the warming trend observed since 1901 in Jones's data were present in data selected from the archive of the Swedish Meteorological and Hydrological Institute. The study, however, lacked statistical rigour and the individual temperature records used were selected on basis of earlier experience, where proper references to homogeneity test results could not be made. The large discrepancy found in relation to Jones's data implied that it is of importance to perform of a more thorough study. Such a study is presently

undertaken, where the six new grid box temperature series are used for SNHT-testing the corresponding Jones's data and for analyses of temperature trends in the regions represented by the grid boxes. At the time of writing, only preliminary results are at hands. Definite results will be presented at the conference.

The Stockholm air temperature record

The Stockholm air temperature record has frequently been used in analyses of climatic changes of the past c. 250 years in Europe. This temperature record has sometimes in the older literature been considered to be homogeneous. However, Moberg (1992) and Alexandersson (unpublished manuscript B) demonstrated that the record has clearly been affected by an urban heating, at least during the present century. Moberg also pointed out some possible causes of non-homogeneities in the older part of the record. Comparisons (Moberg) of the Stockholm temperature record with a composite reference series indicated a warming by 1.0 °C of the annual temperature in Stockholm in relation to the surroundings during the period 1860-1970. In a similar study, covering only the present century, Alexandersson observed a warming by 0.54 °C during the period 1925-45. The difference between these two results is so large that not both of them can be considered as good estimates of the urban heating trend in Stockholm.

Therefore, a more thorough study is presently undertaken, where the set of reference stations is selected on basis of results from the homogeneity tests made within the grid box study. The urban heating trend is estimated by using the newly developed SNHT for a trend of arbitrary length. Comparisons are also made with the long temperature record from Uppsala, beginning in 1722. While this study is made simultaneously with the grid box temperature study, the results presently at hands are also only preliminary. The final SNHT results and analyses of temperature changes in Stockholm and Uppsala since the mid-1700s will be presented at the conference.

References

Alexandersson, H. 1986. A homogeneity test applied to precipitation data. J. Climatology 6: 661-675.

Alexandersson, H. (unpublished manuscript A). Temperature variations in Sweden. Part I: A homogeneity test for linear trends.

Alexandersson, H. (unpublished manuscript B). Urban effects on Nordic temperature data.

Jones, P.D. 1994. Hemispheric surface air temperature variations: A reanalysis and an update to 1993. J. Climate 7: 1794-1802.

Moberg, A. and Alexandersson, H. (unpublished manuscript). Urban bias trend observed in the Swedish part of gridded temperature data.

Moberg, A. 1992. Lufttemperaturer i Stockholm 1756-1990. SMHI Meteorologi 83. Sveriges Meteorologiska och Hydrologiska Institut. Norrköping, 45 pp. (English abstract)

The "cold-wet" famines of the years 1695 - 1697 in Finland and manifestations of the Little Ice Age in Central Europe

Jan Munzar

Institute of Geonics, ASCR
P.O.B. 23, CZ - 613 00 Brno, Czech Republic

Introduction

The nineties of the seventeenth century belong to the coldest decades of the Little Ice Age in Europe. The unusual course of weather in the years 1695 - 1697 has resulted in a great famine that has struck Finland, Estonia and today's Latvia and Lithuania. It was estimated that the casualties only in Finland have reached 25-33%, and in Estonia around 20% of the total population (Neumann and Lindgrén 1979, Vesajoki and Tornberg 1994).

At present an intensive work is being done on the reconstruction of the course of weather in Europe in the historical age, and the period of the end of the 17th and beginning of the 18th centuries is considered a "key period for studying rapid climate change in Europe" (Wanner and Pfister 1994). Within the bounds of monitoring the historical environmental changes for the needs of looking for an analogue of the future development we have therefore raised a question how has the above period manifested itself in Central Europe.

Weather in Finland in the years 1695 - 1697

It is documented in historical sources that both 1695 and 1696 were highly exceptional, with variable weather, cold summers and failed harvests, resulting in a severe famine. What was the concrete course of the "confused seasons" of this period like?

The beginning of the year 1695 is said to have been colder than any winter since 1658. Spring came late and was so cold that sowing could not be completed before midsummer. The summer was cold too and rainy, and the cereals could not ripen before a devastating frost came in September. In the good agricultural area of the province of southern Finland the harvest did not amount to more than one third of "normal". Furthermore, the autumn was rainy, which made it impossible to carry out the autumn sowing in many areas.

The first months of 1696 were mild. In the southernmost part of Finland the snow and· ice melted, and the leaves came out on the trees and bushes as early as in January. Then, on March 7th, winter returned. Lakes and bays of the sea froze again so that people could drive across them. Spring arrived late, and the summer was so rainy that the ripening of the crops proceeded slowly. On the night of August 17th to 18th, the first frost occured, and in the morning the ears of cereals were coated with a layer of ice. Two weeks later four consecutive nights of frost completely destroyed the crops as a whole (Vesajoki and Tornberg 1994).

These miserable conditions are reflected in the tree-ring record too. Early spring followed by a cold early summer have caused that the ring for the year 1696 was the narrowest of the whole reconstructed period of 1450 - 1984. Thus it may be concluded that the weather in Finland has never been as unfavourable as it was in 1696 (Eronen. et al. 1994).

The year 1697·has begun as cold, and the spring was long. Although the weather was more or less favourable during the following period of the year, in comparison to the preceding years this one became an even worse "year of mass death" because of the total lack of seed (Vesajoki and Tornberg 1994).

Weather in the Czech Republic and the neighbouring countries in the years 1695 - 1697

In Germany the year 1695 has been characterized as uncommonly cold and wet, and as one of the coldest years of the Little Ice Age (Lindgrén and Neumann 1981). It can be supposed that a severe winter of 1695 has also occured in the territory of the Czech Republic as it was recorded in Slovakia as well; for the time being, however, it has not been documented (this is probably connected with a low density of information about weather from this period). For the present we only have data on warm half-year from Bohemia and Moravia (Munzar 1995 a).

June of 1695, when an exceptional fall in temperature has occured, was especially unfavourable. From June 2nd three severe ground frosts have been reported in north-west Bohemia which have destroyed vineyards. In Moravia the cold first half of June 1695 has been documented in many localities. In Brtnice a hard frost and an ice layer at the thickness of two fingers has been mentioned from June 2nd to 15th. In Boskovice it was snowing on June 3rd and the frost was so hard that both the water in the square and the field crops have frozen. The overall damage to the cereals caused by frost has been made even worse by a comparatively wet July and an unusual number of mice before harvest. In north Bohemia frost has set in again on August 25th; there was soft rime in the morning, and from September 15th to 19th 15 cm of snow has fallen. The crop was poor and grapes did not ripen at all.

A mild winter is confirmed - analogously to Finland - in 1696. In north Bohemia a short winter is mentioned so that rye and oats could have been sowed in January. It was similar in Moravia where people ploughed at Shrovetide. In his evaluation of the winter' of 1695/96, a Slovak chronicler confirms the "confused seasons" in the following way: "Some would swear that seasons have changed. There was the last summer and

winter, and now winter is changing into summer to such a degree, that there is nothing winter-like in winter. Even in the usually coldest months there is no cold, no frost, no snow, shortly winter has been the warmest season" (Réthly 1962).

A cold spring with numerous ground frosts has followed (Bohemia). In the second week of Lent (between March 11th and 17th, 1696) it snowed in Moravia, and the snow lasted for a week. On April 23rd it again snowed so much that people could sledge, and even more snow came on May 1st, 1696. According to a chronicler of Bratislava, there were similarly quite hard frosts in Slovakia at the end of March. The weather was very severe, there was frost and snow at night, but it did not last long and changed into rain during the day. April also was not milder; in accordance with the nature of April the weather was very unsettled... Spring resembled winter very much and not spring but winter diseases emerged (Réthly 1962). In north Bohemia an unusual frost was mentioned on June 10 th, 1696, which has damaged vineyards, and there was also a locust invasion in the same year. In Moravia the year 1696 is, generally evaluated as lean with high cost of living.

As far as the character of tree-rings of this period is concerned, in comparison to Finland the exceptionality of the year 1696 was not corroborated. The oldest tree-rings have been registered with beech trees in the region of Moravskoslezské Beskydy (Mts.) for the year 1660. In the period of 1694/95 the beech trees of this region have relatively maximum increments followed by a slow decrease: although in the year 1696 the tree-rings already show a considerably subnormal width there is, however, a further decrease in 1697 to the extreme minimum of the year 1700 (Müller-Stoll 1951).

There is a shortage of data about winter 1696/97 both for the territory of Germany and the Czech Republic. A report has been preserved only from Slovakia stating that from December 21st, 1696 to March 21st, 1697 the winter in Northern Europe has analogously been most severe, and it has not grown milder during this period at all. The Danube in Bratislava has frozen over right away in January, and this ice bridge has lasted for 8 weeks which seldom happens in this region. It was interesting to note, however, that even under an even, deep layer of snow the soil has not frozen so that after removing the snow digging was possible as easily as in spring. Under this layer of snow everything has rotted, even those varieties that can easily endure winter frosts and weather. When the snow melted, everything has remained as a rotten fertilizer. For this reason there was a shortage of cereals and feed of all kinds (Réthly 1962).

In north Bohemia occurence of snow pellets has been recorded on June 2nd, 1697, followed by a night frost on June 3rd which has resulted in serious damages to cereals and vine (Litoměřice). The inhabitants of the Most region were excused from taxes because of frosts on June 4th and 5th that have caused damages on cereals and vineyards. Frosts on June 2nd and 3rd, 1697 were also mentioned in Moravia, where, apart from other things, walnuts have frozen; the year 1697 is generally evaluated as lean.

Conclusion

On the grounds of the above reconstruction of weather in the territory of the Czech Republic during the period of 1695 - 1697 it is possible to state that some extremes of the weather during this period have been corroborated. Nevertheless, on the basis of further information about weather in this part of Central Europe (Munzar 1995 b) it can be stated that the problem of local occurence (beginning, course and end) of the Little Ice Age still remains open; it will necessitate a more detailed research.

References

Brázdil, R., Dobrovolný, P., Chocholáč, B., Munzar, J. 1994. Reconstruction of the climate of Bohemia and Moravia in the period of 1675-1715 on the basis of written sources. In: Climatic trends and anomalies in Europe 1675-1715, edit. B.Frenzel, 109-122. G.Fischer Verlag Stuttgart-Jena-New York.

Eronen, M., Lindholm, M., Zetterberg, P. 1994. Extracting palaeoclimatic information from pine tree rings in Finland. In: Climatic trends and anomalies in Europe 1675-1715, edit. B.Frenzel, 43-50. G.Fischer Verlag Stuttgart-Jena-New York.

Lindgrén, S., Neumann, J. 1981. The cold and wet year 1695 - A contemporary German account. Climatic Change 3 : 173-187.

Müller-Stoll, H. 1951. Vergleichende Untersuchungen über die Abhängigkeit der Jahrringfolge von Holzart, Standort und Klima. E.Schweizerbartsche Verlagsbuchhandlung Stuttgart, 93 pp.

Munzar, J. 1995 a. The cold and wet year 1695 - also on the territory of the Czech Republic? In: The Jehuda Neumann Memorial Symposium on Mesoscale modelling and climate, Jerusalem, Israel, January 4-6, 1995, Abstracts, 135-136.

Munzar, J. 1995 b. The sources for reconstruction of weather and climate on the territory of the Czech Republic in preinstrumental period. Brno, manuscript.

Neumann, J., Lindgrén, S. 1979. Great historical events that were significantly affected by the weather: 4. The great famines in Finland and Estonia, 1695-1697. Bulletin of the American Meteorological Society 60 : 775-787.

Réthly, A. 1962: Weather events and calamities in Hungary up to 1700 /in Hungarian/. Akadémiai Kiadó Budapest, 450 pp.

Vesajoki, H., Tornberg, M. 1994. Outlining the climate in Finland during the pre-instrumental period on the basis of documentary sources. In: Climatic trends and anomalies in Europe 1675-1715, edit. B.Frenzel, 43-50. G.Fischer Verlag Stuttgart-Jena-New York.

Wanner, H., Pfister, C. 1994. The late Maunder Minimum /1675-1704/ - a key period for studying rapid climate change in Europe. In: Contemporary climatology, edit. R.Brázdil, M.Kolář, 574-579. Masaryk University Brno.

Arentz's Observations of Precipitation in Bergen, 1765-70

Øyvind Nordli

Norwegian Meteorological Institute
P.O.B. 43 Blindern, N-0313 OSLO

Introduction

In Bergen precipitation measurements were performed during the years 1765-1770 by Fredrik Christian Holberg Arentz, a teacher at the Bergen Cathedral School. Monthly values of his observations were published by The Royal Scientific Society in Copenhagen, (Arentz, 1777).

Arentz's observations are later discussed by Leopold von Buch (1807). His paper comprises only the annual values. Later the monthly values are printed by Føyn (1910). Føyn states that the observations, being the oldest in Norway, do not depart much from later observations at the Lungegård Hospital.

The observations seem not to have been subject to much attention from later climatologists probably because there is a gap of almost 100 years to the regular observations in Bergen. Without neighbouring stations the gap is almost impossible to fill and thus obtain a consecutive series.

Observational procedure

Arentz tells nothing of the site of the gauge. His observational procedure, however, is described in details. The gauge was a box with a hole in the bottom from which the liquid was allowed to flow into a bottle.

Arentz points out that he uses the concept of volume for his calibration. *..af Vandets Voulmen at beregne dets Heyde*. For measuring purposes he used two bottles, one large and the other small, both of them were calibrated from known hydrostatic rules. *Disse flaskens rigtige Indhold søgte jeg neye at bestemme efter hydrostatiske Regler*. The results of calibration, i.e. the corresponding volumes and amounts of precipitation, were listed in tables.

Arentz seems to be concerned of inaccuracies in his measurements and discusses the liquid's attraction to the glass. His bottles were narrow in the upper parts and he therefore concludes that the attraction errors were very small. It should also be noticed that the construction reduced evaporation to a minimum although he did not seem to be aware of this problem.

No reference is so far found to his original observations. Probably observations were not taken daily. He tells us that the last amount of water from one observation not sufficient to fill the small bottle, was left for the next one. When not measuring the rest precipitation, he obviously not aimed accurate daily values.

The precipitation in Bergen 1765-1770

Arentz's precipitation observations are published in its original form in decimals of Danish lines. (1 foot = 12 inches, 1 inch = 12 lines. From 1683 1 Danish foot = 0.31407 m). His use of the decimal system is remarkable because the system was not common in those days.

First of all Arentz's means and sums in Danish lines were checked and no miscalculations were found. However, in calculating the monthly mean values of the entire 6 years period, he has obviously omitted hundreds of a line, the consequence being that 0.8 mm is lost in the mean annual value. In table 1 Arentz's observations are listed in mm. The values compared to those of Føyn (1910) differ with an amount of about 2 mm or less in the annual sums.

Table 1 Arentz's precipitation observations in Bergen. Monthly and annual values in mm.

	Jan	Feb.	March	April	May	June	July	Aug.	Sep.	Oct.	Nov.	Dec	Year
1765	81.8	54.3	137.0	114.5	68.3	66.1	119.1	117.1	323.7	245.6	222.2	192.6	1742.2
1766	168.4	145.3	216.4	63.0	63.9	69.8	136.3	246.7	292.0	304.0	231.0	124.3	2061.1
1767	108.6	181.7	112.1	99.9	60.9	203.1	208.9	317.6	332.2	410.9	284.4	156.6	2476.8
1768	97.7	144.6	145.3	155.3	42.3	17.7	81.8	106.7	113.4	133.0	306.0	241.2	1585.0
1769	176.4	60.0	154.4	168.8	105.6	138.7	102.1	138.9	218.3	85.5	240.8	282.2	1871.8
1770	192.1	301.2	109.1	38.8	44.5	155.5	133.3	188.9	94.4	161.2	155.5	148.7	1723.2
Mean	137.5	147.8	145.7	106.7	64.2	108.5	130.2	186.0	229.0	223.4	240.0	191.0	1910.0
Max.	192.1	301.2	216.4	168.8	105.6	203.1	208.9	317.6	332.2	410.9	306.0	282.2	2476.8
Min	81.8	54.3	109.1	38.8	42.3	17.7	81.8	106.7	94.4	85.5	155.5	124.3	1585.0

Bergen is known as the town between the seven mountains. In this rough topography precipitation varies considerably within small distances. Moreover the capture efficiency of the gauges also depends of the sites. Thus several series near the centre of the town differ up to 20%. This should be kept in mind when the series of Arentz is compared with later observations in Bergen.

Arentz's mean values (1765-1770) are shown in figures 1 and 2 together with a homogenised series mainly from 50560 Bergen - Fredriksberg for the 100 years period 1895-1994. It is seen that the mean values in his 6 years period exceed the mean values of the 100 years period in

August and November, but in the other months the opposite is true. The mean values of Arentz's 6 years period is 1910 mm compared with 2156 mm within the 100 years period which gives a quotient of 0.89.
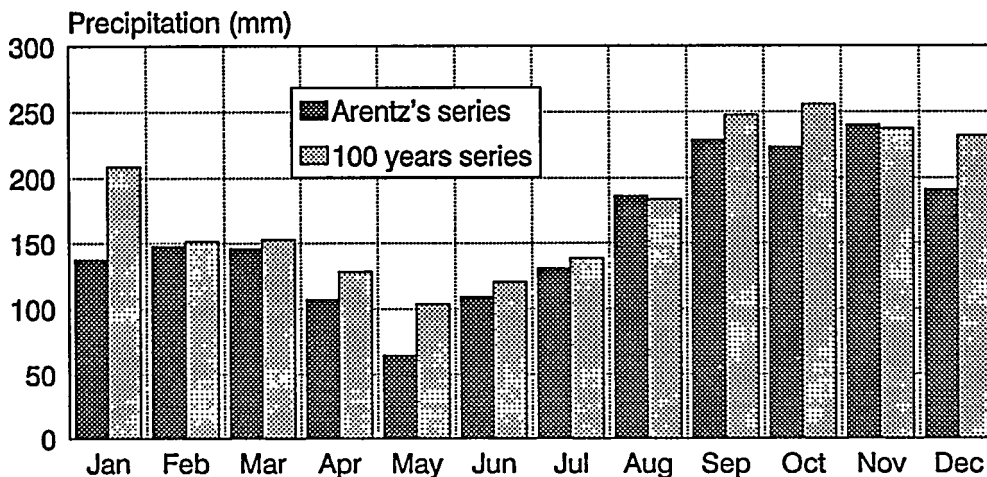
Precipitation (mm)

Fig. 1 Monthly precipitation in Bergen. Arentz's observations, 1765-1770, and a homogenised series 1895-1994, mainly from Bergen - Fredriksberg, but adjusted to be valid for Bergen - Florida.

During the 6 years observational period of Arentz the driest year was 1768 with an annual sum of only 1585 mm. This is not an extreme as there exist 9 years below this limit within the 100 years period. The previous year (1767) was the only really wet year in the Arentz's series, 2476 mm. In that year June and July precipitation exceeded 200 mm, August and September 300 mm followed by October with 411 mm.

No. of years
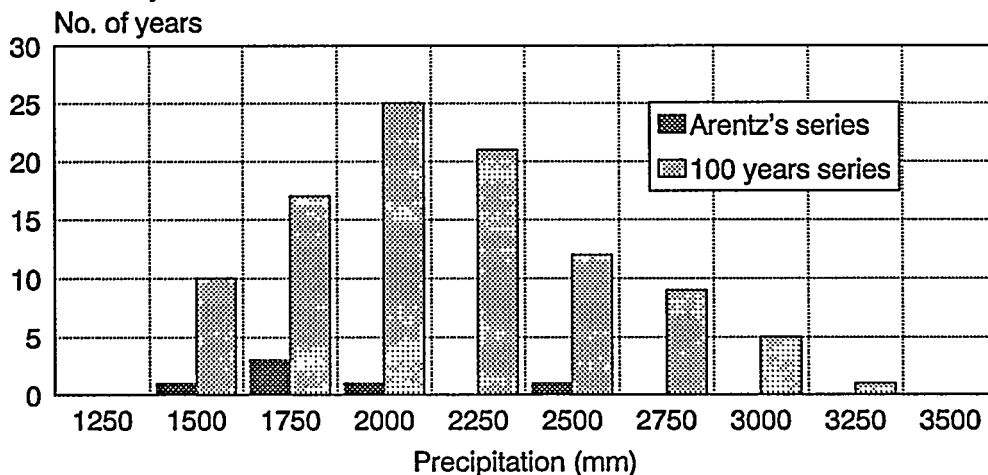
Fig. 2. Frequency distributions of annual precipitation in Bergen. A homogenised series 1895 - 1994 (light shaded bars) and Arentz's observations in the years 1765-1770 (dark bars).

The distribution of monthly sums of the 6 years and 100 years periods are shown in figure 3. Arentz's highest value occurs in October 1767, but it is exceeded by several others in the 100 years period, among them the highest one, 596 mm in 1967. The lowest value of Arentz occurs

in June 1768, only 17.6 mm. The lowest one in the 100 years period is only 4.2 mm in June 1982.
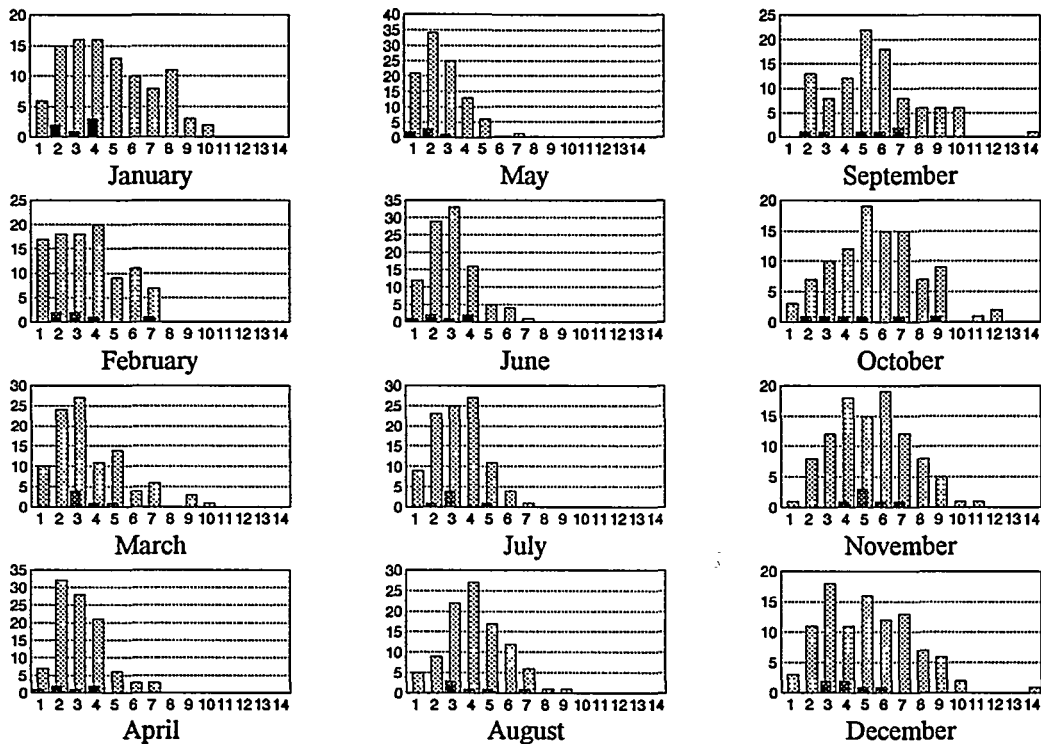
Fig.3 Frequency distributions of 100 years precipitation series in Bergen (light shaded bars) and of Arentz's observations in the years 1765-1770 (dark bars). Each bar (marked 1 to 14) comprises an interval of 50 mm monthly precipitation. Starting with the first interval from 0-50 mm, no. 14 corresponds to the interval 650-700 mm.

Concluding remarks

Arentz's description of the observational procedure as well as his effort of calibration are the main reasons for concluding that his observations should be considered highly reliable. This suggestion is strengthen taking into account the mild climate in Bergen which means that even in winter a great part of the precipitation may fall as rain. This is important because the capture efficiency for rain is far better than for snow and consequently reliable measurements are more easily established.

The mean values of Arentz's 6 years period (1765-1770) is 246 mm (11 %) lower than the mean of the 100 years period 1895-1994. Drier periods are easily found also in the 100 years period. The driest one (1940 - 1945) is 13 % lower. These comparisons, however, are not realistic if the combined series is inhomogenous. Because of the lack of neighbouring stations homogeneity tests do not exist during the 18th century.

Arentz's main concern was the surplus of rain in Bergen. He concluded that the precipitation amount in Bergen was at least the double of the ones found in other places in Europe.

References

Arentz, F.C.H. 1777. Observationer af Regnes Mængde i Bergen med nogle derhos føyede Anmerkninger. The Scientific Society in Copenhagen. Volume XI, 81-92.

Buch, L. von. 1807. Geognostische und physikalishe Beobactungen über Norwegen. The Scientific Society in Copenhagen. Volume ?, 318-332..

Føyn, N.J. 1910. Das Klima von Bergen. Yearbook for The Museum of Bergen. No. 2. Bergen. Norway.

Acknowledgement

"The country's ancient enemy": Sea-ice variations in Iceland in historical times and their social impact

Astrid E. J. Ogilvie

Institute of Arctic and Alpine Research
University of Colorado
Campus Box 450
Boulder, Colorado 80309-0450
U. S. A.

Introduction

Traditionally, Iceland takes its name from the sea ice which frequents its coasts. In Landnámabók, an historical source which lists the early settlers in Iceland,one of the first Norse visitors to Iceland, Flóki Vilgerdarson, is said to have reached Iceland around the year A.D. 865. It is written there that Flóki and his companions made land at Bardastrand in the west of Iceland. They spent the summer fishing and neglected to gather in hay for the livestock, which subsequently starved to death during the winter. It is written that the spring was rather cold. Flóki climbed up a high mountain and saw a fjord which was full of sea ice and "because of this they called the country Iceland".

There are textual problems associated with this account and it cannot be regarded as a reliable source (Ogilvie,1991). Nevertheless, whether or not we believe the story of Floki, it is interesting for a variety of reasons, not least because of the naming of Iceland. It also describes a pattern which ocurred over and over throughout Iceland's history: a poor hay crop leading to insufficient fodder to keep the livestock alive over the winter, leading to hunger and starvation amongst the human population and related problems. Furthermore, it closely associates the presence of sea ice with these difficulties.

In this paper, an analysis of sea-ice incidence from the twelfth century to ca. 1900 will be considered. Some of the social and economic implications of the effects of the proximity of the sea ice will also be presented. The main emphasis will be on the period 1750 to 1850. Sea-ice data are taken primarily from historical sources discussed in Ogilvie, 1991; 1992; 1995.A brief discussion of these sources, and the nature of the sea ice, follows.

Discussion and Results

Icelandic historical records of sea ice are excellent, in particular after c.A.D. 1600. The major sources used here are the later Icelandic annals, weather diaries and official government records.some interesting earlier sources such as a description of Iceland from the sixteenth century will also be discused.

The Arctic drift ice is carried southward to the shores of Iceland by the East Greenland current and is a most important feature of the climate of Iceland.The presence or absence of the sea ice has a considerable influence on the climate of Iceland, both directly (because of its nature as a major heat sink) and indirectly (through the influence of sea ice on the atmospheric circulation over the hemisphere as a whole). The proximity of the ice to the Icelandic coastline thus means a fall in both land and sea temperatures.The correlation between sea ice and temperature has been established for 'some time (Bergthórsson,1969;Ogilvie,1984,1992). Nevertheless, the relationship is a complex one.

Sea ice occurs most frequently off the coast of Iceland from late winter to early spring, but during severe seasons it can remain far into the summer or even the autumn. The ice usually affects the northwest, north or east coasts; it is rare for it to reach the southwest or south.The extent of the sea ice is highly variable on all time scales..

The East Greenland ice and the sea ice off Iceland have been the subject of much discussion.However,the classic work on the subject is by Lauge Koch (1945).Koch's general methods of analysis have been followed here. However, unreliable data usedby Koch have been omitted and many new data, little used by previous researchers, have been included.

A decadal sea-ice index has been reconstructed for the period A.D. 1600 to 1850 (see Ogilvie,1994,1995).From this diagram the variability of the incidence of sea ice may be seen. Thus a relatively ice-free period occurred from around 1630 to 1680. The years from c. 1700 to 1740 were also comparatively ice-free. The 1690s and 1740s were severe, and the 1780s to c. 1840 extremely so. The 1840s saw a return to an ice-free period. Some severe sea-ice years which will be discussed are: 1695; 1699; 1714; 1728; 1729; 1745; 1750; 1756; 1772; 1782; 1783; 1784; 1791; 1798; 1801; 1802; 1807; 1808; 1811; 1812; 1817; 1821; 1822; 1827; 1835; 1837; and 1840.

Conclusions

The presence of the sea ice affected people in a variety of ways; not all of them negative. Thus, useful products,such as driftwood and marine mammals, for example whales and seals, could accompany the ice. However, the lowering of temperatures undoubtedly

affected the growth of the all important grass crop (Ogilvie, 1982;1984). As has been observed many times,but first in Landnámabók, mentioned above, a lack of hay with which to feed the livestock meant that they were likely to die of starvation. As the Icelandic economy was based largely on animal husbandry , the loss of the all-important livestock frequently meant loss of human life as well.Other social consequences followed, such as the desertion of farms. The presence of the sea ice off the coasts caused other problems such as the prevention of fishing and access by trading vessels. Not without reason did the Icelandic poet Matthias Jøchumsson call the sea ice *landsins forni fjandi* - "the country's ancient enemy".

References

Bergthórsson, P. 1969. An estimate of drift ice and temperature in 1000 years. Jökull 19: 94-101.

Koch, L. 1945. The East Greenland ice. Meddelelser om Grønland 130 (3). Udgivne af kommissionen for videnskabelige undersøgelser I Grønland. Copenhagen.

Ogilvie, A.E.J. 1982. Climate and society in Iceland from the medieval period to the late eighteenth century. Thesis. University of East Anglia, 504 pp.

Ogilvie, A.E.J. 1984. The impact of climate on grass growth and hay yield in Iceland. In, Climatic changes on a yearly to millenial basis. N.-A. Mörner and W. Karlén (eds). D. Reidel, Dordrecht. 343-352.

Ogilvie, A.E.J. 1991. Climatic changes in Iceland A.D. c. 865 to 1598. In, The Norse of the North Atlantic (presented by G. F. Bigelow) Acta Archaeologica 61-1990. Munksgaard, Copenhagen. 233-251.

Ogilvie, A.E.J. 1992. Documentary evidence for changes in the climate of Iceland, A.D. 1500 to 1800. In, Climate since A.D. 1500. R.S. Bradley and P.D. Jones (eds). Routledge, London and New York. 92-117.

Ogilvie, A.E.J.1994. Documentary records of climate from Iceland during the late Maunder Minimum period A.D. 1675 to 1715 with reference to the isotopic record from Greenland. In, Climatic trends and anomalies in Europe 1675-1715. B. Frenzel (ed.). Special Issue: ESF Project European Palaeoclimate and Man 8. European Science Foundation, Strasbourg. 9-22.

Ogilvie, A.E.J. 1995. Sea-ice conditions off the coasts of Iceland 1601-1850 with special reference to part of the Maunder Minimum period. AmS-Rapport, 7, Stavanger. (in press).

Climate in the 'Low Lands' in the 13th - 14th century

Aryan van Engelen

Royal Netherlands Meteorological Institute,
P.O.B. 201, 3730 AE De Bilt

Introduction

In the eighties, the European Community launched a number of climatological research projects under the heading "Reconstitution of Past Climates". KNMI's contribution to this program have been two projects on historical weather observations.

The first project aimed to set up an inventory of Dutch meteorological observations, carried out with early instruments before the foundation of the KNMI in 1854. A database was set up with, in general, three times a day observations of temperature, precipitation, pressure, winddirection and windspeed and state of the sky, noted down at 12 different locations and extending back to 1706. Station-dictionaries with comprehensive descriptions of the used instruments, units of measurements, observers, conditions of observations and other relevant information have been composed for over 125 observational places.
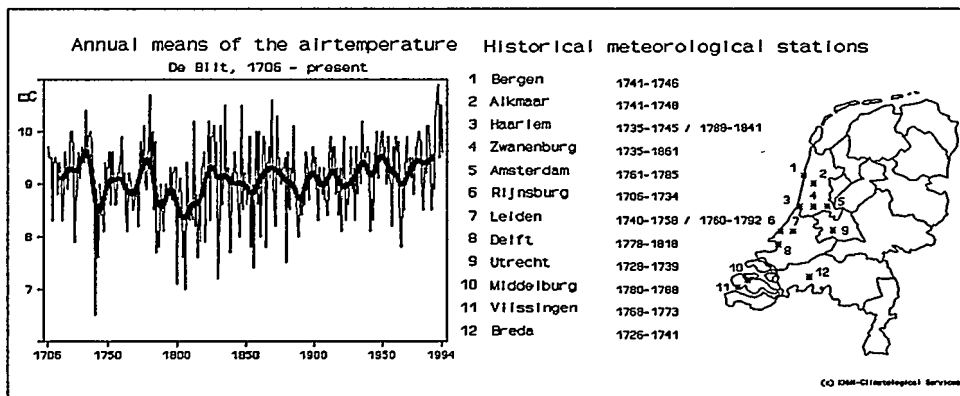
Exploring the archives for historical instrumental data, it became obvious that they contained also enough source-material to make a reconstruction of the climate in the pre-instrumental era, back as far as ca. 800 AD.
The second project will provide a series of four books, each containing some 700 pages, with detailed descriptions of weather and climate in the Netherlands and neigbouring countries from year to year and from season to season. Next to qualitative descriptions, quantitative classifications will be included of winter- and

summertemperature, droughts and wet periods, riverfloods, stormsurges and storms that caused severe dammage. The first volume covers the period 800-1300 AD and appeared last spring. The following volumes will each cover an approximately two hundred year period and will be published within a timespan of about 2 years.

The paper will deal with the specific historical sources we explored and analysed and which formed the base of the reconstruction of the Dutch climate in past centuries and the techniques we developped in order to classify the qualatitive information into instrumental terms. The results will be presented as some of the interpretations we made of the climate in the 'Low Lands' in the 13th and 14th century.

Sources

Sources that provided us with usefull information about the weather in the past can be subdivided in two main categories: the tangible sources and the non tangible sources like toponyms, folk customs and songs. Tangible sources can either be written or non-written as paintings, archeologica, tree rings and proxy series of vintage, harvest and ice data. In our studies we focussed mainly on written sources as presented by the numerous historical documents we found in the archives and libraries of not only the Netherlands but also abroad in Britain, Germany, Denmark, Belgium and France.
Extremely usefull information was hidden in the 'Low Land' series of accounts of townships, shipcargo's, agriculture, water- and windmills and accounts of rivertolls.

Classifications of temperature

We adopted and developped techniques to set up quantitative classifications of categories of temperature-production of the winter (DJF), summer (JJA) and winter and summer halfyear and were able to express the discerned categories into degrees Celsius on the base of non-instrumental information. To that purpose we awarded marks for instance to three aspects, characteristic of many winters: a thermical aspect, an aspect of duration and the aspect of intensity. The total of the marks is then a measure of the seasonal temperature.

Results

The graph of 'decadal means of the winter severity index', covering the period 1000 AD to present, is just one example of the reports of the climate in the past that can be found in our books. Other examples are represented by the graphs of winter (DJF) and summer (JJA) temperatures covering the 13th and 14th century.

We are not certain about the temperatures in the 9th and 10th century: too many sources and data lack. We can assume however that the average temperature of the 9th century was below average and times were wet.

winter (DJF) temperatures 1200 - 1400   Netherlands

summer (JJA) temperatures 1200 - 1400   Netherlands
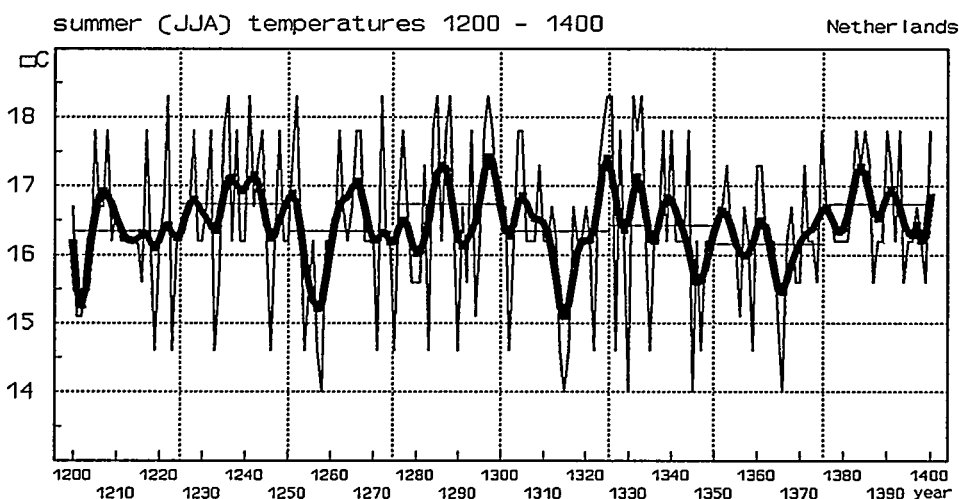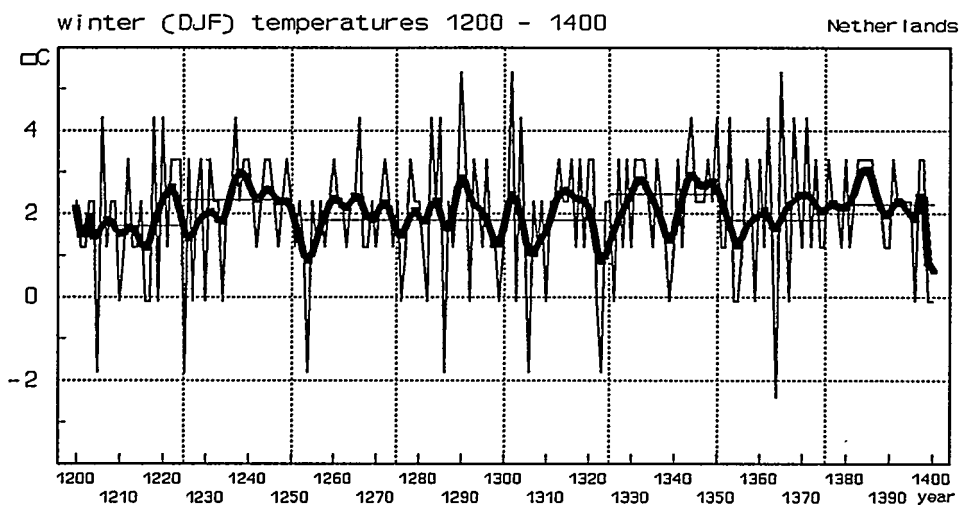
In the tenth century we find many cold winters but also warmer summers and sometimes periods of drouht. Afterwards we see a gradually rising of the temperatures and a decreasing amount of wet periods.

The 12th century shows a quite average pattern without many extremes. During the first quarter of the 13th century winters are somewhat colder but the second quarter recovers, in the summers predominantly. Remarkable is the great number of warm and dry summers of the last quarter of this century.

Winter- and summertemperatures of the 14th century are rather high, except for some curious relapses. For the first, with the wet years 1314 to 1316, we have no explanation. At the second, around 1364 we may possibly relate to the extremely heavy and desastrous vulcanic eruption of the Oeraefajökull in Iceland in 1362.

The socio-economic detoriation of the 14th century is often ascribed to a

decadal means of winter severity index
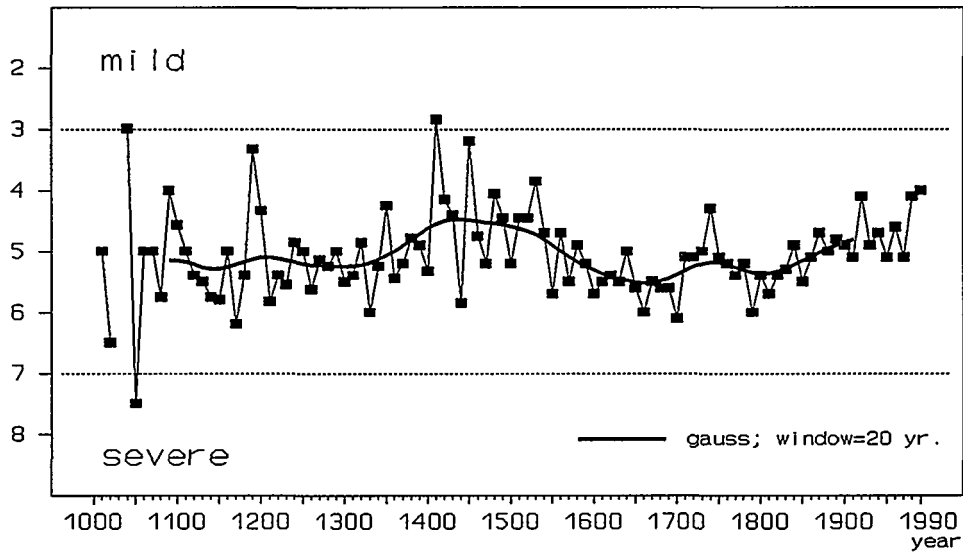
detoriating climate. Though we found several climatic events that certainly had a negative impact, the all-over picture is one of a century with generally good climate conditions.

The well known Middle Age climate-optimum with its many warm and dry summers starts somewhere in the second half of the 11th century and lasts until around 1450. There we find the onset of a 100-year transient period to the Little Ice-Age that begins around 1550 and ends in the second half of the 19th century. Afterwards temperatures are generally rising and variability is lowering, except for the last decades.

Early temperature records from Tornio, northern Finland, 1737-1749

Heikki Vesajoki, Mika Narinen and Jari Holopainen

Department of Geography and Regional Planning, University of Joensuu
P.O.B. 111, FIN-80101 Joensuu

Introduction

The longest meteorological journal from the first half of the 18th century in Finland comes - perhaps surprisingly - from a small northern town, Tornio, where a local clergyman, Abraham Johannes Fougt, started regular observations in 1737. The obvious background for the initiation of observations was the French expedition of de Maupertuis measuring the shape of the globe in the Tornionjoki river valley in 1736-37. De Maupertuis' expedition had among other equipment instruments like barometers and thermometers, for measuring meteorological phenomena. Some of these instruments were obviously left to Fougt, who started to make observations three days before the departure of the expedition. One of the participants of the expedition was Anders Celsius, who inspired learned men in Sweden and Finland to start the observation of meteorological phenomena. There is a note at the beginning of the journal stating that the first records were made under the guidance of Celsius. Another person who was perhaps involved in the initiation of these observations was Anders Hellant, who acted as guide and interpreter to the expedition and was also interested in studying natural phenomena. (Johansson 1913).

Fougt started the observations on 6 June 1737 and continued them until 16 July 1749 (all dates changed to the Gregorian calendar). The site of observation was the parsonage located on the northern head of Pirkkiö island (65°50'N; 24°08'E) at the mouth of the Tornio River. The observations included instrumental measurements of air pressure and temperature, observations of wind direction and strength, cloudiness and precipitation and occasional notes on sunspots, comets, etc. The thermometer seems to have been a mercury one with a Réamur scale, i.e. the same type the French expedition used in their measurements (Outhier 1975). More detailed information concerning the exact placing of the thermometer is, however, missing.

The number of observations per day varied from one to four, although in most cases they were made three times a day, always noting the exact time. The most usual observation times were as follows: in the morning at 7 a.m. (70 %), at about midday at noon (37 %) or at 1 p.m. (39 %), in the evening at 9 p.m. (66 %). Because of Fougt's work journeys, on some days the observations are totally missing. Besides these minor

interruptions there are three longer gaps in the series: December 1742 - February 1743 (3 months), June - July 1746 (2 months) and January - February 1747 (2 months), together 7 months. The reason for the longest interruption was the war between Sweden and Russia, the so-called "Small Hate".

Preliminary notes on mean temperatures and their reliability

The monthly mean temperatures of the Tornio series were calculated simply according to the formulae $T = 1/3 \ (t_{morning} + t_{midday} + t_{evening})$, where $t_{morning}$ represents the mean of the morning records of the month in question, etc. (Table 1). In order to preliminarily evaluate the record of temperatures the monthly means were compared with those of the Uppsala series (Bergström 1990), which - although possessing many uncertainties - represents the best possible reference series in Fennoscandia from that time. It turned out that, despite the more than 700 km long distance between the places, the correlation coefficients of the monthly means of the series show a covariation from moderate to strong (Tab. 2) and the reference graphs of seasonal and annual means display quite similar patterns (Fig. 1).

Table 1. Monthly and annual mean temperatures in Tornio 1737-1749. The reference series 1961-90 from Haparanda (SMHI 1991).

	Jan	Feb	Mar	Apr	May	June	July	Aug	Sept	Oct	Nov	Dec	Year
1737	-	-	-	-	-	11.8	16.3	15.3	10.1	3.5	-1.7	-4.1	-
1738	-3.3	-9.3	-7.6	0.4	5.5	13.6	17.5	17.7	10.4	7.1	-2.6	-10.3	3.3
1739	-14.3	-17.4	-8.6	-2.3	4.7	10.5	17.5	14.5	8.9	0.9	-3.7	-6.9	0.3
1740	-12.5	-10.0	-6.4	0.5	3.6	12.6	13.1	14.7	10.3	-1.4	-8.1	-5.5	0.9
1741	-11.2	-6.8	-4.6	-1.3	5.7	11.1	15.8	13.9	9.3	3.8	-3.9	-5.4	2.2
1742	-8.1	-5.8	-8.5	-2.0	4.8	12.2	17.1	13.2	8.6	4.6	-4.2	-	-
1743	-	-	-4.3	0.9	5.4	15.9	16.9	15.8	9.3	2.1	-0.7	-8.9	-
1744	-4.7	-6.7	-5.7	4.0	7.7	14.8	19.0	15.1	7.7	1.8	-4.1	-7.8	3.4
1745	-7.3	-12.9	-8.7	1.6	7.7	17.5	15.1	14.1	9.2	3.4	-4.8	-4.7	2.5
1746	-5.3	-11.6	-6.9	1.6	6.5	-	-	14.5	10.8	3.9	-3.1	-7.4	-
1747	-	-	-5.4	0.4	7.9	15.6	15.3	12.7	10.3	6.0	-2.1	-6.1	-
1748	-10.2	-4.4	-9.8	0.5	5.8	15.1	16.8	14.7	10.1	4.8	-4.7	-9.6	2.4
1749	-9.8	-11.2	-4.7	1.8	9.8	10.5	-	-	-	-	-	-	-
1737 -49	-8.7	-9.6	-6.8	0.5	6.3	13.4	16.3	14.7	9.6	3.4	-3.7	-7.0	2.3
1961 -90	-12.1	-11.4	-6.8	-0.5	6.1	12.8	15.4	13.2	8.0	2.5	-4.2	-9.5	1.1

Fig. 1. Graphs representing the annual and seasonal temperature means in Tornio and (1737-1749) and in Uppsala (1739-1750). Source for Uppsala: Bergström 1990.

Autumn (C°) — Tornio / Uppsala, 1735–1750

Winter (C°) — 1735–1750

Spring (C°) — 1735–1750

Summer (C°) — 1735–1750

Annual (C°) — 1735–1750
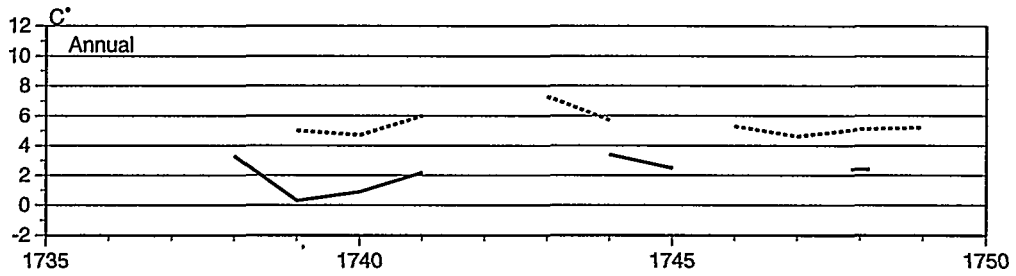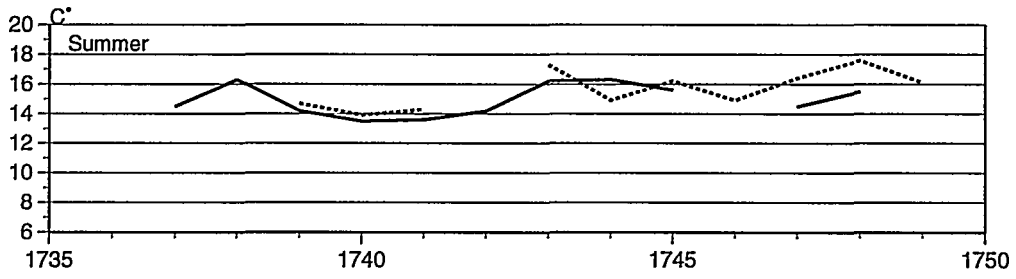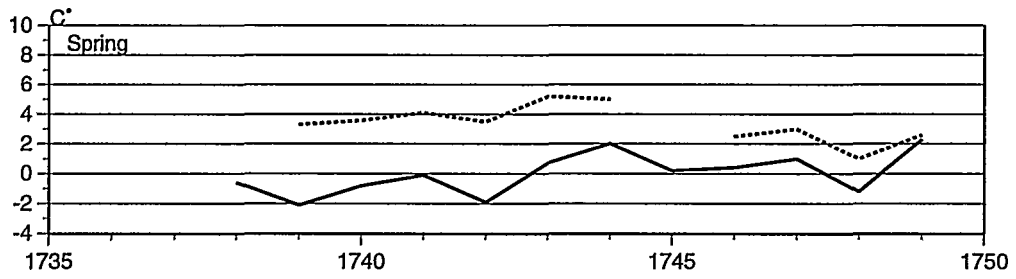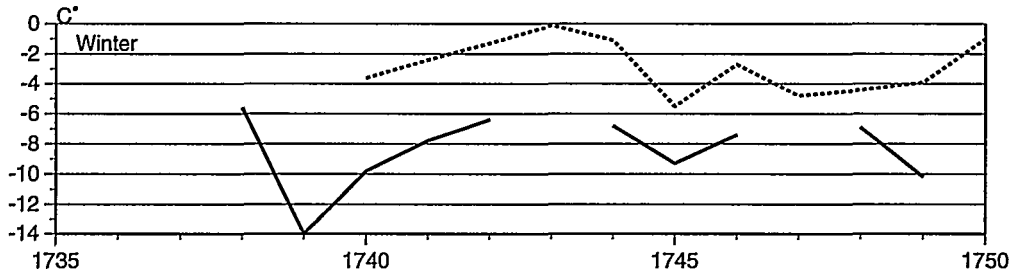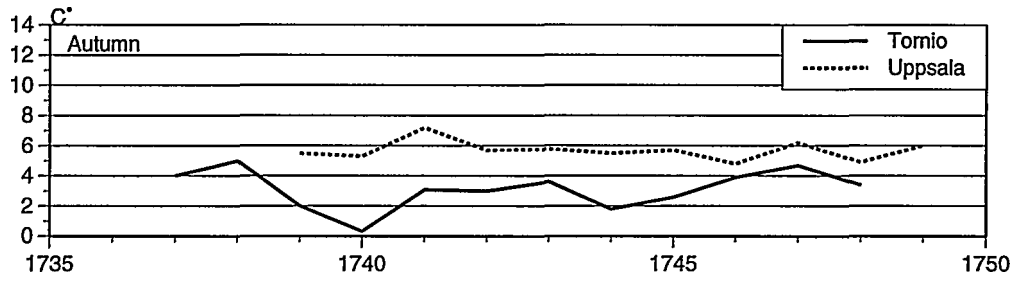
Table 2. Coefficients of correlation between the Tornio and Uppsala series in 1739-1749.

January	0.68	August	0.46
February	0.73	September	0.54
March	0.53	October	0.76
April	0.41	November	0.83
May	0.77	December	0.94
June	0.77		
July	0.55	Year	0.61

Concluding words

Compared with the present record series of the neighbouring town, Haparanda, located on the opposite (Swedish) side of the river (in Tornio there is no observation point), the 18th century temperatures seem to be higher all year round and especially during the winter months (Table 1). The lowest recorded temperature in the journal, however, is -22.2°R (-27.75°C), which seems strange considering the number of winters the observation period covers and that the French expedition had measured as low as below -30°R temperatures in the previous winter 1736/37 (Outhier 1975). This suggests that either the scale of the thermometer used by Fougt did not reach lower temperatures (Johansson 1913) or the instrument was exposed in a "well-ventilated north-facing fireless room" according to the recommendations of James Jurin, which were followed until the middle of the 18th century, at least in England (Manley 1952). So, taking into account the location of the early observation point in Tornio, close to the river, as well as the lack of information concerning the exact placement of the thermometer, we cannot, on the basis of previous figures, draw any definite conclusions about the development of temperature climate in Tornio. To achieve that goal more investigation is needed to clarify the actual measurement procedures. One source of information could be the possible correspondence between Fougt and Celsius.

References

Bergström, H. 1990. The early climatological records of Uppsala. Geogr. Ann. 72 A (2): 143-149.

Fougt, A.J. 1737-1749. Meteorological Journal 1737-1749. The Swedish State Archive.

Manley, G. 1974. Central England Temperatures: monthly means 1659-1973. Quart. J. Roy. Meteorol. Soc. 100: 389-405.

Outhier, R. 1975. Matka Pohjan perille 1736-1737 (Journal d'un Voyage au Nord). Otava, Keuruu, 179 pp.

SMHI (Swedish Meteorological and Hydrological Institute) Väder och Vatten 1991.

Digitizing Norwegian logbooks 1867-1890: A final round to reach the objectives of the international conference of 1853 in Brussels on obtaining meteorolgical data from the ocean

Erik Hauff Wishman

Archaeological museum in Stavanger
P.O.B. 478, N-4001 Stavanger, Norway

Introduction

In 1990 Archaeological museum in Stavanger (AmS) was given a grant from the Norwegian Research Council under its "Climate and Ozone programme" to carry out its project: "Establishment of a historic climatological data base at the Archaeological museum in Stavanger". The data base should comprise historic climatological data from Norway with the Svalbard Islands, and the adjacent seas. During the run of the project, AmS was made aware of about 600 logbooks containing meteorological data, which had been observed on Norwegian sailing ships during the period 1867-1890, and now stored at the Norwegian Meteorological Institute (DNMI). All together, the observational records amount to more than 500 000, and all oceans are represented in the sample.

Because of limitations imposed by the telegraphic communication still on an elementary stage, the observations could only be utilized to a limited degree during last century. In agreement with DNMI, the COADS data base (Comprehensive Ocean-Atmospheric Data Set) in Boulder, USA and AmS, the logbook data are now being digitized and transferred to the COADS within its so called Release-2 updating programme, which is expected to be run for another couple of years. The objective of the AmS project is 1) to secure the data for international climatological research, and 2) at the same time supply AmS with necessary maritime climatological data from the North Atlantic, for the use in historic climatological research in Norway.

Copies of original and digitized pages of the logbooks are shown in Fig 1a and 1b below.
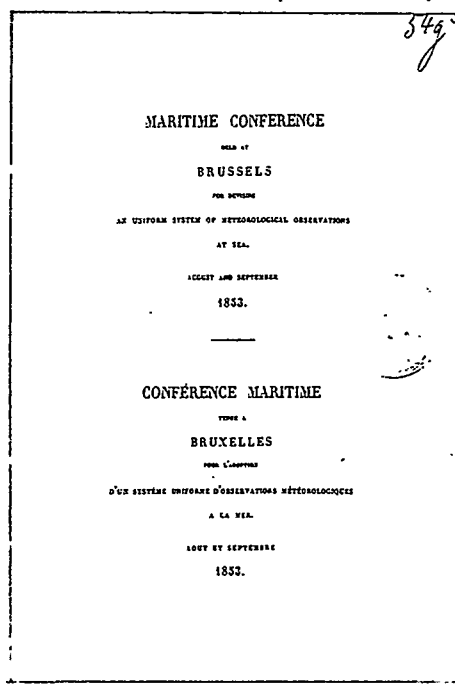
Fig. 2 Title page of the final document after the Brussels agreement about collecting meteorological observations from the oceans.

By this time, a few smaller or bigger projects on obtaining contemporary meteorological observations from a network of meteorological observatories on land had already been run in different regions. Most famous was the Societas Meteorologica Palatinas (SMP), established in 1780 in Mannheim, Germany. Its observatories had been equipped with instruments, and the observations were carried out by observers according to common instructions. According to Kington (1988), the landbased Palatinate network included by the mid 1780s over 50 observatories extending from Siberia across Europe to Greenland and eastern North America. The main object of the SMP organization was to gain experience in predicting weather. Although the activities of SMP came to an end by 1795 as a consequence of the Napoleonic wars (Kington, op. cit.), many of the stations which had been established survived in the following decades, and new observatories were erected by private persons and scientific societies. Thus, by middle of the 19th. century, by the time of the maritime conference in Brussels, several hundred landbased meteorological stations, were at work in Europe and America.

Among the nations represented at Brussels were Belgium, The Netherlands, Great Britain, Sweden, Denmark and Norway. One objective of this joint international investment by shipping nations, was of course to learn about the climatology of the oceans, for the benefit of international trading and transport between the continents by sailing ships. Another objective was to improve the basis for predicting weather development, to protect lives and property.

189

Fig. 1a Part of a logbook page of observational records.

```
 C.nr  Date     Hour  Lat.  NS Long. EW Btem Airp Airt Seat Wdi Wf Cc Wea S Remarks
 ------ -------- ----- ----- -- ----- -- ---- ---- ---- ---- --- -- -- --- - -------
 Shipname: Ovos         From:LIMERICK           To:CHARLESTON          Ocean: 3

 12181 22.12.78   8                    250 7645 250 260 NE   3 00  3 Shooting star from NE to SW.
 12181 22.12.78  12  1826 N  4740 W    260 7650 250     NE   3 00  3
 12181 22.12.78  16                    250 7630 250     NE   3 00  4
 12181 22.12.78  20                    250 7640 250 260 NE   3 00  4
 12181 23.12.78   0                    250 7650 250     NE   3 05  4 Increasing cloudcover with rain from N.
 12181 23.12.78   4                    260 7645 250     NE   3 05  4
 12181 23.12.78   8                    250 7645 250 250 NE   3 00  4 Clear air.
 12181 23.12.78  12  1844 N  5136 W    250 7645 250     NE   3 00  4 Flying fish and some whales from time to time.
 12181 23.12.78  16                    250 7640 250     NE   3 03  4
 12181 23.12.78  20                    250 7640 250 250 NE   3 05  4
 12181 24.12.78   0                    240 7650 240     NE   3 05  3
 12181 24.12.78   4                    250 7640 250     NE   3 05  3
 12181 24.12.78   8                    240 7640 240 250 ENE  3 05  3 Some flying fish and a couple of whales.
 12181 24.12.78  12  1913 N  5517 W    250 7640 250     ENE  3 05  4
 12181 24.12.78  16                    250 7630 250     ESE  3 05  3 Clear air. Clouds shape cirro cumulus.
 12181 24.12.78  20                    250 7640 250 250 ESE  3 08  3
```

Fig. 1b Same part of logbook page as presented in Fig. 1a in digitized format.

History

The work with the Norwegian logbooks has uncovered the history of the joint international effort on organizing and implementation of a systematic plan for collecting meteorological observations from the oceans. This grand project had its formal basis in an agreement reached between 10 shipping nations at the maritime conference held at Brussels in 1853. (Fig. 2).

Thanks to the increasing number of meteorological observations from the Atlantic, adding to available contemporary observations from the continents of both sides of it, it became for the first time possible to construct weather maps, which gave a continous picture of the meteorological events in space and time right across the North Atlantic from Eastern America to Ural (fig. 3). Studies of the continous behaviour of the pressure and weather systems visualized on the maps, together with increased knowledge of theoretical meteorology, contributed fundamentally to the discovery of the <u>Polar Front</u> and the <u>Polar Front Cyclones</u> by V. Bjerknes et al. in about 1919. One may say that by this discovery, the fundamental objective of the pioneers of meteorology, namely producing reliable weather forecasts at least one day in advance, had been reached.
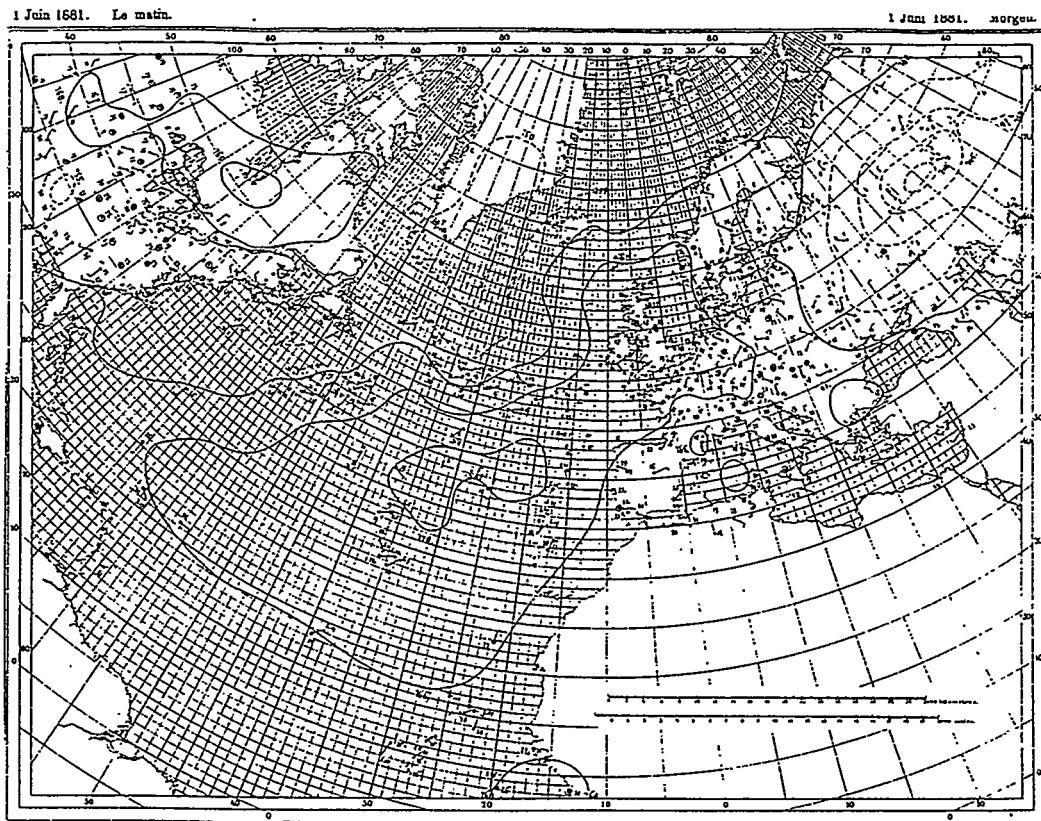
Fig. 3 Weather map of 1. June 1881 (morning) for the North Atlantic Ocean.

The present climatological challenge of "Global Warming"

Perhaps the most prominent climatological challenge of today is the "Global Warming" problem. But the reality of the observed rising trend of global temp since about 1850, depends very much on the quality and amount of data available from the oceans, which cover more than 70% of the surface of the planet. Data from the period 1867-1890 are very sparse. This is a main idea behind the agreement with DNMI and COADS on the "logbook project". We believe that the more than 500 000 records, transferred to the COADS data

base, and quality controlled by a meteorologist before sending, may contribute positively to determining the historical trend of the global air temperature more excactly. This objective would be in agreement with the intentions of the "Climate and Ozone programme" of the Norwegian Research Council. In change for our carrying out the transferring operation, AmS will receive maritime meteorological data products of the Atlantic Ocean from the COADS for historical climatological research in Norway.
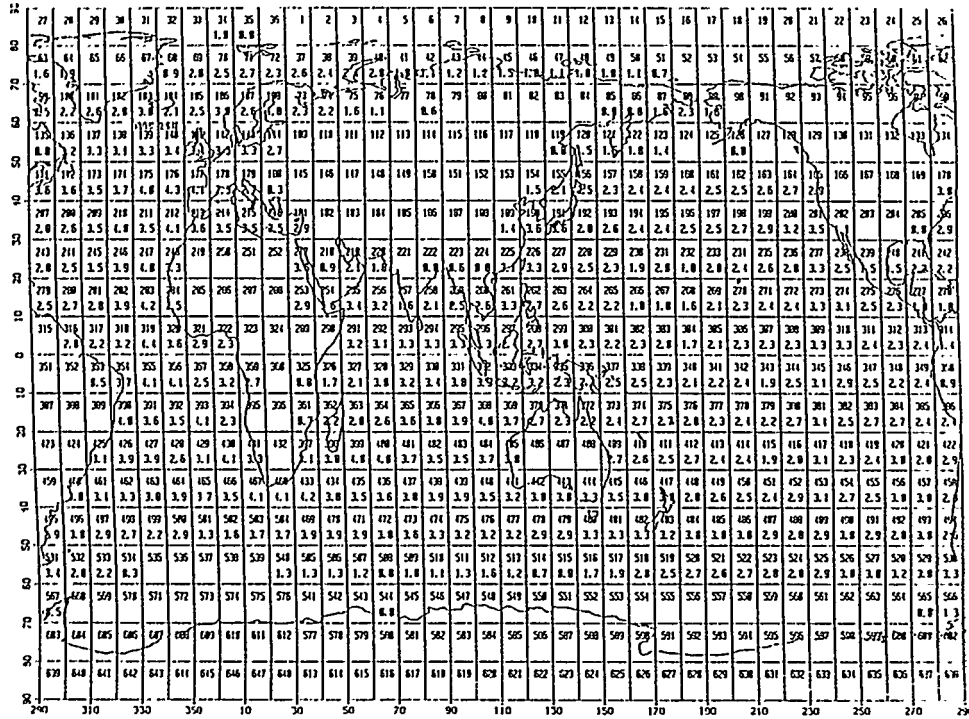
Fig. 4 Number of observations (logaritm of reports) within 10x10 deg. boxes during 1870-1879 (After COADS, Release 1, April 1985)

Conclusions

Perhaps the "logbook project" of AmS may be seen a model for the other European countries which were represented at the Brussels conference of 1853. Of course, the completed logbooks achieved by the respective countries represented at the Brussels conference, have been taken securely care of in archives. However, much of their content are not fully utilized and still unavailable for modern international climatological research. The climate of European regions may to a large extent be understood as modifications of the climate of the Atlantic Ocean. The climatological content of the European logbooks will give important contributions to the understanding of the climate history of Europe. It would be the best if they could be brought up in the light for quality control of their content and stored in a modern maritime climatological data base as basis for common climatological research.

It has been suggested that two climatological challenges have stimulated the sciences of meteorology and climate. Firstly, the variability of the weather, which ultimately, after 150 years of collecting meteorological data, improving of instruments, and research, resulted in the discovery of the Polar Front and the Polar front cyclones.

Then, the present challenge of "Global Warming" (or more generally, the variability of global climate). This has initiated the need for developing dynamic models of the climatic system, for studying how it works when exposed to internal or external impacts.

For this sake, there is a need for improved data over the last couple of hundred years, from land and sea. In this historical context one must also see the EURO-CLIMHIST project, which builds up a basis for studying climate variability of Europe during historic times. In addition, this historic climatological data base ultimately will include all available information about man and society's adaptation to the climatic challenge.

Acknowledgements

I am indebted to Dr. Gaston René Demarée for the information he has given me about the international maritime conference held at Brussels in 1853.

References

Kington, John. 1988. The weather of the 1780s over Europe. Cambridge University Press, 164 pp.

COADS (Comprehensive Ocean-Atmosphere Data Set) Release 1. Boulder Colorado. April 1985.

Elms, Joe D., Woodruff, Scott D., Worley, Steven J. & Hanson, Claire S. 1993. Digitizing Historical Records for the Comprehensive Ocean-Atmosphere Data Set (COADS). Earth System Monitor, Vol. 4, No. 2:4-10

Some Seasonal Climatic Scenarios in Continental Western Europe Based on a Dataset of Medieval Narrative Sources, A.D. 708 to 1426

Zhongwei Yan (1), Pierre Alexandre (2) and Gaston R. Demaré(3)

(1) Institute of Atmospheric Physics
Beijing 100029, China

(2) Royal Observatory of Belgium
B - 1180 Brussels, Belgium

(3) Royal Meteorological Institute of Belgium
B - 1180 Brussels, Belgium

Abstract

The climatic variations over the last 2000 years still remain far from being well-known. Some recent analyses (Jones and Bradley, 1992; Hughes and Diaz, 1994) showed large regional differences even for the periods such as the Medieval Warm Epoch (MWE) and the Little Ice Age (LIA), which used to be regarded as worldwide and persisting for a few centuries. An important step in improving our knowledge is to properly extract the significant signals from independent data sources which may, hence, provide a base for dynamical and multi-type-of-data synthesis. The work depicts some regional historical climates inferred from independent narrative sources. In this paper, the databank used for this purpose is an enlarged and upgraded version of the one described by Alexandre (1987). All selected climatological information has passed the thorough criteria of historical criticism.

The narrative sources of the Middle Ages in Western Europe mainly record the extreme events on seasonal, monthly or sub-monthly time scale. One of the scientific tasks concerned in this paper is, therefore, how to link the limited historical information to the more general and digitized climatological information of the modern times. An analysis of the relationship between the modern instrumentally observed climates and their reconstruction from extreme records was carried out, which highlighted the reliability of the reconstructed medieval climates.

The 30 year moving average time series for temperature and for precipitation were constructed for the following 4 continental west-european sub-regions: northwestern Europe, northcentral Europe, the Mediterranean region and Switzerland. A warming trend from the early to the late Middle Ages seems to have occurred but with considerable decade-to-century scale fluctuations different between the sub-regions. The mean warm season temperature level during the late 14th to early 15th century might have been 0.3øC higher than that of the present century. The narrative data used for this study recorded most of the strong climate signals at the decade-to-century scale which were also reflected in the natural climatic archives data sources.

Detection of climate changes from the instrumental record
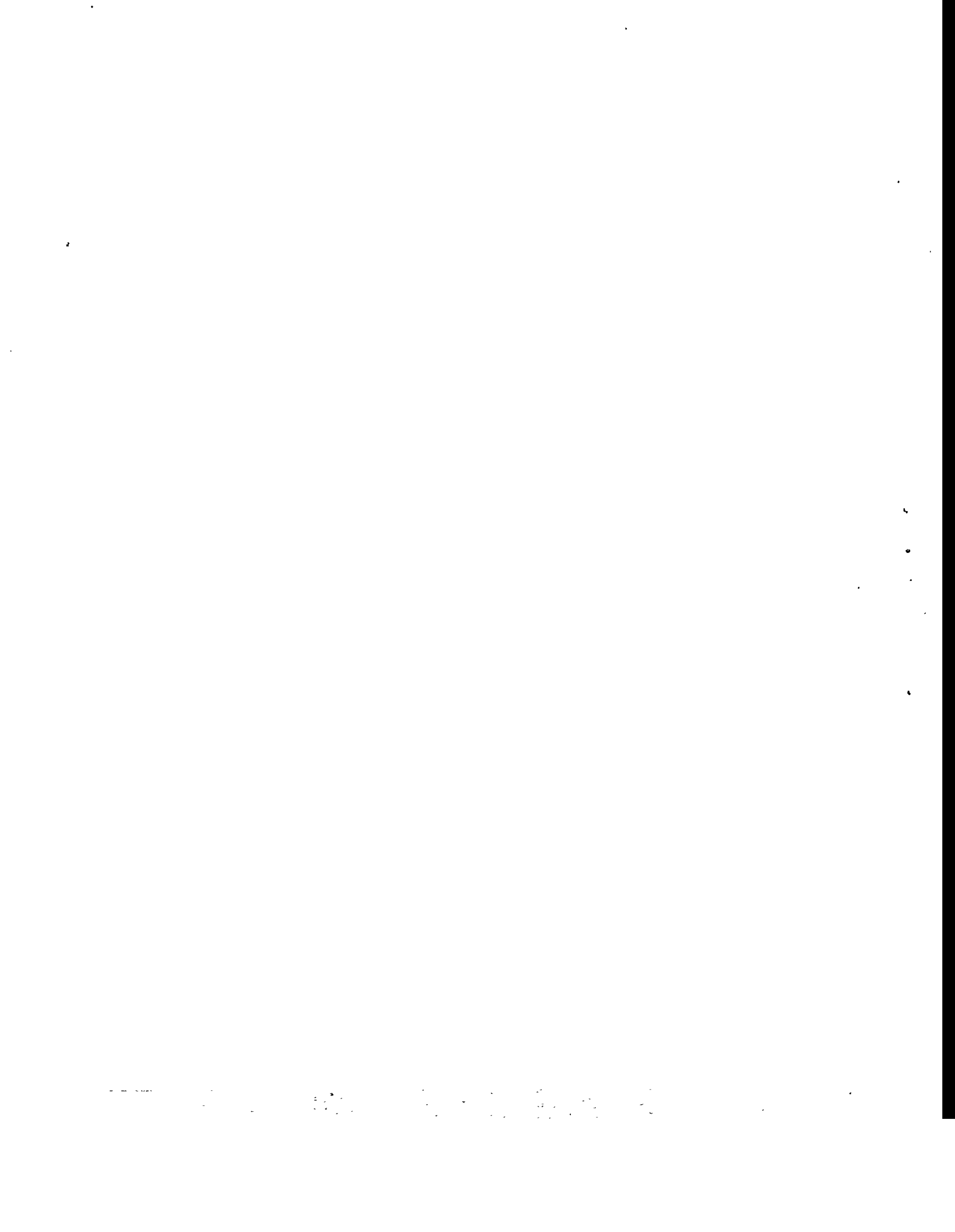
Detecting and Communicating Information on Climate Change: The Role of Indices

Thomas R. Karl

NOAA/National Climatic Data Center
151 Patton Avenue Asheville, NC 28801-5001 USA

Although there has been a substantial amount of work that has addressed changes in monthly, seasonal, and annual temperature and precipitation, relatively little information exists regarding multi-decadal changes of precipitation frequency and intensity and temperature variability. Using data sets of daily precipitation and temperature over the USA, Russia, China, and Australia, precipitation and temperature changes and variations have been analyzed. Results indicate that there are some significant changes in precipitation intensity that are not well reflected in seasonal or annual totals. Moreover, changes of temperature variability are observed to be spectrally dependent.

The question arises as how best to integrate these changes with observed changes in the mean quantities and to convey this information to non-specialists. Observed changes in climate within the contiguous United States are used as an example of how one might go about developing a Climate Extremes Index (CEI) and a Greenhouse Climate Response Index (GCRI). The CEI is based on an aggregate set of conventional climate extreme indicators, and the GCRI is composed of indicators that measure changes in the climate that have been projected to occur as a result of increased emissions of greenhouse gases. These indices may help non-specialists to better understand the rich diversity of climate change.

The CEI in the U.S. supports the notion that the climate has become more extreme, but this may merely be the results of natural climate variability. The U.S. GCRI reflects a significant increase in the index. Still, the rate of change of the GCRI is not large enough to unequivocally reject the possibility that the increase in the GCRI may have resulted from other factors including natural climate variability, although this is not a likely explanation (about a 5 to 10% chance). Both indices increased rather abruptly during the 1970s, at a time of major circulation changes over the Pacific Ocean and North America.

Significance of the $R(t)$ trends

In the previous section we showed that for certain seasons, the $R(t)$ time series for surface temperature signals from the TP experiment with combined CO_2 and sulphate aerosol forcing show large, positive linear trends over the last 40-60 years. Such trends are qualitatively consistent with the hypothesis that sulphate aerosol-induced cooling could have obscured an enhanced greenhouse effect warming signal. But are these trends statistically significant? This is a difficult question to answer. In order to make meaningful statements about trend significance, we need information about the characteristics of 'unforced' $R(t)$ trends due solely to the effects of internally-generated natural variability on decadal-to-century timescales.

The observational data are probably contaminated by anthropogenic influences. In this study, we employ model-generated noise data. In the model world, we can examine output from experiments with no external forcing in order to estimate the magnitude and spatial properties of natural variability noise. Near surface temperatures data were taken from a 600-year control integration with the Hamburg A/OGCM, and a 1,000-year integration of the GFDL coupled model. In order to determine the significance of the $R(t)$ trends, we need first to establish the sampling distributions of trends in these statistics in the absence of external forcing. The method we use is similar to that employed by Santer et al., (1995b).

Using these distributions, $R(t)$ trends for the SC signal are significant for trend lengths of 50 years in JJA and SON. This result does not depend on the model used to define natural variability noise, at least not for the two control runs examined here. It indicates that, in these seasons, there is an evolving expression of the SC signal pattern in the observed data, independent of any trend in global-mean temperature.

Conclusions

Our results indicate that in summer (JJA) and autumn (SON), the pattern of near-surface temperature change in response to combined sulphate aerosol and CO_2 forcing shows increasing similarity with observed changes over the last 50 years. The results from the individual CO_2-only and sulphate-only experiments suggest that at least some of this increasing spatial congruence is attributable to areas where the real world has cooled.

In the absence of reliable information on the magnitude and spatial characteristics of long timescale natural variability in the real world, we use data from multi-centennial control integrations performed with two different coupled atmosphere-ocean models to estimate the sampling distributions of trends in $R(t)$ on timescales of 10-50 years. For the combined CO_2/sulphate aerosol experiment, the 50-year $R(t)$ trends for the JJA and SON signals are significant relative to the trends obtained in the absence of external forcing. Results are robust in that they do not depend on the choice of control run used to estimate natural variability noise properties. The $R(t)$ trends for the CO_2-only signal are not significant in any season.

The caveats regarding the signals and natural variability noise which form the basis of this study are numerous. Most important is that GCMs of this kind at present probably

underestimate natural variability by a factor of at least two when compared to syntheses of long paleoclimatic time series (Bradley and Jones, 1993; Barnett et al., 1995). Nevertheless, we have provided first evidence that both the large scale (global-mean) and smaller scale (spatial anomalies about the global mean) components of a combined CO_2/anthropogenic sulphate aerosol signal are identifiable in the observed near-surface air temperature data. If the coupled model noise estimates used here are realistic, we can be highly confident that the anthropogenic signal we have identified is distinctly different from natural variability noise. The fact that we have been able to detect the detailed spatial signature in response to combined CO_2 and sulphate aerosol forcing, but not in response to CO_2 forcing alone, suggests that some of the regional scale background noise (against which we are trying to detect a CO_2-only signal) is in fact part of the signal of a sulphate aerosol effect on climate. The large effect of sulphate aerosols found in this study demonstrates the importance of their inclusion in experiments designed to simulate past and future climate change.

References

Barnett TP, 1986: Detection of changes in global tropospheric temperature field induced by greenhouse gases. *J Geophys Res* 91, 6659-6667

Barnett TP, and Schlesinger ME, 1987: Detecting changes in global climate induced by greenhouse gases. *J Geophys Res* 92, 14772-14780

Barnett TP, Santer BD, Jones PD, Bradley RS and Briffa KR, 1995: Estimates of low frequency natural variability in near-surface air temperature. *Science* (submitted)

Bradley RS and Jones PD, 1993: 'Little Ice Age' summer temperature variations: their nature and relevance to recent global warming trends. The *Holocene* 3, 367-376

Charlson RJ and Wigley TML, 1994: Sulfate aerosol and climate change. *Sci Amer* 270, 48-57.

Hegerl GC, von Storch H, Hasselmann K, Santer BD, Cubasch U, Jones PD, 1995: Detecting Anthropogenic climate change with an optimal fingerprint method. *J Climate* (in press)

Jones PD and Briffa KR, 1992: Global surface air temperature variations during the twentieth century: part 1, spatial, temporal and seasonal details. The *Holocene* 2, 165-179

Madden RA and Ramanathan V, 1980: Detecting climate change due to increasing carbon dioxide. *Science* 209, 763-768

Meehl GA, Washington WM and Karl TR, 1993: Low-frequency variability and CO_2 transient climate change. *Climate Dynamics* 8, 117-133.

Santer BD, Wigley TML and Jones PD, 1993: Correlation methods in fingerprint detection studies. *Clim Dynamics* 8, 265-276

Santer BD, Taylor KE, Wigley TML, Penner JE, Jones PD and Cubasch U, 1995a: Towards the detection and attribution of an anthropogenic effect on climate. *Climate Dynamics* (in press)
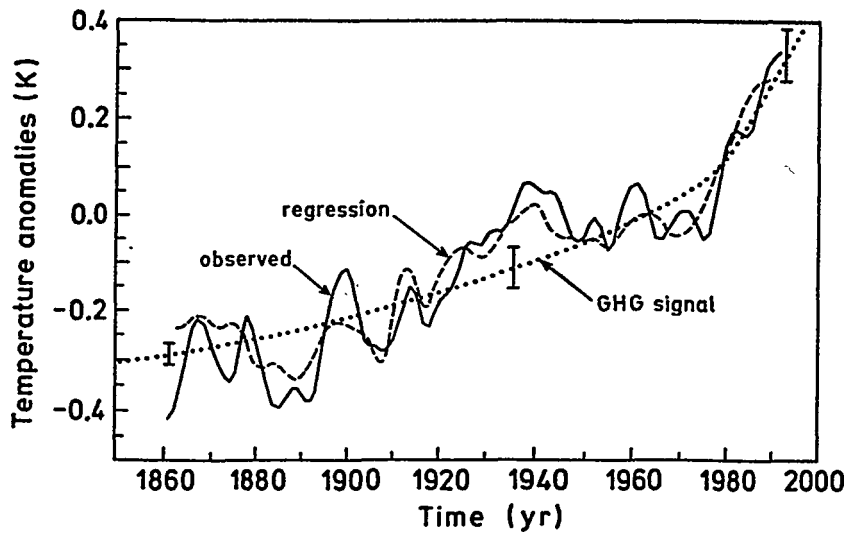
Fig. 1 Observed (Gaussian) 10 yr low-pass filtered global surface air temperatures 1861-1992, solid line, reproduction by the best-fit MRM (see text), dashed line, and MRM-deduced anthropogenic enhanced GHG signal, dotted line.
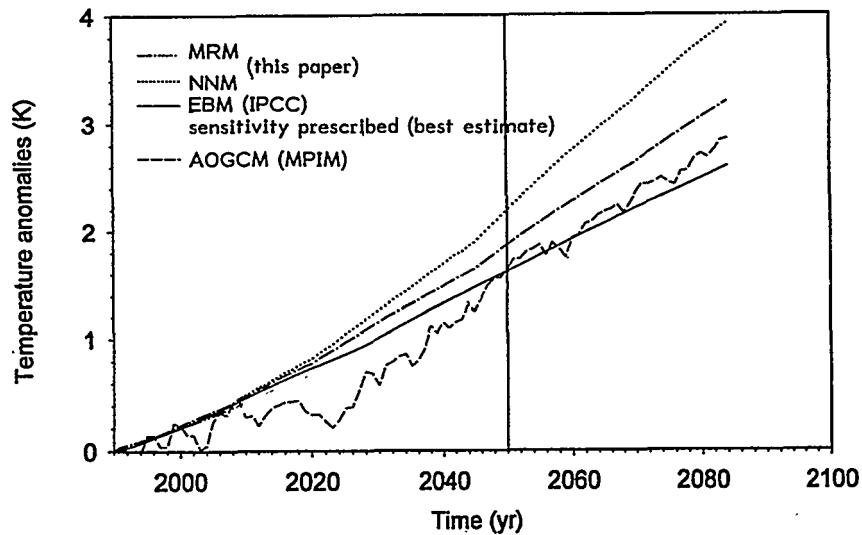
Fig. 2. Comparison of the projected GHG signal 1990 (reference) - 2084 using the following models: EBM (IPCC 1992 best estimate, see also Wigley and Schlesinger 1985, Wigley et al. 1991), AOGCM (Cubasch et al. 1992, 1994), MRM, and NNM (multiple regression and neural network model, this paper).

Table 1   Equilibrium   and transient GHG signals as derived from selected AOGCM experiments compared with the EBM IPCC best estimate and statistical assessments (MRM and NNM, this paper; GFDL = Geophysical Fluid Dynamics Laboratory, Manabe et al. 1992; MPIM = Max Planck Institute for Meteorology, Cubasch et al. 1992; CRU = Climate Research Unit, Wigley et al. 1991; UF = University of Frankfurt, this paper).

Model type	AOGCM	AOGCM	OD-EBM	MRM	NNM
Institution	GFDL	MPIM	IPCC/CRU	UF	UF
CO_2 inital	300 ppm	390 ppm	300 ppm	300 ppm	300 ppm
CO_2 increase	1% yr^{-1}	IPCC A	IPCC A	IPCC A	IPCC A
Equilibrium signal:					
$2 \times CO_2$ (ΔT_{2x})	3.5 K	2.6 K	(2.5 K)$^+$	2.3 ± 0.5 K	2.7 K
Transient signal:					
$2 \times CO_2$	2.3 K	1.3 K^l	1.4 K	1.6 ± 0.3 K	1.8 K
1700 - 1990	-	-	0.8 K	0.7 ± 0.1 K	0.6 K
1875 - 1990	-	-	0.65 K	0.6 ± 0.1 K	0.5 K
1990 - 2050	?	1.6 K	1.5 K	1.8 ± 0.3 K	2.2 K

$^+$ prescribed (CO_2 doubling sensitivity, IPCC best estimate)

Table 2   Comparison of the GHG ('industrial'), volcanic, solar, and ENSO signals in the surface air temperature, global mean (see Fig. 1) and seasonal-regional (meridional) maximum, as deduced from MRM.

Forcing	Best estimate	range	seasonal-regional maximum	explained variance
GHG	+ 0.6 K	0.6 - 0.8 K	~ 7 K	35 - 50 %
volcanic	- 0.15 K	0.1 - 0.4 K$^{a)}$	~ 3 K$^{a)}$	15 - 30 %
solar	+ 0.1 K	0.1 - 0.2 K$^{a)}$	~ 1.5 K$^{a)}$	5 - 15 %
ENSO	+ 0.2 K	0.2 - 0.3 K$^{b)}$	~ 2 K$^{b)}$	5 - 10 %

a) fluctuations, year-to-year and longer time scales
b) fluctuations, year-to-year time scale

since 1800 (carbon dioxide concentration of c. 280 ppm) is considered and the natural forcing parameter time series in the MRM are varied. In case of the mean northern or southern hemisphere temperatures, respectively, the GHG signals are nearly identical although the deviations (year-to-year and decadal fluctuations) from the long-term non-linear trend are much more pronounced in the former case (northern hemisphere, figures not shown).

In a similar way neural networks (feed-forward and back-propagation, see e.g. Smith 1993) are applied to this problem. They lead to very similar GHG signals which may be derived from observations. Furthermore, all these statistical signal assessments are extrapolated into the future (1990-2084) based on the IPCC 'business-as-usual scenario, also called scenario A, in order to enable an intercomparison with EBM (energy balance models) and GCM (general circulation models) projections where in case of EBM the IPCC (1992) best estimate (model based on Wigley and Schlesinger 1985 or Wigley et al. 1991) and in case of GCM coupled atmosphere-ocean models (AOGCM; Manabe at al. 1992, Cubasch et al. 1992) are used. The results are summarized in Table 1 and Fig. 2. (For seasonal and regional signal assessments see Schönwiese & Stähler 1991, Schönwiese & Bayer 1995.) Finally, in Table 2, using again MRM assessments, the GHG signals so far ('industrial', carbon dioxide equivalents) are compared with those from volcanic, solar, and ENSO forcing.

Conclusions

The statistical approach based on observational data indicates that the enhanced anthropogenic GHG signal so far ('industrial') in the global mean surface air temperature amounts to 0.6-0.8 K and the seasonal-meridional maximum may have a magnitude of roughly 7 K. The transient carbon dioxide doubling signal assessed in the same way is 1.3-1.9 K (global average) compared to 1.3-2.3 K using EBM (IPCC) and AOGCM projections. (The IPCC 1995 Second Assesment Report seems to evaluate very similar numbers.) So, there is a fair agreement of statistical and deterministic model simulations of the enhanced GHG signal at least in respect to the global mean surface air tremperature. The natural signals considered statistically in this paper are smaller than the 'industrial' GHG signal.

Acknowledgements

References

Carbon Dioxide Information Analysis Center (CDIAC) 1994. Trends '93. A Compendium of Data on Global Change. Publ. No. ORNL/CDIAC-65, Oak Ridge, 984+28 pp.

Cubasch, U., et al. 1992. Time-dependent greenhouse warming computations with a coupled ocean-atmosphere model. Clim. Dyn. 8: 55-69. - 1994. Priv. Comm.

Hansen, J. & Lebedeff, S. 1987. Global trends of measured surface air temperature. J. Geophys. Res. 92(D11): 13345-13372. - 1993. Priv. Comm. and GISS data on magnetic tape.

Intergovernmental Panel on Climate Change (IPCC, Houghton, J.T. et al., eds.) 1992. Climate Change 1992. The Supplementary Report to the IPCC Scientific Assessment. Cambridge Univ. Press, Cambridge, 200 pp. - 1994. Radiative Forcing of Climate Change. IPCC/WMO/UNEP, Geneva, 28 pp. - 1995. Second Assessment Report, in prep.

Jones. P.D. 1988. Hemispheric surface air temperature variations: recent trends and an update to 1987. J. Climate 1: 654-660.

Jones, P.D. 1994. Hemispheric surface air temperature variations: a reanalysis and an update to 1993. J. Climate 7: 1794-1802. - Priv. comm.

Manabe, S., Spelman, M.J. & Stouffer, R.J. 1992. Transient responses of a coupled ocean-atmosphere model to gradual changes of atmospheric CO_2. J. Climate 5: 105-126.

Schönwiese, C.-D. & Stähler, U. 1991. Multiforced statistical assessments of greenhouse-gas-induced surface air temperature change 1890-1985. Clim. Dyn. 6: 23-33.

Schönwiese, C.-D. & Bayer, D. 1995. Some statistical aspects of anthropogenic and natural forced global temperature change. Atmósfera 8: 3-22.

Smith, M. 1993. Neural Networks for Statistical Modeling. Van Nostrand Reinhold, New York, 235 pp.

Wigley, T.M.L. & Schlesinger, M.E. 1985. Analytical solution for the effct of increasing CO_2 on global mean temperature. Nature 315: 649-652. - Wigley, T.M.L. et al. 1991: Sea level and temperature change under the greenhouse effect (STUGE), User's Manual, Climatic Research Unit, University of East Anglia, UK.
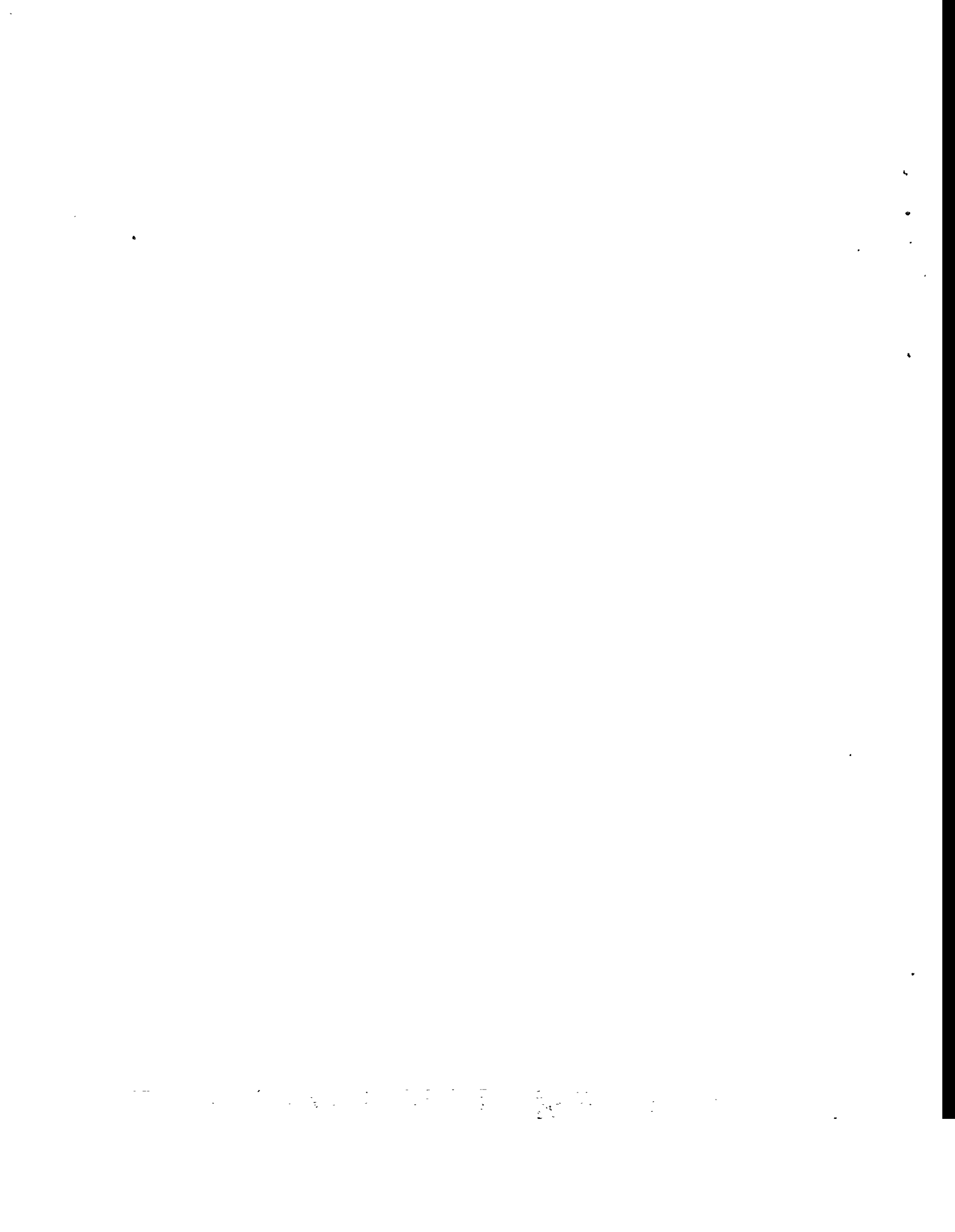
Analysis of climate records: local and regional aspects
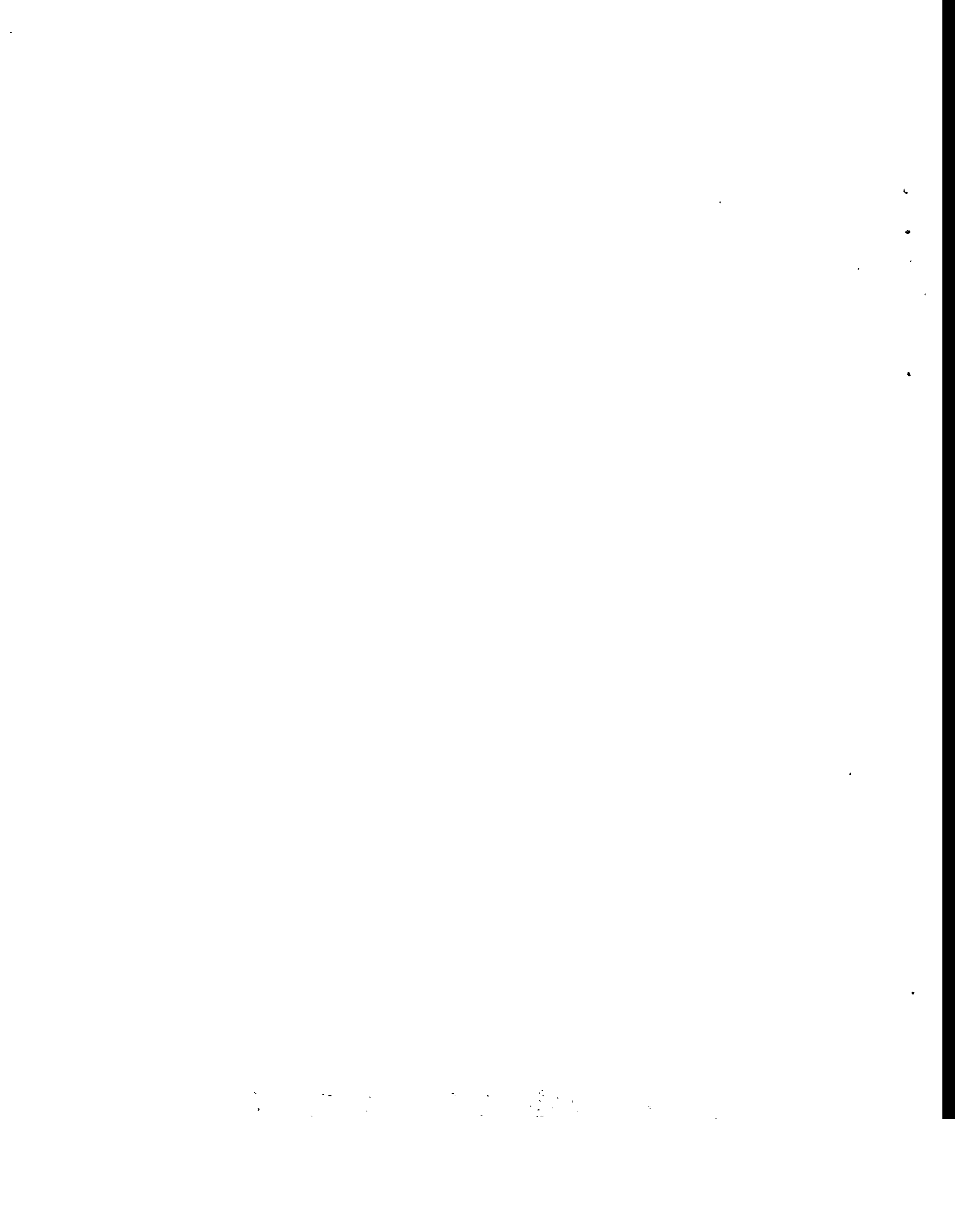
Extreme precipitation events - time series analyses of Viennese data

Ingeborg Auer

Central Institute for Meteorology and Geodynamics,
Hohe Warte 38, Vienna

Introduction

There is much uncertainty about increase or decrease of extreme weather events due to an artificially enhanced greenhouse effect (Auer, Boehm and Steinacker, 1995). In the case of precipitation one assumption is that a warmer atmosphere should contain more water and by that an increase of extreme precipitation should follow, sometimes including simultaneously the intensification of dry spells. At first guess this seems to be a logical idea in some aspects. On the other hand such a simple idea was relativized by Auer and Böhm, 1994 showing that the warming from the 19th to 20th century has led to a spatial quite differently long-term precipitation behaviour in a quite small area like Austria. In this study daily precipitation measurements are used to create time series of some derived elements in order to investigate their long-term development.

The question of data quality and homogeneity

Precipitation has been measured in Vienna since 1845, the time series of monthly precipitation amounts was tested for homogeneity in Auer (1993) and turned out to be homogeneous between 1873 and 1992. For this period it was assumed that also daily precipitation data should be homogeneous during this time interval. Since 1993 an automatic precipitation measuring system has been in operational use, however, there is no experience of homogeneity for the last two years, as the time interval was too short for homogeneity testing.

Extreme daily precipitation sums

The time series of the Rx (abbreviation referring to NACD) for the year and the four seasons are shown in Fig.1. Taking into account only the highest daily precipitation sum of each year it turns out that the two highest values of this time series occurred during the 1880ies within two successive years, looking at the highest 10% there is no special accumulation observable during the last decades. For the seasons, as well, no increasing frequency during the last few decades can be found.
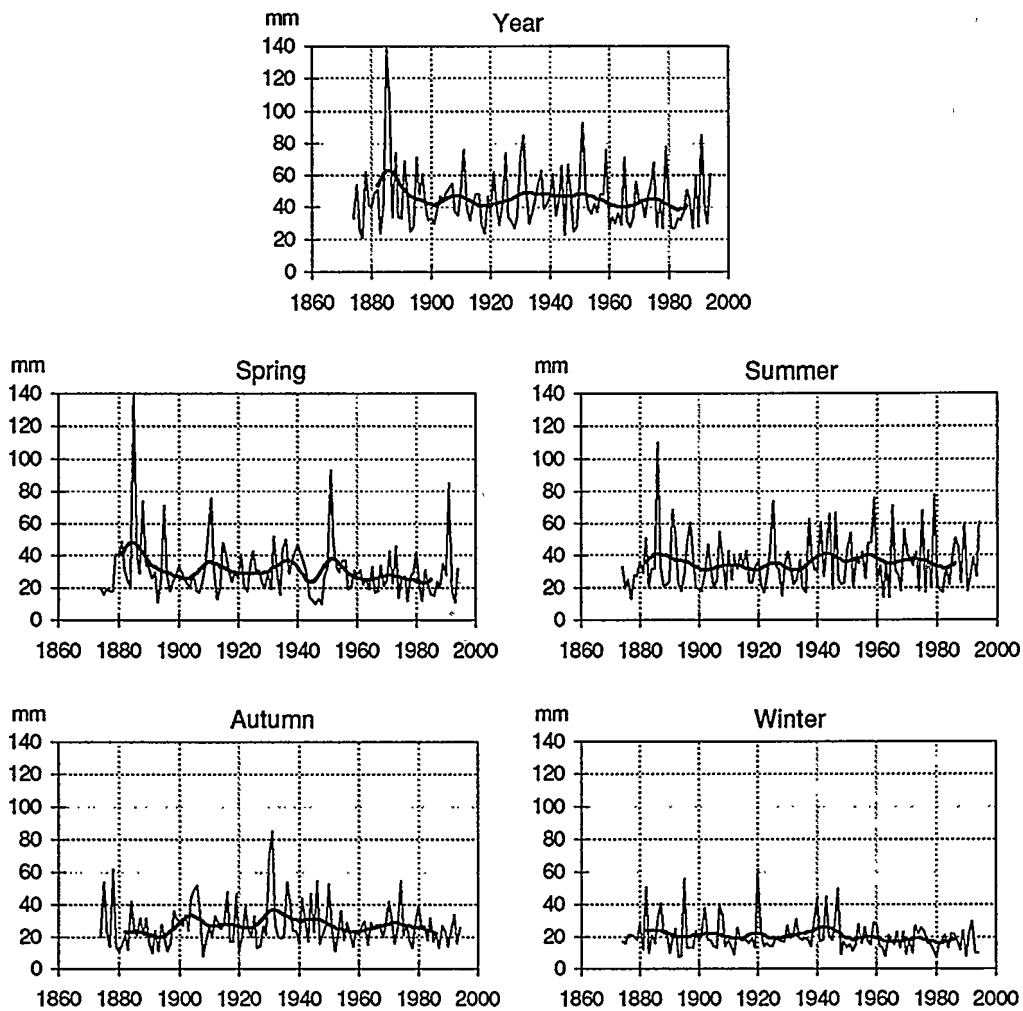
Fig. 1 Time series of maximum daily precipitation for the year and the seasons in Vienna, 1874 - 1994 ——— single values ——— filtered T*=20y

Table 1 Linear regression analysis of monthly, seasonal and annual extreme daily precipitation sums in Vienna, 1874-1994.

	J	F	M	A	M	J	J	A	S	O	N	D
Trend	-0,7	1,2	-2,7	-3,09	-8,1	2,4	0,4	-0,5	-1,6	-1,6	2,3	-5,1
TNR	-0,12	0,14	-0,32	-0,33	-0,42	0,14	0,03	-0,04	-0,14	-0,12	0,22	-0,51

	Sp	Su	Au	Wi	Year	TNR Trend to noise ratio
Trend	-8,1	4,1	-1,0	-5,0	-5,5	(1,0 = 68%, 2,0 = 95%
TNR	-0,46	0,24	-0,08	-0,51	-0,3	significance for existing trend)

Table 1 gives additional information about linear regression analyses for the last 121 years of this meteorological element. The result is quite clear: Except summer all the seasons as well as the year show more likely a decrease. The amounts however, including that for the slight summer increase, are beyond any statistical significance.

To go into more detail the time series were divided into subintervals, to be precise according to times of increasing and decreasing temperature level (Boehm, 1992). The question was, does increasing temperature cause an increase of extreme precipitation too and vice versa. Table 2 shows the same information as Table 1 for the subintervals, but only for the seasons and the year.

Table 2 Linear regression analysis of extreme daily precipitation sums for the year and the seasons for special subintervals, Wien Hohe-Warte, 1874-1994

	Year	Spring	Summer	Autumn	Winter
	1874-1890	1877-1948	1874-1914	1874-1913	1874-1890
Trend	26,8	-12,2	2,8	4,8	5,5
TNR	0,84	-0,65	0,16	0,37	0,51
	1890-1949	1948-1957	1914-1949	1913-1964	1890-1917
Trend	1,2	-1,8	5,0	-5,4	-0,3
TNR	0,08	-0,08	0,33	-0,36	-0,02
	1949-1973	1957-1994	1949-1966	1964-1973	1917-1941
Trend	-10,7	4,4	0,0	-1,5	2,8
TNR	-0,66	0,20	0,00	-0,14	0,26
	1973-1994		1966-1994	1973-1994	1941-1994
Trend	1,0		2,9	-9,0	-6,7
TNR	0,06		0,17	-0,90	-0,62

A certain increase of the annual extreme precipitation sums can be observed between 1874 and 1890, a time interval with decreasing temperature level but high annual precipitation amounts around 1880, but again TNR does not reach the level of statistical significance. The latest warming phase starting at different dates during the different seasons was accompanied by slight increases for the year, spring and summer, but TNR is near to zero. On the contrary, the warming periods in autumn and winter go ahead with decreases of daily extreme precipitation in autumn (TNR = 0,9) and winter.

Frequencies of number of precipitation days $\geq$ 20,0 and $\geq$ 50,0 mm

The next derived climatological elements that should be investigated are the number of days $\geq$ 20,0 and 50,0 mm, quantities with mean occurrences of about 5 days per year and 0,25 days per year respectively in Vienna, normally concentrated during the warmer season. Fig. 2 show the time series of these two climatological elements since 1872.

The linear trend analyses for the annual number of days ≥ 20 mm shows that no change at all has taken place during the last 120 years, in detail that a slight decrease during the summer season was compensated by a slight increase during the winter.

The very rare occurrence of days ≥ 50,0 mm shows no increase during the last decades.
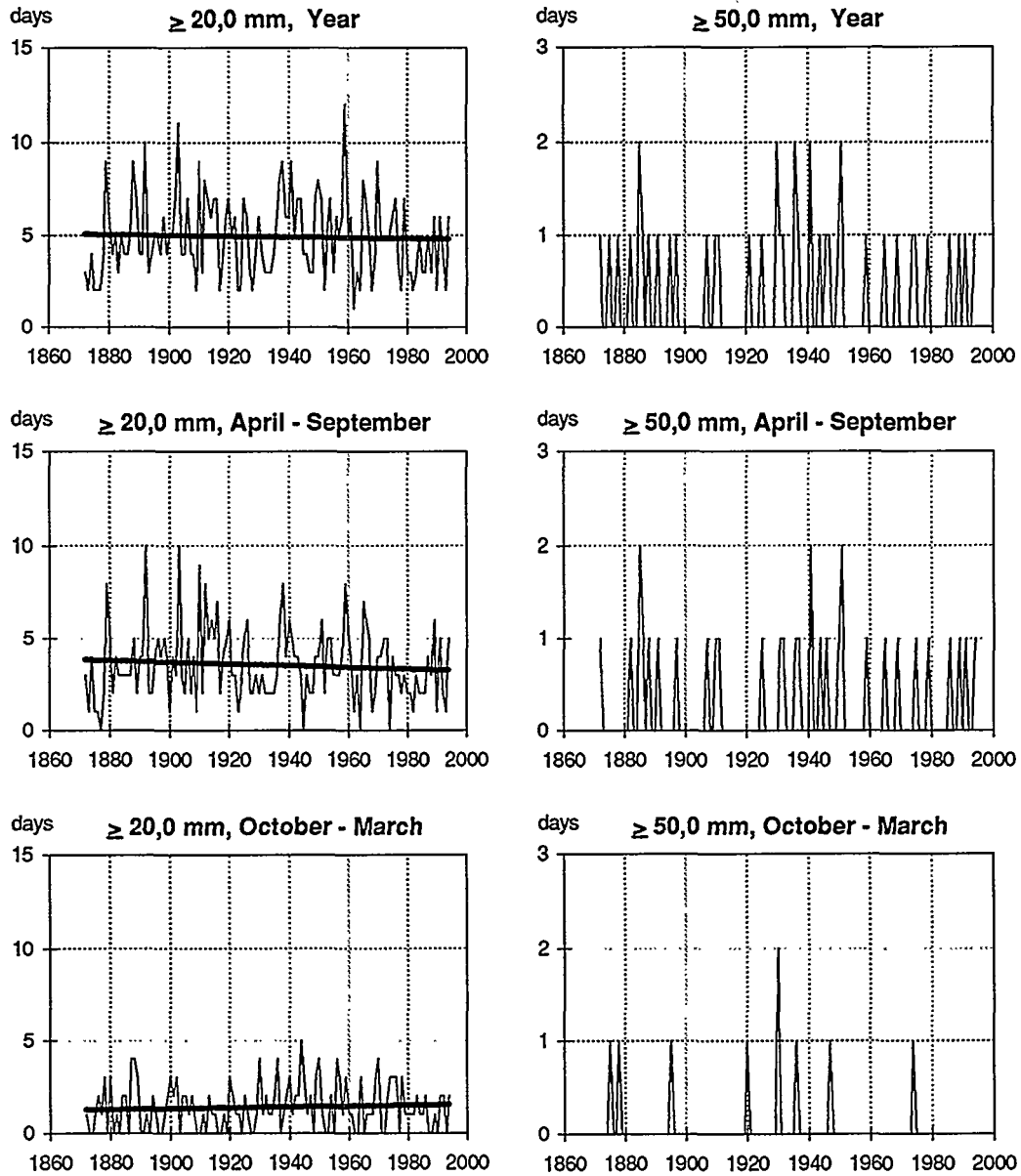
Fig. 2 Time series of the number of days with precipitation ≥ 20,0 mm and ≥ 50,0 mm, Wien Hohe Warte, 1872 -1994.

Days without precipitation

Another often heard speculation is that drought duration is becoming more intensive within the ongoing warming of our climate. To study this topic time series of the number of days without precipitation (noR) for the whole year as well as for summer season and winter season are given in Fig. 3. Practically no change has taken place in the winter season, trend as well as TNR are very near 0. On the contrary an increase of about 8 days since 1874 in the summer season causes practically the same increase for the whole year. But taking into account TNR the increase turns out to be not statistically significant.
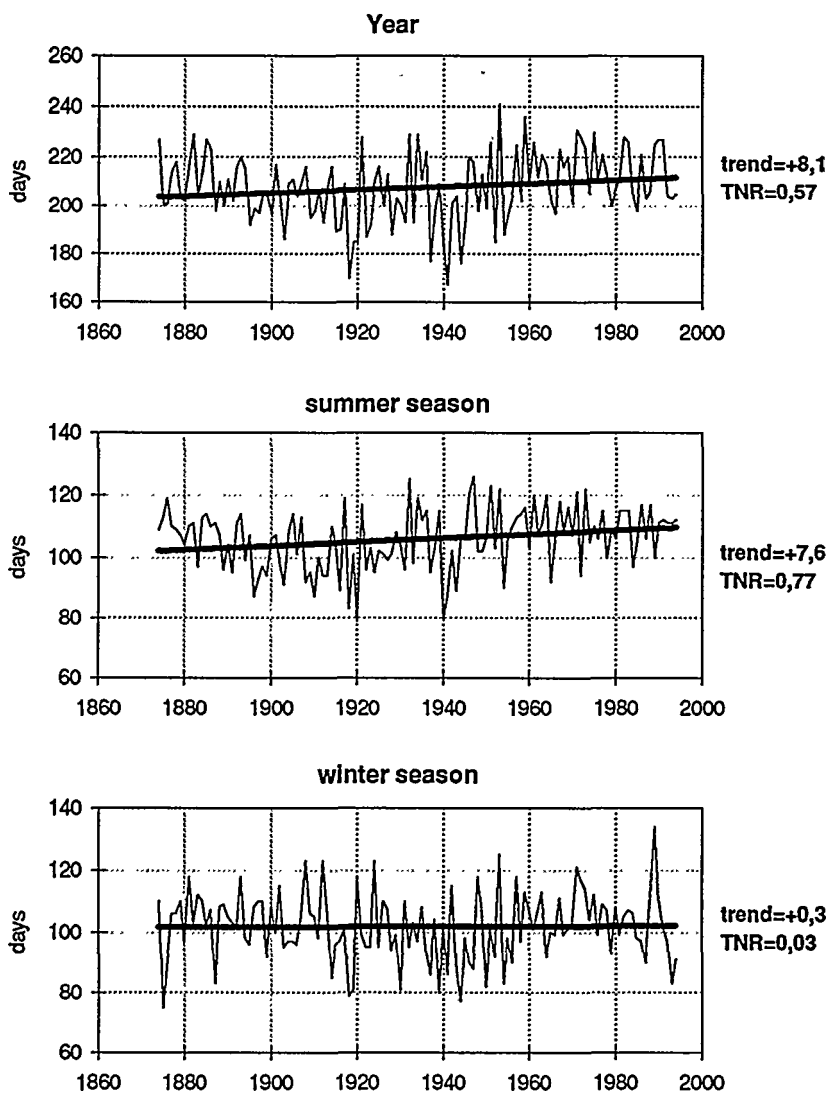
Fig. 3 Time series of the number of days without precipitation, Wien-Hohe Warte, 1874-1994

Correlation between monthly precipitation sums and extreme events

For each month the correlation coefficients between Rsum and Rx are greater than 0,7, in April, June and October the values exceed 0,8. In general between Rsum and R20 r is smaller, especially from November till March when those events are of rare occurrence. This fact is the principle case for the correlation between the very rare R50 and Rsum. For noR r is a little bit smaller than for Rx, except February.

Table 3 Annual course of the correlation coefficients r between precipitation sums (Rsum) and some derived climatological elements describing extreme precipitation events (1874-1993).

Correlation coefficients												
	J	F	M	A	M	J	J	A	S	O	N	D
Rsum/ Rx	0,79	0,72	0,71	0,84	0,79	0,83	0,79	0,70	0,78	0,85	0,72	0,72
Rsum/R20	0,41	0,58	0,61	0,73	0,80	0,73	0,78	0,80	0,79	0,75	0,59	0,50
Rsum/R50	*	0,18	*	0,31	0,51	0,53	0,49	0,22	0,36	0,54	0,13	0,39
Rsum/no R	-0,70	-0,73	-0,56	-0,56	-0,61	-0,53	-0,50	-0,57	-0,63	-0,69	-0,60	-0,68

	Sp	Su	Au	Wi	Year							
Rsum/ Rx	0,54	0,65	0,66	0,60	0,34							
Rsum/R20	0,68	0,78	0,69	0,49	0,67							
Rsum/R50	0,28	0,49	0,43	0,47	0,33							
Rsum/no R	-0,52	-0,62	-0,69	-0,69	-0,56							

* no occurrence during observation period

Summary

The often claimed supposition that extreme precipitation events have been increasing with a simultaneous increasing of dry spells due to an artificially enhanced warming of our atmosphere is investigated with the help of extreme daily precipitation sums, no. of days ≥ 20 and ≥ 50 mm as well as of days without precipitation on monthly basis. None of the enumerated derived climatological elements shows a statistically significant change during the period of investigation. The study was done for one single point of Austria in a region with decreasing precipitation regime since 1940. It is clear that more work has to be done in extending to more than one single point, especially to regions with an observed increase of precipitation regime during the last years, as it could be found for example (Auer, 1993) in some western parts of Austria.

References

Auer, I. 1993. Niederschlagsschwankungen in Österreich seit Beginn der instrumentellen Beobachtungen durch die Zentralanstalt für Meteorologie und Geodynamik. Österr. Beitr. zu Meteorologie und Geophysik, Heft 7, 73pp, Vienna.

Auer, I. 1993. Trend and variations in precipitation in Austria since 1845. Zeszyty Naukowe Uniwersytetu Jagiellonskiego MCXIX, Prace Geograficzne * Z. 95, pp 173-182.

Auer, I. & Boehm, R. 1994. Combined Temperature-Precipitation Variations in Austria During the Instrumental Period. Theor. Appl. Climatol. 49, 161-174.

Auer, I., Boehm R. & Steinacker, R. 1995. 32 questions concerning climate change (results of a questionnaire): to be printed in SILMU report, 1995.

Boehm, R. 1992. Lufttemperaturschwankungen in Österreich seit 1775. Öster. Beitr. zu Meteorologie und Geophysik, Heft 5, Vienna.

Frich, P. 1994. North Atlantic Climatological Dataset (NACD) - objectives, methodology and present status. P. 17-23 in Pre-prints from 19. Nordic Meteorology Meeting, 6.-10. June 1994, Kristiansand, Norway.

Short term variability of air temperature at three meteorological stations in Bucharest

Constanţa Boroneanţ

National Institute of Meteorology and Hydrology,
Sos. Bucureşti-Ploieşti 97, 71552 Bucharest, Romania

Introduction

During the last decades the global warming of the atmosphere has been documented in the series of global air temperature mean. Various hypotheses such as greenhouse gases effect and changes in the natural variability of the climate have been forwarded. Several authors (Brázdil et al., 1994, Karl et al., 1993) pointed out on asymmetric trends of daily maximum and minimum temperature. The daily maximas are strongly influenced by the incoming radiation while the daily minima are mainly forced by the long-wave radiation budget. Consequently, these daily extremes are responsible for the evolution of daily temperature mean and the mean daily temperature range.

The variability of annual and seasonal series of air temperature mean (MT), maxima mean (TMAX), minima mean (TMIN) and mean of daily temperature range (DTR) is examined for three stations in Bucharest during the period 1951-1994. The meteorological stations Filaret (44°25'N, 26°06'E), Băneasa (44°30'N, 26°08'E) and Afumaţi (44°30'N, 26°13'E) are shown on the Bucharest map. In present, Filaret is considered as representative for urban conditions while the other two stations for the geographical conditions the Bucharest city belongs to.

Fig. 1 Location of the considered meteorological stations on the Bucharest map

Station	Winter		Spring		Summer		Autumn		Annual	
	$\bar{x}$ °C	change-point year	$\bar{x}$ °C	change-point year	$\bar{x}$ °C	change-point year	$\bar{x}$ °C	change-point year	$\bar{x}$ °C	change-point year
MT										
Filaret	-0.2	1961↓	11.3	1965↑	21.9	1966↓,1984↑	11.8	1970↓	11.2	1968↓,1987↑
Băneasa	-0.7	1961↓,1987↑	10.7	1965↑	21.3	1967↓,1985↑	11.0	1970↓	10.6	1972↓,1987↑
Afumaţi	-0.7	1961↓,1970↑	10.6	1965↑	21.2	1966↓,1984↑	11.0	1969↓	10.5	1988↑
TMAX										
Filaret	3.7	1970↑	17.5	1965↑	28.6	1965↓,1984↑	18.0	1959↑,1970↓	17.0	1980↑
Băneasa	3.4	1961↓,1987↑	17.0	1965↑	28.3	1966↓,1985↑	17.5	1959↑,1970↓	16.6	1968↓,1987↑
Afumaţi	3.3	1961↓,1987↑	16.8	1965↑	28.0	1965↓,1985↑	17.4	1959↑,1970↓	16.4	1968↓,1988↑
TMIN										
Filaret	-3.1	1970↑,1984↓	6.3	1965↑	16.1	1972↓,1985↑	7.3	1959↑,1969↓	6.6	1965↑
Băneasa	-3.9	1969↑,1977↓	5.2	1957↑,1975↓	14.9	1972↓	6.1	1956↑,1970↓	5.6	1956↑,1972↓
Afumaţi	-4.1	1969↑,1984↓	5.1	1965↑	14.8	1972↓	6.0	1959↑,1969↓	5.4	1959↑,1975↓
DTR										
Filaret	6.8	1984↑	11.2	1982↑	12.5	1965↓,1984↑	10.7	1981↑	10.3	1982↑
Băneasa	7.3	1974↑	11.9	1974↑	13.4	1956↓,1976↑	11.4	1956↓,1976↑	11.0	1956↓,1976↑
Afumaţi	7.3	1986↑	11.7	1980↑	13.3	1968↓,1985↑	11.4	1965↓,1981↑	10.9	1963↓,1980↑

Table 1 Seasonal and annual means of MT, TMAX,TMIN and DTR and the change-point year of these series given by the Pettitt test for three meteorological stations in Bucharest

This study is aimed at pointing out the differences in evolution of the temperature parameters taken into consideration at the urban station (Filaret) and the other two stations outside to town (Băneasa and Afumați). In the same time, we search to find out at these stations common characteristics such as trend, change points that could be attributed to those factors responsible for short term climatic changes.

Data and methods

The seasonal and annual temperature means (MT), maxima means (TMAX), minima means (TMIN) and daily range means (DTR) were calculated from the corresponding daily values at all three considered stations during the period 1951-1994.

The statistical analysis has been performed using the methodology proposed by Sneyers (1990, 1992). To test the trend and the change points in the series mean, the non-parametric test Mann-Kendall, in the sequential manner, and the Pettitt tests have been used.

Results and discussion

As the Table1 shows, the seasonal and the annual means calculated for MT, TMAX, TMIN and DTR indicate differences between the values at the urban station (Filaret) and both stations outside of the town (Băneasa and Afumați). The greatest differences appear for TMIN in summer and autumn (1.3°C) while the smallest differences appear for TMAX (0.7°C) in spring.

The change-point years given by the Pettitt test indicate a shift in the series mean. Its values suggest the existence of two moments, one located in the 1960's characterised by the decreasing TMAX and increasing TMIN and another one located in the 1980's characterised by the increasing TMAX and decreasing TMIN, associated with the corresponding increasing of DTR.

References

Brázdil, R., Machu, R. and Budíkova, M. 1994. Temporal and spatial changes in maxima and minima of air temperature in the Czech Republic in the period of 1051-1993, in Brázdil, R. and Kolár, M. (eds.) Contemporary Climatology, Brno, pp.93-102.

Boroneanţ, C. and Râmbu, N., 1992. Some aspects of the air temperature regime as appearing at selected stations in Romania, Meteorology and Hydrology, vol. 22, 2, pp. 17-21

Karl, T.R., Jones, P.D., Knight, R.W., Kukla, G., Plummer, N., Razuvayev, V., Gallo, K.P. , Lindseay, J., Charlson, R.J. and Peterson, T.C. 1993. A new perspective on recent global warming: Asymmetric trends of daily maximum and minimum temperature, Bull. Amer. Meteor. Soc., 74, 1007-1023.

Sneyers, R., 1990. On the statistical analysis of series of observations, W.M.O., Technical Note No. 143, Geneva, 192p.

Sneyers, R., 1992. Use and misuse of statistical methods for the detection of climate change, 12th Conference on Probability and Statistics in the Atmospheric Sciences, Amer. Meteor. Soc. pp. J76-J81.

TRENDS OF MAXIMUM AND MINIMUM DAILY TEMPERATURES IN CENTRAL EUROPE

R. Brázdil[1], M. Budíková[2], I. Auer[3], R. Böhm[3], T. Cegnar[4], P. Faško[5], M. Gajić-Čapka[6], M. Lapin[5], T. Niedźwiedź[7], S. Szalai[8], Z. Ustrnul[7], R.O. Weber[9] and K. Zaninović[6]

[1] Department of Geography, Masaryk University, Brno, Czech Republic
[2] Department of Applied Mathematics, Masaryk University, Brno, Czech Republic
[3] Central Institute for Meteorology and Geodynamics, Vienna, Austria
[4] Hydrometeorological Institute, Ljubljana, Slovenia
[5] Slovak Hydrometeorological Institute, Bratislava, Slovak Republic
[6] Meteorological and Hydrological Service, Zagreb, Croatia
[7] Institute of Meteorology and Water Management, Cracov, Poland
[8] Hungarian Meteorological Service, Budapest, Hungary
[9] Paul Scherrer Institute, Villigen, Switzerland

INTRODUCTION

Minimum daily temperatures (TMIN) of 37 % of the global land mass increased three times more quickly than the maximum daily temperatures (TMAX) during the period 1951-1990 (0.84 and 0.24 $^\circ$C, respectively) (Karl et al. 1993). The resulting decrease in the daily temperature range (DTR defined as the difference of TMAX and TMIN) corresponded with the increase in mean temperature (MT) and was observed in all seasons of the year. Similar results were also found for about 50 % of the Northern Hemisphere land mass (corresponding values for TMAX, TMIN and DTR were 0.20, 0.80 and -0.56 $^\circ$C respectively) (Karl et al. 1993). These trends might be related to the greenhouse gas effect because the daily maxima are strongly influenced by incoming radiation, while the daily minima are mainly forced by the long-wave radiation. But in some parts of eastern North America, southern India, Antarctica and parts of Europe and Oceania (Karl et al. 1994) DTR showed little change or even an increase during 1951-1990. Considering the pure coverage of the European region in the above paper this study dealt with a corresponding analysis for the Central European region.

DATA AND METHODS

Seasonal and annual MT, TMAX as well as TMIN for nine selected countries or regions in central Europe (Fig. 1) in 1951-1990 were used for investigation. Only stations whose records are well checked and considered to have no inhomogeneities are used. These stations are mainly located outside the direct impact of the urban heat island. But for some regions their spatial coverage is small. The central European

series of MT, TMAX, TMIN and DTR were compiled by the area-weighted averaging of the series of areal means calculated for each of nine selected regions in the form of deviations from the mean of the period of 1961-1990.
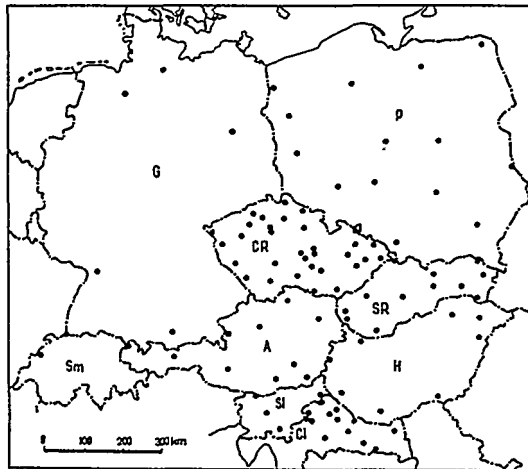
Fig. 1 Geographical distribution of stations used for calculation of the Central European series: Germany (used abbreviation is G - 5 stations), Switzerland - midland (Sm - 2), Poland (P - 14), Czech Republic (CR - 32), Austria (A - 10), Slovenia (SI - 4), Slovak Republic (SR - 12), Hungary (H - 8), Croatia - lowland (CI - 13)

The central European series were analysed by the method of linear trend with t-tests of statistical significance, by the method of a change point identification in the mean and by the method of kernel smoothing (see Brázdil et al. 1995).

RESULTS AND DISCUSSION

The increase in annual TMAX in central Europe during the 1951-1990 period was slightly lower than that of TMIN (0.52 $^{\circ}$C and 0.60 $^{\circ}$C, respectively). The resulting decrease in DTR by -0.08 $^{\circ}$C was smaller than the value of the warming (increase in MT by 0.40 $^{\circ}$C). In central Europe, with the exception of spring TMIN, corresponding changes in other seasonal characteristics are non-significant (Fig. 2). There is practically no agreement between the linear trends of seasonal and annual MT and the DTR values. These results, valid for 1.03 % of the Northern Hemisphere land mass and for 0.69 % of the Globe land mass do not coincide with the results obtained by Karl et al. (1993) on the global scale and for the Northern Hemisphere. On the other hand, the central European series are significantly correlated (α=0.01) with the Globe land-mass series (Karl et al., 1993) for the annual TMAX (0.440 in 1952-1989) and for the annual TMIN (0.454) which does not hold for the annual DTR (0.124). But due to low correlation of both series for annual TMAX, TMIN and DTR their fluctuations show different features (Fig. 3).

Negligible non-significant trends in DTR in central Europe are probably related to small cloud cover changes in this region (mainly a decrease between 1 and 6 % in cloud cover for selected regions during 1951-1990). TMAX values are more closely connected with the cloud cover than the TMIN values, mainly in spring and summer, but also in autumn when radiative effects are more important than circulation effects. Correlations of the DTR with the mean daily cloud cover explain usually 50 to 90 % of

the common variance (see e.g. Brázdil et al. 1995). The remaining unexplained variance may be related to the influence of other meteorological variables, such as air humidity, evaporation, snow cover, aerosols, etc.
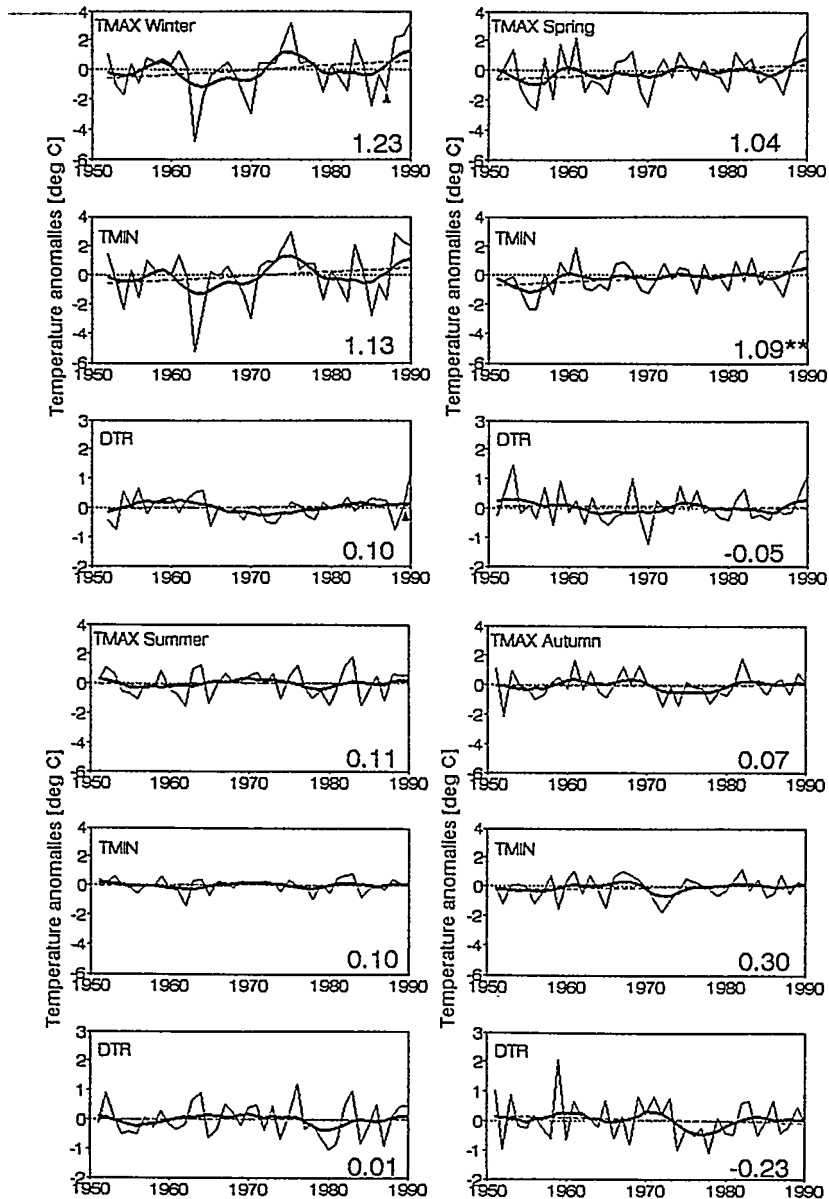
Fig. 2 Variation of seasonal anomalies of TMAX, TMIN and DTR (in °C) for central Europe in 1951-1990 smoothed by the method of kernel smoothing and with linear trend (its value is given by the number for 1951-1990, * - trend significant at the 0.10 level, ** - trend significant at the 0.05 level). Reference period 1961-1990. Significant change points are denoted with an arrow
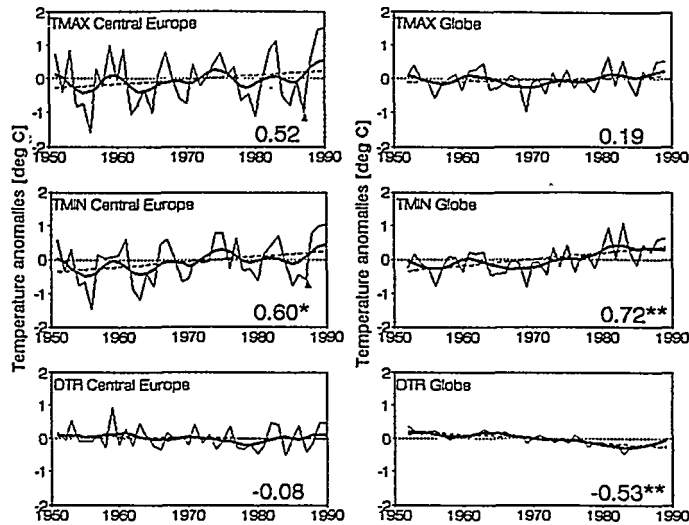
Fig. 3 Text see Fig. 2, annual anomalies, central Europe (1951-1990) and the Globe land mass (1952-1989) (Karl et al., 1993)

The obtained results do not confirm the simplified hypothesis about a faster increase in TMIN in comparison with TMAX and a resulting decrease in DTR for the period of increasing greenhouse gas concentration in the central European region. The observations support the idea about different impacts of global effects in several parts of the Globe as a consequence of possible variations in circulation patterns.

Acknowledgements: The authors thank the following person and institutions for kindly providing the data: Dr. P.D. Jones, University of East Anglia, Norwich; German Weather Service, Offenbach a. M.; Czech Hydrometeorological Institute, Prague; Swiss Meteorological Institute, Zürich.

REFERENCES

Brázdil, R., Budíková, M., Auer, I., Böhm, R., Cegnar, T., Faško, P., Gajić-Čapka, M., Koleva, E., Lapin, M., Niedźwiedź, T., Szalai, S., Ustrnul, Z., Weber, R.O. & Zaninović, K. 1995. Trends of maximum and minimum daily temperatures in central and southeastern Europe - natural variability or greenhouse gas signal? Manuscript, Brno, 36 pp.

Karl, T.R., Easterling, D., Peterson, T.C., Baker, C.B., Jones, P.D., Kukla, G., Plummer, N., Razuvayev, V.N. & Horton, B. 1994. An update on the asymmetric day/night land surface warming. In: Sixth Conference on Climate Variations, Amer. Meteorol. Soc., Nashville, Tennessee, pp. 170-172.

Karl, T.R., Jones, P.D., Knight, R.W., Kukla, G., Plummer, N., Razuvayev, V., Gallo, K.P., Lindseay, J., Charlson, R.J. & Peterson, T.C. 1993. A new perspective on recent global warming: Asymmetric trends of daily maximum and minimum temperature. Bull. Amer. Meteor. Soc. 74:1007-1023.

Snow conditions in Finland during the last century

Achim Drebs

Climatology Division, Finnish Meteorological Institute
P.O.Box 503, FIN-00101 Helsinki, Finland

Introduction

The knowledge of snow cover extension and snow depth during the winter have a great importance in many ways to people in northern countries. For example, the power industry needs snow cover information for water regulation. Nowadays, the tourist sector wants to find areas with long snow cover period and with good infrastructure. On the long run, snow cover and snow depth data can be used as an indicator for climate changes.

The first attempts of measuring snow cover extensions and snow depth were made at the end of the 19th century. They were wide spread but unfortunately not very continuous. Only at the meteorological institute in Helsinki continuous measurements extend back to 1892. From 1911 the snow cover and snow depth were measured.

Data

The data used in this overview is based on the published daily data from the meteorological yearbooks. Due to the ongoing research work this data is not quality controlled. Three stations from the south to the north (Helsinki-Jyväskylä/Kajaani-Sodankylä) are presented. This overview covers the same period, 1911-1994, for all stations. The calendar year is used. Kajaani data is used in the snow depth comparison due to the missing data from Jyväskylä 1959 - 1983. In the course of time, the definition of snow cover days has been changed. Therefore snow cover days were calculated for the period 1911 - 1936 only when snow depth was greater than 0 cm. All measurements were made with snow sticks.

Station:	co-ordinates:	founded:	snow observation since:
Helsinki	60°10' N 24°57' E	1829	1882
Jyväskylä	62°14' N 25°40' E	1883	1911
Kajaani	64°17' N 27°41' E	1887	1911
Sodankylä	67°22' N 26°39' E	1908	1911

Discussion

Snow cover days show a greater variability in Southern Finland than in Central or Northern Finland. In Helsinki, the number of days with snow cover varies between 57 and 180 days with a trend to smaller variability and to a decreasing number of days with snow cover since 1940. For Jyväskylä the extremes are 104 to 205 with no significant trend of change in the variability but with a slight increase of days with snow cover. The data from Sodankylä shows the same patterns except of the local maximum of snow cover days in the late sixties (Fig. 1). The study of the variability of snow cover days during the spring and autumn months shows that warming during one season does not causes remarkable influence on the number of snow cover days at whole winter. The variability of days with snow cover decreases from the south to the north and from the coast to the inland.
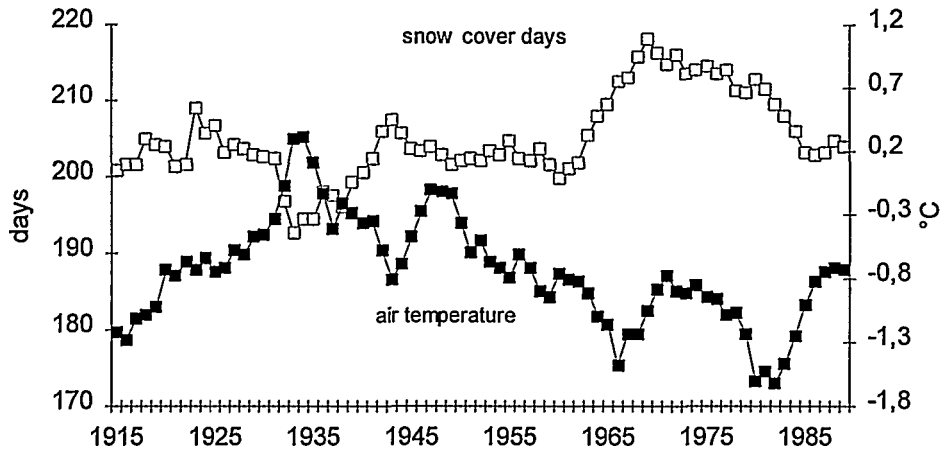
Fig. 1   10-year moving averages of snow cover and air temperature at Sodankylä, observatory, 1911 - 1994.

The snow depth maximum in Helsinki, 109 cm at 23 March 1941, is the event only over 1 m in Helsinki. The relation between high winter precipitation and snow depth maximum is not significant for Helsinki. For Kajaani, the variability of snow depth slightly decrease. There was no significant trend up to the last decade. Recently the snow depth maximum has begun to decrease. The snow depth maximum varies from 25 to 99 cm. In Sodankylä, the trends are vice versa. The largest snow depth maximum (116 cm) was measured 1993 and the variability of snow depth maximum is growing. The range lies between 52 and 116 cm. However, there is from the south to the north a great variability from year to year in snow depth results at all stations

References

Heino, R., 1994: Climate in Finland during the period of meteorological observations. Finnish Meteorological Institute Contributions 12, 209 p

CHANGES IN "NORMAL" PRECIPITATION IN NORWAY AND THE NORTH ATLANTIC REGION.

Eirik J. Førland and Inger Hanssen-Bauer
Norwegian Meteorological Institute, P.O. Box 43 - Blindern, N-0313, Norway

Introduction

Climatic data are often more useful when they are compared with reference values. The International Meteorological Committee in 1872 decided to compile mean values over a uniform period in order to assure comparability between data collected at various stations. At the meeting of the "International Meteorological Organization" in Warzaw in 1935 it was agreed to calculate such mean values ("normal values") for the period 1901-30. Succeeding normal periods were decided to be at 30-years intervals (i.e. 1931-1960, 1961-1990, etc).

When deciding the length of the normal period, one requirement was that the length of the normal period should be sufficient to reflect climatic changes. Too long a period might prove insensitive to real climatic trends, whereas too short a period would be over-sensitive to random climatic variations. Normal values are commonly used as reference values for a number of purposes (engineering constructions, agriculture planning, climate change analysis, etc.). To judge the representativity of the new normals, it is important to know to which extent they differ from the previous normals and from long-term means.

Ratio between precipitation normals 1961-90 and 1931-60

The international cooperation between 11 countries within the NACD-project (Frich, 1994) gave an excellent opportunity to compose maps showing the differences between the new (1961-90) and old (1931-60) normals. This analysis revealed that the normal annual precipitation (figure 1) has increased over large parts of the North Atlantic area, and most pronounced in western parts of both UK, Netherlands, Denmark, Sweden, Norway and in eastern parts of Poland. In northern parts of Iceland, Finland and Norway the annual precipitation has increased by more than 10%. However in eastern parts of both UK, Belgium, Denmark (Jutland), southern Norway and Sweden, the normal annual precipitation is lower than in the previous normal period. In most of these areas the decrease is less than 5%,- but some eastern areas in England and Scotland have experienced a decrease of more than 5%.

Detailed analysis of the series demonstrated the importance of using homogenous series,- inhomogeneity breaks may cause artificial differences of more than 10 % between succeding annual precipitation normals (Hanssen-Bauer & Førland, 1994a).
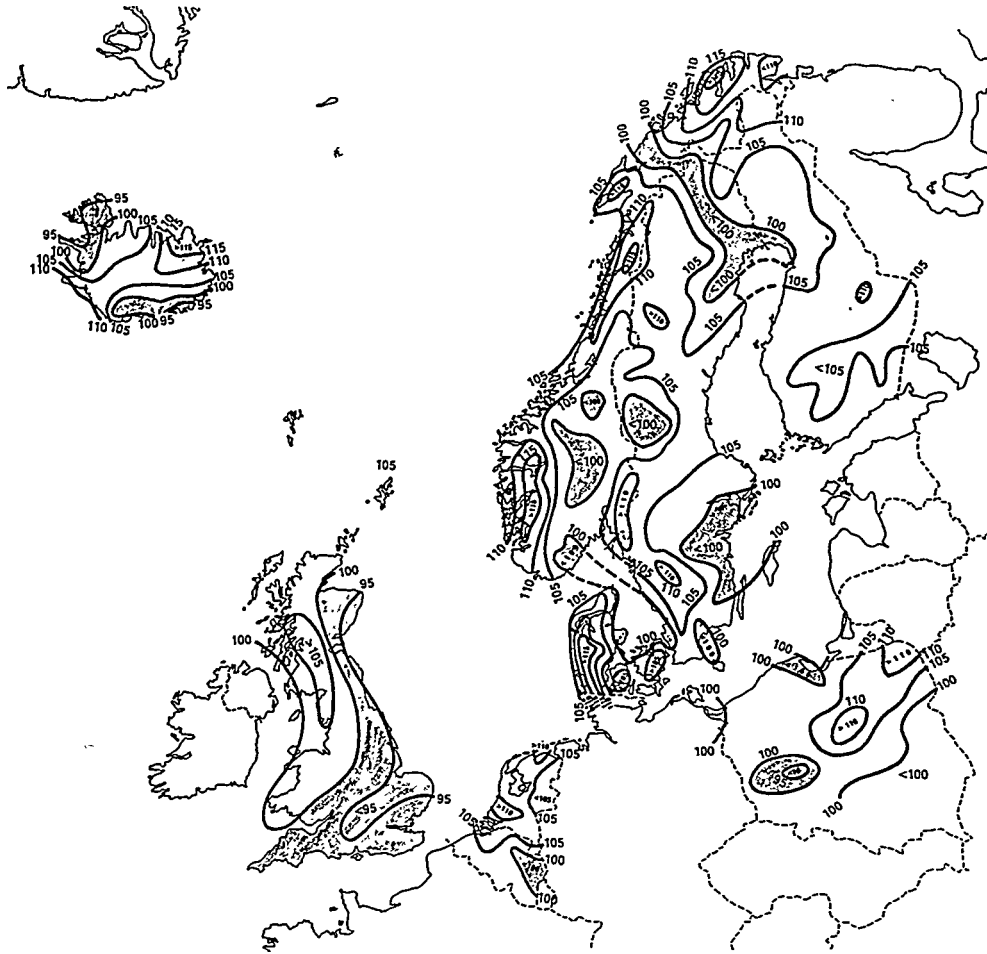
Fig. 1. Ratio (percent) between new (1961-90) and old (1931-60) annual precipitation normals.

The anomali pattern in figure 1 indicates that the changes in normal annual precipitation are caused by changes in the circulation pattern. Areas exposed to orographic precipitation from the humid westerlies from the North-Atlantic have experienced increased precipitation. On the other hand, the annual precipitation has decreased in areas on the leeward side of hills and mountains in UK, Belgium, Norway and Sweden.

The changes in normal precipitation are even larger on seasonal and especially monthly basis. While the summer precipitation has decreased over most of the North-Atlantic region, most areas have experienced increased precipitation during autumn, winter and particularly during the spring. For large parts of the area the spring precipitation has increased by more than 15% and in some areas in southern Norway by more than 30%. Most of this increase in Norway is caused by a dramatic rise in the March precipitation. At several stations in southwestern and southeastern parts of Norway, the new precipitation normals for March are more than twice as high as the 1931-60 normal. Comparison with old values indicates that it is the 1931-60 normals that are "abnormal": the 1901-30 normals are at the same level as the 1961-90 normals.

Long-term variations

While the choice of length of the normal period was based on scientific considerations, practical reasons made choosing 1901 as the starting year in the first normal period. This year also decides the start of the succeeding standard normal periods. Would the normals in this century have been different if another starting point had been chosen ?

This may be illustrated by studying 30-year moving averages. The graph for Samnanger in Western Norway (Figure 2) shows that the 30-year averages were quite stable (3130-3310 mm/year) between the periods 1901-1930 to 1958-87. However in the last five 30-year periods it has increased dramatically, to 3496 mm in the period 1965-1994. For Samnanger the normal precipitation for the 1931-60 period is one of the lowest 30-year averages in this century, while the 1961-90 normal is one of the highest. The 30-year average for 1965-94 is more than 200 mm (7 %) higher than the long-term mean for the whole 1901-1994 period.
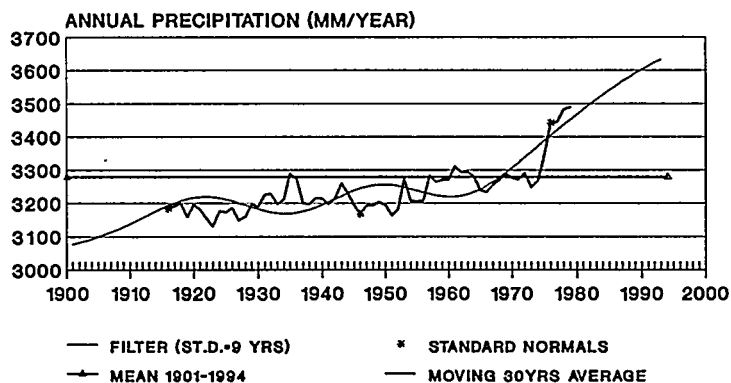
Fig. 2. Long-term variation of annual precipitation at Samnanger, Western Norway.

It should be stressed that the difference between the new and old normal values (and also maps like figure 1 is based solely on two points on graphs similar to figure 2, and does not give an unambigous measurement for climatic change.

Another feature of moving 30-year averages is that the smoothed series may seem periodic, even if the original series is not (Parkinson, 1989). Therefore, no conclusions about climatic trends should be drawn just from moving averages. For Samnanger low pass filtered trend curves show a relatively constant precipitation level from 1900 to the middle of the 1960s, after which there has been an increasing trend of about 10 % (figure 2).

Preliminary analyses of 140 filtered precipitation series from Norway, show that the normalised trend curves of homogenous neighbouring stations exhibit almost identical trend curves, while there were large differences between different regions (Hanssen-Bauer & Førland, 1994b and this volume). By using comparative trend analysis, five main regional groups of trend curves were identified for Norway. For all regions, the trend curves showed that the precipitation level at the end of this century is lower than at the beginning.

Conclusions

a). Normal values should be based on homogenous (or homogenised) series
b). The 30-year moving averages may change rapidly within a few years
c). Normals may represent "abnormal" values among 30-year moving averages.
d). Normals may deviate significantly from long-time means
e). The difference between normal periods does not give an unambigous measurement for climatic change.

Is 30 years a reasonable length of the "normal periods" ? The large differences between the two latest normal periods indicate that 30 years is too short averaging period to get stable mean values. But on the other hand, normal values should reflect real climate changes (e.g. by increased greenhoues effect). Also by using longer averaging periods, it will be still more difficult to get homogenous (or homogenised) series covering the whole period.

The use of the word "normal" may not be proper, because it is often understood as the usual state or condition. In addition arithmetic mean values (or normal values) may be a misleading statistic for non-normal distributions Førland (1994). In spite of the criticisms presented above, the 30-year standard normal periods should therefore still be maintained in climatology. But bearing point a)-e) above in mind, the normals should mainly be used for comparative purposes.

References

Frich, P., 1994: North Atlantic Climatological Dataset (NACD), towards an European Climatic Data centre (ECDC). In: "Climate variations in Europe". Proceedings of the European Workshop on Climate variations, Finland, 15-18 May 1994, p.81-96.

Førland, E.J., 1994: Are the normals really normal ? (In Norwegian). Proceedings from the XIX Nordic Meteorological Meeting, Kristiansand, Norway, 6-10. June 1994, p.33-38

Hanssen-Bauer, I. & E.J.Førland, 1994a: Homogenizing long Norwegian precipitation series. J. Climatol, Vol.7, No.6, 1001-1013.

Hanssen-Bauer, I. & E.J.Førland, 1994b: Regionalization of Norwegian precipitation series. Norwegian Met.Inst. Report KLIMA 13/94, Oslo, 44 pp.

Hanssen-Bauer,I. & E.J. Førland, 1995: Regionalisation of Norwegian precipitation trends. (This volume).

Parkinson, C., 1989: Dangers of multiyear averageing in analyses of long term climate trends. Climate Dynamics, 4: 39-44.

Temperature variations over Switzerland 1864 - 1990

Othmar Gisler

Swiss Meteorological Institute,
P.O.B., CH-8044 Zurich, Switzerland

Introduction

The climate in Switzerland was described in detail during the years after 1960, in form of complementary texts to the yearbooks of the Swiss Meteorological Institute (Klimatologie der Schweiz [Climatology of Switzerland], 1960 ff.). The description of the regional climatic behaviour was written in 1978/79 as an important part of this publication. The discussion about climatic fluctuation and climatic change is actually going on in many places and on the most different levels. Descriptions of regional climate are equally revised, newly interpreted or written down.

This study is the beginning of climatological investigations using several climatic elements and long time series to perform a description of regional climatic variability and related questions in Switzerland.

Data

Data material in form of several long temperature series actually help us in our research. Some of these series were yet homogenized on the occasion of former processing; they had, however, to be extended up to 1864 or 1990 respectively. A verification and adaptation of the annual mean series, which are used in this case, was done as well. Data from different sources had been processed, corrected and tested in respect of homogeneity before they were accepted for this study (Maurer, Billwiller, Hess, 1910; DB SMI, Schüepp, 1961; Annalen SMA 1864ff., Alexandersson, 1986).

In this study we consider only annual mean temperature time series from ten locations. All stations are situated in small to medium sized cities since 1864, except the locations in the alpine region. The number of stations in each region varies from 2 to 4. This is not ideal, but longer time series with high quality data are not yet ready for use. The set of observation sites covers the important areas of central and western Switzerland. Bearing in mind the different density and expositions of observation sites per region, one can deduce only careful interpretations. Nevertheless, general results can also be extracted.

Regional time series of annual mean air temperature

Series of mean values for every region are deduced from the data of the various stations. These series can be compared with each other, and the regional temperature behaviour can be studied as well. Figure 1 reveals the temperature series for the Swiss Plateau and the alpine region, based on several stations. The annual mean temperatures show the known warming since the middle of the last century. The movement of the temperature during these 127 years was characterized by two or three pronounced variations within a short time. In less than 20 years temperature fell and rose by barely 1°C (around 1890 and 1948). This significates a temperature variation of barely 1°C/10 years.The overall temperature warming trend for the Swiss Plateau from 1864 to 1990 amount to 1.21°C/127 years (= 0.95°C/100 years).

Swiss Plateau

Swiss alpine region
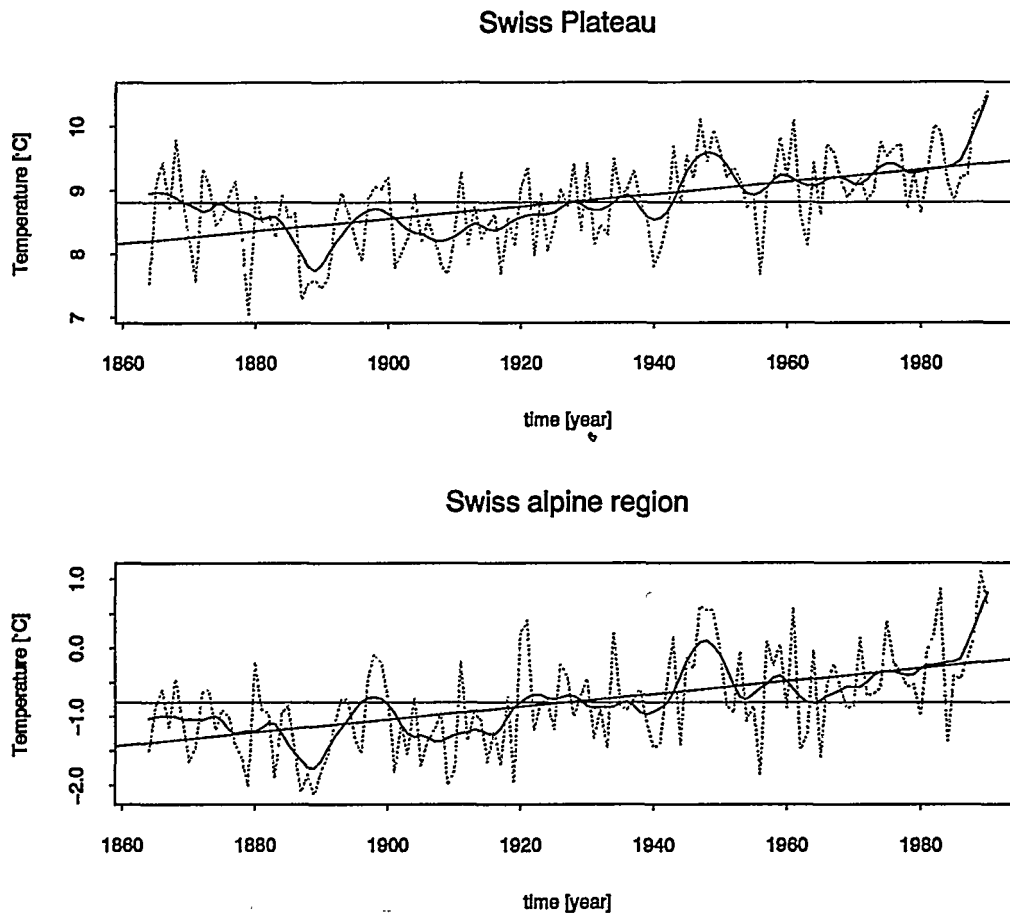
Fig. 1 Annual mean temperature variation of the Swiss Plateau and the alpine region 1864-1990 (Solid lines show mean, 10-year locally-weighted, smoothed data and linear trend).

Temperature gradients

Temperature movements were not identical in all regions. Figure 2 reveals the absolute difference between two regional temperature curves. The air layer between the lower and the higher region was not exposed to the same influences at the same time. In fact, the synoptic situation plays an indirect part. Its influence, represented by curves of other climatic elements related to temperature, has still to be studied. The temperature gradients in Switzerland were calculated for different types of stations and expositions within the scope of former works (Gensler, Schüepp, 1978/79). The behaviour of temperature gradients can be studied by means of regional temperature series. As urban measuring stations are missing in the alpine region, this area can be considered as not influenced by the urban heat island effect. We study the behaviour of some regional gradients during these 127 years.

a)

b)
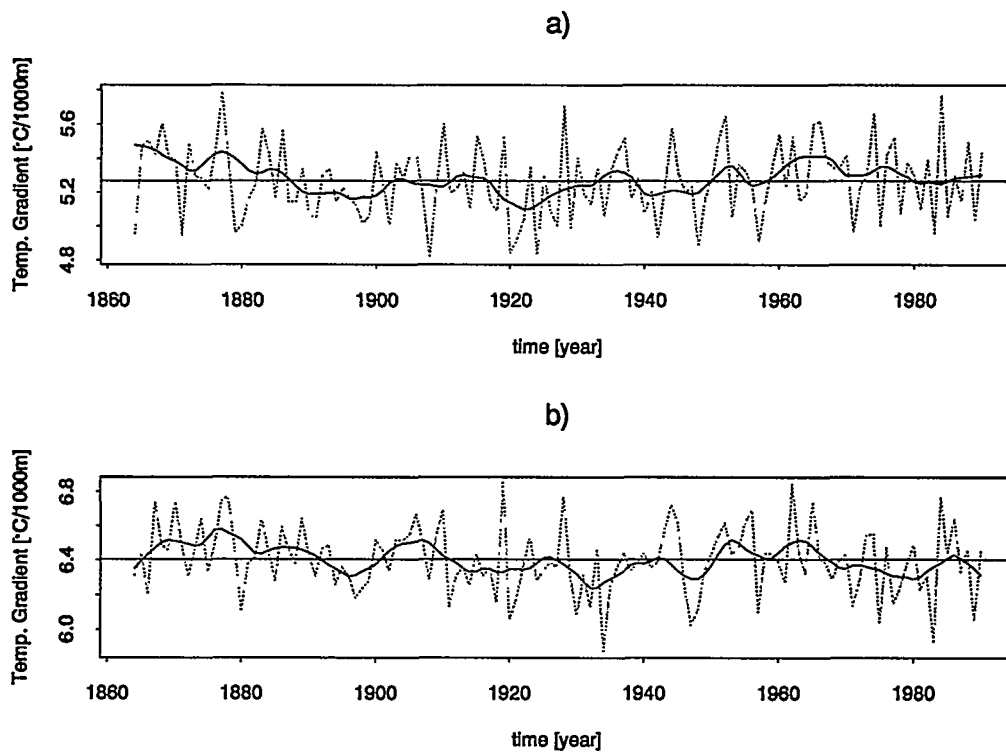
Fig. 2 a) Annual mean temperature gradient between the Swiss Plateau and the alpine region 1864-1990. b) Annual mean temperature gradient between the southern part of Switzerland and the alpine region 1864-1990. (Solid lines show mean and 10-year locally-weighted, smoothed data).

References

Alexandersson, H. 1986. A homogeneity test applied to precipitation data. Journal of Climatology 6:661-675.

Annalen SMA 1967. Annalen der Schweizerischen Meteorologischen Anstalt 1864ff., Zürich.

DB SMI. Climatological Database of Swiss Meteorological Institute, Zurich.

Gensler, G. & Schüepp, M. et al. 1978/79. Klimatologie der Schweiz, Band I+II, 2 Teile, Regionale Klimabeschreibungen. Beiheft zu den Annalen der Schweizerischen Meteorologischen Anstalt 1960. Zürich, 437 pp.

Klimatologie der Schweiz 1960 ff. Beiheft zu den Annalen der Schweizerischen Meteorologischen Anstalt 1960 ff. Zürich.

Maurer, J., Billwiller, R. & Hess, C. 1910. Das Klima der Schweiz. 2 Bände. Huber. Frauenfeld, 519 pp.

Schüepp, M. 1961. Klimatologie der Schweiz. Heft 2/C. Lufttemperatur 2. Teil. Beiheft zu den Annalen der Schweizerischen Meteorologischen Anstalt 1960. Zürich, 62 pp.

Regionalisation of Norwegian precipitation trends.

Inger Hanssen-Bauer and Eirik J. Førland
Norwegian Meteorological Institute, P.O. Box 43 - Blindern
N-0313 Oslo, Norway

Introduction

Precipitation may differ greatly over small distances, both in amount and in variability and trends. Regionally averaged precipitation series, or precipitation series "representative" for certain areas are thus generally more difficult to obtain than similar series of air pressure or temperature. A denser network of stations is needed to give the same reliability. Additionally, the results are often influenced by choice of methods or averaging procedures. It is thus important to choose a method which serves the purpose of the investigation on hand. For instance, is it desired that the series reflect the changes in the total amount of rain which has fallen in a certain area, or should it rather be an expression of the dominating relative precipitation trends in the area? In the present study, 140 precipitation series of 70-100 years duration were used to investigate trends and variability in precipitation in Norway during the last century. Two different methods were used in order to regionalize the series. Influence on the results of inhomogeneities in the precipitation series and density of the station network were examined.

Data

The 140 precipitation series used in the present analysis covers the Norwegian mainland fairly well. They were all homogeneity tested (Hanssen-Bauer and Førland 1994) and, in case of inhomogeneities, adjusted on an annual basis. A subset of the stations was also adjusted on a seasonal basis. General results from homogeneity testing demonstrate that inhomogeneous series may show major artificial trends, making them unsuitable for trend studies. The tests also revealed that the adjustment factors for the inhomogeneities found in the dataset were not symmetrically distributed around unity: There was a bias towards increased catch efficiency both for inhomogeneities caused by introduction of wind shields, and for inhomogeneities caused by changes in the local environment of the gauges. Consequently, trend analyses of untested precipitation series may give dubious results for groups of series, as well as for single series.

Methods

Standardization

The aim of the present investigation was to find representative trends of precipitation. In Norway annual precipitation varies from less than 300 mm at some stations to nearly 4000 mm at others. To suppress the influence of the large differences in precipitation amounts, all precipitation series were standardized by dividing by their respective 1961-1990 average (PN_{61-90}). The reason for standardizing in this way, is that it is easy to reverse the process and extrapolate a time series (in mm) for any station just by multiplying by the official normal values. It is also convenient to standardize all series by comparing with data from the same period, as differences between stations in working periods would otherwise affect the relative levels of the curves (cf. Førland and Hanssen-Bauer, this volume).

Regionalisation

The regionalisation problem was approached using two different methods. The "comparative trend analysis" includes subjective grouping together of filtered precipitation series showing similar trends. This method has the advantage of not demanding complete data series from all stations. The principal component analysis, on the other hand, needs complete series from all stations, and the number of available data series thus rapidly decreases as the length of the analysed period increases. The advantage of the PCA that it is less time consuming to accomplish, as it is available in several statistical computer packages. It is also basically an objective method, even if the interpretation of the results often will include subjective considerations.

Comparative trend analysis

Two low pass filters, F1 and F2, including Gaussian weighting coefficients were used to describe variability and trend of the standardized precipitation series. The standard deviation of the Gaussian distribution was 3 years for filter F1, and 9 years for filter F2. Five years were cut from each end of the filtered time series, as the ends of filtered curves depend highly on the first or last few values, which thus may seriously influence the trends.

The 140 standardized precipitation series were plotted, both as annual sums and as filtered values. Series with similar precipitation variations and trends were then grouped together. The precipitation series were divided into 13 groups with different patterns of precipitation variation in time, using the comparative trend method. The groups included from 3 to 29 stations. It was possible to associate each of the 13 groups with a geographical region. Most regions consisted of series showing a distinct variation pattern, with clearly definable local

maxima and minima. For such regions, it was usually easy to decide whether or not a station belonged to the region. The precipitation trend was similar from one end to the other of these "trend regions". Some groups, however, included series with a less distinct variation pattern. In these regions it seemed to be a systematic change in the trend curves from north to south or from east to west. They may thus be classified as "transitional regions" rather than as a trend regions.

For each region, the standardized precipitation curve was defined as the average of the standardized precipitation curves from all stations within the region. Series of standard deviations between the individual curves within the regions were also calculated, in order to get a measure of the significance of regional precipitation variation relative to the interregional variation. The precipitation trend for any point on the Norwegian mainland may now be estimated by multiplying the regional trend curve by the 1961-1990 precipitation average, which may be deduced from the official precipitation normal maps (Førland 1993). The standard deviations give a measure for the uncertainty of the estimate.

Principal component analysis (PCA)

PCA (i.e. Preisendorfer 1988) may be applied to either correlation or covariance matrices. Mills (1995) summarizes the advantage of using the covariance matrix. The covariance matrix was also used in the present work. However, to avoid influence on the principal components of differences in precipitation levels, the standardization introduced in the first paragraph of this chapter was applied. Thus, the precipitation series of an arbitrary point may be estimated simply by using the PCs, their respective loadings found from maps, and the precipitation normal. In order to study the influence of density of the station network, PCA was performed using networks of different density.

Results

Regional trends

The comparative trend analysis resulted in thirteen 13 regions, which formed 5 main regions. The results showed good agreement with regional patterns from the PCA.

For each region, representative curves of annual and seasonal precipitation trends were computed. In all regions, there has been an increase in the level of annual precipitation from 1900 to the present. In most regions the increase was 8-13%. In southeastern regions the increase occured mainly in the period 1900-1930. In western regions, the annual precipitation increased mainly after 1960. In northern coastal regions, the increase was more evenly distributed throughout the century, while the northern inland areas experienced the increase mainly in the period 1940-1970.

There are also regional differences concerning the contribution to the increase in annual precipitation from precipitation within the individual seasons. In southern regions, most of the annual increase is due to increased precipitation during fall. In northern Norway, however, there seems to have been an increase in precipitation during all seasons. The regional pattern indicates that the different trends in precipitation may be explained by changes in the circulation pattern.

Effects of including inhomogeneous series in the analyses

Results from analyses based upon adjusted and unadjusted series, respectively, were compared. The main problem with inhomogeneities so far seems to be a generally increased "noise level" in the data. In the comparative trend analysis, the standard deviations within the groups increased considerably, using unadjusted series. In the PCA, the scattering of the loadings was greater using unadjusted series. Consequently, an eventual "signal" of climatic change will be easier to detect when using homogeneous and/or adjusted series.

In order to perform trend analysis on a seasonal basis, the series should also be adjusted on a seasonal basis, as adjustment factors may differ substantially from one season to another.

References

Førland, E.J., 1993: Årsnedbør. (Annual precipitation.) *National Atlas for Norway, map 3.1.1*, Statens Kartverk.

Førland, E.J., and I. Hanssen-Bauer, 1995: Changes in "normal" precipitation in Norway and the North Atlantic Region. *This volume.*

Hanssen-Bauer, I. and E.J. Førland, 1994a: Homogenizing long Norwegian precipitation series. *J. Climate,* Vol.7, No.6, 1001-1013.

Mills, G.F., 1995: Principal Component Analysis of Precipitation and Rainfall Regionalization in Spain. *Theor. Appl. Climatol.,* 50, 169-183.

Preisendorfer, R.W, 1988: *Principal Component Analysis in Meteorology and Oceanography,* Elsevier, 425 pp.

Long-term climatic trends in Estonia during the period of instrumental observations

Jaak Jaagus

Institute of Geography, University of Tartu
Vanemuise 46, EE2400 Tartu, Estonia

Introduction

Estonia is located on the eastern coast of the Baltic Sea in the transition zone from the maritime climate type to the continental one. In spite of its comparatively small territory, climatic differences in Estonia are significant. For example, mean air temperature in January varies from -2.5°C on the western coast of Saaremaa Island to -7.5°C in the East Estonia. Also, temporal variability of meteorological values has been high.

Weather conditions in Estonia directly depend on cyclonic activity at the Northern Atlantic. Long-term fluctuations of its intensity clearly reflect on meteorological anomalies. On the base of high variability of weather conditions it can be expected that Estonia should be a sensitive region for probable climate change. The aim of this study is to determine long-term periodical fluctuations and trends in meteorological time series during instrumental observations in Estonia.

Data

In this study, time series of six climate components - air temperature, precipitation, snow cover, sunshine, air pressure and wind - are analyzed. Proceeding from the statistical peculiarities, individual approach to each of the component is necessary.

High spatial variability is characteristic for precipitation and snow cover data measured in a great number of stations. Hereby, time series of spatial mean annual and seasonal precipitation and snow cover duration are analyzed. Territorial averaging of precipitation data was made by spatial interpolation into grid cells for the period 1866-1994.

Spatial mean values of snow cover duration in Estonia were found by means of geographical information system. IDRISI raster images were created to represent snow cover fields. Mean value of all raster elements on terrestrial part of Estonia was calculated for 124-year time series of winters (1891/1892-1994/1995).

Territorial variability of the other meteorological characteristics is much lower. Four stations in different climatic regions in Estonia and with the longest observation periods were chosen for discribing trends and fluctuations of air temperature - Tallinn in North Estonia (1828-1994), Tartu (1866-1994) in the continental part of Estonia in south-east, Pärnu (1842-1994) on the coast of the Gulf of Riga in south-west and Vilsandi (1865-1994) on a small island with the most maritime climate west from Saaremaa Island.

Wind speed measurements strongly depend on the openness of the meteorological station. Buildings and trees can highly decrease wind speed. Here are used 104-year

series of wind speed (1891-1994) from three coastal stations (Pärnu, Vilsandi, Pakri). Sunshine duration and air pressure were studied only in Tartu during the periods of 1901-1994 and 1881-1994 correspondingly. Lacks of observation are replaced by values calculated on the base of data measured at neighbouring stations.

Time series not only annual but also seasonal values were analyzed. Fluctuations in intensity of cyclonic activity occur, first of all, in seasonal pattern. Seasonal values were calculated by three months. For example, spring means the period from March to May, summer - from June to August etc.

A problem of homogeneity of the time series is of a great importance. Usually, meteorological time series are not entirely homogenuous. During a long time, locations of stations, surroundings of observation places, times of measurements, gauge types and measuring techniques are changed. Hereby, published meteorological data are not corrected and possible inhomogeneity is taken into account in the analysis of results.

Results and discussion

Linear trend analysis was used to determine trends and autocorrelation and spectral analyses to estimate periodical fluctuations in meteorological time series in Estonia. In some cases, significant trends and also periodicities are found, in another cases not. It is important to emphasize that fluctuations of meteorological times series are not exactly cyclic but more like quasi-periodical. It means that the alternation of maximum and minimum values is clearly distinctable but time interval between them varies.

Temporal course of air temperature is coherent with large-scale temperature changes in the Northern Hemisphere. Significant increasing trend existed during the period from the middle of last century to the 1930s (Fig. 1). Then followed a stable period. But the last decade was the warmest also in Estonia. The warming is observed in spring, autumn and winter but not in summer. Remarkable periodicities in air temperature series were not determined. Fluctuations of at the four stations were rather coherent.

The strong increasing trend of precipitation (Fig. 2) is mostly caused by improvement of gauges and measuring technique. Reliable trend was detected only for autumn. Clear periodical fluctuations of precipitation were with periods of 50-60, 25-30 and 5-7 years. The most important periods of high precipitation were observed at 1866-1873, 1923-1935 and 1978-1990. These maxima appear in annual and also in autumn totals of precipitation. There are weaker secondary maxima between them at 1897-1906 and 1952-1962. They correspond to periodicity of 25-30 years that is mostly expressed in time series of annual precipitation. During summer season only period of 5-7 years is determined. In case of spring rainfall, another periodicity (22-23, 45-47 years) was observed. Winter precipitation series was inhomogenuous and was not analyzed.

Time series of snow cover duration (Fig. 3) has a decreasing trend. During 104 years the mean number of days with snow cover have changed by 14 days - from 121 to 107. The first half of the period is characterized by a very strong trend while during the latter half the trend is very weak. Time series of IDRISI raster images of snow cover duration at 1920/1921-1994/1995 is quite homogenuous and representative because of sufficient number of observations from the all parts of Estonia. Decrease of snow cover duration for that period was only 2 days. Figure 3 expresses significant periodical fluctuations of 13-18 years. Periods of mild winters with lower duration of snow cover were regularly observed. Snow cover duration has slowly decreased during this century.

Annual mean wind speed data at three stations (Fig. 4) evidence a high variability and the great influence of local factors on wind speed. There is no reliable trend in wind speed. The variance is cause by changes in surroundings and in measuring technique.
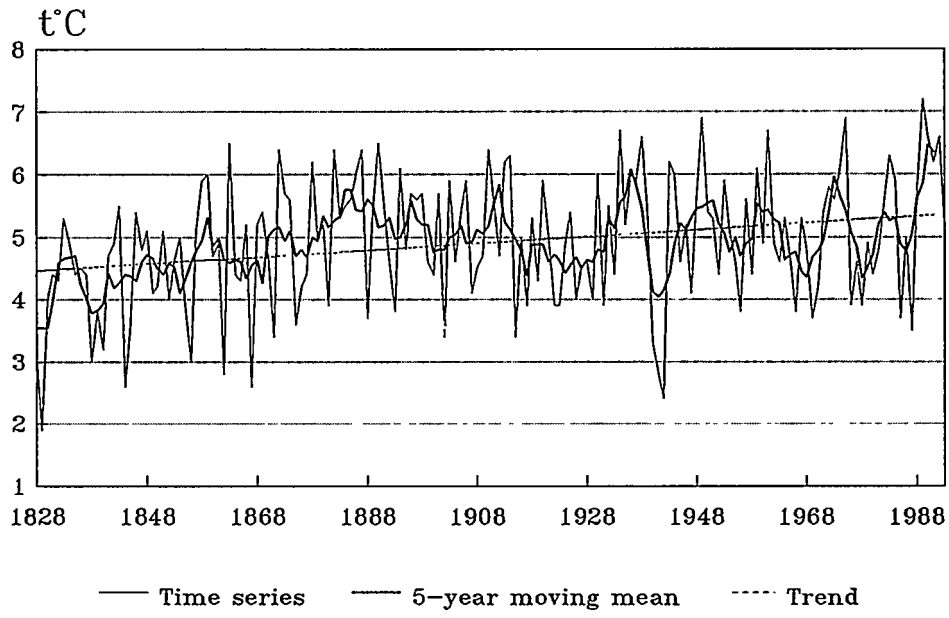
Fig. 1 Annual air temperature in Tallinn
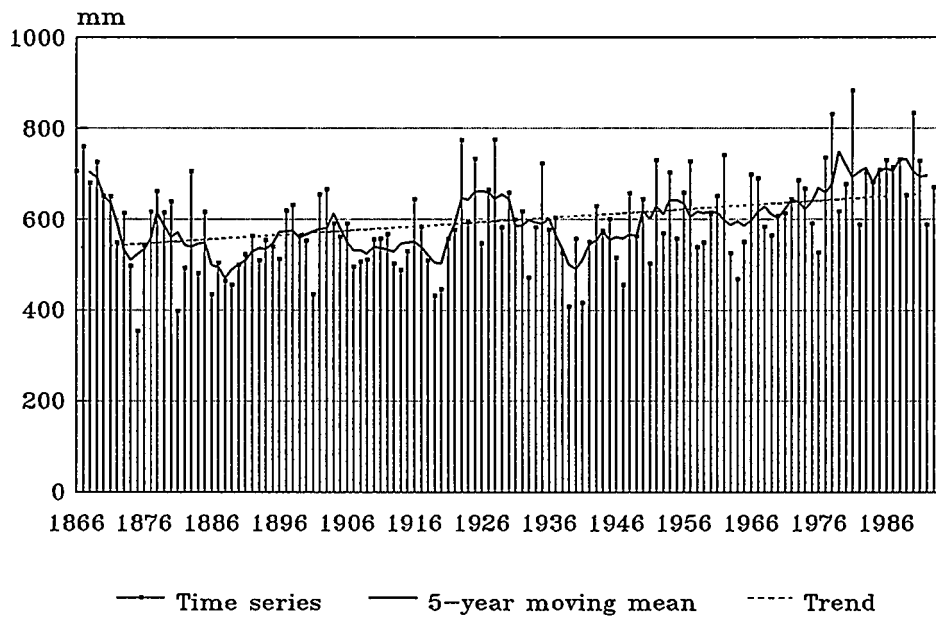
Fig. 2 Annual precipitation in Estonia
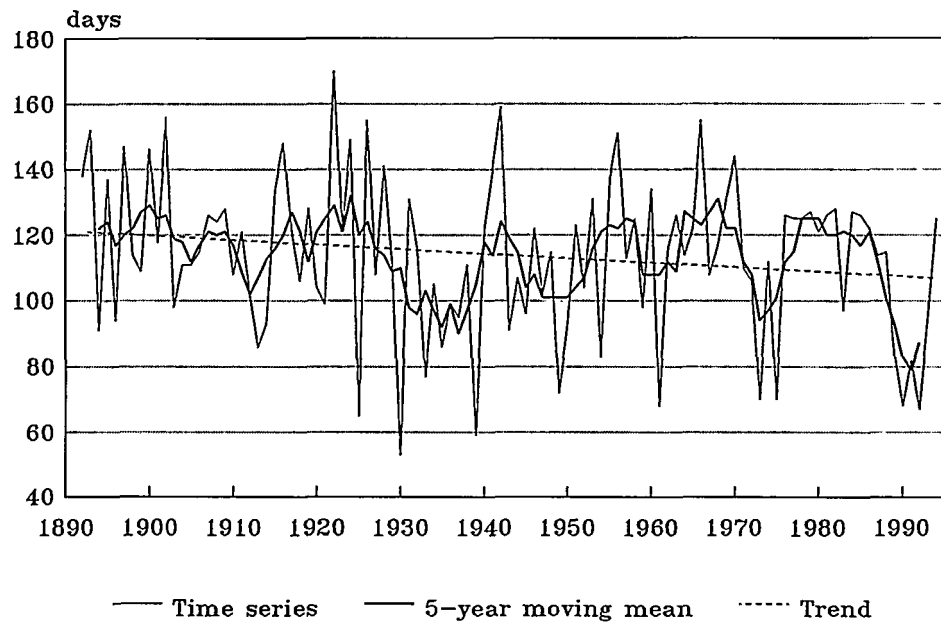
Fig. 3 Snow cover duration in Estonia
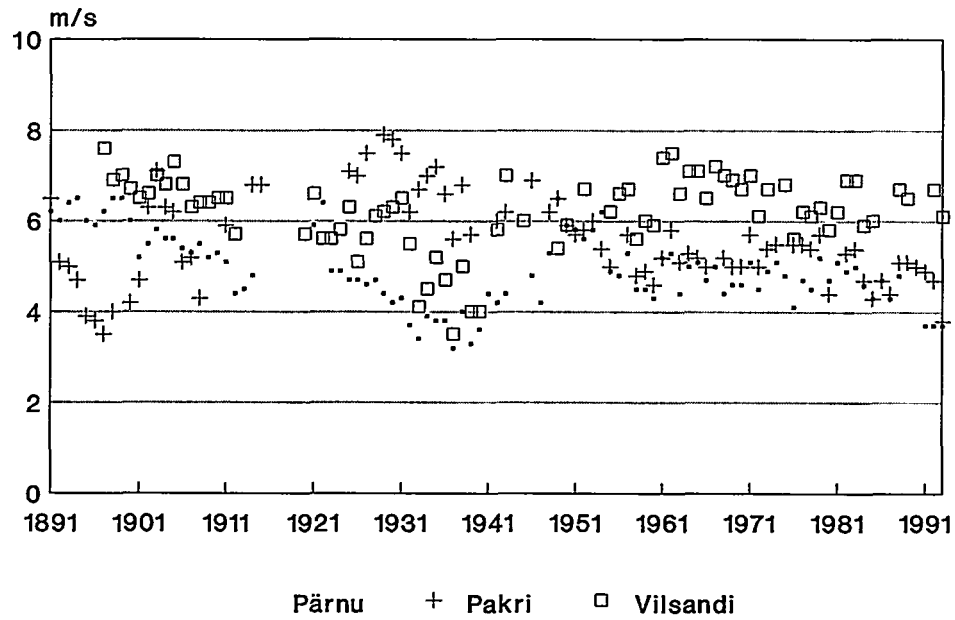
Fig. 4 Annual mean wind speed

The variation of temperature and humidity in the atmosphere over Poland

Zenobia Lityńska

Institute for Meteorology and Water Management
Centre of Aerology
Zegrzyńska str. 38, 05-119 Legionowo, Poland

The homogenity of polish upper-air data series 1971 - 1990 was analysed.

The annual cycles of temperature, dew point, relative humidity and precipitable water in the troposphere are typical for middle and high latitude continental humidity regime (Gaffen et al.JGR 1992).

The results of linear regression trend analysis of temperature and relative geopotential, calculated for main isobaric levels show positive annual trends in the lowest troposphere and statistically significant large positive trends in April in the lower troposphere and in October in the whole troposphere (up to 250 hPa) Hence, the final result of tropospheric warming since 1970 in Poland is demonstrated as prolongation of warm season - earlier, warmer spring and later, warmer autumn.

The relative humidity trends are consistent with temperature trends - significant negative for the same months. No trends were found for potential precipitation and specific humidity.

The dynamical background of tropospheric warming over Poland is discussed.

The temperature and relative geopotential variations in the stratosphere are analysed and discussed against the results achieved for northern hemisphere (Labitzke and Van Loon J.Met.Soc. Japan, 1994).

Variability of temperature in Italy 1870-1980

Guido LO VECCHIO and Teresa NANNI

Istituto FISBAT-CNR, via Gobetti 101,
40129 BOLOGNA, ITALY

Introduction

Hansen and Lebedeff (1987) determined a global surface temperature increase of about 0.6 °C occurred between 1880 and 1980.

In a preceeding paper (Lo Vecchio and Nanni, 1995) we verified whether the above results regarding a large area such as in their boxes, are valid also for restricted zones like the Italian territory which has furthermore a peculiar orography. We performed this study having at disposal the historical temperature series (about 100 years) of 27 stations distributed over the Italian territory. Then, according to the variance of the temperature series, we separated these stations in two climatically homogeneous groups.

Another important question about a subject frequently discussed at present is if the climate variability has changed significantly during the last century (Malcher and Schönwiese, 1987, Parker et al., 1994; Solow, 1987). Wallén (1985), hereafter W, studied the fluctuations in variability of winter temperature during the past century at eight selected European stations.

In this paper we first verify if the HL considerations about global temperature trends fit local behaviours, then we analyze the temperature variability of Italy to integrate the results with those obtained by W.

We determined, by statistic method, two different climatic regions corresponding to the continental and the peninsular zone respectively. For both series groups, hereafter indicated with N (northern Italy) and S (central and southern Italy), we computed the mean annual (YT), winter (WT) and summer (ST) temperatures, considering, year by year, all the available data. Then for WT and ST in N and S we compute the 10-year running variance.

Results and discussion

In figs. 1 and 2 the ST and WT variances of N and S are represented. To each variance series are associated its mean M and two levels M±2.σ corresponding to a 95% confidence interval ; this is possible because we know that the variance of a series has a χ^2 distribution. It appears clearly that the ST presents a maximum of variability in correspondence of the period 1940-1960 (for N the significativity is about
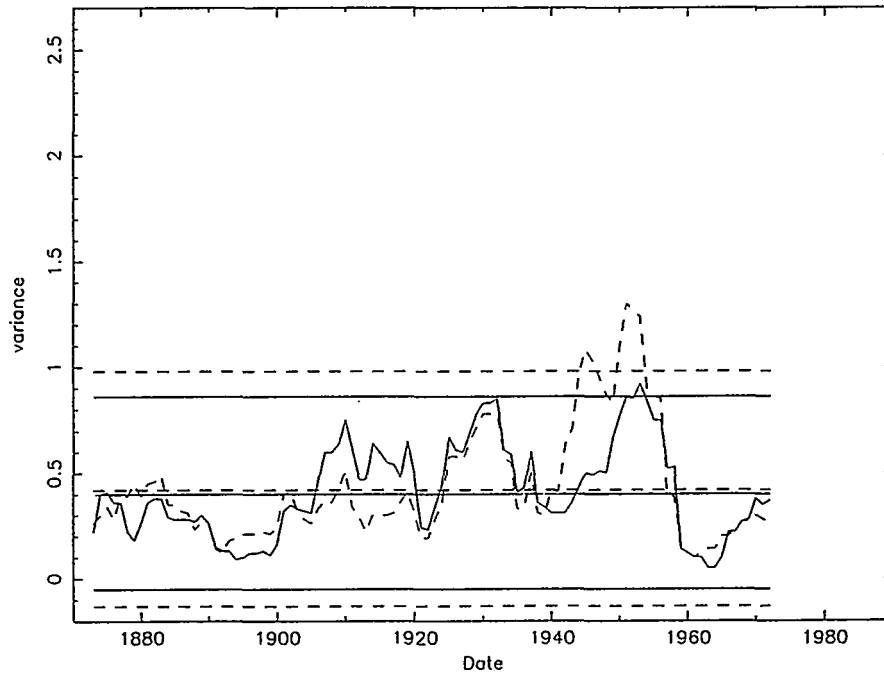
Fig. 1. 10-years running variance (°C)^2 of WT for N (dashed line) and S (continuous line). The horizontal lines are respectively M and M±σ referring to the variance of WT for N and S.
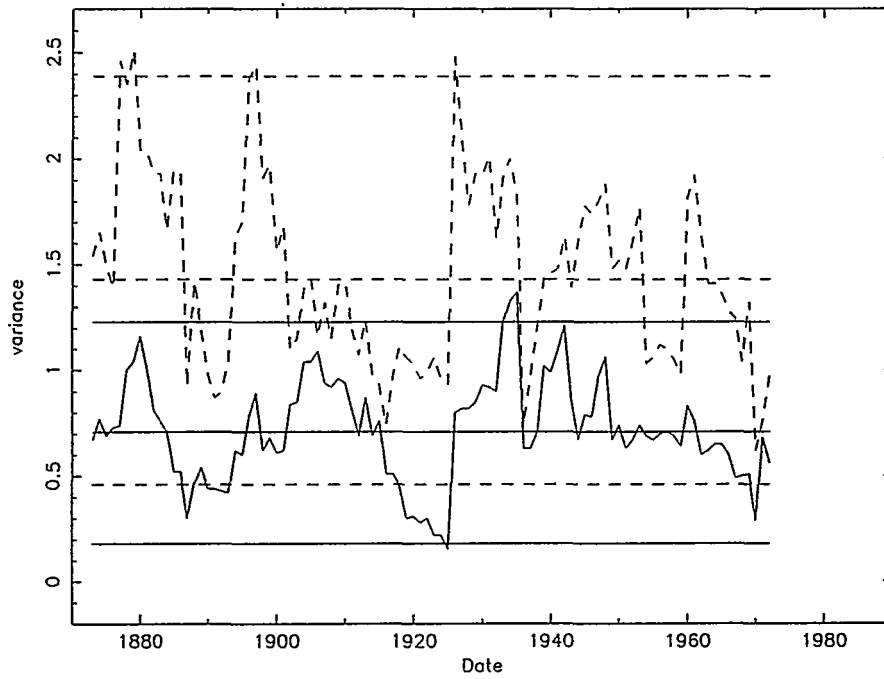
Fig. 2. Like in fig. 1 but for ST.
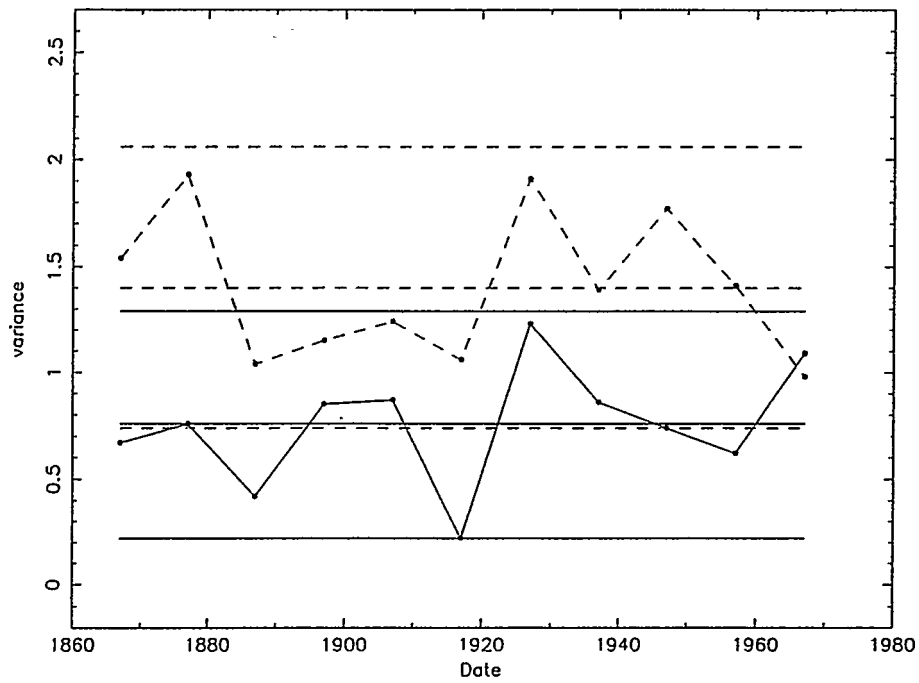
Fig. 3 Interannual variability of WT for N (dashed line) and S (continuous line) shown as variances (°C)^2 by consecutive decades from 1867-1976. The horizontal lines are respectively M and M ±σ referring to the variance of WT for N and S.
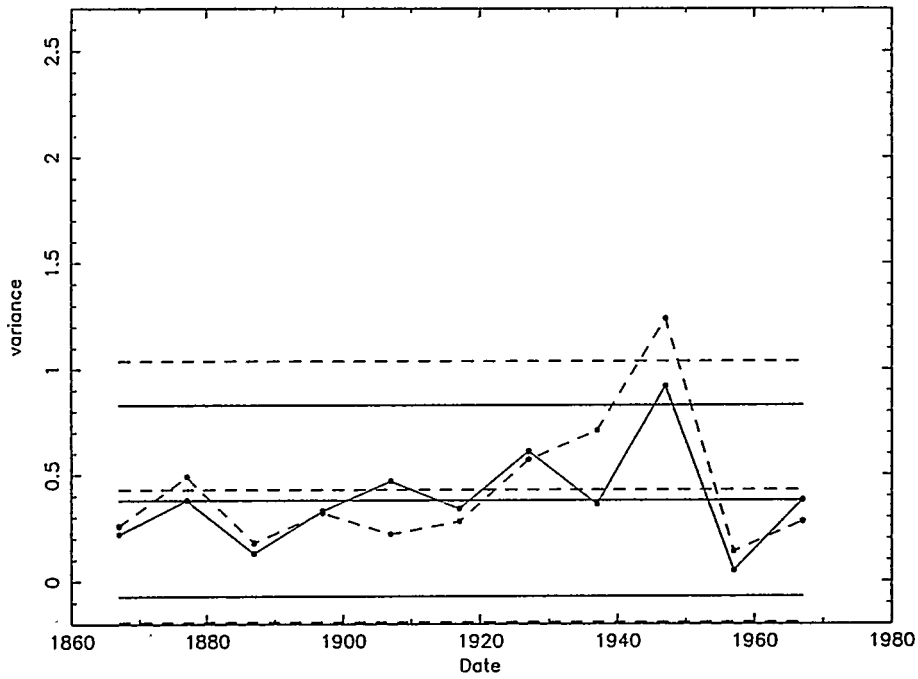
Fig. 4.Like in fig.3 but for ST.

99%, for S is about 95%). WT presents significant (about 95%) variability, minimum in correspondence of the period 1920-1930 but only for S.

The other peaks in fig. 2 are in our opinion to be considered statistical fluctuations. In fact, in order to compare our results with those of Wallén, we also calculated the fluctuations of the variance for consecutive 10-year periods from 1867 to 1976. The results reported in figs. 3 and 4 support our choice.

So our results does not completely agree which those of Wallén; in fact, considering only the winter and spring season he found a minimum of temperature variability in the period 1900-1920 and the maximum in the period 1930-1950.

Subtantially our results, for winter, present a minimum of variability only for S shifted of about ten years in relation to those of W, for N there are not significant peaks of variability. For summer there are no W results so a comparison is not possible. But we observe that our results present a maximum shifted of ten years in respect to that found by W for winter.

On the basis of the consideration presented in the paper we think that this disagreement could be explained considering that the stations selected by Wallén are very distant from one another all over central and northern Europe while our stations are very concentrated and located in the south of Europe in a peculiar geographical position.

References

Hansen, J., Lebedeff, S., 1987: Global Trends of Measured Surface Air Temperature. J.Geophys.Res., 92,13345-13372.

Lo Vecchio G. and T. Nanni, 1995: The atmospheric temperatures in Italy during the last one hundred years and its relationship with solar output, Theor. Appl. Climatol.,in press.

Malcher J., and Ch.-D. Schönwiese, 1987: Homogeneity, Spatial Correlation and Spectral Variance Analysis of Long European and North American Air Temperature Records, Theor.Appl. Climatol., 38, 157-166.

Parker, D.E., P.D. Jones, C.K. Folland, A. Bevan, 1994: Interdecadal changes of surface temperature since the late nineteenth century, J. Geophys. Res., 99, 14373-14399.

Solow A. R., 1988: Detecting Changes through Time in the Variance of a Long-Term Hemispheric Temperature Record: An Application of Robust locally Weighted Regression, J. of Climate, 1, 290-296.

Wallén C.C., 1986: Variability and Extremes of Winter Temperatures in Europe 1870-1980, Arch. Met. Geophys. Biocl, Ser. B, 173-188.

Temperature variation in Poland in the period of instrumental observations

Miroslaw Mietus

Institute of Meteorology and Water Management
Maritime Branch, Waszyngtona 42, PL–81–342 Gdynia, Poland

Intoduction

Studies on the variability of climatic conditions since the time when regular instrumental observations began are aimed to consist of investigations on the natural changes and the changes due to the human activity. Identification of anthropogenic changes can be carried on in two aspects: to detect statistically significant changes induced by this activity and to look for the relations between the change of the climate element and the change in the associated anthropogenic factor itself. The detection of pure climatic changes is difficult due to the fact that the effects of anthropogenic influences are overlapping the natural changes of given climatological element, so that additional observations of untainted background would be needed for comparison, and these often are lacking. Therefore, though the factors causing the natural changes are well known it often is impossible to clearly distinguish an anthropogenic signal from a natural one.

The sort of detection applied in contemporary climatology, being statistical in character, demands for long series of data and, regrettably, is often barred by limited lengths of observation series. The series available (chiefly of air temperature and precipitation) usually do not exceed 100 to 200 years of regular meteorological measurements. They nevertheless are an invaluable source of direct information on the present changes in the variability of these elements. And in spite of this that they are short as compared with the non–instrumental series of meteorological data of the 'proxy' – type, only they can be used to investigate the present features of the climatic changes, to the detection of the changes and to the numerical modellilng.

Data and their quality

Problems with data series of different derivation. As already said, proper estimation of the variability of the main climatological elements and the detection of changes in the character of this variability meets with different hindrances, as for instance lack of data series long enough, or gaps in the indispensable 'meta–data'. This problem is of special

importance when Poland's observation series are considered. This follows from the fact that this country for more than the whole nineteenth century – and this was the time when the principles for the European system of meteorological observations were formed – did not exist as an independent state and its provinces remained under the administration of the invador states. Thus, within the borders of to-day's Poland, until the end of the second decade of the twentieth century, three different meteorological services were functioning: the Russian, Prussian and the Austrian ones. In consequence, when Polish observation series are considered, many problems arise regarding the differences resulting from the non-uniform observing systems (different observation hours, meteorological screens, rules used for computing mean values, and so on). Besides, there are problems of gaps in the source material and in the history of stations. Further, in many cases the continuity of observation series is broken due to the heavy and repeated military operations of the I and II World War. All these reasons do not allow to construct a station net of both very long observation time and well documented station history. The first places where in the first decades of nineteenth century the first meteorological observations were established were usually the developing centres of administration and bigger academic, research or cultural centres. At first the stations were of private status, until in the eighties of nineteenth century the growing institutionalism led to inclusion of these stations into the national networks. The stations in towns were located usually in the city, quite often in the observer's rooms, sometimes upstairs, several meters above the ground. Temperature readings were made twice or three times a day, be means of thermometers mounted before a window. In cases when sun rays struck the thermometer directly (e.g. in early morning hours) a shelter was fastened before it or two thermometers were used, fastened before two differently exposed windows, depending on the day's hours. It was often a normal practice to shift the reading hours following the sun risehours, according to the season of the year. Location of the stations changed very often, due to the observer's changung his dwellings.

In the seventies of nineteenth century the growing institutionalism succeeded in accomplishing the unification of observing practices during less than twenty years and in establishing some meteorological stations in small towns, rural institutions or estates. In this way the observations moved outside the urban and industrial regions. Nevertheless, running the station in rural regions was not easy, especially due to lack of observing personnel. Therefore the really long series of observations from the extra-urban regions are scarce; this is a pity, because they are of great importance to the investigations, as they can serve as a background for the series gained in big centres (provided, both stations are not very far apart).

Regions and time considered. Respecting all the above mentioned circumstances – indispensable corrections were calculated and applied to the series of annual means of air temperature. Then the Standard Normal Homogeneity Test by Alexandersson (1986) was applied to prove the homogeneity of the series. For the analysis of variability of air temperature in Poland could be selected some long series of observations in big centres, as Krakow (1881–1990, Morawska–Horawska 1991), Warszawa (1881–1990), Wroclaw (1881–1990, Pyka 1991), Szczecin (1881–1990), Bydgoszcz (1881–1990),

Gdynia (1923–1990) and some in rural environment, as Pulawy (1881–1990), Hel (1881–1990), Poswietne (1900–1990) and Rozewie (1923–1990).

Results and discussion

Analysis of the century's temperatures. To characterize the variability of air temperature the usual criteria were adopted: when the mean temperature of a given year deviated from the long term (1881–1990) annaul mean for the station considered by less than 1 standard deviation, this year was classified as a normal one; when the departure was closed between 1 and 2 standard deviations the year was classified as subnormal, and when it differed by more than 2 standard deviations from the long–term mean it was classified as far subnormal or far overnormal, respectively.

Using these criteria we can say that – comparing to the long–term mean of 1881–1990, which varied from 7.6 °C to 8.6 °C depending on station – the beginning of twentieth century was subnormally cool and far subnormally cool; the first half of the secend decade of this century was warm and subnormally warm; the fourth decade was subnormally or even far subnormally warm; the early forties were subnormally cool or even far subnormally cool. After these cold years some separate overnormally warm years followed: 1943, 1944, 1949, 1953, 1961, 1974, 1975, 1985 and 1990. Also some separete years subnormally cool were encountered in 1956, 1966, 1985 and 1987. In general, 70 per cent of years could be classified as thermally normal (of annual temperature differing by not more than $\pm 1\delta$ from the long–term mean), 25–27 per cent were classified as subnormal (cool or warm, respectively) and only 3–5%, depending on stations, as far subnormal. During this time of more than hundred years (1881–1990) there were, depending on station, 18–22 overnormally warm years and 26–29 subnormally cool ones.

The analysis of deviations of the mean values for the successive decades (1881–1890, 1891–1900, 1901–1910,....) from the long–term mean reveals a regularity: the sign of the deviation changes from a negative one in the first five decades of the time considered, through zero in the four following decades (until 1961–1970) to become positive in the two last decades (1971–1980 and 1981–1990).
Compared to the air temperature anomalies on some selected stations in northwestern and central Europe, e.g. Foerder Fyr, Goeteborg, Visby, Putbus, Berlin, considered in above described manner, the anomalies on Polish stations reveal very similar variability.

Linear trends. The Gaussian loww–pass filter with 10 and 30 years window applied to the temperature series allowed to eliminate very short–term fluctuations and to stress the short and middle term variability. Results gained by means of this operation prove that the filtered variability curves are of the same character on all the Polish stations considered, differing only slightly from station to station. The variability of temperature differs only by a small degree in respect to amplitudes (by 0.0 to 0.8 °C) and the time of persistence of particular peaks (by 1 to 2 years). By means of fitting the regression lines to the series of particular station, both the magnitude and the rate of temperature changes could be estimated They amounted from 0.002°C/year in Wroclaw and Warszawa to as much as 0.015 °C/year in Krakow. These values were derived by the

verification of zero–hypothesis on the non–existence of linear trend, which gave evidence that there exists a statistically significant positive trend of the above given values. The such very high trend coefficient in Krakow is evidently connected with a very dynamic urban and industrial development of this town during 1951–990, when the metallurgic and chemical industry grew rapidly there.

Local anthropogenically conditioned trends. In order to detect the influence of local factors (influence exerted by human activity in developing centres) analysed were annual air temperature differences between stations in bigger towns and stations in environment only slightly modified by men. As an example could be taken series from station Gdynia, Hel and Rozewie, lying not very far from each other (18–38 km) and all of them coastal stations. Gdynia is a town which, from a small fisherman village until 1923 grew within 16 years – and further, until now – to an important sea port and industrial centre, reaching nearly 300.000 inhabitants. Hel is a small resort of 5.000 inhibitants, on the end of a narrow and flat penninsula, with a sea port mainly for fishing purposes. Rozewie is a place on a cliff shore with a lighthouse, and only few scattered single buildings: nearest villages and small resorts are 2–5 km away.

The analysed variability of annual temperature differences between so differently developing localities allows to show the existence of statistically significant positive tendencies of 0.003°C/year between Gdynia and Hel and of 0.004 °C/year between Gdynia and Rozewie. The magnitude is to be accepted as an effect of impact of the local anthropogenic sources (in this case – of Gdynia) contributing to the trends possible in the variability of greater, may be global, scale.

Conclusions

Following features can be attributed to the long–term variability of air temperature in Poland:
- character of these variability in the years 1881–1990, both in big industrial centres and in rural environment was similar and in agreement with the regional features;
- a positive, statistically significant trend of 0.002 °C/year to 0.014 °C/year was detected, depending on region;
- the rate of temperature increase in big urban and industrial centres due to big local impact is greater than in the rural environment.

It must be also kept in mind, when dealing with long series, that due to inuniformities in observational material detailed corrections and homogenization are indispensable.

References

Alexandersson H., 1986. A homogeneity test applied to precipitation data., J. of Clim., 6: 661–675.

Horawska–Morawska M, 1991. The influence of the growth of the town and of and the global warming on the rise of the air temperature in Cracow in 100–years period 1881–1980, Rev. of Geophysics., 4:321–328 (in polish).

Pyka J., 1991. Air temperature and precipitation at Wroclaw, 1881–1980. Acta Univ. Wratislaviensis, No 1237, Papers of Inst. of Geography, s.A, VI, 19–53 (in polish).

LONG-TERM VARIABILITY IN THE PRECIPITATION FLUCTUATIONS OVER THE RUSSIAN PLAIN AND ITS RELATIONSHIP WITH GLOBAL CLIMATIC CHANGES

V. Popova

Institute of Geography
Russian Academy of Sciences
29, Staromonetny str., Moscow,
109017, Russia

Introduction

The diagnosis of climate fluctuation of regional scale and their relationship with global warming and cooling processes as well as changes of general atmospheric circulation is integrated to the decision of such problems as determination of fluctuations spatial scale and allocation of long-term components as well. It acquires the special significance while researching atmospheric precipitation characterized by discretion in time and space and distinguished by smaller fluctuations relationship in space in comparison with air temperature.

The present work is devoted to study of spatial and temporal structure of the precipitation fluctuations over the Russian plain for period of tool observations with the purpose of long-term variability revealing connected to climate fluctuations, in particular, with changes of general atmospheric circulation.

Results and discussion

Delimitation of the homogeneous regions according to the precipitation fluctuation over the Russian plain (Popova, 1992) carried out on the basis of data on both annual precipitation and precipitation of cold period averaged for the area (Efremova, 1976, Meshcherskaya, et al. 1988) has allowed to determine spatial scales of the precipitation fluctuations which are defined by the size of regions within the limits of which fluctuations are synchronous. These scales make 600 km on a longitude and 1000 km in latitudinal direction. The main components method was fixed in the basis of delimitation of the homogeneous regions according to the precipitation fluctuations. That allowed to divide 44 series of spatially averaged precipitation appropriate to centers of administrative areas into 5 groups

depending on variable significance on first three vectors containing a main share of general precipitation variability over the Russian plain territory. These 5 groups have formed 5 regions: north-west of the Russian plain, western part, central part, east of the Russian plain including the Middle Volga and southern regions including Caspian and Black sea steppe areas (Fig. 1a). We shall note that the points on whole considered territory appropriate variable included in each allocated group have lain in a kind of homogeneous areas. This circumstance as well as quantity of allocated regions, their geographical location and extent specifies objectivity of their allocation and on the fact that their availability is stipulated by occurrence of the common factors instead of local conditions.

Delimitation of the homogeneous regions according to precipitation of cold period over the Russian plain obtained by the same method has also resulted in delimitation of five regions, location of which basically coincides with location of regions got for annual precipitation (Fig. 1b).

Delimitation of regions with homogeneous precipitation fluctuation permits to establish a long-term annual cycle of precipitation and precipitation of cold period as well for each of delimited regions on the Russian plain territory for period 1891 - 1982 by averaging on the area and to reveal features of its temporary structure. For this purpose we shall consider spectra of annual precipitation fluctuations. The spectral analysis was conducted with use of parametrical assessment process method developed by V.E. Privalsky (1985). Spectra of annual precipitation fluctuations indicated on Fig. 2a,b show that the contribution of low-frequency fluctuations (with periods of 10 and more years) exceeds the contribution of high-frequency component into general variability of precipitation in two regions - on the north-west and on the east of the Russian plain. Thus the parity of a share of high-frequency and low-frequency fluctuations in both regions is about identical. The spectra of precipitation fluctuation in the north and in the west represent itself so called "white noise", i.e. uniform distribution of spectral density on frequency. In centre of the Russian plain spectral density accrues to the area of a two-year cycle but does not fall outside the limits of trustworthy interval and as appear, specifies only some tendency to existence of two-year cyclic recurrence in this region.

Let us compare a long-term variation of annual precipitation in each of five regions delimited on the Russian plain territory with change of atmospheric circulation according to B.L.Dzerdzeevsky classification. As it is known, allocation of elementary circulating mechanisms (ECM) and determination of their main characteristic which is treated as the zone or meridionality lies in the basis of Dzerdzeevsky classification (1981). In the first case this is the zone west transfer in moderate latitudes, in the second one - infringement of zone. Thus the zone circulation in moderate and subtropical bands corresponds to latitudinal or close to latitudinal trajectories of baroformations, meridional circulation corresponds to southern cyclones and polar invasion into moderate bands.

Change of circulating processes of the last century according to B.L.Dzedrzeevsky classification reflect the global climate fluctuations, about than a rather high correlation of zone types ECM duration and air temperature in non-tropical latitudes testifies (correlation factor 0,50). Linear correlation factors between annual precipitation variation and ratio of
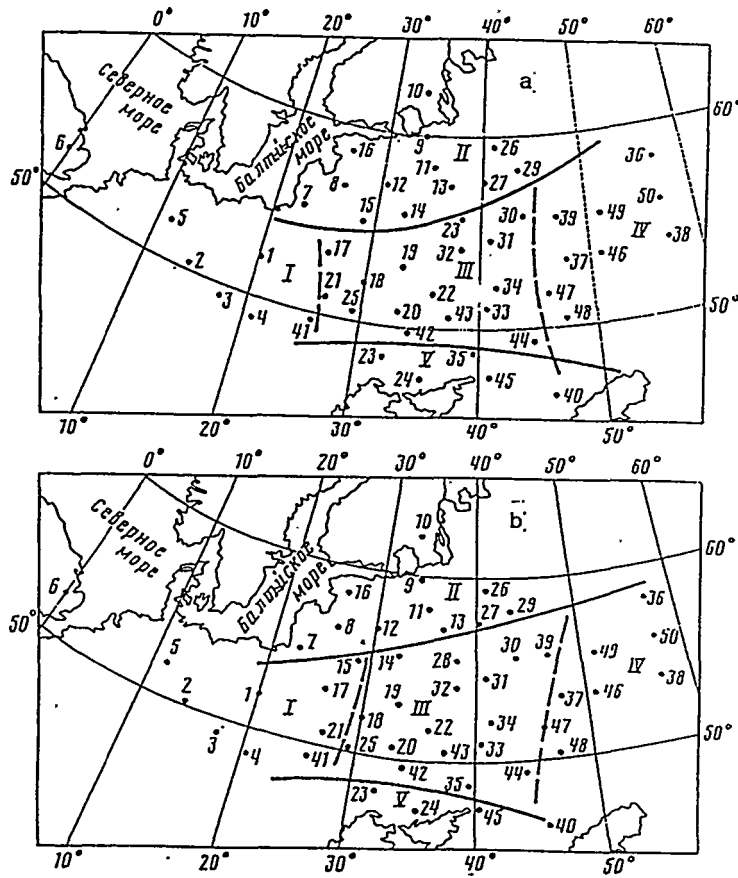
Fig. 1. Borders of regions with homogeneous fluctuations of annual precipitation (a) and precipitation of cold period (b) over the Russian plain territory. 1 - 50 - centres of administrative areas (oblasts).
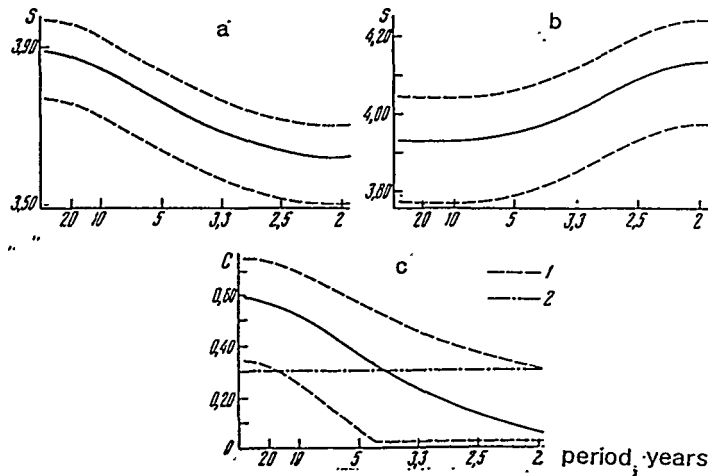
Fig. 2. Function of spectral density of precipitation fluctuations in north-west (a) and in east (b) of the Russian plain as well as function of mutual coherence of precipitation fluctuations in eastern part of the Russian plain and duration of zone circulation types action to meridional ones according to B.L. Dzerdzeevsky (c).

1 - boundaries of 90% trustworthy interval; 2 - significance level of mutual coherence function.

zone ECM action duration to meridional one have statistically significant values only for two regions - central part and east part of the Russian plain, the significance of correlation factors are negative for both regions but not high. At the same time, for more extended than one year of periods this relationship is essential as mutual spectra of annual precipitation fluctuations and changes of circulation show (Fig. 2c). In an interval of periods till 5 years the relationship is absent but with increase of period length it grows and becomes closest within the periods of 20 - 30 years where mutual coherence function reaches 0,5 for central part and 0,6 for east part of the Russian plain.

In conditions of cold period humidifying the relationship between atmospheric precipitation fluctuations and changes in general atmospheric circulation appears statistically significant for all five regions delimited on the Russian plain territory, and for central and eastern parts of the considered territory it becomes closer. Correlation factor between fluctuations of ECM zone action duration and precipitation of cold period reach -0,41, -0,45. The lowest values of correlation factors (-0,25) are marked for north-west part of the Russian plain, and they make accordingly -0,33 and -0,28 for south and western parts.

Thus, the prevalence of long-term component in precipitation fluctuations is found out in north-west and east parts of the Russian plain. Equal contribution of long-term and high-frequency precipitation fluctuations is characteristic of for central regions of the Russian plain. At the same time the relationship of humidifying with global climatic changes is marked only for eastern and central parts of the Russian plain. Precipitation falls less over central and eastern parts of the Russian plain during prevalence of zone type circulation (according to Dzerdzeevsky classification) conterminous with periods of global warming, but precipitation exceed their average long-term values during activization of meridional processes. For annual sums of precipitation this distinction as was shown early on empirical data (Popova, 1988) makes on the average 40-50 mm. It is obvious that determined distinctions in years and periods from several years till several decades which are differ depending on prevalence of zone or meridional ECM action duration, effected the environment, in particular, rivers outlets and levels of closed water reservoirs that is confirmed by fluctuations of the Caspian sea level this century.

References

1. Popova V.V., 1988. Long-term fluctuations of precipitation on the USSR European territory and their relationship with global circulation.// Meteorological Researches, N 14, IGC AS USSR, 120-125 pp.

2. Popova V.V., 1992, Spatial and temporal structure of atmospheric precipitation fluctuations on the East and Central Europe territory.// Water Resources, N 4, 124-130 pp.

3. Efremova N.I., 1979. Month atmospheric precipitation average both for the USSR European and Northern Kazakhstan territory. Trudy VNIIGMI-MCD, edition 58, 41-60 pp.

4. Meshcherskaya A.V., Boldyreva N.A., 1988. Long-term series of average month regional precipitation in cold period of a year for the main agricultural zone of the USSR.// L., Gidrometeoizdat, 285 pp.

5. Dzerdzeevsky B.L., 1968. Circulating mechanism in the atmosphere of Northern hemisphere in XX century.// Meteorological Researches, M.: IGC AS USSR, 173 pp.

6. Privalsky V.E., 1985. Climatic variability. M., Nauka, 181 pp.

The warmest decade in Finland - the 1930s

Heikki Tuomenvirta

Finnish Meteorological Institute, Climatology Division,
Box 503, 00101 Helsinki, Finland

Temperature anomalies

The warmest ten year period in Finnish annual mean temperature series (Heino 1994) is decade 1930-1939 (Fig. 1). According to temperature series from Helsinki, the.1930s has been the hottest ten year period at least in 170 years in Finland. Short review on literature reveals that in Norway (Aune 1994), Sweden (Alexandersson and Eriksson 1989) and in an area extending close Iceland, the 1930s has been the warmest decade. According to Nordli (1995), the same feature can be seen in High Arctic series from Spitsbergen. In Central Europe, e.g. in Germany (Dahlström 1994), the 1930s is only a local maximum and warmer decades can be found. Also the Baltic states and European part of Russia north of 60N and up to the Ural mountains belong to area where 1930s was the warmest period of at least past 110 years (Groisman 1995).
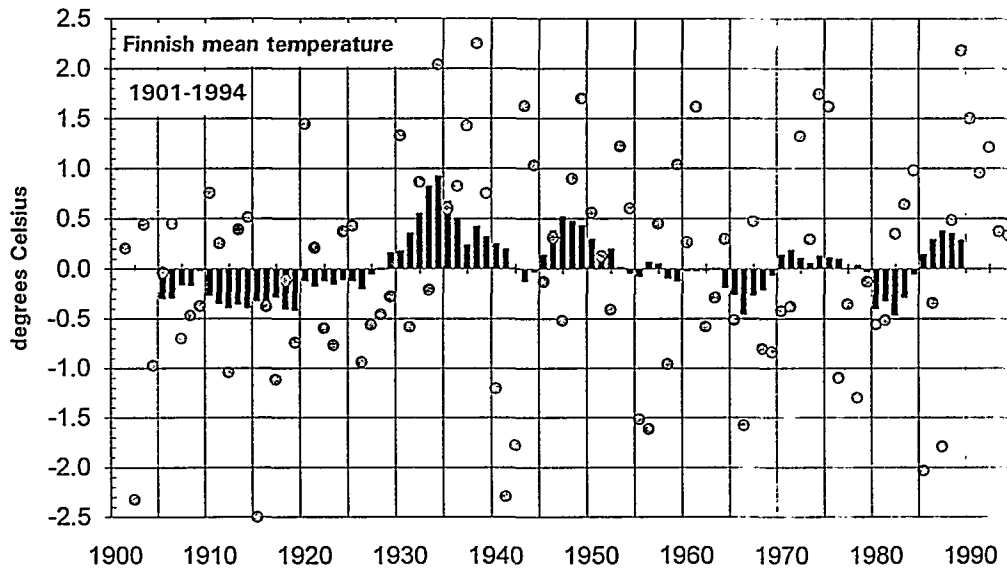
Figure 1. 10-year moving averages (bars) of Finnish annual mean temperature (dots) anomalies from the period 1961-90 mean value.

In Finland, temperature anomalies of the 1930s were about one standard deviation (calculated from the normal period 1961-90). The annual anomalies were largest in the north, where winter was the season with largest deviation from the normal (Table 1). In Southern Finland anomalies were slightly smaller and summer anomalies were largest. The springs of 1930s were close to the normal period, but autumns were warm.

Table 1. Temperature anomalies of the period 1930-39 from normal period 1961-90 expressed in degrees (italics) and in standard deviation of normal period (bold). Stations are from north to south. Seasons are three month periods, e.g. summer is June- August.

	Annual		Winter		Spring		Summer		Autumn	
Sodankylä	1.4	1.1	3.4	1.0	0.0	0.0	0.8	0.7	1.2	0.7
Oulu	1.2	1.0	3.1	0.9	-0.2	-0.1	0.9	0.8	1.0	0.7
Kajaani	1.0	0.8	2.5	0.7	0.0	0.0	0.7	0.6	0.8	0.5
Jyväskylä	0.8	0.7	2.1	0.6	0.2	0.1	0.4	0.4	0.6	0.5
Lappeenranta	0.9	0.8	2.0	0.7	0.1	0.1	0.8	0.7	0.7	0.6
Helsinki	0.8	0.8	1.6	0.6	0.2	0.2	1.0	1.0	0.5	0.5

Precipitation, snow cover and cloudiness

Generally, precipitation amounts show large spatial variation. This was true also during the 1930s. At some stations it was the wettest decade during this century, but there are also stations where the 1930s was the driest decade. Northern half of Finland, except areas close to Norwegian border, received more precipitation than normal. In Southern Finland anomalies were small or, at some stations, clearly negative.

The mean duration of snow cover in the 1930s was close to the normal. However, the length of snow cover season was short during winters 1936-37 and 1937-38, according to observations from Jyväskylä and Sodankylä. Helsinki experienced record short 'snow winter' in 1929-30.

The observations made at the Central Institute in Helsinki and in Sodankylä Observatory were used for cloudiness analysis. Due to subjectivity of cloud amount observation, even the results from these high quality stations must be analysed with care. The summertime cloudiness was below normal during 1930s at both stations. In Helsinki, winter cloudiness was higher than normal and slightly above normal in Sodankylä. The intermediate seasons did not show any anomalies.

Geostrophic wind

Geostrophic winds used in this study were calculated by Lahti (1994) in triangle formed by stations Mariehamn, Helsinki and Vaasa in South-western Finland. Correlation analysis of seasonal geostrophic wind vectors and temperature series (mean of Helsinki and Kajaani) in period 1895-1992 (Fig. 2) confirms that westerly winds (= wind vector pointing east) bring mild winters to Finland. The variation of wintertime 30-year running correlation was fairly large, from 0.5 to 0.8. Correlation in spring and summer are weak. The coolness of autumn can be said to come from the northeast. The warm

winters of the 1930s can partly be explained by westerlies, but they were also warmer than would be expected from wind speeds (squares are above circles in Fig. 3).
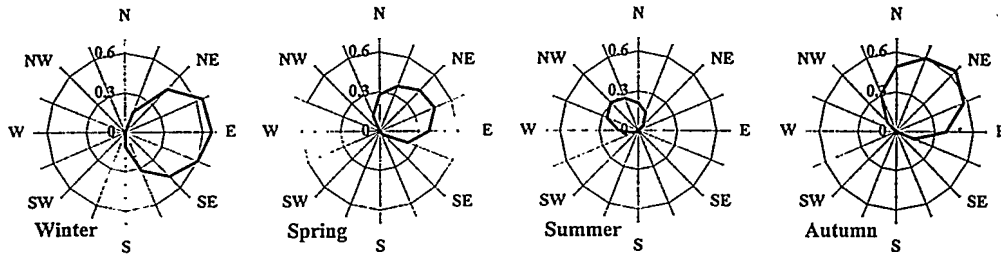
Figure 2. Seasonal correlation between geostrophic wind vector and temperature in Southern Finland. Only positive correlation is shown.
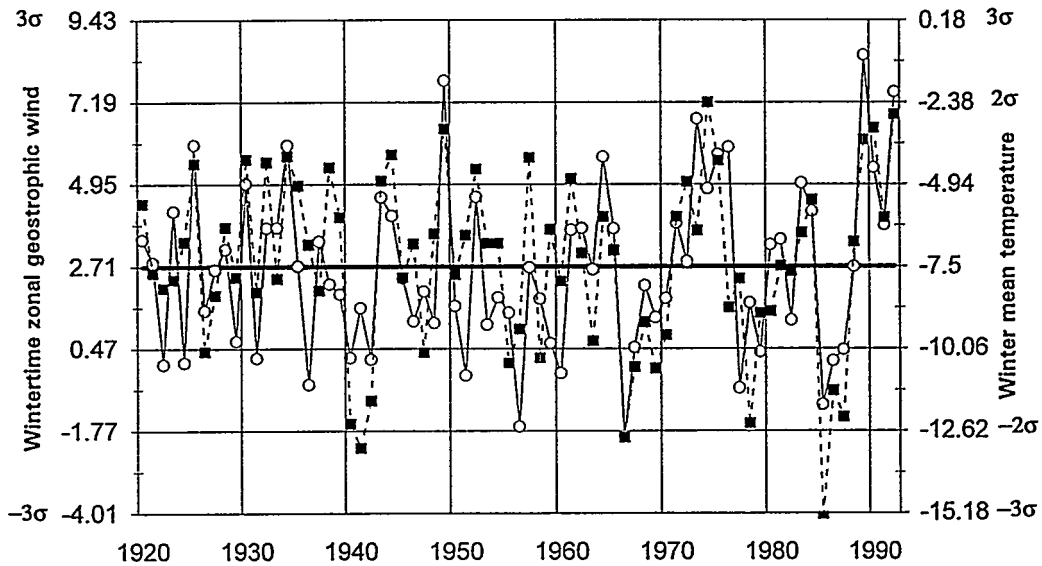
Figure 3. Wintertime zonal geostrophic wind (open circles, left axis) and mean temperature (black squares, right axis) in Southern Finland 1920-1992. Wind is in m/s and temperature in degrees Celsius. Major gridlines are spaced every one standard deviation from the mean (period 1895-1992).

The 1930s as a scenario

At least, Kettunen et al. (1989) have used the 1930s in studies of future crop yields. Carter et al. (1995) constructed climatic scenarios for Finland based on three transient GCM simulations. They account for two major uncertainties (the range of possible future greenhouse gas emissions and range of estimates of climatic sensitivity). 'Policy-scenarios' are defined as spatially uniform seasonal trends over Finland with possible range of temperature change. According to 'central' scenario, we have to wait until the

first quarter of 21st century before temperatures have risen on the same level as in 1930s. However, uncertainty is large, e.g. 0.9 degree rise of long-term annual mean may happen already in 2005, or as late as 2080, the 'best' estimate being 2013.

Table 2. Finnish temperature anomaly of period 1930-39 from normal period 1961-90 and corresponding years with similar temperature rise in three SILMU policy-oriented scenarios. Temperature anomalies are in degrees Celsius.

SILMU 'policy scenario'	Annual	Winter	Spring	Summer	Autumn
Central	2013	2028		2013	2008
Low	2080	2174		2083	2060
High	2005	2021		2006	2002
Anomaly from 1961-90 mean	0.9	2.3	0.0	0.7	0.7

References

Alexandersson, H. and B. Eriksson, 1989: Climate fluctuations in Sweden 1860-1987. *SMHI Rep. Met. Clim. Nr 58*, 54 p.

Aune, B., 1994: Climate variations in Norway in the period of instrumental observations. In: *Heino, R. (Ed.), Climate Variations in Europe. Proceedings of the European Workshop held in Kirkkonummi (Majvik), Finland 15-18 May 1994.* Publications of the Academy of Finland 3/94, Helsinki, 97-102.

Carter, T., M. Posch and H. Tuomenvirta, 1995: SILMUSCEN and CLIGEN User's Guide. Guidelines for construction of climatic scenarios and use of a stochastic weather generator in the Finnish Research Programme on Climate Change (SILMU). *Publications of the Academy of Finland 5/95*, Helsinki, 62 p.

Dahlström, B., 1994: Short term fluctuations of temperature and precipitation in Western Europe. In: *Heino, R. (Ed.),op cit.*, 30-38.

Groisman, P.Ya., 1995: Personal communication

Heino, R., 1994: Climate in Finland during the period of meteorological observations. *Finnish Meteorological Institute Contributions 12*, 209 p.

Kettunen, L., J. Mukula, V. Pohjonen, O. Rantanen and U. Varjo, 1988: The effects of climatic variations on agriculture in Finland. In: Parry, M.L., T.R. Carter and N.T. Konijn (Eds). *The Impact of Climatic Variations on Agriculture. Volume 1. Assessments on Cool Temperate and Cold Regions.* Kluwer, Dordrect, The Netherlands, 511-614.

Lahti, M., 1994: Linear trends in surface and geostrophic winds in Finland. In: *Heino, R. (Ed.),op cit.*, 306-313.

Nordli, P., 1995: Long time series of temperature in Norway. *Proceedings of the Sixth International Meeting on Statistical Climatology, June 19-23, 1995, Galway, Ireland* (submitted).
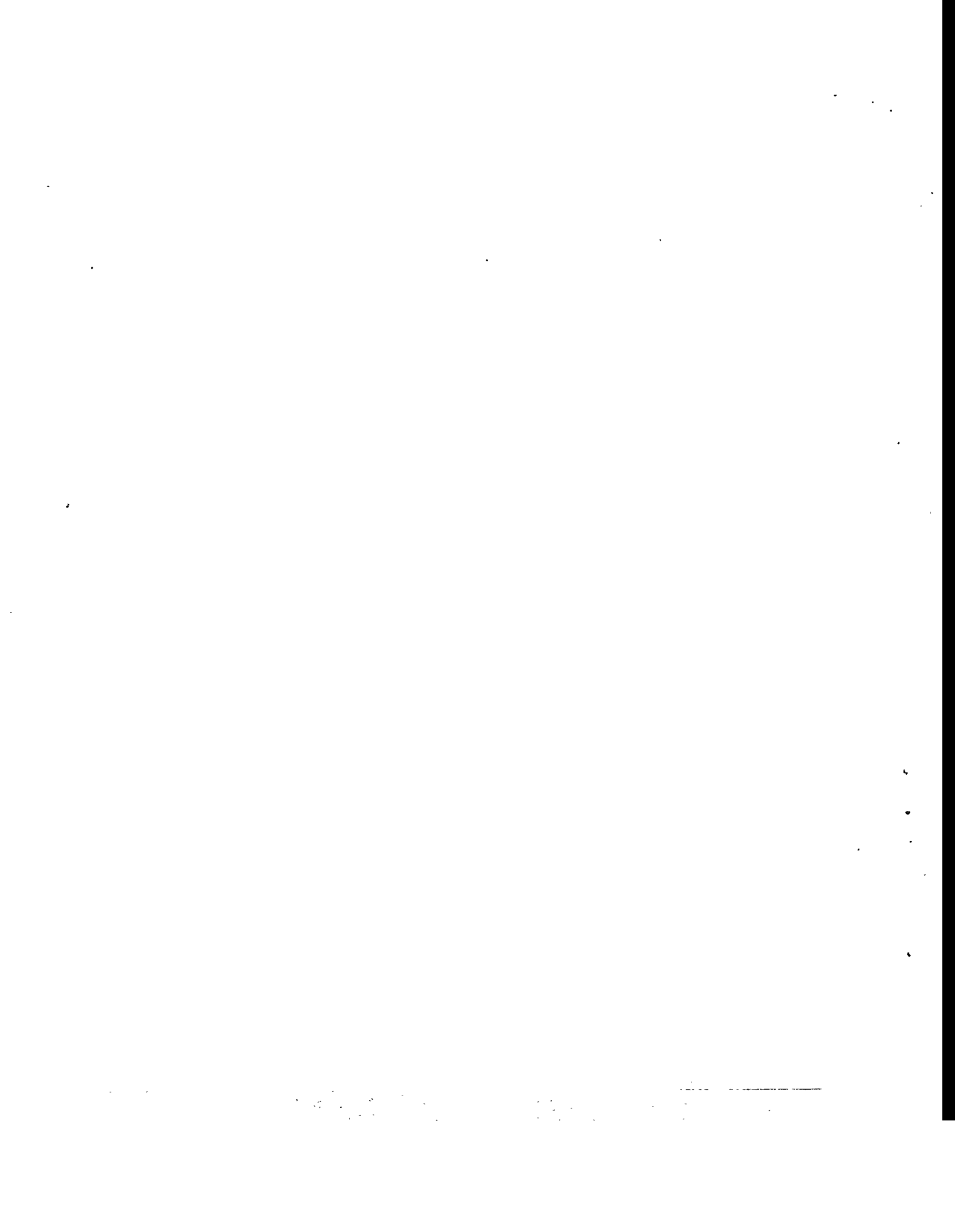
Analytical methods /
analysis of observations
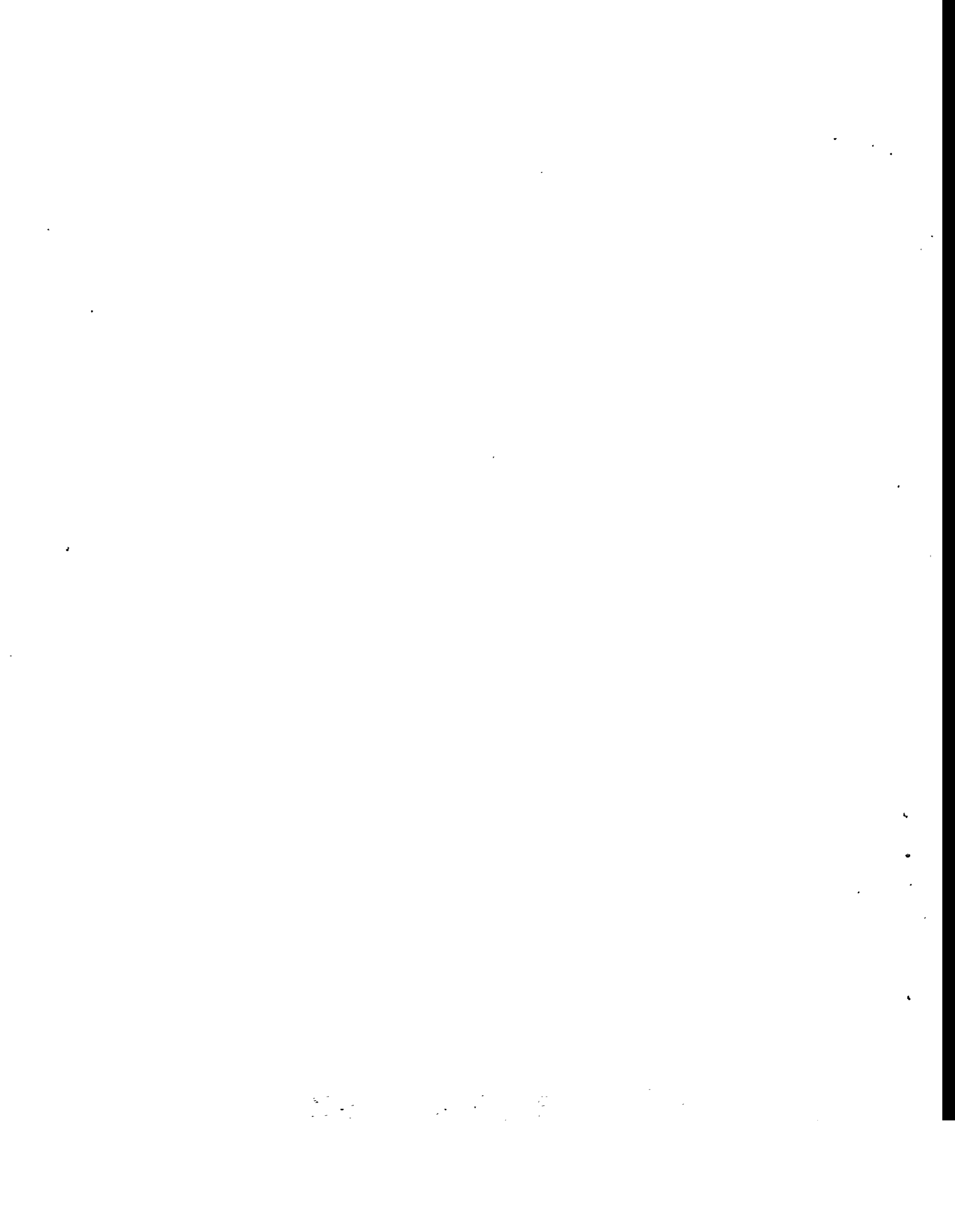
Land ice and sea level change

Conrads, Louis A.

Institute for Marine and Atmospheric Research, Utrecht University in co-operation with the University of Amsterdam, the Free University (Amsterdam)

sponsored by

Sea-level change is an important issue in the greenhouse problem. All workers agree that predictions made so far have a high degree of uncertainty. Comparable contributions to this uncertainty come from limited knowledge of future emissions of greenhouse gases, different opinions concerning the response of the climate system, and inadequate knowledge of the sensitivity of land ice to climate change.

The goal of this project is to improve estimates of the contribution of land ice masses to sea-level change in the coming 150 years.

MASS BALANCE OF THE GREENLAND ICE SHEET

The mass balance of the Greenland ice sheet has been studied with an energy balance model. The mass balance is generated from climatological input. Data from several field experiments have been used to improve the parameterization of energy transfers between atmosphere and surface. The grid resolution is 20 km.

The picture below shows the calculated surface mass balance for the "reference case". Sensitivity tests reveal that

a 1K warming implies a 0.30 mm/year sea-level rise
a 1K warming $(+\delta P)$ implies a 0.21 mm/year sea-level rise
a 10% increase in cloudiness implies a 0.02 mm/yr sea-level drop
a 0.02 decrease in albedo implies a 0.17 mm/year sea-level rise

[δP is a change in precipitation in proportion to saturation vapour pressure]

m of water equivalent per year
(nonlinear scale)

+ 2.0

+ 1.0

+ 0.5

+ 0.25

+ 0.0

- 2.0
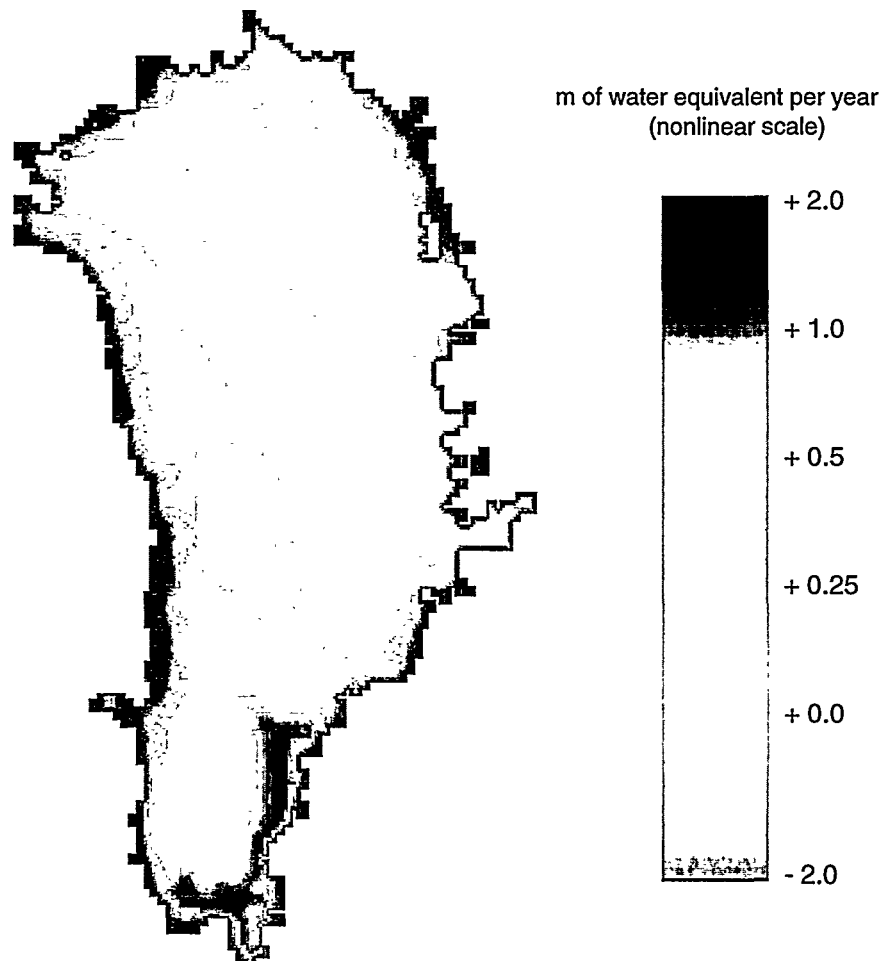
Greenland ice sheet, +1K: 0.21 mm/year sea-level RISE (*best estimate*)

GLACIERS AND SMALL ICE CAPS

A model has been designed that simulates mass balance profiles on glaciers. It has been tested on 12 glaciers for which good observations exist. After careful calibration a large number of sensitivity tests have been carried out. There appears to be a significant correlation between glacier sensitivity and precipitation regime. The figure below shows the result for an experiment with uniform 1K warming and an increase in precipitation proportional to saturation vapour pressure of the air. The mean loss of ice, averaged over the entire glacier, is shown for the 12 glaciers studied.
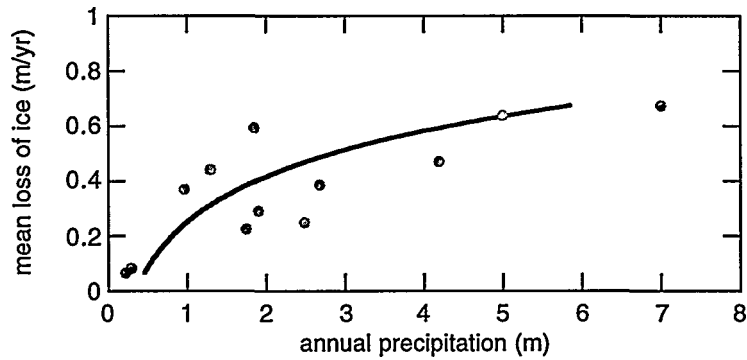
Extrapolation of this result to all glaciers and small ice caps outside Greenland and Antarctica yields a sea-level rise of 0.46 mm/yr for a uniform 1K warming (this includes increasing precipitation). This is about half the value of the 1.2 ± 0.6 mm/yr used in IPCC-1990.

The difference is due to an earlier overestimation of glacier sensitivity in the dry subpolar regions, where a large amount of glaciers and small ice caps are located (see below).
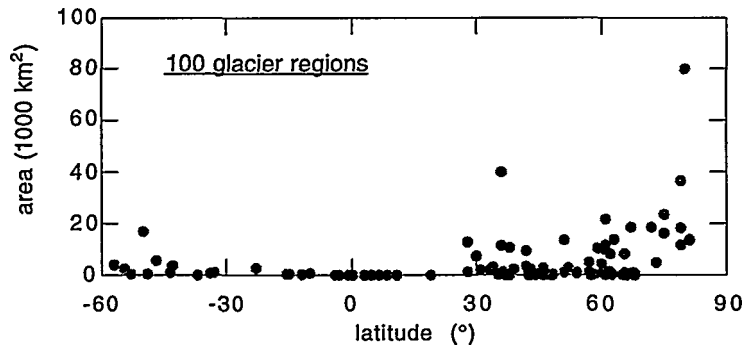
| Glaciers and ice caps, +1K: 0.45 mm/year sea-level RISE (*best estimate*) |

A MODEL FOR SNOW ACCUMULATION ON THE ANTARCTIC ICE SHEET

A simple meteorological model has been developed to simulate the temperature and precipitation distribution over the Antarctic continent. The model is two-dimensional (vertical plane, see figure below), and has 4 layers: stratosphere, troposphere, boundary layer and surface of the ice sheet. It has a detailed radiation scheme for short and long wave radiation.

The katabatic outflow is explicitly calculated and drives the circulation over the ice sheet. The boundary layer has two shear zones: one at the ice sheet surface and one at the top of the boundary layer, where significant entrainment takes place. Boundary layer depth is a prognostic variable.
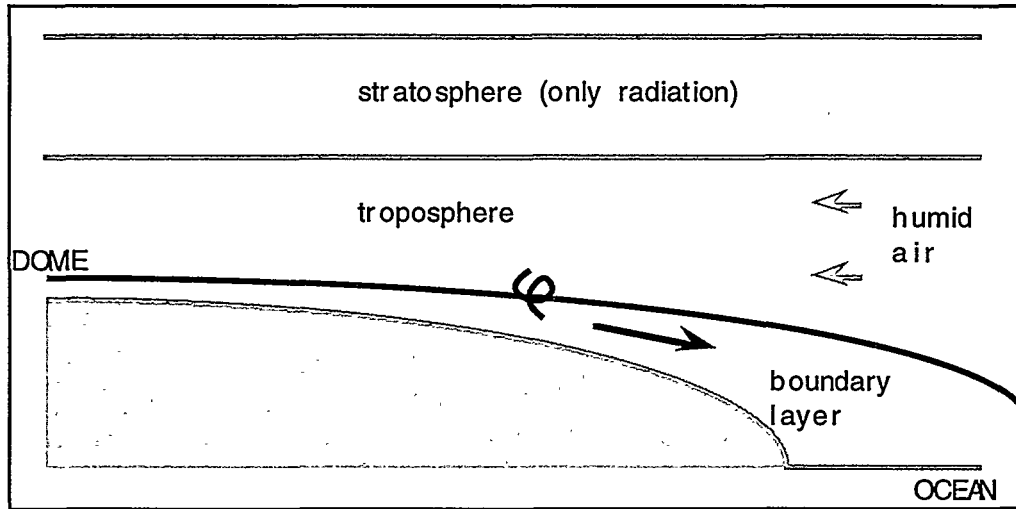
Moisture is brought to the ice sheet by the return flow in the free troposphere. Precipitation occurs because of cooling of the air (due to uplift and a negative radiation balance). The moisture budget at the surface has four contributions:

- precipitation
- riming
- evaporation
- divergence of snow drift

When run with appropriate boundary conditions (annual mean insolation and temperature at the ocean boundary), the model gives a satisfactory simulation of the meridional profiles of temperature and accumulation on the Antarctic ice sheet (annual mean state).

In case of a warmer climate, snow accumulation increases because the "moisture pump" intensifies. The increase is partly compensated by larger evaporation on the steep slopes of the ice sheet, however. For a uniform 1K warming, the model predicts an increase in snow accumulation that is equivalent to a 0.27 mm/year sea-level drop.

Antarctic ice sheet, +1K: 0.27 mm/year sea-level DROP (*best estimate*)

Volcanic and El Niño signal separation in GCM simulations with neural networks

M. Denhard, M. Klein and C.-D. Schönwiese

Institut für Meteorologie und Geophysik,
Postfach 111932, D-60054 Frankfurt a.M.

Introduction

A variety of internal relations and external forcings determine the climate system dynamics. In this study the effects of volcanic aerosols and the El-Niño-phenomenon are analysed. The model results from experiments with the ECHAM2-T21 climate model (Kirchner & Graf 1994) build the data base for this study. Three experiments have been designed. One with El-Niño forcing, one with vulcanic forcing and finally one with both forcings. The experiments are performed in a perpetual January mode. Every first January is initialised with the same solar parameters and with the resulting fields of the end of the previous January simulation. The data are in the form of spatial anomaly fields for a variety of parameters. The aim is to find a relation between volcano and El-Niño signals in the GCM-Climate.

Methods

The GCM experiments are designed to study the interaction between volcanic and El Niño forcing. A crude but desirable suggestion is that both isolated anomaly patterns simply add up to the combined forcing signal. Certainly, this is not true because of the complexity and the nonlinearity of the model climate. A rather more complex relation may exist:

$$VOEN = f(ENSO, VOLC)$$

This equation presupposes the validity of f on the whole globe. Otherwise, the existence of teleconnections in the atmosphere leads to the assumption that this relation should have at least regional validity. The nonlinearity of f and the differences of f on the regional scale are the main subjects of our investigation. With the intension to analyse the character of the relation a linear multiple regression analysis is applied. A main interest was given to nonlinear connections of the signals. A two layered Feedforward-Backproppagation-Neural Network is used to find a global nonlinear f (Widrow & Lehr 1990) . Further on, the abreviation MRM refers to the multiple linear regression analysis and NNM refers to the Neuronal-Network-Model.

Table 1: Global statistical analysis of combined volcanic and El Niño forcing signals. The coefficients a_V (volcanic) and a_E (El Niño) are derived from multiple regression. EV MLR and EV NN denote the explained variance of the regression model and the neural network model, respectively.

	a_V	a_E	EV MLR	EV NN
T850	0.62	0.48	76	82
T50	1.06	0.16	96	98
U50	0.62	0.83	88	93
U200	0.17	0.89	87	90
Z500	0.22	0.65	58	80

Results

In the upper troposphere and the stratosphere the explained variances of the MRM and NNM have almost equal values. This indicates a linear relation of the two forcings. In the lower troposphere the nonlinar influence of the relation is increasing. This is seen in the diffrerences between the explained variances of MRM and NNM.

The regression coefficients indicate the strenght of each isolated signal (table 1) of in the combined experiment. The volcanic forcing dominates over temperature effects, El-Niño mainly influences the circulation. The following interpretation concentrates on the influence of the volcanic forcing on the tropospheric and stratospheric circulation. The volcanic signal in the combined experiment is significant in the stratosphere but rather supressed in the troposphere.

The large difference between the regression coefficents, as it is found for the zonal wind-speed in 200 hPa (table 1), indicates a suppression of the volcanic signal to the benefit of the El-Niño signal. In this case a linear model can simulate the relation satisfactory. For the geopotetial height at 500 hPa (Z500) the regression coefficents do not differ so much but there is a large difference in the explained variances of the MRM and NNM. This indicates a growing nonlinear character of the relation. The further interpretation focuses on Z500. The nonlinearities appear in the Atlantic/European region only (figure 1 and 2). In other regions a linaer approximation leads to satisfactory results. Anomalies in the Atlantic/European area which appear in the seperated experiments vanish in the combined experiment. This phenomenon does not appear in other regions. Concluding from this a global relation f must be nonlinear. There is one negative anomaly which appears as an extraordinary feature. It can not be simulated even by NNM.

References

Kirchner , I und Graf, H. F 1994: Volcanos and El-Niño- Signalseparation in winter. Accepted for publication in Climate Dynamics (also Max-Planck-Institut f'ur Meteorologie, Report 121).
Widrow, B. & Lehr, M. A. (1990): 30 Years of Adaptive Neural Networks, Proc. IEEE, 78, 1415-1441.

a) VOEN-MRM, Z500
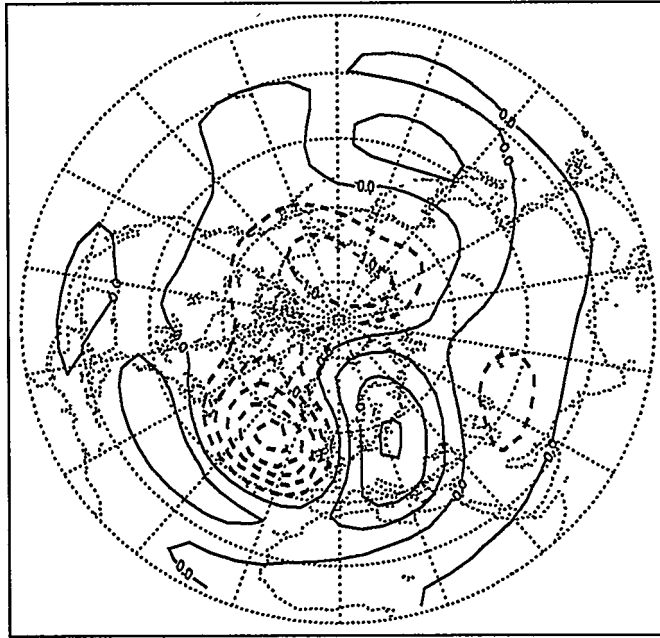
Figure 1: **The differences between the VOEN experiment and the multiple linear regression (MRM) for the geopotential height at 500 hPa.**

b) VOEN-NNM, Z500
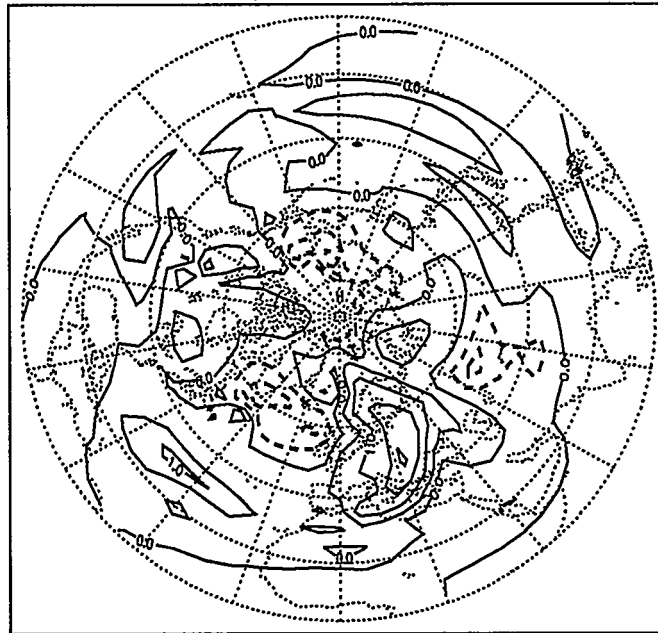
Figure 2: **The differences between the VOEN experiment and the neural network model (NNM) for the geopotential height at 500 hPa.**

Table 1

	winter	spring	summer	autumn
Moscow	+ + -	- - -	+ + +	- - -
Caspian Sea	+ + -	- - -	+ + -	- - -
Khabarovsk	+ + -	+ + -	+ + -	+ + -
Yakutsk	- + -	- - -	- - -	- + -
Prague	- - -	- - -	- + -	- - -
Sydney	- - -	- - -	- - -	- - -
Beijing	+ + -	+ + -	+ + +	+ + -
East America	- - -	- - -	+ + +	+ + -
West America	- - -	- - -	+ + +	+ + -

Table 2

	winter	spring	summer	autumn
Moscow	- + -	- - -	+ - +	- - -
Caspian Sea	- + -	- - -	+ + -	- - -
Khabarovsk	- + -	- + -	+ + -	+ + -
Yakutsk	- + -	- - -	- - -	- + -
Prague	- + -	- - -	- + -	- - -
Sydney	- + -	- + -	- + -	- + -
Beijing	- + -	- + -	+ - +	- + -
East America	- + -	- + -	+ - +	- + -
West America	- + -	- + -	+ - +	- + -

Discussion and conclusions

The differences between E1 and E2 may be explained in terms of hydrological characteristics change under global warming and their influence on DTR and blackbody radiative emissivity diurnal range $BD = 4T^3TD$. Demchenko et al. (1994) showed that integral absorption function of the atmosphere F_a has opposite influence on DTR and BD:

$$TD / F_a < 0$$
$$BD / F_a > 0$$

From (Saltzman & Ashe 1976)

$$TD / r_s < 0$$
$$TD / r_a < 0$$
$$TD / c < 0$$

where c is opacity of the atmosphere, r_s is albedo of surface and r_a is albedo of the atmosphere. Cloudiness affects on both absorption function and albedo of atmosphere:

$$TD / n < 0$$
$$F_a / n > 0$$

In this case total cloud amount change (and other cloudiness characteristics) may

change as DTR as blackbody radiative emissivity diurnal range. Then the cloudiness influence may be treated in terms of BD. Resulting effect is the DTR decrease at total cloud amount and soil moisture content increase (both are treated in terms of precipitation difference under doubling CO_2 content in the atmosphere). The change of BD is as a rule opposite to the DTR one. In regions where the total cloud amount and soil mosture content have a decline under global warming the changes in both DTR and BD are positive. The effect of background aerosol is analogous to the cloudiness one owing to its influence on albedo and transmission function of the atmosphere.

The result of this study is the investigation of cloudiness effect on the DTR and blackbody radiative emissivity diurnal range. It is shown that in some cases (particularly in cold seasons) it results in opposite change in DTR and BD at doubled CO_2 atmosphere content. The influence of backgroud aerosol is the same as the cloudiness one.

References

Demchenko, P.F, G.S.Golitsyn, A.S.Ginzburg & N.N.Veltischev. 1994. An estimate of diurnal cycle amplitude of the greenhouse effect in the 1D models of the vertical structure of the atmosphere. Izv. Atmos. Ocean. Phys. 30:595-600.

Karl, T.R., G.Kukla, V.N.Razuvayev, M.J.Cangery, R.G.Quayle, R.R.Heim, Jr., D.R.Easterling & C.B.Fu. 1991. Global warming: evidence for asymmetric diurnal temperature change. Geophys. Res. Let. 18:2253-2256.

Karl, T.R., P.D.Jones, R.W.Knight, G.Kukla, N.Plummer, V.N.Razuvayev, K.P.Gallo, J.Lindseay, T.C.Peterson. 1993. A new perspective on recent global warming: asymmetric trends of daily maximum and minimum temperature. Bull. Amer. Meteor. Soc. 74:1007-1023.

Michaels, P.J., & D.E.Stooksbury. 1992. Global warming: a reduced treat? Bull. Amer. Meteorol. Soc. 73:1563-1577.

Petoukhov, V.K. 1990. Thermodynamical approach to macroturbulent heat, humidity and momentum transfer description in climate models. in: Investigation of eddy dynamics, atmosphere energetics and the problem of climate (eds. E.G.Nikiforov & V.Ph.Romanov), Leningrad, Hydrometeoizdat, p.156-171.

Petoukhov, V.K., & A.V.Ganopolski. 1994. A set of climate models for integrated modelling of climate change impacts. Part II: A 2.5 - dimensional dynamical - statistical climate model (2.5-DSCM). IIASA, WP-94-39, Laxenburg, 96 pp.

Saltzman, B., & S.Ashe. 1976. The variance of surface temperature due to diurnal and cyclone - scale forcing. Tellus XXVIII:307-322.

Vinnikov, K.Ya. & P.Ta.Groisman. 1982. Empirical investigation of climate sensitivity. Izv. Atmos. Ocean Phys. 18:1159-1169.

Does hyperbolic intermittency exist in extreme variability of climatological data? Empirical study of Polish records.

Krzysztof Fortuniak

Department of Meteorology and Climatology, University of Łódź,
Kościuszki 21, 09–418 Łódź, Poland, E–mail: kfortun@krysia.uni.lodz.pl

Introduction

The methods based of fractal concepts and scaling properties of various meteorological parameters have recently attracted considerable attention and have inspired certain trends in data analysis. The scaling property, if indeed it is found to hold, can lead to far–reaching consequences in data collection and interpretation. In the atmospheric science, the fractal methods have been most commonly applied to spatial and temporal analysis of the precipitation and clouds fields (Lovejoy 1985). Recent developments have shown that the originally postulated mono–scaling behaviour is the exception rather than the rule. Thus, the more general multifractal models of the cascade processes have been developed (Tessier at al. 1993). In spite of many affords of finding scaling properties in the climatological time series the question whether they are scaling or not and the physical reasons for this are still disputable issue (e.g. Gupta Waymire 1987, Zawadzki 1987). This paper focuses on extreme variability (intermittency) of climatological time series from selected meteorological stations in Poland. The hyperbolic intermittency means that tail probability, $\text{Prob.}(|\Delta X| > x_{th})$, of random fluctuation ΔX exceeding a fixed threshold x_{th} takes the.form:

$$\text{Prob.}(|\Delta X| > x_{th}) \propto x_{th}^{-\alpha} \tag{1}$$

For such type of fluctuation a hyperbolic intermittency parameter, α, determines convergence of higher moments of distribution. The moment $<\Delta X^h>$ is finite for $h<\alpha$ but diverges for $h>=\alpha$. Although this fact causes some conceptual difficulties, hyperbolic random variables have been fitted to various parameters (Lovejoy 1985, Ladoy at al. 1992). The parameter α is commonly estimated as a slope of cumulative.tail frequencies on a double logarithmic paper. Hereafter, similar graphs are constructed for selected meteorological parameters from Polish, stations. Unfortunately, empirical values do not compose a straight line on the plots. The tail distributions seem to be neither Gaussian nor hyperbolic. Instead they fit well to the exponential function:

$$\text{Prob.}(|\Delta X| > x_{th}) \propto \exp(-b \cdot x_{th}^{a}) \tag{2}$$

which may be regarded as some kind of Gumbel's distribution.

Results and discussion

Empirical probability distributions, $\text{Prob}(|X(t_{i+1})-X(t_i)| > x_{th})$, were calculated for mean daily temperatures (period 1956–90), daily precipitation total (period 1956–90), mean daily pressure (period 1966–90) and mean daily water vapour pressure (period 1966–90). Data from 11 meteorological stations uniformly distributed over area of Poland were
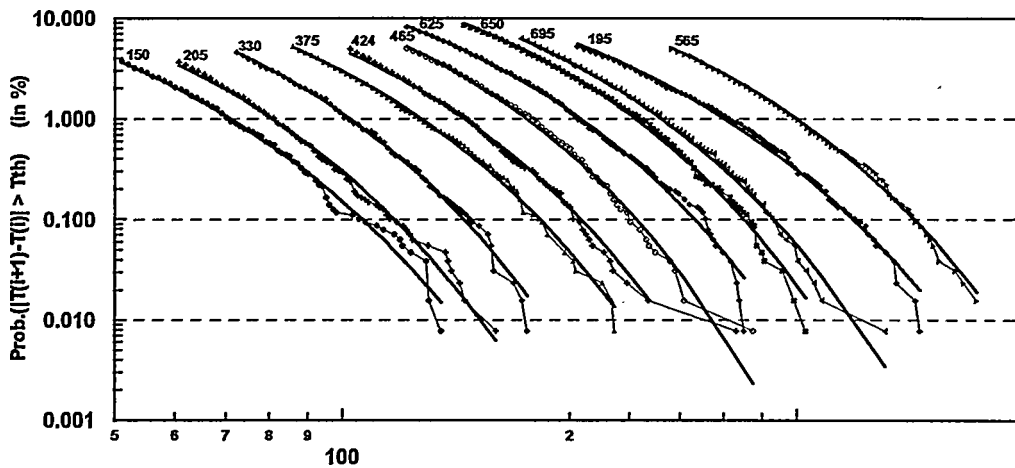
Fig. 1 The tail probability distributions, Prob.$(|T(t_{i+1})-T(t_i)|> T_{th})$, of daily temperatures differences (in daily mean temperatures) from 11 Polish meteorological stations from the period 1956–1990 (12784 days). The OX axis (in 0.1 °C) corresponds with the first curve only and the next lines are successively shifted right. Smooth curves indicate theoretical distributions estimated with the aid of equation (2).

used. The following stations were used: Gdansk (150), Stettin (205), Poznan (330), Warsaw (375), Wroclaw (424), Lodz (465), Cracow (565), Zakopane (625), Kasprowy Wierch (650), and Przemysl (695) (numbers in brackets mean the international station number). Cumulative empirical frequencies were calculated as a percent of events exceeding a fixed threshold for successively growing thresholds with the step taken as a measurement accuracy. Results are showed on double logarithmic plots.
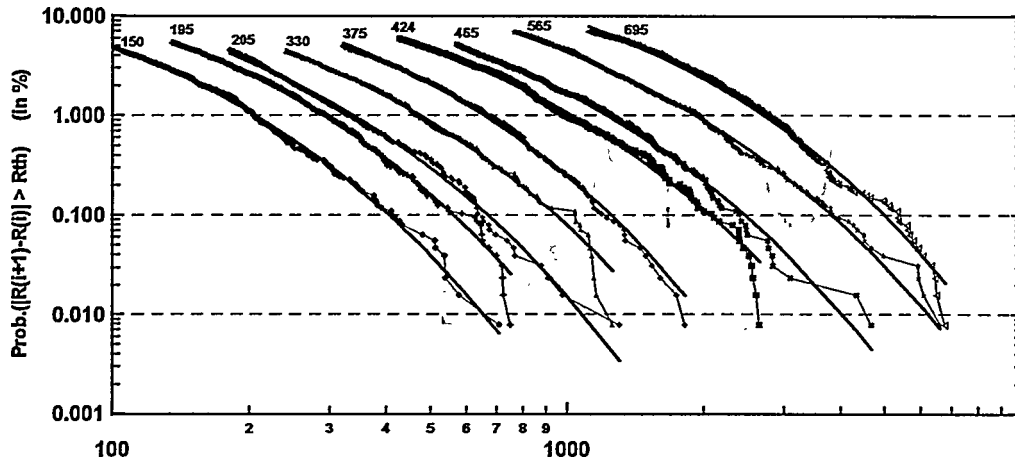
Fig. 2 The tail probability distributions, Prob.$(|R(t_{i+1})-R(t_i)|> R_{th})$, of daily rain accumulations differences (in 0.1 mm) from 9 Polish meteorological stations from the period 1956–1990 (12784 days). The OX axis corresponds with the first curve only and the next lines are successively shifted right. Smooth curves indicate theoretical distributions estimated with the aid of equation (2).
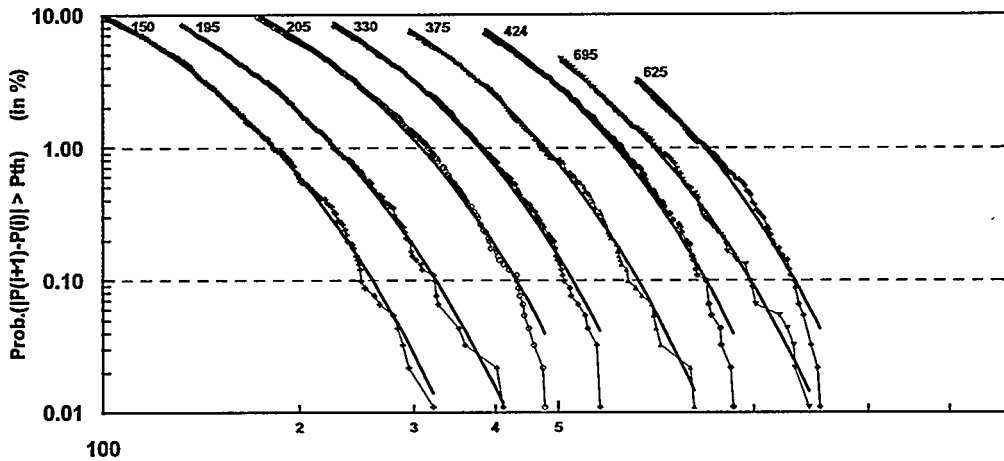
Fig. 3 The tail probability distributions, Prob.$(|P(t_{i+1})-P(t_i)|> P_{th})$, of daily atmospheric pressure (in 0.1 mb) from 8 Polish meteorological stations (numbers mean international station numbers) from the period 1966–1990 (9131 days). The OX axis corresponds with the first curve only and the next lines are successively shifted right. Smooth curves indicate theoretical distributions estimated with the aid of equation (2).

Figure 1 presents tail distribution for temperatures. Because the main goal of this paper is to test the asymptotic behaviour of the probability, frequencies of the inter–diurnal fluctuations higher than 5°C are included only. Lines are initially quite smooth and next reveal a zig–zag pattern. The shapes of curves in the smooth region are similar for all stations whereas for the lower frequencies (which are usually estimated with the aid of singular event of the large fluctuation) it is difficult to draw any general conclusion about
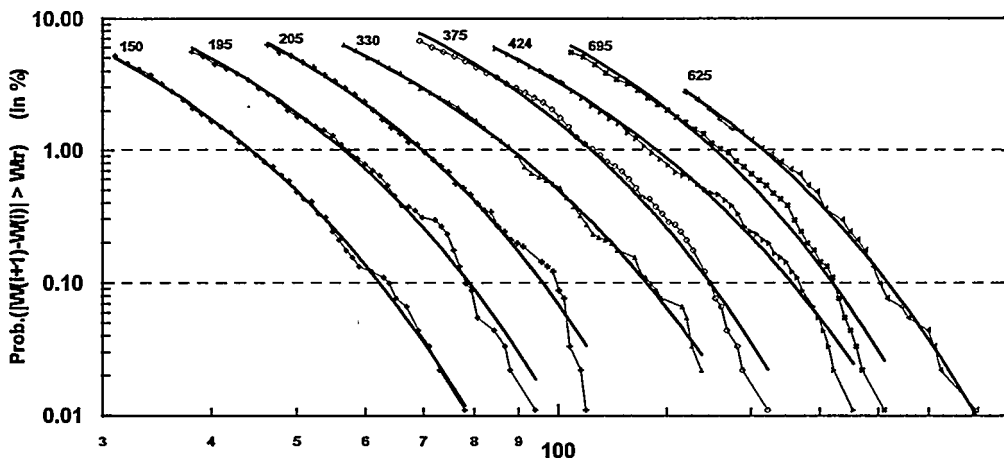
Fig. 4 The tail probability distributions, Prob.$(|W(t_{i+1})-W(t_i)| > W_{th})$, of daily water vapour pressure (in 0.1 mb) from 8 Polish meteorological stations (numbers mean international station numbers) from the period 1966–1990 (9131 days). The OX axis corresponds with the first curve only and the next lines are successively shifted right. Smooth curves indicate theoretical distributions estimated with the aid of equation (2).

their behaviour. Probabilities of fluctuation of the daily rain accumulation displays, in general, the same features. Even if the initial impression could be that the asymptotic distributions are hyperbolic, enlarging of these regions (as it is presented at figure 2 for fluctuations higher than 10 mm) shows curvature of the analysed lines. Similar conclusion could be derived for fluctuations of atmospheric pressure (fig. 3 – fluctuations higher than 10 mb) and water vapour pressure (fig. 4 – fluctuations higher than 10 mb). This is clear from looking at distribution functions shapes that in the case of these parameters the assumption of hyperbolic intermittency cannot hold, either. On the other hand, all tail distributions differ significantly from the Gaussian one. It means that the phenomena may be regarded as temporary intermittent in more general sense (Marsh and Tu 1994). It is believed to indicate that the behaviour of ΔX is largely determined locally more by deterministic than stochastic dynamics. Empirical distributions seem to fit well the theoretical distribution in form (2). The intention of the author here is not to prove the validity of the model, however, the visual evaluation of fitting goodness suggests that it should be regarded as an alternative for estimation of the extremely large fluctuations. Moreover, the same exponential distribution may be theoretically drawn from the model of isotropic turbulence constructed from Navier–Stokes equations (She 1991). The parameter a determines closeness of the distribution to the Gaussian one. Roughly speaking, as a decreases, probability distribution function becomes increasingly non–Gaussian. Although the results presented above do not confirm other authors' conclusions (Loady at al. 1991, Lovejoy 1985) which stress existence of hyperbolic intermittency in climatological time series, they should not be regarded as a proof of non–existence of such asymptotic behaviour in general. At the very end of curves the empirical probabilities are estimated with the aid of single events of large fluctuation only. Thus it is difficult to draw any conclusion on their true character. Some problems appear with the definition what the 'tail' exactly means. It is not clear which sector of curves should be used to estimate asymptotic behaviour. Using daily averaged values can be another source of getting different type of distribution. In spite of this, tests provided with positive and negative differences separately (not included) show that using absolute values does not affect the shape of curve significantly. Concluding, the results of the present work do not solve the problem of the existence of hyperbolic intermittency in climatological time series but rather point out that such concepts, even if they are conceptually attractive, cannot be accepted without any caution.

References

Gupta V.K., Waymire E., 1987, On Taylor's hypothesis and dissipation in rainfall., J.Geophys.Res., 92 (D8), 9657–9660.

Ladoy Ph., Lovejoy S., Schertzer D., 1991, Extreme variability of climatological data: scaling and intermittency., in Non–linear variability in geophysics., Kulwert Academic Publishers, 241–250.

Lovejoy S., 1985, Fractal properties of rain, and a fractal model, Tellus, 35A, 209–232.

Marsch E., Tu C.Y., 1994, Non–Gaussian probability distributions of solar wind fluctuations., Ann. Geophys., 12(12), 1127–1138.

She Z.-S., 1991, Physical model of intermittency in turbulence: near–dissipation–range non–Gaussian statistics., Phys. Rev. Lett., 66(5), 600–603.

Tessier Y., Schertzer D., Lovejoy S., 1993, Universal multifractals: theory and observations for rain and clouds., J.Appl.Meteor. 32 (2), 223–250.

Zawadzki I., 1987, Fractal structure and exponential decorrelation in rain., J.Gophys.Res. 92 (D8), 9586–9590.

Climate variability of atmospheric circulation in the Northern Hemisphere extratropics

G.V.Gruza and E.Ya.Rankova

Institute for Global Climate and Ecology, Moscow, Russia

Synoptic (or dynamic) climatology investigates climate as a result of general atmospheric circulation processes and estimates the climates corresponding to particular circulation (synoptic) regimes. Synoptic (visual) typifications and automated classifications, both are used here to analyze circulation variability and changes.

In the presentation the time series of main circulation forms *frequency* (total number of the days per season/year with particular circulation form) and *mean lifetime* (duration of the period with circulation of the same form) are analyzed for the last century. The time series were obtained on the basis of daily catalogues containing data on day-by-day circulation forms in accordance with macrotypifications by Dzerdzeevskiy and Vangengeim-Girs. Intrasecular variability of these circulation parameters is investigated here as compare to that for the characteristics of the Northern Hemisphere temperature regime.

Data as presently compiled (from 1891-1900 up today) appear to be sufficient to examine the climate variability and regularities in circulation forms alternation more carefully and reliably. The result can help to answer the question: *Is the atmospheric circulation in Northern Hemisphere substantially changing on decadal time scale?*

It is noteworthy that the linear trend for the whole observation period does not reflect the regularities within secular changes in the considered circulation parameters (it is so in the case of both typifications). Instead the emphasis should be placed on the periods of their increase and decrease on a scale of some decades.

Two-dimensional diagrams showing variations in moving statistics with changing of the estimating period limits are suggested as being rather convenient to characterize regularities in variations within secular change. Each point on the diagram *(x,y)* corresponds with the particular period: its duration is ordinate *Oy*, and its final year is abscissa *Ox*. Such diagrams are presented here for the lifetime of circulation forms in Dzerdzeevskiy and Vangengeim

typifications (Fig.a); and for the Northern Hemisphere air temperature characteristics: area-average anomaly and anomality index, or root-mean-square standardized anomaly (Fig.b). The corresponding time series are shown at the top sections; the diagrams for the moving mean anomalies - at the medium, and for the moving linear trend coefficients - at the bottom ones. So, the periods of above and below normal are clearly pronounced from moving means diagrams, while periods of increase and decrease in series are seen from trends' picture.

It is at once apparent that the variability increases when the time scale decreases, while character of the variations is not the same on different time scales and intervals of concern. It is also obvious, that there are many coincidences in the structure of variations in both temperature and circulation indices, which could not have an accidental nature. These oscillations seem to have the same cause, or to be in mutual causal relationship.

To confirm this conclusion, correlations between considered circulation indices and air temperature characteristics were estimated. Significant correlations (up to 0.67) were obtained for the lifetime of all Vangengeim's circulation forms, as well as for frequency of meridional circulation by Dzerdzeevskiy.

An attempt was made to perform an automated classification of synoptic situations, to be used (instead of synoptic visual macrotypifications) to investigate climate variability of atmospheric circulation and the role of circulation regimes alternation in the development of climatic anomalies. Appears to be appropriate to use small-dimensional phase space including different circulation indices rather than station or gridded data. These are Blinova-Rossby zonal circulation index, Kats indices (meridional, zonal, total ones - for the whole hemisphere, and for the sectors), as well as "teleconnections", etc.

To estimate a possibility to perform a simplified typification of 500-hPa height fields, here were used wintertime data on location of the frontal zone axial isohypse. The isoline of 540 dam (L540) was chosen as this isohypse (Khrabrov, 1960). So, 36-dimentional phase space was used, as including the closest to the Pole latitude of 540 dam isohypse on each of 36 meridians (0,10E,20E...).

It is noteworthy that statistics of L540 (as function of longitude) are shown the maximum deviation from normality being occur in the area of the troughs, while the maximum conformity with normal distribution is in the ridges locations.

Interlongitudinal correlation of L540 decreases up to zero as the longitudinal lag is as small as 40-50 deg. Thus, typification should be performed within a limited longitudinal sector not exceeding 160-180 deg. (90^{0}-sector of crosscorrelated processes plus approximately by 40 degree on the both boundaries).

As the first experiment, two automated classifications were carried out by using the simplest cluster analysis algorithm within sector of 80W-100E which is concerned in Vangengeim's typification.

Encouraging results on automated classifications were also obtained on the basis of characteristics of localization and intensity of ridges and troughs. In particular, distribution of the main ridge's top longitude was found to be bimodal so that it can be considered as singular, degenerated into two isolated ones. More detailed analysis of these characteristics shows an existence of three clusters (thus, and three types of ridges) in the frontal zone. Work on such typification continues.

It was appeared that the visual typification did not take any advantage over automated one. Opposite, automated types (even being not the real clusters) have at least such advantage over visual ones that they were obtained using formal computer procedure. They are easy to be used, for example, in comparative analysis of the atmosphere behavior (in terms of circulation type frequency) on modelled and observed data to be aimed at a validation the GACMs.

CONCLUSION

1. Synoptic (visual) typifications, being a useful instrument of atmospheric processes investigation, are the examples of successful grouping of observed situations.

2. While, there is no reliable evidence that these patterns (groups, subspaces) represent clusters in any phase space, these are useful for synoptic climatology and analysis of the climate variability and climate changes reasons. In particular, variance analysis of surface air temperature at some stations over European part of Russia showed the temperature as essentially depending on circulation patterns.

3. Statistical analysis of the frontal zone axial isohypse of 500hPa heights over the Northern Hemisphere showed the automated classification should be carried out within some limited sector, not more than 160-180 deg.

4. Examples of automated classification, resembled to synoptic (visual) typifications, were obtained for Atlantic-Eurasian sector of the Northern Hemisphere extratropics.

a) Mean Annual Lifetime of the Circulation Forms in Macrotypifications:
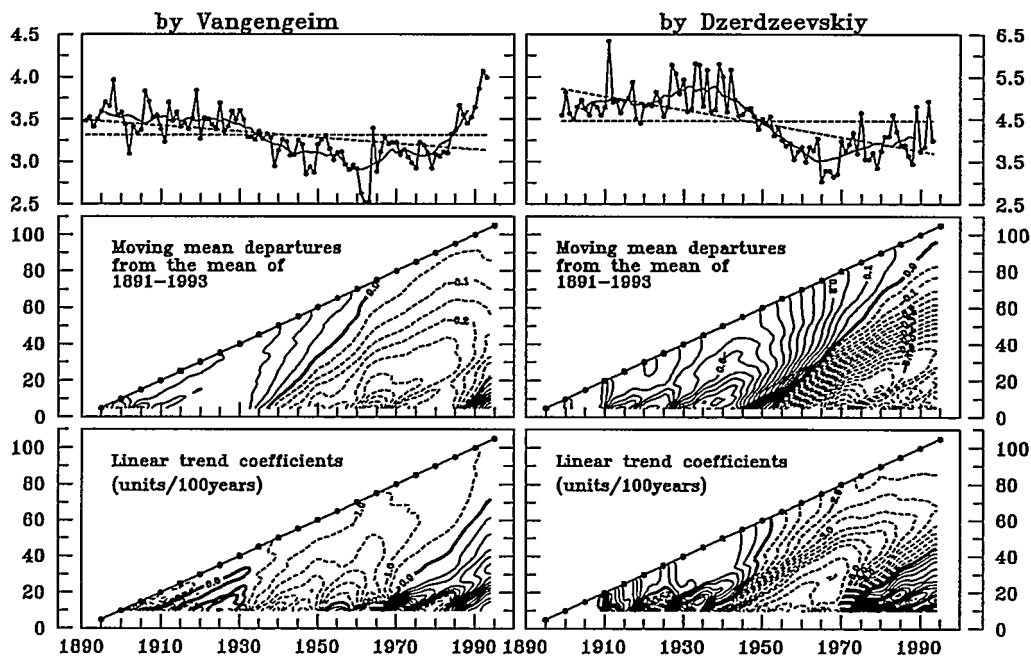
b) Area-average Annual N.H.Surface Air Temperature Characteristics:
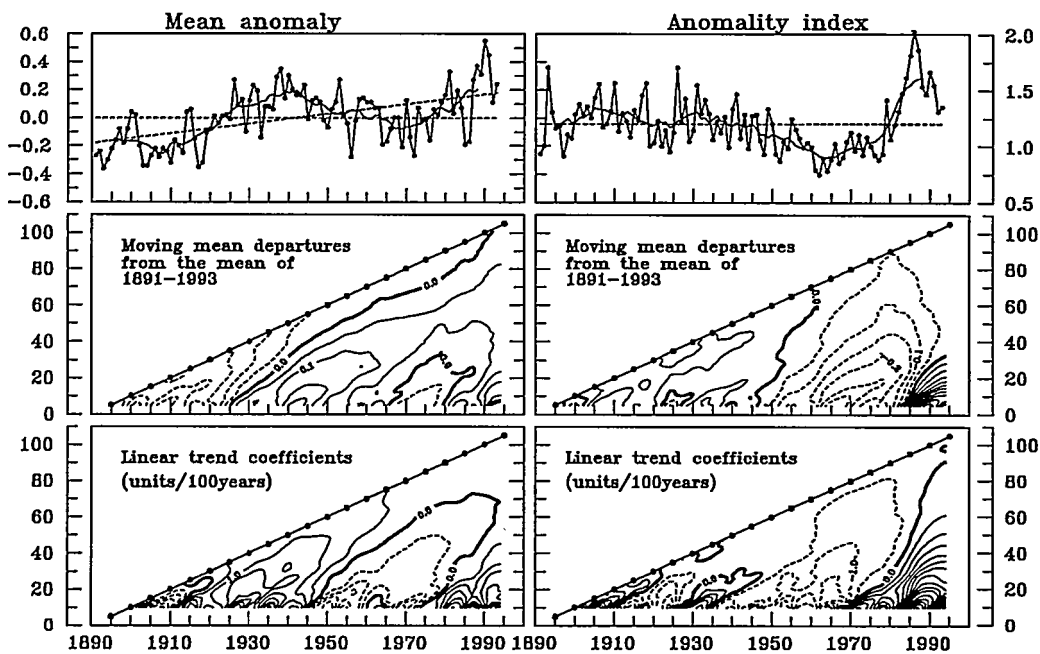
Figure. Time series of climatic parameters and their moving statistics (means and linear trend coefficients) depending on the estimating period: oY – period's length; oX – period's ending year.

A REVIEW OF THE ACCURACY OF METEOROLOGICAL MEASUREMENTS DURING THE PAST HUNDRED YEARS

Seppo Huovila
Sallatunturintie 1 B 15
FIN-00970 Helsinki

Introduction

The accuracy of meteorological measurements is a rather complicated concept. Factors such as the accuracy and reliability of the measuring instrument and a well-defined measuring site are very important, but service and maintenance failures, erroneous methods of measurement and severe weather phenomena may also lead to serious degradation in the accuracy of measurements.

A measuring instrument's accuracy is defined as "the ability of the instrument to give indications approaching the true value of the quantity subjected to measurement" whereas accuracy of measurement is the "closeness of the agreement between the result of a measurement and the true value of the quantity" (Huovila 1991). The distinction between these two definitions can be found e.g. in studies of the accuracy of precipitation measurements. Manufacturers of precipitation gauges and recorders may advertise a certain numerical value as the "accuracy" of their measuring devices, but a closer examination of those instruments probably reveals that the given value is actually nothing more than the smallest digital resolution of the readings of the instruments. The real accuracy of precipitation measurements is subject to much larger, and even unforeseeable, systematic or accidental errors. The prevailing wind (speed, direction, turbulence), the type and intensity of precipitation (rain, hail, snow, dew, rime, hoar frost), the material, dimensions and exposure of the gauge, etc., may be mentioned among the numerous and capricious factors affecting the accuracy of precipitation measurements.

Observations of many other meteorological variables may also be considerably less accurate than the instruments used for their measurements. Very intricate errors can be found in the records of wind speed, relative humidity, sunshine duration, etc.. Long meteorological records made in the past may thus be unusable for climatological purposes, unless the factors affecting the accuracy of measurements can be reconstructed and the data corrected in a reliable way.

Pressure and temperature

Well-made mercury-in-glass barometers and thermometers are very stable and accurate instruments. Calibrations of such instruments have remained practically unchanged over many decades, as proved by several laboratories. No wonder that temperature records are being used as the best instrumental evidence of climatic changes during the past hundred, or in some cases two hundred, years. In principle, barometer records could be used as well, but the smaller number of mercury barometers, problems in their transport and the rather complicated corrections to barometric readings have reduced the significance of barometric records as compared to temperature records.

The overwhelming instrumental accuracy of mercury barometers and thermometers leads to the conclusion that the main problems in the accuracy of pressure and temperature measurements in the past are due to uncertain or less-known measurement methods. In particular, inadequate knowledge of the influence of solar radiation, the measuring height above the ground, micrometeorological conditions at the measuring site, etc., may sometimes affect the usability of the oldest temperature records. Old pressure records, although made in a more stable and better-known indoor environment, may suffer from less accurate instrumental corrections and from indefinite reductions of the measured values to sea level.

Precipitation

Measurements of precipitation, as stated before, are always subject to several errors caused by the instruments, methods of measurement, measurement site and accidental weather conditions. Those errors vary very much from station to station depending on seasons and situational factors, and most errors are liable to reduce the amounts of measured precipitation. Several instrument comparisons (e.g. Goodison et al. 1992) have revealed that systematic corrections of the order of plus 10 per cent to liquid precipitation and up to plus 50 per cent to solid precipitation should be made in order to get observations at open windy stations comparable with precipitation values measured at well-shielded stations.

Corrections of old precipitation series are often difficult or arbitrary because details of instruments, methods and measuring sites cannot be verified any more. Although old precipitation gauges may still be found in museums and they may participate in forthcoming instrument comparisons, details of old measuring sites have been lost for ever. Homogenization of old precipitation data may thus lead to inconsistent results in neighbouring countries unless agreements on harmonized correction procedures are made in advance.

Humidity and wind

The quality of old humidity measurements is very much related to the instruments and methods used and to the frequency and quality of instrument maintenance. In

particular, observations by means of hair hygrometers are subject to continuous degradation in time if the hairs are not changed or regenerated. Use of unventilated psychrometers has led to great reported humidity differences between nearby stations during dry seasons, because the psychrometer constant very much depends on ventilation but the natural ventilation varies from station to station depending on their sheltering from the wind. Aspiration psychrometers used at the main observatories during the past hundred years, if correctly operated, have produced data which can be used as a guidance when estimating long-term humidity changes. Aspiration psychrometers, however, are rather intricate to operate and most of their measuring errors are systematic leading to too high humidity readings.

Wind observations from the past may be contradictory or confused, because unambiguous definitions of wind instruments and their dynamical properties are very recent. Changes in measuring sites or their environment, e.g. new buildings and the growing or felling of trees or bushes in the neighbourhood, may degrade wind data very seriously. The majority of data on wind speed before World War II may be misleading or worthless for strict analysis, but observations of wind direction are more reliable, where they are not entangled with local topographic factors. Some guidance for evaluating the value of old wind data can be sought from comparisons of wind observations with simultaneous weather maps.

Upper-air data

Upper-air data before World War II is mostly limited to pilot balloon observations and rather shallow temperature soundings by means of kites, aeroplanes and a few radiosondes. The drawback of pilot observations was their availability from high altitudes during clear or semi-clear skies only, which makes them worthless or doubtful for climatological purposes during cloudy seasons. The introduction of rawin instruments in the 1950's and 1960's led to continuous and statistically significant upper-wind observations from the troposphere and lower stratosphere. Although these wind data are nowadays quite free of error for calculating means and distributions, all upper-wind observations still underestimate the strongest wind maxima and wind shears. Observations of upper-air temperature and humidity until the 1960's are rather non-uniform and subject to serious radiation and lag errors. Stepwise regional and temporal changes, which are sometimes large, may be found in data recorded by different radiosonde types (Huovila & Tuominen 1990, Gaffin 1993).

Conclusions

The vast majority of studies on climate change deals with temperature changes. The main reason for this is the overwhelming accuracy and explicit nature of temperature measurements as compared to measurements of other common meteorological variables such as precipitation, humidity or wind. In particular, old instrumental data of these variables are often subject to obscure measuring, situational or environmental errors which cannot be reliably reconstructed and corrected today.

Although irritating and inexplainable measuring errors are most commonly found in the

oldest records of meteorological variables, they may still be everyday occurrences in the observation routines of some developing countries (Huovila 1992). The influence of maintenance failures, defects in calibration and comparison of instruments, negligence of station inspections and careless purchasing and installation procedures of the instruments have been identified among the impairing factors in such countries.

References

Gaffing, Dian J. 1993. Historical changes in radiosonde instruments and practices. WMO Instruments and Observing Methods Report No. 50, 127 pp.

Goodison, B., Golubev, V., Günther, T. & Sevruk, B. 1992. WMO Solid precipitation inter-comparison. WMO Instruments and Observing Methods Report No. 49: 161-165.

Huovila, S. & Tuominen, A. 1989. On the influence of radiosonde lag error on upper-air climatological data in Finland 1951-1988. FMI Meteorological Publications 14, 29 pp.

Huovila, S. 1991. How to maintain and improve the accuracy of meteorological measurements. WMO Bulletin Vol. 40 No. 4: 299-301.

Huovila, S. 1992. Factors affecting the accuracy of meteorological measurements in developing countries. WMO Instruments and Observing Methods Report No. 49: 446-449.

References

1. Energy in Europe - Annual Energy Review, EC, 1992

2. Estimation of Greenhouse Gas Emissions and Sinks - Final Report from OECD Expert Meeting, Paris, February/August 1991

3. Koleva, Ek., Yotova, A. (1994): Comparison between global and regional temperature trends - Proceedings of the International Conference "Global Climate Change: Science, Policy and Mitigation Strategies", 5 - 8 April 1994, Phoenix, Arizona, USA

4. Trends'91: A compendium of data for global change - Carbon Dioxide Information Analysis Centre, Oak Ridge National Laboratory, Tennessee, USA

5. Yotova, A. (1994): Bulgarian Case Study in the DECADES Inter-Agency Project framework - Working Material"Planning and Decision Making for the Electricity Sector", IAEA, Vienna, December 1994

Evolution of the Italian meteorological network in the period 1865/1905 and analysis of the data availability

Maurizio Maugeri and Elena Lombardi
Istituto di Fisica General e e Applicata - University of Milan (Italy)

Letizia Buffoni and Franca Chlistovsky
Astronomical Observatory - Brera - Milan (Italy)

Franca Mangianti
Ufficio Centrale di Ecologia Agraria - Rome (Italy)

Introduction

The state of the art of the researches on the European climate of the last 100/150 years, points out two fundamental deficits. In fact at the present a satisfying number of high quality climatic time series is not available and the existing series are often non multi-elemental, but limited to temperature and precipitation.

In this context it appears important to perform a great effort to dispose and to transform in homogeneous multi-elemental climatic sets the data and the metadata information not yet studied but stored in various European archives; at this purpose it is useful to know the historical evolution of the meteorological network of each country.

The objective of this paper is to present a synthesis of the Italian situation for the period 1865/1905, providing also some information on data availability.

The Italian situation before 1860

With the exception of the observations recorded in Toscana from 1654 to 1667 by the Accademia del Cimento, in Italy the regular observation of meteorological parameters began in the eighteenth century, when observatories were founded in Bologna (1716), Padova (1725), Torino (1756), Milano (1763), Roma (1782) and Palermo (1791). In other cities the observations started in the first half of nineteenth century.

However in spite of a relevant number of meteorological observatories, until 1860 in Italy the development of meteorology was negatively influenced by the lack of political unity and by the consequent lack of a national agency able to assure both the homogeneity of the measures and the publication on year-books of all the Italian data.

Initial organisation of the Italian meteorological network

After the Italian Political Unity (1860), it became clear that the development of Italian meteorology needed a strong organisation of all the activities existing in the country. This problem was solved assigning the meteorological and climatological competencies to three Ministries (Agriculture, Industry e Trade, Navy and Public Works).

The centralised collection of all the Italian meteorological data was assigned to the Ministry of Agriculture, Industry and Trade that began this activity on January 14[Th] 1865, inviting all the Italian meteorological observatories to send every ten days their observations to the "Direzione della Statistica dello Stato" (an office of the Ministry). The Ministry suggested also the hours of the observations and the data collection methodologies. Moreover all the stations which met the proposal were equipped with similar instruments and with detailed forms to fill with their data and to send every ten days to the Ministry (L. Palazzo, 1911).

The data collection began on 1[St] March 1865; initially the stations that met the proposal were 21 (Sondrio, Milano, Pavia, Cremona, Guastalla, Torino, Moncalieri, Cuneo, Alessandria, Genova, Sanremo, Bologna, Ferrara, Forlì, Ancona, Firenze, Livorno, Perugia, Napoli Astronomical Observatory, Napoli University and Palermo) and before the end of the year other 14 observatories (Trento, Pallanza, Aosta, Biella, Pinerolo, Modena, Urbino, Siena, Camerino, Roma, Locorotondo, Catanzaro, Reggio Calabria and Catania) enlarged the first group. In about ten years the stations grew up till 100.

The observations sent to the "Direzione della Statistica" were analysed under the direction of Prof. Cantoni and issued in periodical bulletins then collected in year books published with the title "Meteorologia Italiana" (Ministero d'Agricoltura, Industria e Commercio, 1865;......1878). From 1867 another periodical publication ("Supplementi della Meteorologia Italiana") with important studies about meteorological and climatological research was published (Ministero d'Agricoltura, Industria e Commercio, 1867;......1878).

Foundation of the "Ufficio Centrale di Meteorologia"

Even if the Italian meteorological network reached in its first ten years important results, the division of the meteorological and climatological competencies between different Ministries caused some problems. In order both to achieve a better co-ordination and also to met the suggestions of the International Meteorological Conference of Vienna (1873), the Italian Government decided in 1875 to co-ordinate all the meteorological activities. This decision brought to a decree, issued on November 26[Th] 1876, that nominated a National Council of meteorology (composed by 8 members) and prescribed to centralise all the Italian meteorological and climatological activities in a new office (Ufficio Centrale Meteorologico Italiano, 1879). The National Council of meteorology began immediately to work providing to control and to homogenise all the Italian observatories. The competencies of this Council were quite wide. In fact it was assigned to classify the existing observatories, to determine observatories instalments/suppressions, to set the number and type of instruments to use and fix the hours of the observations and finally to establish the methods of data publication. The centralisation of all the Italian meteorological activities began three years later (1879), when Italian Government set up a Central

Office of Meteorology (Ufficio Centrale di Meteorologia). The Staff of this office was completed in 1880 under the direction of Tacchini (which was also member of the Council).

The Office was organised in four sections: Climatology, Weather forecast, Agriculture meteorology, Physical meteorology. The collection of the meteorological data and their publication was assigned to the climatological section. This section provided to issue year books with the title "Annali", that substituted the year books published by the Ministry of Agriculture, Industry and Trade till 1878. The year books issued by the Ufficio Centrale di Meteorologia contain data of 100/150 observatories and of about 400 termo-pluviometric stations. These year books, beside the data, contain also the results of the research of Italian meteorologists and a lot of notices on the stations, the instruments and the measurement methods.

The issue of the year books continued without interruptions till 1900; after this year sometimes the year books were not, or only partially, issued.

After 1914, with the World War and with the great importance of meteorology for Air Force, the Central Office loosed slowly importance and the competencies were again divided between different Ministries.

Time series available for the period 1865/1905

As before seen, from 1865 all Italian climatic data have been published and collected in year books. Table 1 shows the growth of the number of stations of the Italian meteorological network from 1865 to 1905. Table 2 shows the meteorological parameters that are reported on the year books and their time resolution during the considered period. For some periods and for some stations daily time resolution was used (hour of observations: 9 a.m., 3, 9 p.m.) while for other periods and for other stations mean values on ten days and months were reported. This double irregular condition reached till 1886; from this year ten day resolution became usual for all the stations. Even if not reported on the year books, several daily observations, are available in the "Ufficio Centrale di Ecologia Agraria" archives. The Ufficio Centrale di Ecologia Agraria is the government agency that today substitutes the "Ufficio Centrale di Meteorologia". Beside the year books issued by the climatological section of the Office, another essential source of daily observations are the Daily Meteorological Bulletins edited from 1879 by the weather forecast section and also collected in year books (Ufficio Centrale Meteorologico Italiano, 1879;......;1905;......). In these Bulletins, besides daily temperature, pressure, humidity, state of the sky and others important data, also isobaric maps of all Italy are available.

	OBSERVATORIES	TERM. - PLUV. STATIONS
1865	21	
1870	65	
1875	84	
1880	100	
1885	134	506
1890	134	516
1895	136	519
1900	144	484
1905	143	245

Table 1: observatories and termo-pluviometric stations with issued data

	65	67	69	71	73	75	77	79	81	83	85	87	89	91	93	95	97	99	01	03	05
A: daily data																					
Pressure (9 a.m.: 3,9 p.m.)																					
Temperature (9 a.m.; 3,9 p.m.)																					
Relative Umidity (9 a.m.; 3,9 p.m.)																					
Vapor Pressure (9 a.m.; 3,9 p.m.)																					
Cloudiness (9 a.m.; 3,9 p.m.)																					
Total Precipitation																					
Wind Direction (9 a.m.; 3,9 p.m.)																					
Wind Strenght (9 a.m.; 3,9 p.m.)																					
B: data on 10 days and month																					
Mean Pressure (9 a.m.; 3,9 p.m.)																					
Mean Temperature (9 a.m.; 3,9 p.m.)																					
Mean of Daily Min/max Temperature																					
Mean Relative Umidity (9 a.m.; 3,9 p.m.)																					
Mean Vapor Pressure (9 a.m.; 3,9 p.m.)																					
Mean Cloudiness (9 a.m.; 3,9 p.m.)																					
Total Precipitation																					
Duration of precipitations																					
Frequency of Wind Directions																					
Mean wind Strenght (9 a.m.; 3,9 p.m.)																					
Days with rain, snow, hail, thunderstorm																					
Clear, cloudy, overcast days																					

Table 2: Meteorological parameters reported in the year books (1965/1905)

Conclusions

After Political Unity (1860), Italian meteorological network developed fast and in a few years a complete network of stations was organised. The good organisation of this network and the regular issue of bulletins and year books permit now to have a number of multi-element series for the reconstruction of Italian climate of the period 1865/1905. At the present only a small part of these series has been used and no multi-elemental approach has been adopted.

In this frame the objective of the authors is to contribute to transform in homogeneous multi-elemental climatic sets a part of the data and the metadata information available for this period. This work will start from the results of a project sponsored by CNR that allowed to move to magnetic support some Italian termo-pluviometric series (Anzaldi et al., 1980)

References

Palazzo, L. 1911. Meteorologia e Geodinamica. In: cinquanta anni di storia italiana (1860/1910). Accademia dei Lincei, Roma.

Ministero d'Agricoltura Industria e Commercio - Direzione di Statistica 1865;.......1878. Meteorologia Italiana, Roma.

Ministero d'Agricoltura Industria e Commercio - Direzione di Statistica 1867;.......1878. Supplementi alla Meteorologia Italiana, Roma.

Ufficio Centrale Meteorologico Italiano 1879;.......1905;...... Annali dell'Ufficio Centrale di Meteorologia (e Geodinamica), Roma.

Ufficio Centrale Meteorologico Italiano 1879;.......1905;...... Bollettino Meteorico dell'Ufficio Centrale di Meteorologia (e Geodinamica), Roma.

Anzaldi, C. et al., 1980. Archivio storico delle osservazioni meteorologiche. Report of Consiglio Nazionale delle Ricerche: AQ/5/27, Roma.

"MEDCLIVE " (MEDITERRANEAN CLIMATE AND VEGETATION).
An Expert System for Forecasting the Impact of Climate Change on Mediterranean Cultivated and Natural Vegetation .

Fivos Papadimitriou
School of Geography,
University of Oxford,
Oxford OX 1 - 3 TB,
U. K.

Abstract
The expert system "MEDCLIVE" is designed to give for every place (φ,λ) within the boundary of the Mediterranean and time (year form 1990 until 2030) the response of the vegetation type (natural, seminatural and cultivation) to climate change for any climate change scenario. It can also show the sensitivity of the vegetation type to changing climatic parameters for the place and time these parameters are considered. The grid resolution covering the Mediterranean is 2 by 1 degrees longitude and latitude respectively. Thus, it is possible to calculate the dominant vegetation type corresponding to the given climatic parameters on each one of the resulting grid cells for any year (until 2030).

Introduction
MEDCLIVE is an expert system suitable for research, as well as for training purposes. It serves the user by allowing him to make rapid estimations of the impact of possible climate change on vegetation in the Mediterranean. In this context, the term "vegetation" describes both agricultural crops and natural vegetation. The most appropriate climatic parameters and the most representative vegetation types were selected for inclusion in the system´s database.

The Structure of MEDCLIVE
The impact of climate change on vegetation cover in the Mediterranean E.U. countries can be assessed in a straightforward way by calculating the positions of the shifting vegetation boundaries corresponding to the appropriate climatic types (e.g. for thermomediterranean and middlemediterranean climate types). Like all expert systems, MEDCLIVE contains a knowledge base and an inference engine.

a) The Knowledge Base of MEDCLIVE.

All actual climate and vegetation data are allocated on each cell of a grid covering the Mediterranean from 12 deg. long. West to 40 deg.long. East and from 30 deg.lat. North to 46 deg. lat. North. The grid resolution is 2 degrees on longitude divisions and 1 degree on latitude divisions. Thus, the grid was divided in 16 by 26 = 416 rectangles. Altitudinal data were taken from Tomaselli (1976). Altitude enters as a variable and not as part of the grid division (the grid is planar).

The climatic parameters considered are mean annual precipitation (mm), mean annual temperature (degrees Celcius), solar radiation (kcal/ cmsquare * year) and the Penman ratio (P/ PET value).

The crops considered are cotton, citrus fruits, olives, wheat, sorghum, millet, beat, barley.

As far as the natural and seminatural vegetation are concerned, the knowledge base contains 100 of the most characteristic plant species for the entire spectrum of bioclimatic zones from hyper-arid to hyper-humid Mediterranean zones. Emberger's (1956) ecoclimatic and Le Houerou´s (1973) isoclimatic classification and zoning are used as a basis for creating correspondances between vegetation zone, altitude and climate parameters.

Each plant species is allocated a bounded range of climatic and geographical parameters. The climatic parameters change with time and they consequenntly affect the actual (1990) geographical distribution of vegetation. The mechanisms of these changes are built up within the inference engine of the expert system.

b) The Inference Engine of MEDCLIVE.

The inference engine consists in the mechanisms (IF-THEN rules) of MEDCLIVE that allow to compute the vegetation type of any grid cell for every year between 1990 and 2030.

These rules take into account the climatic and geographical ranges of (actually) allowable values for each vegetation type and they provide the user with the final result of the most appropriate vegetation type, that can occur within the altered (by climatic change) range of values for the grid cell the user has made ·the enquiry about.

For any given climate change scenario, MEDCLIVE calculates the corresponding longitudinal, latitudinal and altitudinal distribution of the spatial extent of the vegetation types affected by the climatic change.

For instance, the IPCC scenarios forecast an average temperature increase of +0.5 degrees Cel. for the year 2015. Hence, using the standard diagrams of the Mediterranean climatic zones, it follows that the altitudinal temperature gradient is 100 meters per 0.55 deg. Cel. Consequently, a temperature rise of 0.5 deg.Cel. would correspond to 0.5 * 100 / 0.55 = 90 meters increase in the altitude. This increase means that the boundary between the thermo-mediterranean and the middle-mediterranean zones will shift 90m towards higher altitudes by the year

2015. Given that the boundary is now at 300m altitude, it comes out that the new boundary will be at 390 meters altitude. This example shows how it is possible to derive results that give an overview of the resulting spatial distribution of the major crop and natural vegetation types.

The Main Menu

The MEDCLIVE menu is articulated in three modules which have two different (yet complementary) functions. These modules are the following.

1) *MEDICLIF* (MEDIterranean CLImate Forecasting)
This module allows the user to select the climate change scenario he wishes, by setting the values of the appropriate climate parameters according to the selected climate change scenario.

2) *MEDICLIM* (MEDIterranean CLimate IMpact)
This module allows the user to select a grid cell of the Mediterranean and calculate the impact of climate change on the vegetation type of the chosen grid cell.

3) *MEDISENS* (MEDIterranean SENSitivity)
This module provides the user with a rapid assessment of the sensitivity of the calculated (from the previous module) vegetation types to climate change.

The user must run the system from module to module in an orderly way.
On the basis of the MEDCLIVE forecasts , speculations can be made about the rural policies of the European Union and their landscape ecological and geomorphic consequences.

References

Emberger, L. (1956) "Une classification biogeographique des climats" *Natur. Monspel. serie botanique*, 7, p.3-43.

Le Houerou (1973) " Ecologie, demographie, et production agricole dans les pays mediterraneennes du Tiers- Monde" *Options Mediterraneennes*, 17, p.53-61.

Tomaselli (1976) "La degradation du maquis Mediterraneen " Notes Techniques du MAB, n.2, UNESCO, Paris, p.35-46.

Scenarios of Arctic air temperature and precipitation in a warmer world based on instrumental data

Rajmund Przybylak

**Department of Climatology,
Nicholas Copernicus University
Danielewskiego 6, 87-100 Toruñ
POLAND**

Introduction

There is growing evidence confirming the crucial role of polar regions in shaping the climate of the Earth. We know (e. g. from climate models outputs) that these regions are the most sensitive to climatic changes. As a consequence, the warming and cooling epochs should be seen here most clearly (Polar Group 1980; Jäger, Kellogg 1983). But it is not true for the last decades when the Arctic (here defined after Atlas Arktiki, 1985) shows no or small warming (Chapman, Walsh 1993; Kahl 1993a, b; Przybylak, Usowicz 1994). We agree with Kahl's statement (1993a) that „ this discrepancy suggests that present climate models do not adequately incorporate the physical processes that affect the polar regions". So, our knowledge of the role of the Arctic in global climate is continually insufficient. It is due to awareness of this fact that in 1991 Joint Scientific Committee for the WCRP decided to initiate the new research programme called Arctic Climate System Study. The main observational phase of this project started on January 1, 1994 (WCRP-85 1994).

The main aim of the present paper is to check what was the behaviour of Arctic air temperature (T) and precipitation (P) in different phases of thermic condition in the world in last decades. Such knowledge enable us also to construct scenarios of future climate of the Arctic connected with global warming. To do this we can use two main approaches. One is to construct climatic models and second is to use warm periods as analogues (Wigley et al. 1980; Palutikof et al. 1984; Palutikof 1986). The approach adopted here is to use instrumental data of the last 40 years (1951-1990) to construct warm-world analogues (similarly as Wigley et al. 1980; Williams 1980; Jäger and Kellogg 1983; Palutikof et al. 1984; Palutikof 1986). The 40-year series is rather short, however just since 1951 the density of stations in the Arctic became acceptable to construct regional scenarios. The differences between the highest and lowest seasonal and annual means of T and P were computed in those scenarios using the data from:

i) the ten individual warmest and coldest years from the Northern Hemisphere temperature series (land+sea), 1951-1990 (after Jones 1994),
ii) the warmest and coldest decades from the same Northern Hemisphere series,
iii) the warmest and coldest 20-year blocks from the same Northern Hemisphere series. Here in this abstract we present only the results of the last scenario which in opinion of Palutikof et al. (1984) is the best and most reliable. The 1971-1990 20-year block is the warmest in the whole Jones series (since 1851) and the 1960-1979 one is the coolest since 1926.

Results and discussion

The calculated differences between the highest and lowest mean T and P totals from individual stations are put on the maps and their izarythms are drawn (Fig. 1). The obtained scenarios are probably valid only for the first period of global warming connected with CO_2 doubling.

According to presented scenarios in a warmer world greater part of the Arctic shows also warming (Fig. 1). The pattern of the warming is very similar in winter, spring (not shown) and for the year. The largest increases of T occur in the eastern part of the Arctic, especially over Barents and Kara Seas. The autumn T (not shown) exhibit the most peculiar behaviour. In this season less than half of the Arctic shows the warming. The cooling should occur mostly in its western part (Greenland, Canadian Arctic and Alaska) and Czukocki Peninsula with the largest decreases over Alaska. Arealy the greatest warming show summer T (Fig. 1). The decreases of T are only found over south and west coasts of Greenland, over Baffin Sea and some small parts of the Russian Arctic. The greatest extreme increases (or decreases) of T in a warmer world has winter (in both cases more than 1°C) and the smallest has summer (mostly below 0.3°C). But the largest mean seasonal warming in the Arctic (calculated from 27 stations) are found in spring (0.31°C), much lower in winter (0.17°C) and the least in autumn (0.01°C). Very interesting results gives the comparison of the mean seasonal and annual warming of the Arctic with the hemispheric warming. The intensity of the Arctic warming is greater than for Northern Hemisphere in spring and summer (more than twice), only a little larger in winter and much smaller in autumn. The mean annual warming of the Arctic is 1.6 times greater.

The patterns of P in a warmer world are more complex than those for T (Fig. 1). It is connected with the greater spatial variability of P. In all seasons, except spring, the mean P in the Arctic (computed from 27 stations) is lower in a warmer world. The increase occurs only in spring which, as we remember, shows the most distinct warming. On the contrary, the largest decreases of the mean Arctic P are found in autumn which is characterised by the lack of warming. However, as can be seen in Fig. 1, the greatest part of the Arctic shows decrease of P under warm-world conditions in winter. But these decreases are smaller than in autumn. More than half part of the Arctic shows in all seasons decreases of P. Winter precipitation is expected to increase only over most part of the Atlantic region of the Arctic and Canadian Arctic (Fig. 1). In spring the pattern is very similar; the main difference is the reduced area of P increases. In summer the increases and decreases of P contain equal areas. The largest area of P increase include Alaska, Canadian Arctic, east coast of Greenland and Greenland Sea (Fig. 1). In autumn dominate P decrease in a warmer world, with
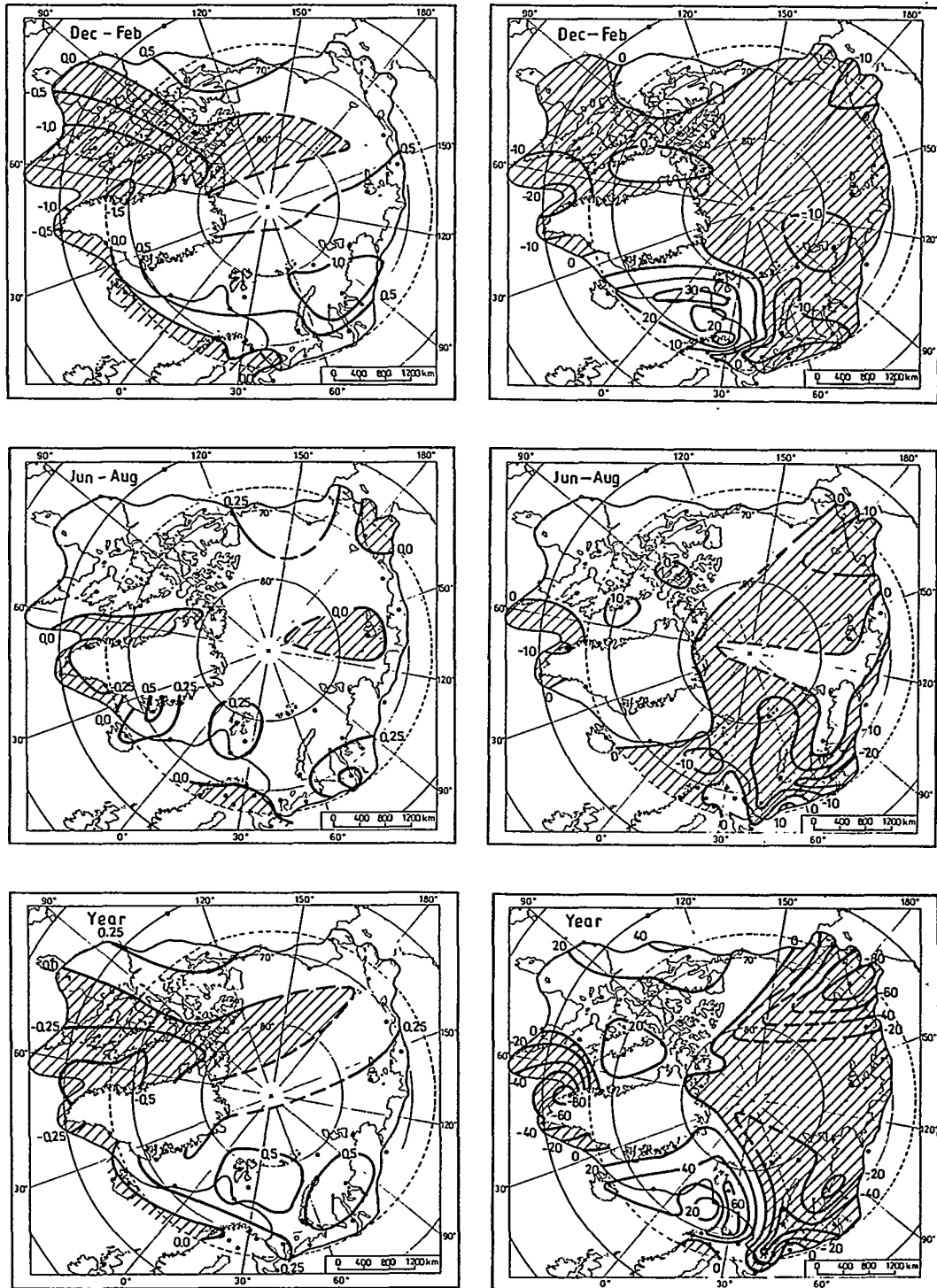
Fig. 1. The changes scenarios of temperature (^{0}C, left panels) and precipitation (mm, right panels) for the Arctic. Areas with decrease of given elements are hatched.

the largest values over south-west Greenland and Czukocki Peninsula (up to 40-50 mm). The increase is expected only over Barents Sea and adjoining islands. The annual P shows the decrease over two areas; the largest one include central and Russian Arctic and the smaller one south part of Greenland with adjoining seas.

In conclusion we can say that in the Arctic a small warming and a decrease of P in the first period of global warming connected with CO_2 doubling is expected. But there is no direct relation between behaviour of T and P. The increases and decreases of P in the Arctic are found in the regions which show both warming and cooling.

References

Atlas Arktiki 1985. Glavnoye Upravlenye Geodeziy i Kartografiy SSSR, Moskva, 204 pp.

Chapman, W.L., Walsh, J.E. 1993. Recent variations of sea ice and air temperature in high latitudes. Bull. of the Amer. Met. Soc. 74, 1:33-47.

Jäger, J., Kellogg, W.W. 1983. Anomalies in temperature and rainfall during warm Arctic seasons. Clim. Change 5: 39-60.

Jones, P. D. 1994. Personal communication.

Kahl, J.D. 1993a. Absence of evidence for greenhouse warming over the Arctic Ocean in the past 40 years. Nature 361:335-337.

Kahl, J.D. 1993b. Tropospheric temperature trends in the Arctic: 1958-1986. J. Geophys. Res. D7:12825-12838.

Palutikof, J.P. 1986. Scenario construction for regional climatic change in a warmer world. Proceedings of a Canadian Climatic Program Workshop, March 3-5, Geneva Park, Ontario, 2-14

Palutikof, J.P., Wigley, T.M.L. & Lough, J.M. 1984. Seasonal climate scenarios for Europe and North America in a high-CO_2, warmer world. U. S. Dept. of Energy, Carbon Dioxide Res. Division, Tech. Report TRO12, 2-14.

Polar Group 1980. Polar atmosphere-ice-ocean processes: A review of polar problems in climate research. Rev. Geophys. Space Phys. 18, 2: 525-543.

Przybylak, R. & Usowicz, J. 1994. Trends and cyclic behaviour of air temperature and precipitation in the Atlantic-European area of the Arctic. In: Contemporary climatology (eds. R. Brazdil & M. Kolar), Brno, 479-485.

WCRP-85 1994. Arctic climate system study (ACSYS), Initial implementation plan. WMO/TD-No. 627, 66 pp.

Wigley, T.M.L., Jones, P.D. & Kelly, P.M. 1980. Scenario for a warm, high-CO_2 world. Nature 283: 17-21.

Williams, J. 1980. Anomalies in temperature and rainfall during warm Arctic seasons as a guide to the formulation of climate scenarios. Clim. Change 2: 249-266.

Variability of the 500 hPa geopotential height field simulated with UKMO and MPI atmospheric general circulation models

Norel Râmbu[1], Sabina Ştefan[1], Constanţa Boroneanţ[2]

[1] University of Bucharest, Faculty of Physics, Dept. of Atmospherics, P.O. Box 5211, Bucharest -Măgurele, Romania, [2] National Institute of Meteorology and Hydrology, Sos. Bucureşti-Ploieşti 97, 71552 Bucharest, Romania

Introduction

The project AMIP is an excelent framework for the intercomparative studies on the ability of various general circulation models to simulate the low frequency variability of the atmosphere. In this paper we deal with a comparative analysis of the variability of the 500 hPa geopotential height field simulated with UKMO and MPI atmospheric general circulation modelas during the 10-year integrations (1979-1988).

Models, data sets and analysys techniques

The UKMO is an atmospheric general circulation model developed at the Hadley Centre for Climate Prediction and Research, Bracknell, UK. The MPI atmospheric general circulation model was developed at the Max-Planck-Institute in Hamburg, Germany. A detailed description of these models is presented in the AMIP reports (Gates, 1992).

In order to simulate the atmospheric variability during the period January 1979 - December 1988, these two models were integrated in the standard AMIP conditions. The data sets of the models consist of monthly means of 500 hPa geopotential height fields over the Northern Hemisphere during the AMIP period.

The analysis techniques used in this study are that recommended by Lau (1981) in a study on 15-year integrations with GFDL atmospheric general circulation model (linear regression, EOF and pattern analysis).

Variability of the 500 hPa geopotential height

The analysis was performed separately for winter and summer Northern Hemisphere seasons. The spatial distribution of the root-mean-square (*rms*) was calculated for each season. The *rms* fields for the UKMO and MPI simulations were compared to the corresponding observed *rms* fields calculated for the period (1946-1988) (Wallace et al., 1993).
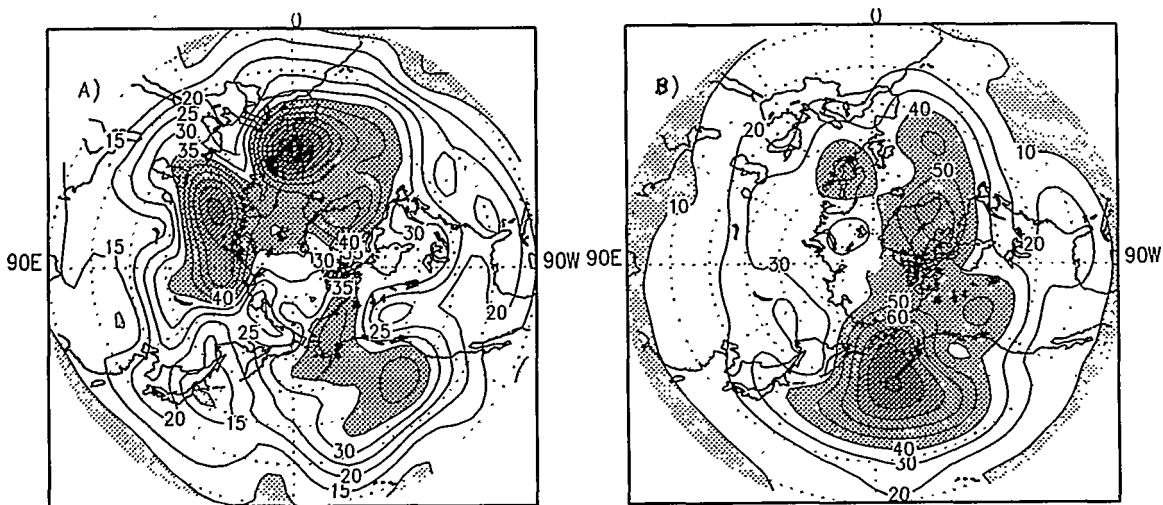
Fig.1 Temporal standard deviation of seasonaly averaged winter time 500-hPa height for the a) UKMO and b) MPI simulations poleward of 20^0N

The spatial distribution of the *rms* field of the winter simulated 500 hPa height in the Northern Hemisphere for the UKMO and MPI simulations are presented in Fig. 1A and Fig. 1B, respectively. Both fields indicate a great variability over the Pacific Ocean. In the UKMO simulation the maximum of the *rms* field in this area is centred on (140W, 40N) and its value is around 40 m. The corresponding maximum of the *rms* field simulated with the MPI model is centred on (175W, 55N) and its value is around 90 m being much more close to the observed *rms* field (not shown) whose maximum is centred on (165W, 45N) and its value is around 80 m. Over the North Atlantic region, in the observed *rms* field (not shown) there are two maxims of 60 m centred on (50W, 65N) and (35W, 45N), respectively. The UKMO simulated field indicates a maximum of

50 m centred on (55W, 65N) which is close both in position and in intensity to the corresponding observed field. The second maximum in this region of 70 m is centred on (5W, 50N), its position being located to the SE from that indicated in the observed field. The *rms* field of the MPI simulation has one maximum of 60 m centred on (70W, 65N) and another one of 60 m centred on (10E, 50N). The *rms* of the observed field shows another 60 m maximum centred on (80E, 80N) which is well simulated by both models.

The spatial distribution of the summer *rms* field is less organised than that during the winter. In the Pacific area the *rms* field of the UKMO simulation presents a well-defined maximum of 35 m centred on (160W, 50N). The *rms* field of the MPI simulation shows a well-defined maximum of 40 m centred on (180W, 45N) being much closer to the corresponding observed field which shows a similar maximum centred in the same position. The region of height variability centred over the Northern Pole is well simulated by both models.

EOF analysis

The results of the models presented in this section are based on the monthly normalised averages of 500 hPa geopotential height for ten simulated winters. The eigenvector analysis was performed on 224 grid points covering a region of the Northern Hemisphere between 20N and 82N. The distributions of the first eigenvector for both models are presented in Fig.2. The EOF1 explains 18.39% of the domain integrated variance (vs. 12.92% for EOF2) for UKMO and 21.75% (vs.14.95% for EOF2) for MPI simulaions.

Fig. 2. Distribution of the EOF1 of the 500 hPa height for A) UKMO and B) MPI models

There exists a spatial correspondence between the essential features of the leading EOFs of the two simulations represented in Figure 2A, B with those obtained from the observed geopotential field presented by Lau (1981). However, differences between the simulated and the observed patterns regarding the exact location of the anomaly centres are significant.

The time series of the expansion coefficients of the EOF1 corresponding to the simulations of the models are very small correlated explaining the significant difference in the time evolution of this mode in both simulations.

Conclusions

The UKMO and MPI simulations fit well the general characteristics of spatial variability in the 500 hPa geopotential field. The discrepances between the model simulations and the observations with respect to the exact details of the anomaly structure could in part be accounted for the dynamical and physical mechanisms not properly represented in these two models.

Acknowledgments

References

Gates, W. L., 1992. AMIP: The Atmospheric Model Intercomparison Project, PCMDI Report, No. 7, 18 pp.

Lau, N.C., 1981. A diagnostic study of recurrent meteorological anomalies appearing in a 15-year simulation with a GFDL General Circulation Model, Month. Weath. Rew., 10, 2287-2311

Wallace, J.M., Zang Y. and Lau K. H. 1993. Structure and sesonality of interannual and interdecadal variability of the geopotential height and temperature fields in the Northern Hemisphere troposphere, Journal of Climate, 6, 11, 2063-2082

Thermal climate from 1931 to 1990 in Finland

A study using downscaling technique and mesoscale analysis in GIS

Aulis Ritari and Vesa Nivala

Finnish Forest Research Institute
Rovaniemi Research Station
P.O.B. 16, FIN-96301 Rovaniemi

Introduction

The question of climate change has been addressed using various approaches. One is to study the existing temperature records and to base future predictions on observed trends. This has limitations due to relatively short time series of directly measured temperature data and the changes in atmospheric forcing, a.o.t. Air temperature records at the height of 2 meters maintained by the Finnish Meteorological Institute now cover two 30- year WMO (World Meteorological Organization) normal periods in the form of series starting from 1931. Solantie (1992) and Heino (1994) have performed detailed studies with the data measured at the climate stations. This type of analysis, however, is not most effective if we are interested in results that need to be weighed by the land area to get unbiased areal estimates, and hence the effect surface related factors must be taken into account. Another shortcoming is the difficulty to see how representative the chosen periods are within the data period due to areal variation.

Luckily enough, GIS (Geographical Information System) can provide good services for us. The aim of this study was to scale down data into a regular mesoscale grid and use the data to analyse annual temperatures in Finland on a monthly or on a yearly basis for the 60 year period.

Model

Our empirical model uses measured air temperatures as an input. Before performing areal interpolation by the KRIGING algorithm, the values are corrected for the effect of the geographical location, elevation and the proximity of seas and inland waters. This was done on a monthly basis. After interpolation the new smoothed temperature surface is returned to the level determined by the combined correction factors. The result is a raster-

form areal presentation of the desired temperature parameters (Ritari and Nivala 1995). As the time series of temperatures for each grid point is in the GIS system, mathematical operations can be performed using these time series and the results presented as temporal and areal averages.

Results and discussion

The maps in Fig. 1a and 1b show the mean annual temperatures of the two normal periods in Finland; from 1931 to 1960 and from 1961 to 1990. The grid size used was 1x1 km. As expected the earlier period was slighly warmer and clearly so in the central and northern parts of the country. This is visible in the difference map in Fig. 2a.

As the general annual mean temperature gradient passes from south-west to north-east, the gradient for standard deviation of temperatures go from west to east (Fig. 2b). This is the result of the more continental conditions in the eastern parts of Finland especially during summer. Not only is it possible to compare temperatures on a yearly basis between the normal periods; it is also possible to compare monthly mean temperatures in the similar way in order to see the seasonal differences. When this was done we could notice that the summer months were clearly warmer in 1931-60 as compared with the period 1961 to 1990.

In order to get insight on how the normal periods differ from each other we also plotted the 60 year annual mean temperatures and monthly temperature differences for the whole country into diagrams. These results can be studied at the poster presentation in detail.

References

Heino, R. 1994. Climate in Finland during the period of meteorological observations. Finnish Meteorological Institute, Contributions 8:1-209.

Ritari, A. & Nivala, V. 1995. Gis and climate modelling in mesoscale. In Proc. International Conference on Global Change and Arctic Terrestial Ecosystems, Oppdal, Norway, 21-26 Aug. 1993 (in print).

Solantie, R. 1992. Lämpötilanmuutos "vanhasta" normaalikaudesta 1931-1960 "uuteen" 1961-1990. Summary: On the change of thermal climate in Finland between the "normal" periods 1931-1960 and 1961-1990. Lapin tutkimusseura, Vuosikirja 33:33-42.

a)

■	- ⁻6.0 °C
▓	⁻5.9 - ⁻5.0
▨	⁻4.9 - ⁻4.0
■	⁻3.9 - ⁻3.0
▨	⁻2.9 - ⁻2.0
□	⁻1.9 - ⁻1.0
□	⁻0.9 - 0.0
▨	0.1 - 1.0
■	1.1 - 2.0
■	2.1 - 3.0
■	3.1 - 4.0
■	4.1 -

©METLA/Rovaniemi

b)

■	- ⁻6.0 °C
▓	⁻5.9 - ⁻5.0
▨	⁻4.9 - ⁻4.0
■	⁻3.9 - ⁻3.0
▨	⁻2.9 - ⁻2.0
□	⁻1.9 - ⁻1.0
▨	⁻0.9 - 0.0
▨	0.1 - 1.0
■	1.1 - 2.0
■	2.1 - 3.0
■	3.1 - 4.0
■	4.1 -

©METLA/Rovaniemi
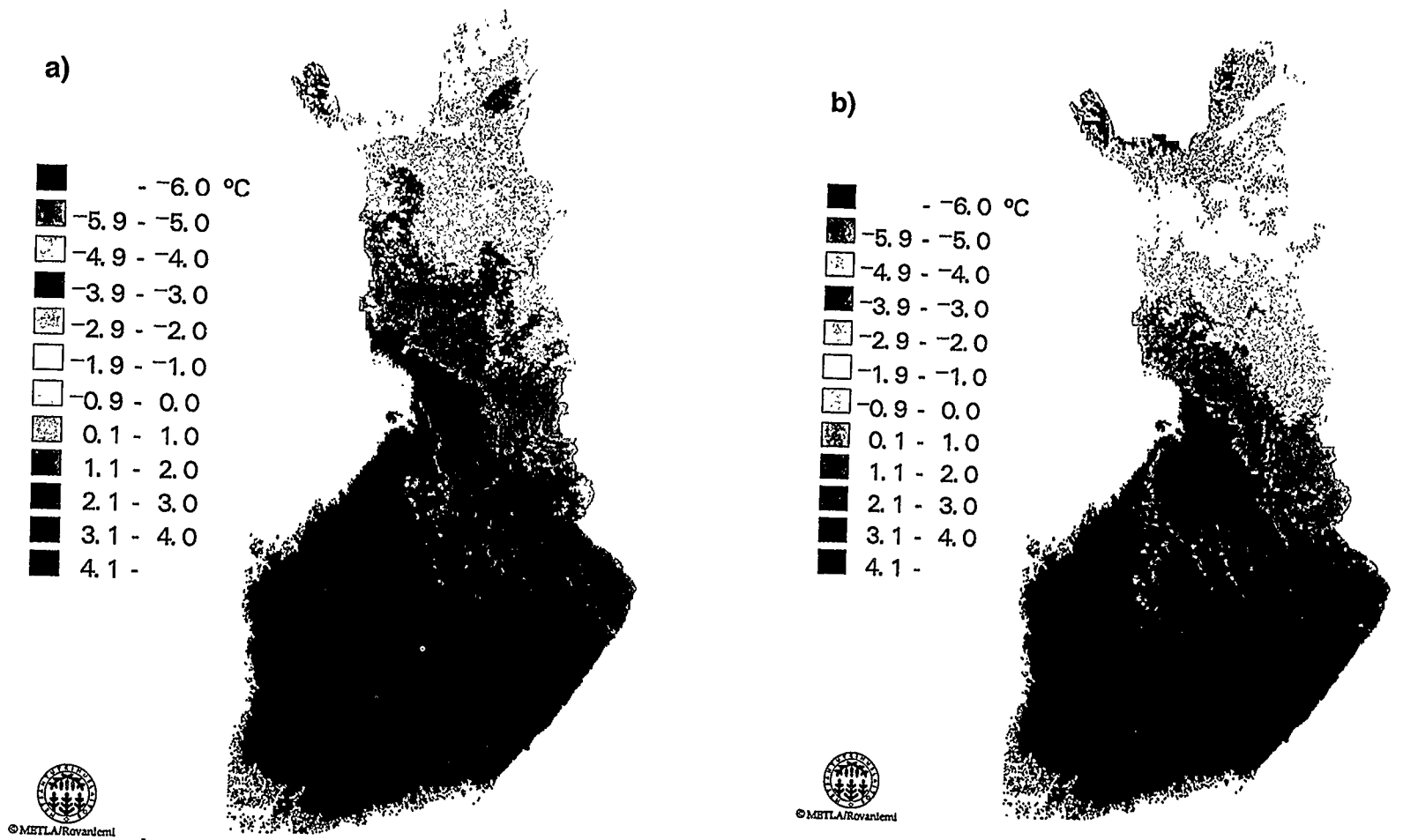
Figure 1. Mean annual temperature in Finland during periods (a) 1931 to 1960 and (b) 1961 to 1990.

b)

■	- 1.0 °C
▨	1. 01- 1. 05
▨	1. 06- 1. 10
■	1. 11- 1. 15
▨	1. 16- 1. 20
□	1. 21- 1. 25
▨	1. 26- 1. 30
▨	1. 31- 1. 35
■	1. 36- 1. 40
■	1. 41-

©METLA/Rovaniemi

a)

■	- ⁻0. 40 °C
■	⁻0. 39 - ⁻0. 20
■	⁻0. 19 - ⁻0. 0
■	0. 01 - 0. 20
■	0. 21 - 0. 40
▨	0. 41 - 0. 60
■	0. 61 - 0. 80
■	0. 81 - 1. 00
■	1. 01 - 1. 20
■	1. 21 - 1. 40
■	1. 41 - 1. 50
■	1. 51 -

©METLA/Rovaniemi

309
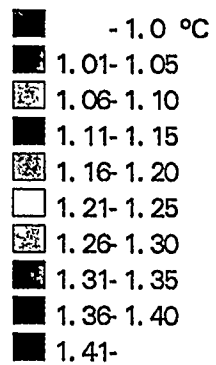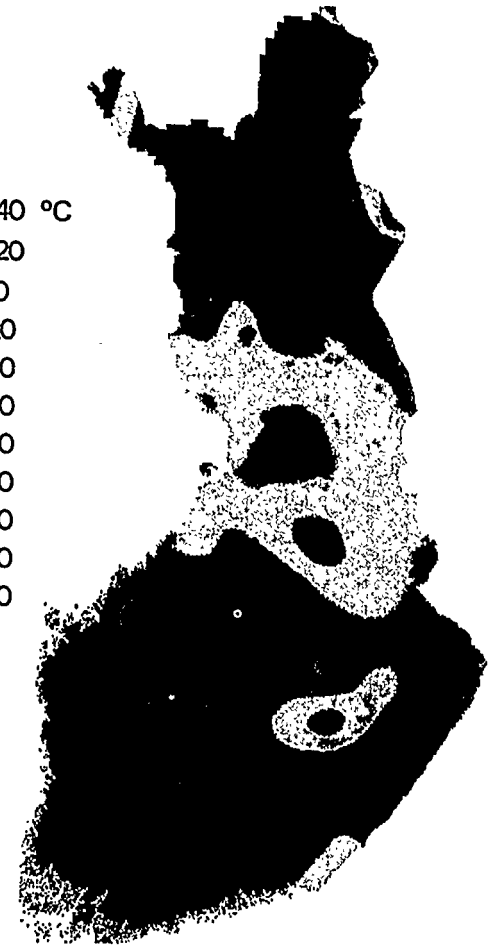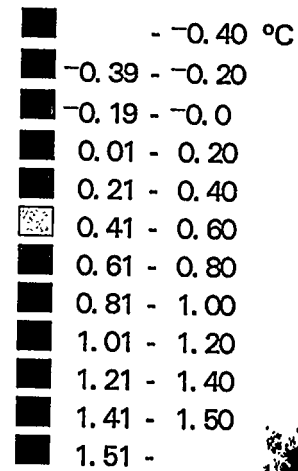
Figure 2. (a) Mean annual temperature differences for the periods from 1931 to 1960 and from 1961 to 1990, (b) standard deviation of mean annual temperatures for the period 1961 to 1990.

Analysis of meteorological observation series in Latvia

Marta Treiliba

Department of Meteorology and Climate
Latvian Hydrometeorological Agency
165, Maskavas Str., Riga, LV-1019
Latvia

In a general sense, two types of mechanisms determine climate change, external and internal. The search for external causes obviously focuses attention on the Sun as the ultimate powerhouse of the atmospheric engine as well as on the variations in the movement of the Earth relative to the Sun. Among internal causes, the capability of the Earth's atmosphere to filter the incoming sunlight before it reaches the surface and so enters the atmospheric engine is of great importance. So anything, significantly affecting the filtering, could be climatically important. An increase in the greenhouse gases concentrations due to human activities during the recent decades could affect the atmospheric filtering and thereby - the climate.

The meteorological observations in Latvia have a long period history. In January 1995, it was 200 years since regular weather observations started at the oldest station Riga. On the border of XX century, Latvia was covered with 16 meteorological stations and 29 posts. Today meteorological observation data are available at 24 stations, i.e. one station per 2650 km^2 with a mean distance between them of 40-50 km, and 80 posts; at 20% of the network they are of up to 100 years long and more.

Data on the air temperature, relative humidity, cloudiness, atmospheric precipitation and sunshine duration were processed with an effort to determine trends in the main meteorological elements over the period of operating of ground - based weather stations in Latvia.

In the first stage of the study the data sets analysis was simplified with an assumption, that variations in the meteorological elements were close to linear over the whole period examined. A method of least squares was used to define the direction coefficient of the regression line.

Air temperature observations show progressive warming over the territory of Latvia. Comparisons made of the values for the recent 100-year period testify to a more rapid rise in the temperature for the second half of the period. During the first 50 years annual mean air temperature become 0,2°C higher on the average without no influence being observed from the populated areas and the level of economic

development. In the second half however, the effect of industrial centres was evident. Mean annual temperature in Riga has increased nearly by 1°C as against 0,5°C for the rest of the Republic (Fig.1).
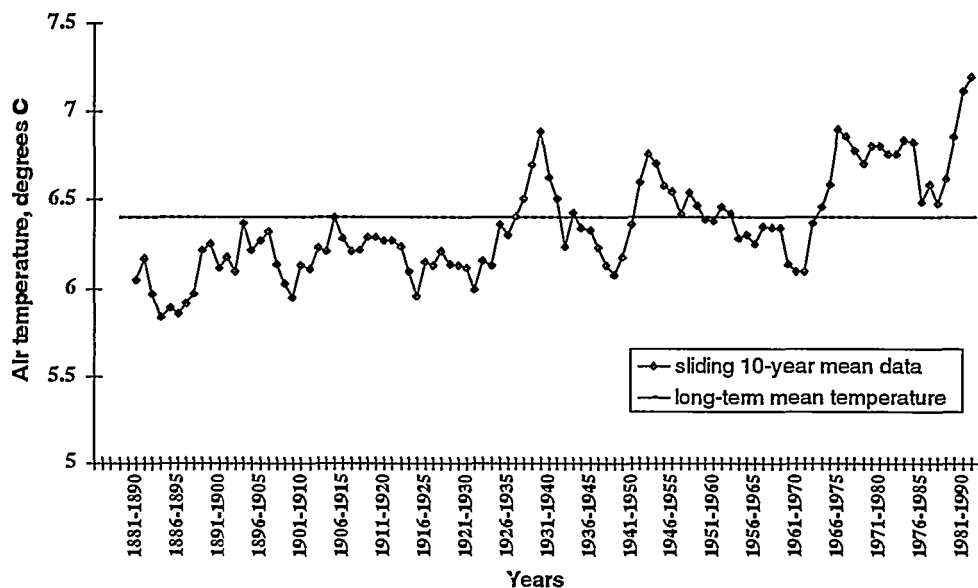
Fig.1. Mean annual air temperature variations in Riga

The air temperature amplitude has become narrower. The greatest positive changes occurred in the winter months, mainly due to rise in temperature at night. Mean annual extreme values have moved closer, and mean minimum was increasing faster than maximum one.

Annual precipitation has become more abundant. The process was more evident in districts, where prevailing winds and the relief fostered ascending of air masses. During the year the increase was more evident early in the cold period.

Total cloud amount remained unchanged, with some reduction in the low cloud amount. Notwithstanding this fact the analysis shows that sunshine duration has become shorter. Mean annual relative humidity remained unchanged.

The influence of circulation on daily temperatures in Łódź in the period 1930-1990

Joanna Wibig

Department of Meteorology and Climatology, University of Łódź
90-418 Łódź, Kościuszki 21, Poland

Introduction

Daily values of minimum, mean and maximum temperature in Łódź in the period September 1930 – July 1939 and 1951–1990 have been analyzed. The annual course and variability of daily temperature in the period 1951 – 1990 is presented on fig.1. It can be seen that the difference between the lowest and the highest mean values is about 20 degree, whereas the annual range (the difference between the highest daily maximum and the lowest daily minimum) exceed 65 degree. The daily ranges change from about 25 degree in summer to about 40 degree in winter.
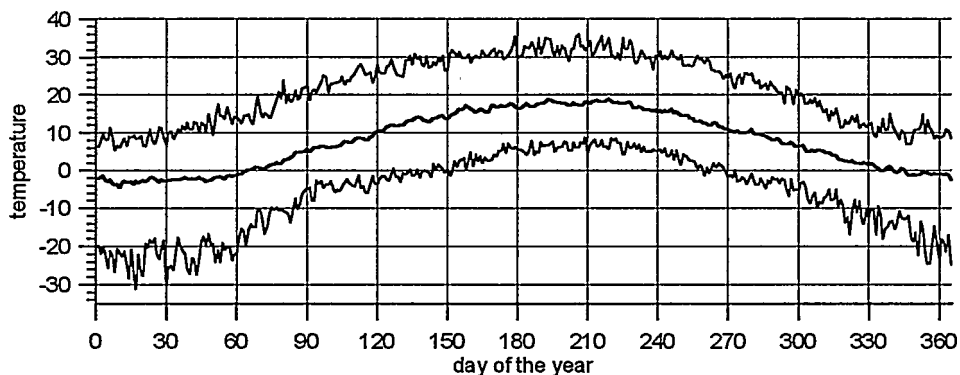
Fig.1. The annual course of daiy temperature: the upper curve – the highest daily values of the maximum temperature, the middle curve – the mean daily temperature and the lower curve – the lowest daily values of the minimum temperature in Łódź in the period 1951–1990.

The relation of temperatures to circulation was analyzed using the classification of circulation types defined for Polish area by Osuchowska – Klein (1978). This classification is based on character of circulation and direction of air mass advection.

Thirteen types are distinguished: six cyclonal, six anticyclonal and one mixed, their definitions and abbreviations are given in Table 1.

Table 1. Circulation types by Osuchowska – Klein

abbreviation	description of circulation type
A	western cyclonal
CB	north–western cyclonal
D	south–western cyclonal
B	southern cyclonal
F	south–eastern cyclonal
E0	north–eastern and eastern cyclonal
C2D	western anticyclonal
D2C	southern and south–western anticyclonal
G	central anticyclonal
E2C	north–western anticyclonal
E	north–eastern anticyclonal
E1	eastern and south–eastern anticyclonal
BE	southern transitional between cyclonal and anticyclonal

The mean values of temperature for each calendar month were calculated and for each day the deviation of temperature from appropriate monthly mean was found. Distributions of these deviations were made separately for each circulation type and then compared. The analysis was performed for minimum, maximum and mean daily temperatures. Results for the four most frequent types and daily mean temperatures are presented on fig.2.

To describe a time variability the mean deviations from appropriate monthly mean values for all circulation types in five subperiods were calculated. The first one takes the period from September 1930 to June 1939, the next four are full ten–year periods: (1951–60, 1961–70, 1971–80 and 1981–90). Fig. 3 shows the winter and summer values for daily mean temperatures. The variability of circulation types during the analyzed period was also examined. On fig. 4 the frequencies of six most popular types in six ten–year periods (from 1931–40 to 1981–90) are presented.

Results

Comparison of distributions of deviations from the mean value for different circulation types shows that most of the distributions differs significantly. Only types A and BE have similar distributions but the type BE is very rare and the analysis of fig. 3 shows that their influence on temperature differ in different seasons.

Some types is always connected with deviations of the same sign. For instance types D and D2C correspond with warmer days, whereas types EO, E2C with the colder ones (fig. 3). But there are also which are connected with warm situations during one season and with cold ones in the other, for instance type A which is cold only in

summer and type E1 which is the hottest one in summer and one of the coldest during winter. It is surprising that the mean deviations variate so strong with time. For type A in winter temperature was 2 degree higher during the period 1981–90 than previously. Similar phenomenon can be observed also for other types (fig. 3).
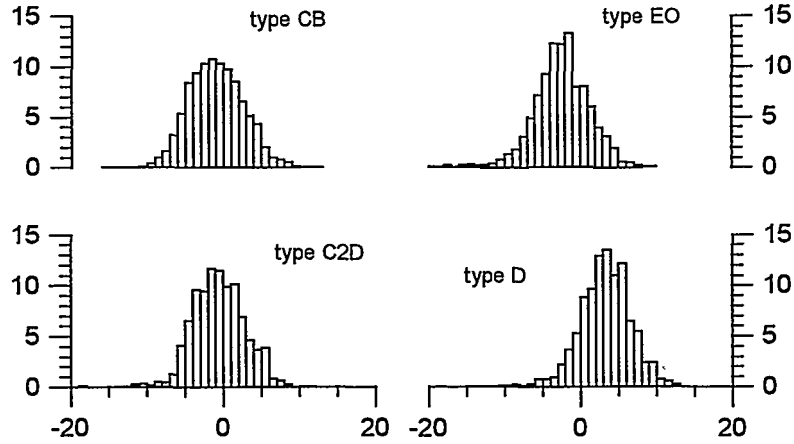
Fig. 2. Relative frequencies of deviations of daily temperature from appropriate monthly mean values for the four most popular circulation types
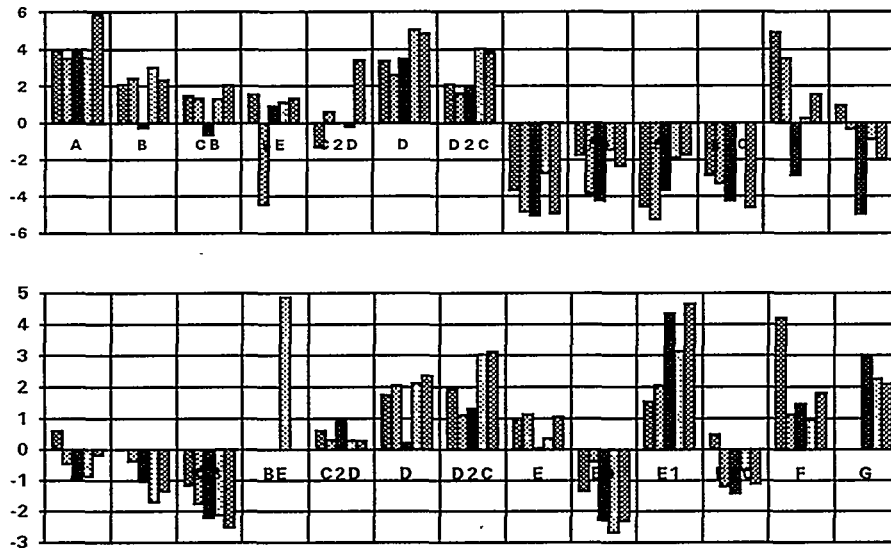
Fig. 3. The mean deviations from appropriate monthly mean temperature for all circulation types in particular ten-year periods (30–39, 51–60, 61–70, 71–80, 81–90) for winter (upper graph) and summer (lower graph)

The annual course of circulation types frequencies and their variability in time are presented on fig. 4. It is seen that frequency of type CB is uniform during the year, whereas type E1 is relatively rare in summer and very frequent during winter. Type E is more frequent during spring and summer than during autumn and winter. The opposite is true for type A. The high variability of frequency in following ten-year periods is also seen. The frequencies of types A in winter, summer and autumn, B and D2C in winter and E1 in autumn decrease evidently from the beginning of analyzed period. On the other hand the frequencies of types B in autumn, F and BE in spring and G in all seasons increase. Comparison of frequencies of circulation types in very cold and very warm season (Wibig, 1995) with results of this paper was also made.
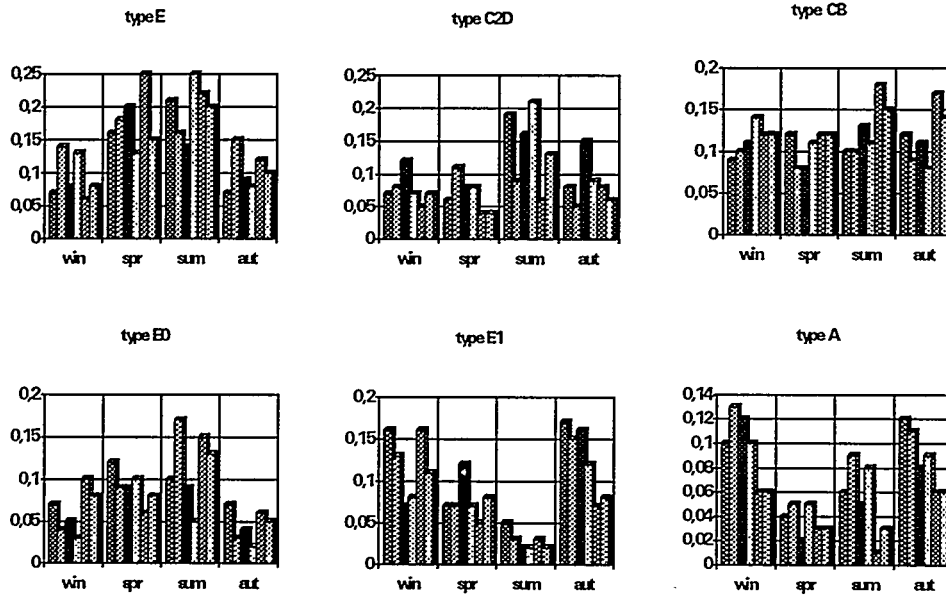
Fig. 4. Relative frequencies of circulation types in different seasons in six ten-year periods from 1931–40 to 1981–90.

References

Osuchowska – Klein, B. 1978. Katalog typów cyrkulacji atmosferycznej. (The catalogue of atmospheric circulation types). Wyd.Kom.i Łączn. (in Polish).

Osuchowska – Klein, B. 1991. Katalog typów cyrkulacji atmosferycznej, 1976 – 1990. (The catalogue of atmospheric circulation types, 1976–1990). IMGW, Warsaw, 50 pp. (in Polish).

Wibig, J. 1995. Daily temperature in Łódź according to circulation patterns, Proccedings of II Greek Conf. on Met., Clim. and Phys. of Atmos., Thessaloniki, Sep. 1994 (in press).

Melting, drainage patterns and frozen lakes on the land ice mass at Jutulgryta in Dronning Maud Land, Antarctica

Jan-Gunnar Winther,
Norwegian Polar Institute, Oslo, N-0301, Norway

Knut Sand,
SINTEF Norwegian Hydrotechnical Laboratory, Trondheim, N-7034, Norway

Carl Egede Bøggild,
The Geological Survey of Greenland, Copenhagen, DK-1350, Denmark

Hallgeir Elvehøy,
Norwegian Water Resources and Energy Administration, Oslo, N-0301, Norway.

Even in the cold environments of Antarctica, surface melting can take place locally during summertime. One example of this is the South Shetland Islands where drainage systems associated with snow melt are studied by Birnie and Gordon (1980). Further, in the dry valleys, summer melting of snow and glaciers and the characteristics of permanently ice-covered lakes are reported by Chinn (1993). Additionally, melting occurs locally close to nunataks due to strong absorption of solar radiation at surfaces with low albedo. However, the melt water drainage channels and melt water accumulation basins (hereafter named frozen lakes) described in this extended abstract are located on the land ice mass in Dronning Maud Land, tens of kilometres away from the closest nunatak and about 130 kilometres from the ice shelf barrier. The features are created by snow melt in a north-sloping area that is favourably exposed to incoming solar radiation. In addition, katabatic winds lead to very low winter snow accumulation.

These large scale melting phenomena like melt water drainage channels and melt water accumulation basins or frozen lakes were surveyed on the land ice mass at Jutulgryta in Dronning Maud Land, Antarctica, during the Norwegian Antarctic Research Expedition in 1989/90 (NARE 1989/90). The largest frozen lake that was observed was close to 1 km wide. These melting features were also detected in a Landsat Thematic Mapper (TM) image recorded on 12 February 1990 (Winther 1993). Image processing techniques such as principal component analysis, band ratioing and histogram-equalising were carried out to emphasise these melting features.

Then, during NARE 1993/94 the area was revisited and a five-year glaciological program was started. The overall objective of the program is to improve our

understanding of climatically significant snow-ice-air processes in this area. The program includes the collection of basic glaciological, hydrological and meteorological data for use in developing a method by which to monitor melting variations in coastal regions of Antarctica. To obtain this objective we make use of remote sensing techniques in conjunction with a field observation programme.

In spite of negative air temperatures and the presence of a frozen ice surface, sub-surface melting and runoff was found within the uppermost metre in blue ice fields. The sub-surface melting is a consequence of solar radiative penetration and absorption within the ice, i.e. the solid state greenhouse effect. The occurrence of a temperature maximum below the surface is a result of solar radiation penetration and absorption inside the snow and the fact that long-wave radiative cooling is restricted to the surface (Brandt and Warren 1993). The solid-state-greenhouse-effect has been described theoretically by Schlatter (1972) and Brandt and Warren (1993). Brandt and Warren (1993) state that this phenomenon is rather questionable within snow, but more likely to occur within blue ice due to its lower extinction coefficient and albedo. Some of the past observations of the solid-state-greenhouse-effect in snow have been affected by factors such as radiative sensor heating or the presence of a dark layer within the snow pack. In Jutulgryta the snow and ice were totally free of visible contamination. Temperatures in blue ice were about 6 °C higher than for snow.

Internal melt and melt water transport was observed throughout the one month of measurements. The blue ice fields feed the frozen lakes with melt water that flows both upon the lake ice surface and below a lake ice cover that has a typically thickness of 10-20 cm. A layer of water with thickness varying between 40 and 83 cm was found between the underlying main ice body and the top ice cover of a frozen lake (Bøggild et al., in press).

The conditions for melting activity to take place in Jutulgryta are probably marginal. A slight increase of air temperatures can result in more "classical" surface melting whereas a cooling may disable sub-surface melting. Further studies of the solid-state-greenhouse-effect melt and frozen lakes in Dronning Maud Land may as well contribute to the understanding of runoff from the Greenland Ice Sheet, since similar surface features, i.e. frozen lakes and blue ice fields intersected by snow fields have been documented near the equilibrium line in both East and West Greenland (Echelmeyer et al. 1991; Reeh et al. 1991).

Surface melting in this area is limited and insignificant for the mass balance budget. However, we anticipate that the sub-surface melt-related features we have identified in Dronning Maud Land are quite sensitive to variations in local and regional air temperature and energy balance. Because of this sensitivity, an understanding and description of the extent and characteristics of these melt features as they change with time can be particularly valuable as a climate change indicator. In light of this opportunity to make a significant contribution to monitoring Antarctic climate variations, we have determined that it is clearly important to analyse how these melt features originate, map their present areal distribution, determine how sensitive they are to climate change and study changes in the past and possible changes in the future.

References

Birnie, R.V. and Gordon, J.E. 1980: Drainage systems associated with snow melt, South Shetland Islands, Antarctica. *Geogr. Ann.* 62, Ser. A, 57-62.

Brandt, R.E. and Warren, S.G. 1993: Solar-heating rates and temperature profiles in Antarctic snow and ice. *J. Glaciol.* 39(131), 99-110.

Bøggild, C. E., Winther, J.G., Sand, K. & Elvehøy, H. 1994: Observations of subsurface melting and temperatures in a blue ice field in Jutulgryta, Dronning Maud Land, Antarctica. *Ann. Glaciol.*, 21, in press.

Chinn, T.J. 1993: Physical hydrology of the dry valley lakes. *Physical and biogeochemical processes in Antarctic lakes. Ant. Res. Ser.*, 59, 1-51.

Echelmeyer, K., Clarke, T.S. & Harrison, W.D. 1991: Surface glaciology of Jakobshavn Isbræ, West Greenland: Part 1. Surface morpology. *J. Glaciol.* 37(127), 368-382.

Reeh, N., Oerter, H. & Neve, J.K. 1991: Supra-glacial lakes on Storstrømmen Glacier Northeast Greenland and their relation to ice dynamics. Abstract in *Programm, Deutche Gesellschaft für Polarforschung, 16.* Internationale Polartagung in Göttingen, April 1991.

Schlatter, T.W. 1972: The local surface energy balance and subsurface temperature regime in Antarctica. *J. Appl. Meteorol.* 11(10), 1048-1062.

Winther, J.G. 1993: Studies of snow surface characteristics by Landsat TM in Dronning Maud Land, Antarctica. *Ann. Glaciol.*, 17, 27-34.

Changes in atmospheric composition

Ozone and aerosol studies

the measurements. In the beginning of a measurement cycle, the hole and the top of the cuvette are closed for seventy seconds by aid of pneumatic air. After this the gas analyzer measures the cuvette CO_2 concentration once in every ten seconds. In the end of the cycle, the hole and the top are opened. In this way the overall environmental conditions of the twig in the cuvette remain very similar to those of the neighboring twigs.

The station is visited by the personel two or three times a week in winter. The more intensive measurements during summer require daily checking of the system to quarantee a sufficient quality of measurements. Hari et al. (1994) have represented the measuring equipment and conditions in more detail.

Experimental results

In Fig. 1 we present the mean and maximum hourly sulphur dioxide concentrations and medians and 25% - 75 % percentiles of particle (CN) concentrations measured in years 1993-1994 at 9m height.

SO_2 is typically observed in Värriö as episodes the background concentration being near the detection limit. Therefore the maximum values for each month are quite high in comparison with the mean SO_2 concentrations. Episodes occur during winds coming from northeastern direction, where the Kola industrial areas are located. CN concentrations are quite low and usually, but not always follow SO_2 -concentrations indicating new particle formation (see e.g. Kulmala et al. 1995). This indicates the magnitude of different nucleation mechanisms in particle formation.

Some results from the profile measurements are presented in Fig. 2. The carbon dioxide concentration difference measured between 9 and 2 meters is highest during summer months when the photosynthetic activity of plants is at its maximum. In daytime the concentration gradient is positive ie. CO_2 is moving towards vegetation. During nighttime the direction of the flux is opposite.

References

Hari, P., Kulmala, M., Pohja, T., Lahti, T., Siivola, E., Palva, L., Aalto, P., Hämeri, K., Vesala, T., Luoma, S. & Pulliainen, E. 1994. Air Pollution in Eastern Lapland: Challenge for an Environmental Measurement Station. Silva Fennica 28(1):29-39.

Kulmala, M., Kerminen, V.-M. & Laaksonen, A. 1995. Simulations on the Effect of Sulphuric Acid Formation on Atmospheric Aerosol Concentrations. Atmospheric Environment 29(3):377-382.
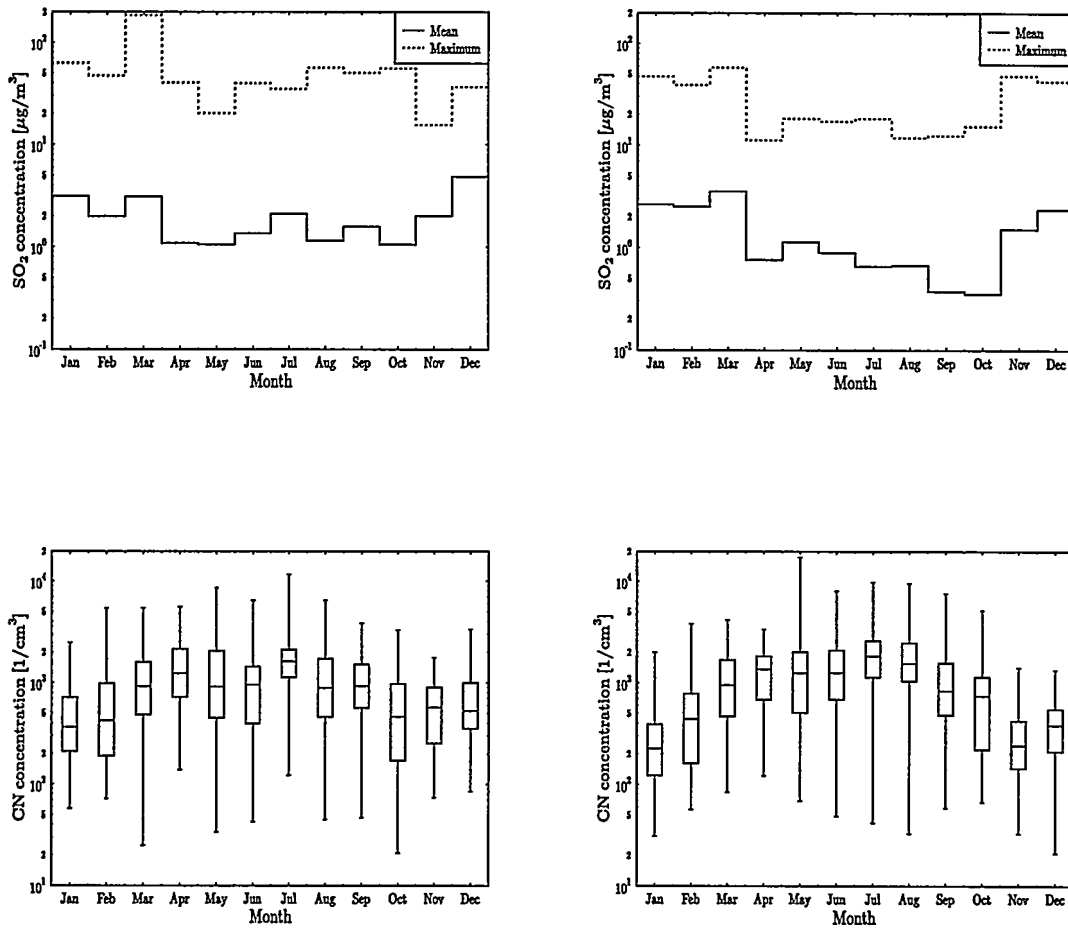
Figure 1: SO$_2$- and particle (CN) concentrations during years 1993 (left) and 1994 (right).

studies considering the exchange of physical and chemical constituents between these two regions. The latitude of Marambio is also excellent for hemispheric comparisons of the stratospheric ozone behaviour. The total ozone measurements at Marambio are done using the Dobson spectrophotometer. Although the solar radiation is available at Marambio throughout the year, during the austral winter the solar zenith angle is too high for reasonable 'dobson-measurements', and consequently measurements of good quality are available from the beginning of August until the end of April. For comparisons with normal total ozone the dataset of Argentine Islands 1957-67 is used. This site is located about 380 km south-west from Marambio (65°15'S, 64°16'W). The ozone soundings are done using the ECC-type ozonesondes. The interval of soundings is roughly one to two times a week during the end of austral winter and whole spring. The rest of the year is covered approximately by one or two soundings per month. The analysis of polar vortex and the air mass origin are accomplished using ECMWF-based potential vorticity analysis and trajectory calculations.

Total Ozone Behaviour above Marambio

Lower than normal ozone column abundance's above Marambio have been observed during the whole period of measurements. The Marambio total ozone distributions during austral winter and spring and the average monthly Argentine Islands total ozone 1957-67 distributions are shown in figure 1. The first four years of measurements have been reported by Taalas and Kyrö (1992), and Taalas (1993). The ozone destruction season above Marambio initiates typically during the end of August or beginning of September, and terminates during the end of November or beginning of December. The total ozone minima are typically found during October. In 1991 the ozone minimum of 163 DU was measured at 21st of October, and the level of ozone destruction was very profound throughout the whole season. In 1992 the situation was somewhat similar to 1991. The absolute minimum over Marambio was 131 DU. In 1992 reliable total ozone measurements were available only from the beginning of September. In 1993 the absolute minimum was 141 DU. The behaviour of total ozone in 1993 is somewhat different in contrast to earlier years. During 1993 relatively rapid changes in total ozone amount were measured in two to six day periods, specially in October. While the lowest total ozone values were around 150 DU (i.e. ~60 % destruction) the covering values were about 200-250 DU (i.e. ~20% destruction). Although similar behaviour is also evident in the whole Marambio dataset (1987-94) the frequency of these changes is greatest in 1993. These relatively rapid changes in total ozone are connected to the movements of the polar vortex. Our case-by-case analysis of ECMWF-based potential vorticities and trajectories show that the lowest values are measured during in-vortex situations when the air mass is originated from inside the vortex. The higher values (typically more than 200 DU) are detected when the site of Marambio is outside the polar vortex, and the air mass has the mid-latitude origin. In 1994 the entire season was characterised by very low values of total ozone, and the record low of 130 DU was measured above Marambio in the 2nd of October.

Using the Marambio total ozone data 1987-94 we have calculated linear slopes for total ozone. For August, September, October, November, December, January, February, and March these linear inclines are − 5.0%, − 29.5%, − 14.1%, − 18.8%, − 3.4%, − 8.5%, − 9.8%, and − 3.7% respectively. The deviations for August,

September, January, February, and March are significant on the 95 % confidence level, while inclines for the other months are not significant. The annual incline for the whole period is − 10.8 % which is significant at 95 % confidence level.
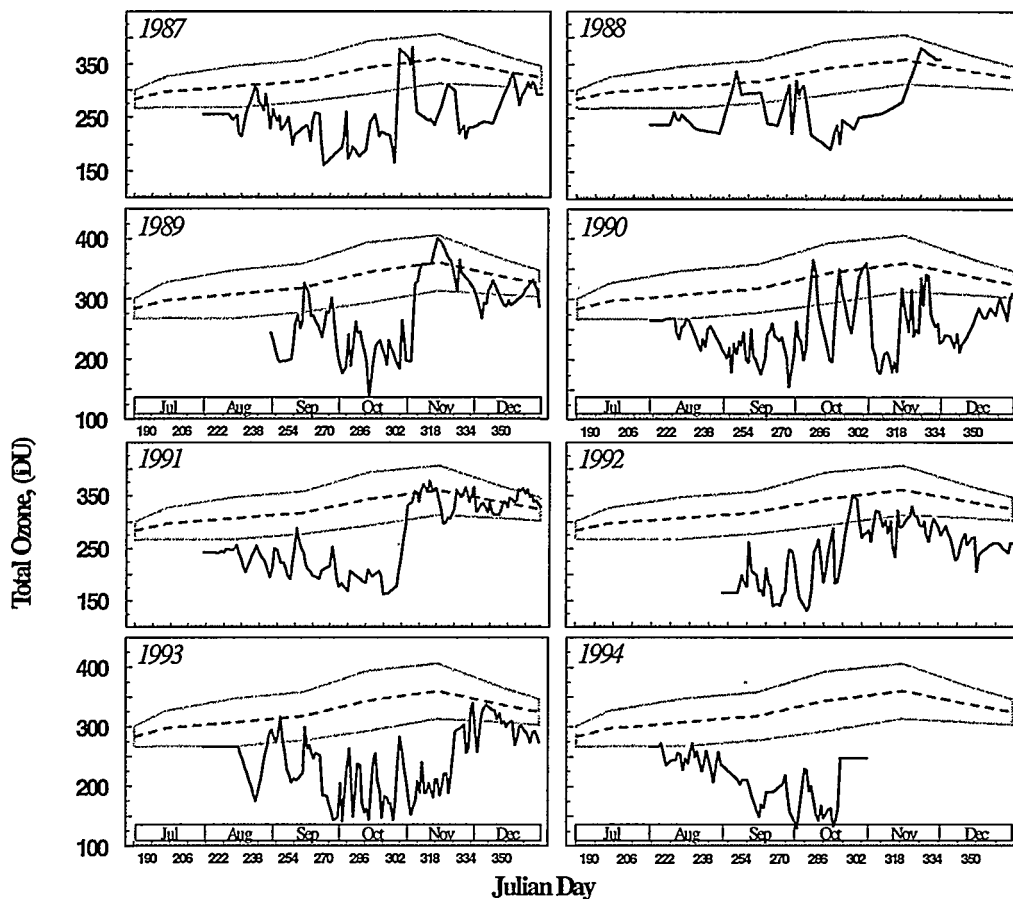
Figure 1. Total ozone distributions at Marambio 1987-94 (solid line). The dashed line represents the Argentine Islands 1957-67 monthly mean values, and the shaded area shows the respective standard deviation.

UV-B-Radiation; Model Results

The effect of total ozone differences to the received amount of UV-B-radiation at the surface is studied using radiative transfer model of Dahlback (Dahlback et al. 1989, Dahlback et al. 1991). In the model the dose rates are calculated at sea level for clear sky conditions, and the surface albedo is assumed to be 20 % globally. The dose rates are defined as the integrated irradiances of both diffuse and direct solar radiation, and the spectral integration is done from 290 nm to 400 nm. The modelled spectra are weighted using biologically active actionspectrum (standard CIE-spectrum; see Dahlback et al. 1989), and the doses are relevant for the human epidermis (i.e. the erythemal dose).

The modelled monthly erythemal UV-B-doses at Marambio are at highest more than 120 kJ/m²/month, and they are received during the austral summer months December and January. Due to the decrease in total ozone during austral spring the October and November UV-B-doses have increased more than 50 % exceeding the dose level of 100 kJ/m²/month. The deviations in August and September are also high (~30%) but since the solar zenith angle is high the increases in dose levels are of minor importance.

Summary and Concluding Remarks

The Marambio total ozone measurements from 1987-94 exhibit lower than normal total ozone amounts throughout the measurement period. The lowest values are typically measured during October. However, unusually low values are also present in late austral winter, as well as in austral summer. The low total ozone values during late winter are characterised by the fact that the latitude of Marambio (~64°S) is sufficient for chemical destruction of stratospheric ozone as early as in middle of August. The low values in summer are usually measured after the destruction of polar vortex. During austral spring the lowest total ozone amounts are connected to in-vortex cases. In out-vortex cases the total ozone is typically of order of 200 DU which is still significantly low compared to long term average (see fig. 1). Conclusion that the total ozone amounts reveal lower than normal values also in mid-latitude air during austral spring and summer is therefore valid at least above Marambio. The total ozone incline for the whole 8-year period at Marambio is –10.8%.

The low values of total ozone at Marambio are also reflected to the received UV-B-doses which have increased roughly 20-80% (compared to long term average) during austral spring and summer. In respective to the total amount of ozone, our model calculations show that during October the UV-B-doses can be at the same level as they should be during normal summer.

References

Austin, J., Butchart, N. & Shine, K.P. 1992. Possibility of an Arctic ozone hole in a doubled-CO2 climate. Nature 360:221-225.

Dahlback, A., Henriksen, T., Larsen, S. & Stamnes, K. 1989. Biological UV-Doses and the Effect of an Ozone Layer Depletion. Photochem. Photobiol. 49:621-625.

Dahlback, A. & Stamnes, K. 1991. A New Spherical Model for Computing the Radiation Field Available for Photolysis and Heating at Twilight. Planet. Space. Sci. 39:671-683.

Taalas, P. & Kyrö, E. 1992. 1987-89 total ozone and ozone sounding observations in Northern Scandinavia and at Antarctica and the climatology of lower stratosphere during 1965-88 in Northern Finland. Journal of Atmospheric and Terrestrial Physics 54:1089-1099.

Taalas, P. 1993. Factors affecting the behaviour of tropospheric and stratospheric ozone in the European Arctic and in Antarctica. Finnish Meteorological Institute, Contributions No. 10, 138 p.

Methane Emissions from Ruminant Animal and Livestock Manure in China

Dong Hongmin   Li Yue   Lin Erda

Agrometeorology Institute, Chinese Academy of Agricultural Sciences, Beijing 100081.

Introduction

Methane is an important greenhouse gas. Its concentration in atmosphere is increasing at a rate of about 0.9% per year. This increase is correlative closely with human activities. Ruminant animals and livestock manure are the major anthropogenic sources of methane emissions. The methane emission from animals and livestock manure account for about 22.2% and 5% of the total methane from anthropogenic sources. China is one of the countries with the largest domestic livestock population. Based on large human population and rapid economic development, the numbers of domestic livestock will increase, which in turn will result in increasing methane emissions. This paper presents a detailed estimations of methane emissions from ruminants animal and livestock manures in China.

Contribution of Chinese Ruminants to methane emission

Methodology

To estimate methane emissions from ruminants in China, emissions factors were developed based on China-specific feed energy systems and production characteristics for representative animal types. Because ruminants in China are mostly fed low quality roughage, which have low rates of growth and milk production, the method recommended by IPCC(1993) are not suitable in China. The emission factors developed in this paper are believed to be more reasonable for estimation of methane emission.

Methane from ruminants

Using the emission factors developed in this paper and animal population, emissions from ruminants are estimated at about 5.80 Tg or about 7.2 per cent of global methane from animals in 1990.

Contribution of livestock manure to methane emission

Methodology

Methane emissions from livestock manure depend on the type of manure, the characteristics of manure management system, and the climatic conditions. To estimate methane emissions from livestock manure in China, emission factors were developed based on method recommended by IPCC(1993) and China's climate region.

Table 1: Total methane emission from Chinese ruminants

Type	Subtype	M(kg/a/head)	Population(10^4)		Methane emissions(Tg)	
			1985	1990	1985	1990
Draft cattle	Breeding cow	48.27	2419.6	3110.0	1.168	1.501
	Young calf	27.88	1019.0	1387.2	0.237	0.322
	Others	45.34	3087.3	3353.1	1.400	1.52
Buffalo	Breeding cow	68.09	730.3	851.5	0.497	0.58
	Young calf	38.3	244.4	271.3	0.078	0.0w
	Others	51.77	1018.7	1046.2	0.527	0.542
Dairy cattle	Breeding cow	70.4	84.0	142.1	0.059	0.100
	Younger calf	38.3	34.8	64.5	0.011	0.021
	Others	51.77	43.9	62.5	0.023	0.032
Sheep	Breeding ewe	7.05	4882.3	5865.6	0.344	0.414
	Others	3.83	4538.7	5416.0	0.139	0.166
Goat	Breeding doe	7.05	2847.5	4585.0	0.201	0.320
	Others	3.83	3319.9	5135.5	0.107	0.157
Camel		58	53	463	0.031	0.027
Total			24323.4	31336.7	4.822	5.796

Current methane emissions from livestock manure

Using the emission factors developed in this paper and animal population in different climate conditions, emissions from livestock and poultry manure are estimated to be about 1.249 Tg or about 5 per cent of global methane from animal manure in 1990. Of the total 1.249 Tg, methane emission from swine manure accounts for 1.027 Tg

or about 82.2 percent of the total.

Table 2: Total methane emission from China's livestock and poultry manure in recent years

Animal Type	1980	1990
Dairy	6.13	23.69
Non-dairy	40.34	60.41
Bufalo	33.15	38.87
Swine	831.92	1027.55
Sheep	11.29	11.72
Goat	10.50	12.51
Camel	0.79	0.59
Horse	13.11	12.49
Mules/Asses	7.42	10.40
Poultry	14.73	51.48
Total	969.38	1249.11

Reference

Blaxter,K.L. and J.L. Clapperton, Prediction of the amount of methane produced by ruminants, British journal of Nutrition, 19:511-522 (1965).

Crutzen,P.J.,I.Aselmann and W.secler, Methane Production by Domestic Animal, Wild Ruminants, Other Herbivorous Fauna, and Humans, Tullus, 38B: 271-284 (1986).

Editing Committee of Agricultural Yearbook of China,Agricultural yearbook of China 1990, Agriculture Press, Beijing(1991).

IPCC/OECD, 1993, Greenhouse Gas Inventory Reference Manual,first draft, Volume 3.

Northeast Agricultural institute, Animal Feeding Science,Agriculture press, Beijing (1981).

OECD, Estimating of Greenhouse Gas Emissions and Sinks, Final Report From the OECD Experts Meeting, 18-21 Feb, Paris (1991).

Professional standard of the P.R.of China, Feeding standard of dairy cattle, Standard Press, Beijing (1987).

USEPA, 1992. Global Methane Emissions from Livestock and Poultry Manure, GCD/ORA, USEPA, Washington,
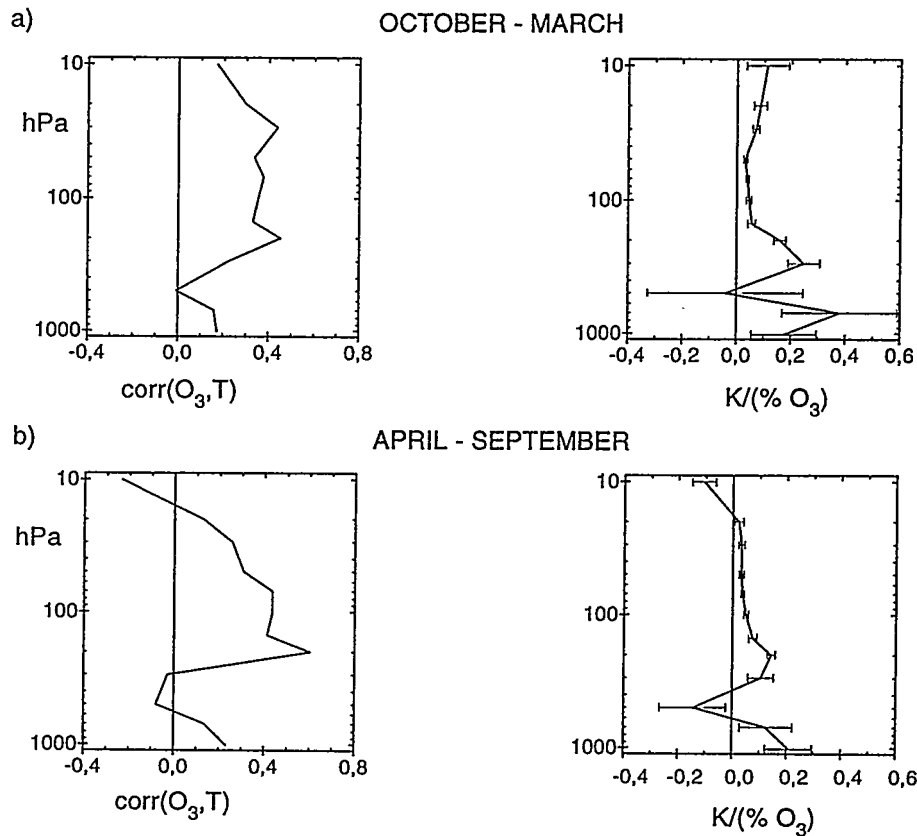
Fig. 2 Average correlation (solid line) and linear relation (solid line plus standard error bars) between residual ozone and temperature over the period 1971-1991, for 8 ozonesonde stations (see text).

during the cold period, the stratospheric ozone depletion is not accompanied by an observed cooling (the temperature trend is even slightly positive, though not significant) indicating perhaps the influence of dynamics on stratospheric temperature at these high latitudes. The calculated equilibrium cooling is quantitively similar to what was calculated by Miller et al. (1992). In the troposphere, the positive ozone trends come from the Japanese stations, and Wallops Island in the warm cycle - Canada showing an on average zero trend for the whole troposphere. What is interesting is that the tropospheric ozone increase during the warm seasons is steadily accompanied by a significant surface warming for the Japanese stations as well as Wallops Island. This seems to indicate a smog-related warming, although the cause-effect relationship is not established.

With the ozone and temperature residuals obtained from the multiple regression analysis, a further statistical analysis is performed to determine the correlation between them and find how they are linearly related. Fig. 2 presents the results for the two half year cycles. Keeping in mind that the tropopause is on average between 200 and 300 hPa, we see a maximum correlation and the highest temperature sensitivity to percentual ozone change in this region. Although based on a different concept, the curve is reminiscent of the sensitivity curve in Lacis et al. (1990), showing equilibrium global surface temperature change to vertical changes in ozone - or the sensitivity curves in Fortuin et al. (1995b), showing FT

and FD forcing values instead. However, the sensitivity curves of Fig. 2 depict average *layer temperature* changes due to changing ozone in the same layer. From radiative theory, the maximum sensitivity around the tropopause is to be expected, as in this region the temperature contrasts most with the surface temperature. The widening of the confidence intervals in the highly variable troposphere is also to be expected. However, the significant and high temperature sensitivity to near-surface ozone changes is somewhat in contrast with the above-mentioned sensitivity studies - where climate forcing due to near-surface ozone changes is almost zero. As mentioned earlier, this points to a local (possibly shortwave) warming caused by smog conditions - the inversion preventing convective transport of the heat to the rest of the troposphere. Also surprising is a higher temperature sensitivity in the cold period - near the tropopause and above 50 hPa - than in the warm period, despite a higher solar and longwave (surface temperature) forcing. Explanations for these findings need to be sought, either in further climate model studies, or in a closer look at the reliability of the sonde measurements on which this study is based.

References

Angell JK, 1988. Variations and trends in tropospheric and stratopheric global temperatures, 1958-1987. J. Climate 1:1296-1313.

Angell JK, 1993. Comparison of stratospheric warming following Agung, El Chichon and Pinatubo volcanic eruptions. Geoph. Res. Lett. 20:715-718.

Fortuin JPF, Van Dorland R, Kelder H, 1995a. Concurrent ozone and temperature trends derived from ozonesonde stations. NATO ARW series 32:131-144.

Fortuin JPF, Van Dorland R, Wauben WMF, Kelder H, 1995b. Greenhouse effects of aircraft emissions as calculated by a radiative transfer model. Ann. Geoph. 13:413-418.

Lacis AA, Wuebbles DJ, Logan JA, 1990. Radiative forcing of climate by changes in the vertical distribution of ozone. J. Geoph. Res. 95:9971-9981.

Logan JA, 1994. Trends in the vertical distribution of ozone: an analysis of ozonesonde data. J. Geoph. Res. 99:25553-25585.

McCormack JP and Hood LL, 1994. Relationship between ozone and temperature trends in the lower stratosphere: latitudinal and seasonal dependencies. Geoph. Res. Lett. 21:1615-1618.

McCormick MP, Veiga RE and Chu WP, 1992. Stratospheric ozone profile and total ozone trends derived from SAGE I and II data. Geoph. Res. Lett. 19:269-272.

Miller AJ, Nagatami RM, Tiao GC, Niu XF, Reinsel GC, Wuebbles DJ and Grant K, 1992. Comparisons of observed ozone and temperature trends in the lower stratosphere. Geoph. Res. Lett. 19:929-932.

Peixoto JP and Oort AH, 1992. 'Physics of climate', AIP, New York, 520 pp.

Tiao GC, Reinsel GC, Xu D, Pedrick JH, Allenby GM, Mateer CL, Miller AJ and DeLuisi JJ, 1986. A statistical trend analysis of ozonesonde data. J. Geoph. Res. 91:13121-13136.

Van Dorland R, 1995. The extension of the ECMWF radiation scheme with trace gases and aerosols for climate modelling purposes: methods and performance. In prep.
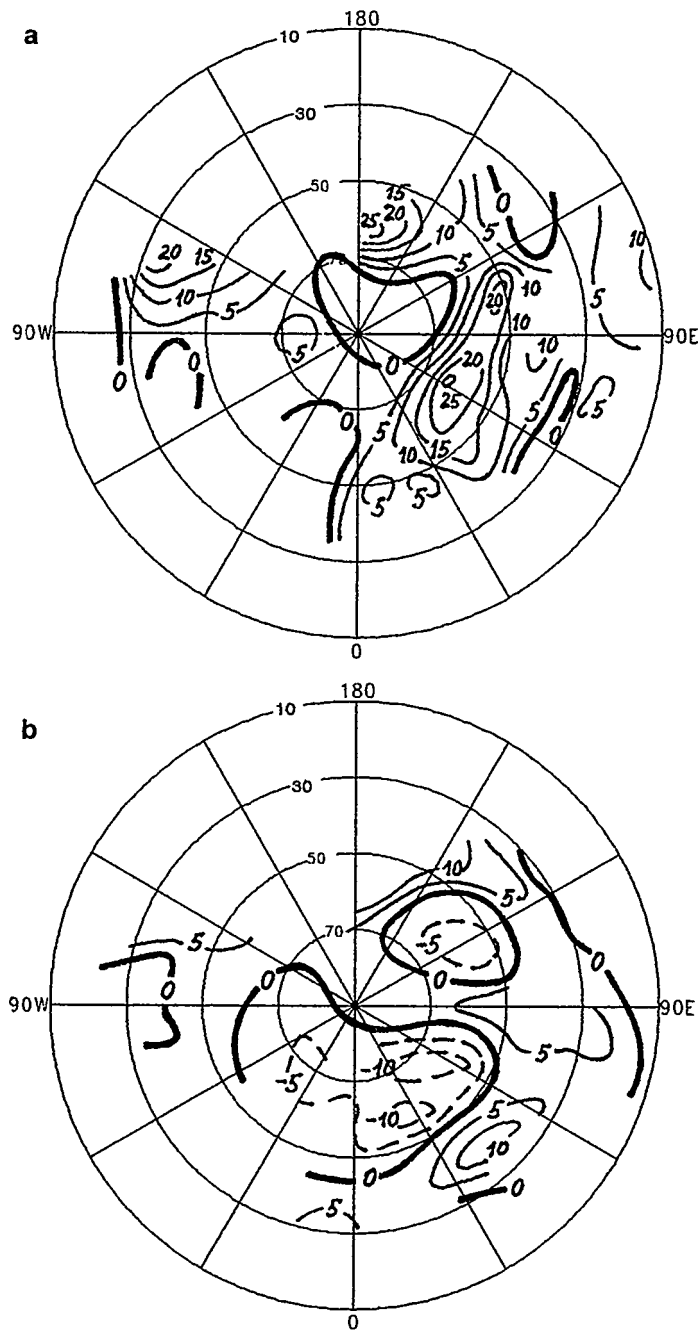
Fig. 3 a) Percent differences in the UV-B dose for generalized DNA damadge, caused by the change of total ozone from contents peculiar to the easterly phase of the QBO of equatorial wind at 50 mb to the content peculiar to the westerly phase, for March. b) As in a) but for July, and the wind QBO is specified at 30 mb

East Europe to Siberia), in the Bering Sea, and in the western part of the USA, approaching there 20-25%. It is worth noting large longitudinal gradients of changes in the UV-B dose, associated with strong regional dependence of the ozone QBO. Similar distribution of possible QBO-related changes in the UV-B dose in July, but related to the QBO phases specified at 30 mb, is presented in Fig.3b. This distribution is quite different and the changes are smaller in absolute value than those for March, but are not of less importance because of larger solar UV-B radiation energy and longer days in summer. The largest increase in the UV-B dose (up to 10%) is possible during the westerly QBO phases in Caucasus region and, again, in the Bering Sea. In the vast region of North Atlantic and North Europe, the UV-B dose increases during the easterly QBO phases, up to 10% in North Europe. It is important that the spatial inhomogeneity of ozone changes makes the biosphere of certain regions extremely prone to damaging UV-B radiation. Some of these regions are clearly seen in Fig.3. The seasonal dependence of the changes in the UV-B dose may be also important, as the sensitivity of certain living organisms to the received UV-B dose can depend on the phase of their life cycle. The magnitude of the changes can be quite large and exceed a half of possible over/all interannual changes (Gruzdev 1995). The quasi-periodicity of a possible biosphere response to the ozone QBO may serve as a basis for searching such a quasi-biennial signal in the behaviour of natural populations.

Strong seasonal and regional dependence of the QBO in ozone is important for correct determination of long-term trends. Statistical trend models should take into account these effects. The following linear regression model is suggested:

$$O_3(t)=\alpha_s+\beta_s \cdot trend+\gamma \cdot annual+\delta_s \cdot QBO+\varepsilon_s \cdot solar+...+residual \qquad (1)$$

where α_s, β_s, γ, δ_s, and ε_s are coefficients to be determined, subscript s denotes seasonal dependence. The annual and solar components can be modelled, for example, according to Stolarski et al. (1991). Taking into account the reported results, the QBO component in (1) can be represented, for example, by $sign(u)$, where u is the zonal equatorial wind at 30 mb, 50 mb or other level, or layer mean wind.

References

Gerstl, S.A., Zardecki, A. & Wiser, H.L. 1981. Biologically damaging radiation amplified by ozone depletion. Nature 294:352-354.

Gruzdev, A.N. 1995. Possible changes in the dose of biologically active ultraviolet radiation received by the biosphere in the summertime Arctic due to total ozone interannual variability. Sci. Total Environ. 160/161:669-675.

Gruzdev, A.N. & Mokhov, I.I. 1992. Quasi-biennial oscillation in the total ozone global field from ground based observations. Izvestiya, Atmos. Oceanic Phys. 28:358-366.

Gruzdev, A.N. & Sitnov, S.A. 1995. Differences of vertical distributions of ozone and meteoparameters in phases of the quasi-biennial oscillation (from ozonesonde data). Izvestiya, Atmos. Oceanic Phys. 31: in press.

Stolarski, R.S., Bloomfield, P. & McPeters, R.D. 1991. Total ozone trends deduced from Nimbus 7 TOMS data. Geophys. Res. Lett. 18:1015-1018.

Growth of nuclei into the CCN size

One of the major problems in modelling the DMS-cloud-climate system is to quantify the growth of newly borne nuclei into a size where they are able to act as CCN. The two main reasons for this are: 1) owing to very few reliable measurements, the gas-phase concentrations of condensational sulfur species are largely unknown in the atmosphere, and in remote marine regions in particular. 2) due to uncertainties in the accommodation coefficients for gaseous sulfur species on particle surfaces, evaluating the condensation rates of these compounds has proven to be extremely difficult.

By combining our model simulations with the information on various kind of gas/particle measurements carried out in remote marine regions, with our current understanding of particle production via homogeneous nucleation, and with the knowledge of how different factors may affect the surface accommodation, we were able to narrow down the above mentioned uncertainties considerably. First, compared to condensation, coagulation between nuclei was shown to have a minor effect on their growth. Second, we pointed out that co-condensation of species other than sulfuric acid and water is unlikely to contribute significantly to nuclei growth in mid/low-latitude marine boundary layers. Third, by assuming that most CCN in these areas are a result of *in situ* nuclei production and subsequent condensational particle growth, either (or some combination) of the two following hypothesis must hold: 1) all marine particles have roughly an equal accommodation coefficient for sulfuric acid vapor, the value of which is smaller than 0.1. This option requires that there is a $H_2SO_4(g)$ source other than gas-phase oxidation of $SO_2(g)$, which might be some unknown route in the DMS oxidation pathway (Bandy et al. 1992). 2) nuclei accommodation coefficient for sulfuric acid is larger than 0.1, while at the same time the bulk of the larger and more aged particles have a considerably lower accommodation coefficient for this species. Both these hypotheses were tested and can be considered viable based on our current understanding on the marine environment.

The effect of clouds on marine CN/CCN production

Marine boundary layers are capped frequently with stratiform clouds. The interaction between a cloud deck and the underlying air is complicated, depending on shear, surface based heating and evaporation, cloud-top longwave radiative cooling, short wave radiative heating together with latent heating/cooling inside the cloud layer, subsidence, entrainment, and drizzle (Moeng et al. 1992). Although a complete microphysical treatment of these processes is impossible at the present, our model can be considered adequate in exploring some basic features related to the marine cloud- CN/CCN production interaction.

The first thing we looked at was nighttime cycling of air through stratus decks, and little effect on both CN and CCN production were found. This was primarily due to the fact that

sulfuric acid, which is depleted efficiently from the gas phase by cloud droplets, has low gas-phase concentrations anyway because of a negligible photochemical source during the night.

In tropical regions, as well as at midlatitudes in the summer, clouds become regularly decoupled from the underlying air during the sunlit hours (Hignett 1991). Hence, daytime interaction between the boundary layer air and clouds is more or less sporadic even when clouds are present. We incorporated this phenomenon by letting the air parcel penetrate the cloud layer a few times per day, and for a relatively short period at a time. Our simulations pointed out the interaction with even a single cloud during the photochemically active period of the day is likely to reduce nuclei production considerably, and may inhibit it altogether. Continual cloud cycling during daytime makes CN production very improbable, and reduces significantly the rate at which nuclei grow in size.

References

Bandy, A.R., Scott, D.L.,Blomquist, B.W., Chen, S.M. & Thornton, D.C. 1992. Low yields of SO_2 from dimethyl sulfide oxidation in the marine boundary layer. Geophys. Res. Lett. 19: 1125-1127.

Charlson, R.J., Lovelock, J.E., Andreae, M.A. & Warren, S.G. 1987. Oceanic phytoplankton, atmospheric sulphur, cloud albedo and climate. Nature 326: 655-661.

Fouquart, Y. & Isaka, H. 1992. Sulfur emissions, CCN, clouds and climate: A review. Ann. Geophys. 10: 462-471.

Hignett, P. 1991. Observations of the diurnal variation in a cloud-capped marine boundary layer. J. Atmos. Sci. 48: 1474-1482.

Kaufman, Y. & Chou, M.-D. 1993. Model simulations of the competing climatic effect of SO_2 and CO_2. J. Climate 6: 1241-1252.

Moeng, C.-H., Shen, S. & Randall, D.A. 1992. Physical processes within the nocturnal stratus-topped boundary layer. J. Atmos. Sci. 49: 2384-2401.

Russell, L.M, Pandis, S.N. & Seinfeld, J.H. 1994. Aerosol production and growth in the marine boundary layer. J. Geophys. Res. 99:20989-21003.
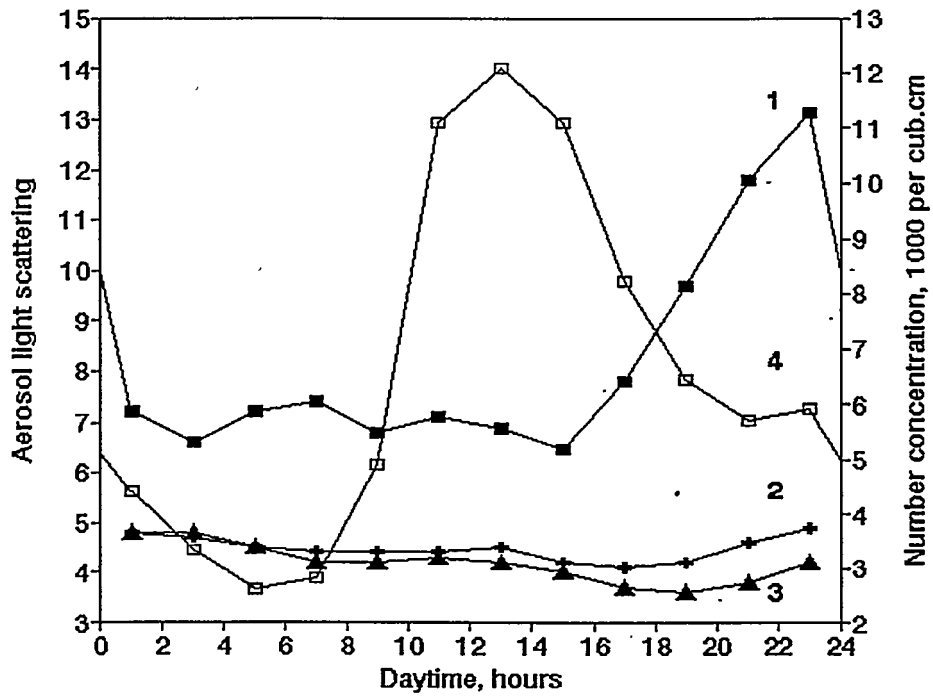
Fig.1 Mean daily evolution of aerosol light scattering in Summer measured at Akademgorodok (1), near Kljutchi (2) and Lake Tchany (3) and of total aerosol number concentration (4), measured near Kljutchi.
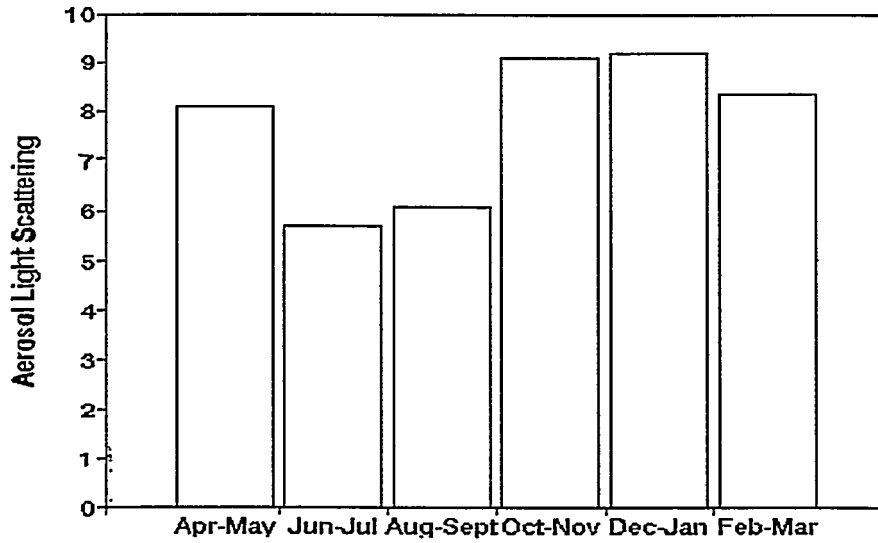

Fig.2 Mean aerosol light scattering measured at Akademgorodok in different seasons.

Formation of Cloud Droplets - The indirect effect

The radiative properties of clouds (the optical depth and the single scattering albedo) depend on their liquid water content and droplet size distribution (e.g. Twomey, 1977). The formation of cloud droplets occurs on pre-existing aerosol particles. The pre-existing particle distribution therefore strongly affects the developing cloud droplet distribution. Field experiments show that usually the pre-existing aerosol particle distribution is composed of particles which include both hygroscopic and insoluble components (Zhang et al., 1993; Svenningsson et al., 1992, 1994).

According to our recent simulations the soluble mass of pre-existing aerosol particles, together with growth dynamics, are the most important factors influencing the activation process (Korhonen et al., 1995). This is due to the fact that hygroscopic material lowers the saturation vapour pressure of water vapour above the surface of a solution droplet and therefore makes the formation of a cloud droplet more likely.

Increasing amounts of sulphur compounds in the atmosphere may lead to an increase in the amount of sulphuric acid and ammonium sulphate particles. This may lead to increased cloud droplet concentrations (see, for example, Charlson et al. 1992; Charlson and Wigley, 1994). We have studied an additional mechanism whereby condensing gaseous pollutants (nitric acid in our example) could influence the number concentration of cloud droplets due to the increased amount of hygroscopic matter in the developing cloud condensation nuclei (Kulmala et al. 1993; 1995a).

Measurements have shown that there is a close nonlinear relationship between the cloud droplet size distribution and the presence of atmospheric pollutants (e.g. Leaitch et al., 1992). Some studies, based on satellite measurements, find higher albedos from the polluted areas of the United States and Asia (see Kim and Chess, 1993) as one might expect, while some other studies find no changes in the albedo of clouds in the northern hemisphere (see e.g. Schwartz, 1988). Thus, it is evident that we do not understand the relationship between air pollutants, the formation of aerosol particles and cloud droplets, and the atmospheric radiative balance and climate sufficiently.

References

Charlson R.J., Langner J., Rodhe H., Leovy C.B. and Warren S.G. (1991). Tellus, 43AB, 152

Charlson R.J., Schwartz S.E., Hales J.M., Chess R.D., Coakley Jr. J.A., Hansen J.E. and Hofmann D.J. (1992). Science, 255, 423

Charlson R.J. and Wigley T.M.L. (1994). Scientific American, 2, 48

Coffmann D.J. and Hegg D.A. (1995). J. Geophys. Res., 100, 7147

Countess R.J. and Heicklen J. (1973). J. Phys. Chem., 77, 444

Curry J.A. (1995). Interactions among aerosols, clouds and climate of the Artic Ocean. *The Science of the Total Environment* (in press).

Girshick S.L. and Chiu C.P. (1990). *J. Chem. Phys.*, **93**, 1273.

Hartmann D.L. and Doelling D. (1991). *J. Geophys. Res.*, **96**, 869

Henry J.F., Gonzales A. and Peters L.K. (1983). *Aerosol Science and Technology*, **2**, 321

Hoppel W.A., Frick G.M., Fitzgerald J.W. and Larson R.E. (1994). *J. Geophys. Res.*, **99**, 14443

Kim Y. and Chess R.D. (1993). *J. Geophys. Res.*, **98**, 14883

Korhonen P., Kulmala M., Hansson H.-C., Svenningsson I.B. and Rusko N., (1995). Hygroscopicity of pre-existing particle distribution and formation of cloud droplets: A model study. Submitted to *Atmos. Res.*

Kulmala M., Laaksonen A., Korhonen P., Vesala T., Ahonen T. and Barrett J.C. (1993). *J. Geophys. Res.*, **98**, 22949

Kulmala M., Korhonen P., Laaksonen A., Vesala T. (1995a). *Geophys. Res. Lett.*, **22**, 239

Kulmala M, Kerminen V.-M. and Laaksonen A. (1995b). *Atmospheric Environment*, **29**, 377

Kulmala M., Mäkelä J., Choularton, T.W., Wiedensohler A. and Hansson H.-C. (1995c). To be presented in European Aerosol Conference, Helsinki.

Leaitch W.R., Isaac G.A., Strapp J.W., Banic C.M., and Wiebe H.A. (1992). *J. Geophys. Res.*, **97**, 2463

Raes F., and Van Dingenen R. (1992). *J. Geophys. Res.*, **97**, 12901

Russell L.M., Pandis S.N. and Seinfeld J.H. (1994). *J. Geophys. Res.*, **99**, 20989

Schwartz S.E. (1988). *Nature*, **336**, 441

Seinfeld J.H. (1986). *Atmospheric Chemistry and Physics of Air Pollution.* John Wiley & Sons, New York

Svenningsson I.B., Hansson H.-C. Wiedensohler A., Ogren J.A., Noone K.J.and Hallberg A. (1992). *Tellus*, **44B**, 556

Svenningsson B., Hansson H.-C., Wiedensohler A., Noone K., Ogren J., Hallberg A. and Colvile R. (1994). *J. Atmos. Chem.*, **19**, 129

Twomey S. (1977). *Atmospheric aerosols*, Elsevier, Holland.

Wyslouzil, B.E., Seinfeld, J.H, Flagan, R.C, and Okuyama, K. (1991). *J. Chem. Phys.*, **94**, 6842

Zhang X.Q., McMurry P.H., Hering S.V. and Casuccio G.S. (1993). *Atm. Env.*, **27A**, 1593

The Estimation of Methane and N_2O Emissions from Agricultural Soils in China

Li Yue Lin Erda Dong Hongmin

Agrometeorology Institute, Chinese Academy of Agricultural Sciences
30 Baishiqiao Road, Beijing 100081, China

Introduction

Both methane and N_2O are important greenhouse gases. The concentrations of these two gases in atmosphere are increasing because of human activities. During 1989-1990, the increase rate of methane and N_2O were 0.80% and 0.25%, respectively(Paul J. Crutzen). The contributions of methane and N_2O to future global warming account for about 18% and 5%, respectively (IPCC 1990).

Agricultural system is an important sector to influence global climate change. It was reported that 60 Tg of methane was emitted from world rice field and 0.05-4.7 Tg N_2O from cultivated soils(Watson et al., 1992). In this paper, the methane emission from China's rice fields and N_2O emission from agricultural soils were estimated.

Review of the methodologies for estimating methane emission from rice fields

In this paper, the methodologies for estimating methane emission from paddies, especially the methodology recommended by IPCC(1993) were reviewed. It is believed that there are too many factors to be considered in the IPCC methodology(1993). It is difficult to be used in China. If the effect of fertilizer on methane emission is considered in the estimation, the statistical data of planting area under different fertilizer conditions will be necessarily available. But anyway, these data will be impossible to be obtained since the fertilizer application varies greatly from place to place in China. So we proposed a simple methodology to estimate methane emission from China's rice fields.

Methane emissions from China's rice fields

In China, It was divided into six rice planting regions according to the climatic

ecological conditions (sunshine , temperature, precipitation, humidity) and geographic biological conditions (topography, soil type and so on).

1. Double *indica* rice in South China
2. Single or double *indica* rice and *japonica* rice in Middle China
3. Indica rice and *japonica* rice in Southwest China
4. Single *japonica* rice in North China
5. Early-maturing rice in Northeast China
6. *Japonica* rice in Northwest China

Middle China, South China and Southwest China are main rice producing regions. The planting area in these three parts accounts for about 93% in 1990.

Based on the division, planting pattern, planting area, flooded days and emission fluxes, the methane emission from rice field of each region was estimated as follows:

Table 1 Methane emission from rice field in each region

Regions	Emission		
	Early rice	Late rice	Single rice
1	1.173	1.659	
2	1.471	2.365	
3			2.051
4			0.159
5			0.133
6			0.187

The total methane emissions from China's rice fields was estimated to be 9.198 Tg in 1990.

N₂O emissions from agricultural soils in China

The N_2O emissions from agricultural soils in China was estimated according to the methodology recommended by IPCC (1993). The amount of mineral N, organic N and biological N fixation applied to agricultural soils are included in the formula.

1. The amount of mineral N applied into agricultural soils was 16.502 Tg in 1990
2. Estimation of organic N applied into agricultural soils in 1990

a. N from straw

Based on the grain yields and the ratio of grain to straw, nitrogen content in the straw, we estimated the total N in the straw. The total straw yield was 578.57 Tg and Total N from straw was 3.04 Tg in 1990. Because there was about 50% of straw as fuel in countryside and 20-30 of straw as animal feed, it is assumed that 25% of straw was directly applied into soils. The total N from crop straw applied to agricultural soils was 0.76 Tg.

b. N from animal manure

It is estimated that there was 60-70% of manure to be applied to agricultural soils. In this paper we assumed that there is 65% of manure applied into soils.

According to the statistics on amount of main livestock the amount of excreta and the amount of N in the excreta, the amount of N in the livestock manure was calculated in China to be 11.209 Tg in 1990. There was about 7.286 Tg N from livestock manure applied into agricultural soils.

3. N from biological N-fixation

The planting area of leguminous crops in China was 10.47 million hectares in 1990. The amount N from N-fixation was estimated to be 1.465 Tg.

The N_2O emission from China's agricultural soils was estimated to be 0.094 Tg using the median emission coefficient in 1990.

Mitigation options

This paper presented some mitigation options for reducing methane and N_2O emission from agricultural soils.

Reference

China Agriculture Yearbook, 1991, Agricultural publishing house
Greenhouse Gas Inventory Reference Manual Volume 3, 1993
IPCC 1990 Climate Change: The IPCC Scientific Assessment, Report Prepare for Intergovernmental Panel on Climate Change by Working Group 1, eds. J.T. Houghton, G.J. Jenkins and J.J. Ephraums, Meteorological Office, Bracknell, UK.
Paul J. Crutzen 1994 Non-CO2 Greenhouse Gases Why and How to Control? Proceedings of an international Symposium, Maastricht, The Netherlands, 13-15 December 1993, edited by J.van Ham, L.J.H.M. Janssen and R.J. Swart PP1-16
Waston, R.T., Meira Filho, L.G., Sanhueza, E., Janetos, A., 1992 Greenhouse Gases: Sources and Sinks, from [Houghton, 1992]

Atmospheric integral transparency coefficient: a climatological parameter

Hanno Ohvril[1], Martti Heikinheimo[2], Arvid Skartveit[3], Hilda Teral[1], Margus Arak[1], Jan Asle Olseth[3], Kristina Teral[1], Leila Laitinen[2] and Margus Roll[1]

[1] University of Tartu, Department of Environmental Physics, Ülikooli 18, Tartu, EE2400 Estonia
[2] Finnish Meteorological Institute, Climatology Division, Vuorikatu 24, P.O.B. 503, SF-00101 Helsinki, Finland
[3] University of Bergen, Geophysical Institute, Allegaten 70, 5007 Bergen, Norway

Introduction

Monitoring for climate research requires considerably more details than are contained in the routine meteorological observations used for operational weather forecasting. Special attention should be paid to variables which will assist in the development and improvement of various scale parametrization for climatological models.

One of such parameters is *transparency of the atmosphere* – a primary measure indicating the state of the atmosphere. Long-term time series of transparency allow one quantitatively to assess the variability of turbidity of air and make climatological conclusions in regard to contamination, radiative exchange, cloud formation, solar engineering.

Transparency in turn may be determined in several ways – by visibility of remote objects, by irradiance of calibrated lamps or known natural sources of light. In meteorological practice the sun – despite of its rotation, sunspot cycles, faculae activities – is considered as a quite stable source of light. According to the well known Bouguer law, the ratio between the intensity of direct solar beam S_m at the earth's surface, and S_0 at the top of the atmosphere, easily gives the coefficient of transparency p_m :

$$ p_m = \left(\frac{S_m}{S_0}\right)^{\frac{1}{m}} , \qquad (1) $$

here m is the *relative optical air mass* or simply *air mass*. As S_m and S_0 correspond to broadband, integral solar spectrum, coefficient p_m may be considered as *Atmospheric Integral Transparency Coefficient – AITC*. Due to simplicity of AITC p_m , numerous actinometrists tried from 1920s to introduce it as a character of atmospheric turbidity (Kondratyev 1969). Unfortunately AITC has not found wide use. The difficulties are mainly of two kinds:

1) high quality pyrheliometers used in measuring of direct solar radiation S_m are expensive but vulnerable instruments, their use in automatized measurements always contains risk of damage by precipitation; unfortunately cheap and more robust Actinometers AT50 (developed at the Main Geophysical Observatory in Leningrad), considered to reach acceptable accuracy, are hardly available now;

2) because of the Forbes' effect (caused by the selective spectral attenuation of direct solar radiation in the atmosphere) the AITC depends on solar elevation even in the case of stationary and azimuthally homogeneous atmosphere.

The problem of vulnerability of pyrheliometers needs to be solved by development of instruments better constructed or better protected. Until these kinds of development are available, the solution would be: 1) the manual use of pyrheliometers, 2) measurement of S_m by pyranometers as difference of global and diffuse solar radiation.

Methods to reduce the Forbes' effect were in principal solved in 1960s by Sivkov and Mürk. Methods were upgraded to be more user-friendly by Yevnevich & Savikovskij (1989) and Mürk & Ohvril (1988, 1990). It is generally accepted to reduce the AITC p_m from the actual air mass m to p_2 which corresponds to air mass $m = 2$ (solar elevation $h = 30°$). We have used the next formula of Mürk:

$$p_2 = \left(\frac{2}{m}\right)^{\frac{\log p_m + 0.009}{\log m - 1.848}} \tag{2}$$

Initial databases

In this research data on direct solar radiation during last 30 years were used from 4 meteorological stations:

1) Bergen, Norway, 60°24' N, 5°19' E, 1965-1994; values of S_m were calculated as differences of global and diffuse solar irradiances (Eppley PSP pyranometers); an original method was applied to select cloudless situations (Olseth & Skartveit 1989);

2) Jokioinen, Finland, 60°24' N, 25°41' E, 1967-1991; Ångström pyrheliometers Å130 and Å601 were operated manually;

3) Sodankylä, Finland, 67°22', N, 26°39' E, 1967-1991; silver disk (S182) and Ångström pyrheliometers (Å598) were operated manually;

4) Tiirikoja, Estonia, 58°52' N, 26°58' E, 1956-1994; actinometer AT50 was operated manually or by solar tracker.

Months November, December and January were absent in Finnish and Norwegian data; the year 1985 was not entirely used at Estonian station Tiirikoja.

Results and discussion

In Fig 1 all measured at Tiirikoja from 1975 to June 1994 instant values of p_2 are presented. In total 3774 points demonstrate a great variability of AITC.
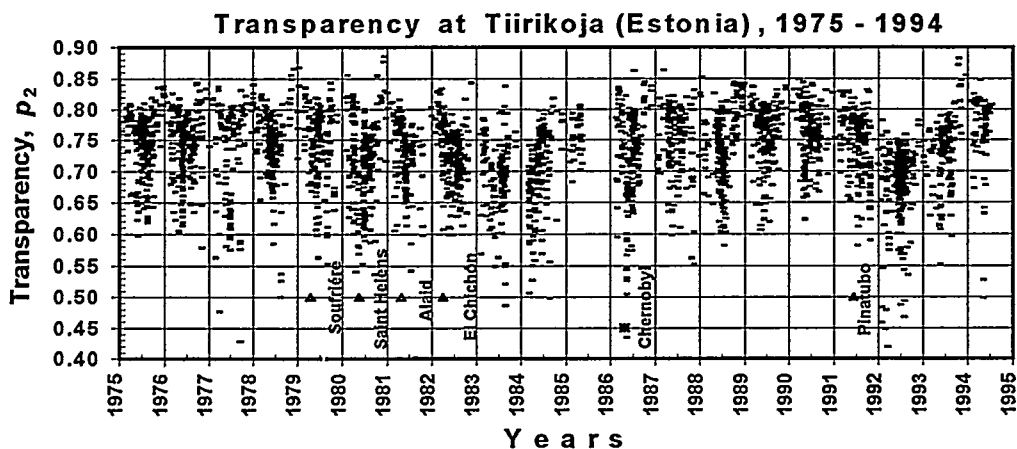
Fig 1 Instant values of AITC at Tiirikoja during 1975-1994, ▲ - greatest volcanic eruptions, ■ - Chernobyl accident.

Nevertheless, averaging over days, months and years, certain regularities in variability of transparency may be revealed (Fig. 2). The diminishing trend of AITC until 1984 and correlation with volcanic eruptions (especially with eruptions during 1979-1982 and eruption of Pinatubo in 1991) are evident. Correlation with Chernobyl accident needs additional analysis.
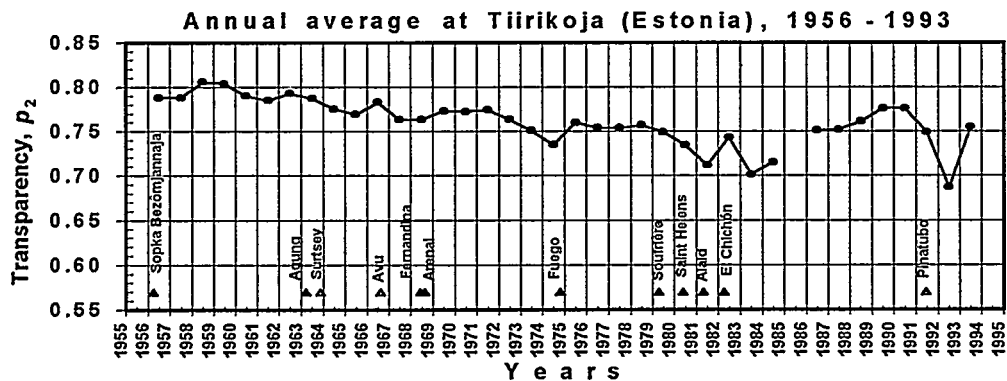
Fig. 2 Mean annual values of AITC at Tiirikoja (the year 1985 is not presented),
▲ - greatest volcanic eruptions.

Average station values of AITC were calculated for each calendar month (by weighting with the number of analyzed days), which enabled us to study the seasonal cycle in great detail. Annual courses of monthly values of transparency are quite similar at all stations under consideration (Fig. 3-6). The lowest transparency one meets during summer, which is typical at middle and temperate latitudes. In August water vapor content starts to decrease, rains wash dust from the lower atmosphere — and AITC starts to increase. The clearest air is at Sodankylä which is the northernmost station of considered ones. Even during summer the long-term average of p_2 is higher than 0.76 at Sodankylä. The most turbid air is at Tiirikoja where the long-term average

al. (1987, 1990). It is based on the NASA/GISS GCM (Hansen et al., 1983; Rind et al., 1988). CTM21 and it has a global domain and a horizontal resolution of 7.8° in latitude and 10° in longitude. In the vertical, there are 21 layers, and the top is fixed at the level of 0.002 hPa (about 91 km). The nine lowest layers use σ as the vertical coordinate. Constant pressure coordinates are used above. The model domain is depicted in Fig. 1. The formal grid-point resolution is considerably better in practice, due to the applied SOM-advection technique (Prather, 1986).

CTM21 uses realistic meteorology from NASA/GISS GCM (Rind et al. 1988). Chemical model runs with CTM21 are initialised with modelled 2-dimensional chemical fields. Photodissociation rates have been calculated according Isaksen et al. (1977) and Jonson and Isaksen (1991).
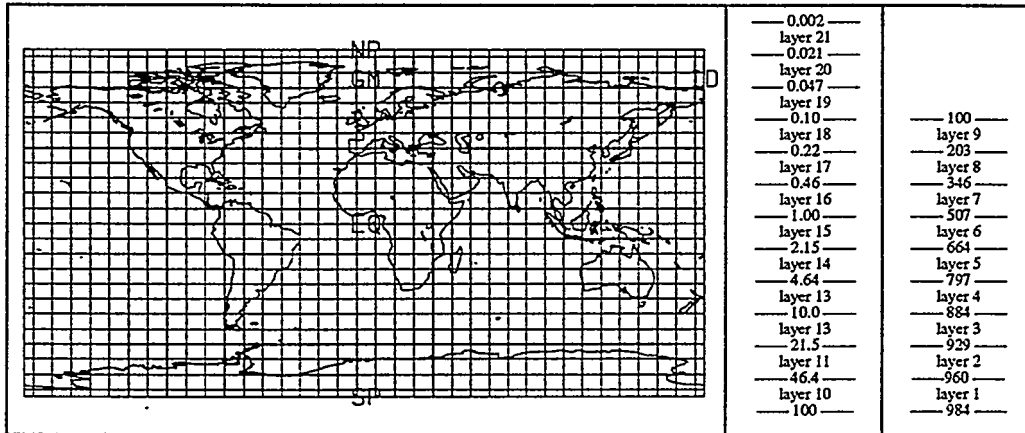
Fig.1. CTM21 model structure: Horizontal grid, upper levels, and σ-levels corresponding to surface pressure of 984 hPa. Layer edges are in [hPa].

Simulations have been done to test the transport characteristics and the numerical interface between model chemistry and transport routines. For example, CTM21 has been run for two years with the three long-lived chemical species of CFC-11, CFC-12 and N2O, parameterised sources and a simple photochemistry. These species have ground-level sources and their removal is dominated by photodissociation in the middle atmosphere. In order to separate chemical effects from pure advection, similarly initialised inert tracers were also run in the simulation.

Results

The three modelled species all show the same general behavior. Results are shown for CFC-12. In Fig. 2a, the zonally averaged initial distribution of CFC-12 is given. In Fig. 2b, the corresponding field is shown for the end of the run for CFC-12, treated as an inert tracer, whereas the final state for CFC-12 with photodissociation is given in Fig. 2c. The effects of photodissociation are visible in Fig. 2c. There has been an overall increase in the global amount of CFC-12 but no pronounced spreading over the model domain, indicating that the photodissociation sink is of the right order of

magnitude and suggesting that the transport in the model is realistic. These modelled
results compare well with measured vertical distributions of CFC-12 in 1991-92
(Schmidt et al., 1994), given that CTM21 operates with climatological meteorology.
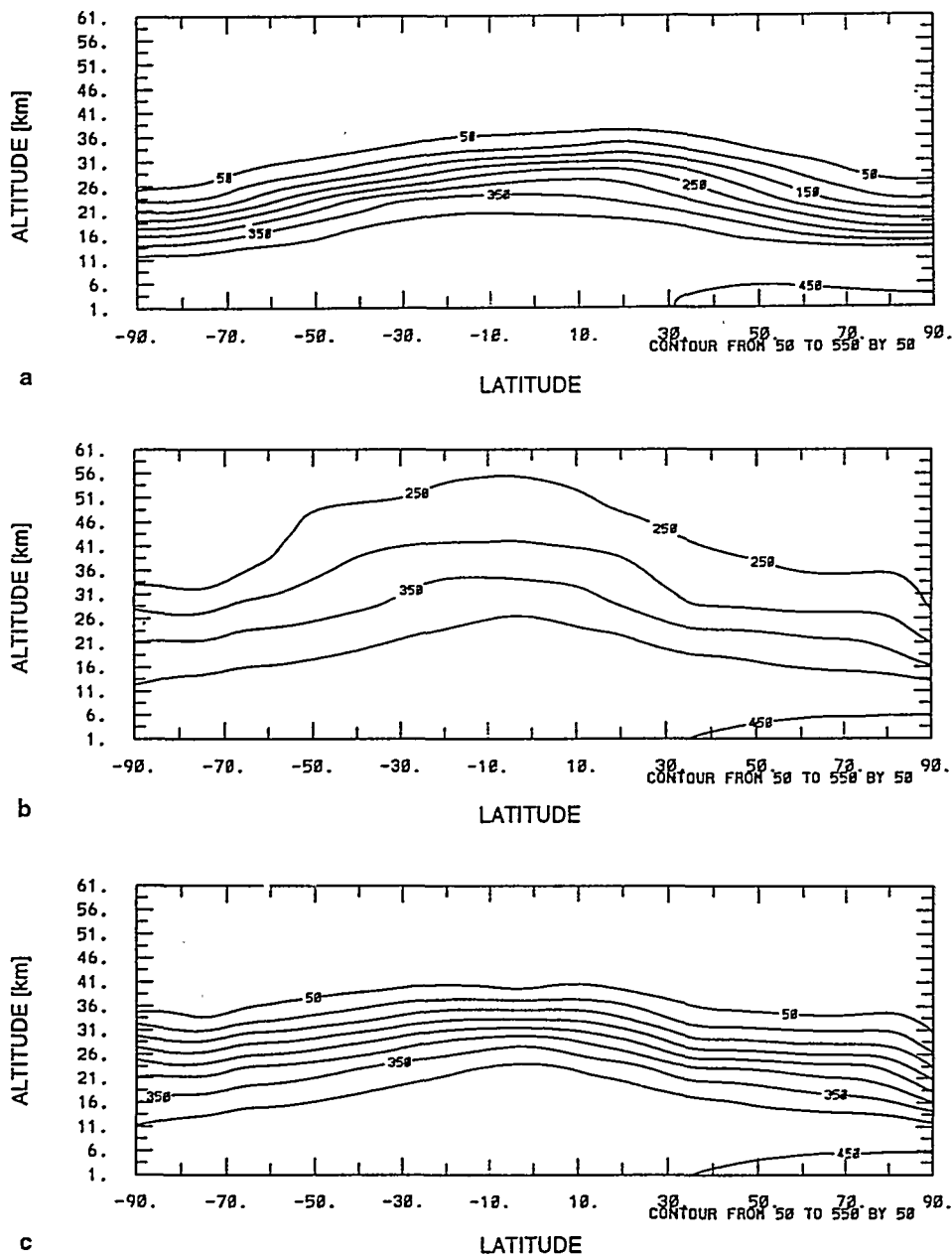
Fig. 2 CFC-12 [pptv] in a) the beginning of a two year simulation with CTM21, and in the
end of the simulation, b) run as an inert tracer, c) run with photodissociation.

Synoptic weather observations and global, diffuse and reflected solar radiation observations are performed at all stations. Several decades of meteorological sounding observations are available from Jokioinen, Tikkakoski and Sodankylä stations.

Following modelling tools/data are in use at FMI at present:

*ECMWF global meteorological analysis fields: 3-d trajectories, potential vorticity & temperature data
*UVSPEC & UVDOSE radiative transfer models
*NCAR 2-d chemistry/dynamics model

Co-operation with NCAR and with the Univ. of Oslo in the field of modelling of stratospheric chemistry/dynamics may lead to use of additional models at FMI.

Data from other sources are also used at FMI: UARS & TOMS records of NASA and old total ozone records back to the 1930's.

Stratospheric Climatology

Stratospheric meteorology is highly controlling the variations of regional ozone distribution as well as the chemical ozone loss processes. The meteorological sounding observations performed since early 1960's at Jokioinen (1961-) and at Sodankylä (1965-) in Finland have been analysed. At both stations cooling of lower stratosphere and warming of lower and middle troposphere has been detected during 1961-93. The stratospheric cooling has been strongest in January, e.g. 4.75 K during 1965-93 at Sodankylä. The cooling has increased the possibility to detect temperatures below 195 K, which may have led to enhanced formation of polar stratospheric clouds in the European Arctic.

Stratospheric ozone anomalies at high latitudes 1988-95

A strong decline of lower stratospheric ozone has been detected at high latitudes of both hemispheres. At 64 S, Marambio a negative trend of -11 % has been observed during 1988-1994. At 67 N, Sodankyla, the trend has been -12 %. At Northern Hemisphere the trend is closely related to unusually low lower stratospheric ozone concentrations during 1992-95.

In the Arctic major part of stratospheric ozone deviations are observed outside the polar vortex, whereas at Antarctica the major ozone anomalies are related to chemically induced ozone loss inside the polar vortex.

The morphology of stratospheric ozone deviations in the Arctic and at Antarctica and their meteorological background will be presented. It may be concluded that additional information about lower stratospheric/upper tropospheric ozone and its precursors are needed for better understanding of the ozone deviations observed in the Northern Hemisphere during recent years.

The effect of ozone variations on UV-B radiation

The regional intensity of solar UV-B radiation is controlled by the solar zenith angle, cloudiness, surface albedo/geometry and the vertical distribution of ozone, aerosols, SO_2 and NO_2. Although ozone loss has been a major factor behind interest towards UV radiation research, its role has sometimes been overestimated.

The Antarctic ozone may have led to occasional doubling of the intensity of solar UV-B radiation according to model calculations made for the 64 S latitude. The highest UV-B doses at 64 S have exceeded those of subtropics (30 S).

In the Arctic the largest ozone deviations have been observed during winter-early spring. The role of those deviations for the annual UV-B dose are often rather small, although relative UV-B changes may be large. More important are the intensified UV-B doses related to ozone deviations during late spring and summer. Observed ozone and UV-B records will be presented, as well as modelled UV-B doses at both hemispheres.

The future levels of solar UV-B radiation are partly linked to the future development of atmospheric ozone content. A worst-case UV-B scenario, as based on the CO_2 doubling scenario by Austin et al. (1992) is used as an example to demonstrate the risks of atmospheric CO_2 increase for the Arctic.

Tropospheric ozone at high latitudes

The ozone sounding programmes carried out at Sodankylä, European Arctic and at Marambio, Antarctic Peninsula are interesting for tropospheric ozone research, since no previous routine ozone sounding programmes have been carried out at these regions.

Influences of European emissions on the lower tropospheric ozone profiles have been detected. Advection of NO_x/HC-rich airmasses from the major European source areas during photochemically favourable weather conditions has led to detection of high ozone concentration in about 2 km thick layers close to the ground. On the other hand ozone-

- annual variation, e.g. of monthly means and their standard deviations (MOHP: March: high mean value and high standard deviation; July: monthly mean equal to annual mean, lowest variation, which is double the ten year trend reduction).
- day to day ozone variations: "Miniholes" are strong decreases of total ozone within 5 to 7 days (e.g. MOHP: 1.-8.2.90 from 340 to 220DU or - 32% total ozone).

There is a big contrast between the actual long term trend in ten years and „normal" variation within some days, and annual variation of monthly means. How is it possible that biological systems cope with values resulting from 60 -100 DU below the mean, but the trend reduction of 1 DU per year is expected to cause significant extra harm?

Biological damage related to ozone depletion is caused through changing UV radiation, ozone effects are therefore modified by the local insolation conditions.

IV. Biological UV damage: ozone variation and trend effect

Action spectra or biological weighting functions quantify the spectral sensitivity of a biological (damage) reaction to radiation. Ozone changes the spectral composition of UV radiation. Action spectra translate such spectral changes of UV in biological quantities: dose rates (i.e. integrals of biologically weighted spectral irradiances). Biological damage is taken to be determined by the product of dose rate and corresponding exposure time. Time integrals of dose rates are taken to determine damage. We want to show changes in dose rates, due to the ozone variations and trend.

Ozone variations and trend effects for dose rates (MOHP data):

- Ozone trend depletion increases by 4.5% in 10 years the mean July noon dose rate for erythema.
- Standard deviation for July (two times the trend) indicates, that even the trend mean values in 20 years have been 'regular events' up to now.
- If day to day changes are considered: Miniholes cover 104% jumps of effective noon dose rates within 7 days in February and 25% jumps in July.

The relative effect of ozone variations depends on insolation conditions and weighting function. The value of 104% for erythema translates into a value of 140% for a DNA action spectrum.

In the face of this, the ozone trend value has to be taken as only one way to describe the changing ozone layer. We ask for experiments that prove, whether the trend based calculation, based on action spectra, is useful for the prediction of the biological damage, caused by man-made ozone destruction.

V. Experiments with artificial UV

The main problem for experiments with artificial UV is the knowledge of the action spectrum of the reaction at question. For such experiments exposure times have to be calculated as the ratio of natural (present or future) effective daily dose and effective dose rate for the artificial UV source. Dose and dose rate calculated with the spectral sensitivity of the reaction at question. Only then the spectral difference between natural and artificial UV radiation is adequately considered.

To show the importance of this consideration, we calculated exposure times for a UV lamp (Philips TL12, with UVC foil, which is very common in biological experiments) and for an elaborate light plant (Seckmeyer, 1993, Thiel, 1993) and mean July conditions.

Action Spectrum	UV-Lamp	Light Plant
Parsley (Wellmann)	18h	22h
Erythema (McKinley)	3h	17h
DNA (Tevini)	1h	23h
DNA (Madronich)	2h	25h

Tab.1: Exposure times for different action spectra, calculated as ratio of July daily dose and dose rate for two laboratory UV spectra.

Considerable differences result from action spectra as well as from the light sources. A change of 100% in exposure time can result from the use of two alternative DNA spectra from literature (see UV lamp times). Only parsley gives similar exposure times for both UV sources (it has a low UV sensitivity).

This tabular illustrates a fundamental problem for UV sensitive reactions: Realistic exposure times (<<24) for future conditions are created with unrealistically high short wave UV. This leads to a strong dependence of exposure time on the spectral sensitivity of the reaction (see exposure times for the UV lamp). Controls for experiments with artificial UV are thus necessary to test results against the influence of spectral differences between natural and artificial UV.

VI. Conclusion

Trend Arguments: At present biological damage predictions are burdened with uncertainties about the correct spectral sensitivity and the question, if ozone trend is the relevant aspect of changing UV radiation. On this background, the positive arguments for (exclusively) trend based predictions will be shortly discussed:

1. Argument for trend based prediction: Organisms simple integrate dose rates over the total exposure time. That is, the integration over all actual conditions would give the same total value as the simple trend calculations. This would correspond to the general dependence of biological damage on total dose, and never on dose pattern.

Research on UV induced human carcinoma proposes both possibilities, the first for basal cell carcinoma the second for melanoma. This means, that the relevance of overall trend calculations is possible, but it has to be (specially) tested for the prediction of each damage reaction.

2. Argument for trend based prediction: Trend calculations correspond (roughly) to observable damages, because the action spectrum involved, describes (roughly) an overall effect: the action spectrum represents a mean or long term action spectrum. This is an approach behind so called 'generalized action' spectra.

Action spectra raw data are low resolution data, the DNA spectra for Tab. 1 are different approximations of the Setlow DNA data (Setlow ,74). Even rough estimates of the consequences of moving data points in action spectra are very difficult to perform: Exposure times for UV experiments were shown to be eventually very sensitive to spectral differences (compare parsley and the two DNA times). Differences in noon dose rates for the DNA versions and spring cover almost 100%.

Any construction of mean action spectra out of similar looking action spectra has to be performed in the face of the of resulting dose rate, dose and RAF value effects.

Experiments with Artificial UV Sources and Future Ozone Conditions:

Control Experiments: In the face of the demonstrated uncertainty and unknown relevance of ozone variation it is necessary to ask the organism, if the presumed normal conditions are realistic for the reaction at question and for a present or future atmosphere. One has to ask, if all, but ozone conditions are normal for the organism or reaction. Radiation conditions have to be proven suitable for predictions, to do this, control experiments have to be performed:

- with identical spectral radiation, but
- exposure times for non reduced ozone conditions

Controls should yield the same reactions as natural non reduced UV. Mean conditions might be adequate for non reduced ozone conditions.

This, of course, is not sufficient to prove whether a biological effect gives realistic data for a prediction (on the radiation level), but it is a necessary condition for such experiments: it is a prove that the spectral differences and variation differences have not dominated the results.

Controls, which use filters to eliminate the UVB part of experimental UV radiation are not adequate to prove experimental results as relevant for future ozone conditions.

Acknowledgment:

References:

Claude, H. (1994): Ozonbulletin des Deutschen Wetterdienstes Nr.12. in DWD Abteilung Forschung: Arbeitsergebnisse Nr24, Offenbach.

Köhler,U., W.Vandersee (1995): Total Ozone data kindly provided.

Madronich, S. (1994). DNA spectrum kindly provided. This spectrum is used in Madronich (1991).

Madronich, S., L.O. Björn, M. Ilyas and M.M. Caldwell (1991). Changes in biologically active ultraviolet radiation reaching the earth's surface in environmental effects of zone depletion 1991 update, in United Nations Environment Programme, Nairobi, 1991, pp. 1-13.

McKinlay, A.F., B.L. Diffey (1987): A reference action spectrum for ultraviolet induced erythema in human skin. Comparison Internationale de l'Eclairage (CIE)-J. 6, 17-22.

Setlow, R.B. (1974). The wavelength in sunlight effective in producing skin cancer: A theoretical analysis. In: Proceedings of the National Academy of Science, 71, pp. 3363-3366.

Seckmeyer, G. and H.-D. Payer (1993): A new sunlight simulator for ecological research on plants. J. Photochem. B: Biol. 21, 175-181.

Tevini, M., J. Braun, G. Fieser, U. Mark, J. Ros, M. Saile. Effekte solarer und künstlicher UVB-Strahlung auf Wachstum, Funktion und Zusammensetzung von Nutzpflanzen. GSF Forschungsberichte 5/90, S. 30.

Thiel, S. (1993): Messung strahlungsphysikalischer Eigenschaften eines Sonnensimulators. Diplomarbeit Sektion Physik, L.M. Universität München.

Wellmann, E. (1983): UV-radiation in photomorphongenesis. In: Encyclopedia of plant physiology. Vol. 16, 745-756. Springer Verlag, Berlin, Heidelberg.

Total ozone measurements with a laboratory spectrometer in Estonia

U. Veismann, T. Kübarsepp, K. Eerme, M. Pehk

Institute of Astrophysics and Atmospheric Physics,
EE2444 Tõravere, Estonia

The standard instruments presently used to measure atmospheric total ozone are the Dobson and Brewer spectrometers. These instruments are too expensive for newly independent countries and it is necessary to search for more acceptable possibilities. For ultraviolet radiation spectra analysis and future UV-B radiation monitoring at ground level the spectro-radiometric equipment is still preferred.

The instrument used in this study is a commercially available laboratory spectrometer designed at LOMO (St. Petersburg). The optical configuration consists of a double monochromator with changeable gratings, concave mirrors and objective lens input optics and a photomultiplier tube detector with amplifier. The characteristics of the spectrometer are the following:

diffraction gratings	1200 mm^{-1},
max. energy concentration	300 nm,
linear dispersion	1.25 mm/nm,
spectral interval	300-340 nm.
scanning rate	20 nm/min,

A coelostat device for Sun tracking was built at the institute. PMT FEU-39A with bialkali photocathode was used (today replaced with solar blind PMT FEU-142) as a detector. An IBM PC is used to control the data acquisition, with a 14-bit analogue-to-digital converter (Enari Electronics, Tallinn). Two wavelength markers (0.1 nm and 2.5 nm) are built in spectrometer drive. The instrument spectral response is calibrated using the Optronics 1000 W standard lamp DXW. The instrument has been tested for stray light, non-linearity of response, wavelength repeatability and accuracy as well as radiometric stability. The

experimental bandwidth is 1 nm (FWHM), the wavelength accuracy is more than 0.3 nm.

For analysing the uncertainty related to the instrumentation setup the data set obtained during 1993-1994 was applied. Preliminary analysis of the uncertainty has revealed that the most critical individual sources of error are the following:

- standard lamp calibration and operating accuracy;
- wavelength scale shift;
- signal noise;
- drift of the system during the scanning of spectra.

The three first sources listed above are of random character, while the fourth is due to systematic error of the measurement method. The total uncertainty of 3 % (1σ) was estimated for regular ozone amount measurements with spectroradiometric apparatus described in the present paper, and does not include the error arising from Dobson's algorithm.

The direct solar spectra measurements as well as the measurements looking at the zenith have been carried out since the spring of 1993 at Tõravere ($58^0 16$'N, $26^0 28$'E). The total time for a scan is about 2 min. The data reduction was made using standard Dobson method. Whereas the full spectra are recorded, it is possible to use the Brewer retrieval algorithm as well as Dobson's. Still there are some uncertainties with instrumental constants for the Brewer's retrieval. The comparatively long recording time of spectra is seriously restricting the use of the cloudy sky measurements. For this reason the winter season is poorly covered with data. Most of the measurements are taken directly from the Sun. During 1994 and early 1995 the data set was collected to check the suitability of these clear zenith sky charts of the European and Canadian Dobson networks with our results. For the values from 325 to 425 DU the agreement is ±7 %. The larger and smaller values have been sporadic. The derivations up to ±20 % of total ozone from the seasonal mean were recorded in the spring and autumn of 1994. The midsummer total ozone behaviour was found to be usual.

ZENITH

SOLAR
RADIATION

SUN
TRACKING
MIRROR

SPECTROMETER
SDL-1

DATA
ACQUISITION
SYSTEM

PMT

LENS

3 3 2 3 3

SCANNING DRIVE

$\Lambda\Lambda$ 2.5 nm

0.1 nm
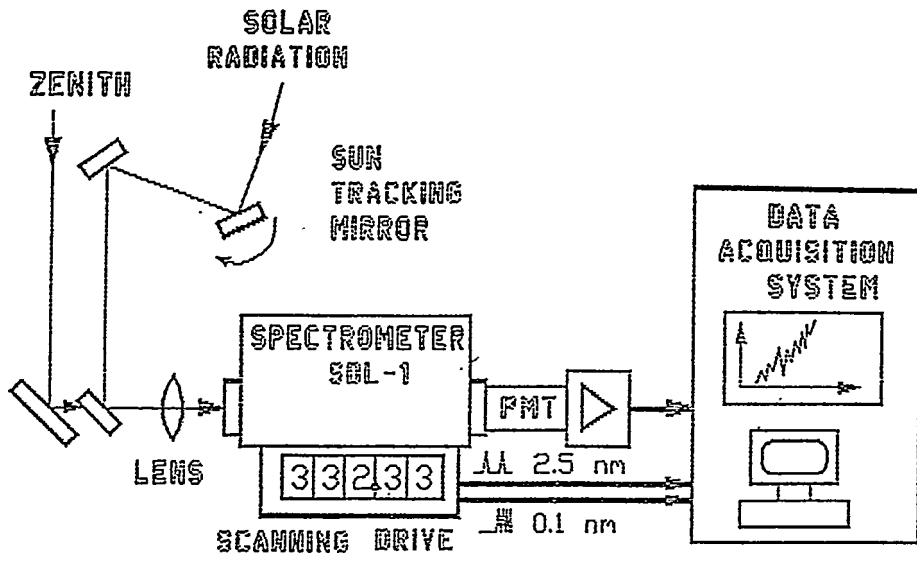
Total ozone in Tôravere
1994

Total ozone (D.U.)

Day number
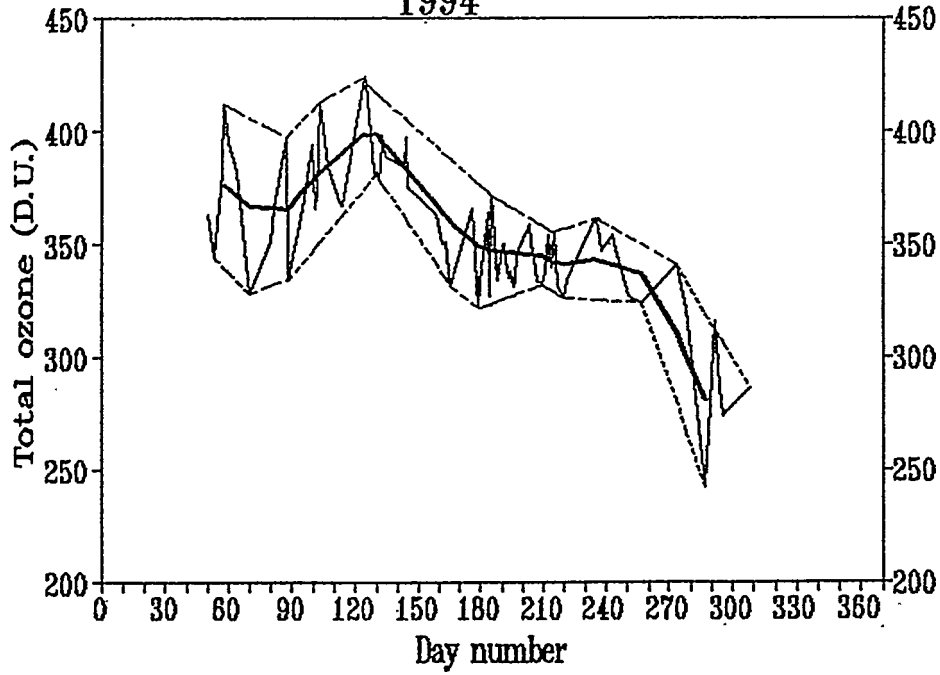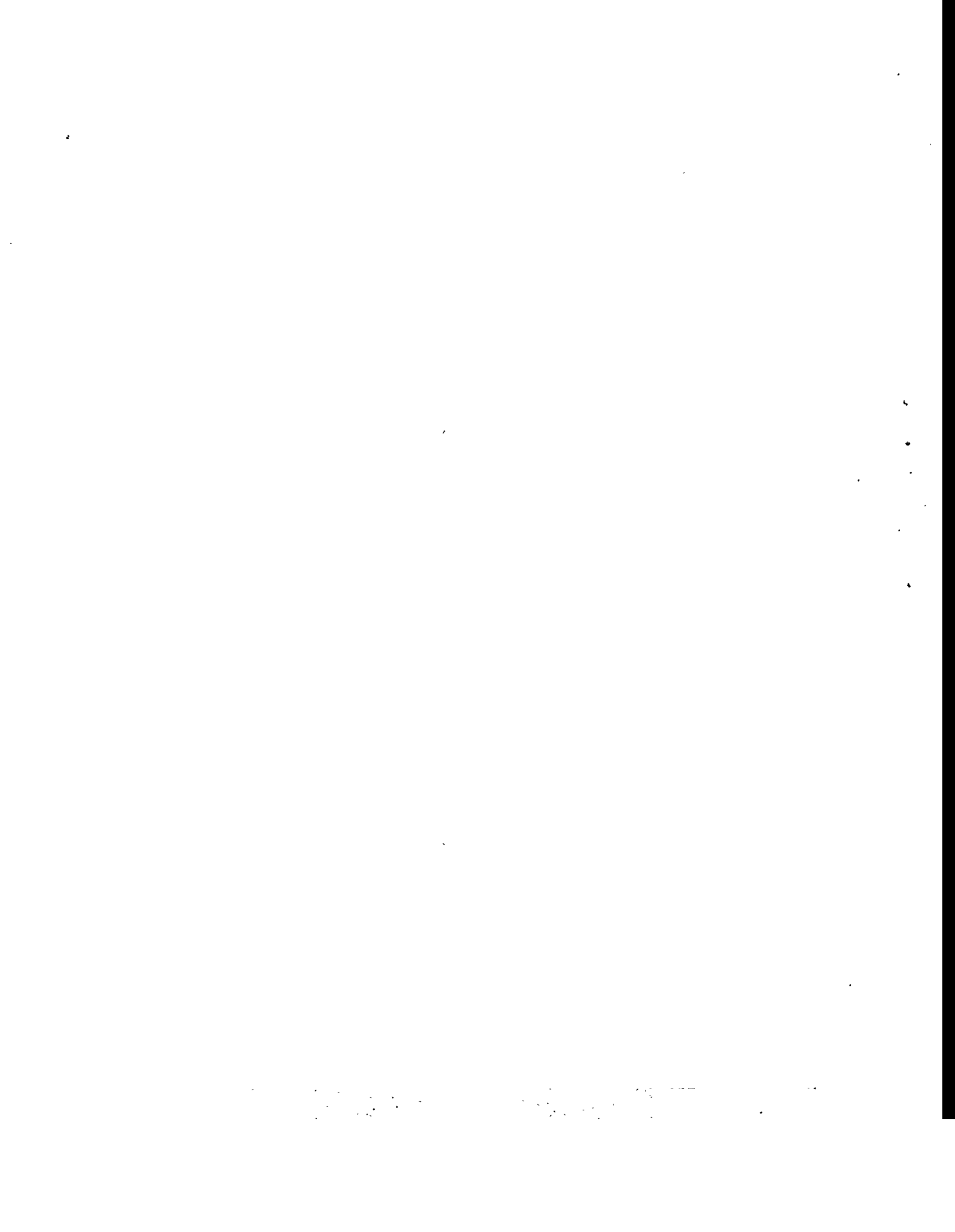
UV radiation
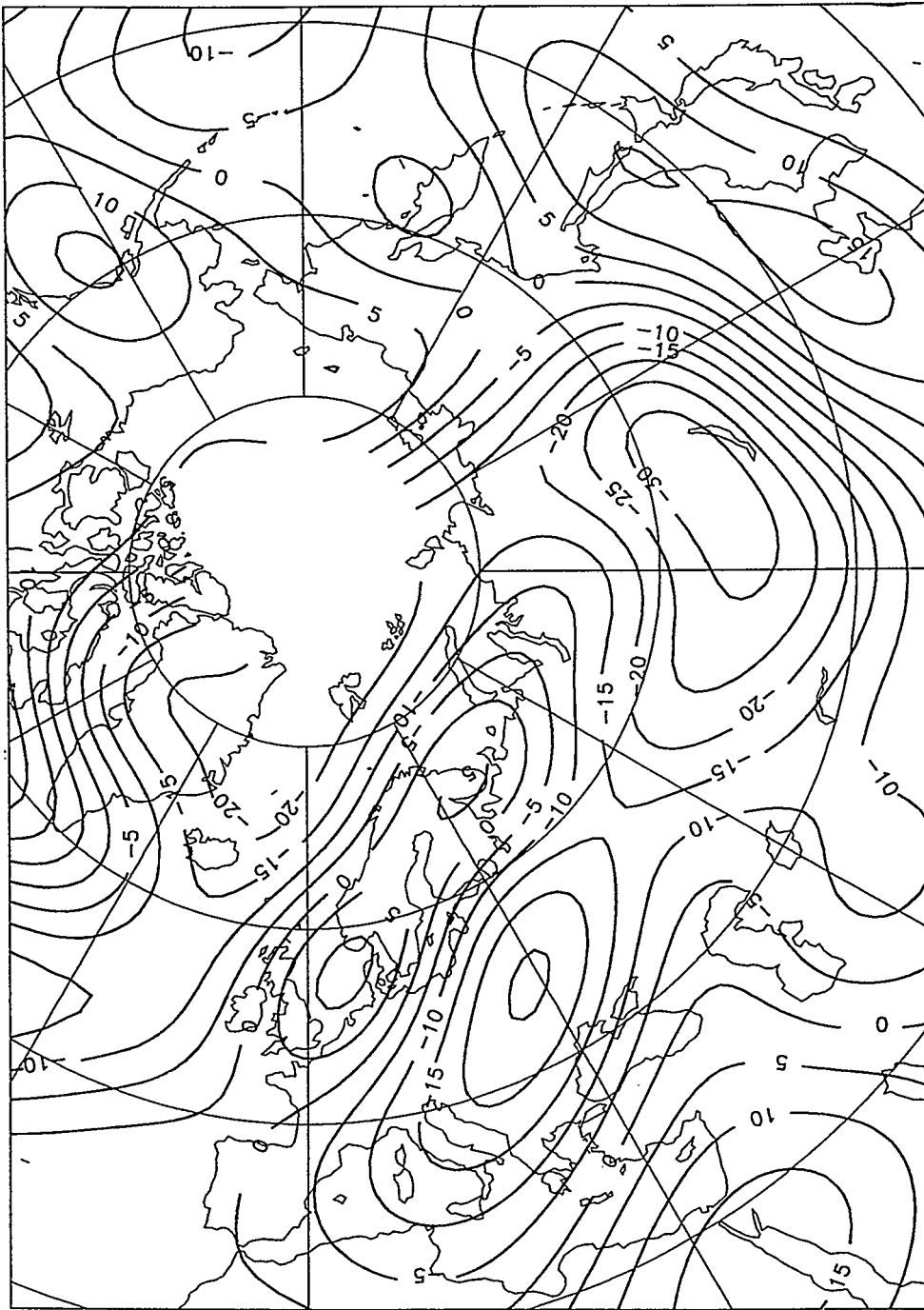
Fig. 1a TOMS/Meteor-3 total ozone values for 12 March 1994, expressed in terms of percent deviations from long-term means. Central Aerological Observatory, Moscow.
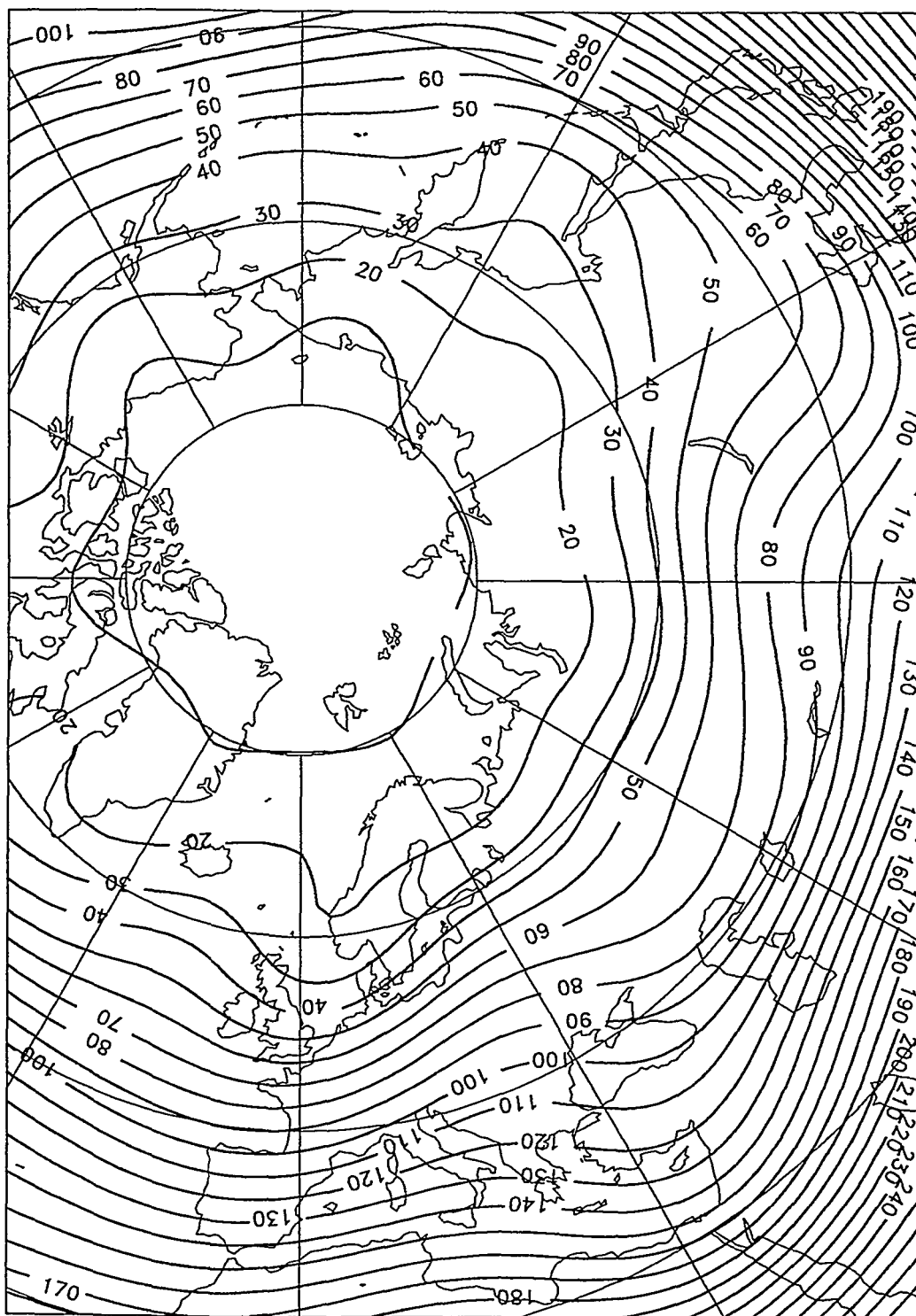
Fig. 1b Noontime erythemal UV levels for 12 March 1994, mWt/m²

observed variations may be attributed mainly to the variations of aerosol optical thickness (see Fig.1a) or may be connected by uncertainties in ozone vertical profiles which can differ in real conditions from model ones. The sharpest relative influence of solar elevation is in the shortwave spectral region (<310nm). Changes of h from 11 to 40 lead to 40-50 times increase of irradiance on 300 nm, and only 4.5-6.5 times on 350nm. This relation expressed in terms of Rp is presented in Table. One can see the growth of Rh to the shorter wavelengths due to strong increase of ozone absorption.

Table. Rh examples for different wavelengths and erithemal radiation (clear sky)

wave	ozone amount	Rh(meas)	Rh(calc)
	BARROW		
l=300 nm		4.4	4.9
l=310 nm	348 D.U.	2.7	2.3
Erithemal radiation (McKinlay & Diffey 1987)		2.1	2.0
	MO MSU		
l=310 nm	351 D.U.	2.1	2.3
l=320 nm		1.3	1.6
l=310 nm	343 D.U.	1.9	2.3
l=320.5 nm		1.2	1.6
Erithemal radiation (McKinlay & Diffey 1987)		1.7	2.0
	SUVS-M		
l=310	313 D.U.	2.6	2.3
l=319.5		2.1	1.6

Ozone influence. There is a strong spectral dependence of UV irradiance on total ozone amount (X). Rx is used to define quantitative characteristics of spectral UV irradiance attenuation. Due to model simulation Rx is shown to decrease (in absolute units) approximately for two times in UVB region with growth of h from 20 to 60; Rx for erithemal radiation changes contrarily due to relative growth of shorter wavelengths with h increasing. Cloud optical thickness as well as aerosol optical thickness variations appear to have a weak effect on Rx values. Figure 1b demonstrates distinct Rx spectral dependence obtained from measurements.

Aerosol influence. A good agreement in relative changes of UV irradiance and aerosol optical thickness (ta) (i.e. Rta) has been obtained both from spectral data and model simulations. According to model calculations for continental type of tropospheric aerosol the typical value of Rta is about -0.11 in UVA spectral region and slightly decreases in the shortest region of spectrum (to Rta=-0.15 at l=300nm). The Rta values evaluated from spectral measurements by spectroradiometer of MO MSU usually found to be in the range -0.12- -0.15 with standard deviation 0.007-0.014.

Albedo influence. Albedo influence was analyzed by comparison of spectral UV irradiance under the snow (QA) and snowless (Q) conditions when UV surface albedo is very low (A=0.01-0.02). Fig.1c shows distinct spectral dependence of

R=QA/Q for both measurements and model data for clear sky conditions with maximum in the spectral range 320-340 nm. In this range of spectrum snow cover can increase UV radiation level by up to 50%. Almost all analyzed data have better compliance with model curve at A=0.95. These high values of snow albedo are possible (Blumthaler & Ambach 1988) for new dry snow.
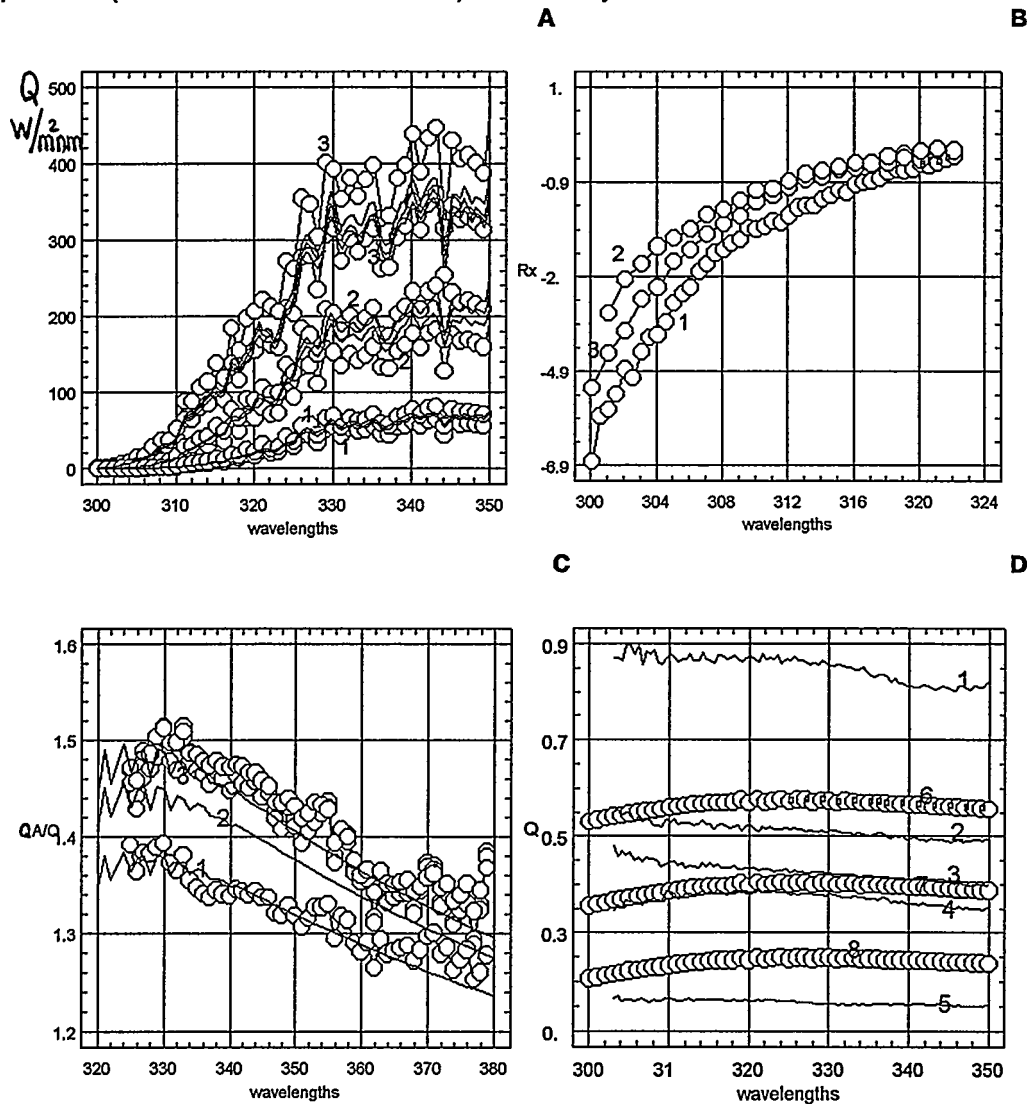
Fig. 1 Comparison of measured and modeled results. A,B,C- clear sky conditions. A. Spectral irradiance at solar elevation: 1 - h=11, 2 - h=24, 3 - h=40. Model simulations with ta(550nm)=0.05 and 0.3. B. Rx spectral dependence, 1,2 - measurements, 3 - model calculation. C. Spectral dependence of R=QA/Q, h=35-37, Barrow. Calculations: 1 - A=0.8, 2 - A=0.9, 3 - A=0.95 (thin lines). D. Cq spectral dependence in conditions with extended low layer cloudiness. Measurements, 10/10 Stratus (1-5), X=325-336 D.U., h=29-31. Model calculations for tcl=10 (6), tcl=20 (7), tcl=40 (8)

Cloud influence. Cloud influence was analyzed by ratio Cq=Q/Q0, where Q is global spectral radiation in cloudy conditions, Q0 is the same but in clear sky. Fig.1d shows the spectral dependence of Cq values obtained from measurements under extended low layer clouds (10/10, Stratus) and from model calculations. There is a slight spectral dependence of Cq values with maximum at 315-325nm decreasing for 3-9% towards 350nm and for 8-23% towards 299nm due to model data. UV losses by clouds change from 20% to more than 80% due to variability of cloud optical thickness.

Conclusions

1. It was shown the possibility of using Rp conception for different atmospheric parameters in their wide range.
2. Agreement was found in Rh and Rta values obtained both from spectral measurements and modeling. Also distinct spectral dependence of Rh and Rx values was evaluated.
3. Snow albedo influence on UV radiation was shown to have distinct spectral dependence with the maximum at 320-340nm; the growth of UV radiation due to fresh snow cover may reach 40 - 50%.
4. According to model calculations and spectral data the slight spectral dependence of extended clouds influence have been obtained. UV losses by clouds may reach 80%.

Acknowledgments

References

Blumthaler M, & Ambach W.1988. Solar UVB-albedo of various surfaces, Photochemistry and Photobiology, v.48, No 1:85-88

Dorokhov, V.M., V.U. Khattatov, T.N. Klimova, A.V. Pankratov, V.A. Torgovichev, 1989. An Automated Spectral Complex for Measurements of Atmospheric Ozone and UV-Radiation. Ozone in the Atmosphere,. A Deepak Pub. Co., Hampton; 766-771

McKinlay A.F. & Diffey B.L.,1987. A reference action spectrum for ultraviolet induced erythema on human skin. - Human exposure to ultraviolet radiation:83-87.

NSF Polar Programs UV Spectroradiometer Network 1991-1992 Operations Report, Biospherical Instruments Inc., 1992

Visotsky A.V. et al. 1982. The developing of instruments for ultraviolet monitoring. Monitoring of background pollution of nature. Gidrometeoizdat Publishing House.

CLOUD INFLUENCE UPON UV RADIATION: RESULTS OF LONG-TERM MEASUREMENTS AND MODELING

Nataly Ye. Chubarova
Meteorological Observatory, Moscow State University, 119899, Russia

Introduction

Ultraviolet radiation (UV) impact on human beings is widely discussed during last decades due to decreasing of ozone levels. Contradicting results of either increase or decrease of UV radiation were shown in (Scotto et all. 1988, Kerr & McElroy 1993). Cloudiness also may be one of the causes of observed discrepancies. Different cloud types and cloud amount can change UV radiation in different way. According to long-term ground measurements of global UV radiation (less than 380nm) and hourly observations of cloudiness in Meteorological Observatory of Moscow State University (MO MSU) the influence of different types of extended clouds and cloud amount on global ultraviolet radiation has been analyzed. UV measurements are carried out in MO MSU since 1968 with the original type of instrument.

The influence of clouds is analyzed by ratio Cq=Q/Q0, where Q is global UV radiation in cloudy conditions, Q0 is the same but in clear sky. Snow and snowless periods are examined separately to take into account the differences between the surface with different albedo.

Results and discussions

Due to model calculation (delta-Eddington scheme) Cq values (in spectral region I<380nm) for extended clouds have been shown to be determined mainly by cloud optical thickness (tcl). Other factors (effective size of cloud droplets, cloud height, aerosol and ozone conditions, etc.) change Cq less than 10% in a reasonable range of their variability. Therefore influence of different extended cloud types on UV radiation is mainly connected with their tcl. Figure 1 demonstrates fitted probability density functions (a,c,d) and histogram (b) of Cq values for upper (a), middle (b) layer clouds and different types of low layer clouds (c,d) in summer and winter conditions.

The effects of UV radiation increasing due to high surface albedo and multiplied reflectance between surface and extended cloud layer can be determined from

13 452844D
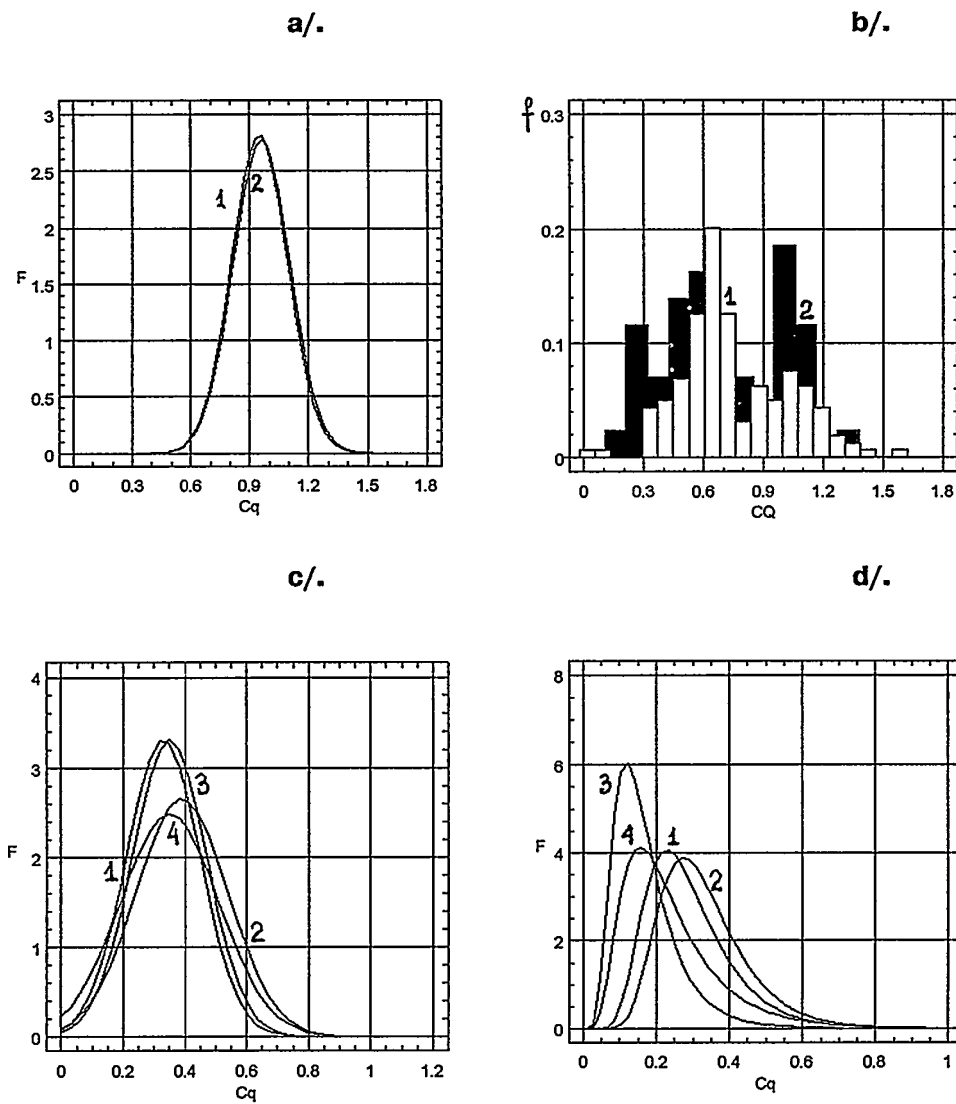
Fig. 1 Probability density functions of Cq values for different extended cloud types. a/ upper layer clouds; 1-winter period, 2-summer period, b/ Histogram of Cq values for middle layer clouds; 1-winter period, 2-summer period, c/ low layer clouds, winter period, 1 - Sc, 2 - St, 3 - Ns, 4 - Cb, d/ low layer clouds, summer period

the following expression obtained by modeling:

$$Q = Q[A=0]/\{1 - A*(0.34 + 0.58*\{1 - Cq[A=0]\})\}, \quad (1)$$

where
A - spatial surface albedo. (In winter it is much lower than measured one in a concrete point at ground due to great influence of "dark" objects: buildings, trees, etc). Effects of UV surface albedo in summer can be neglected. It is clearly seen that snow albedo impacts increases greatly with decreasing of UV transmittance. i.e. with the growth of cloud optical thickness.

Figure 2 demonstrates Cq values dependence on low layer cloud amount N. It differs from the curve (Bais et all.,1993) when N is high and can be approximated by the following expressions:

$$Cq = 1-0.1*N, \qquad \text{for N less 0.3}$$
$$Cq = 1.071-0.34*N, \qquad \text{for N=0.3-0.9}$$
$$Cq = 5.17 - 4.9*N, \qquad \text{for N higher 0.9} \qquad (2)$$

The effects of different amount of upper layer clouds up to N = 1.0 are comparable with the aerosol influence.
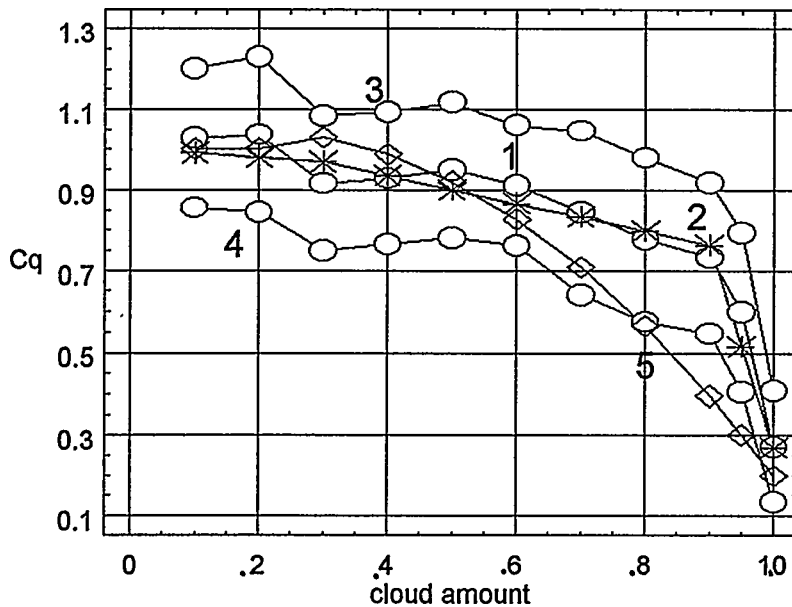
Fig.2 Cq values versus low layer cloud amount. Summer conditions (1981-1990). 1 - mean values, 2 - approximation curve (according to (2)), 3,4 - standard deviation of the above means, 5 - approximation curve from Bais et all.,1993.

According to model simulations a very slight difference in Cq values between I<380nm and erithemal radiation have been obtained. Cq values obtained from measurements by MO MSU instrument (I<380nm) and by Biometer 501 (erithemal radiation) are also compared in various cloudy conditions according to several months of observations. There are small differences between them but in some cases discrepancies can reach 20%; the reason may be in the uncertainties of ozone vertical profiles or amount of cloud layers. We examine Cq peculiarities which may be caused by multi-layer cloudiness. The results are shown in Table. Multi-layer cloudiness has stronger influence on erithemal radiation; the effects increase when upper cloud layers become crystalline (g=0.7).

Table. Multi-layer influence on Cq values in different spectral regions and erithemal radiation (McKinlay & Diffey 1987). (Model simulations, X=300 D.U., subarctic conditions, h=40).

1-Cq(multi)/Cq(one),%	tcl	(I<380 nm)	(I<320 nm)	erithema
g low=g middle=	40	2	10	13
=g upper=0.848	70	4	18	22
g low=g middle =0.848,	40	9	36	24
g upper=0.7	70	12	46	34
g - asymmetry factor of cloud particle				

Conclusions

Great impacts of extended low level clouds on UV radiation have been shown on the base of continuous ground measurements. Simple equations were obtained to take into account effects of surface albedo and cloud amount. Slight spectral dependence have been obtained for different UV integrals. Possible influence of multi-layer cloudiness (especially of crystalline type) on the increasing of spectral Cq distinctions has been demonstrated.

References

Bais A.F., Zerefos C.S., Meleti C., Ziomas I.C., and Tourpali K. 1993. Spectral measurements of solar UVB radiation and its relations to total ozone , SO2, and clouds , J.Geophys.Res., 98(D3):5199-5204.

McKinlay A.F.& Diffey B.L. 1987. A reference action spectrum for ultraviolet induced erythema on human skin. - Human exposure to ultraviolet radiation:83-87.

Scotto J. et al. 1988. Biologically effective Ultraviolet radiation: Surface Measurements in the United States, 1974 to 1985, Science, 239:762-764.

Modeling UV radiation transfer through broken cloudiness and comparison with measurements.

I. V. Geogdzhaev, T. V. Kondranin

Moscow Institute of Physics and Technology
141700, Institutsky per., 9, Dolgoprudny, Moscow Region)

A. N. Rublev

Russian Scientific Center "Kurchatov Institute". Institute of Molecular Physics
123182, Kurchatov sq. 1, Moscow, Russia)

N.E.Chubarova

Meteorological Observatory, Moscow State University
Vorobievy Gory, GSP3, Moscow, 119899, Russia)

Introduction

A significant portion of biologically active ultraviolet (UV) radiation is obtained by living organisms in the broken cloudiness conditions. Horizontal inhomogeneity and statistical variability of broken clouds dramatically affect radiation field. To perform a model study of surface UV levels we had developed an accurate technique to compute shortwave radiation through a stochastic cloud field.

Model of broken cloudiness

The broken (cumulus) cloud field with horizontal dimensions of L^2=50x50 km and the cloud bottom height 1 km is included into stratified plane-parallel clear-sky atmosphere model. We used standard atmosphere model (WMO, 1986), representing subpolar summer and continental and stratospheric aerosol model. Geometrical structure of the broken cloudiness is modeled based on the stochastic Gaussian field $Z(x,y)$, isotropic in the (x,y) plane and bounded from the bottom on a certain level h_0. Zenith cloud amount n_0, mean cloud bottom diameter $\overline{D}$ and cloud form coefficient $k_f = \overline{H}/\overline{D}$, where $\overline{H}$ is mean cloud height serve as input model parameters.

Fig. 1 shows vertical cross-section of the cloud field and the relation between mean field height z_0, truncation level h_0 and the height of the cloud layer H_{bottom}. Cloud aerosol optical properties (phase function, scattering and extinction coefficients) are specified based on the C1 cloud model (Deirmendjan, D. 1969) in all points coordinates (x,y,z) of which satisfy the condition $H_{bottom} < z < Z(x,y)$.

The surface $Z(x,y)$ is represented by a two dimensional spatial Fourier series:

$$Z(x,y) = z_0 + \sum_m \sum_n P_{m,n} \, \exp\left[i\left(\frac{2\pi m}{L}x + \frac{2\pi n}{L}y\right)\right]$$

where coefficients $P_{m,n}$ are independent between each other random numbers having Gaussian distribution with zero mean.
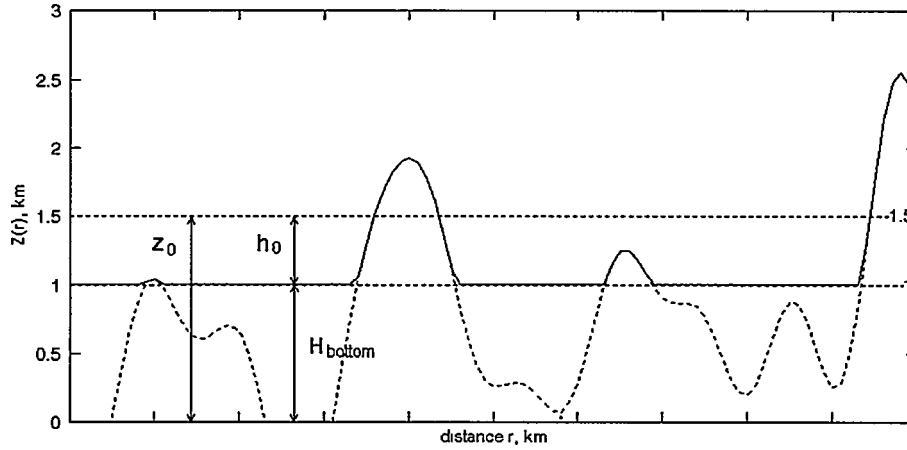
Fig. 1 Vertical cross-section of the random cloud field. The figure demonstrates relation between the mean field height z_0, truncation level h_0 and the height of the cloud layer H_{bottom}.

Since $Z(x,y)$ is a real function, $P_{m,n}=P_{-m,n}$, and the variances of the coefficients $P_{m,n}$ are:

$$\sigma^2_{m,n} = \left(2\pi/L\right)^2\left(1/4\right)W\left(2\pi m/L, 2\pi n/L\right).$$

The function $W(p,q)$ where $p = 2\pi m/L, q = 2\pi n/L$ is related to the correlation function $\eta(\vec{\rho})$ by the Fourier transformation:

$$(p,q) = \sigma_z^2/\pi^2 \int_{-\infty}^{+\infty}\int_{-\infty}^{+\infty}\eta(\rho_x, \rho_y)\exp(-ip\rho_x - iq\rho_y)d\rho_x d\rho_y,$$

where σ_z^2 is the field variance.

Let $\beta = h_0/\sigma_z$, then, since the field is Gaussian, $\beta = \Phi^{-1}(1-n_0)$, where $\Phi(\beta)$ is the probability function.

Let us determine the mean field points height $\overline{h}$ above the truncation level h_0.

$$\overline{h} = (1/n_0)\int_{h_0}^{\infty}(1/\sqrt{2\pi})\exp(-z/\sigma_z^2)(z - h)dz$$

Assuming the approximate equality $\overline{h} \approx \overline{H}/2$, (which becomes exact when, for instance, clouds are assumed to be paraboloids) one can found that

$$\sigma_z = \sqrt{\pi/2}k_f Dn_0/\left[\exp(-\beta^2/2) - \sqrt{2\pi}\beta n_0\right]$$

Taking the correlation function in the form $\eta(\rho) = \exp(-\alpha\rho^2)$ (where α is a constant), which provides for the existence of the mean diameter $\overline{D}$ we obtain

$$(p,q) = (\sigma_z^2/\pi\alpha)\exp(-p^2/4\alpha)\exp(-p^2/4\alpha),$$

and, from the expression for β we have $\alpha = 32(n_0^2/\overline{D}^2)\exp(\beta^2)$

The above equations determine the algorithm of the modeling of random cloud fields in a closed form.

In the simulations described below total of five cloud fields were used calculated for cloud amount $n_0 = 0.1, 0.3,..., 0.9$. Mean cloud diameter changed from 1.2 to 1.55, and the form coefficient was adopted to be from 0.5 to 1.0 based on the (Shmeter, S.M., 1987; Central Aerological Observatory (CAO), 1977). Both mean cloud diameter and form coefficient increase with the cloud amount increasing.

Radiative transfer code.

Spectral and biologically active ultraviolet (UV) irradiances under the broken cloudiness conditions were calculated using Monte Carlo technique. The technique is based on the tracing of the photon trajectories in the atmosphere. It takes into account aerosol (including clouds) scattering and absorption, molecular scattering and ozone absorption, and radiation reflection from the Earth surface.

Two specific modifications of Monte Carlo method for horizontally homogeneous and broken clouds layers are applied to speed up calculations. Spectral irradiance on the Earth's surface $F_\lambda(\theta_0)$ for the sun zenith angle θ_0 is calculated as

$$F_\lambda(\theta_0) = \left\langle \sum_{n=0}^{N} Q_n \exp(-\tau_{\lambda n})\Delta_n \right\rangle, \text{ where}$$

- Q_n is a weighting factor, taking into account photon energetic value;
- $Q_0 = S_\lambda \cos\theta_0$, S_λ is spectral solar constant
- $\tau_{\lambda n}$ absorptive optical depth accumulated alone the photon trajectory
- Δ is an indicator equal 1 if the photon has reached the Earth's surface and zero otherwise.

Results and discussion

Based on the developed approach a numerical investigation of UV surface irradiances dependence under broken cloudiness was made. For that purpose the ratio of surface irradiance in cloudy conditions to that under clear sky C_q was used. In ultraviolet (290 - 400 nm) C_q depends feebly on the wavelength having a small maximum at 310-320 nm and decreasing on the shorter wavelengths due to the stronger ozone absorption. This is similar to the spectral dependence of the surface UV irradiance under overcast cloud layers. The dependence of C_q on the solar height is also small. For example we found that $C_q(350)$ changes by only 5% as the solar height grows from 20° to 50° for the cloud amount 0.5.

Based on model simulations the dependence of global UV irradiance on broken cloud amount was found. It was compared with a similar relationship obtained from experimental long-term measurements of integral global UV radiation shorter 380 nm. The results of the comparison are presented at Fig. 2.

The experimental curve is based on the analysis of measurements of global UV radiation and hourly observations of cloud amount which were carried out at the Meteorological Observatory of Moscow State University (MO MSU) during the period of 10 years (1981-1990). These data sets gave an opportunity to choose the cases when
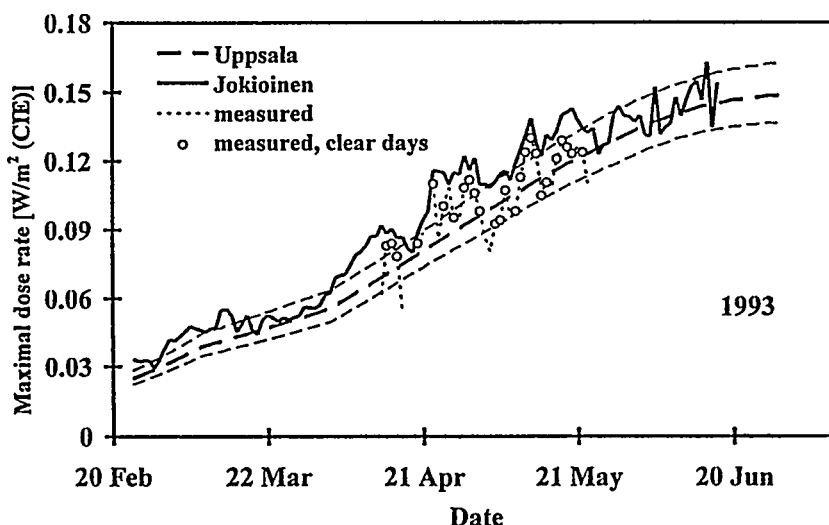
Fig.1 Measured and computed daily maxima of the erythemally effective UV dose rate in Helsinki in spring 1993. The long-term reference curve based on Uppsala ozone data is shown together with the standard deviation of monthly averages represented as thin dashed lines. The circles represent relatively clear days during the measurements. The theoretical clear day curve for 1993 (irregular thick line) was computed using the ozone data from the Meteorological Observatory of Jokioinen.

In spring 1993 the theoretical clear day UV dose rates were considerably above the normal values, in contrast to spring 1994 when there was no increase. In 1993 the theoretical clear day dose rates at noon were on average 17, 25, and 14 % higher in March, April and May, respectively, compared with the long term mean based on the Uppsala ozone. Maximal increase occurred on 23 April when the theoretical increase of the dose rate was 41 %. Measured UV levels increased less than the theoretical levels and even on most clear days the increase was not statistically significant due to the ±11 % uncertainty in the measurements. There were, however, more measured data points above the mean curve, and on some days the significance level of 11 % is exceeded. The maximal measured increase in the dose rate at noon was 34 %, when compared with the Uppsala reference.

To study the combined effects of ozone depletions and snow, erythemal doses (clear day) were computed by varying UV-reflectivity of the ground (Fig.2). To simulate the exposure received by the face the daily doses were computed for vertical surfaces. The lower smooth curve was obtained by using the long term mean of the total ozone values measured in Uppsala (59.9°N, 17.6°N) and in Tromsø (69.7 N°, 18.9 E°). The upper smooth curve present the results corresponding to a depletion of 30 % from the long-term mean. The irregular lines give the UV doses based on the total ozone measured in 1993 by the meteorological observatory in Sodankylä (Esko Kyrö, personal communication). The average local snow season was derived from the statistics of the Finnish Meteorological Institute. For the winter, a reflectivity of 0.8 was adopted, which

decreased linearly to the summer value of 0.04 during the period of 25 days before the end of the snow season. To achieve this reflectivity the terrain must be treeless up to several kilometers from the observation point. The first peak in the April clearly demonstrates how great the effect of snow is for the facial exposure. In April the facial and ocular exposures are equal or higher than the midsummer values although the horizontal doses are considerably smaller. The decreased ozone levels in 1993 resulted in a theoretical increase of 8.8 % in facial doses in Northern Finland.
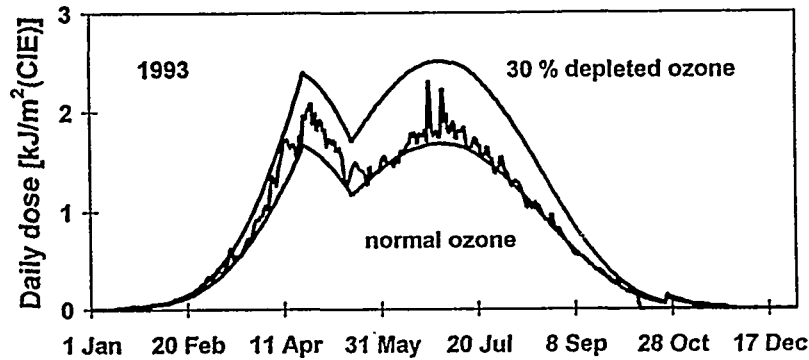
Fig.2 Computed vertical UV doses as a function of date on clear days in Saariselkä for long-term mean of total ozone (lower smooth line), 30 % depleted ozone (upper smooth line), and measured ozone (irregular line) in 1993.

Annual erythema doses, both horizontal and vertical, were computed using the measured total ozone data from Sodankylä from 1989 to 1994 for Northern Finland (Fig.3). The results were plotted as points in Figure 3. The straight lines were computed by using trend estimates derived from TOMS satellite data. There are great year to year variations but some trend for increasing UV levels can be noted as well as the exceptional increase in 1993.

In summary, in 1993 both theoretical and measured results indicated increase in erythemally effective UV in Finland. The reflection from snow increases facial and ocular UV doses in Northern Finland.
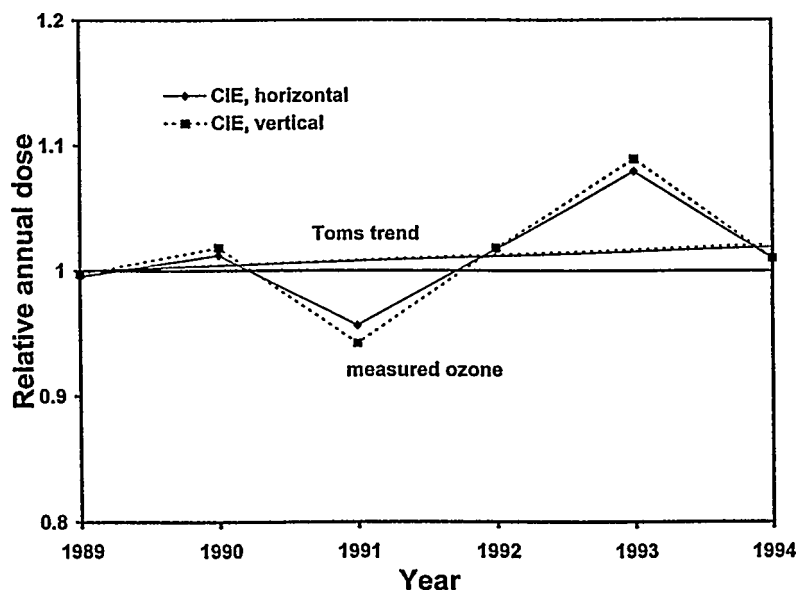
Fig.3 Computed relative annual UV doses for Saariselkä from 1989 to 1994.

References

Jokela, K., Leszczynski, K., Visuri, R. 1993. Effects of arctic ozone dpletion and of snow on UV exposure in Finland. Photochem and Photobiol. 58:559-566.

Jokela, K., Leszczynski, K., Visuri, R. & Ylianttila L. 1995. Increased UV exposure in Finland in 1993. Accepted in Photchem. and Photobiol.

Leszczynski, K., Jokela, K., Visuri, R. & Ylianttila L. 1995. Calibration of the broadband radiometers of the Finnish solar UV monitoring network. Accepted in Metrologia.

Taalas, P., Damski, J., Korpela, A., Koskela, T., Kyrö, E. 1995. Connections between atmospheric ozone, the climate system and UV-B-radiation in the Arctic. In: W.C. Wang (ed.) Ozone as a Climate Gas. NATO ASI Series, 2/1995.

Detector-based calibration of a solar UV spectroradiometer

Petri Kärhä, Heidi Fagerlund, Antti Lassila, Farshid Manoochehri and Erkki Ikonen

Metrology Research Institute, Helsinki University of Technology,
Otakaari 5 A, FIN-02150 Espoo

Kari Jokela, Kirsti Leszczynski and Reijo Visuri

Non-Ionizing Radiation Laboratory, Finnish Centre for Radiation and Nuclear Safety,
P.O.B. 14, FIN-00881 Helsinki

Introduction

The accuracy of the Finnish solar UV monitoring network is based on intercomparison of the network instruments with an accurately calibrated reference spectroradiometer. The uncertainty of the lamp-based calibration of the reference spectroradiometer is 3,6 % (2σ) and the overall uncertainty of solar UV irradiance measurements is 8% (at 310 nm) [1]. Hence, the improvement of the calibration methods and development of new standards with lower uncertainties are of primary importance.

Cryogenic absolute radiometers [2, 3] are currently the most accurate devices to measure optical power. Uncertainties as low as 0,04 % may be achieved in detector calibrations [4].

In this report we present a new detector-based method for UV irradiance calibration and some critical aspects encountered during the development work. Transferring the accuracy of the cryogenic absolute radiometer to the desired UV-wavelengths requires specific transfer standard radiometers. The characterization of these radiometers requires careful measurements of e.g. aperture area, filter transmittance and spectral responsivity of the detector. In addition to these, accurate temperature control is needed.

Standard detectors of optical power

In the Helsinki University of Technology the cryogenic absolute radiometer is operated twice a year to calibrate secondary transfer standard detectors. The methods used in calibrations have been thoroughly presented in [4]. Usually a trap detector [5] is used as a transfer standard, but also other type of detectors e.g. pyroelectric radiometers

may be calibrated. The calibration is performed using a power- and frequency-stabilized 543,5 nm He-Ne laser as the light source.

The trap detector consists of three photodiodes arranged in such a way that the light undergoes multiple reflections from the photodiode surfaces as depicted in Fig. 1. This arrangement reduces the reflection of incident light to a negligible level which is a desired feature in a radiometric system. In addition to the low reflectance, trap detectors have predictable spectral responsivity in the visible, high sensitivity, low noise characteristics and good spatial responsivity. They are also linear, stable in time and relatively cheap.

The responsivity of the trap detector is not predictable in the ultraviolet range. Therefore a pyroelectric detector with a flat spectral responsivity is also needed in UV calibrations. A pyroelectric detector by itself is not sufficient for UV calibrations for several reasons. They tend to be unstable, insensitive and have a poor spatial responsivity.
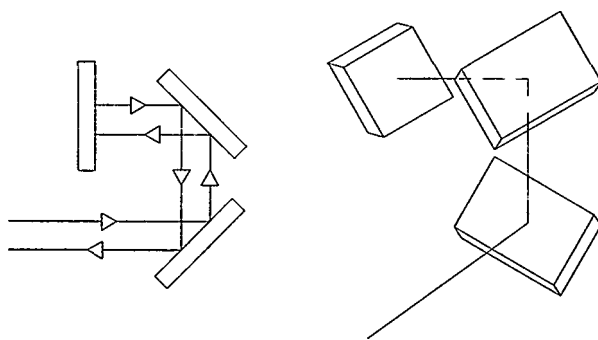
Fig. 1 Arrangement of the photodiodes in a trap detector. A three dimensional configuration reduces sensitivity to polarization of the incident light.

A setup to compare detectors in the UV and visible spectral ranges has been constructed using a 1 kW xenon lamp and an irradiance monochromator. The relative spectral responsivity of the trap detector is compared with the flat spectral responsivity of the pyroelectric detector. Combined with the absolute responsivity calibration against the cryogenic absolute radiometer this gives the absolute responsivity of the trap detector at UV wavelengths.

Scheme for detector-based UV calibration

A setup for calibrating the standard lamps used in the calibration of the solar UV spectroradiometer is presented in Fig. 2. A special wavelength selective filter radiometer is formed using a trap detector, a precision aperture and a UV bandpass filter. All the components are packed closely together to form a compact radiometer. A temperature controller keeps the temperature of the bandpass filter stable during the measurements in the vicinity of a high-power lamp.

Temperature controller
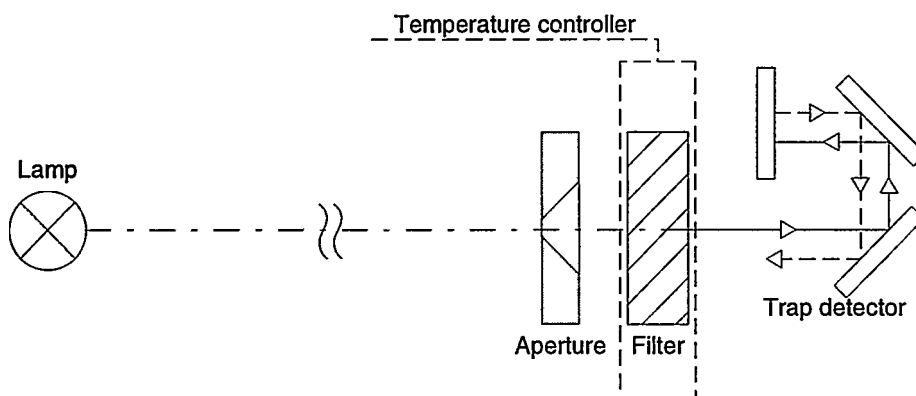
Fig. 2 Setup for the detector-based calibration of the UV standard lamp.

The photocurrent of the filter radiometer is calculated as

$$i = A \int E(\lambda) \, T(\lambda) \, R(\lambda) \, d\lambda, \tag{1}$$

where $E(\lambda)$ [W cm^{-2} nm^{-1}] is the spectral irradiance of the lamp, A [cm^2] is the area of the aperture, $T(\lambda)$ is the filter transmittance and $R(\lambda)$ [A W^{-1}] is the responsivity of the trap detector.

Parameters A, $T(\lambda)$ and $R(\lambda)$ can be determined separately. The *shape* of the lamp irradiance $E(\lambda)$ can be measured using the spectroradiometer within the narrow transmission band of $T(\lambda)$. Substituting the measured photocurrent into Eq. (1) gives the irradiance of the lamp and thus the calibration of the spectroradiometer within the passband of the filter.

Results and discussion

So far only preliminary results have been achieved using the detector based calibration system.

The spectral transmittance of an interference filter with a center wavelength of 312 nm and a bandwidth of 10 nm (full width at half maximum) was determined using a reference spectrometer with a deuterium lamp as the light source. The spectral responsivity of a trap detector was calibrated in the spectral region 280-340 nm. The areas of three precision apertures with nominal diameters 3,0, 3,5 and 4,0 mm were measured optically using a laser interferometer.

The characterized filter radiometer was compared with a 1 kW halogen standard lamp which is traceable to the spectral irradiance scale of NIST. The measured photocurrent was 8 % higher than the value based on the specified lamp irradiance. This may be considered as a fair first result taking into account the complexity of UV measurements. There are several possible reasons for the difference.

Of main concern are the properties of the interference filter. Great care should be taken in making the transmittance measurements. The filter has steep slopes which are very difficult to measure. Accurate measurements require a good wavelength scale. Also the blocking of the filter outside its passband is critical.

The filter transmittance was measured in the region from 400 to 800 nm to check for any leakage, none was found. However, the resolution of the measurements was 5×10^{-6}, and a leakage of this order of magnitude in longer wavelengths can cause considerable errors. It was calculated that e.g. a leakage with a maximum transmission of 5×10^{-6} at 700 nm wavelength would cause a 5 % error, assuming a bandwidth of 100 nm for the leakage. This is due to the spectral characteristics of the halogen lamp and the trap detector.

Some error may also be caused by the interreflections between the filter and the aperture and between the filter and the trap detector.

The effect of the aperture size on the responsivity of the radiometer was also studied. It was noted that increasing the aperture diameter from 3,0 mm causes slight decrease in the responsivity (approximately -0,8 % with the 3,5 mm and -1,5 % with the 4,0 mm diameter aperture). This is due to the limited angular response of the trap detector.

Acknowledgements

References

[1]   K. Leszczynski, K. Jokela, R. Visuri and L. Ylianttila, "Accuracy problems in solar UV radiation measurements" (this conference).

[2]   J. E. Martin, N. P. Fox and P. J. Key, "A cryogenic radiometer for absolute radiometric measurements", *Metrologia* 21, 147 (1985).

[3]   T. Varpula, H. Seppä and J.-M. Saari, "Optical power calibrator based on a stabilized green He-Ne laser and a cryogenic absolute radiometer", *IEEE Trans. Instrum. Meas.* 38, 558 (1989)

[4]   P. Kärhä, A. Lassila, H. Ludvigsen, F. Manoochehri, H. Fagerlund and E. Ikonen, "Optical power and transmittance measurements and their use in detector-based realization of the luminous intensity scale", *Optical Engineering* (in press).

[5]   N. P. Fox, "Trap detectors and their properties", *Metrologia* 28, 197 (1991)

Preliminary results from the WMO/STUK solar UV radiometer intercomparison

Kirsti Leszczynski[t], Kari Jokela[t], Reijo Visuri[t], Lasse Ylianttila[t] and
Mario Blumthaler[tt]

[t]Non-Ionizing Radiation Laboratory, Finnish Centre for Radiation and Nuclear Safety,
P.O.Box 14, FIN-00881 Helsinki

[tt]Institute of Medical Physics, University of Innsbruck, A-6020 Innsbruck, Austria

Introduction

To improve accuracy and compatibility of solar measurements carried out by UV
monitoring networks an intercomparison of erythemally weighted radiometers will be
arranged in Helsinki by the Finnish Centre for Radiation and Nuclear Safety (STUK) in
late spring and early summer 1995. Geographical span of the UV monitoring sites of the
16 participating countries covers latitudes approximately from 62°S to 79°N. The overall
number of meters belonging to the networks participating the project is around 100. The
five types of the participating radiometers are Solar Light Model 500 and Model 501
radiometers (denoted SL 500 and SL 501), Vital BW-20 and BW-100 radiometers and
YES UVB-1 Pyranometer. The intercomparison is supported by the World
Meteorological Organization (WMO).

Scope of the project

The intercomparison has two stages. At the beginning of the intercomparison the meters
will be tested in the optical laboratory of STUK, where the following tests will be carried
out: 1) measurement of the spectral responsivity function (SRF), 2) measurement of the
cosine response and 3) stability tests with a 1 kW quartz-halogen lamp. As the second
stage of the comparison the broadband radiometers will be intercompared in solar
radiation at elevation angles from approximately 10° to 53°. Simultaneously spectral
measurements will be carried out with two spectroradiometers, the Optronic 742
(denoted OL 742) of STUK and the Bentham DM150 of the Institute of Medical Physics
of the University of Innsbruck. The spectral measurements confirm or re-establish the
calibration of the broadband radiometers. The test and calibration results can be used
to reduce global differences in absolute calibration and to reduce errors arising from
non-ideal characteristics of the instruments.

Materials and methods

Instrumentation

The laboratory tests are carried out in a dark room the temperature of which is stabilized to 22 ± 1°C. Besides the spectroradiometer OL 742, the instrumentation of STUK for solar UV radiation measurements, radiometer tests and calibrations includes broadband SL 500 and SL 501 radiometers, 1000 W FEL and 200 W DXW quartz-halogen standard lamps, an irradiance monochromator consisting of a 1000 W xenon lamp Oriel 6271 and a monochromator Oriel 77200, a solar radiation simulating filtered metal halide lamp Philips HPA 400 W and low pressure mercury lamps.

Halogen lamps are operated by utilizing Optronic OL 65 or OL 83DS Precision Current Sources, and a shunt resistor (Cambridge Instruments 10 mΩ Manganin No L-201388) together with a Keithley 182 Sensitive Digital Voltmeter are used to monitor the lamp current. The shunt resistor and voltmeter are calibrated at the National Standards Laboratory of Finland. The estimated uncertainties of the resistance and voltmeter are ± 0.002% and ± 0.001%, respectively. Besides calibrations, halogen lamps are used for measuring the cosine response of the spectroradiometer and temperature sensitivity tests. Irradiance monochromator is used for the spectral response measurements, solar simulator is utilized for the cosine response measurements of the broadband meters and mercury lamp is used for measuring the slit function and calibration of the wavelength scale of the OL 742.

The calibration of the OL 742 is based on 1000 W FEL lamps traceable to NIST and the uncertainty of the calibration is estimated to be ± 3.6% (2σ). An overall uncertainty of ± 8% (2σ) has been achieved for the solar UV irradiance measurements at 310 nm and for the erythemally weighted irradiance by applying numerical corrections to minimize the errors caused by the cosine response, shift of the wavelength scale and temperature sensitivity of the optics head (Leszczynski et al. 1994, Leszczynski et al. 1995a, Leszczynski et al. 1995b).

The Bentham DM150 doublemonochromator of the University Innsbruck is operated with a slit width of 0.7 nm and the solar spectrum is measured from 290 to 500 nm at 0.5 nm steps. Its calibration is based on a 1000 W halogen lamp which is operated at 8.00000 A, provided with a computer controlled power supply. The high quality of calibration and stability has been demonstrated in the successful participation at three European spectrometer intercomparisons. Just prior to the measurement campaign in Helsinki, the DM150 will be tested at another European spectrometer intercomparison in Ispra, Italy, so that the agreement of the spectral measurements with the joint quality level of several instruments in Europe will be achieved. With the method of simultaneous spectroradiometry (Blumthaler et al., 1994) the absolute accuracy of the measurements in Helsinki can be improved. The additional possibility to determine total ozone content and aerosol optical thickness with the DM150 by spectral measurements of direct solar irradiance (Huber et al., 1995) is a great advantage in characterising the measurement conditions of the STUK/WMO intercomparison, and it also assists in global generalizing of the results of this campaign.

Intercomparison in solar radiation

The broadband radiometers are intercompared with the spectroradiometric measurements in solar radiation on clear days at solar elevation angles from approximately 10° to 53°. During the measurements the optical axis of each instrument is directed towards the zenith. During the spectral scan from 290 to 400 nm the instantaneous readings of all the broadband radiometers are simultaneously recorded. From the spectral measurements the dose rate value is derived by computing the erythemally effective irradiance by convolving the solar irradiance with 1) the CIE action spectrum (McKinlay and Diffey 1987) and 2) the measured spectral responsivity function of the meter in the range of from 290 to 400 nm and converting the irradiance to dose rate (1 MED/h = 200 J/m²h = 0,0555 W/m²). For each broadband meter the average of the readings recorded simultaneously with the spectroradiometer wavelengths of 290, 300, 310, 320 and 330 nm is calculated and compared with the dose rate values based on the spectroradiometric measurements.

Results

Preliminary results will be given at the conference and the final results will be reported in WMO report series.

References

Blumthaler M., Webb A.R., Seckmeyer G., Bais A.F., Huber M., Mayer B. 1994. Simultaneous spectroradiometry: a study of solar UV irradiance at two altitudes; Geophys Res Let 21, 2805-2808.

Huber M., Blumthaler M., Ambach W., Staehelin J. 1995. Total atmospheric ozone determined from spectral measurements of direct solar UV irradiance; Geophys Res Let 22, 53-56.

Leszczynski, K. 1994. Materials and methods, In: T. Koskela (ed.), NOGIC-93: The Nordic Intercomparison of Ultraviolet and Ozone Instruments at Izaña (INM) from 24 October to 5 November 1993, Finnish Meteorological Institute Contributions, pp. 27-49.

Leszczynski K., Jokela K., Visuri R., Ylianttila L. 1995a. Calibration of the broadband radiometers of the Finnish solar UV monitoring network., Metrologia Vol 32, in press.

Leszczynski K., Jokela K., Visuri R., Ylianttila L. 1995b. Quality assurance of the Finnish solar UV network measurements, poster presented in Critical Issues in Air Ultraviolet Metrology Workshop at the National Institute of Standards and Technology, May 26-27, submitted to be published in a special publication of NIST.

McKinlay A.F., Diffey, B.L., CIE-Journal, 1987, 6, 17-22.

Accuracy problems in solar UV radiation measurements

Kirsti Leszczynski, Kari Jokela, Reijo Visuri and Lasse Ylianttila

Non-Ionizing Radiation Laboratory, Finnish Centre for Radiation and Nuclear Safety, P.O.Box 14, FIN-00881 Helsinki

Introduction

Ground-based solar ultraviolet (UV) radiation monitoring is necessary for evaluating the impact of UV on human health and Earth's ecosystems (WMO 1992). Spectral measurements of highest precision are required for detecting UV trends associated with the depletion of stratospheric ozone and for providing data for evaluating radiative transfer models. On the other hand, for constructing a global terrestrial climatology, relatively simple broadband, e.g. erythemally weighted radiometers, as low-cost and easy-to-operate instruments, might be the only choice to establish networks of numerous monitoring sites.

Common problems shared with all methods applied for solar UV measurements are (i) lack of primary sources simulating the terrestrial solar spectrum, (ii) uncertainties associated with transfering the calibration from laboratory working standards to solar UV monitoring networks, (iii) the complicated geometry of the solar UV measurements and (iv) non-ideal angular and spectral responsivities of the solar UV radiometers. At present, within the spectroradiometric measurements of the solar UV irradiance, the absolute uncertainty (2σ) of ±15 to $\pm20\%$ is commonly exceeded, and the uncertainty of even the highest precision solar UVR measurements is limited to the level of ±5 to $\pm6\%$. This ultimate limit is set by the uncertainties associated with both the primary and secondary standards (Tegeler 1993, Walker 1991).

Ultraviolet radiation measurements in Finland

Solar UVR measurements have been carried out in Finland since 1989 by the Finnish Meteorological Institute (FMI) and the Finnish Centre for Radiation and Nuclear Safety (STUK). The present solar UV monitoring network of FMI consists of seven sites equipped with erythemally weighted broadband radiometers Solar Light Model 501A (denoted SL 501A), and two of the sites are equipped with a Brewer spectroradiometer. In 1995, two additional broadband UV monitoring sites equipped with erythemally weighted broadband SL 501A radiometers together with two Solar Light UVA radiometers will be established by the University of Helsinki (UH).

All the broadband radiometers of FMI and UH are calibrated and radiometrically characterized by STUK by measuring the spectral and cosine responses before they are put into use (Leszczynski et al. 1995a, Leszczynski et al. 1995b, Leszczynski 1995). The measuring instrumentation of STUK includes an Optronic 742 (OL 742) spectroradiometer and a SL 501 radiometer. The solar measurements by STUK are not carried out on regular basis, but rather for calibration and testing purposes and for collecting solar UV data for research and UV climatology purposes (Jokela et al. 1993, Jokela et al. 1995).

Improved accuracy of the solar UVR measurements

Spectral measurements

The accuracy of spectral solar UV measurements with the OL 742 spectroradiometer has been improved with respect to the most significant sources of error, e.g. the non-ideal cosine response, inaccuracy of the wavelength scale and the temperature sensitivity of the optics head (Leszczynski 1995, Leszczynski et al 1995b). The cosine response of the OL 742 has been measured and the cosine error is minimized by applying an elevation angle dependent cosine correction function, see Fig. 2(a). The accuracy of the wavelength scale is improved during every scan by measuring the 253.65 nm Hg line and correcting the results with respect to the shift of the wavelength scale. The temperature response of the optics head has been determined, and the results are corrected with respect to the difference between the calibration and measurement temperatures. The remaining uncertainty components (2σ) associated with the non-ideal cosine response, inaccuracy of the wavelength scale and temperature sensitivity are estimated to be ±5%, ±3% and ±3%, respectively. The absolute calibration of the OL 742 is based on 1000 W FEL lamps traceable to the National Institute of Standards and Technology (NIST) in the U.S., and the calibration uncertainty is estimated to be ±3.6%. When adding all the uncertainty components in root square an estimate of ±8% is obtained for the overall uncertainty (2σ) at 310 nm in solar UV measurements. This is also the uncertainty of the erythemally effective dose rate.

Broadband measurements

The accuracy of the broadband measurements has been improved by calibrating the erythemally weighted radiometers against the OL 742 spectroradiometer in solar radiation. Altogether eight SL 501 V.3 radiometers have been calibrated. In Fig. 1 there are shown calibration results for one SL 501A unit (#1452). Calibrations were performed on clear days at solar elevation angles from 22° to 53°. The total ozone values varied from 313 to 397 Dobson units. The pattern of the calibration factors is representative for all the tested SL 501 V.3 meters and the average calibration factors varied from 1.00 to 1.18.

To investigate the reason for the systematic increase of the calibration factors towards lower elevation angles, the measured spectral and angular responses were used to calculate elevation angle dependent correction functions to eliminate the effects of non-ideal cosine and spectral responses, see Figs. 2(a) and 2(b). Here, the CIE-action

spectrum (McKinlay and Diffey 1987) is taken as an ideal spectral response. In Fig. 3 are shown the calibration factors after applying the correction factors shown in Fig.2.
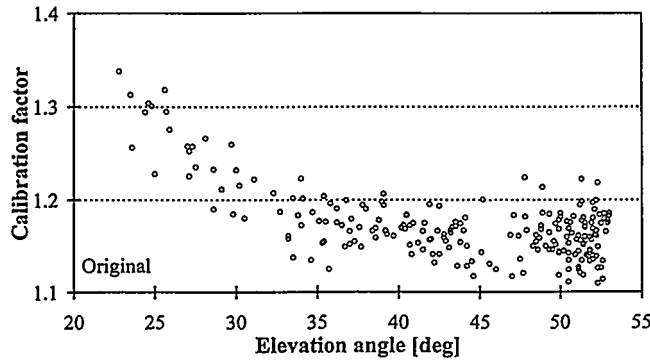
Fig. 1. The calibration factors of an erythemally weighted radiometer type SL 501A V.3 (#1452) based on spectroradiometric calibrations in solar radiation on clear days.

(a)

(b)
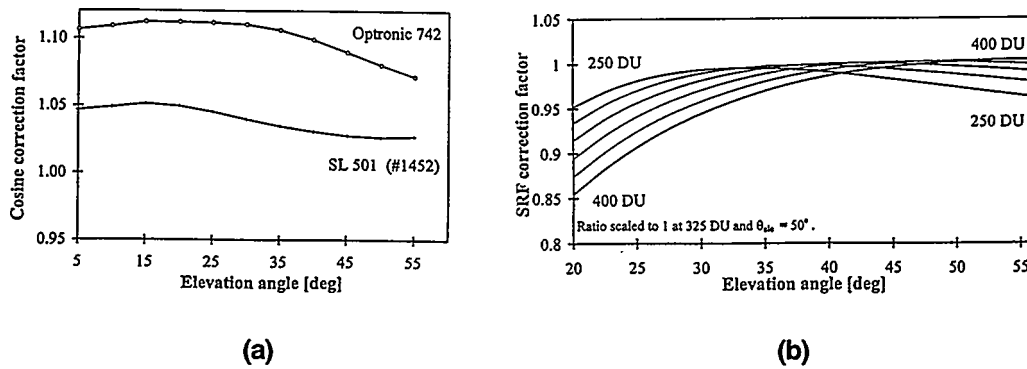
Fig.2. Correction factors for the radiometer SL 501A V.3 (#1452) due to non-ideal cosine response (a) and non-ideal spectral response (b) as a function of elevation angle. The cosine correction function for the spectroradiometer OL 742 has been included for comparison in Fig. 2(a).
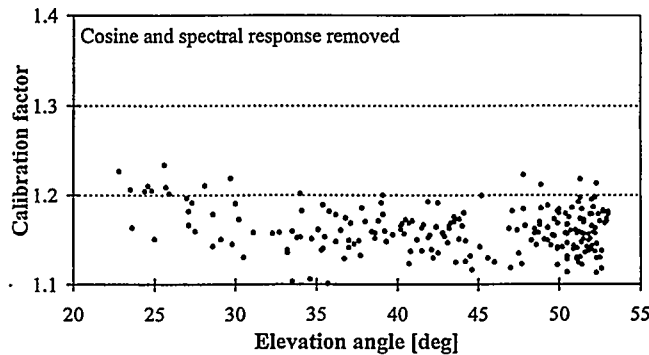
Fig 3. Calibration factors for the SL 501A radiometer (#1452) after removing the effect caused by the non-ideal angular and spectral responses using the correction factors shown in Fig.2.

Conclusions

Within the highest precision solar UV irradiance measurements the absolute uncertainty is limited at the level of ±5 to ±6%. This is due to the disagreement up to 4% between the primary standards. The uncertainty below ±10% in spectroradiometric measurements is possible to achieve only by 1) measuring the radiometric characteristics like angular and spectral responses as well as temperature sensitivity and 2) by applying numerical corrections based on measured characteristics and theoretical calculations.

In broadband measurements with temperature stabilized instruments, an uncertainty comparable with many spectroradiometric measurements is achievable by thorough characterization of every unit and by spectroradiometric calibration in solar radiation at various elevation angles.

Acknowledgements

References

Jokela K., Leszczynski K., Visuri R. 1993. Photochem. and Photobiol. 58, 559-566.

Jokela K., Leszczynski K., Visuri R., Ylianttila L. 1995. Photochem. and Photobiol., in press.

Leszczynski K. 1995. Assessment and comparison of methods for solar ultraviolet radiation measurements, Report STUK-A115, Finnish Centre for Radiation and Nuclear Safety, in press.

Leszczynski K., Jokela K., Visuri R., Ylianttila L. 1995a. Calibration of the broadband radiometers of the Finnish solar UV monitoring network., Metrologia Vol 32, in press.

Leszczynski K., Jokela K., Visuri R., Ylianttila L. 1995b. Quality assurance of the Finnish solar UV network measurements, poster presented in Critical Issues in Air Ultraviolet Metrology Workshop at the National Institute of Standards and Technology, May 26-27, submitted to be published in a special publication of NIST.

McKinlay A.F., Diffey, B.L., CIE-Journal, 1987, 6, 17-22.

Tegeler E., Metrologia, 1993, 30, 373-374.

Walker J.H., Saunders R.D., Jackson J.K., Mielenz K.D., J. Res. Natl. Inst. Stand.Technol., 1991, 96, 647- 668.

WMO, Scientific Assessment of Ozone Depletion: 1991, World Meteorological Organization Global Ozone Research and Monitoring Project - Report No. 25, pp. 11.1 11.14, 1992.

Factors affecting the accuracy of long term UV radiation monitoring.

Marian Morys and Daniel Berger

Solar Light Company, Inc.
721 Oak Lane
Philadelphia, PA 19126

Introduction

The observed ozone layer depletion is causing mounting concern for the potential it poses for increasing UV-B exposure and its effects on the biosphere. Due to the complicated nature of processes taking place in the atmosphere ground UV-B levels can only be known from direct measurement.

In addition to the complex variations imposed on UVB reaching the ground are the uncertainties inherent in any measuring device.

Limitations of measurement techniques result in substantial uncertainty of the measurement result. Proper identification and quantification of all uncertainty components is essential in order to interpret the results in a meaningful way. Full characterization of the radiometer is the first step of that process.

The measured signal must be characterized as well, since the measurement uncertainty depends on its properties. The wide dynamic range, large temporal variability and strong diffuse component of the solar UV-B radiation make it especially difficult to measure.

A commonly stated requirement for UV-B monitoring equipment is that it should be able to detect a trend of the total UV-B dose in the order of several percent per decade. To meet this requirement both the stability of the instrument and precision of its calibration have to be assured.

The errors associated with radiometric measurement are:
- Random and systematic errors of the instrument calibration,
- Instrumental errors, such as non-ideal angular or spectral response, instrument response time, etc.
- Drifts of the instrument

The focus of this analysis is an identification of the various error sources for a UV-B radiometric measurement based on the Solar Light Company's UV-Biometer Model 501. Empirical and analytic methods to quantify the uncertainty are shown. These methods are universal and provide an example of a practical approach to the problem of radiometer calibration.

Results and discussion

Characterization of the instrument

The spectral response of the UV-Biometer Model 501 follows the McKinlay-Diffey Erythema Action Spectrum (Figure 1). The angular response is within 5% of the ideal cosine for incident angles <60°. The phosphor based Robertson-Berger UV-B sensor is thermally stabilized at 25°C making the temperature effect negligible.

—⊞— UV-Biometer   —▽— Erythema Action Spectrum
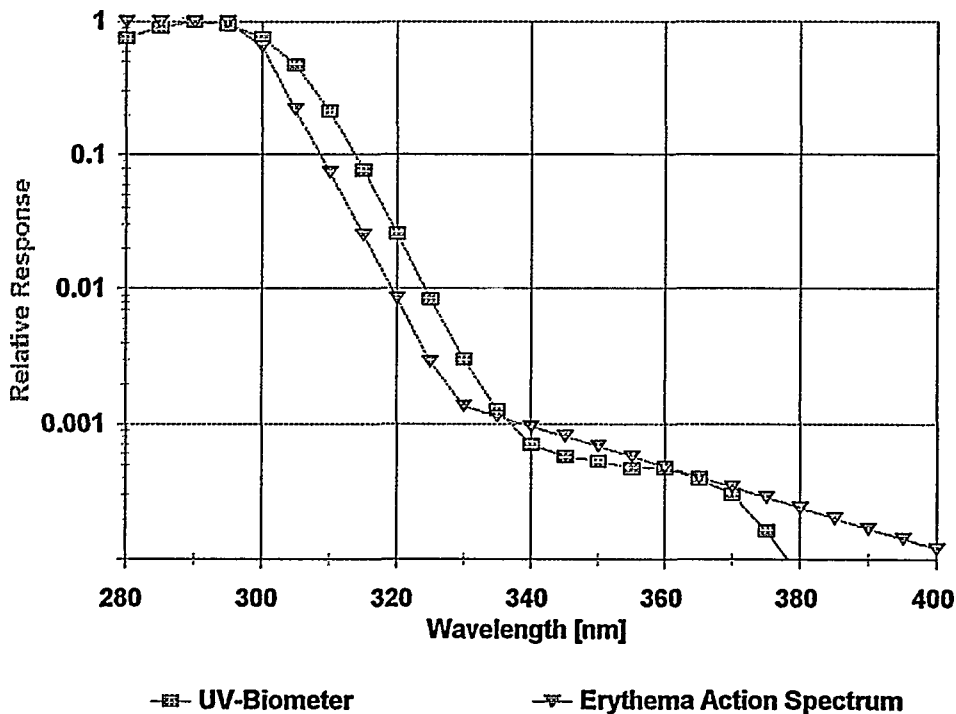
**Figure 1 Typical spectral response of the UV-Biometer Model 501 and the Erythema Action Spectrum**

Characterization of the solar ultraviolet radiation

Typically the erythemally weighted irradiance does not exceed $30\mu W/cm^2$. Most of the effective radiation comes from the 300-320nm region. It is measured the in presence of a strong visible and IR component so high stray light rejection is important.

A study was conducted to quantify the temporal variations of the UV-B radiation. The signal from the UV-Biometer was sampled every second in 5 minute intervals over a period of 2 weeks. Within each interval, the maximum, minimum and average was recorded. Only samples with sufficient S/N ratio were taken into account. About 16% of all samples showed a UV irradiance change less than 5% within 5 minutes. A change of 5-20% in irradiance was recorded in 43% of 5 minute intervals. In 41% of all samples the irradiance changed by 20% or more. The variability was more severe during cloudy days. The variability of the radiation should be taken into account when evaluating the required response time of the instrument, as well as the settings of the data logging and processing equipment.

Calibration of the radiometer

A method of calibrating the radiometer by spectroradiometric transfer from a standard lamp is described along with an analysis of its uncertainties. This calibration is performed in a laboratory, eliminating the influence of changing field conditions. Characterization of the instrument is a part of the procedure. The standard deviation of the random uncertainty component is estimated at 1.6%. The systematic component is within -6.2 to +4.7%.

The calibration should be performed on a yearly basis. In addition, frequent comparisons between radiometers within a network and with other types of instruments is recommended to assure measurement homogeneity within a given geographical area.

Instrumental errors

The departure of angular response from the ideal cosine causes a measurement error which changes with weather conditions. While relatively constant for a cloudy day, it changes in a course of a sunny day. Based on a numerical model, assuming an isotropic distribution of the diffuse component across the sky, the error was estimated at less than 1% for solar zenith angle (SZA) up to 50° and increases to 3% at 70° SZA.

The difference between nominal erythema action spectrum and the actual spectral response of the meter causes a measurement error changing with the spectral irradiance of solar radiation. Thus makes comparison difficult between radiometers with different spectral responses. However, this does not pose a major problem for the detection of long term trends, as long as the spectral response remains stable.

The installation and maintenance of the instrument can have a significant impact on the quality of the collected data. Assuring unobstructed view of the sky during the entire year as well as removal of dust, snow and ice from the entrance optics are important maintenance requirements for a radiometer..

Measurement of long term trends

The statistical significance of the trend determined from a series of measurements depends on the overall uncertainty of each measurement, particularly on its random

Table 1 An idealized example of increased detectability of a trend as the number of calibrations within the trend period increases. Calibration precision for 1 sigma is 1.6%. Calculation based on a linear trend and equal calibration spacing.

Number of calibration during the period of monitoring	Trend uncertainty contribution [%/period]
5	2.6
10	1.9
20	1.4

component. The random uncertainty of the radiometer calibration can be reduced by frequently performing the calibration.

If possible, the estimation of the uncertainty figures for the measurement and of the projected trend detection should be done prior to the installation of the UV monitoring network ,so appropriate project goals can be set.
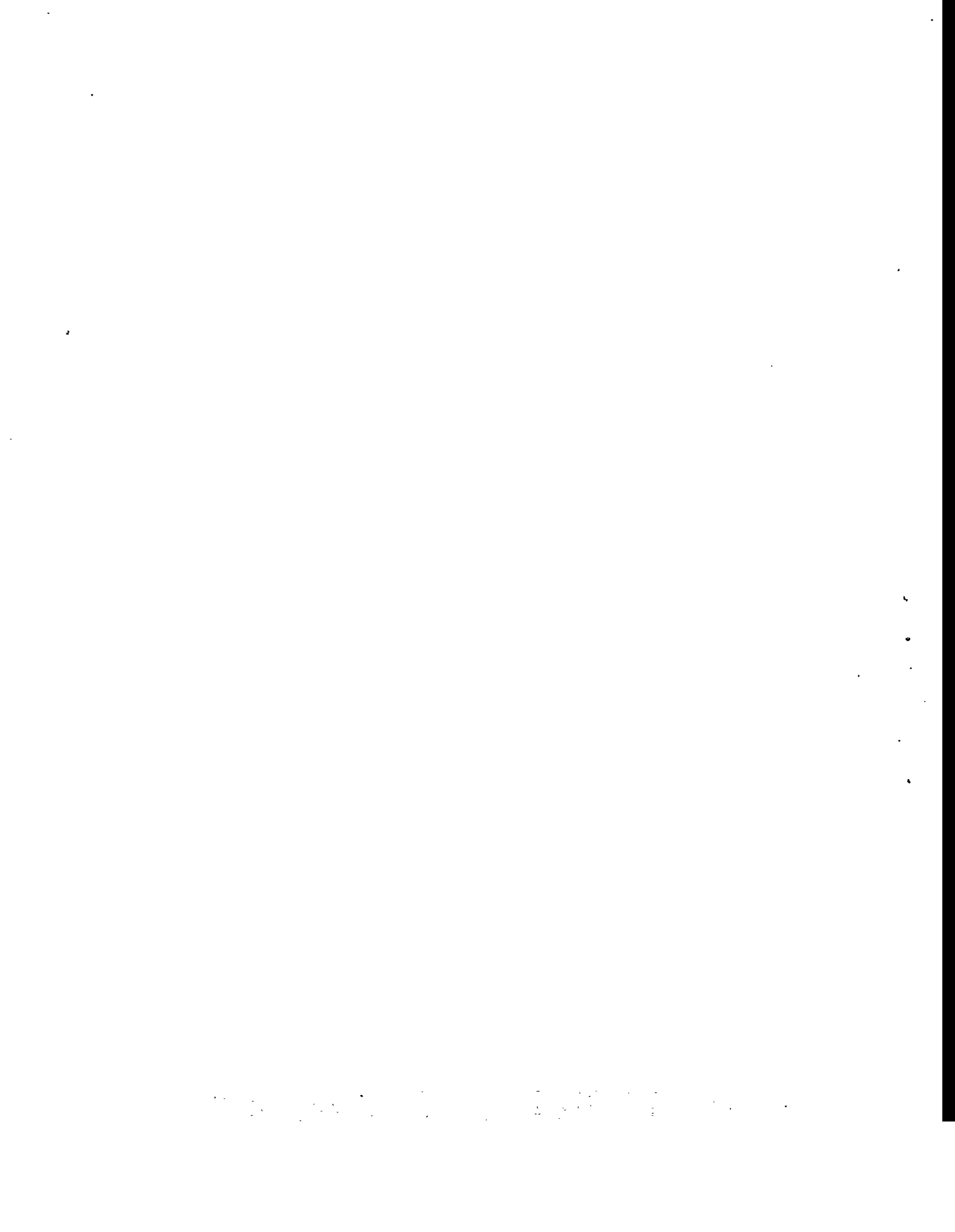
Predicting future climate

The results

Fig. 1 shows the time evolution of the globally averaged near surface temperature of the two aerosol experiments, the experiment without aerosols as well as the observations after Jones and Briffa (1992). The near surface temperature average has only been calculated in those areas which have an adequate observational coverage. One can clearly see that the three curves run close together until about 1970. This means that the model is quite capable to reproduce the observed temperature and that the aerosol effect was of no great importance until then. From 1975 onwards the CO_2 only experiment shows a temperature rise of about 0.3 K per decade, the aerosol experiments only ca. 0.2 K per decade. The curve of the observation appears to be closer to the curves of the aerosol experiment than to the CO_2 only experiment.

Fig. 2 shows the regional change of the near surface temperature for the experiments for the years 2041-2050 for summer and winter. The aerosols have a particularly large effect in the Northern hemisphere, since one finds here the main sources of the aerosols. In this hemisphere one can also find a clear seasonal signal. In summer the aerosols have a larger impact than in winter, since due to the larger insolation their albedo effect is more effective. The impact of the aerosols on the Indian monsoon circulation is particularly remarkable. While without the aerosols most models predict a reinforcement of the monsoon, the aerosol experiment indicate rather a decrease of the monsoon and the rainfall. This is caused by the local cooling over the Tibetan plateau caused by the aerosols, which damps the monsoon circulation (Lal et al, 1995).

The question if by the inclusion of the sulphate-aerosols the detection of the anthropogenic climate change can be improved, has still to be answered.

Acknowledgements

Literature

Cubasch, U., B. D. Santer and G. Hegerl, 1995a: Klimamodelle - wo stehen wir? Phys. Bl. **51**, 269-276.

Cubasch, U., G. Hegerl, A. Hellbach, H. Höck, U. Mikolajewicz, B. D. Santer and R. Voss, 1995b: A climate change simulation starting 1935. *Climate Dynamics,* **11**, 71-84.

Hasselmann, K., R. Sausen, E. Maier-Reimer and R. Voss, 1992: On the cold start problem in transient simulations with coupled ocean-atmosphere models. *Climate Dynamics,* **9**, 53-61.

Hasselmann, K., L. Bengtsson, U. Cubasch, G. C. Hegerl, H. Rohde, E. Roeckner, H. von Storch, R. Voss and J. Waszkewitz,(1995): Detection of Anthropogenic Climate Change using a Fingerprint Method. submitted to *"Science"*

Hegerl, G. C., H. von Storch, K. Hasselmann, B. D. Santer, U. Cubasch and P. D. Jones, 1994: Detecting anthropogenic climate change with an optimal fingerprint method. accepted by "Climatic Change".

IPCC, 1992: Climate change: The supplementary report to the IPCC scientific assessment. Eds. J. Houghton, B. A. Callendar and S. K. Varney, Cambridge University Press, 198pp.

Jones, P. D., and K. R. Briffa, 1992: Global surface air temperature variations during the twenties century: Part 1, spatial, temporal and seasonal details. The Holocene 2, 2, pp. 165-179

Lal, M., U. Cubasch, R. Voss and J. Waszkewitz, 1995: The transient response of greenhouse gases and sulphate aerosols on monsoon climate. submitted to *Climate Change*

Mitchell, J. F. B, T. J. Johns, J. M. Gregory and S. B. F. Tett, 1995: Transient climate response to increasing sulphate aerosols and greenhouse gases. submitted to *Nature*

Roeckner, E., T. Siebert and J. Feichter, 1995: Climatic response to anthropogenic sulfate forcing simulated with a general circulation model. In: *Aerosol forcing of climate*, Charlson, R. J., und J. Heintzenberg (Eds), John Wiley and Sons, in press

Santer, B. D., K. E. Taylor, T. M. L. Wigley, J. E. Penner, P. D. Jones and U. Cubasch, 1995: Towards the detection and attribution of an anthropogenic effect on climate. PCMDI Report No. 21, PCMDI/LLNL, Livermore, Ca.

Taylor, K., and J. Penner, 1994: Climate system response to aerosols and greenhouse gases: a model study. *Nature*, 369, 734-737.
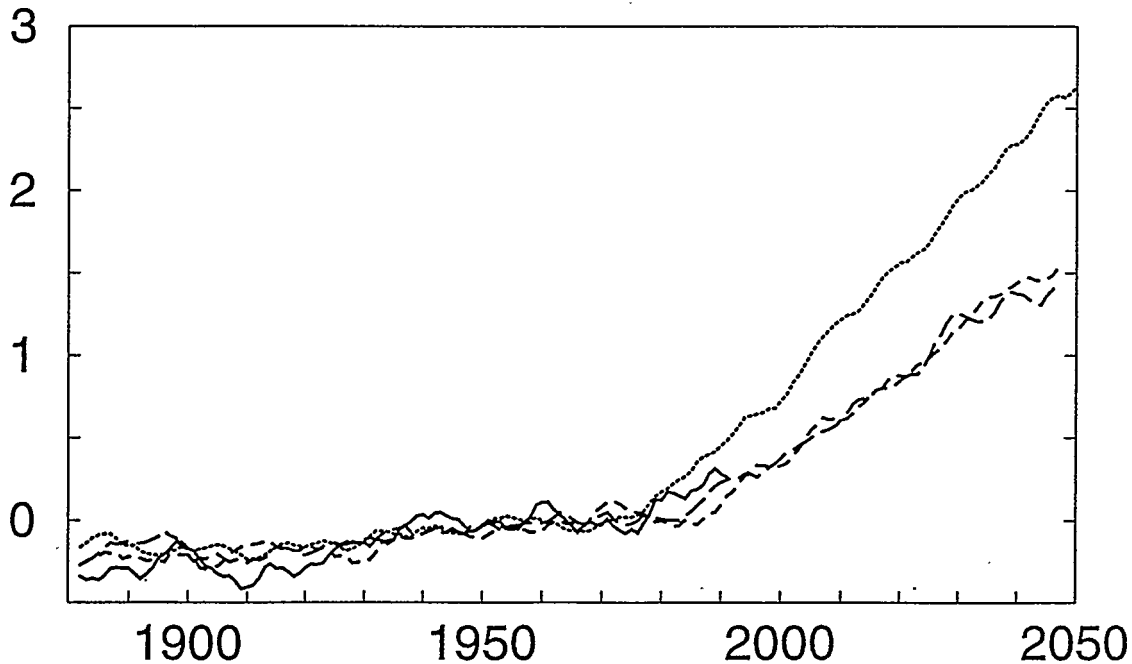
Figure 1: The time evolution of the near surface air temperature for the experiments with only the CO_2 forcing (dotted), for both the aerosol experiments (dashed) and the observations (solid line). The x-axis describes the years, the y-axis the relative temperature change to the years 1951 to 1980.
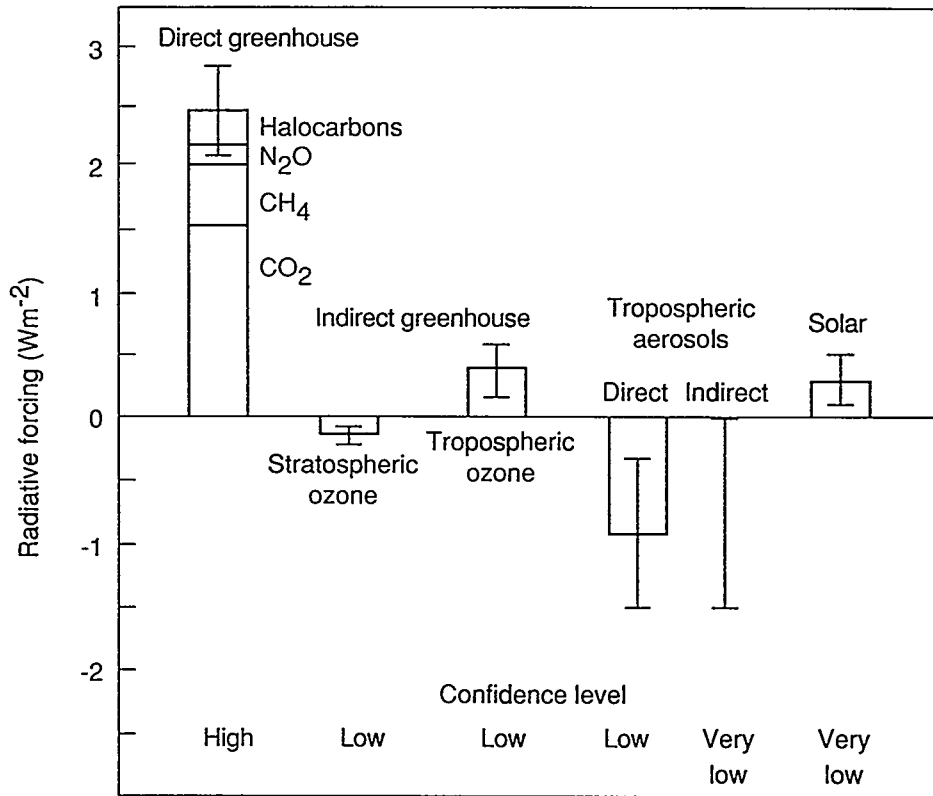
Fig. 1 Estimates of the globally averaged radiative forcing due to changes in greenhouse gases and aerosols from pre-industrial times to the present and changes in solar variability from 1850 to the present day. (From IPCC/WG1 1994, Fig. 3)

Due to many feedback processes occurring in the climate system, however, the radiative forcing, although an interesting quantity by itself, does not tell much about climate change. Estimation of the latter requires the use dynamical climate models.

Dynamical models of the climate system

The climate system consists of several components: atmosphere, oceans, cryosphere (snow and ice) and soil (including vegetation). All these components are essential for the distribution of climatic elements such as temperature, precipitation, wind, etc. The vegetation, for example, regulates the exchange of energy and water between the soil and the atmosphere and is thereby important in shaping the distribution of temperature and moisture in the atmosphere.

A dynamical climate model has, in principle, as many components as the real climate system. The atmospheric model component consists of a set of equations and a set of numbers. The equations are mathematical expressions for the laws of physics (e.g. conservation of energy, angular momentum, and mass) that govern the changes in the atmosphere. The numbers give the values of the independent variables (temperature,

pressure, wind, humidity) at an arbitrary moment; the values change with time as determined by the equations. The oceanic component of a dynamical climate model is in principle similar to the atmospheric one. An important ingredient of the soil component of a climate model is the equation for soil moisture changes. As in nature, such changes depend also in the model on precipitation, evapotranspiration and runoff, and are regulated by the vegetation.

Model results on the man-made climate change

Two types of model results are available for the man-made climate change. One is called "equilibrium climate change", the other "time-dependent climate change" (IPCC/WG1 1990). The equilibrium climate change is the potential climate change to which one is committed if the greenhouse gas concentration (or any other radiative forcing factor) is changed and the climate system, initially in equilibrium, is allowed to find a new equilibrium. In the time-dependent climate change calculations the forcing factors as well as the climate are allowed to change gradually. The time-dependent calculations take into account the delays caused by the World Ocean. At any given time, the results from the time-dependent calculations are expected to be closer to reality than those from the equilibrium calculations. The equilibrium calculations require, however, much less computer resources than the time-dependent calculations.

In the calculations of the time-dependent climate change it has become apparent that, when the atmospheric concentrations of the greenhouse gases increase, the ocean current systems tend to change, especially around Antarctica and in the Atlantic (e.g. IPCC/WG1 1990, ch. 6). Several models indicate that the heat transport capacity of the Atlantic Ocean may weaken in connection with the enhancement of the atmospheric greenhouse effect. These changes are due to freshenig of the ocean surface waters in high latitudes in the model, and appear to diminish the air temperature change. In North Atlantic and the surrounding areas the climate predictions are therefore more uncertain than elsewhere in the Northern Hemisphere.

The effect of atmospheric aerosols is discussed in length in IPCC/WG1(1994, 1995). It appears that aerosols affect not only the amplitude but also the geographical pattern of the man-made climate change.

Räisänen (1994) has compared the performance and predictions of several climate models in northern Europe, and Carter et al. (1995) have suggested climate change scenarios for Finland for impact studies. In the climate models, whose results have been used in these studies, the man-made increase of greenhouse gases but not that of aerosols has been considered.

There are many sources of uncertainty in the climate models, for example clouds which strongly influence the magnitude of the climate change, and oceans which influence the timing and geographical pattern of the climate change. However, there are good prospects for improving these models, which are our only rigorous tool to understand the climate and possibly to predict its forthcoming changes.

Detection issue

When is the "signal" (i.e. man-made climate change) clearly visible in the observations, which contain a lot of "noise" (i..e. natural low-frequency variability)? This is the important detection issue. We cannot yet be definitely sure that we already see the man-made climate change in the observations. It appears, however, that accounting in climate models for both the increased greenhouse gas effect and the increased aerosol effect gives for the past few decades a better correspondence between the observed and predicted temperature change patterns than what is obtained in the case when only the enhanced greenhouse gas effect is included (Kerr 1995; IPCC/WG1 1995).

Concluding remarks

The first major man-made environmental problem was the soil acidification, caused primarily by the massive industrial emissions of sulphur dioxide. Then came the problem of ozone depletion, caused by the emissions of man-made halocarbons. More recently, the possibility of man-made climate change has received a lot of attention. These three man-made problems are interconnected in fundamental ways. and require for their solution interdisciplinary and international approach.

Narrowing of the scientific uncertianties connected with the problems mentioned above can be expected through international "Global Change" programmes such as the World Climate Research Programme (WCRP) and the International Geosphere- Biosphere Programme (IGBP). Periodic assessments of the type produced by the IPCC will clearly be needed. Also in the future such assessments should form the scientific basis for international negotiations and conventions on the climate change issue.

References

Carter, T. & H. Tuomenvirta and M. Posch, 1995: *SILMUSCEN and CLIGEN User´s Guide. Guidelines for the construction of climatic scenarios and use of a stochastic weather generator in the Finnish Research Programme on Climate Change (SILMU)*. Publications of the Academy of Finland 5/95, 62 pp.

IPCC/WG1, 1990: *Climate Change - The IPCC Scientific Assessment* (Eds. J.T. Houghton, G.J. Jenkins and J.J. Ephraums). Cambridge Univ. Press, 365 pp.

IPCC/WG1, 1992: *Climate Change 1992-The Supplementary Report to the IPCC Scientific Assessment.* (Eds. J.T. Houghton, B.A. Callander and S.K Varney). Cambridge University Press, Cambridge, 200 pp.

IPCC/WG1, 1994: *Climate Change 1994-Radiative forcing of climate change and an evaluation of the IPCC IS92 Emission Scenarios.* (Eds. J.T. Houghton, L.G. Meira filho, J. Bruce,Hoesung Lee, B.A. Callander, E. Haites, N. Harris and K. Maskell.). Cambridge University Press, Cambridge, 339 pp.

IPCC/WG1, 1995: *Climate change - The Second IPCC Assessment* (in preparation)

Kerr, R.A., 1995: Studies say - tentatively - that greenhouse warming is here. *Science*, **268**, (16 June 1995), 1567-1568.

Räisänen, J., 1994: A comparison of the results of seven GCM experiments in northern Europe. *Geophysica*, **30**, 3-30.

Global climate change: Facts and hypotheses

Prof. K.Ya. Kondratyev, Research Centre for Ecological Safety,
Russian Academy of Sciences; Co-Chairman of the Board,
Nansen International Environmental and Remote Sensing Centre,
18 Korpusnaya Str., 197042 St. Petersburg, Russia

Documents produced by the UN Conference on Environment and Development (Rio-de-Janeiro, 1992), the UN Conference on Population and Development (Cairo, 1994), the World Summit on Social Problems (Copenhagen, 1996) have clearly emphasized the crucial importance of environmental changes from the viewpoint of development, as well as the coupled nature of development and environment. Global climate change has doubtless been the focus of all environmental considerations. This has been specifically expressed in the Framework Convention on Climate Change containing (as a non-binding document) strong recommendations to reduce greenhouse gases (GHGs) emissions to the level of 1990 by the year 2000. Very authoritative assessments of the state of global change studies have been given in the Intergovernmental Panel on Climate Change (IPCC-1990- and -1992) Reports.

It may seem paradoxical, but the results of research published during the recent few years raised a number of important and yet unsolved problems; hence the necessity to identify facts and hypotheses:

1) There is firmly established evidence of the growth of the CO_2 concentration and a global temperature rise during the past century, but there only are certain hypotheses about the cause-and-effect relationships. Although the annual mean global-averaged surface temperature increase is a fact, there is a strong need to further carefully analyze the inhomogeneous geographical patterns of not only temperature fields, but also other meteorological parameters (cloudiness, precipitation, soil moisture, etc.). Special emphasis should be made on further satellite observations and their analysis. High-resolution paleoclimatic data deserve special attention in this context. Further detailed and precise substantiation of requirements to a Global Climate Observing System (first of all, from the viewpoint of its optimization) is urgently needed (also as a prerequisite to identify a greenhouse climate signal).

2) A recent new wave of interest to aerosol impact on climate resulted in a number of assessments of the significant contribution of anthropogenic sulphate aerosols to global climate change. Several unsolved aspects of the problem require further studies, however, (the role of aerosol impact on cloud properties, the contribution of absorbing aerosols, etc.). Some results of the CAENEX and GAAREX Programmes may be instructive in this respect (e.g., for planning future field studies).

3) The mysterious solar activity impact on climate has actually been neglected, although considerable progress in satellite solar constant measurements has recently been achieved, and some new results of high-altitude surface spectral solar radiation measurements have been obtained which indicate important changes in stratospheric energetics due to solar activity.

These and other, new and old results indicate a necessity in a fresh look on the problem of global climate change, especially in view of the preparation of the next IPCC Report.

References

1. K.Ya. Kondratyev, A.P. Cracknell. Observing Global Climate Change.Taylor & Francis. 1995 (in press).
2. K.Ya. Kondratyev, H. Grassl. Global Climate Dynamics in the Context of Global Change. Springer-Verlag, Berlin, Heidelberg. 1995 (in press).

Climate models - Diagnostics, validation and sensitivity studies
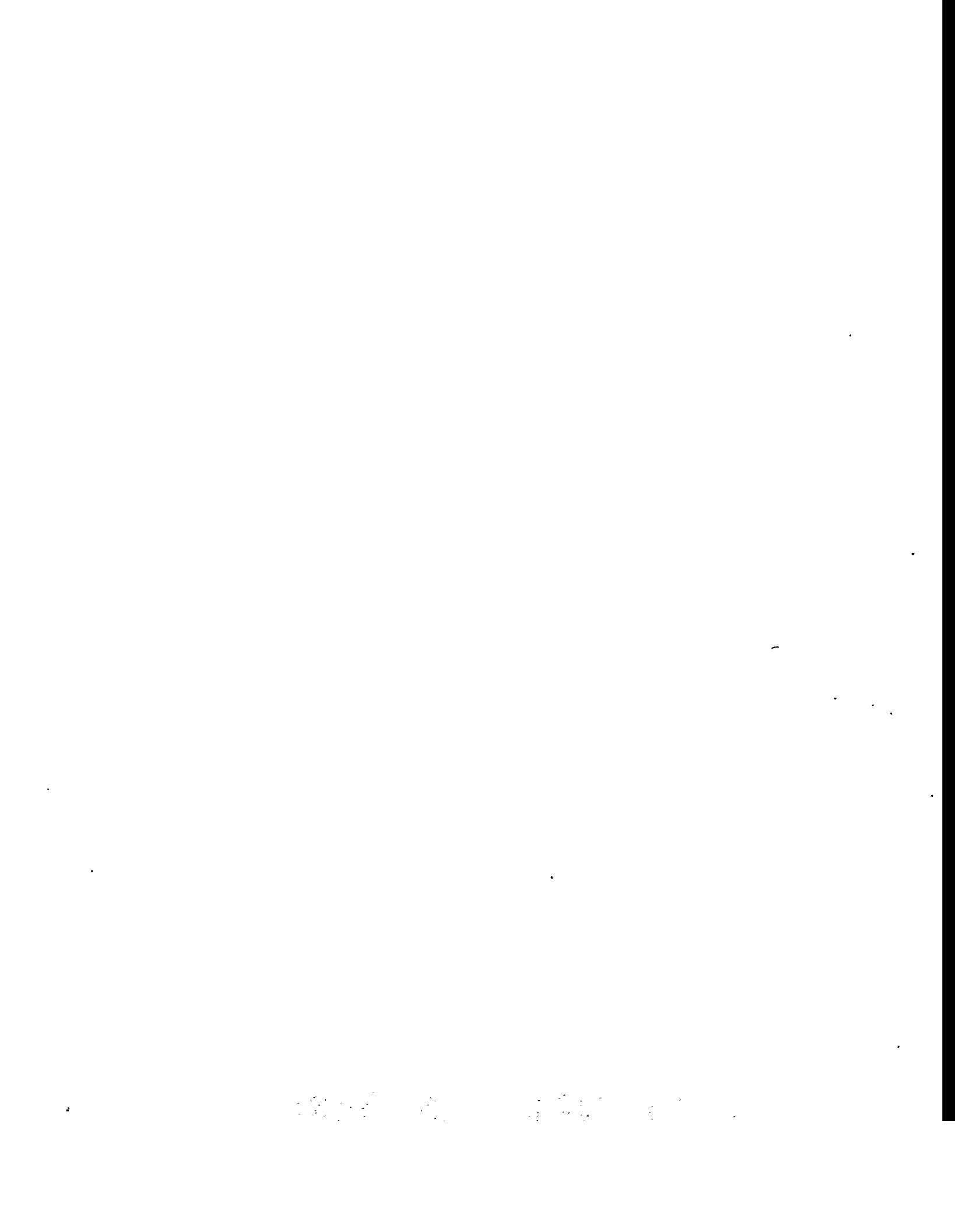
# On the causes of interannual climate variability

Carl Fortelius

Department of Meteorology, P.O. Box 4 (Hallituskatu 11)
FI-00014 UNIVERSITY OF HELSINKI

Introduction

The climate at any location near sea level is principally determined by the latitude. Nevertheless, on scales up to several thousands of kilometres, the climate may vary as much in the zonal (east-west) direction as in the meridional (north-south) one. The zonal variation is related to wave-like patterns in the time-mean upper air flow, known as stationary waves. The stationary waves ultimately owe their existence to the asymmetric forcing exerted at the earth's surface, primarily by flow over mountain ranges and by zonally-varying diabatic heating associated with the distribution of oceans and continents. They are further affected by momentum and heat fluxes associated with travelling cyclones and anticyclones, ("transient eddies"). Finally, stationary waves interact significantly with each other.

The stationary wave pattern of a given season varies from year to year, and these fluctuations actually account for the majority of the interannual climate variability in the middle latitudes. On the longer term, a global climate change is likely to be accompanied by changes in the stationary wave pattern. Such changes may significantly alter the relationships between the local and the zonally or globally averaged climate. Thus compelling reasons exist for studying the mechanisms behind the stationary waves and their fluctuations.

Starting from general equations describing the atmospheric dynamics, it is possible to derive expressions for the stationary waves as functions of a "basic state" consisting of the zonally-averaged time-mean flow fields, "forcing terms" associated with orography, diabatic heating and transient eddies, and "interaction terms" representing the effect of the stationary eddies on themselves and on each other. The basic state and the forcing and interaction terms can be computed from meteorological observations or, alternatively, from a climate simulation carried out with a general circulation model. Such

a) observed   b) linear model
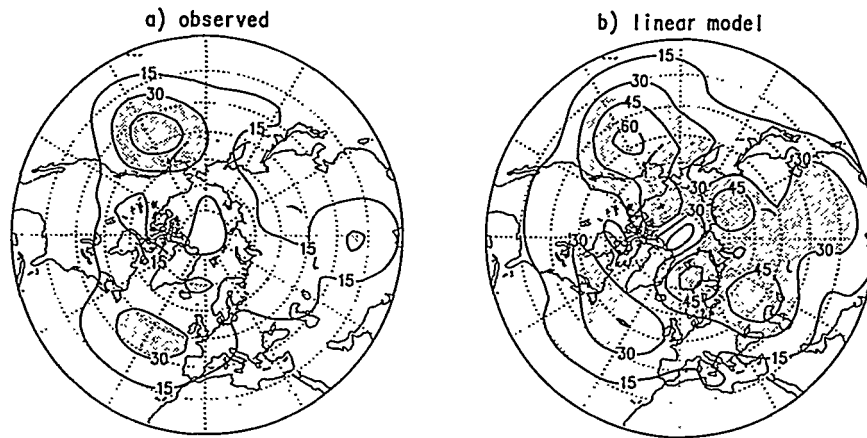
Fig. 1. Standard deviation of the interannual variability of the zonally asymmetric wintertime height field at 850 hPa as observed (a) and reproduced by the linear model using the total forcing (b). The contour interval is 15 m and values in excess of 30 m are indicated by shading. (From Fortelius 1995)

an analysis, however, by itself tells very little about the mechanisms maintaining the observed (or simulated) waves.

More insight can be gained if one inserts the empirically determined basic state and forcing and interaction terms into the general equations as externally specified functions. Doing so, one obtains a linear system of equations that can be solved for the stationary waves corresponding to any combination of the empirical parameters, and the relative importance of various forcing mechanisms may thus be assessed.

In the present study the linear climate model of Ruosteenoja (1993) is used to investigate the mechanisms that cause the northern hemisphere winter-time stationary wave field to fluctuate from year to year. The empirical parameters were computed from operational analyses compiled by the European Centre for Medium-Range Weather Forecasts (Hoskins et al. 1989), spanning the ten winters of 1979/80 through 1988/89.

Results

Figure 1 shows the standard deviation of the observed (1a) and simulated (1b) interannual variability of the wintertime zonally asymmetric 850 hPa height field. The overall shape of the distributions is similar: the two oceanic maxima are reproduced with the correct relative intensity and the relative minimum over eastern Asia as well as the maximum near the Tibetan plateau are present in both panels. On the other hand,

a) orographic forcing

b) diabatic heating

c) transient eddies

d) stationary eddies
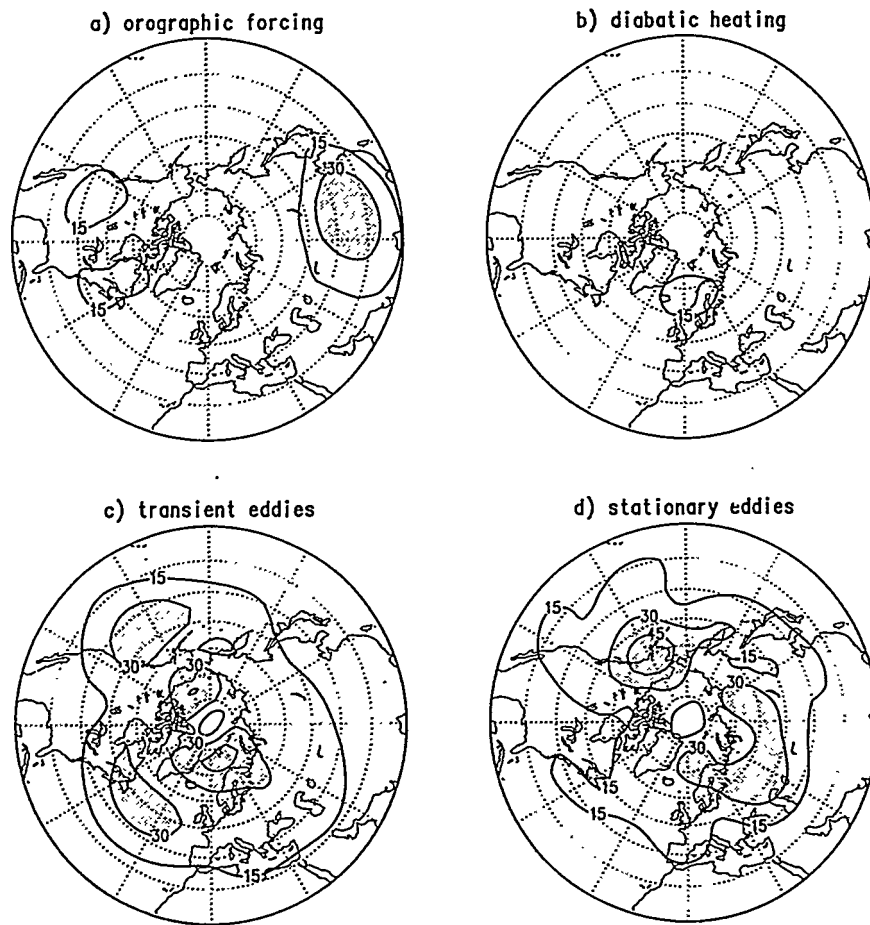
Fig. 2. Standard deviation of the interannual variability of the zonally asymmetric height field at 850 hPa computed separately for the forcing due to (a) orography, (b) diabatic heating, (c) transient eddies and (d) stationary eddies). The contour interval is 15 m and values in excess of 30 m are indicated by shading. (From Fortelius 1995).

the model severely overestimates the variability over the Eurasian continent and in the polar region.

Figure 2 shows the interannual standard deviation at 850 hPa of the linear responses to the different forcings. Most of the simulated variability is clearly due to anomalous forcing by transient eddies (2c) and anomalous interaction between stationary waves (2d). Actally the best correspondence (correlation of 0.7 at 850 hPa) between observed and simulated variability is obtained by letting only these two vary from year to year, while keeping the diabatic heating and mountain forcing fixed at their climatological values (Fortelius 1995). If, by contrast, either the forcing by transient eddies or the interaction term is kept fixed, virtually all correlation is lost. Further

types over the whole length of record, although there are numerous multi-decadal trends.

The use of weather types for weather generation

Traditional weather generators all possess a similar structure. Precipitation is considered to be the primary variable. Depending on whether the day is wet or dry, other meteorological variables are determined by regression relationships, maintaining the cross-and auto-correlations between and within each of the variables. The realism of the procedure rests primarily on the method of precipitation generation (Hutchinson, 1986). An alternative to the generation of wet and dry sequences is to use weather types, either those generated by observed data (see section 4) or using weather types derived from GCM output. The sequences of wet and dry days will be incorporated in the weather types. Generating weather at neighbouring stations should be simpler with weather types because the interstation correlations are an inherent property of the types. More parameters of a generator may be required as each of the basic weather types necessitates a different distribution to determine the precipitation amount on wet days. Figure 1 shows an example of such distributions, seasonally for cyclonic WTs, using precipitation data for Durham in the UK (1932-1990). The length of the LWT and daily rainfall series in the UK means that the consistency of the relationships between the large and small scale can be tested in different epochs of the observations. Current work is attempting to relate these distributions to additional information incorporated in the objective weather types such as the strength of the flow and vorticity over the region. These variables may improve the distributions fitted in a similar way to how the incorporation of weather fronts improved the relationships between types and precipitation totals (Wilby, 1994).

Applications to GCMs - some concluding remarks

All the ideas and techniques described in this paper may be theoretically applied to GCM data, providing the weather typing scheme is objective with certain decision rules. Application of the LWTs to GCM control run integrations shows that the monthly counts of weather types differ somewhat from reality (Hulme et al., 1993). Furthermore the relationships in the GCMs between the weather types and surface weather differ from those evident in reality. This is a serious impediment to the use of weather types for GCM downscaling. It should not be considered as a drawback, however. Indeed, the lack of similarity between reality and the GCM is more apparent when weather types are used, whereas these differences may be hidden in the mathematical detail of techniques such as canonical correlation analysis.

The development of downscaling methods is a response to the need for the appropriate spatial and temporal scale data for climate impact assessment studies. Many applications require sequences of future weather for design purposes. Without climate change these would come from long observational series or synthetically generated weather series when records were short. GCMs are the best tool for incorporating the effects of climate change through transient integrations including the effects of increasing levels of greenhouse gases and sulphate aerosols. Transient scenarios for the future, however, will have the climate changing by a sufficient amount on the decadal timescale to violate the stationarity constraints recognised for

designs. GCMs cannot be run for specific design criteria. Therefore there will be a need for weather type generation to produce long sequences with the characteristics of a future time period suitable for design purposes.

References

Hulme, M., Briffa, K.R., Jones, P.D. and Senior, C.A., 1993: Validation of GCM control simulations using indices of daily airflow types over the British Isles. *Climate Dynamics* 9, 95-105.

Hutchinson, M.F., 1986: Methods of generation of weather sequences. In (A.H. Bunting ed.) *Agricultural Environments*. C.A.B. International, Wallingford, 149-157.

Jones, P.D., Hulme, M. and Briffa, K.R., 1993: A comparison of Lamb circulation types with an objective classification scheme. *International Journal of Climatology* 13, 655-663.

Lamb, H.H., 1972: British Isles weather types and a register of daily sequence of circulation patterns, 1861-1971. *Geophysical Memoir* 116, HMSO, London, 85pp.

Wilby, R.L., 1994: Stochastic weather type simulation for regional climate change impact assessment. *Water Resources Research* 30, 3395-3453.

Wilby, R.L., 1995: Simulation of precipitation by weather pattern and frontal analysis. *J. of Hydrology*, in press.

Wilby, R.L., Barnsley, N. and O'Hare, G., 1995: Rainfall variability associated with Lamb weather types: the case for incorporating weather fronts. *International Journal of Climatology*, in press.

Acknowledgements

Observations   Model
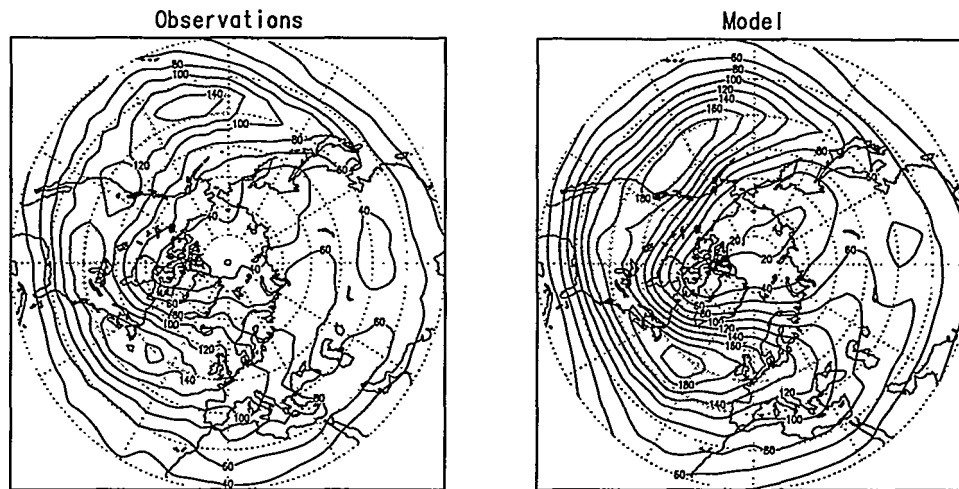
FIG. 1. Transient eddy kinetic energy at 250 hPa calculated from high-pass filtered fields from ECMWF analyses (left panel) and ECHAM3 control climate (right panel) during the Northern Hemisphere winter. Contours every 40 m^2s^{-2} with values larger than 120 m^2s^{-2} shaded.

al. (1983). The results of this study indicate (not shown) that at the downstream ends of the storm tracks the high-pass eddies in the model exert too weak a deceleration of jets. At the same time the vertically averaged zonal wind is stronger than observed, which suggests that in the model too strong high frequency eddies play a role in the maintainance of excessive barotropic component of westerlies at the end of storm tracks.

The cyclone climatology of ECHAM3 inferred from the frequency distribution of cyclone events, was calculated from the model data by using a simple method (Lambert 1988). In this method the cyclone event is defined as a local minimum in the 1000 hPa height field without applying any treshold values for gradients and with no restriction to the lifetime of cyclones. The horizontal distribution of cyclone events is quite well simulated (not shown). The total number of cyclones is underestimated only slightly by ECHAM3.

Propagation of planetary-scale waves in ECHAM3 is compared with observations by using a lag correlation method. The characteristic zonal wavelength and group velocity calculated from the unfiltered model data is close to that observed. The phase speed is towards east in the model while the observed waves are quasi-stationary. This problem stems from the low-pass filtered (periods longer than 10 days) part of the spectrum. The bandpass filtered (periods 2.5 to 6 days) waves in the model have phase speed and wavelength close to the observations. The essential characteristics of vertical wave propagation from the troposphere to the stratosphere is simulated by the model. In this context it is also noted that ECHAM3 is capable of generating "sudden stratospheric warming" phenomenon with three major warmings during the period of nine analysed winters (DJF).

Results from the lag-correlation analysis indicate that the characteristics of the wave propagation of ECHAM3 during the northern winter resembles in some respects the observed diagnostics for the Southern Hemisphere winter. It is speculated that this problem might be caused by the shortcomings of orographic forcing in ECHAM3. The systematic error of the zonal mean temperature, zonal wind and of the 500 hPa height field also are indicative of too weak an orographic forcing.

The methods used in this study for the simulation of present climate are also applied to an experiment of future climatic conditions (Perlwitz et al. 1994). In this run the greenhouse gas concentrations of the model correspond IPCC scenario A at the end of next century, ie. at the time of tripling of CO_2 and sea surface temperatures are taken from a previous low-resolution coupled ocean-atmosphere run.

References

Hoskins, B. J., I. N. James and G. H. White, 1983: The shape, propagation and mean-flow interaction of large-scale weather systems. *J. Atmos. Sci.*, **40**, 1595-1612.

Hoskins, B. J., H. H. Hsu, I. N. James, M. Masutani, P. D. Sardeshmukh and G. H. White, 1989: Diagnostics of the global circulation based on ECMWF analyses 1979-1989. WCRP-27, WMO/TD No. 326. WMO, Geneva, Switzerland, 217 pp.

Lambert, S. J., 1988: A cyclone climatology of the Canadian Climate Centre general circulation model. *J. Climate*, **1**, 109-115.

Perlwitz, J., U. Cubasch and E. Roeckner, 1994: Simulation of greenhouse warming with the ECHAM-3 model using the time-slice method. In G. Boer (ed): Reseach Activities in Atmospheric and Oceanic Modelling. WMO/TD -No. 592.

Randel, W. J., 1988: Further modification of time-longitude lag-correlation diagrams: application to three-dimensional wave propagation. *Tellus*, **40A**, 257-271.

Roeckner, E., K. Arpe, L. Bengtsson, S. Brinkop, L. Dümenil, M. Esch, E. Kirk, F. Lunkeit., M. Ponater, B. Rockel, R. Sausen, U. Schlese, S. Schubert and M. Windelband, 1992: Simulation of the present-day climate with the ECHAM model: Impact of model physics and resolution. *Report No. 93, Max-Planck-Institut für Meteorologie*, Hamburg, Germany, 172 pp.

Sensitivity of storm track activity and blockings to global climatic changes: Diagnostics and modelling

Igor I. Mokhov, Vladimir K. Petukhov and Andrey O. Senatorsky

Institute of Atmospheric Physics, Russian Academy of Sciences,
Moscow, Russia

Introduction

The aim of this paper is to estimate the trends in cyclonic and anticyclonic activity characteristics and to examine their interrelationship and co-evolution in the extratropical atmosphere accompaning the global-scale climate changes in the Northern and Southern Hemispheres based on different observational data sets and model results (Arsky et al., 1989, Mokhov et al., 1992a,b; Mokhov et al., 1993; Mokhov et al., 1994).

Data

To evaluate the tendencies of cyclonic and anticyclonic activity in the atmosphere under large-scale long-term temperature change we used different observational data sets including data obtained in Russian Hydrometeorological Center (RHMC) in 1949-1990 and in US National Meteorological Center (USNMC) in 1980-1988 (Mokhov et al., 1993).

Monthly mean data for total cyclones/anticyclones duration in 1949-1988 and for cyclogenesis/ anticyclogenesis (including local and non-local eddy-genesis) in 1962-1986 for the NH extratropical regions are described in (AFCPNH, 1979; Mokhov et al., 1992a,b; Mokhov et al., 1993). To estimate the tendencies of blocking activity characteristics in the NH we also used different data and criteria of blocking identification, particularly from Lejenas, Okland, 1983; the Catalog of Parameters of Atmospheric Circulation (CPAC, 1988), Monitoring of Climate - 87, 1989; Gruza and Korovkina (1991), Bulletin of Monitoring of Atmospheric General Circulation (MAGC, 1992) for the Northern Hemisphere (see Mokhov et al., 1994).

Results and discussion

According to the daily RHMC data analysis (Mokhov et al., 1992a; Mokhov et al., 1994) a general tendency of the cyclogenesis increase in extratropical latitudes with an increase of the hemispheric surface temperature (TH) is exhibited during last decades in the Northern Hemisphere. Remarkable correlation of cyclone frequency with TH (from Vinnikov et al., 1990) is noted at the 60-s latitudes (especially over land), at 30-s latitudes over ocean, at 40-s latitudes over land. There are also latitudinal belts with negative correlation. The closest negative correlation is noted for 50-s. The analysis

of the daily RHMC data for a period 1949-1988 shows a remarkable tendencies of decrease of the total duration (eddy-days) of extratropical cyclones and anticyclones in winter and in summer with an increase of the hemispheric surface temperature TH in the Northern Hemisphere (Mokhov et al., 1993). On the other hand it was noted the tendency of increase of the total duration of extratropical deep cyclones in January with the increase of TH. A remarkable trends are exhibited for a separate regions. In particular, a remarkable tendency of decrease was noted for a strong January anticyclones in the 50-70N latitudinal belt under the hemispheric warming. A significant trends were noted during 1980-s. So, the tendency of the increase was exhibited for the total duration of deep cyclones in polar latitudes. The analysis of the characteristic life-time of extratropical cyclones and anticyclones in different seasons shows remarkable interannual variations. Statistically significant decrease of life-time with the increase of TH was noted, in particular for summer extratropical cyclones in the Northern Hemisphere. Variations in storm track activity were analyzed for different regions, including the North Atlantic and Mediterranean cyclone tracks (Mokhov et al., 1993). In particular, the statistically significant tendency of increase of cyclonic activity over Caspian Sea basin accompaning the increase of the Northern Hemisphere surface temperature during 1980-s (1980-1988) was estimated by use of the USNMC data analysis. This tendency is more pronounced for the summer and autumn seasons. Such character of changes can be responsible in part for a significant hydrological cycle changes in the Caspian Sea basin during last decades with the sharp increase of the Caspian Sea level since the end of 1970-s (Golitsyn et al., 1995). According to Christoph (1994) the storm track intensity increases over Caspian Sea region (up to 6%) in winter under warming due to triple CO_2 content in the atmosphere in the ECHAM3 (T42) general circulation model experiments.

It should be noted that from the USNMC data analysis significant anomalies of cyclone characteristics (including the frequency, intensity, characteristic size) in different latitudinal zones are associated with the El-Nino effects.

Schinke (1993) found the increasing trend in the number of deep cyclones over Europe and the North Atlantic in 1930-1991. However, he noted that no connection between the deep cyclone frequency and the increase of the NH surface air temperature seems to exist. According to our results (Mokhov et al., 1993; Mokhov et al., 1994) this result can be related to the size of analyzed region. In particular, remarkable correlations of eddy characteristics with the NH surface air temperature but of different signs were found in (Mokhov et al., 1993; Mokhov et al., 1994) for different sub-regions inside the Europe - North Atlantic region.

Remarkable interannual and interdecadal variations were noted in Mokhov et al. (1994) for the total number and the distribution function of blocking anticyclones in extratropical latitudes of NH for a period 1949-1992 from different data, particularly from the Catalog of Parameters of Atmospheric Circulation (CPAC, 1988), Gruza and Korovkina (1991), Bulletin of Monitoring of Atmospheric General Circulation (MAGC, 1992). In particular, a statistically significant increase was noted for a number of blocking anticyclones with a duration from 5 to 9 days under TH increase during the 35-years period (1949-1983) by the data from CPAC (1988). The analysis of these data shows also the statistically significant increase of the total number and total duration of blocking cases in the 30-70N

latitudinal belt with the increase of TH (Mokhov et al., 1994). The characteristic linear size L_{ba} and life-time τ_{ba} of splitting and Ω types of blocking anticyclones can be estimated using the kinematic condition of stationarity of the pair and the three of barotropic vortices in the quasi-zonal barotropic flow U (Obukhov et al., 1984) and the balance equation for the kinetic energy of barotropic perturbation (Dymnikov and Filatov, 1990). In the case of proportionality of the characteristic blocking size L_{ba} to its intensity H_{ba} (Lupo et al., 1995) we can obtain

$$L_{ba} \propto H_{ba}/U ,$$

$$\tau_{ba} \propto L_{ba}/U \propto H_{ba}/(U^2) ,$$

where $H_{ba} = k\, f\, U\, L_{ba}/g$ (f - Coriolis parameter, g - gravitational acceleration). H_{ba} can be determined by the geopotential height perturbation at the anticyclone center relative to the ambient geopotential height field (Lupo et al., 1995). Parameter k is different for different types of blockings, in particular for splitting and Ω types. It should be noted that τ_{ba} is proportional to $\cos\phi(L_{ba}/U)$ or to $(g\cos\phi/f)H_{ba}/(U^2)$, where ϕ is latitude. In the case of latitudinally independent values of L_{ba} and H_{ba} the τ_{ba} has to be maximum at 45° latitude. In the considered approximation the dependence of τ_{ba} on L_{ba} has a minimum about 5 days at $L_{ba} \sim L_0$ (L_0-Obukhov scale). The formulae for L_{ba} and τ_{ba} can be used to evaluate their sensitivity to climate change impacts such as increase of CO_2 content in the atmosphere. Sensitivity parameters of L_{ba} and τ_{ba} to the temperature (T) change can be represented as follows

$$\frac{1}{L_{ba}}\frac{dL_{ba}}{dT} = \frac{1}{H_{ba}}\frac{dH_{ba}}{dT} - \frac{1}{U}\frac{dU}{dT} ,$$

$$\frac{1}{\tau_{ba}}\frac{d\tau_{ba}}{dT} = \frac{1}{L_{ba}}\frac{dL_{ba}}{dT} - \frac{1}{U}\frac{dU}{dT} = \frac{1}{H_{ba}}\frac{dH_{ba}}{dT} - \frac{2}{U}\frac{dU}{dT} .$$

According to these estimates the blocking anticyclones have to be more persistent in the warmer atmosphere with the weaker zonal circulation. The blockings with decreased, unchanged or slightly increased sizes have also to be weaker, while blockings with strongly increased sizes have to intensify. These results are in general agreement with observational data from (AFCPNH, 1979; CPAC, 1988) and with results of the general circulation model simulations (Lupo et al., 1995).

References

Analysis and Forecast of Cyclonic Processes in the Northern Hemisphere (AFCPNH). 1979. Kazan State University. Kazan. 215 pp. (in Russian)

Arsky, A.A., Mokhov I.I. & Petukhov V.K. 1989. Modeling of trends of the characteristics of

variability of the thermodynamic regime of the Earth's climatic system. Atmos. Oceanic Phys. 25: 3-13.

Catalog of Parameters of Atmospheric Circulation. Northern Hemisphere (CPAC). 1988. ASRIHMI-WCD. Obninsk. 452 pp. (in Russian)

Christoph, M., 1994. Zeitliche und raumliche Variabilitat hochfrequenter Fluktuationen (Stormtracks) in der realen Atmosphare und im Modell. Heft 99. Institut fur Geophysik und Meteorologie der Universitat zu Koln. 140 pp.

Dymnikov, V.P. & Filatov A.N. 1990. Stability of Large-Scale Atmospheric Processes. Gidrometeoizdat, Leningrad, 237 pp. (in Russian)

Golitsyn, G.S., Meleshko, V.P., Meshcherskaya, A.V., Mokhov, I.I., Pavlova, T.V., Galin, V.Ya. & Senatorsky, A.O. 1995. GCM simulation of water balance over Caspian Sea and its watershed. Proceedings of the First AMIP Conference. (submitted)

Gruza, G. V. & Korovkina L.V. 1991. Climatic monitoring of blocking processes of the middle of westerlies in Northern Hemisphere. Meteorol. Hydrol. 8:11-17.

Lejenas, H. & Okland, H. 1983. Characteristics of Northern Hemisphere blocking as determined from a long time series of observational data. Tellus 35A:350-362.

Lupo, A.R., Oglesby, R.J. & Mokhov, I.I. 1995. Climatological features of blocking anticyclones: A study of Northern Hemisphere CCM1 model blocking events in present-day and double CO_2 concentration atmospheres. Clim. Dyn.

Mokhov, I.I., Mokhov, O.I., Petukhov, V.K. & Khairullin, R.R. 1992a. Effect of global climatic changes on the cyclonic activity in the atmosphere. Atmos. Oceanic Phys. 28:7-18.

Mokhov, I.I., Mokhov, O.I., Petukhov, V.K. & Khairullin, R.R. 1992b. Cloud effect on the atmospheric eddy activity at climate change. Meteorol. Hydrol. 1:1-6.

Mokhov, I.I. 1993. Diagnostics of the Climate System Structure. Gidrometeoizdat, St.Petersburg, 272 pp. (in Russian)

Mokhov, I. I., Doronina T. N., Gryanik V. M., Petukhov V. K., Senatorsky A. O., Tevs M. V., Khairullin R. R., Naumov E. P., Korovkina L. V., Lagun V. E. and Mokhov O. I. 1994. Extratropical cyclones and anticyclones: Tendencies of change. In: The Life Cycles of Extratropical Cyclones, Vol. II. Ed. by S. Gronas and M. A. Shapiro. Geophysical Institute, University of Bergen, Bergen. P. 56-60.

Monotoring of Climate - 87. 1989. Leningrad, Gidrometeoizdat. 45pp.

Obukhov, A. M., Kurgansky M. V. and Tatarskaya M. S. 1984. Dynamical conditions for the origin of droughts and other and other large scale weather anomalies. Meteorol. Hydrol.10:5-13.

Schinke, H. 1993. On the occurrence of deep cyclones over Europe and the North Atlantic in the period 1930-1991. Beitr. Phys. Atmosph. 66:223-237.

Vinnikov, K.Ya., Groisman P.Ya. & Lugina K.M. 1990. Empirical data on contemporary global climate changes (temperature and precipitation). J. Climate 3:662-677.

The influence of local mountain forcing on stationary waves

Kimmo Ruosteenoja

Department of Meteorology
P.O.Box 4, 00014 University of Helsinki, Finland

Introduction

The local climate is determined by the zonal mean state and deviations from it. These deviations, called stationary waves, are primarily forced by diabatic heating and the vertical velocities at the lower boundary due to zonally-varying orography. In addition, the distribution of stationary waves is modified by nonlinear fluxes of heat and momentum in transient eddies. Global climate changes affect the distribution of stationary waves, and therefore it is essential to understand the behaviour of the waves in order to be able to forecast changes in local climate.

The importance of various factors in forcing stationary waves can be studied by simulating the waves with equations linearized about the temporally averaged zonal mean state. A linear model works well in middle latitudes, i.e. in areas where the zonal mean zonal velocity $[u]$ is far from zero. Close to the so called critical latitudes (CL) where $[u]$ vanishes, linear simulation fails. As discussed in Held (1983), stationary wave activity cannot pass the CL, but must be either absorbed or reflected. In the real atmosphere, the major sources of stationary waves exist in the middle latitudes. From these areas stationary waves propagate equatorward towards the critical layer (a zone with small $[u]$ surrounding the CL) in the subtropics. An essential question in the theory of stationary waves is to which extent the waves are reflected from the critical layer back into the middle latitudes. Previous studies give quite contradictory estimates of the degree of reflection.

This poster presents tentative results from a general circulation model (GCM) simulation (ECMWF cycle 34 model, T42 truncation) in which the effect of the critical layer on stationary waves is studied. In the real atmosphere, wave forcing occurs everywhere, and consequently it is impossible to isolate any wave component reflected by the CL from the total wave field. In the present experiment the waves are forced by local topographical forcing that is situated far from the CL. Thus there can be a latitude belt between the forcing and the CL where wave forcing/dissipation is small. In such a latitude belt, it is possible to separate the northward-directed component of the wave activity flux from the southward-directed one (Ruosteenoja 1989; Held and Phillips 1990).

In the experiment, the Earth surface consists almost entirely of ocean with uniform temperature in the zonal direction. The only factor that forces stationary waves is a 4000 m high
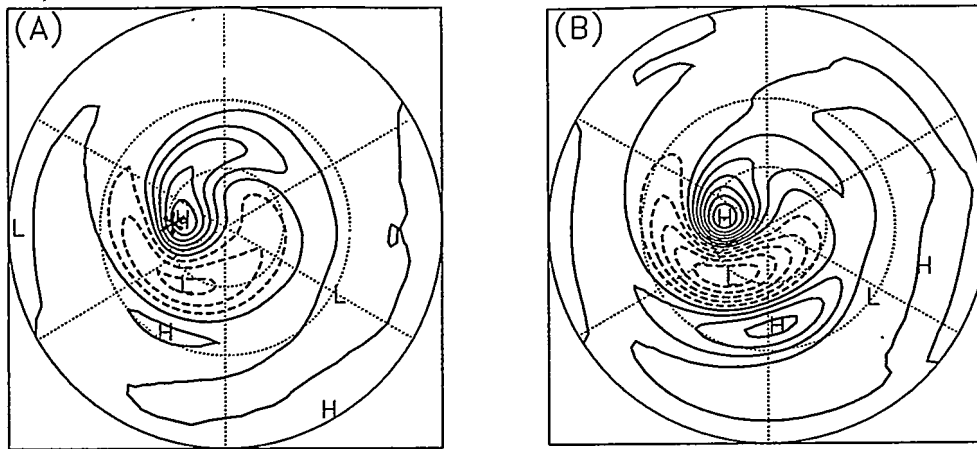
Fig. 1. Stationary eddy height field at 300 mb as simulated by a) the GCM and b) the linear model. Contour interval 50 m, negative contours dashed. The location of the mountain top is depicted by an asterix in panel a.

gaussian mountain with a half width of 1000 km, centered at the latitude 65°N. The total length of the simulation was 2700 days, from which a spinup period of 300 days was excluded.

In order to check that the waves are indeed mainly forced by the orography, and that there is no strong forcing between the mountain and the CL (e.g., that caused by transient eddies), the stationary waves are partitioned into components due to various forcing factors using a linear primitive equation model. The properties of this model are discussed in Ruosteenoja (1993). The forcing functions required in the linear simulation were derived from the output of the GCM.

Simulation of stationary waves

The distribution of stationary waves simulated by the two models is given in Fig. 1. The linear model reproduces the pattern given by the GCM very well, the spatial correlation between the two being 0.89. On the other hand, linear simulation produces too high wave amplitudes; in the GCM air may flow around the mountain, and thus vertical velocities at the lower boundary in the GCM are not as large as those predicted by linear theory.

A partition of the linear simulation showed that the direct response to mountain forcing dominates. The amplitudes of responses to other forcing functions were less than ~20% of the response to mountain forcing.

Flux of wave activity

The horizontal fluxes of stationary wave activity (for a definition, see Plumb 1985) are shown in Fig. 2. Both in the GCM and in the linear simulation, the flux is emitted from the area close to the mountain, and is directed to the southeast. In the GCM simulation, strongest wave absorption takes place near 30°N, i.e. somewhat to the north of the CL. In the linear simulation, absorption is strongest near the CL, although significant absorption occurs slightly poleward as well. A partitioning of the flux showed that this non-CL absorption is mainly

(a)

(b)
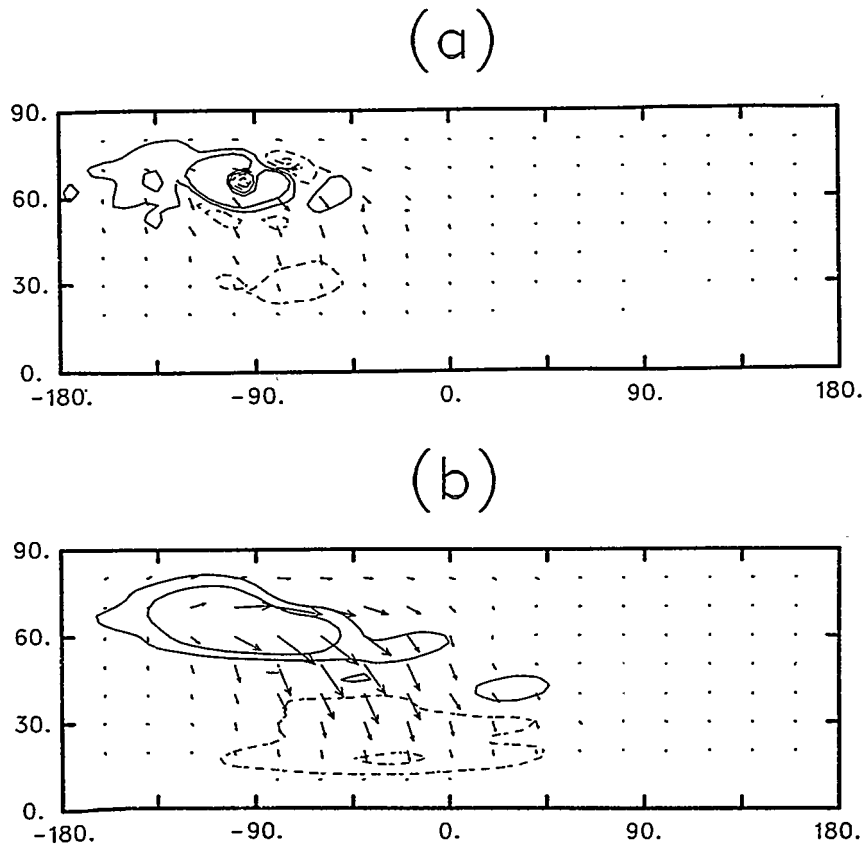
Fig. 2. The flux of wave activity (vectors) at 300 mb derived from (a) the GCM simulation and (b) the linear model response. Contours show the isolines of ± 2.5 × 10^{-6} and ± 7.5 × 10^{-6} m/s² of flux divergence. The CL is located at ~ 15°N.

caused by forcing due to transient eddies. In both cases, there is a belt of weak absorption between the mountain forcing and the critical layer, in accord with linear theory.

In both cases, the flux is southward-directed everywhere, i.e., there is no reflected component so strong that it would be discernible in the vector representation. The distribution of the correlation between the stationary wave velocity components u and v (Ruosteenoja 1989; Held and Phillips 1990) in the GCM results showed that the ratio of the northward to southward flux component was 0.2-0.3. This northward component includes both the wave activity reflected by the CL and the one forced by subtropical diabatic heating and transient eddy forcing.

Conclusions

When stationary waves are forced by local orography, a linear model simulates the pattern produced by the GCM surprisingly well. This is evidently related to the fact that in the GCM there is little wave reflection from the CL; a model linearized about the GCM mean state could not reproduce such reflection. In the GCM, the wave absorption takes place somewhat to the north of the CL. This is presumably so because the meridional group velocity of stationary waves is small when the basic flow [u] is weak. Thus stationary wave activity flux "spends

a long time" in the zone with small [u] north of the CL, and damping mechanisms work effectively.

References

Held, I. M., 1983: Stationary and quasi-stationary eddies in the extratropical troposphere: Theory. Large-scale dynamical processes in the atmosphere. B. Hoskins and R. Pearce, Eds., Academic Press, London. 127-168.

Held, I.M. and P.J. Phillips, 1990: A barotropic model of the interaction between the Hadley cell and a Rossby wave. J. Atmos. Sci., 47, 856-869.

Plumb, R. A., 1985: On the three-dimensional propagation of stationary waves. J. Atmos. Sci., 42, 217-229.

Ruosteenoja, K., 1989: Simulation of the partial reflection by the critical latitude with a linear model. Part I: Methods of regulating the reflectivity. J. Atmos. Sci., 46, 3487-3504.

Ruosteenoja, K. 1993: An isobaric coordinate multi-layer linear model of stationary waves. Technical Report No. 8, Dept. of Meteorology, Univ. of Helsinki. 20 pp.

Climate projections and scenarios

32 questions concerning climate change
(results of a questionnaire)

Ingeborg Auer*, Reinhard Böhm* and Reinhold Steinacker**

*Central Institute for Meteorology and Geodynamics, Vienna, Austria
**Institute for Meteorology and Geophysics, University of Vienna, Austria
both: Hohe Warte 38, A-1190 Vienna, Austria

Introduction

Climatologic research has gained much public attention specially in the field of questions about an oncoming or an already ongoing anthropogenic climate change. This high degree of public awareness has hit a field of research at an early stage of its development. In public opinion and in mass media the whole question about the existence and the the future development of an anthropogenic greenhouse effect seems to be solved already and public discussion concentrates only on the possible impacts and how to control or minimize them. Public opinion has surpassed quickly the development of science itself. Public opinion and mass media have taken over the topic to such an extent that in the meantime it begins in some way to repenetrate and influence scientific discussion. Not only scientific terms and methods to gain knowledge nowadays are present in scientific discussion but arguments like "the majority of scientists believes"and others are to be heard more and more. Not the "truth" in the sense of natural science- verificated by falsification - seems to be an argument but much guessing and believing dominates. Although the authors strongly believe the former to be the only method to be appropriate to gain knowledge and new insight in natural science, they are confronted so frequently with arguments based on the latter, that they decided to try to test themselves, what "the majority of scientists" really believes or guesses to know for sure.

The sample

A catalogue of popular assumptions about climate change topics circulating in public opinion was easy to collect. 32 popular climate change related statements about 12 items were collected, formulated into a questionnaire and distributed among climatologists.

Quite a large number of questionnaires is travelling round nowadays within the scientific community and it is not easy to raise the necessary attention of colleagues for a new one. To distribute our questionnaire we chose the method of personal contacts on scientific conferences, and at the occasions of visits at institutes to keep the return rate high. About 250 questionnaires were distributed by that method between June and September 1994 and 101 were sent back until March 1995 . Only 4 colleagues prefered to stay anonymous, 97 declared their names and institutes so that a good description of the sample characteristics was possible. Only one had to be eliminated of quality reasons. We express our thanks to our friends and colleagues who spent their time answering our questions:

The following number of answers came from the following countries:
33 from Austria, 8 from the USA, 7 from Germany, 5 from the Czech Republic, Norway and Switzerland, 4 from Belgium, 3 from Bulgaria, Finland, Slowenia and United Kingdom, 2 from Hungary, Poland, Portugal and Romania and one from Australia, Canada, Denmark, France, Greece, India, Sweden and Spain. 74 of the answering persons could be recognized as climatologists, 10 were glaciologists (which usually have also close connections to climatological questions), 12 were meteorologists or students not specialized in climatology and 4 stayed anonymous.

The sample therefore can be described as an international one with strong "Eurocentric" and even stronger "Austrocentric" tendency, but consisting to the overwhelming part of climatologists or persons having studied meteorology or closely related sciences. It is a sample consisting mainly of European professional scientists in climatology. The Austrocentric tendency was too strong to allow the presentation of statistics for the whole sample, it had to be devided into Austrian and international answers, which in some cases were significantly different. In this presentation we will show some examples and a short summary of the whole number of answers only for the international sample, without the 33 Austrians. An extended paper for the whole sample and the whole number of answers is in work and will be published elsewhere.

Results

The intention of the inquiry was to investigate the opinion within the scientific community about climate change questions that are believed to be already well solved in the public opinion. 32 questions were formulated that deal with 12 main assumptions about the existence, the predictability and the impacts of climate changes due to an artificially enhanced greenhouse effect. The possibilities to answer reached from "sure yes" , over "guess yes", "not answerable or no opinion" to "guess no" and "sure no". There were additional questions about the way the answers were gained: "by own research", "by studying scientific literature or discussion with colleagues" and "by mass media consumption". In the following some of the key assumptions about climate change topics will be discussed as the predictability of future evolution of climate by climate models and the detectability of an artificially enhanced greenhouse effect in climate time series. The other assumptions can be shown here only in the form of a comprehensive overview.

Predictability of greenhouse gas induced climate change

This topic is of main importance for the whole question of climate change. Its appropriate scientific description is the criterium for all impact studies which need quantitative solutions of the reaction of climate to greenhouse forcing. Todays advanced climate change research uses coupled atmosphere-ocean general circulation models to simulate climate with present and with future greenhouse gas forcing. There have been advances during the last years in including the oceans (e.g. Cubasch et al., 1991). Spatial resolution is one of the major problems in global climate modeling. Recently the step from T21 to T42 model resolution is being tried, a better resolution for global models seems not to be possible in the near future (von Storch, 1995). To get regional results methods of statistical downscaling or the construction and application of "limited area models" (LAM) recently are and will be used in the near future.

The topic of the predictability of greenhouse gas induced climate change has been formulated within the following three questions, referring to different scales. Figs.1, 2 and 3 show the corresponding opinion spectra within the international sample.
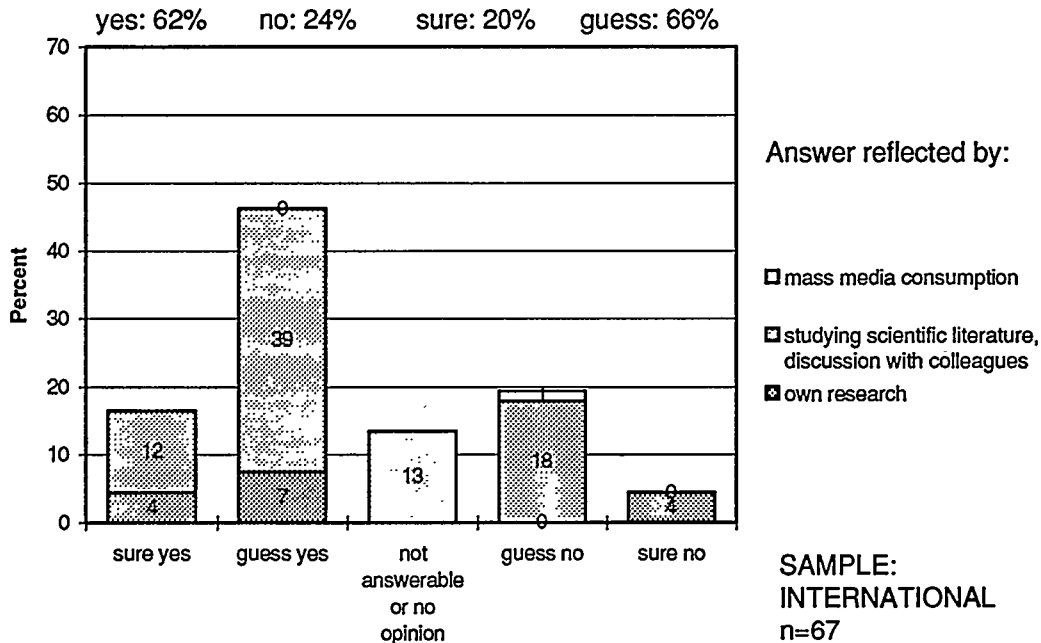
Fig.1 Assumption 1a: General circulation models are already successful in forecasting climate change due to enhanced greenhouse forcing in global scale.
Opinion spectrum (in percent) within the international sample

yes: 22% no: 62% sure: 28% guess: 56%
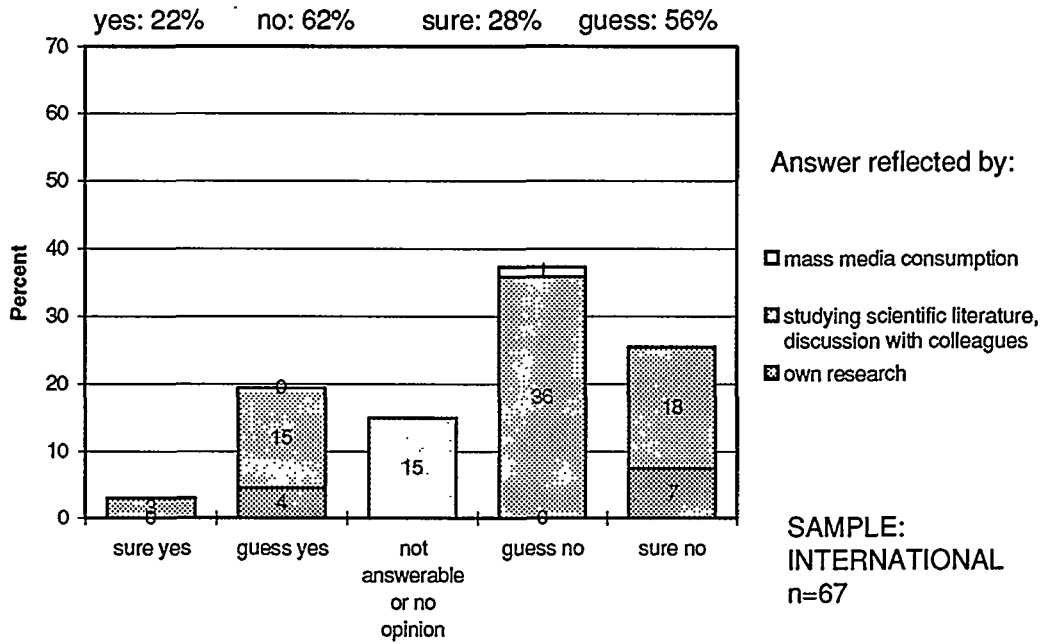
Fig.2 Assumption 1b: General circulation models are already successful in forecasting climate change due to enhanced greenhouse forcing in regional scale.
Opinion spectrum (in percent) within the international sample

yes: 2% no: 83% sure: 52% guess: 33%
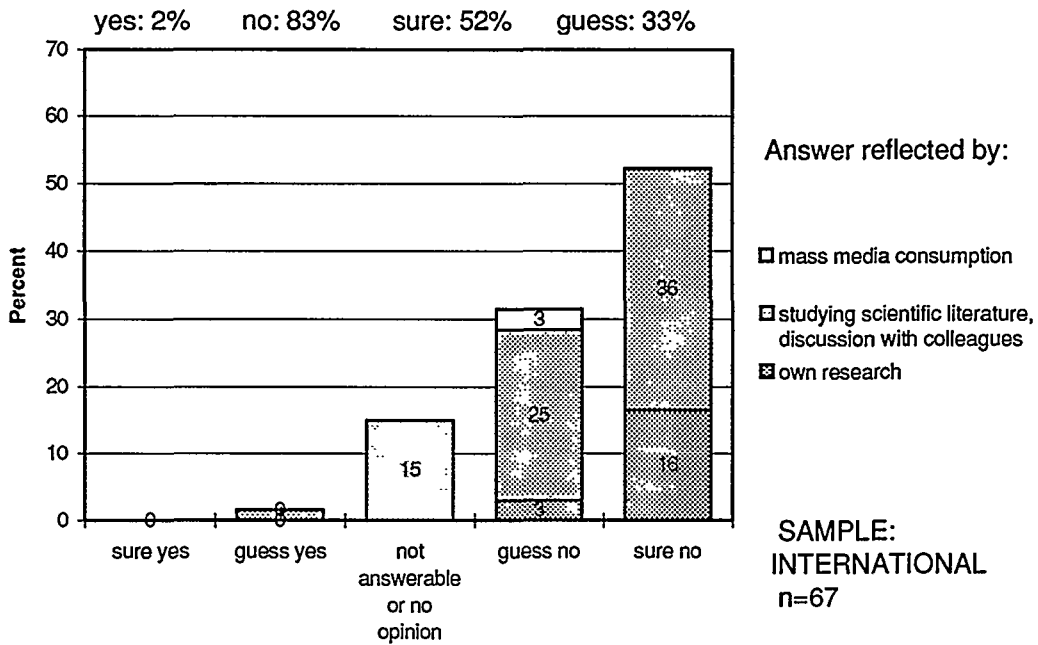
Fig.3 Assumption 1c: General circulation models are already successful in forecasting climate change due to enhanced greenhouse forcing in local scale.
Opinion spectrum (in percent) within the international sample

In the contrary to public opinion, which seems to be sure about the predictability of the oncoming climate changes and discusses only the possible impacts, the opinion spectrum of climatologists is different. A majority of climatologists (but not all of them) only believes in the ability of models to describe climate change in a global scale. The smaller the scale the less is the trust of climatologists in regional or local model results. Austrians are slightly more sceptical against model results than their international colleagues, a feature that can be seen in nearly all the following opinion spectra.

The existence of an anthropogenic greenhouse signal in climatic time series

The climate change topic has strongly been pushed into public attention by the fact that there has been a global warming since mid 19th century and a strong one during the last ten years. (Jones, 1994). The general public opinion seems to take this as a proof for the already ongoing anthropogenic climate change. More sophisticated reflexions about the difficulties to extract the "greenhouse signal" from high frequent statistical noise and from possible natural variability are not very popular. Fig.4 shows the opinion spectrum within climatologists.

yes: 44%   no: 52%   sure: 27%   guess: 69%

Answer reflected by:

□ mass media consumption

□ studying scientific literature, discussion with colleagues

☒ own research

SAMPLE:
INTERNATIONAL
n=67
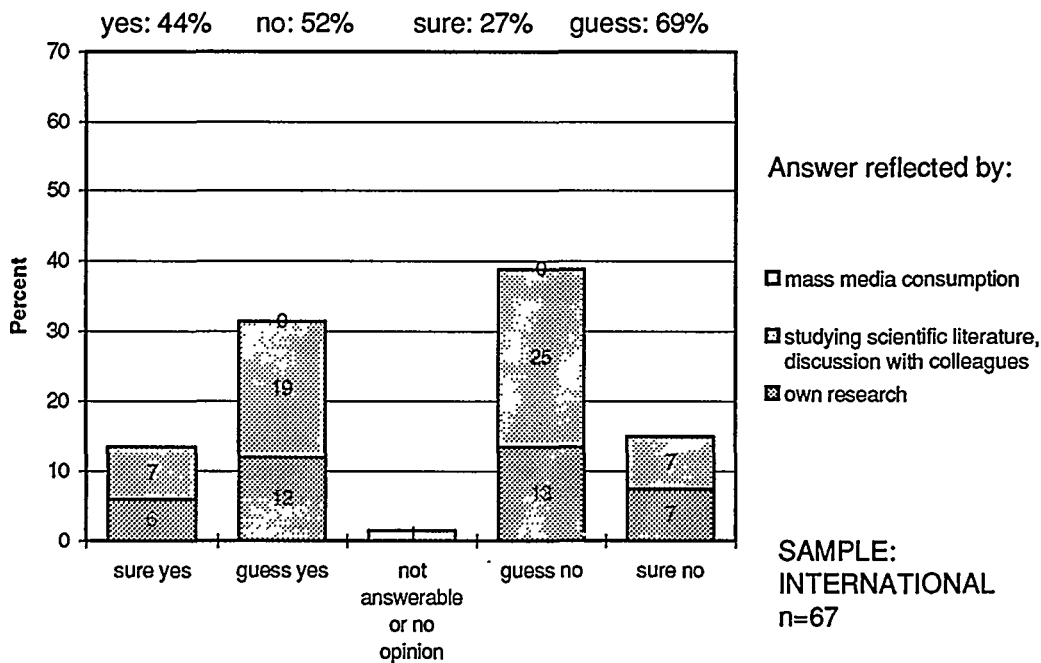
Fig.4 Assumption 2: Analyses of climate time series already show an additional greenhouse effect.
Opinion spectrum (in percent) within the international sample

Here the scientific community is sharply divided into believers and disbelievers, the latter slightly dominating the former. The amount of sure knowledge is rather small,

also a feature which can be seen also in most of the other topics. The opinion spectrum is a typical one for an unsolved scientific problem with a rather symmetric distribution and with much more "guessing" than "knowing". Therefore the quite common argument that the global warming since 1850 already was an artificial one is not favoured by a majority of the climatologists of our sample and should not be used as a "proof" for climate models at the moment.

The impacts of climate change

The next assumptions that were tested by the opinion poll deal with impacts of climate change which are believed to have serious mainly negative consequences for the human society. The following topics were tested by 28 questions about 10 kinds of possible impacts:

The question of extreme events
The question of desertification
Tropical and extratropical storms
Sea level rise
The expected amount of temperature rise in relation to historic time series
The speed of climate change.
The impact on vegetation
The extraordinary last ten years
Impact of climate change on tourism
Greenhouse effect and glaciers

The answers to the 10 impact items showed a widespread opinion spectrum, the opinions differing from topic to topic. To bring some system into the single opinion spectra two subsamples were built for assumptions concerning an expected anthropogenic greenhouse effect in the future and for those concening presently already effective anthropogenic greenhouse effects. The two subsamples turned out to be significantly different. About 30 % of the assumptions were declared as "not answerable" or as "no opinion about them". The sources of knowledge were between 5 and 10 % own research (slightly more concerning a present, slightly less concerning a future effectivity of an anthropogenic greenhouse effect). The majority got information from scientific literature or discussions with colleagues. This ratio seems to be a typical one for modern highly specialized research in a rather interdisciplinary field like the climate change topic. Only very few of the colleagues mentioned mass media to be a source of knowledge which is a sign of quality of the sample.

The subdivision into future related and present related questions brought significantly different frequency distributions of the answers. A majority of nearly 50% believes in a future effectivity of an anthropogenic greenhouse effect (about 20% do not). A minority of only 20% on the contrary believes that such an effect is already effective at present, 45% don't. Fig.5 shows the average opinion spectra about the present and future impacts of an anthropogenic greenhouse effect.
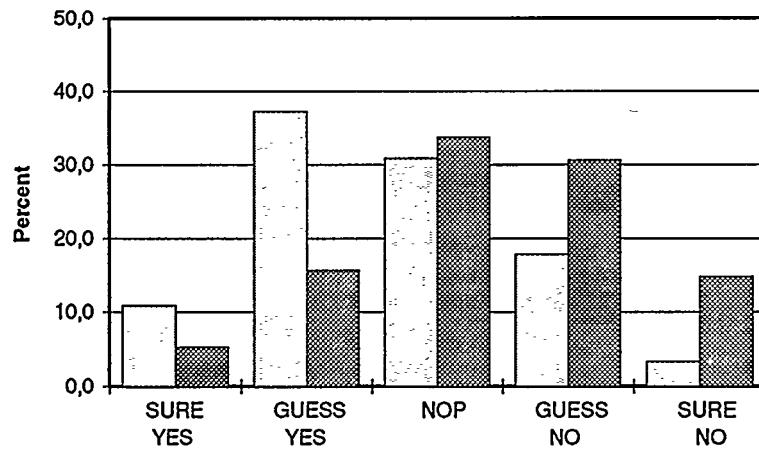
Fig. 5 Average opinion spectra within the International sample (n=67) about the present (dark) and the future (light) Impacts of an anthropogenic greenhouse effect.

Conclusions

In a very comprehensive form the results of the inquiry could be described in the following :

A weak majority of climatologists believes today's climate models to be able to describe a greenhouse gas induced climate change in global scale - much less in regional scale and not in local scale.

A majority of climatologists believes an anthropogenic greenhouse gas forced climate and its impacts to be developing in the future but not already at present.

The shape of the opinion spectra is in most cases far from that of a scientifically solved problem - a lot of work still has to be done.

References

Cubasch, U., K. Hasselmann, H. Höck, E. Meier-Reimer, U.Mikolajawicz, B.D. Santer, R. Sausen 1992. Time-dependent greenhouse warming computations with a coupled ocean-atmosphere model. Clim.Dyn., Vol.8, 55-69

Jones, P.D. 1994. Hemispheric surface air temperature variations: A reanalysis and an update to 1993. Journal of Climate, Vol.7, 1794-1802

von Storch, H. 1995. Inconsistencies at the interface of climate impact studies and global climate research. Met.Z., N.F. 4, H.2, 72-80

The development of climatic scenarios for assessing impacts of climate change

Timothy Carter[1], Maximilian Posch[2] and Heikki Tuomenvirta[1]

[1] Finnish Meteorological Institute, Box 503, FIN-00101 Helsinki, FINLAND
[2] National Institute of Public Health and the Environment (RIVM/MTV), P.O. Box 1, NL-3720 BA Bilthoven, NETHERLANDS

Introduction

There is a growing recognition that mitigation measures for limiting future global changes in climate due to the enhanced greenhouse effect are unlikely to prevent some changes from occurring. Thus, if climate changes appear to be unavoidable, there is an increased need to evaluate their likely impacts on natural systems and human activities.

Most impacts of climate change need to be examined at a regional scale, and their assessment requires up-to-date information on future regional climate changes. Unfortunately, accurate predictions of regional climate are not yet available. Instead, it is customary to construct *climatic scenarios*, which are plausible representations of future climate based on the best available information.

This paper outlines seven principles of climatic scenario development for impact studies, briefly describing some of the strengths and weaknesses of available methods and then illustrating one approach adopted in Finland.

Principles of climatic scenario development

Seven general principles are useful as a guide for developing climatic scenarios. These relate to: comprehensiveness, representativeness, the baseline, resolution, time horizon, consistency and accessibility.

Comprehensiveness points to the need to embrace all available information on future climate changes in a region before selecting from alternative options. There are many groups engaged in climate research and new results are continually being reported, though not always in published form, so it is important to be aware of ongoing activities.

Representativeness describes the requirement that scenarios should provide a fair reflection of existing estimates of regional climate, including the range of uncertainties surrounding predictions.

The *baseline* is the period used as a reference to describe the present climate, against which future projections are compared. Conventionally a thirty-year period (e.g., 1961-1990) is adopted as the climatological baseline.

Resolution is the spatial and temporal scale of the scenario. This should be appropriate for the scale of impact being examined. The spatial resolution of global model outputs is generally coarse, and downscaling procedures based on statistical methods or on numerical modelling are commonly employed to obtain regional scenarios. Similarly, global models are not able to provide reliable high resolution (daily) temporal outputs for use in impact assessment, and stochastic weather generators are sometimes used to downscale from monthly or seasonal model outputs.

The *time horizon* of a scenario should be selected according to the projection period over which impacts need to be assessed, but will also depend on the period for which climate predictions (and associated factors such as greenhouse gas concentrations) are available.

Consistency is desirable on at least four counts. First, changes in any one climatic variable (e.g., temperature, global irradiance, precipitation) should be consistent with changes in all other climatic variables. Second, changes in regional climate should be consistent with changes in other regions and globally. Third, a climatic scenario should be consistent with related non-climatic projections adopted in an impact assessment (e.g., of atmospheric carbon dioxide concentration or economic development). Fourth, it is desirable to have some consistency between the scenarios adopted in different impact studies, to allow for the intercomparison of results.

Accessibility refers to the availability of information for developing climatic scenarios and the ease of applying them in impact studies. One reason for the lack of consistency between scenarios adopted in previous impact studies has been the practical problem of insufficient access to common methods and data for scenario construction.

Types of climatic scenario

Four main types of scenario are commonly adopted in impact assessments: synthetic, analogue, model-based and composite scenarios. These are described briefly below and are reviewed in detail elsewhere (e.g., Giorgi & Mearns, 1991; Pittock, 1993).

Synthetic scenarios describe techniques where particular climatic elements are changed by realistic but arbitrary amounts. Given their arbitrary nature, these are not scenarios in the strict sense, but they do offer useful tools for constructing "response surfaces", which describe the sensitivity of a system or activity to climatic variations.

Analogue scenarios are constructed by identifying recorded climatic regimes which may serve as analogues of the future climate in a given region. These records can be obtained either from the past (temporal analogues) or from another region at the present (spatial analogues). The main virtue of both types is that they represent climatic conditions which have actually occurred. An important drawback of temporal analogues

is the uncertainty about the physical mechanisms and boundary conditions giving rise to a changed climate in the past, which may be different from those involved in greenhouse gas induced climate change. One problem with spatial analogues is that non-climatic features of the analogue region which are important in estimating impacts (e.g., daylength, soils, economic development) may not correspond closely with the same features in the study region.

Model-based scenarios are representations of the future global and regional climate under changed concentrations of greenhouse gases and other atmospheric constituents, as simulated by global climate models, usually three dimensional general circulation models (GCMs). The main problem with these models is their inability to resolve regional climate with any confidence. However, they are the most credible method of predicting future climate, since they attempt to simulate the physical processes that determine the global climate response to changing atmospheric composition.

Composite scenarios embrace a range of methods of combining some of the above techniques of scenario construction to obtain regional scenarios. These include qualitative analysis using expert judgement and more quantitative averaging and downscaling methods. Composite scenarios are useful integrators of knowledge, and can be used to indicate uncertainties in projections. Their major drawback is a lack of internal consistency when combining different approaches.

Climatic scenarios for Finland

In this section an example of climatic scenario development is presented for Finland. The scenarios were designed for impact studies in the Finnish Research Programme on Climate Change (SILMU).

The process of scenario development began with discussions on the needs of impact assessors working in different research disciplines in Finland. In order to obtain some guidance from experts involved in climate prediction and scenario development, an international workshop was held in Finland. This addressed the state-of-the-art of climate prediction over the Nordic region and the most appropriate methods of scenario development (Carter *et al.*, 1993). Based on the workshop recommendations, a number of scenarios were subsequently developed for SILMU (Carter *et al.*, 1995).

The scenarios are of two types: policy-oriented scenarios and scientific scenarios. The policy scenarios are generalised for the whole of Finland and represent uncertainties concerning greenhouse gas emissions and global climate response by including high, central ("best guess") and low estimates (Table 1). The scientific scenarios (not shown) have more regional and temporal detail, and reflect uncertainties in modelling regional climate change. The baseline climatology used in SILMU is from the period 1961-1990.

All scenarios are based on a composite approach which combines information from a simple global model framework (MAGICC - Hulme *et al.*, 1995) with recent information from coupled ocean-atmosphere GCMs. This approach has also been followed by the IPCC as part of its international review of potential impacts of climate change (TSU,

Table 1   SILMU policy-oriented scenarios for 2020, 2050 and 2100. Temperature and precipitation changes are annual for Finland; CO_2 concentration and sea-level rise are global means (data from Carter et al., 1995).

Year and attribute	SILMU Policy Scenarios		
	1 (Central)	2 (Low)	3 (High)
2020:			
CO_2 concentration (ppmv)	425.6	408.8	433.7
Temperature change (°C)	1.2	0.3	1.8
Precipitation change (%)	3.0	0.8	4.5
Sea-level rise (cm)	8.9	2.1	19.2
2050:			
CO_2 concentration (ppmv)	523.0	456.1	554.8
Temperature change (°C)	2.4	0.6	3.6
Precipitation change (%)	6.0	1.5	9.0
Sea-level rise (cm)	20.8	4.6	43.3
2100:			
CO_2 concentration (ppmv)	733.3	484.9	848.2
Temperature change (°C)	4.4	1.1	6.6
Precipitation change (%)	11.0	2.8	16.5
Sea-level rise (cm)	45.4	7.4	95.0

1994). MAGICC provides a range of estimates over the period 1990-2100 of the time evolution of global mean annual temperature change and global sea-level rise for different assumptions of greenhouse gas emissions reported by the Intergovernmental Panel on Climate Change (IPCC, 1992). The GCMs provide the regional pattern of climate change corresponding to a given global temperature change at different time slices in the future. The performance of these GCMs in the Nordic region has been evaluated in a separate study (Räisänen, 1995).

MAGICC also computes the globally-averaged effect of projected sulphate aerosol loading on climate, which offsets some of the greenhouse gas induced warming. However, it does not account for the regional effects of sulphate loading as demonstrated by more recent GCM simulations (e.g., Taylor & Penner, 1995; Hadley Centre, 1995).

The scenarios are available on a diskette (Carter et al., 1995), allowing changes in climate to be linearly interpolated for any point in Finland and any year (1990-2100). More sophisticated spatial downscaling techniques were not applied due to time constraints. In addition, stochastic daily time series can be obtained for any of the given scenarios using a weather generator also included on the diskette (Posch, 1994). Note that the global scenarios obtained from MAGICC of CO_2 concentration (which affects plant growth) and sea-level rise (important in low-lying regions not subject to rapid isostatic uplift) may also be required in impact assessments (cf. Table 1).

Conclusions

As predictions of future atmospheric composition and climate improve, so the range of uncertainties should begin to narrow. For this reason, the detail provided by climatic scenarios generally has a limited "shelf-life", and is soon superceded. However, if scenarios are to be useful in decision-making and planning, it is imperative that they embrace most foreseeable changes. The Finnish policy-oriented scenarios illustrate an attempt to account for some (though not all) of these uncertainties. The ultimate objective is a set of scenarios for which any modification based on new information would merely be an exercise of fine tuning rather than a complete re-appraisal of the future climatic regime.

References

Carter, T., Holopainen, E. & Kanninen, M. (Eds). 1993. Techniques for Developing Regional Climatic Scenarios for Finland. Publications of the Academy of Finland 2/93, Helsinki, 63 pp.

Carter, T., Posch, M. & Tuomenvirta, H. 1995. SILMUSCEN and CLIGEN User's Guide: Guidelines for the Construction of Climatic Scenarios and Use of a Stochastic Weather Generator in the Finnish Research Programme on Climate Change. Publications of the Academy of Finland 5/95, Helsinki, 62 pp. plus diskette.

Giorgi, F. & Mearns, L.O. 1991. Approaches to the simulation of regional climate change: a review. Rev. Geophys. 29: 191-216.

Hadley Centre 1995. Modelling Climate Change: 1860-2050, Hadley Centre, Bracknell, UK, 13 pp.

Hulme, M., Raper, S. & Wigley, T.M.L. 1995. An integrated framework to address climate change (ESCAPE) and further developments of the global and regional climate modules (MAGICC). Energy Policy (in press).

IPCC 1992. Climate Change 1992: The Supplementary Report to the IPCC Scientific Assessment. J.T. Houghton, B.A. Callander & S.K. Varney (Eds), Cambridge University Press, 200 pp.

Pittock, A.B. 1993. Climate scenario development. In: A.J. Jakeman, M.B. Beck & M.J. McAleer (Eds). Modelling Change in Environmental Systems. John Wiley, pp. 481-503.

Posch, M. 1994. Development of a weather generator for Finland II. In: M. Kanninen & P. Heikinheimo (Eds). The Finnish Research Programme on Climate Change. Second Progress Report. Publications of the Academy of Finland 1/94, Helsinki, pp. 323-328.

Räisänen, J. 1995. A comparison of the results of seven GCM experiments in northern Europe. Geophysica 30: 3-30.

Taylor, K.E. & Penner, J.E. 1994. Response of the climate system to atmospheric aerosols and greenhouse gases. Nature 369: 734-737.

TSU 1994. Climatic Scenarios and Socioeconomic Projections for IPCC WGII Assessment. IPCC WGII Technical Support Unit, Washington, D.C, 12 pp. plus appendices and diskettes.

Atmospheric thermal regime evolution in the next decades due to anthropogenic emissions according to IPCC scenarios

Victor A. Frolkis, Igor L. Karol, and Andrey A. Kiselev

Main Geophysical Observatory
St.Petersburg, 194018, Russia

The influence of atmospheric anthropogenic pollution on radiative-thermal regime has constantly increased during the last decades. This tendency is likely to keep in the near future. As a result of human activity the atmosphere is regularly polluted by dozen compounds varying in chemical composition and radiative properties. It is of great importance to find out what kind of influence the emission of each of these compounds exerts on thermal behavior of the lower atmosphere and to determine which gas emission is the most "dangerous". For this purpose a varying with time vertical profile of air temperature due to the anthropogenic emission of one or a few gases is calculated based on 1-D radiative photochemical model that allows one to calculate the vertical profiles of 44 main gaseous air components and atmospheric temperature in the 0-50 km layer. Model definition is described by Karol (Ed. 1986).

Two scenarios of greenhouse gas emissions are used. Emission scenario A of twenty anthropogenic gases (N_2O, NO_x, CO, CH_4, CO_2, CH_3CCl_3, CCl_4, CH_3Br, CFC-11, -12, -22, -113, -114, -115, -123, -124, -141b, -142b, Halon-1211, -1301) during 1985-2050 is taken from IPCC (1992). Scenario B differs from scenario A in a more intensive emission of six gases (CCl_4, CH_3Br, CH_3CCl_3, CFC-11, -12, -113) during 1992-2010. Scenario A obeys the actual international restrictions on production and application of ozone destructing compounds (CFCs, Halons), while scenario B meets these demands only partially. In scenario A, in particular, during 1985-2050 surface mixing ratios (SMRs) of N_2O and CH_4 will increase by 17.7% and 51.2%; mixing ratio of CO_2 by 46.9%; SMRs of NO_x = NO + NO_2 and CO by 74.7% and 78.0%, respectively; SMRs of CFCs and Halons are found to be maximum in 1993-1996 with subsequent decrease, the only exception being CFC-22, whose SMR will increase till 2019. In scenario B SMRs of CFC-12 and CCl_4 will increase till 2006; SMR of CFC-11 and -113 will grow till 1995-1996; CH_3Br increases during the whole period. Some of the above gases (e.g. CO_2) exert a direct influence on the atmospheric radiative regime, being chemically passive. Others (e.g. CO) affect radiative regime only indirectly, causing photochemical changes of radiatively-active air components. The third (e.g. CH_4) exert both direct and indirect influence.

The following computation procedure has been used. The vertical profiles of gaseous constituents and temperature have been calculated during 1985-2050, considering the anthropogenic emissions that are constant in time and equal to those of 1985. Then another variant is calculated in which the emissions of one or of a few anthropogenic gases changed with time according to scenarios A or B, with all other gases having constant emission of 1985. Temperature differences of these two variants allow one to estimate the emission effect of each gas on temperature changes at any moment of time. It should be emphasized that a separate gas emission always changes the contents of all gases because of their photochemical interactions. Thus, the temperature changes depend on the response of all atmospheric gas contents to the emission of the gas under consideration. Vertical thermal transfer in the model is parameterized by the lapse rate y equal to standard $y_c = -6.5$ K/km in the model. To estimate the model sensitivity to such parameterization other variants of y are used: $y_0 = -5.5$ K/km, $y_{\pm} = -(5.5 \pm 0.11 \cdot \Delta T_s)$ K/km (where ΔT_s is a surface temperature deviation from the undisturbed state (Gulev et al. 1991)), and the moist adiabatic gradient y_w.

Fig. 1 shows temperature deviations ΔT (for y_c) in the layer 0-50 km during 1990 - 2050 caused by the N_2O (A), NO_x (B), CH_4 (C), CO (D), CO_2 (E) emissions according to scenario A. Vertical ΔT profiles due to the emissions of N_2O, NO_x and CO are very close to ΔT in the layer considered and attain maximum $\Delta T = -1.1 \ldots -1.2$ K in the upper stratosphere. In the lower stratosphere ΔT are 0.2 ... 0.4 K, and at the 30-km level ΔT are practically absent. It is also interesting to note a weak temperature variation with time for the emissions of N_2O, NO_x, and CO. Temperature variations caused by the emission of CH_4 are somewhat lower, and maximum temperature decrease ΔT (≈ 0.8 K) in the upper stratosphere will occur in 2010, later ΔT will decrease due to the ozone content increase in the upper stratosphere, while the continuing emissions of N_2O, NO_x, and CO will lead to ozone depletion there. Fig. 2 presents a temperature deviation for the joint emission of all CFCs and Halons (A for scenario A, B for scenario B). The influence of CFC on temperature occurs only in the upper stratosphere where even at a considerable emission decrease after 1996 (scenario A) temperature deviations ΔT will be twice as great by 2010 as those due to the emission of N_2O, NO_x, or CO. This effect is connected with ozone content decrease in the upper stratosphere, rather than with the greenhouse cooling of the stratosphere. During 2010-2050 a considerable decrease of CFCs emissions will contribute to the stratosphere ozone growth and, hence, to the decrease of stratosphere cooling. Comparison of Figs. 2A and 2B shows that scenario B "provides" further temperature decrease approximately by -1.0 K in the upper stratosphere by 2010. Fig. 3 presents temperature variations ΔT (for y_c) in the 0-50 km layer as a result of simultaneous emissions of all anthropogenic gases according to scenarios A (A) and B (B). Comparison of Figs. 1E and 2A shows that after 2020 the total thermal effect in the upper stratosphere due to all the emissions will be less than that due to the emission of CO_2 alone. Emissions of CO_2, N_2O, NO_x, and CH_4 cause the greenhouse cooling of the stratosphere, however their total greenhouse effect is reduced by due to absorption bands overlap. The total emission of anthropogenic gases leads to ozone enhancement at the altitudes

over 30 km, which also reduces the stratospheric cooling. Surface temperature increase (and that of the whole troposphere) due to the greenhouse effect proceeds almost linearly in time, with surface temperature increment
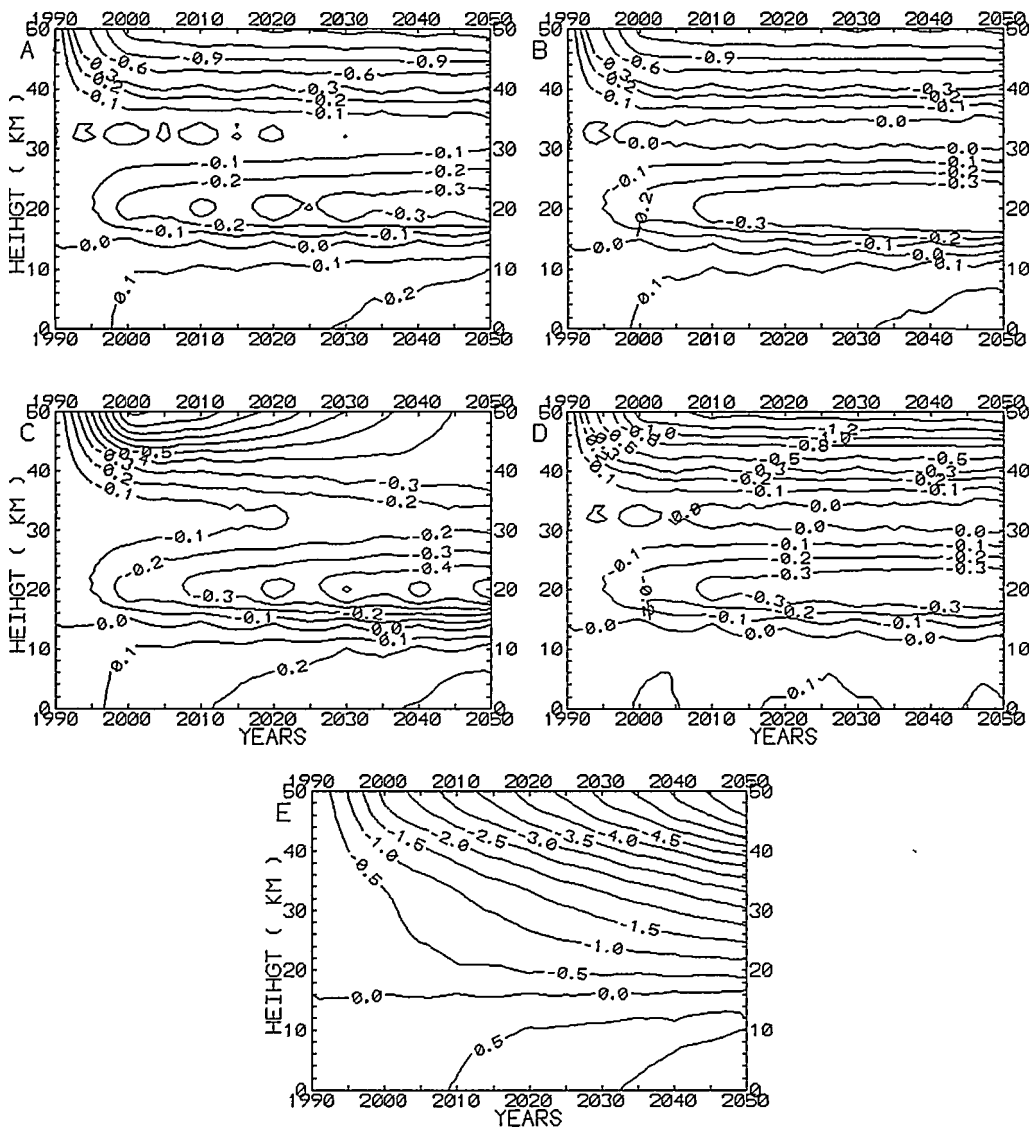

Fig. 1. Temperature deviations ΔT (K) caused by emission of N_2O (A), NO_x (B), CH_4 (C), CO (D), CO_2 (E) according to scenario A.

for emissions of N_2O, NO_x by 0.2 K, for emission of CH_4 by 0.3 K, and for that of CO_2 by 1.5 K by 2050; the total value 2.3 K is approximately equal to the surface temperature increment caused by the total emission of all gases. Surface temperature enhances the faster the higher is the lapse rate $|\gamma|$, and by 2050 the surface temperature will rise by 1.4, 1.6, 1.7, and 2.4 K for γ_-, γ_w, γ_0, and γ_+, respectively. Parameterization γ_+ at which convec-

tive mixing intensity and surface temperature growth T_s leads to the greater tropospheric warming in the quasistationary regime, it enhances the greenhouse effect of anthropogenic gases. Parameterization y_{-} results in the convective mixing intensity decrease and leads to less tropospheric warming, hence, it weakens the positive connection between gas emissions and greenhouse warming.
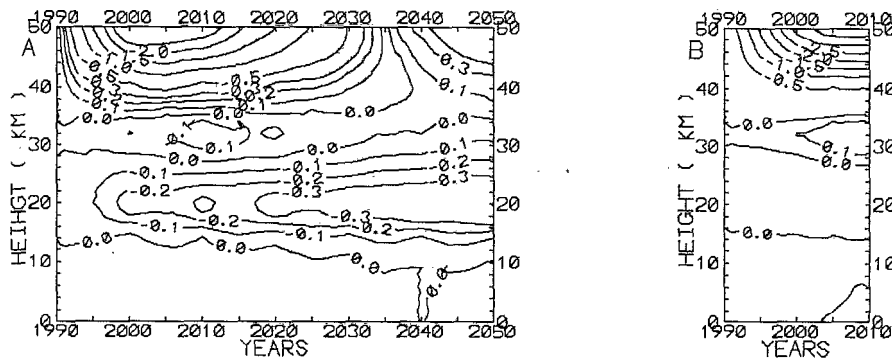
Fig 2. Temperature deviations ΔT (K) caused by emission of CFC for scenario *A (A)*, scenario *B* (B).
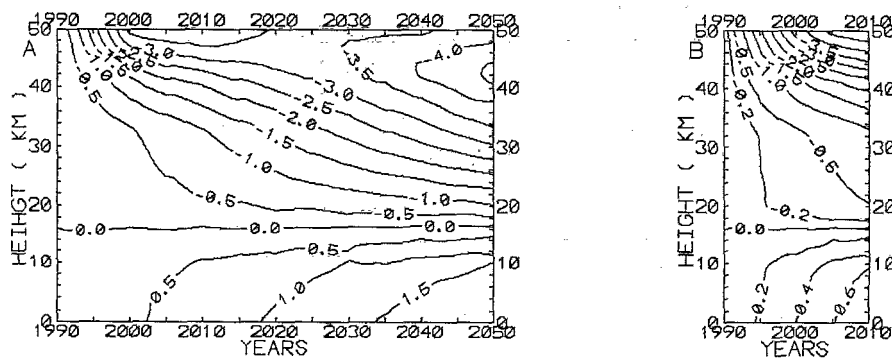
Fig 3. Temperature deviations ΔT (K) caused by the simultaneous emission of all anthropogenic gases according to scenarios *A* (A) and *B* (B).

Reference

IPCC 1992. Climate change 1992. The supplementary report to the IPCC scientific assessment. 1992. /Houghton, J.T., Callender, B.A. & Varney, S.K. /Eds.// Cambridge Univ. Press, 365 pp.

Karol, I.L. /Ed./ 1986. Radiative-Photochemical Models of the Atmosphere (in Russian). Gidrometeoizdat, Leningrad, 192 pp.

Gulev S.K., Zveryaev, I.I & Mokhov, I.I. 1991. Troposheric vertical temperature gradient depending on surface temperature regime (in Rus.). Izv. Russ. Acad., Atm. Oceanic Phys. 27:419-430

Possible Future Climates;
The IPCC-scenarios simulated by Dialogue

Jeljer Hoekstra
KEMA-KES
P.O. Box 9035, 6800 ET Arnhem, The Netherlands
e-mail: hoekstra@mta6.kema.nl

Introduction

Global warming is an environmental problem that increasingly attracts the attention of governments, (inter)national organizations and the general public. Policymakers that want to attack this problem need to understand the causes and effects of all related aspects. For this reason integrated assessment tools are developed that allow policymakers to analyze and evaluate climate change scenarios.

Dialogue is such an integrated assessment tool. This paper presents the results of Dialogue when the socio-economic parameters of the six well-known IPCC-scenarios, IS92a-f (IPCC 1992) are taken as a point of departure. Using as input, variables as population growth and the energy intensity of an economy, Dialogue goes through a chain of processes and finally determines climatic changes in temperature and precipitation.

Dialogue

Dialogue computes the emissions and concentrations of several greenhouse gases (including SO_2) in ten regions. After that it computes radiative forcing and hence, change in surface temperature and in precipitation. In future versions of Dialogue we will add impacts of climatic change as well.

For each step in the chain from emissions to climate change, more than one established model is used. The resulting different outcomes are then used to calculate the maximum, minimum and median values that serve as an indication for the uncertainty. This multi-model approach is an elegant and simple way of expressing the uncertainties that arise because of the lack of scientific knowledge about physical and economic processes and insufficient datasets to estimate parameters. It also shows where uncertainties are large and can direct future research into those areas. The uncertainty propagates through the chain and will inevitably become bigger. Dialogue shows at each step the combined uncertainty of all previous steps.

Results and discussion

The socio-economic parameters of the IPCC-scenarios (IPCC 1990, Pepper 1992) are used as input for Dialogue. This leads to emissions of greenhouse gases in each region. The emissions are summed and used as input for the concentration module. The atmospheric CO_2 concentrations are shown in figure 1.
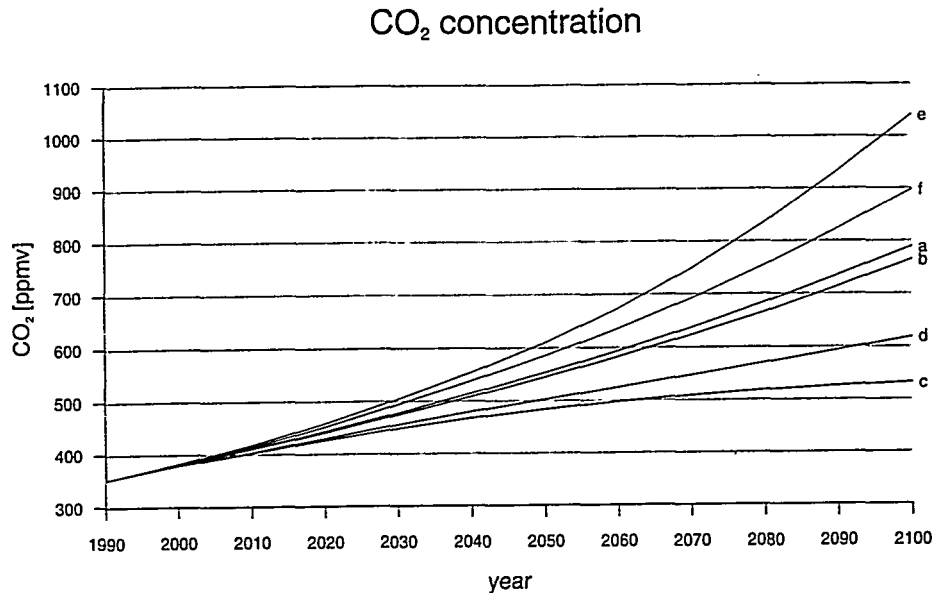
CO_2 concentration

Figure 1, Global CO_2 concentration for every IPCC-scenario (IS92a-f)

The increased greenhouse gas concentrations result in climatic changes, through a change of the radiative forcing. Figure 2 shows the temperature increase relative to 1990 in Western Europe for IS92a and IS92c. It also shows the uncertainty band. This is the combined uncertainty of every process sofar, i.e. uncertainty in emissions, concentration, radiative forcing and in temperature. The uncertainty band is wider for IS92a than for IS92c, which may in a very extreme case even lead to less global warming in scenario a than in c. This is caused by the SO_2 aerosol. There is large uncertainty over the magnitude of the cooling effect of SO_2. In IS92c less SO_2 is emitted thus there is less cooling and caused by the resulting smaller uncertainty, global warming could be less in scenario a than in scenario c.

Temperature increase in W. Europe
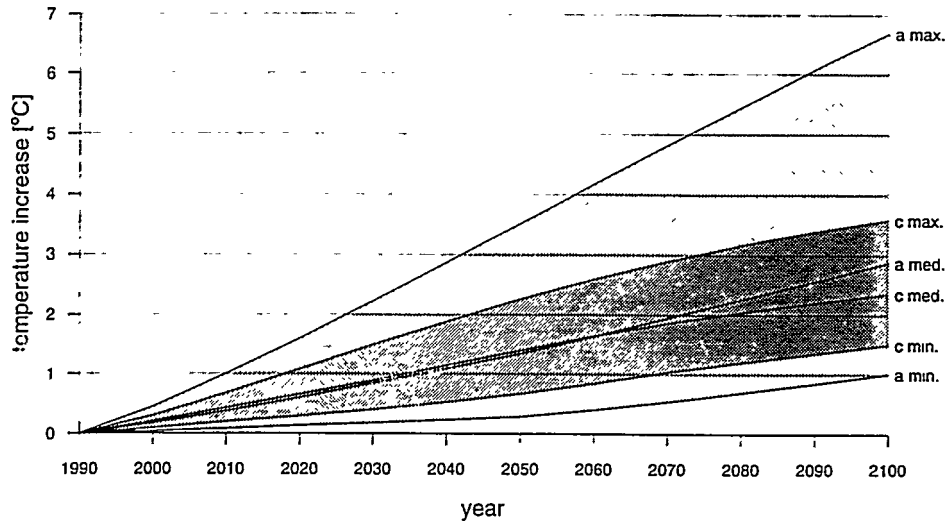
Figure 2, Temperature increase in Western Europe relative to 1990 for IS92a and IS92c with uncertainty range.

Figure 3 shows the global temperature increase for all the IPCC-scenarios. Due to the many lags in the climate system differences between the six scenarios cannot be seen in the global average temperature until about 2040. The curves seem to be grouped in clusters that have the same assumption about population growth. This shows that population is a very important factor for climate change.

The distribution of climatic changes over the globe are shown in figure 4 and 5 for IS92a for temperature and precipitation in the year 2100. The latitudes closer to the poles and especially the landmasses experience the greatest warming. There is a decrease as well as an increase in precipitation. Rainfall in India increases and so does rainfall in the Sahara. However, despite a 20% increase, the Sahara will remain a very dry area. Decreases in precipitation occur over the oceans at latitudes close to 30N and 30S.

References

IPCC (Houghton, J.T., B.A. Callander and S.K. Varney (eds.)), 1992. Climate Change 1992, The Supplementary Report to the IPCC Scientific Assessment, Cambridge University Press, Cambridge.

Pepper, W.J., J.A. Legget, R.J. Swart. J. Wasson, J. Edmonds and I. Mintzer, 1992. Emission Scenarios for the IPCC -an update: Background Documentation on Assumptions, Methodology and Results. US EPA Washington D.C.

Global warming
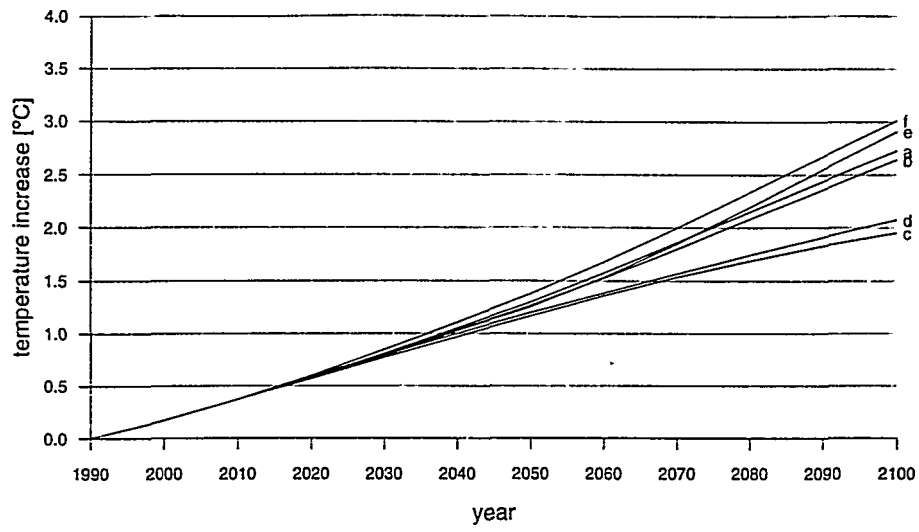
Figure 3, Global temperature increase relative to 1990 for IS92a-f

Scenario a
## global warming in 2100
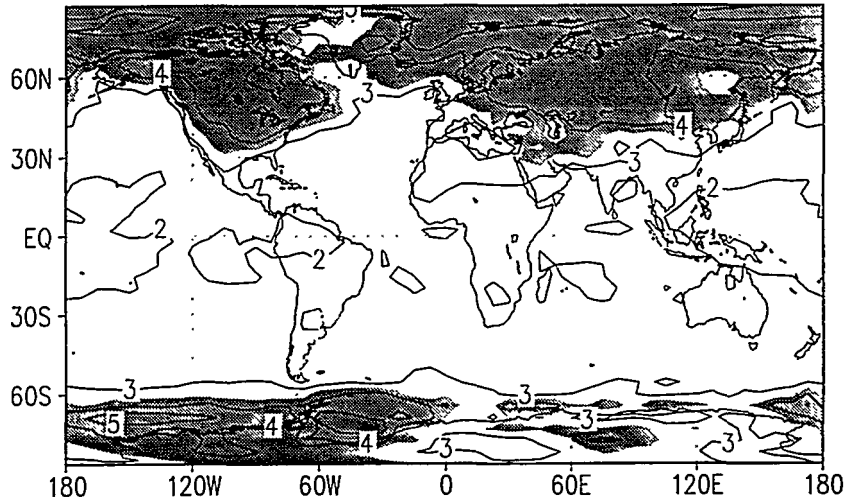

Scenario a
precipitation change in 2100
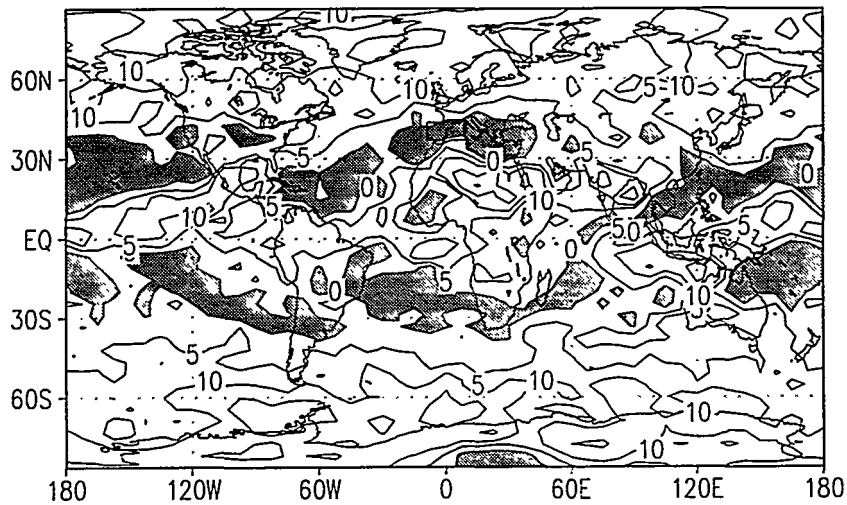
Figure 4, Maps of temperature (top) and precipitation (bottom) change in 2100 for IS92a, a temperature increase > 3.5°C and a precipitation decrease are shaded grey

Scenario a
global warming in 2100
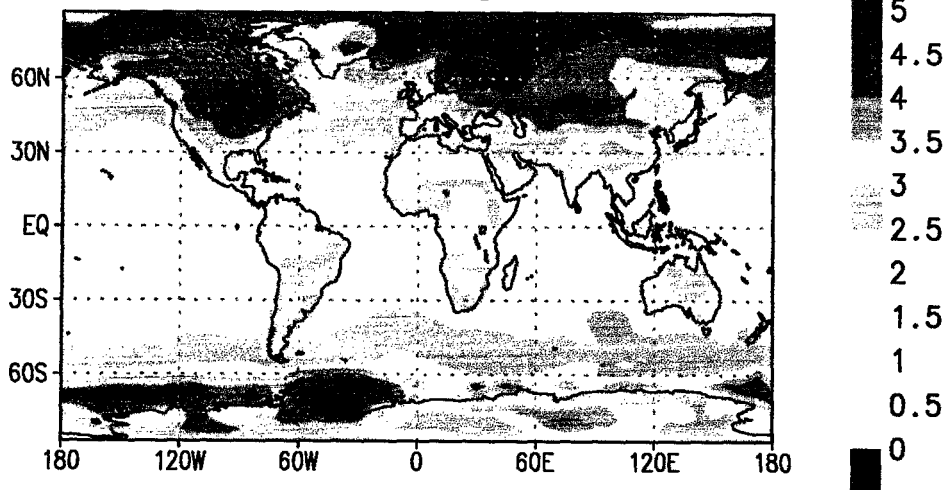
Scenario a
## precipitation change in 2100
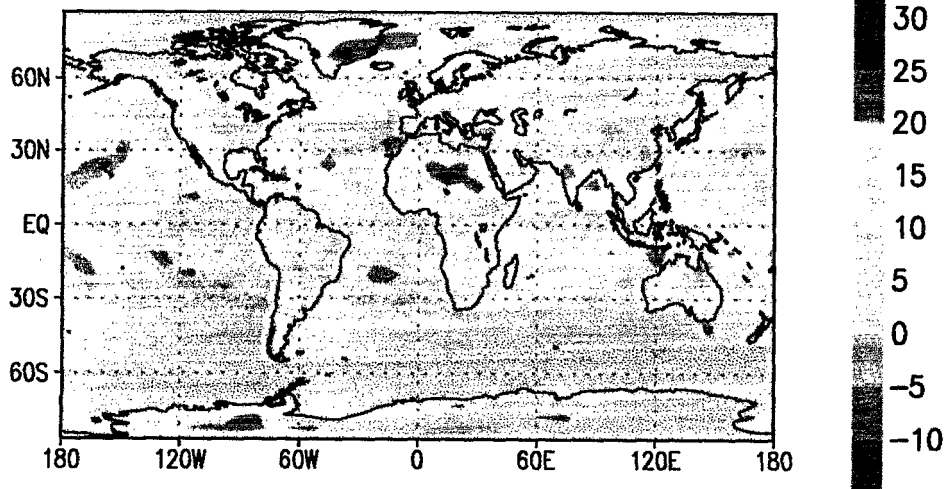
Figure 4, Maps of temperature (top) and precipitation (bottom) change in 2100 for IS92a

Some GCM simulation results on present and possible future climate in northern Europe

Jouni Räisänen

Department of Meteorology, University of Helsinki
P.O.B. 4, FIN-00014 Helsinki

Introduction

The Intergovernmental Panel on Climate Change initiated in 1993 a project entitled "Evaluation of Regional Climate Simulations". The two basic aims of this project were to assess the skill of current general circulation models (GCMs) in simulating present climate at a regional level and to intercompare the regional response of various GCMs to increased greenhouse gas concentrations. The public data base established for the comparison included simulation results from several modelling centres, but most of the data were available in the form of time-averaged seasonal means only, and important quantities like precipitation were totally lacking in many cases. This paper summarizes the intercomparison results for surface air temperature and sea level pressure in northern Europe. The quality of the control simulations and the response of the models to increased CO_2 are addressed in both winter (December-February) and summer (June-August). A more detailed discussion of the same subject is provided by Räisänen (1994).

## Comparison of control simulations with observed climate

Altogether, data were available for seven experiments, five of which have been conducted with coupled atmosphere-ocean GCMs [two experiments (hereafter ECHAM1 and ECHAM2) from MPI and one from each of GFDL, NCAR and UKMO; for references, see Räisänen (1994)] and two with atmospheric GCMs connected to a mixed-layer ocean (GFDL and UKMO). To separate from each other the GFDL (UKMO) experiments of the former and the latter type, the terms GFDL/coupled and GFDL/mixed (UKMO/coupled and UKMO/mixed) are used in the following. All the data were given on a grid with a mesh size of 5.6° latitude X 5.6° longitude. The statistics for the control simulations were in most cases computed by using a 10-year averaging period.

Surface air temperature

Fig. 1a shows the wintertime area averages of surface air temperature in the land areas of northern Europe (bordered from the south by the latitude 50°N and from the east by the longitude 60°E) in the seven control simulations and according to observational data extracted from a data bank maintained by the Carbon Dioxide Information Analysis Center, Oak Ridge, USA. Strikingly, all seven models produce area average temperatures colder than observed. This bias is relatively small in the

two GFDL runs, but it is of the order of 10°C in the NCAR and the two UKMO simulations. In many cases, the cold bias grows towards northeast and the horizontal temperature gradient across the continent is consequently too large.
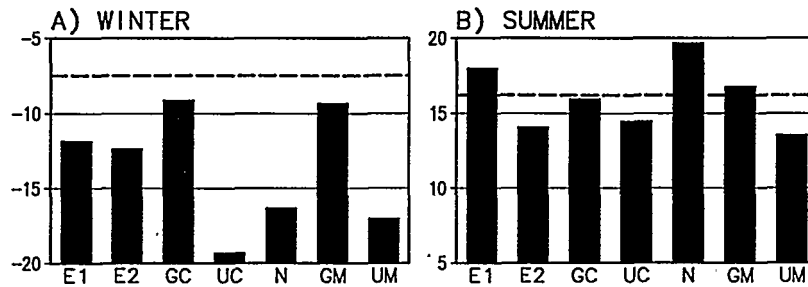

Fig. 1 The simulated (bars) and observed (dashed lines) area average temperatures (°C) in the continental northern Europe in (a) December-February and (b) June-August. E1 = ECHAM1, E2 = ECHAM2, GC = GFDL/coupled, UC = UKMO/coupled, N = NCAR, GM = GFDL/mixed and UM = UKMO/mixed.

In summer (Fig. 1b), the errors in area average temperature vary in sign and are generally smaller than in winter. However, the simulated north-south temperature gradient is typically somewhat too large, most markedly in the ECHAM1 and NCAR experiments.

Sea level pressure

The accuracy of the simulated sea level pressure distributions is characterized in Fig. 2 by the spatial correlations with the climatological fields obtained from the ECMWF analyses for 1979-1989 (Hoskins et al. 1989). In addition to the continental northern Europe, the domain used in this comparison (50°-75°N, 30°W-60°E) includes the northeastern North Atlantic and a part of the southern Arctic Ocean. In winter (Fig. 2a), four of the seven models succeed relatively well (correlation with the observed pressure distribution near 0.9) but the other three considerably worse. The climatological Icelandic low is typically fairly well simulated (apart from the ECHAM1 run, in which this low is located much too far to the south), but there are somewhat larger discrepancies over the continental northern Europe. In some models, most markedly in ECHAM1, UKMO/coupled and NCAR, the simulated pressure distribution implies a somewhat too easterly flow over northern Europe. This is one the possible causes for the cold bias in the simulated temperatures.
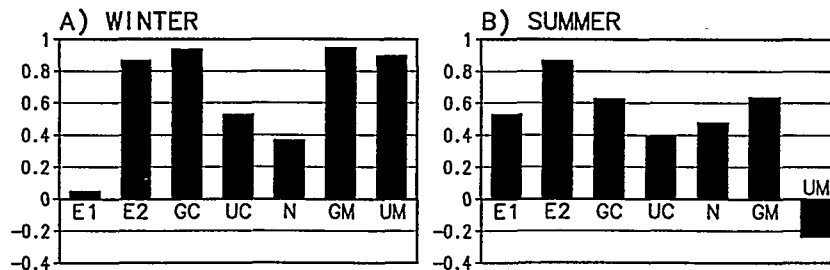
Fig. 2 Spatial correlation between simulated and observed mean sea level pressure fields within the area (50°-75°N, 30°W-60°E) in (a) December-February and (b) June-August.

In summer (Fig. 2b), the correlation coefficients are in most cases lower than in winter. Since the climatological summertime pressure distribution within the area considered here is relatively flat, however, this does not in all cases result from large absolute errors. Nevertheless, according to subjective judgement also, the ECHAM2 pressure simulation is clearly the best and the UKMO/mixed simulation (which is dominated by a spurious southward protruding Arctic high) the worst of the seven.

Simulated response to increased greenhouse gas concentrations

The results of the greenhouse runs were averaged over a 10- or 20-year time slice, which in four of the five transient simulations conducted with the coupled atmosphere-ocean GCMs was centred at the doubling of equivalent CO_2. In the NCAR experiment, however, the corresponding increase was only 65%, hence this experiment is not directly comparable with the others. The results from the two models with a mixed-layer ocean represent an equilibrium response to doubled CO_2 with the assumption of no changes in ocean currents.

Surface air temperature

Area averages of the simulated change (greenhouse run — control run) in surface air temperature are depicted in Fig. 3a. For each experiment, three bars are shown, the first two of which give the winter- and summertime means over the continental northern Europe and the last the global annual mean. In all seven experiments, the simulated area average warming over northern Europe in winter exceeds the warming in summer. It may be noted, though, that the difference is smallest in the ECHAM2 and GFDL experiments, which appeared to provide the most realistic control simulations over the area. The ratio of the warming in northern Europe to the global annual mean
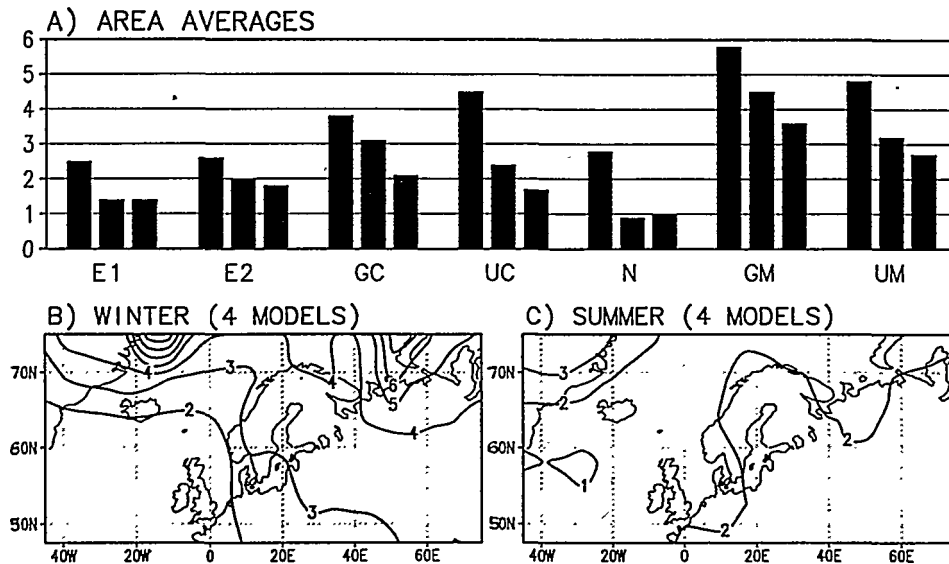

Fig. 3 (a) The simulated area average warming (°C) over the continental northern Europe and the whole globe (see text). (b) The arithmetic mean of the simulated December-February temperature changes in those four transient experiments (E1, E2, GC and UC) in which the doubling of CO_2 was achieved. (c) As (b) but for June-August.

varies, depending on the model, from 1.5 to 2.7 in winter and from 0.9 to 1.5 in summer. Not surprisingly, the two equilibrium experiments yield both globally and in northern Europe a larger warming than any of the transient experiments. In qualitative terms, however, the area averages reveal no large differences between the results of the transient and the equilibrium experiments.

Figs. 3b and 3c show the geographical distribution of the simulated winter- and summertime warming averaged over those four transient experiments (ECHAM1, ECHAM2, GFDL and UKMO) in which the doubling of CO_2 was achieved. In winter, this composite reveals a minimum of warming over the Atlantic and an increase towards the continental interior and the Arctic Ocean. The Atlantic minimum is also present in summer, but the gradients are weaker in this season. Due to the large variability from model to model and the relatively short averaging periods used, the finer geographical details deserve little attention.

Sea level pressure

Analogously to Figs. 3b-c, four-model averages of the simulated changes in sea level pressure are shown in Fig. 4. In the composite for winter (Fig. 4a), the changes are strongest over the northern North Atlantic, where the pattern implies a slight northward shift of the Icelandic low and a minor strengthening of westerly winds. In summer (Fig. 4b), a small but widespread pressure decrease is indicated. A comparison of the individual simulations suggested that this general summertime pressure decrease may actually be a more robust finding than the wintertime changes over the Atlantic. This conclusion was also supported by a statistical t-test conducted for the one experiment (ECHAM2) for which information about interannual variability was available.
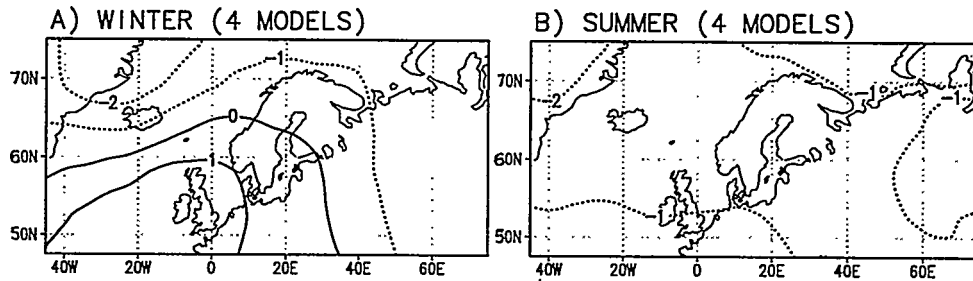
Fig. 4 .As Figs. 3b-3c, but for changes in sea level pressure (hPa) in (a) December-February and (b) June-August.

References

Hoskins, B. J., H. H. Hsu, I. N. James, M. Masutani, P. D. Sardesmukh, and G. H. White, 1989. Diagnostics of the Global Atmospheric Circulation Based on ECMWF analyses 1979-1989. WCRP - 27, WMO/TD - NO. 326, 217 pp.

Räisänen, J., 1994: A comparison of the results of seven GCM experiments in northern Europe. Geophysica, 30, 3-30.

Climate without atmospheric ozone

Petri Räisänen, Petri Hoppula and Niilo Siljamo

Department of Meteorology, University of Helsinki
P.O.B. 4, FIN-00014 Helsinki

Introduction

In the course "Laboratory in numerical meteorology" held at the Department of Meteorology, the University of Helsinki in autumn term 1994, several climate model experiments were performed. Our group investigated the effect of removing all atmospheric ozone.

Model and experiment

The model used in the experiment was the Cycle 34 version of the ECMWF atmospheric model. It had 19 layers in the vertical, the uppermost one at the height of 10 hPa. Because of limited computer resources, fairly low horizontal resolution (triangular truncation T21) was used. Likewise, in order to get statistically significant results from relatively short simulations, perpetual January insolation conditions were assumed. Apart from those already mentioned, the major limitations of the model included: prescribed sea surface temperatures, prescribed distributions of deep soil temperature and humidity, and the lack of gravity wave drag parameterization.

The climatic effects of removing ozone were investigated by comparing the results of a "ozoneless run" (no ozone in the atmosphere) with those of a "control run" (unperturbed gas concentration). The total length of the ozoneless run was 705 days; the last 400 days of the run were taken to represent the adjusted climate. For the control run, the corresponding period for calculating statistical quantities was 420 days.

Results

In agreement with earlier experiments (e.g., Manabe & Strickler 1964, Kiehl & Boville 1988), the removal of ozone led to very low stratospheric temperatures (Fig. 1). The change (i.e., the temperature difference between the ozoneless run and the control run) was largest (about -90 °C) at the 10 hPa level over Antarctica, whereas in the high northern latitudes, the stratospheric temperatures decreased by 30 °C or less. (It may be noted, however, that even the temperatures in the control run were somewhat colder than observed in that region.) No major changes occurred in tropospheric temperatures.
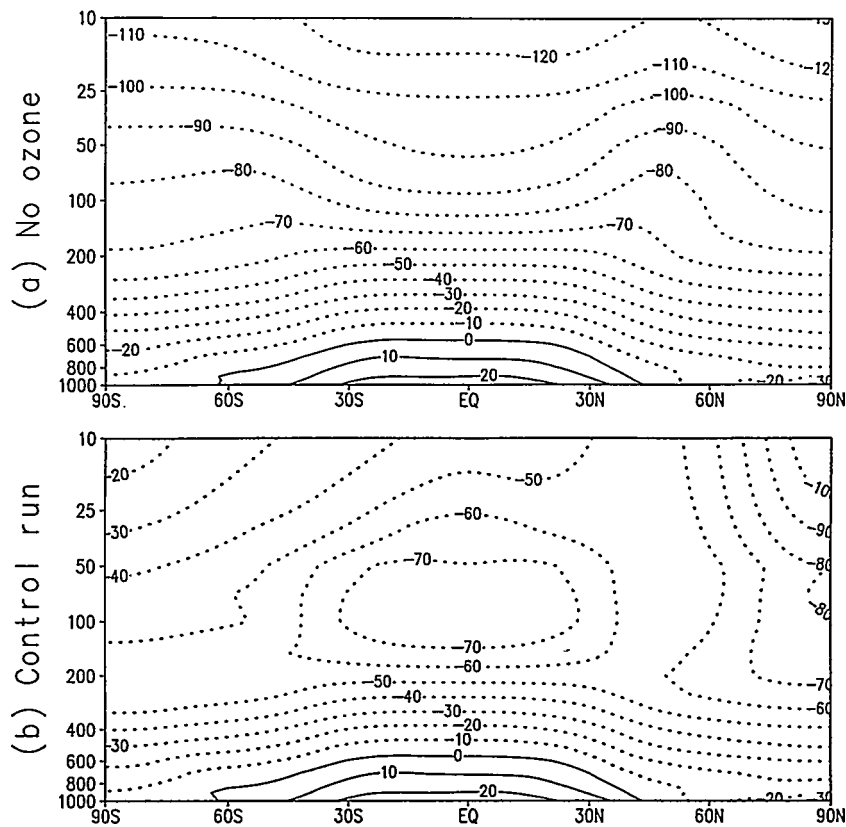
Fig. 1 The zonal mean temperature (°C) as a function of pressure (hPa) and latitude in the ozoneless run (a) and in the control run (b).

The change of the temperature distribution induced considerable changes in the mean zonal winds in the stratosphere (not shown). Both the westerly polar night jet and the easterly jet in the tropics were weaker in the ozoneless run than in the control run. In the midstratosphere over Antarctica, the easterly winds of the control run were replaced by westerly winds, which now prevailed throughout the atmospheric column. This feature deviates from the results of Kiehl & Boville (1988), and was accompanied by substantially increased spatial and temporal variations in the midstratospheric geopotential field. The theory presented in Holton (1992, p. 414) provides an explanation for this: stationary waves can propagate vertically only in the presence of westerly winds weaker than a certain critical value. In both hemispheres, the upper tropospheric westerly jets were a bit more intense and slightly higher-located than in the control run.

The mean meridional circulation was slightly more intense in the ozoneless run than in the control run. This feature is probably related to the weaker stability in the stratosphere and near the tropopause.

The removal of ozone also had significant effects on the distribution of surface pressure (Fig. 2). The mean pressure decreased over large areas extending from western Atlantic to eastern Siberia, locally by up to 13 hPa. On the other hand, in

North America, the northern Pacific area and south Asia the mean pressure was slightly higher in the ozoneless run than in the control run. A modest, but quite widespread, increase of surface pressure took place in the tropics. The differences in surface pressure between the two runs may stem from different reflection of long stationary waves from the top, associated with differences in stability and zonal mean winds in the stratosphere. This conclusion is supported by the large horizontal scale of the pressure changes.
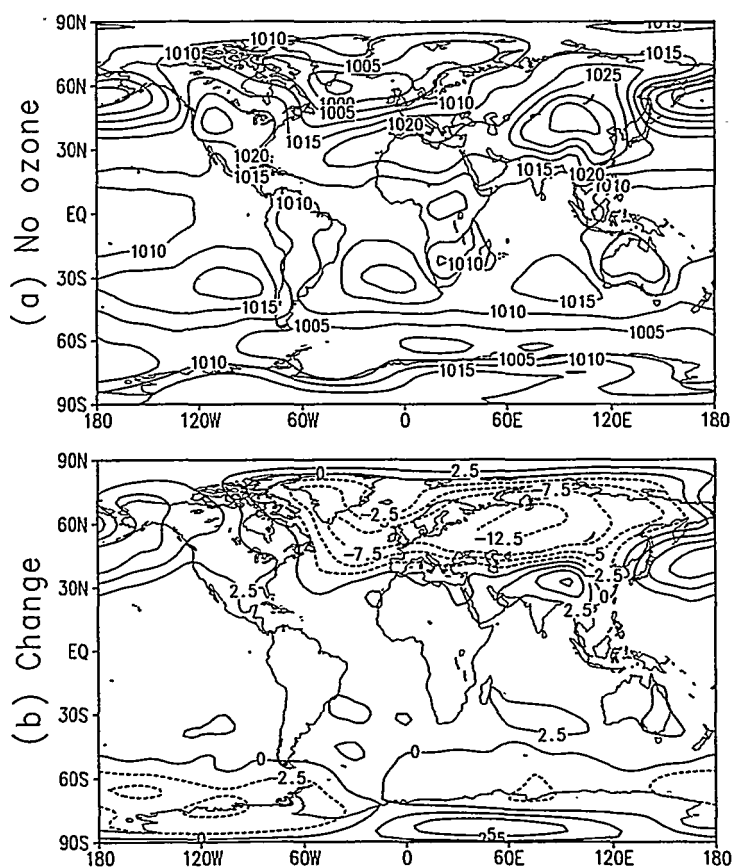
Fig. 2 The average sea level pressure (hPa) in the ozoneless run (a) and the difference between the ozoneless run and the control run (b).

The largest changes in the average surface temperature, about + 6 °C, took place in central Asia, consistently with the weakening of the climatological cold anticyclone in that area. The most notable change in the distribution of precipitation was an increase in an area extending from northern Atlantic via central Europe to southwestern Siberia. This feature is likewise related to the change of the average surface pressure distribution. In accord with the intensified meridional circulation, the globally averaged precipitation was about 5% larger in the ozoneless run than in the control run.

No major changes occurred in the diagnosed amounts of low and middle clouds. However, a curiosity of interest is that the very low temperatures in the ozoneless run

led to the occurrence of clouds in the stratosphere. As the absolute amount of stratospheric water vapour was substantially smaller than in the control run, these clouds were evidently extremely tenuous.

Globally averaged, the reflected solar radiation at the top of the atmosphere was about 5 Wm^{-2} larger in the ozoneless run than in the control run, whereas the outgoing longwave radiation was about 5 Wm^{-2} smaller. The average surface radiation balance was slightly more positive (by about 5 Wm^{-2}) in the ozoneless run, but this was, on the average, compensated by slightly larger fluxes of sensible and latent heat. However, there were large local differences in the surface energy balance between the two runs. In the Gulf stream region, the energy flux from the ocean was larger in the ozoneless run, locally by up to 100 Wm^{-2}. In the region of the Kurosio stream east of Japan, a decrease of the same magnitude took place. These changes were associated with differences in the distribution of surface air temperature and wind speed. In reality (and in a more sophisticated climate model), changes so large could lead to considerable changes in sea surface temperatures.

References

Holton, J.R. 1992. An introduction to dynamic meteorology, Third edition. International geophysics series, Vol. 48. Academic Press, 511 pp.

Kiehl, J.T. & Boville, B.A. 1988. The radiative-dynamical response of a stratospheric-tropospheric general circulation model to changes in ozone. J. Atmos. Sci. 45: 1798-1817.

Manabe, S. & Strickler, R.F. 1964. Thermal equilibrium of the atmosphere with a convective adjustment. J. Atmos. Sci. 21: 361-385.

Radiative forcing due to greenhouse gas emission and sink histories in Finland and its future control potential

Ilkka Savolainen, Jukka Sinisalo and Riitta Pipatti

VTT Energy (Technical Research Centre of Finland)
P.O.Box 1606, FIN-02044 VTT, Finland

Introduction

The effective atmospheric lifetimes of the greenhouse gases like carbon dioxide (CO_2),nitrous oxide (N_2O) and many of the CFCs are of the order of 100 years. Human activities, as an example GDP, very often change at rates of a few per cents per year,corresponding time constants of some tens of years. Also the forest ecosystems have time constants of this order. Even the human population of the globe is increasing by about two percent per year. Because so many natural and human-linked processes, which are relevant to global warming, have slow change rates of about same order, a time-dependent consideration of the greenhouse warming and its control can give useful information for the understanding of the problem.

The objective of the work is to study the anthropogenic greenhouse gas emissions and sinks in Finland and their greenhouse impact as a function of time. The greenhouse impact is expressed in terms of radiative forcing which describes the perturbation in the Earth's radiation budget. Radiative forcing allows a comparison of the impact of various greenhouse gases and their possible control options as a function of time. The idea behind the calculations is that Finland should in some way steer its share of the global radiative forcing and greenhouse effect.

Calculation model

The removal of carbon dioxide from the atmosphere in the REFUGE model (Korhonen et al. 1993) is based on the pulse-response functions obtained with a three-dimensional ocean model by Maier-Reimer and Hasselmann. The removal of methane, nitrous oxide, CFCs and their substitutes from the atmosphere are depicted with exponential models based on one time constant for each gas.

Radiative forcing arising from increased concentrations is calculated with a method given by IPCC in 1990 and by Wigley. The REFUGE model examines the direct impacts of gases on radiative forcing, which are considered to be fairly precisely known. In the case of methane also the indirect impacts are considered using an atmospheric adjustment time and an estimate for the contribution of methane-induced increase of tropospheric ozone and stratospheric water vapour.

Model applications

The REFUGE model has been applied to study a wide range of emission types and control possibilities: 1) Scenarios for the fossil CO_2 emission control in Finland (Korhonen el al. 1993; Savolainen and Sinisalo 1994), 2) Role of forest carbon sink in the control of the net CO_2 emissions in Finland (Kanninen et al. 1993), 3) Impact of anthropogenic CH_4 and N_2O emissions on radiative forcing (Pipatti et al. (in press)),
4) Impact of CFC emissions and their substitutes on radiative forcing and chlorine load of the atmosphere (Pipatti and Sinisalo 1994), 5) Greenhouse impacts of peat and wood based energy production chains (Savolainen et al. 1994), 6) The Nordic anthropogenic greenhouse gas emission history and caused radiative forcing, 7) The greenhouse impact of peatland draining.

References

Kanninen, M., Korhonen, R., Savolainen, I. & Sinisalo, J. 1993. Comparison of the radiative forcings due to the CO_2 emissions caused by fossil fuel and forest management scenarios in Finland. In: Kanninen, M. (ed.) Carbon Balance of the World's Forested Ecosystems: Towards a Global Assesment. IPCC/AFOS workshop held in Joensuu, Finland, 11-15 May 1992. Publ. Acad. of Finland 3/93. Pp. 240-251.

Korhonen, R., Savolainen, I. & Sinisalo, J. 1993: Assessing the impact of CO_2 emission control scenarios in Finland on radiative forcing and greenhouse effect. Environmental Management Vol. 17, No. 6, pp. 797-805.

Pipatti, R., Savolainen, I., Sinisalo, J. (in press): Greenhouse impacts of anthropogenic CH_4 and N_2O emissions in Finland. Accepted to be published in Environmental Management.

Pipatti, R. & Sinisalo, J. 1994: Scenarios for halocarbon emissions in Finland and estimates of their impact on global warming and chlorine loading in the stratosphere. Journal of Environmental Management Vol. 40, No. 3, July 1994, pp. 259-275.

Savolainen, I., Hillebrand, K., Nousiainen, I., Sinisalo, J. 1994: Comparison of radiative forcing impacts of the use of wood, peat, and fossil fuels. Fifth Global Warming Science and Policy International Conference (GW5), 4-7 April 1994, San Francisco, Calif., U.S.A. Published in World Resource Review 6(2), p. 248-262, June 1994.

Savolainen, I. & Sinisalo, J. 1994: Radiative forcing due to greenhouse gas emissions in Finland - estimating the control potential. The Science of the Total Environment, 151 (1994) 47-57.

Sensitivity of climate change in Europe to the Northern Atlantic warming

B. Timbal, J.-F. Mahfouf and J.-F. Royer

Centre National de Recherches Météorologiques (CNRM), Météo-France
42 Av. G. Coriolis, 31057 Toulouse Cedex, France

Introduction

The increase in atmospheric carbon dioxide since the beginning of the industrial revolution has raised the question of its impact on climate. Anthropogenic release of carbon dioxide is an extra source in the complex carbon cycle involving the ocean, the atmosphere and the biosphere. Three-dimensional general circulation models have been used world-wide over the last decade to perform climate research (Houghton et al., 1990 and 1992). Complete global change experiments need to couple an atmospheric model with an oceanic one and a thermodynamical and dynamical sea-ice model. Therefore realistic scenarios of greenhouse gas increases can be studied. These computer-time expensive experiments cannot be reproduced as often as necessary. A commonly used approach is to perform time-slice experiments at the equilibrium with an atmospheric GCM forced by Sea Surface Temperature (SST) anomalies. Several sensitivity experiments using higher resolutions or more sophisticated physical parameterisations can be performed (Mahfouf et al., 1994). As the resolution increases, one can study the result over special areas of interest, such as Europe.

Models, experimental designs

The atmospheric GCM is the climatic version of the ARPEGE/IFS code developed jointly by METEO-FRANCE and the European Centre for Medium-Range Weather Forecasts (Courtier et al., 1991) that has been adapted for climate studies. The version used in these experiments has been described in detail by Déqué et al. (1994). The model has a spectral T42 triangular horizontal truncation. The reduced Gaussian grid has a horizontal resolution of about 2.8° in latitude and longitude. Such resolution allows a focus on regional changes in selected areas over continents as proposed in the IPCC report (Houghton et al. 1990). The model has comprehensive physical parameterisations similar to those used for previous climate change studies (Mahfouf et al. 1994).
Three time-slice integrations have been performed. Five annual cycles were integrated and averaged, which appears sufficient to obtain a rather stable mean annual cycle. In the control run, the atmospheric carbon dioxide is set to 345 *ppmv*. The prescribed SSTs and sea-ice extents (with constant depth)

are 1979-1988 averages of the COLA-CAC sets used for AMIP simulations. For the two doubled CO_2 experiments the same technique was applied. Mean sea-ice extents and SSTs from the two coupled AOGCMs were used. One coupled model was the ECHAM1/LSG developed at the Max-Planck-Institut für Meteorologie (MPI) in Hamburg (Cubasch et al. 1992). The SST anomalies were calculated between the control run and the transient perturbed run in which the concentration of CO_2 increased at the rate of $1.3\%year^{-1}$. They are averaged over ten years (2041-2050) corresponding to the doubled CO_2 period according to IPCC scenario A. The other coupled model is that developed at the Hadley Centre (HC) of the United Kingdom Meteorological Office coupled with an ocean model derived from Cox (1984) (Murphy 1994, Murphy and Mitchell 1994). In this transient experiment the rate of increase of CO_2 concentration is $1\%year^{-1}$ and the doubled period is the last ten years of the 75-year transient run.
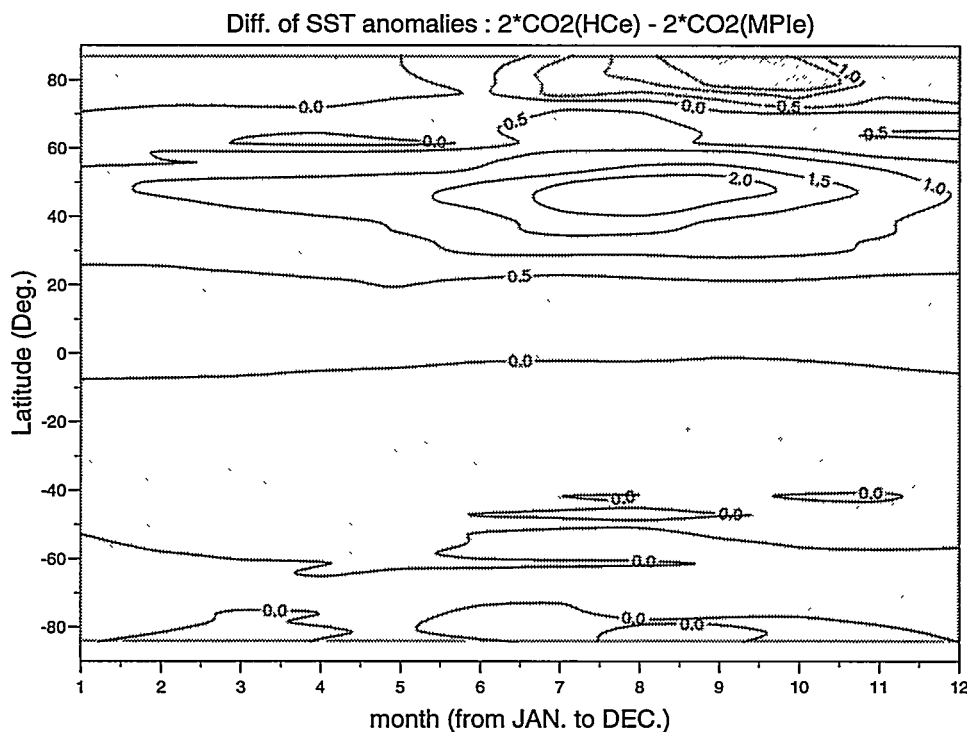
Figure 1 : *Seasonal cycle of the zonal mean of the difference in the SST anomalies (°C) imposed in HCe minus that imposed in MPIe.*

It is interesting to use the results of the two coupled models since the zonal mean SST anomalies imposed were rather different (Fig 1), at least in the Northern Hemisphere. The stronger forcing of the HC model is mostly located between 30° and 60°N with a strong annual cycle. The maximum difference is obtained in August and its amplitude is reinforced by a negative difference at higher latitude over the North Pole later in autumn. The geographical

repartition of this difference proves that it is mostly situated over Northern Atlantic where the warming is particularly strong in summer. Nevertheless, in both coupled experiments, the warming over Northern Atlantic is limited compared to previous simulations with a mix-layer ocean due to deep-water formation. This is discussed in the IPCC report (Houghton et al., 1990).

Discussion on the signals over Europe
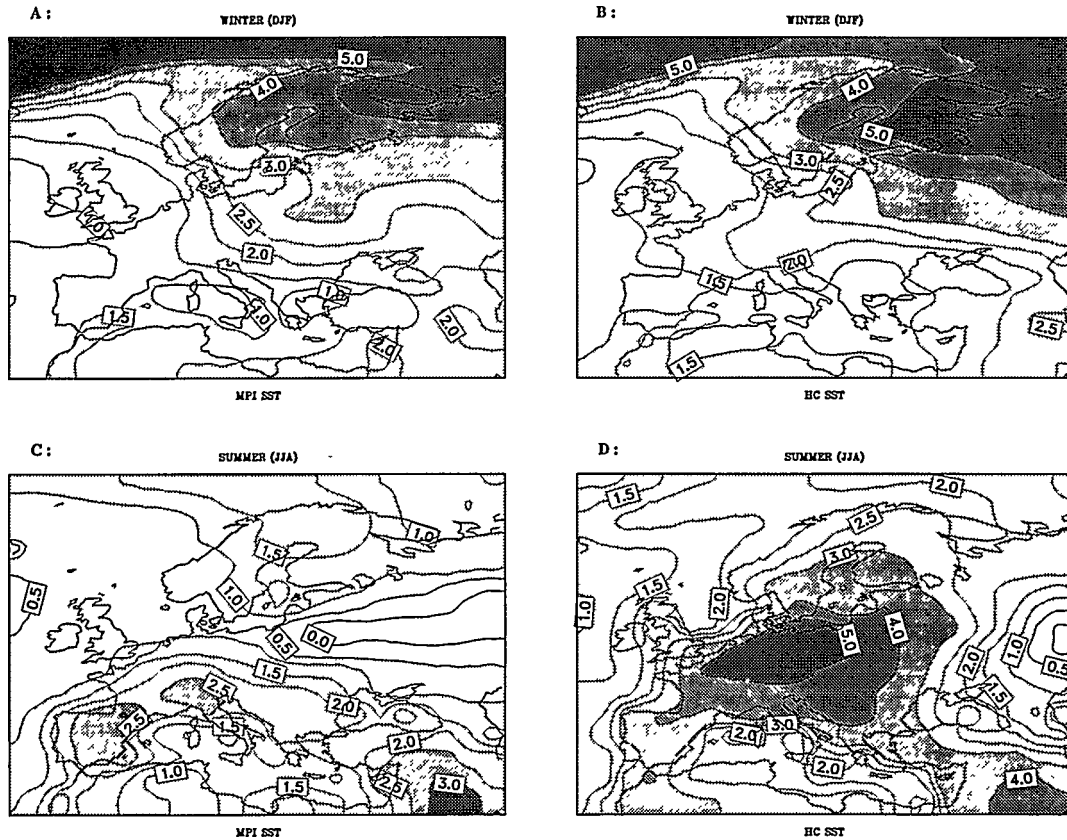
Figure 2 : *Anomalies of temperature (°C) in winter (A and B) and in summer (C and D) for MPIe and HCe, over Europe and the Mediterranean area.*

During winter, the patterns of the temperature anomalies in both experiments are rather similar. The warming increases with the latitude due to snow and sea-ice feedbacks and is more important over the continents (a minimum over the Mediterranean basin). In summer the model response is different according to the oceanic forcing. Limited to 2 to $3°C$ around the Mediterranean sea, the warming is up to $5°C$ in HC over Northern Europe while a cooling appears in MPI.

A similar annual evolution is observed for soil moisture. In winter, the Mediterranean basin get dryer, while in Northern Europe, soil moisture increases. This

is due, in both experiments, to an increase and a shift northward of the Islandic low which shifts the penetration of humid air over Europe more northward. In summer, when evaporation is strong, the patterns are related to the surface warming and differ in the two experiments. A very strong pattern is visible in HC (up to $3\,mm$ of soil moisture reduction equivalent to 15% of the total reservoir) and not in MPI. This is also due to the precipitation anomalies in each case.
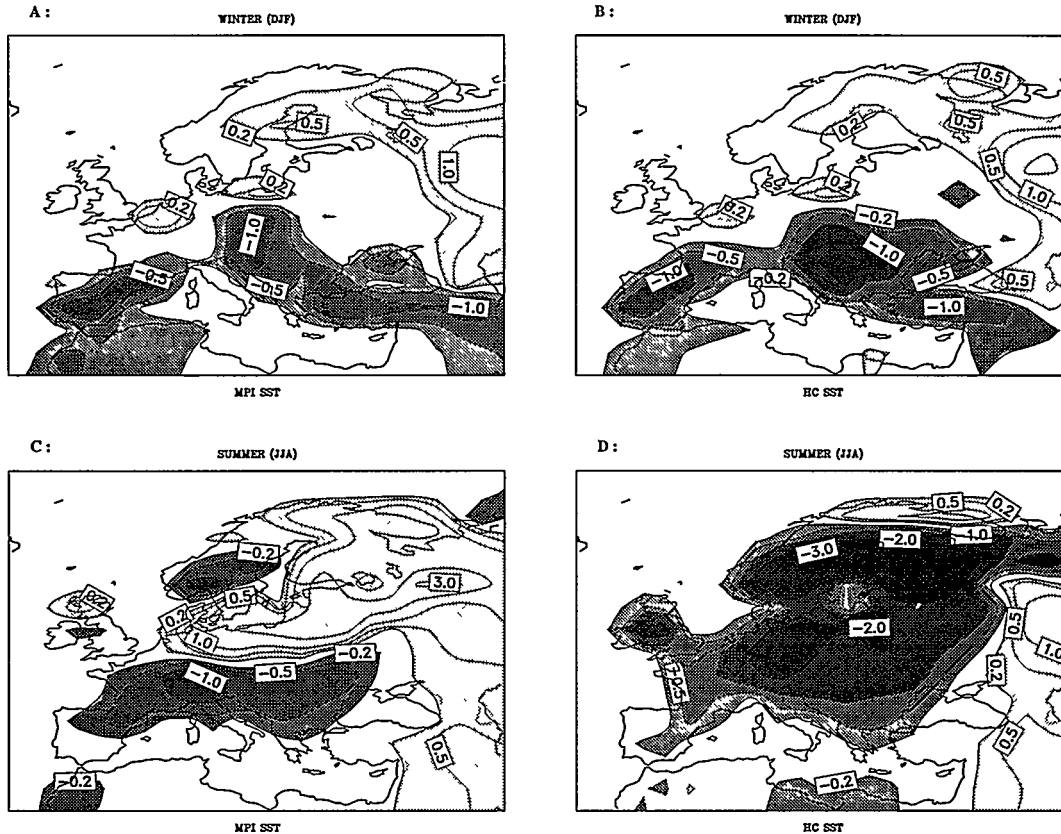
Figure 3 : *As in Fig 2 but for soil moisture in mm.*

Conclusions

The temperature response over Northern Europe is directly related to the warming of the Atlantic ocean. This pattern directs the response of the hydrological cycle over the European continent. Thus the global climate change simulated by any model is closely related to the way the oceanic influence is taken into account. Therefore it is necessary to use global coupled models which can simulate the formation of deep-water in the Northern Atlantic.

References

Courtier Ph., Freydier C., Geleyn J.-F., Rabier F., Rochas M. (1991) The ARPEGE project at Météo-France. In: Workshop on Numerical methods in atmospheric models, vol II, ECMWF, pp 193–231

Cox M.D. (1984) A primitive equation, three dimensional model of the ocean. Technical report N°1, GFDL/Ocean group

Cubasch U., Hasselmann K., Höck H., Maier-Reimer E., Mikolajewicz U., Santer B.D., Sausen R. (1992) Time-dependent greenhouse warming computations with a coupled ocean-atmosphere model. Climate Dynamics, 8: 55–69

Déqué M., Dreveton C., Braun A., Cariolle D. (1994) The ARPEGE/IFS atmospheric model: a contribution to the French Community Climate modelling. Climate Dynamics, 10: 249–266

Houghton J.T., Callander B.A., Varney S. K. (1992) Climate Change 1992, the supplementary report to the IPCC Scientific Assessment. Intergovernemental Panel on Climate Change IPCC, University Press, Cambridge

Houghton J.T., Jenkins G.J., Ephraums J.J. (1990) Climate Change, the IPCC Scientific Assessment. Intergovernemental Panel on Climate Change IPCC, University Press, Cambridge

Mahfouf J.-F., Cariolle D., Royer J.-F., Geleyn J.-F., Timbal B. (1994) Response of the METEO-FRANCE Climate Model to Changes in CO_2 and Sea-Surface-Temperature. Climate Dynamics, 9: 345–362

Murphy J.M. (1995) Transient response of the Hadley-Centre coupled Ocean-Atmosphere model to increase in carbon dioxide. Part I: Control Climate and flux adjustement. Journal of Climate, 8: 36–56

Murphy J.M., Mitchell J.F.B. (1995) Transient response of the Hadley-Centre coupled Ocean-Atmosphere model to increase in carbon dioxide. Part II: Spatial and temporal structure of response. Journal of Climate, 8: 57–80

Operational Long-Lead Seasonal Climate Outlooks Out to One Year: Rationale

Huug M. van den Dool

Climate Analysis Center, W/NMC51
5200 Auth Rd., Washington, DC 20233 U.S.A.

As of January 1995 there have been several major changes in the operational long range US-NWS forecasts. For many decades we have known the Monthly and Seasonal *Weather* Outlooks. These were developed by Jerome Namias (1940's, etc) and Donald Gilman (1970's, etc) and collaborators. The origin of long-range forecasts is thus in the days well before Numerical Weather Prediction (NWP) played a role even in the short-range weather forecasts.

From the beginning, the Outlooks were usually released just before the first date of validity. For example, the February forecast would be released on or about Jan 30. Taking into account also the slow delivery system (by regular mail) it is fair to speak of a zero-lead forecast. The "lead" is defined as the amount of time between release and first moment of validity.

The biggest changes introduced consist of three aspects:

1. The lead of all monthly and seasonal forecasts will be 2 weeks or longer. For example, the February forecast will be released around the middle of January. The term Long Lead (LL) refers to the change from a zero to a two week lead operation.

2. Every month there will be a suite of 13 seasonal forecasts going forward in time in overlapping fashion with steps of one month out to the next year. For instance, around the middle of January 1995, there were forecasts for FMA95, MAM95, AMJ95........to FMA96. The forecast for FMA96 (for instance) will be updated every month until Jan 15, 1996 when the final FMA96 forecast is issued. {This is, in design, much like running a NWP model out to 10 days every days.} There will be a monthly forecast at two week lead, but only for the first upcoming month.

3. The third change, implied by the first two, is a change in emphasis from weather forecasts (as an initial value problem) to climate forecasts. By eliminating the first two weeks there is virtually no skill left due to knowing the initial atmospheric condition, and all remaining skill is thus based on knowing global boundary condition, climate change, etc.

The rationale or justification for these changes is as follows:

The change from zero-lead to two week lead. We are assuming that NWP is covering days 1-7 individually, (or averaged in small groups, such as days 3-5), followed by a 2nd week forecast (days 8-14 averaged) which will replace the 6-10 day forecast (also a NWS

product) sometime late in 1995. There is thus no need to repeat and combine the first two weeks into a monthly and seasonal mean. Rather, the longer averages should start beyond two weeks.

Forecasts out to a year. In-house experimentation with the tools to be used (see below for a list of tools) has shown that the skill of seasonal forecasts over 1956-present is much more a function of the target season than of the lead. There are two maxima in skill, one at the end of winter (JFM), the other at the end of summer (JAS), with two minima in between. This characteristic two peak-two vally structure (which, interestingly does not exist in day-to-day weather forecasting) can be seen regardless of lead. For the times in the year of maximum skill one can state that whatever little we know, we know it well in advance, i.e. the skill at leads of 1 and 4 months are quite close, and skill remains non-zero out to at least a year. Considering utility as well there is no reason to withhold this information until the last minute. On the other hand, some three month periods during the transition seasons (late fall in particular) are almost impossible to forecast, even at the shortest leads.

The LL forecasts are based on the three following tools:

1. Canonical Correlation Analysis (CCA) (Barnston 1994, J.Climate, p. 1513)
2. Coupled Model Forecasts (CMF) (Ji et al. 1994, Tellus, p398)
3. Optimal Climate Normals (OCN) (Huang and Van den Dool, 1995, J.Climate, in press). {More tools could be added in the future.}

CCA essentially determines a relationship between the predictor fields in 4 previous seasons and the US seasonal mean T and P at a later time. For the US, near global SST turns out to be the most valuable predictor, but NH 700mb heights and the predictand at an earlier time are also offered. In determining the skill of CCA on independent data, "cross-validation" is used extensively over 1956-present.

CMF is like NWP, i.e. based on the familiar equations of motion, temperature etc, applied to both the atmosphere **and the ocean**. At this point only the tropical Pacific is coupled interactively to the atmosphere. The CMF is run each month in ensemble fashion out to about 7 months ahead, both with forecast SST and with persisted SST (no two way coupling in the latter case).

OCN boils down to persistence of the average of the anomaly observed in last ten years in the same season at the same location. Anomaly is relative to the WMO 30 year normal. A verification record over 1961-present has been established. Because of the very low frequency nature of OCN the skill at leads of 1 and 2 years are almost the same. Therefore, OCN becomes the dominant tool at leads of 9 months or longer. The fact that OCN has skill proves that **the climate is not constant.**

As always: A-priori estimates of skill for each tool are important. For OCN and CCA we have extensive skill information based on a 30+ year record. For CMF we have a proxy skill record over 1982-93 based on runs with prescribed perfect SST. The a-priori skill estimates are used as a mask on top of real time forecasts by each tool. Forecast values are considered only in areas where the a-priori skill estimate is >0.3 in terms of local temporal anomaly correlation. For any given tool this leaves large portions of the US blank, particularly for

precipitation and longer leads.

The consolidated forecast is ideally constructed in the following objective way. If A, B, C denote the forecast anomalies by tool A, B and C respectively, the official forecast as a function of element, lead, location and season will be:

$$\text{Official} = a^*A + b^*B + c^*C$$

where the coefficients a,b,c are determined from a large set of honest hindcasts by the three methods. Solving for a, b, and c entails the calculation of the Cov(A,B), Cov(A,C), Cov(B,C) and Cov(A,Obs), Cov(B,Obs), Cov(C,obs). In the last three covariances we recognize traditional anomaly correlations. The first three measure the relative redundacy among methods on the 30+year data set. There is clearly a limit to how much more new information can be gained out of yet another forecast method, even if the latter has good skill on its own.

By absolute standards the skill of these forecasts is fairly low. In the best seasons (JFM) when ENSO is believed to have the most stereotypical impacts on the US in some of the years, the nation averaged anomaly correlation over 30+ years is at best 0.4, although certain areas in the Southeast and Northwest may exceed that number.

The forecast map has four options:

1. Forecast for above normal/median: **A**
2. Forecast for below normal/median: **B**
3. Forecast for confident near-normal/median: **N**
4. No forecast at all because of lack of skill in all tools. Advise climatological (**CL**) probabilities for the three classes based on the 1961-90 WMO base period.

The last two options are a novelty. We use three equiprobable classes and the forecasts are in probability anomaly format.

The no-forecast or **CL** option is important. It is an up-front admission of lack of skill (by current tools) in certain areas/seasons and it is thus appropriate to refrain from a forecast and use the climatological "fall-back" forecast. This will help our credibility for those occassions/locations where/when we do issue a forecast.

The forecast will no longer be distributed by mail. Distribution through regular NWS channels (AFOS, DIFAX ..etc) will continue as before. In addition we will distribute the forecasts (official, and forecast by each tool) on internet with address http://nic.fb4.noaa.gov. All a-priori skill estimates are to be found on internet as well. Therefore, the user will know about as much as we do, and can reproduce the official forecast from the tools.

These new forecasts are named Climate Outlooks so as to distinguish them from traditional weather forecasts. The Climate Outlook tells little or.nothing about the weather on any given day in the season.

Stratospheric ozone reduction and its relation to natural and man made sources

Ivar S. Isaksen
Department of Geophysics, University of Oslo

Abstract

Approximately 90% of the total ozone mass is in the stratosphere (between approximately 12 and 50 km), the rest is in the troposphere (below 12 km). Since we are primarily interested in ozone's role as a protecting shield for harmful radiation from the sun we are interested in changes in the stratospheric ozone. The global distribution of ozone in the stratosphere and its variation over time have been studied extensively over several decades. These studies include observations by ground based instruments (e.g. Dobson instruments), instruments on airborne platforms (e.g. ozone sondes) and on satellites, and model studies which simulate the chemical and dynamical behaviour of the stratosphere. These studies have given us good information about the processes which determine the ozone distribution, and how man made emissions affect the distribution.

variations in stratospheric

ozone concentrations occur, during winter and spring months. For instance, during the 1992/1993 winter ozone reductions up to 25 to 30 %, compared to the long term mean, were observed. Measurements from the last winter (1994/1995) performed by the European SESAME campaign have shown similar and even larger ozone decreases in the lower stratosphere. Model studies give strong indications that a substantial fraction of the reduction is due to the enhanced chemical loss through chemical reactions involving chlorine compounds (ClO and Cl). Calculations give chemical ozone loss in the lower stratosphere in excess of 1 % per day for extended periods (weeks) during spring. The chlorine involved in the ozone destruction is released from CFSs in the stratosphere.

The enhanced ozone loss which has occurred since 1991 coincides with enhanced particle formation in the stratosphere from the Mt.Pinatubo volcanic eruption in 1991, and enhanced formation of Polar Stratospheric Clouds (PSC) due to extremely low stratospheric temperatures, which were particularly pronounced in the winters of 1992/193 and 1994/1995. The particles activate the ozone destruction by chlorine reactions. Model studies have shown that the ozone loss process was strongly enhanced due to the presence of aerosol particles and PSCs during the last four winter seasons, and could account for the observed ozone reductions. The man made impact of stratospheric ozone is therefore more pronounced during periods with high particle and PSC concentrations than during periods with low concentrations.

Observations have also shown that the 11 year solar cycle variation affects stratospheric ozone on a short time scale (a few years) and has to be taken into account when observations are analysed.

Chlorine levels in the stratospheric have increased steadily mainly due to the increase in CFCs in the atmosphere. It is estimated that approximately 80 % of chlorine in the stratosphere today is due to the man made emissions of different chlorine compounds. The strong regulations in the emissions of CFCs imposed by the Montreal agreement, have led to a slower growth in stratospheric chlorine during the last two to three years than previously. It is estimated that stratospheric chlorine will level off within the next five years, whereafter it will decrease slowly during the next century. This is estimated to lead to a levelling off in the ozone decrease and a slow increase in stratospheric ozone over the next 50 to 100 years towards values which were observed prior 1970.